ISSN 0711-6659

canadian acoustics
acoustique canadienne

Journal of the Canadian Acoustical Association - Revue de l'Association canadienne d'acoustique

SEPTEMBER 2023
Volume 51 - - Number 3

SEPTEMBRE 2023
Volume 51 - - Numéro 3

canadian acoustics

acoustique canadienne

Canadian Acoustical Association

Canadian Acoustics publishes refereed articles and news items on all aspects of acoustics and vibration. Articles reporting new research or applications, as well as review or tutorial papers and shorter technical notes are welcomed, in English or in French. Submissions should be sent only through the journal online submission system. Complete instructions to authors concerning the required "camera-ready" manuscript are provided within the journal online submission system.

Canadian Acoustics is published four times a year - in March, June, September and December. This quarterly journal is free to individual members of the Canadian Acoustical Association (CAA) and institutional subscribers. **Canadian Acoustics** publishes refereed articles and news items on all aspects of acoustics and vibration. It also includes information on research, reviews, news, employment, new products, activities, discussions, etc. Papers reporting new results and applications, as well as review or tutorial papers and shorter research notes are welcomed, in English or in French. The Canadian Acoustical Association selected **Paypal** as its **preferred system** for the online payment of your subscription fees. Paypal supports a wide range of payment methods (Visa, Mastercard, Amex, Bank account, etc.) and does not requires you to have already an account with them. If you still want to proceed with a manual payment of your subscription fee, please Membership form and send it to the Executive Secretary of the Association (see address above). - - Dr. Roberto Racca - Canadian Acoustical Association/Association Canadienne d'Acoustique c/o JASCO Applied Sciences 2305–4464 Markham Street Victoria, BC V8Z 7X8 - - secretary@caa-aca.ca

Association canadienne d'acoustique

L'**Acoustique Canadienne** publie des articles arbitrés et des informations sur tous les aspects de l'acoustique et des vibrations. Les informations portent sur la recherche, les ouvrages sous forme de revues, les nouvelles, l'emploi, les nouveaux produits, les activités, etc. Des articles concernant des résultats inédits ou des applications ainsi que les articles de synthèse ou d'initiation, en français ou en anglais, sont les bienvenus.

Acoustique canadienne est publié quantre fois par an, en mars, juin, septembre et décembre. Cette revue trimestrielle est envoyée gratuitement aux membres individuels de l'Association canadienne d'acoustique (ACA) et aux abonnés institutionnels. L'**Acoustique canadienne** publie des articles arbitrés et des rubriques sur tous les aspects de l'acoustique et des vibrations. Ceci comprend la recherche, les recensions des travaux, les nouvelles, les offres d'emploi, les nouveaux produits, les activités, etc. Les articles concernant les résultats inédits ou les applications de l'acoustique ainsi que les articles de synthèse, les tutoriels et les exposées techniques, en français ou en anglais, sont les bienvenus. L'Association canadienne d'acoustique a sélectionné **Paypal** comme solution pratique pour le paiement en ligne de vos frais d'abonnement. Paypal prend en charge un large éventail de méthodes de paiement (Visa, Mastercard, Amex, compte bancaire, etc) et ne nécessite pas que vous ayez déjà un compte avec eux. Si vous désirez procéder à un paiement par chèque de votre abonnement, merci de remplir le formulaire d'inscription et de l'envoyer au secrétaire exécutif de l'association (voir adresse ci-dessus). - - Dr. Roberto Racca - Canadian Acoustical Association/Association Canadienne d'Acoustique c/o JASCO Applied Sciences 2305–4464 Markham Street Victoria, BC V8Z 7X8 - - secretary@caa-aca.ca

CANADIAN ASSOCIATION
ACOUSTICAL CANADIENNE
ASSOCIATION D'ACOUSTIQUE

ORGANIZING COMMITTEE

- **Gauthier Bezançon** (ÉTS): Environmental sustainability coordinator
- **Julien Biboud** (Mecanum): Exhibitor and sponsor chair
- **Victoria Duda** (Université de Montréal): CAA Student prize coordinator
- **Olivier Doutres** (ÉTS): Conference chair
- **Pierre Grandjean** (Université de Sherbrooke): Proceedings preparation
- **Cécile Le Cocq** (ÉTS): Proceedings preparation
- **Mael Lopez** (ÉTS): On-site coordinator
- **Thomas Padois** (IRSST): Scientific chair
- **Simon Prenant** (ÉTS): Website coordinator
- **Jérémie Voix** (ÉTS): Social convener / CAA president

Conference website: https://awc.caa-aca.ca

INTRODUCTION

It is with great joy that we warmly welcome all participants to this year's Acoustics Week in Canada 2023. Montreal, a renowned cultural hub, provides the ideal setting for this conference. Its streets resonate with a blend of tradition and innovation. Beyond the exciting scientific exchanges at the *Plaza Centre-Ville*, participants will have the opportunity to (re)discover this city, its vibrant activities, and its unique acoustic environments. From the tranquility of Mont-Royal Park to the liveliness of markets and the hubbub of traffic and construction, the city becomes a true sonic canvas, characteristic of our ever-evolving societies.

This conference is already a resounding success with over 160 scheduled presentations. Key topics will be covered, such as environmental noise, materials for noise and vibration control, building and architectural acoustics, hearing protection, and speech and auditory sciences. Experts from various acoustic fields will lead sessions, offering fresh perspectives and fostering stimulating discussions. In addition, various scientific tours (e.g., visit to the Montreal Symphony House, different university laboratories and research centers, etc.) and social activities (i.e., gala evening, city noise mapping) are planned to provide a full experience.

At the heart of this conference are the invited speakers, representing the pinnacle of knowledge in three highly active research areas in Canada. We are honored to host distinguished experts, including Professor Christian Giguère from the University of Ottawa, Professor Noureddine Atalla from the University of Sherbrooke, and Professor Fabrice Marandola from McGill University. Their contributions promise to illuminate multifaceted aspects of acoustics, ranging from vibroacoustics to percussion and cultural conception of music, as well as warning sound perception.

Each edition of the Acoustics Week in Canada offers great visibility to local scientists (generally from the host province and neighboring ones) and a unique opportunity for everyone to meet and exchange ideas. Beyond their crucial role in advancing scientific knowledge, national conferences play an essential role in providing local solutions for researchers and contributing to the global effort to reduce CO2 emissions associated with air travel. As participants and organizers of this conference, we are in a way committing to the sustainable future of our planet. Every step we take towards hosting national conferences reinforces our role as agents of positive change. Together, we demonstrate that the pursuit of knowledge and innovation can harmoniously align with environmental responsibility.

Lastly, we express our gratitude to the sponsors who make this conference possible. Their commitment to promoting acoustics underscores the importance of collaboration between the academic world and industry.

We wish you an enriching conference, filled with exchanges and discoveries!

CANADIAN ACOUSTICAL ASSOCIATION
ASSOCIATION CANADIENNE D'ACOUSTIQUE

COMITÉ ORGANISATEUR

- **Gauthier Bezançon** (ÉTS): Coordinateur du développement durable
- **Julien Biboud** (Mecanum): Responsable des exposants et des sponsors,
- **Victoria Duda** (Université de Montréal): Coordinatrice CAA des prix étudiants
- **Olivier Doutres** (ÉTS): Président de la conférence
- **Pierre Grandjean** (Université de Sherbrooke) : Préparation des actes
- **Cécile Le Cocq** (ÉTS) : Préparation des actes
- **Mael Lopez** (ÉTS): Coordinateur sur site
- **Thomas Padois** (IRSST): Directeur scientifique
- **Simon Prenant** (ÉTS): Coordinateur du site web
- **Jérémie Voix** (ÉTS): Responsable des évènements sociaux
président de la CAA

Site internet de la conférence : https://awc.caa-aca.ca

INTRODUCTION

C'est avec une grande joie que nous accueillons chaleureusement tous les participant.e.s à la Semaine canadienne de l'acoustique de cette année 2023. Montréal, un pôle culturel renommé, offre le cadre idéal pour cette conférence. Ses rues résonnent d'un mélange de tradition et d'innovation. Une fois sorti des échanges scientifiques palpitants du *Plaza Centre-Ville*, les participant.e.s auront la chance de (re)découvrir cette ville, ses animations et ses environnements acoustiques si particuliers. Du calme du parc du Mont-Royal à l'animation des marchés jusqu'au brouhaha du trafic et des travaux de construction, la ville devient en elle-même une véritable fresque sonore si caractéristique de nos sociétés en perpétuel mouvement.

Cette conférence est d'ores et déjà un succès retentissant avec plus de 160 présentations programmées. Des sujets clés y seront abordés, tels que l'acoustique environnementale, les matériaux acoustiques pour le contrôle du bruit, l'acoustique architecturale, la protection auditive et les sciences de l'audition et de la parole. Des expert.e.s de multiples domaines de l'acoustique animeront les sessions, offrant de nouvelles perspectives et favorisant des discussions stimulantes. De plus, diverses visites scientifiques (e.g., visite de la Maison symphonique de Montréal, de différents laboratoires et centres de recherche universitaires, etc.) et activités sociales (i.e., soirée de gala, cartographie du bruit de la ville) seront proposées pour offrir une expérience complète.

Au cœur de cette conférence se trouvent les conférenciers invités, qui représenteront le summum des connaissances dans trois domaines de recherche très actifs au Canada. Nous aurons l'honneur de recevoir des experts éminents, dont le professeur Christian Giguère de l'Université d'Ottawa, le professeur Noureddine Atalla de l'Université de Sherbrooke, et le professeur Fabrice Marandola de l'Université McGill. Leurs contributions promettent d'illuminer les domaines multifacettes de l'acoustique : de la vibroacoustique à la percussion et la conception culturelle de la musique en passant par la perception des signaux d'alerte.

Chaque édition de la Semaine canadienne de l'acoustique offre une belle visibilité aux scientifiques locaux (généralement de la province d'accueil et celles des environs) ainsi qu'une opportunité assez unique pour toutes et tous de se rencontrer et d'échanger. Au-delà de leur rôle crucial dans l'avancement des connaissances scientifiques, les conférences nationales jouent donc un rôle essentiel en apportant des solutions locales aux chercheu.r.se.s et en contribuant à l'effort mondial de réduction des émissions de CO2 liées aux déplacements en avion. En tant que participant.e.s et organisat.eur.rice.s de cette conférence, nous prenons en quelque sorte un engagement envers l'avenir durable de notre planète. Chaque pas que nous faisons vers la tenue de conférences nationales renforce notre rôle en tant qu'agents du changement positif. Ensemble, nous démontrons que la quête du savoir et de l'innovation peut se marier harmonieusement avec la responsabilité environnementale.

Finalement, nous exprimons notre reconnaissance envers les sponsors qui rendent cette conférence possible. Leur engagement à promouvoir l'acoustique souligne l'importance de la collaboration entre le monde universitaire et l'industrie.

Nous vous souhaitons une conférence enrichissante, riche en échanges et en découvertes!

DIAMOND SPONSOR

Pliteq is deeply committed to continued engineering research and development of its many products and manufacturing processes. We have new inventions under development at all times and multiple patents registered in the United States, Canada and other countries worldwide.

Testing is what sets us apart. Our engineers have completed over 2000 laboratory tests in the last ten years with a commitment to a monthly testing schedule as we consider only recent testing to be relevant for engineering purposes.

Over 50 technical sales engineers and sales team support members are focused throughout all major metropolitan areas in North America, throughout the UK and Europe, the Middle East and Asia Pacific. Throughout history Pliteq has completed over 10,000 commercial projects globally, focused on our commitment to engineering and development.

Pliteq is on a steady growth trajectory and will continue to be a leading innovator in architectural acoustics, vibration and sound control on a global scale.

It's not magic, it's engineering.®

SILVER SPONSORS

The **IRSST** contributes to workers' health and safety through research, its laboratories' expertise, and knowledge dissemination and transfer, with a view to promoting prevention and sustainable return to work. Their Acoustics Laboratory is the only one accredited with CLAS (Calibration Laboratory Assessment Service) in Canada. The instruments that can be calibrated include sound level meters, dosimeters, and acoustic calibrators.

Engineered by a company with over 45 years' experience in the field, the **LogiSon Acoustic Network** has been installed in many hundreds of millions of square feet for clients in commercial offices, hospitals, call centers, banks, hotels, military facilities, and more. This award-winning sound masking technology is available worldwide.

Sound and Vibrations Solutions is a Canadian manufacturers representative with over 25 years experience with providing measurement solutions. We provide integrated solutions with equipment, support, and measurement consulting. Our passion and focus with Acoustic and vibration products help our customers deploy rapid, accurate solutions.

EXHIBITORS

An exhibition area is available on Wednesday, October 4, and Thursday, October 5, showcasing various acoustical equipment, products, and services. We highly encourage you to visit the booths, where you can explore the latest cutting-edge equipment and materials, as well as best practices in the field. A **prize drawing** is being organized to encourage participants to visit the booths, featuring remarkable prizes generously contributed by our exhibitors.

DALIMAR INSTRUMENTS
AN AMPHENOL COMPANY

HBK
HOTTINGER BRÜEL & KJÆR

Scantek
A RION COMPANY
LISTEN – FEEL – SOLVE

ENVIRONMENTAL
NOISE CONTROL

Soft dB

Mecanum
We build silence

FPInnovations

ramo

MJM CONSEILLERS EN ACOUSTIQUE INC
MJM ACOUSTICAL CONSULTANTS INC

Other contributors

eers Global

TOURISME / MONTRÉAL

ÉTS
Le génie pour l'industrie

CONFERENCE PROGRAM

DAY 1	Tuesday October 3			
15:00-18:30	CAA Board of Directors (on invitation only); Room : DOLLARD			
16:00-22:00	Advanced Registration			
18:30-20:30	Welcome Reception; Room: FOYER REGENCE ABC			

DAY 2	Wednesday October 4			
8:30-17:30	Exhibition / Trade show ; FOYER REGENCE ABC			
8:50-9:00	Welcome Note; REGENCE BC			
9:00-10:00	**Keynote : Christian Giguère (Univ. of Ottawa);** REGENCE BC			
10:00-10:20	Coffee break - Supported by Dalimar - FOYER REGENCE ABC			
Room	REGENCE A	VICTORIA	CARTIER A	CARTIER B
10:20-12:20	**Architectural and Building Acoustics**	**Hearing Protection**	**Speech and Hearing**	**Environmental Noise**
12:20-13:20	Lunch - REGENCE BC			
13:20-15:00	**Architectural and Building Acoustics**	**Hearing Protection**	**Speech and Hearing**	**Education in Acoustics**
15:00-15:20	Coffee break - Supported by HBK - FOYER REGENCE ABC			
15:20-17:20	**Architectural and Building Acoustics**	**Hearing Protection**	**Speech and Hearing**	**Artificial Intelligence in Acoustics**
17:20-18:00		**General Acoustics**		
18:15-20:00	Reception at EERS (open to all, on reservation only) / Beer&Pizza (only for students and volunteers)			

DAY 3	Thursday October 5			
8:30-17:00	Exhibition / Trade show ; FOYER REGENCE ABC			
8:50-9:00	Welcome Note ; REGENCE BC			
9:00-10:00	**Keynote : Noureddine Atalla (Univ. of Sherbrooke)**; REGENCE BC			
10:00-10:20	Coffee break - Supported by LogiSon - FOYER REGENCE ABC			
Room	REGENCE A	VICTORIA	CARTIER A	CARTIER B
10:20-12:00	**Architectural and Building Acoustics**	**Hearing Protection**	**Speech and Hearing**	**Materials for noise and vibration control**
12:00-13:00	Lunch - REGENCE BC			
13:00-15:00	**General Acoustics**	**Environmental Noise**	**Speech and Hearing**	**Materials for noise and vibration control**
15:00-15:20	Coffee break - FOYER REGENCE ABC			
15:20-17:00	**General Acoustics**	**Aeroacoustics**	**Biomedical Acoustics**	**Materials for noise and vibration control**
17:15-18:15	CAA Annual General Meeting (open to all CAA members) (REGENCE A)			
18:15-19:00	Coktail (FOYER REGENCE ABC) + PowerPoint Karaoke (REGENCE A)			
19:00-21:30	Gala Banquet - Supported by Pliteq (included to all delegates with the 3-day registration) (REGENCE BC)			
21:30-22:30	Music Jam Session (open to all)			

DAY 4	Friday October 6			
8:50-9:00	Welcome Note ; REGENCE BC			
9:00-10:00	**Keynote : Fabrice Marandola (Univ. McGill)**; REGENCE BC			
10:00-10:20	Coffee break - Supported by EERS; FOYER REGENCE ABC			
Room	REGENCE A	VICTORIA	CARTIER A	CARTIER B
10:20-12:20	**General Acoustics**	**Environmental Noise**	**Underwater Acoustics**	**Materials for noise and vibration control**
12:30-13:00	Award Ceremony and Closing Remarks			
12:20-13:00	Lunch - REGENCE BC			
14:00-16:00	Visit 1: Exclusive tour of CIRMMT (reservation required) Visit 2 : Exclusive tour ICAR (reservation required) Visit 3 : Exclusive visit of the Maison symphonique (reservation required)			

Note #1: All contributed presentations are scheduled for 18 minutes (15 minutes + 3 for questions)

Note #2: A "NoiseCapture" party is scheduled during this acoustic week to map the noise of Montréal. Download the app and input the code "AWC23" when conducting your measurements. Make sure to visit our booth for further details (and calibrate your smartphone).

MAP OF THE CONFERENCE CENTER

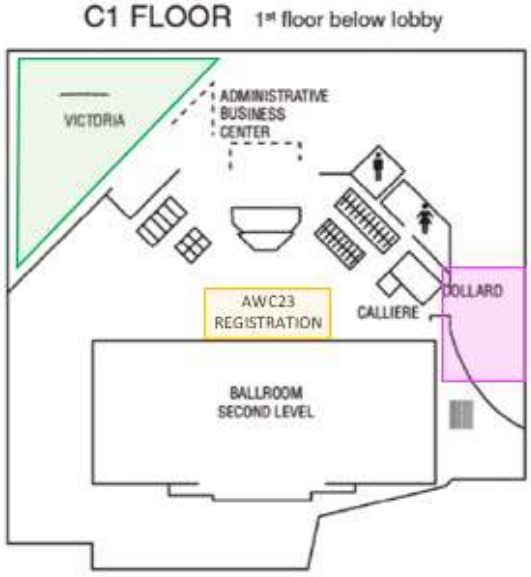

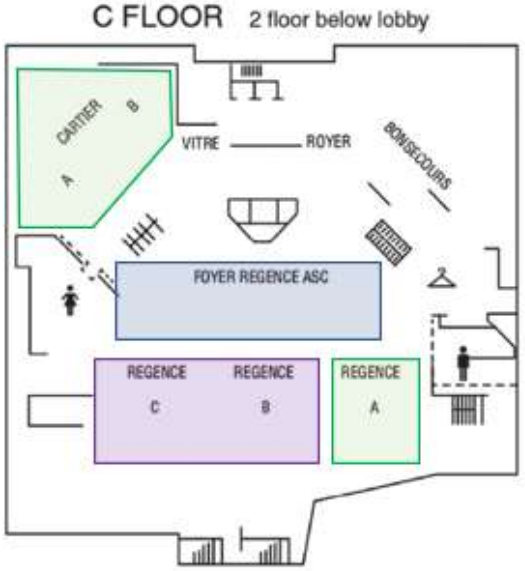

Parking is easy there, as is access to public transportation and the Central Station.
Plaza centre-ville: 777, boul. Robert-Bourassa, Montréal, QC, H3A 0B1
Parking lot entrance: 800 rue Gauvin
Web site: **https://plazapmg.com/plaza-centre-ville/**

PLENARY SPEAKERS

Christian Giguère is Professor in Audiology and Speech-Language Pathology at the Faculty of Health Sciences at the University of Ottawa. He teaches courses in acoustics, speech science, instrumentation in audiology, and hearing aids. His research interests include speech communication, warning sound perception, hearing protection, and hearing loss prevention. He has authored over 150 journal articles, conference proceedings and book chapters. Professor Giguère is active in standards organisations and member of several national (CSA, ANSI) and international (ISO) technical workgroups on topics related to occupational hearing loss, hearing protection and audiology. He was president of the Canadian Acoustical Association (2007-2013), co-chair of the International Commission on the International Commission on the Biological Effects of Noise (2008-2014), and chair of the Technical Committee on Occupational hearing loss with the Canadian Standards Organisation (2016-2022). He is currently Associate Editor with The International Journal of Audiology and Member of the NHCA's Task Force on Auditory Situational Awareness. He is a Distinguished International Member of the Institute of Noise Control Engineering (INCE-USA).

The keynote presented by Christian Giguère is entitled: *Back-up alarms on heavy vehicles: We are moving forward!* Audible back-up alarms are installed on heavy trucks and mobile equipment to alert workers and pedestrians of safety risks during reverse operations. Prompt reaction to back-up alarms by individuals nearby reversing vehicles depends on many acoustical (e.g., sound propagation pattern behind the vehicle) and psychoacoustical (e.g., perceived urgency and ability to localize alarm, effect of hearing loss and hearing protection) factors that are not comprehensively addressed in applicable standards such as SAE J994 and ISO 9533. This presentation will summarize results from a series of four collaborative studies conducted by the University of Ottawa and the IRSST in Montreal in the past twelve years. The focus was in comparing the relative benefits of two types of devices, the widely used tonal alarm and the emerging broadband alarm.

Noureddine Atalla is a professor of Mechanical Engineering at Université de Sherbrooke. His core expertise is in computational vibro-acoustics and acoustic materials. He has authored over 200 papers in acoustics and vibration, encompassing a wide range of domains. His research includes the modeling of poroelastic and viscoelastic materials, the study of coupled fluid-structure problems, the investigation of the acoustic and dynamic response of sandwich and composite structures, as well as computational vibroacoustics. In addition to his scholarly articles, he has co-authored a book on the modeling of sound porous materials and another book on finite and boundary elements in structural acoustics and vibrations.

Over the last decade, the author's team has explored various topics related to the modeling, characterization, and development of lightweight structures and their added sound packages, with a special focus on aircraft and aerospace applications. This talk will present a review of part of this body of research. In particular, the talk will demonstrate the effectiveness of employing the transfer matrix method, along with its numerous extensions, for accurately predicting the vibroacoustic response of a wide array of lightweight structures and noise control materials. The predictive capability of the method will also be illustrated for various types of excitations and systems with structured elements judiciously placed within the structure or the materials.

Fabrice Marandola is an Associate Professor of Percussion and Contemporary Music at the Schulich School of Music of McGill University (Montreal). Previously, he was a professor of percussion at the conservatories of Angers and Grenoble in France, a pedagogy instructor at the Conservatory of Paris, and an invited professor at the Crane School of Music (SUNY-Potsdam, NY). A founding member of Canadian percussion ensemble Sixtrum, he has an active career on the New Music scene, commissioning, performing and recording new works for solo and chamber ensembles. His artistic activities have received numerous distinctions and awards from Conseil Québécois pour la Musique, Académie Charles-Cros and Montreal English Theatre Awards. Marandola holds a PhD in Ethnomusicology from Paris IV-Sorbonne and has conducted in-depth field research in Cameroon with the Langues-Musiques-Sociétés Laboratory (CNRS, France). He is currently the Director of the Centre for Interdisciplinary

Research in Music Media and Technology of Montreal (CIRMMT). As Senior Research Chair at Sorbonne-Universités (2015-16), Marandola led a multidisciplinary research project on Musical Gesture (Geste-Acoustique-Musique). Author of over 30 scientific papers, his current research focuses on the study of the conception, production and perception of instrumental gestures in percussion performance, using 3D Motion Capture and wearable eye-tracking systems.

The keynote presented by Fabrice Marandola is entitled: *From cultural conception to expert performance*. The organization of pitches and durations plays a very important role in the characterization of musical systems and may vary greatly from one culture to another. Since studies on music and sound often relate to models and examples based on the Western musical tradition, it is important to keep in mind that there are a significant variety of principles that rely on different modes of organization found across the globe: for example, not all musical systems rely on a fixed number and distribution of intervals within an octave, nor does an octave always play a structural role within a musical scale. Concrete examples taken from my field work in different cultures of Cameroon will illustrate several modes of organization of musical scales in instrumental and vocal music. While the parameters that define musical systems are implicitly or explicitly known by all members of a cultural group, individuals within these groups have their own ways to build mental representations of the music they are performing. Uncovering the layers that constitute these mental representations reveals fascinating differences between performers that share the same culture. It also brings to the forefront how expert musicians develop consummate control of their movements in time and space. Research based on motion capture and gestural analysis, as well as on experiments realized with performers playing with or without their instruments (air-playing) will illustrate how musicians develop a signature in their sound production gestures, while remaining within the parameters of their cultural musical system.

SCIENTIFIC AND SOCIAL EVENTS

Welcome reception:

The AWC 2023 Welcome Reception will take place on the evening of Tuesday, October 3. All participants are cordially invited to attend. It's an ideal opportunity to make contacts in a friendly atmosphere with other scientists, engineers and conference participants.

Gala Dinner Event:

The AWC organizing committee is planning a congress banquet after the technical sessions on Thursday, October 5. Attendance at the gala is free of charge for all participants (except those attending the individual days on Tuesday, Wednesday and Friday).

Powerpoint Karaoke:

Powerpoint Karaoke (also called Powerpoint Roulette or Battledecks) is an improv game where volunteers give a presentation from a slide deck they've never seen, taken randomly from various slide decks presented in AWC2023. The name "Powerpoint Karaoke" comes from combining "PowerPoint", the presentation software, and "karaoke," the popular singing performance game. It is a game that tests the presenter's improvisation skills, gets people laughing, and keeps everyone wondering what will happen next… Simply register for this event by selecting the appropriate option during your registration process. It will also be possible to register at the last minute at the registration desk. (Picture credits: https://www.unix-ag.uni-kl.de/~guenther/powerpoint-karaoke-logo.html)

NoiseCapture Party:

Join us during AWC23 as we embark on an exciting endeavor to map the sound environment in Montréal, not only around the conference venue but also beyond. Wondering how to accomplish this task efficiently and objectively? We have the perfect solution for you - the NoiseCapture application. This Android app, developed as part of the NoisePlanet project by CNRS and Université Gustave Eiffel, is free and open-source. With NoiseCapture, you can easily measure and share your sound environment data. To facilitate your participation, Professor Olivier Robin (an ambassador and user of NoiseCapture) along with Professor Olivier Doutres (a user of the app), have set up a dedicated booth. At the booth, we will assist you in calibrating your phone and provide all the essential information about the app. You can also explore real-life examples of how NoiseCapture has been utilized in research and education. Our collective challenge during the conference is to surpass 1000 measurements, and we will provide daily updates on our progress. So, don't miss this opportunity to contribute to the sound mapping initiative and be part of an impactful project. See you at the booth! (Picture credits: https://www.uneoreilleavertie.com/quoi-de-neuf/noise-capture-party-et-hyperacousie).

Visit 1: Exclusive tour of CIRMMT

The Centre for Interdisciplinary Research in Music Media and Technology (CIRMMT pronounced "kermit") is housed at the Schulich School of Music at McGill University, just a couple blocks north of the AWC2023 venue. CIRMMT is a multidisciplinary research group that seeks to develop innovative approaches to the scientific study of music media and technology, to promote the application of newer technologies in science and the creative arts, and to provide an advanced research training environment. CIRMMT occupies a unique position on the international stage having developed intense research partnerships with other academic and research institutions, as well as diverse industry partners throughout the world. Several volunteers of the AWC2023 local organising committee are regular members of CIRMMT and a special tour has been arranged to let AWC2023 delegates discover this unique center and visit its new Music Multimedia Room.

Visit 2: Exclusive tour ICAR

The ICAR laboratory (Infrastructure commune en acoustique pour la recherche ÉTS-IRSST) is housed at ÉTS (École de technologie supérieure), just a couple blocks away from the AWC2023 venue. ICAR is a training and research laboratory for industrial acoustics. Its creation results from the successful collaboration between ÉTS university and IRSST occupational health research institute. ICAR allows to test, improve and develop new products or processes that are more acoustically efficient: industrial machines, tools, transportation vehicles, household appliances, acoustic materials and metamaterials and hearing protection devices. The ultimate goal of ICAR activities is to increase the comfort, health and safety of workers (and the general public) through the operation of state-of-the-art acoustic testing facilities that meet the needs of both industry and academic researchers.

Visit 3: Exclusive visit of the Maison symphonique

Inaugurated in 2011, the Maison symphonique is internationally recognized for the excellence of its acoustics. What criteria were used to achieve this excellence? Located in the heart of downtown near the metro and numerous construction sites, how was it ensured that no noise would interfere with the music played inside? How was the hall designed so that each of the 2100 spectators would benefit from the same sound quality? From the shape of the hall to the choice of materials, from the design of the seats to the choice of the ventilation system, come and discover why the Maison symphonique is a true musical showcase. The tour of the hall will be guided by Romain Dumoulin, acoustician, senior consultant at Soft dB, together with SNC Lavalin and/or Artec.

Cocktails, Labs & Ghosts:

EERS Global Technologies Inc is a Montreal-based company that sponsors the "ÉTS-EERS Industrial Research Chair in In-Ear Technologies (CRITIAS)" led by Prof. Jérémie Voix. EERS specializes in enhancing hearables with advanced hearing protection, biometric and in noise communication solutions. Nick Laperle, CEO and founder of EERS, is conveying all AWC2023 delegates interested to attend a cocktail (registration free but mandatory through the online form), at its creative facilities located on the 7th floor of INGO Innovation building at 355 Peel Street (across the street from ETS), on Wednesday October 4th, from 5:30 to 8:00 pm. Technical tours of the EERS and CRITIAS laboratories will be offered to guests followed by a famous Ghost Tour of Griffintown. For those interested in the famous Ghost Tour of Griffintown facilitated by EERS, you can find more details here: https://hauntedmontreal.com/haunted-griff. It will be offered at the discounted price of 21$ per person. The tour is approximately 90 minutes, entirely on foot and outdoors. It concludes about a 5-minute walk from the start location. A theatrical guide/storyteller is included, who will walk the group to each haunted location and tell the ghost story and history. This is classic ghost storytelling, no other actors or jump scares.

ARCHITECTURAL AND BUILDING ACOUSTICS

Chair: Wilson Byrick (Pliteq), Joonhee Lee (Concordia) and Mahn Jeffrey (CNRC)

Wednesday October 4

- **Room REGENCE A**

10:20-10:40 *Apparent Transmission Loss through Stud Walls with Mass Timber Flanking Assemblies*
Jeremy Thorbahn

10:40-11:00 *Repeatability and Reproducibility of Apparent Sound Transmission Class (ASTC) Measurements*
Henning Schlechtriem

11:00-11:20 *Case Study: Variation in ASTC Ratings with Loudspeaker Position when Using Directional Loudspeakers*
Anil Joshi

11:20-11:40 *Comparison of Predicted and Measured ASTC in a Mass Timber Structure*
Sarah Mackel

11:40-12:00 *Airborne Sound Transmission in Cross-Laminated Timber Buildings: The Influence of Building Height*
Erik Nilsson, Sylvain Ménard, Delphine Bard

12:00-12:20 *Incidence des meneaux d'un mur-rideau sur l'indice ASTC de cloisons intérieures*
Julien Fenninger

LUNCH

13:20-13:40 *Recent Experience in the Design of Music Recital Halls*
Bill John Gastmeier, Mandy Chan

13:40-14:00 *Acoustique d'un établissement hospitalier – l'agrandissement du Centre hospitalier de l'Université de Montréal (CHUM)*
Vincent Chavand

14:00-14:20 *The Acoustical Challenges for Modular Buildings used for Residential Purposes*
Paul Marks

14:20-14:40 *Amplifying Change for Music Venues in Montreal: Rethinking the Technical Regulatory Framework Towards Harmonious and Sustainable Nightlife*
Romain Dumoulin

14:40-15:00 *Quantifying the Reduction in Sound Insulation and Speech Privacy in Offices Due to Typical Design and Workmanship Errors*
Roderick KT Mackenzie

COFFEE BREAK

15:20-15:40 *Critical Importance of Acoustical Design in New Developments*
Zoe Razavi

15:40-16:00 *Publication of a New Guide from the Gouvernement du Québec About Noise Protection of Dwellings*
Jean-Philippe Migneron, Jean-Gabriel Migneron, André Potvin

16:00-16:20 *Acoustic Properties of High-Rise Wood Residential Buildings*
Raphaël Duée, Hugo Vasseur

16:20-16:40 *Acoustic Design of Floor Ceiling Assemblies in High Seismic Zones*
Aedan Callaghan, William Thrall

16:40-17:00 *Physical and Perceptual Comparison Between Single and Multiple Diffraction for Thick Edge*
Clément Girin, Alain Berry, Philippe-Aubert Gauthier, Louis-Xavier Buffoni

17:00-17:20 *Apparent Impact Insulation Class (AIIC) Testing of Various Roof Terrace Assemblies and Evaluating the Need for Additional Mitigation*
Jessica Tsang

17:20-17:40 *Online Evaluation of Floor Impact Sounds: Who is More Likely to be Annoyed? Canadians, Germans or Koreans?*
Sabrina Skoda, Markus Müller-Trapet, Young-Ji Choi, Iara Batista da Cunha, Jeffrey Mahn

17:40-18:00 *Field Measurement and Finite Element Modeling of Vibration Propagation from Heavy HardIimpacts on Fitness Flooring*
Giulio Puglielli, Simon Edwards, Brian Howe

Thursday October 5

- **Room REGENCE A**

10:20-10:40 *Contextualizing Speech Privacy Criteria in WELL/LEED Guidelines*
Dorsa Fardaei

10:40-11:00 *Speech Level Variations by Office Type and Work Environments*
Rewan Toubar, Roderick Mackenzie, Joonhee Lee

11:00-11:20 *Evaluating Ambient Noise and Reverberation in Classrooms: A Case Study of a Native school*
Daniel Paromov, Victoria Duda, Julie McIntyre, Phaedra Royle, Adriana Lacerda

11:20-11:40 *Novel Method for Reverberation Time Measurements in Natatoriums*
Adam Collins

11:40-12:00 *Noise and Sleep Quality of Aging Adults -- An Open Question*
Iara B Cunha, Ashley Nixon, Jennifer A Veitch, Hiroshi Sato, Jeffrey Mahn, Markus Müller-Trapet, Sabrina Skoda

HEARING PROTECTION

Chair: Hugues Nélisse (IRSST) and Franck Sgard (IRSST)

This session is organized in memory of our colleague and friend Simon Benacchio [1988-2023], who worked with fervor on the enhancement of artificial ears and hearing protectors.

Wednesday October 4

- **Room VICTORIA**

10:20-10:40 *Effect of Aging on the Ear Canal Morphology: Measurements on Human Subjects*
Robin Petit, Pierre Buyssens, Gwenolé Nexer

10:40-11:00 *Effect of Aging on the Ear Canal Morphology: A Large Scale Study*
Pierre Buyssens, Robin Petit, Gwenolé Nexer

11:00-11:20 *Statistical Shape Modeling of the Human Ear Canal for Designing Hearing Protection Devices and Auditory Wearables*
Farshid Ghezelbash, Katrin Braun, Amir Jafari Bidhendi, Jacob Bouchard-Roy

11:20-11:40 *Functional Discomfort of Earplugs and its Influencing Variables*
Bastien Poissenot-Arrigoni, Alessia Negrini, Djamal Berbiche, Franck Sgard, Olivier Doutres

11:40-12:00 *Evaluating Mechanical Comfort of Ear Tips: An Experimental-Computational Approach*
Amir J Bidhendi, Katrin Braun, Jacob Bouchard-Roy, Farshid Ghezelbash

12:00-12:20 *Experimental Investigation of the Static Mechanical Pressure Induced by Roll-Down Foam Earplugs*
Luiz G. C. Melo, Ahmed Dalaq, Franck Sgard, Olivier Doutres, Éric Wagnac

	LUNCH
13:20-13:40	*3D Printed Meta-Earplug for Minimizing the Occlusion Effect* **Kévin Carillo, Franck Sgard, Olivier Dazel, Olivier Doutres**
13:40-14:00	*Design Considerations to Optimize Occlusion Effect Mitigation with Acoustic Noise Cancelling Hearing Protection* **Vincent Nadon**
14:00-14:20	*Assessment of the Effect of Earplug Type, Insertion Depth and Background Noise Level on the Occlusion Effect in Laboratory Conditions* **Hugo Saint-Gaudens, Hugues Nélisse, Franck Sgard, Olivier Doutres**
14:20-14:40	*Bandwidth Extension of In-Ear Speech Through Machine Learning-Based Dynamic Equalization* **Ajin Tom, Antoine Bernier**
14:40-15:00	*Finite Element Simulation of the Ear Canal Wall Vibrations* **Simon Kersten, Chalotorn Möhlmann, Michael Vorländer**
	COFFEE BREAK
15:20-15:40	*Effects of the Hardness of Acoustic Test Fixtures' Ears on the Evaluation of Earplug's Direct Transmissions Facing High-Level Impulse Noises* **Cyril Blondé-Weinmann, Pascal Hamery, Véronique Zimpfer, Thomas Joubaud**
15:40-16:00	*Development of a Realistic Artificial Ear Dedicated to Earplugs Attenuation Measurements* **Said Ezzaf, Luiz Melo, Bastien Poissenot-Arrigoni, Hugo Saint-Gaudens, Alain Berry, Franck Sgard, Olivier Doutres**
16:00-16:20	*Measurements in the Open and Closed Ear Canal: Comparison Between Different Artificial Head Concepts* **Véronique Zimpfer, Cyril Blondé-Weinmann, Pascal Hamery, Thomas Joubaud, Franck Sgard**
16:20-16:40	*Time Domain Numerical Investigation to Assess Noise Reduction Allowed by a Non-Linear Passive Earplug Facing Impulse Noises.* **Christophe Ruzyla, Pascal Hamery, Sébastien Roth, Cyril Blonde-Weinmann**
16:40-17:00	*On the Use of Wide Dynamic Range Compression and Other Algorithms to Improve Hearing Protection of Workers with Hearing Impairment: A Preliminary Study on Speech Intelligibility* **Solenn Ollivier, Hugues Nélisse, Jérémie Voix**
17:00-17:20	*Towards Adjustable Loudness Compensation in Hearing Protectors for Musicians* **Elliot Drees, Eugénie Segers, Caroline Traube, Jérémie Voix**

Thursday October 5

- **Room VICTORIA**

10:20-10:40	*Source-Separated Dosimetry in an Active Hearing Protection Device* **Max Henry**
10:40-11:00	*Providing Focused Hear-Through on Active Hearing Protection Devices Using Dipole and Omnidirectional Outer-Ear Microphones.* **Hugo Besnard**
11:00-11:20	*Binaural Beamformer: An early Proof of Concept for Wearables Audio Devices* **Stéphane Dedieu, Thomas Padois, Jérémie Voix**
11:20-11:40	*The Effect of Training Material on the Personal Attenuation Rating Achieved by an Initially Untrained Population* **Lucas Carneiro, Lydia Behtani, Antoine Bernier**
11:40-12:00	*Development of the Subjective Evaluation Method of Hearing Protectors* **Farhad Forouharmajd, Adrian Fuente, Hadi Asady, Siamak Pourabdian**

SPEECH AND HEARING

Chair: Victoria Duda (U. de Montréal) and Rachel Bouserhal (ÉTS)

Wednesday October 4

- **Room CARTIER A**

10:20-10:40	*A 3D Voice-Hearing Simulator Co-Created by Voice Hearers and Researchers: Preliminary Sound Quality Evaluation* **Philippe-Aubert Gauthier, Kevin Zemmour, Sylvain Grignon, Bálint Demers, Catherine Lejeune, Sandrine Rousseau, Mouloud Boukala, Sofian Audry, Sylvio Arriola, Alain Berry, Kevin Whittingstall**
10:40-11:00	*Timing of Perioral Muscle Suppression in Smiled Speech* **Yadong Liu, Kyra Hung, Melissa Villasenor, Shannon Colcleugh, Eunhee Chung, Bryan Gick**
11:00-11:20	*Biomechanical Simulation of Lateral Asymmetry in Tongue Bracing* **Jasia Azreen, Connor Mayer, Yadong Liu, Arian Shamei, Ian Stavness, Bryan Gick**
11:20-11:40	*Tongue Adjustments in the Chest-Head Register Transition of Operatic Singers* **Grace Bengtson, Elena Massing, Cindy Zhao, Maria Samarskaya, Jahurul Islam, Bryan Gick**
11:40-12:00	*VOT Analysis of L1 and L2 Speakers of Itza'* **Jack Mahlmann**
12:00-12:20	*Perceptual Compensation of Intrinsic F0 Effects in English Monolingual Speakers* **Connie Ting, Meghan Clayards**
	LUNCH
13:20-13:40	*Articulation and Acoustics of Korean Liquids: A Case Study in Loanword Adaptation* **Naim Lim, Alexei Kochetov, Yoonjung Kang**
13:40-14:00	*Vowel Articulation in Closed-Skull Concussion Patients with no Language Impairment* **Arian Shamei, Bryan Gick**
14:00-14:20	*Prenasal Coarticulation and Allophonic Merger of /ɪ/ and /ɛ/ Across Dialects of English* **Irene Smith, Morgan Sonderegger**
14:20-14:40	*Variation in Articulation Rate in New Brunswick French* **Wladyslaw Cichocki, Luke Hagar, Yves Perreault**
14:40-15:00	*Creaky Voice in Canadian English: An Acoustics-Focused Method* **Jeanne Brown**
	COFFEE BREAK
15:20-15:40	*The Acoustics of Borrowed /ɚ/ in Quebec French* **Massimo Lipari**
15:40-16:00	*Speech Rate Effects on Length Distinctions in Japanese Vowels and Stops* **Hironori Katsuda, Yoonjung Kang**
16:00-16:20	*The Glottal Stop in Garo* **Cheman Baira A'gitok**
16:20-16:40	*Acoustic Variation in Speech: Contrasting Initial and Later Stages of Conversations Showing Opinion Convergence and Divergence* **Charlize Ma, Jahurul Islam, Effie Kao, Raechel Kitamura, Stephanie Wang, Marcell Maitinsky, Bryan Gick**
16:40-17:00	*Size of Velopharyngeal Opening and Nasality Measurements from Acoustic Features* **Jahurul Islam, Bryan Gick**
17:00-17:20	*Elimination of Nasality in Typical Speakers Using Forward Voice Focus, Phonetic Replacement, and Biofeedback* **Somayah Al-Ees, Tim Bressmann**
17:20-17:40	*Acoustic Analysis for Automatic Identification and Classification of Nasality in Simulated Oral-Nasal Balance Conditions using only the nasal speech signal* **Fatemeh Abnavi, Heather Flowers, Hilmi Dajani, Suzy Ahn, Tim Bressmann**
17:40-18:00	*The Temporal Modulation of Infant Directed Speech and the Role of Positive Affect* **Samin Moradi, Linda Polka**

Thursday October 5

- **Room CARTIER A**

10:20-10:40 *A New Individualized, Ecological and Immersive Approach to Measuring Noise-Related Annoyance: Feasibility Study*
Pierre H Bourez, Guillaume T Vallet, François Bergeron, Nathalie Gosselin, Philippe Fournier

10:40-11:00 *Hearing Health in Remote Quebec: A Case Study from a Native School*
Daniel Paromov, Victoria Duda, Julie McIntyre, Phaedra Royle, Adriana Lacerda

11:00-11:20 *Tinnitus Residual Inhibition Through Contralateral Acoustic Stimulation*
Bérangère Margaux Villatte, Arnaud Norena, Sylvie Hébert

11:20-11:40 *Improving the Detectability of Alarms by Adding High Harmonics*
Connor Wessel, Michael Schutz

11:40-12:00 *Classifying Sounds Encountered in Two Million YouTube Videos: Insights for the Future of Auditory Perception Research*
Andrés E. Elizondo López, Michael Schutz

LUNCH

13:00-13:20 *Investigating Gender Differences in the Perception of Human Infant Vocalizations as a Cuteness Component*
M. Fernanda Alonso Arteche, Leatisha Ramloll, Lucie Menard, Linda Polka

13:20-13:40 *A Listening Effort Based Comparative Analysis of CROS Hearing Aids and Bone-Anchored Hearing Devices for Single-Sided Deafness Patients*
Olivier Valentin, François Prévost, Don Luong Nguyen, Alexandre Lehmann

13:40-14:00 *Development of a Method to Assess In-Ear Speech Intelligibility Through Listening Effort*
Alexis Pinsonnault-Skvarenina, Philippe Chabot, Ajin Tom, Antoine Bernier

14:00-14:20 *The Analysis of Speech Perception with the Use of Hearing Protection Earplugs using the Canadian Digit Triplet Test*
Ahmed El Mawazini

14:20-14:40 *Electroacoustic Performance of Alternative Listening Devices: Candidates for Individuals with Mild to Moderate Hearing Loss?*
Alexis Pinsonnault-Skvarenina, Fabien Bonnet, Mathieu Hotton, Hugues Nélisse, Jérémie Voix

14:40-15:00 *Psychoacoustic Parameters and Ear Canal Role*
Hadi Asady, Siamak Pourabdian, Adrian Fuente, Mehdi Jalali, Ali Ahmadi, Fatemeh Ansari, Farhad Forouharmajd

MATERIALS FOR NOISE AND VIBRATION CONTROL

Chair: Thomas Dupont (ÉTS) and Raymond Panneton (U. of Sherbrooke)

Thursday October 5

- **Room CARTIER B**

10:20-10:40 *Assessment of Equivalent Properties for Multilayered Panels*
Diego Martin Tuozzo, Noureddine Atalla

10:40-11:00 *On the Use of Condensation Models for Describing Highly Damped Multilayered Structures*
Rafael da Silva Raqueti, Noureddine Atalla, Morvan Ouisse, Emeline Sadoulet-Reboul

11:00-11:20 *Adding Layers of Gypsum Board Inside the Cavity of Double Stud Walls. A Sound Idea?*
Jeffrey Mahn, Sabrina Skoda, Markus Müller-Trapet, Iara Cunha

11:20-11:40 *Added Viscous Damping of a Microperforated Plate in an Acoustic Non-Linearity Regime*
Lucie Gallerand, Mathias Legrand, Thomas Dupont, Raymond Panneton, Philippe Leclaire

11:40-12:00 *In-Situ Measurement of Acoustic Impedance in Presence of Grazing Flow*
Xukun Feng, Zacharie Laly, Noureddine Atalla

	LUNCH
13:00-13:20	*CFD Simulations of the Static Airflow Resistivity of a Perforated Solid: Effects of Size and Flow Velocity* **Alla Eddine Benchikh Lehocine, Tenon Charly Kone, Maël Lopez, Raymond Panneton, Thomas Dupont, Kévin Verdière**
13:20-13:40	*Engineered Materials for Acoustics: Metamaterials, Sonic Crystals and Calculated Microstructures* **Raymond Panneton**
13:40-14:00	*Investigations on a Periodic Acoustic Metamaterial for Multi-Tonal Noise Attenuation* **Zacharie Laly, Christopher Mechefske, Sebastian Ghinet, Behnam Ashrafi, Charly T. Kone**
14:00-14:20	*On the Use of Weakly Coupled Absorber for Low Frequency Sound Absorption* **Mohamed Amin Ben Lassoued, Edith Roland Fotsing, Annie Ross**
14:20-14:40	*Sonic Crystal Acoustic Attenuation Applied to Exhaust Air Systems* **Jeremy Plé, Tenon Charly Kone, Allaeddine Benchikh Lehocine, Raymond Panneton**
14:40-15:00	*Bragg Bands Generation in Beams and Plates for Mass Reduction and Vibroacoustic Performance* **Nicolas Bohmwald, Vania Gonzalez, Olivier Robin, Viviana Meruane**
	COFFEE BREAK
15:20-15:40	*Acoustic Metamaterials for Low-Frequency Noise Reduction: A Review* **Niloofar Rastegar Dehkordi, Davide De Cicco, David Vidal, Annie Ross**
15:40-16:00	*Method for Characterizing the Acoustic Properties of Thin Metamaterials Capable of Attenuating Broadband Noise at Low Frequencies* **Tenon Charly Kone, Sebastian Ghinet, Raymond Panneton, Anant Grewal**
16:00-16:20	*Finite Element Study of Perfect Sound Absorbing Porous Material with Periodic Conical Hole Profile* **Zacharie Laly, Noureddine Atalla, Raymond Panneton, Sebastian Ghinet, Christopher Mechefske**
16:20-16:40	*Mass-Spring Model for a Resonant Metamaterial at High Sound Pressure Level* **Maël Lopez, Alla Eddine Benchikh Le Hocine, Charly Tenon Kone, Thomas Dupont, Raymond Panneton**
16:40-17:00	*Creating Optimized Sound-Proofing Structure Via Concentrated Emulsions* **Mina Saghaei, Annie Ross, Edith-Roland Fotsing, Louis Fradette**

Friday October 6

- **Room CARTIER B**

10:20-10:40	*Development of an Eco-Acoustic Absorber Based on Local Recycled Granular Materials* **Islam Ben Amara, Raymond Panneton, Richard Gagné**
10:40-11:00	*Novel Acoustic Materials Made from Wood Processing Residues* **Suzhou Yin**
11:00-11:20	*Waste Corn Husk Fibers for Sound Absorption Applications* **Umberto Berardi**
11:20-11:40	*Mycelium Based Acoustic Panels* **Alexis Boisvert, Saïd Elkoun, Olivier Robin, Félix-Antoine Bérubé Simard**
11:40-12:00	*Acoustic Properties of Cork Fiber Reinforced Micro-Perforated Panel Made with Polylactic Acid Through Additive Manufacturing* **Umberto Berardi**
12:00-12:20	*Predicting Acoustic Absorption in Additively Manufactured Porous Microlattices: A Sensitivity Analysis Approach* **Ayoub Ait Aariba**

GENERAL ACOUSTICS

Chair: Viken Koukounian (Parklane), Mathias Legrand (McGill) and Thomas Padois (IRSST)

Wednesday October 4

- **Room VICTORIA**

17:20-17:40 *Turbulence Distortion Effect on Leading Edge Noise from Wind Turbine Blades*
Vasishta Bhargava Nukala, Chinmaya Prasad Padhy

17:40-18:00 *Characterization and Sustainable Acoustic Correction of the Mosque. Case study of two Mosques in Constantine, Algeria*
Zohra Bemaghsoula Hammou

Thursday October 5

- **Room REGENCE A**

13:00-13:20 *Value Engineering 'Acoustics' into Projects*
Michael Bolduc, Viken Koukounian

13:20-13:40 *On the Robustness of a Decoupling Procedure Used in Conjunction with an Indirect Method to Assess the Full Mobility of an Aircraft Hydraulic Pump*
Simon Prenant, Thomas Padois, Manuel Etchessahar, Olivier Doutres

13:40-14:00 *A Criterion Based on the Calculation of a Solid Angle to Assess the Quality of Acoustic Images Obtained With a Spherical Microphone Array*
Kevin ROUARD, Julien St-Jacques, Olivier Doutres, Franck Sgard, Hugues Nélisse, Loic Boileau, Alain Berry, Nicolas Quaegebeur, François Grondin, Thomas Padois

14:00-14:20 *Influence of the Scattering Effect on Acoustic Image Obtained with a Spherical Microphone Array*
Julien St-Jacques, Kevin Rouard, Franck Sgard, Hugues Nélisse, Alain Berry, Nicolas Quaegebeur, François Grondin, Loic Boileau, Olivier Doutres, Thomas Padois

14:20-14:40 *Robust Continous Health Monitoring and Occupational Safety with Hearables*
Alexandre Petrosky, Jérémie Voix, Rachel Bouserhal

14:40-15:00 *Digital Earplug Featuring Combined Noise Dosimetry and Electrocochleography: A Proof of Concept*
Adélaïde Douchet, Alexis Pinsonnault-Skvarenina, Gabrielle Crétot-Richert, Malo Richard, Valentin Pintat, Jérémie Voix

COFFEE BREAK

15:20-15:40 *Assessing Automatic Musical Mode Extraction*
Konrad Swierczek, Michael Schutz

15:40-16:00 *Use of Carillons in Building New Musical Instruments*
Rama Balike Bhat

16:00-16:20 *Detectability and Reducing Annoyance of Alarm Design Using Acoustic Structures of Musical Instruments*
Andres Eugenio Elizondo Lopez, Joseph Schlesinger, Michael Schutz

16:20-16:40 *Dynamics of Harmonic Active Sound Control with a Harmonic Acoustic Pneumatic Source*
Alexandre Schiavini

16:40-17:00 *Rigid Body Motion of Nail Guns: Modal Analysis and 2D Dynamic Modelling*
Maxime Vincent, Marc-André Gaudreau, Thomas Dupont, Pierre Marcotte

Friday October 6

- **Room REGENCE A**

10:20-10:40 *Étude sur la fréquence d'apparition d'aptonymes acoustiques et musicaux en France métropolitaine*
Odile Clavier, Nicolas Trompette, Stéphanie Viollon, Jérémie Voix

10:40-11:00 *Characterization of Typical Music Activities in China: Identification, Classification and Quantification*
Chang MIAO

11:00-11:20 *How Does Interpretation of Acoustic Features Affect Perceived Musical Emotion?*
Cameron Anderson, Jamie Ling, Michael Schutz

11:20-11:40 *Deaf Gain: Enhancements in Vibrotactile Rhythm Perception for Deaf Individuals*
Sean Alexander Gilmore, Frank Russo

11:40-12:00 *Sign Language Handshapes, Similarly to Speech Sounds, Exploit Biomechanical Endpoints*
Oksana Tkachman, Shannon Hsu, Maria Samarskaya, Cindy Zhao, Bryan Gick

12:00-12:20 *Preliminary Numerical and Experimental Studies of Active Acoustic Control of Double-Glazed Partition Walls*
Jonathan Mifundu Nzengi, Pierre Grandjean, Alain Berry, Philippe Micheau

ENVIRONMENTAL NOISE

Chair: Anthony Gérard (Soft dB), Olivier Robin (U. of Sherbrooke) and Joana Rocha (Carleton University)

Wednesday October 4

- **Room CARTIER B**

10:20-10:40 *Relationship Between Community Complaints and Noise Level During the Construction of a Large Road Infrastructure in Montréal*
Alexis Pinsonnault-Skvarenina, Véronique Guay, Renaud Leblanc-Guindon, Mathieu Carrier, Tony Leroux

10:40-11:00 *Effective Methods for Reducing Construction Noise in Densely Populated Environment*
Loic Sauvageot

11:00-11:20 *Design and Dissemination of Environmental Noise Maps: Recommendations for the Province of Québec*
Frédéric Hubert, Jean-Philippe Migneron

11:20-11:40 *Urban Noise Observatory and Management Tool - Application to Quebec Case*
Raphaël Duée, Paul Otis-Bouchart D'Orval, Djesone Gomis

11:40-12:00 *Noisemonitor: A Python Package for Sound Level Monitor Analysis*
Valérian Fraisse

12:00-12:20 *The Introduction of Acoustics in Environmental, Social and Governance (ESG) Frameworks*
Viken Koukounian, Ethan Bourdeau, Michael Bolduc

Thursday October 5

- **Room VICTORIA**

13:00-13:20 *... empty slot...*

13:20-13:40 *Designing and Evaluating Public Space Sound Installations: A Collaborative Research-Creation Approach*
Valérian Fraisse, Étienne Legast, Simone D'Ambrosio, Catherine Guastavino

13:40-14:00 *Lessons Learned Monitoring Near and Further from Wind Turbines*
William Keith Gregory Palmer

14:00-14:20 *Auralisation: A Valuable Consultation and Engagement Tool for Infrastructure Projects – Case Study of Airspace Change for a Regional Airport*
Vincent Jurdic, Calum Sharp, David Hiller, Ryan Biziorek, Caroline Harvey

14:20-14:40 *Bridging the Gap Between Sound and Non-Sound Professionals with Virtual Reality*
Richard Yanaky, Catherine Guastavino

14:40-15:00 *Effect of Acoustic Treatment and Table Dividers on Diners' Experience in a Montreal Restaurant*
Catherine Guastavino

Friday October 6

- **Room VICTORIA**

10:20-10:40 *Vibration Impacts of Tunneling in Transit Construction*
Christopher Bosyj

10:40-11:00 *Manufacturers' Sound Data – Application Experiences*
Pier-Gui Lalonde

11:00-11:20 *Is Friday the New Saturday? The Impact of Using Standard Traffic Distribution Models for Friday Traffic Data on Noise Assessment*
Kathryn Joanne Katsiroumpas, Morgan Austin

11:20-11:40 *Impact of Speed and Throttle Adjustments on FTA Noise Model in Transit Rail Analysis Including Case Study*
Ian Matthew, Anthony Amarra

11:40-12:00 *Predicting the Noise Impact of Large-Scale Battery Storage Sites in Ontario*
Hillary Fung

ARTIFICIAL INTELLIGENCE IN ACOUSTICS

Chair: François Grondin (U. of Sherbrooke)

Wednesday October 4

- **Room CARTIER B**

15:20-15:40 *Enhancing Noise Management Through Siamese Convolutional Neural Networks for Identification of Principal Sound Sources*
Jean-Pierre Côté, Marc-André Gaudreau, Sousso Kelouwani

15:40-16:00 *Wall-Pressure Spectrum Model Based on Artificial Neural Networks Predictions*
Andrea Arroyo Ramo, Michaël Bauerheim, Stéphane Moreau

16:00-16:20 *Deep Learning-Based Approach for Acoustic Source Localization in Turbulent Flows*
Arnav Joshi, Jean-Pierre Hickey

16:20-16:40 *Use of Logistic Regression Models as a Supervised Learning Algorithm to Identify Impulsive Sounds in Monitored Sound Data*
Harry Ao Cai

16:40-17:00 *Accuracies in Algorithmic Predictors of Musical Emotion*
Jackie Zhou, Cameron Anderson, Michael Schutz

17:00-17:20 *Enhancing Automatic Speech Recognition of a Regional Dialect: A Pilot Study with Québécois French*
Xinyi Zhang, Lucia Eve Berger, Duc-Hoa Tran, Rachel Bouserhal

17:20-17:40 *Modeling of Field Sound Insulation for Multi-Layered CLT Floor Assemblies Using Artificial Neural Networks*
Mohamad Bader Eddin

17:40-18:00 *Detecting Ringed Seal Vocalizations Using Deep Learning*
Karlee Zammit, William Halliday, Fabio Frazao, Stan Dosso

UNDERWATER ACOUSTICS

Chair: Pierre Cauchy (Université du Québec à Rimouski)

Wednesday October 4

- **Room CARTIER A**

10:20-10:40 *Assessment of Propeller Cavitation Inception Speed Based on Onboard Vibration Data*
Kamal Kesour, Paul Camerin, Jean-Christophe Gauthier Marquis, Cédric Gervaise

10:40-11:00 *Multi-Domain Approach for Prediction of Vortex-Induced Hull Pressure Fluctuations on a Model-Scale Ship*
Duncan McIntyre, Shameem Islam, Peter Oshkai

11:00-11:20 *Ship Noise Quantification and Source Level Estimation in the Arctic Ocean*
Najeem Shajahan, William D Halliday, Stephen J Insley

11:20-11:40 *The MARS Database – Source Levels Measured for the Fleet Navigating the St-Lawrence Estuary*
Pierre Mercure-Boissonnault, Pierre Cauchy, Faniry Fitiavana Rabetoandro, Cédric Gervaise, Guillaume St-Onge, Jeanne Mérindol, Cécile Perrier de la Bathie, Hugo Catineau

11:40-12:00 *Analysis of the Variability of Ship Acoustic Signatures Measured as a Function of Hydrophone Configuration*
Cecile Perrier de la Bathie, Pierre Cauchy, Guillaume St-Onge

12:00-12:20 *Measurement of Vessel Underwater Acoustic Signature at The MARS Station – Repeatability and Uncertainties Assessed on a 1000 Vessels Database*
Pierre Cauchy, Pierre Mercure-Boissonnault, Cécile Perrier de la Bathie, Faniry Rabetoandro, Guillaume Saint-Onge, Cedric Gervaise, Sylvain Lafrance

BIOMEDICAL ACOUSTICS

Chair: Nicolas Quaegebeur (U. of Sherbrooke)

Thursday October 5

- **Room CARTIER A**

15:20-15:40 *Miniaturized Acoustic Concentrators for Local Generation of Ultrasonic Waves*
Ibrahima Touré, Nicolas Quaegebeur

15:40-16:00 *Printing Beyond Barriers Using Ultrasound in Direct Sound Printing*
Mohsen Habibi, Shervin Foroughi, Muthukumaran Packirisamy

16:00-16:20 *Characterization of Noise Produced During Continuous and Sparse Sampling Functional Magnetic Resonance Imaging*
Olivier Robin, Félix Le Moigne - Le Dem, Pascal Tétreault, Domnique Lorrain, Vivien Staehle

16:20-16:40 *Numerical Analysis of Energy Density Distribution in the Human Lungs Under Low-Frequency Acoustic Excitation*
Arife Uzundurukan, Sébastien Poncet, Daria Camilla Boffito, Philippe Micheau

AEROACOUSTICS

Chair: Joana Rocha (Carleton University) and Marlène Sanjosé (ÉTS)

Thursday October 5

- **Room VICTORIA**

15:20-15:40 *Derivation of an Empirical Model for the Estimation of Power Spectral Density in the Turbulent Boundary Layer of Aircraft with Machine Learning Regression Techniques*
Zachary Huffman, Joana Rocha

15:40-16:00 *Aeroacoustic Optimization of a Metacage to Block the Noise Emitted by an Exhaust Fan*
Marco Lizotte, Jean-Bernard Piaud, Raymond Panneton, Tenon Charly Kone, Jean-Christophe Cuillière, Vincent François

16:00-16:20 *Interaction Noise for a Rotor-Stator Assembly in a Short Duct*
Marlene Sanjose, Baahirham Shanthalingam

16:20-16:40 *Evaluation of Wall Pressure Spectrum Models for Fan Noise Prediction*
Marlene Sanjose, Natacha Galand, Teddy Garnier, Stéphane Moreau

16:40-17:00 *High-fidelity Acoustic Simulation of a Recorder Using Powerflow*
Elissa El Hajj, Davide De Cicco, Annie Ross, David Vidal

EDUCATION IN ACOUSTICS

Chair: Olivier Robin (U. of Sherbrooke)

Wednesday October 4

- **Room CARTIER B**

13:20-13:40 *Teaching Architectural Acoustics Using Project-Based Learning with Real-World Building Projects*
Christoph Hoeller, Adrian Bloedt

13:40-14:00 *Understanding the Skill Gap of Post-Secondary Graduates Entering the Acoustic Consulting Profession*
Abigail Farkas

14:00-14:20 *Teaching Concepts of Acoustical Waves in Air - Part 2*
William John Gastmeier

14:20-14:40 *Noise Evaluation at the École de Technologie Supérieure Campus in Montréal: A Student Project*
Olivier Doutres, Maël Lopez, Kévin Rouard, Louis-Philippe Campagna, Titouan Cougoulic, Anthony Jutras, David Lauzon, Pierre-Luc Pépin-Pagé, Alexis Purson

14:40-15:00 *Improving Audiology Student Training by Clinical Simulation of Tinnitus: A Glimpse of Tinnitus Lived Experience*
Pierre H Bourez, Guillaume T Vallet, Philippe Fournier

GENERAL PAPERS - SUJETS GÉNÉRAUX

INCREASING DETECTABILITY AND REDUCING ANNOYANCE OF ALARM DESIGN USING ACOUSTIC STRUCTURES OF MUSICAL INSTRUMENTS

Andres E. Elizondo Lopez *[1,2], Joseph Schlesinger †[3] and Michael Schutz ‡[1,2]
[1]Psychology, Neuroscience & Behaviour, McMaster University, Hamilton, Ontario, Canada
[2]McMaster Institute for Music and the Mind, McMaster University, Hamilton, Ontario, Canada
[3]Electrical and Computer Engineering, McGill University, Montréal, Québec, Canada

1 Introduction

Auditory alarms are critical to relaying crucial information in high-consequence industries. For example, in a healthcare context these alerts convey important information on patient physiologic status, with potentially catastrophic consequences for missed alarms. The current auditory alarm standard within hospitals [1] uses simplistic tones with non-temporally varied structures (flat tones), whose drawbacks have been discussed extensively [2]. Hospital alarm design have a 'better safe than sorry' approach, leading to an excess of sounds. Alarm rates in hospitals can hover around 350 alarms per patient per day [3], with only 0.5% indicating life threatening events [4]. This sheer numerosity of non-urgent alarms causes alarm fatigue which has led users to ignore or silence alarms, which can lead to negative consequences for staff and even patient deaths [5].

As many issues with alarms are intractable (i.e., numerosity), our team focuses on one specific and readily addressable issue—the lack of temporal and harmonic complexity. We have found that tones with varied amplitude envelopes and more complex harmonic structures reduce annoyance and increase detectability [6], although their relative scarcity in auditory psychophysics [7] seems to have led to lesser use in auditory interfaces [8]. The percussive triangle instrument is capable of piercing through the rich acoustic wall produced by large orchestras without being annoying, making it an interesting source of information on improving alarm efficacy.

In this study we test whether the complexity of musical triangle instrument can increase detectability (experiment 1) while reducing annoyance (experiment 2).

2 Methods

2.1 Participants

We conducted all experiments with psychology students at McMaster University in Hamilton, Ontario, who received course credit for completing in person and online experiments.

2.2 Apparatus

We used *Psychopy* [9] for the creation of all the experiments, which is hosted on the online experimental services *Pavlovia*.

For experiment 1 of detection, participants ran through trials in an IAC Controlled Acoustical Environment room to reduce any excess sounds and used Sennheiser HAD 200 over-ear monitor headphones throughout the study.

For experiment 2 on perceived annoyance, a new set of participants used their own computer and headphones and told to maintain the same volume level across the experiment.

2.3 Procedure

For experiment 1, we used a coordinated response measure (CRM) to test for detectability [10]. Participants listened to a target voice with an assigned callsign directing them to press one of the 16 coloured/numbered square on a computer monitor. Two additional voices 500ms prior and 500ms after the target acted as distractors. In addition to these three voices, participants listened for a tone, which sounded at one of six signal-to-noise ratios (SNRs, figure 2 left). Participants pressed the "space" key on their keyboards whenever they detected a tone. The triangle tone or the standard flat tone was presented randomly at each SNR level with a total of 216 trials, lasting 45 minutes.

For experiment 2, participants completed a two-alternative forced choice task evaluating the relative annoyance tones presented in pairs. Each tone was randomly presented to the participants, using the six signal amplitude levels measured in Root Mean Squared decibels (RMS dB, figure 2 right), the same levels used from the prior procedure. A randomly selected tone-RMS pairing was played and simultaneously the letter "A" was presented on screen. After three seconds the letter "B" appears on the screen and randomly plays another tone without replacement. A prompt asked the participant, "Which tone is more annoying?" and asked to press "A" or "B" on their keyboard to indicate the tone with higher perceived annoyance. The study continued until all comparisons of tones-RMS pairings are completed, with a total of 132 trials lasting 30 minutes.

2.4 Stimuli

Each experiment used a single set of stimuli, consisting of two kinds of sounds (a) "standard flat" and (b) "triangle inspired" tone seen in figure 1. We synthesized all sounds using the *MAESTRO* software [11], built in the *Supercollider* sound synthesis program [12].

The standard flat tone consists of a constant amplitude with a 20ms rise, 20ms fall, and 960ms sustain at every component containing a flat amplitude envelope. With five harmonic components at 261, 523, 783, 1046 and 1305 hertz (Hz), all components have equal energy.

The triangle inspired tone is based on a sample from *Spitfire Audio's BBC Orchestra* sample library [13]. We selected

* elizonda@mcmaster.ca
† joseph.shlesinger@mcgill.ca
‡ schutz@mcmaster.ca

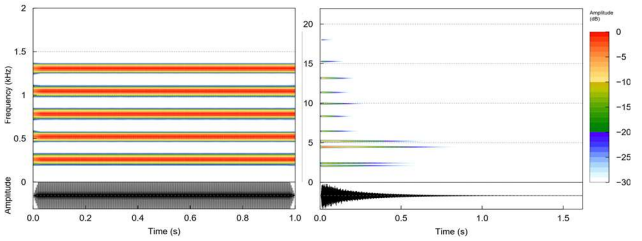

Figure 1: Power spectra and waveforms of the standard flat (left) and triangle inspired (right) tones. Y-axis for power spectra represents Frequency in kHz, and the Y-axis for the waveform represent relative amplitude. X-axis is time in seconds.

the twelve most prominent frequency peaks along with their durations and varied temporal amplitude changes. Its frequencies are 2093.0, 2430.01, 4462.1, 5202.8, 6462.5, 8344.9, 9941.7, 11361.0, 13161.9, 15265.6, 18010.5, and 20778.3 Hz, with relative amplitudes at 0.31, 0.32, 1, 0.6, 0.3, 0.35, 0.34, 0.31, 0.43, 0.17, 0.1, 0.01. The triangle inspired stimuli consist of a 5ms attack, 5ms sustain, 1.6s delay and an off curve of -10 for a percussive amplitude envelope. Both tones have equated RMS.

3 Results

3.1 Experiment 1 – Signal Detection

We used an analysis of variance (ANOVA) to analyze detection between the standard flat and triangle inspired tones, with a total of 31 participants. We analyzed the effect of SNR on tone detection with a 2x6 factorial ANOVA, revealing a significant effect on tone type $F(1,408)=37.3$, $p=<.001$, and SNR $F(5,408)=4.19$, $p=<.01$. We found no significant interaction between SNR and tone type $F(5,408)=1.61$, $p=0.15$.

We also analyzed the effect of each tone alone on SNR with a one-way ANOVA. We found a significant effect of SNR on the standard flat tone $F(5,204)=7.06$, $p=< .001$. However, there no significant effect of SNR on the triangle inspired tone $F(5,204)=0.43$, $p=0.83$.

3.2 Experiment 2 – Perceived Annoyance

For this second experiment, we used a chi-square test (X^2) to analyze perceived annoyance for all 34 participants. We found a significant effect for RMS $X^2(5, N=4488)=478.01$, $p<.001$ and for tone type $X^2(1, N=4488)=36.0$, $p < .001$.

4 Discussion

Reductions in energy lowered the detectability of the standard flat tone but had no effect on the triangle-inspired tone. Consequently, it appears sounds based on the triangle can be played at a greatly reduced volume without sacrificing detectability relative to standard designs—although they lead to significantly less annoyance.

5 Conclusion

This study shows one way in which musical sounds can offer useful insight to improve the efficacy of auditory alarms design in high consequence industries.

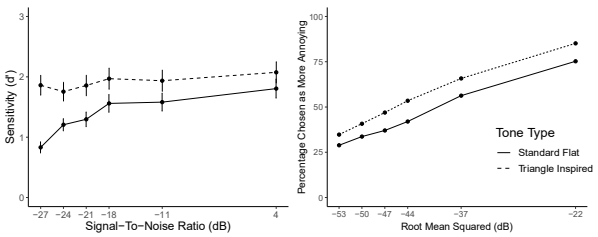

Figure 2: Experiment 1 (left), y-axis measures sensitivity measured in d prime, x-axis represents signal-to-noise ratio (SNR) in decibels (dBs). Error bars: 95% confidence interval. Experiment 2 (right), y-axis measures the percentage chosen as more annoying, x-axis represents root mean square (RMS) in decibels (dB).

Acknowledgments:

This work was supported by Natural Sciences and Engineering Research Council of Canada (NSERC), the Canadian Foundation for Innovation, and the Auditory Performance Division of the US Navy and the Office of Naval Research Grant N00014-22-1-2184.

References

[1] International Electrotechnical Commission. Medical Electrical Equipment. Part 1–8: general requirements for basic safety and essential performance–collateral standard: general requirements, tests and guidance for alarm systems in medical electrical equipment and medical electrical systems. *International Standard IEC 60601-1-8*; 2006.

[2] Edworthy J. Medical audible alarms: a review. *J Am Med Inform Assoc* 2013; **20**: 584–9

[3] Sendelbach S, Funk M. Alarm fatigue: a patient safety concern. *AACN Adv Crit Care* 2013; **24**: 378–86

[4] O'Carroll TM. Survey of alarms in an intensive therapy unit. *Anaesthesia* 1986; **41**: 742–4

[5] Rayo MF, Patterson ES, Abdel-Rasoul M, Moffat-Bruce SD. Using timbre to improve performance of larger auditory alarm sets. *Ergonomics* 2019; **62**: 1617–29

[6] Foley L, Schlesinger JJ, Schutz M. More detectable, less annoying: temporal variation in amplitude envelope and spectral content improves auditory interface efficacy. *J Acoust Soc Am* 2022; **151**: 3189–96

[7] Schutz M, Gillard J. On the generalization of tones: A detailed exploration of non-speech auditory perception stimuli. *Sci Rep* 2020; **10**(1), 9520

[8] Foley L, Schutz M. High time for temporal variation: improving sonic interaction with auditory interfaces. *IEEE* 2021; **24**(7), 4–9

[9] Peirce JW, Gray JR, Simpson S, MacAskill M, HЄochenberger R, Sogo H, Kastman E, Lindeløv, JK. PsychoPy2: Experiments in behavior made easy, *Behav. Res* 2019; **51**(1): 195–203.

[10] Eddins DA, Liu C. Psychometric properties of the coordinate response measure corpus with various types of background interference. *The J Acoust Soc Am*, 2012; **131**: 2

[11] Ng M, Schutz M. Seeing sound: A new tool for teaching music perception principles. *Can Acoust* 2017; **45**(3), 104–105

[12] McCartney J. SuperCollider, a New Real Time Synthesis Language. *ICMC* 1996.

[13] Spitfire Audio, BBC Symphony Orchestra Professional [Audio Sample Library] n.d.

THE INTRODUCTION OF ACOUSTICS IN ENVIRONMENTAL, SOCIAL AND GOVERNANCE (ESG) FRAMEWORKS

Viken Koukounian*[1], Ethan Bourdeau†[2] and Michael Bolduc‡[1]
[1]Parklane Mechanical Acoustics, Oakville, Ontario, Canada
[2]International WELL Building Institute, New York, United States of America

1 Introduction

First referenced in a report in 2006 by the Principles for Responsible Investment (PRI) the purpose of Environmental, Social and Governance (ESG) frameworks is to contribute to a more sustainable global financial system. The consideration of ESG issues has been found to affect portfolio performance, including materially improving risk-adjusted returns [1].

The implementation of ESG strategies is complex for at least two reasons—it is nebulous to determine relevant metrics, and the associated data is exceptionally variable. The complexities of the data include subject (e.g., climate change, indoor environmental quality, social justice, equality), size of datasets, measurement frequency, and so on. Understandably, it is nearly impossible to effectively set, manage and report on sustainability goals without meaningful metrics and data.

In 2015, 193 countries adopted the Sustainable Development Goals (SDGs). Their purpose is to establish a shared plan to "end extreme poverty, reduce inequality, and protect the planet by 2030" [2]. The 17 interlinked objectives are to provide a "shared blueprint for peace and prosperity for people and the planet, now and into the future" [3]. It may be said that the successful adoption of SDGs has been facilitated by ESG frameworks, predominantly by the Social pillar.

The following paper uses the same process to design, develop and deliver the context that is necessary to institutionalize acoustical principles that can be adopted by ESG frameworks by discussing 'how' acoustics has or can have environmental impacts (e.g., materials use, energy performance and efficiencies, community and environmental soundscapes), social impacts (e.g., acoustical equity, health and wellbeing, social engagement, individual agency), and impacts on governance (e.g., holistic approach to architectural and environmental acoustics) [4, 5].

2 SDGs

Herein we contemplate opportunities to relate acoustical principles to SDGs. The intent is not to force 'inclusion' or to make 'absolute' claims but rather to promote rationale that may be relevant to different organizations (and their stakeholders). Many of the presented concepts build upon fundamental and advanced acoustical concepts—whether specific to acoustics (i.e., physics of acoustic energy and its transmission) or psychoacoustics (i.e., perception of sound and associated physiological effects). For the latter, the thought-exercise builds upon the principal factors affecting the acoustical experience of occupants, which are generally assessed via questionnaires to qualify acoustical satisfaction (i.e., communication, acoustical privacy, acoustical comfort) rather than acoustic measurement, or via health assessments.

2.1 SDG 3: Good health & well-being

The public is well-aware of the risks of sudden or sufficiently prolonged exposure of elevated levels of sound. Agencies and noise regulations have successfully communicated the auditory impacts (e.g., hearing loss) resulting from 'noise exposure' and 'noise pollution.' In contrast, the effects of sound on our non-auditory health (i.e., psychological, physiological; e.g., cardiovascular system, cognitive, physical health) is, generally, incorrectly assumed.

While 'noise' has negative effects on our non-auditory health, our assessment of sound as 'noise' depends on its characterizations (i.e., 'dimensions): (1) temporal, (2) spectral and (3) spatial. The combination of these physics, not only 'sound level' (i.e., 'noise exposure'), affect our assessment of our environments (i.e., 'noise sensitivity').

Ultimately, 'sound' is omnipresent and an essential baseline to our lives. The 'mindset' should never be about 'eliminating' noise but rather 'managing' its transmission from 'disturbing' sources (e.g., industrial, transportation).

2.2 SDG 4: Quality education

Though about access to 'good education,' there is ample evidence indicating the need to consider acoustics in schools. Academic and industry research has found that classrooms having poor acoustical privacy (i.e., intrusion of external noise) negatively impact students' learning.

2.3 SDG 7: Affordable & clean energy

There is increasing pressure on manufacturers to design 'better' and 'more efficient' solutions, while also meeting a growing number of stricter constraints (including 'quieter'). While the authors respect the good intentions, it is more important to assess 'context.' By way of example, 60 dBA from a washer/dryer unit may be acceptable when installed in an isolated location (e.g., basement) and unacceptable in a UK/European-style home (e.g., kitchen). Developing this further—it is more important to improve the performance and efficiency of a system than an individual component.

Although a challenging exercise, optimization of critical system components may benefit from relaxation of noise criteria in particular spaces. Case-specific studies are needed to assess the short- and long-term benefits of systems operating with looser constraints but with appropriate controls for

* viken@parklanemechanical.com
† ethan.bourdeau@wellcertified.com
‡ michael@parklanemechanical.com

noise, such as HVAC in open-plan spaces with masking sound, mechanical rooms with greater acoustical isolation, and building systems (e.g., generators, chillers air-handling units,) with plenums, silencers, and barriers.

2.4 SDG 8: Decent work & economic growth

The effects of noise on productivity in workplaces is a popular research topic in acoustics. Intuitively, distractions in the workplace lead to poorer employee performance, comfort, and satisfaction scores. Continued research is needed to describe the economic benefits of having 'good acoustics' on Return On Investment (ROI) metrics (e.g., productivity, absenteeism, retention) [6].

2.5 SDG 9: Industry, innovation & infrastructure

Holistic frameworks centering the needs of occupants empower building professionals to design and build spaces more efficiently. For example, an understanding acoustical privacy—the parameters affecting its signal-to-noise equation—can lead to accurate specification of wall construction (e.g., architectural applications) or of noise mitigation solutions (e.g., environmental applications).

Effectively, complex concepts (such as acoustical satisfaction) can be inferred via measurable acoustic metrics. Sensorial experiences (e.g., acoustical privacy, acoustical comfort, communication) can be 'calculated' using traditional acoustic metrics (which, when used individually, cannot). Better design is the result of the intentional planning and specification of criteria of acoustical features.

2.6 SDG 10: Reduced inequalities

Many forms of inequality exist, and the authors support the movements demanding that all forms of discrimination be curtailed. Herein, we address a 'simpler' notion of [acoustical] equity: suggesting that people have equal right to similar acoustical experiences—whether it be the right to acoustical privacy (from noise intrusions) at home, to similar working conditions at work (e.g., ability to perform tasks) [5], access to consistent quality of healthcare [6], in classrooms [7]. Other initiatives, such as on topics of Diversity, Equity and Inclusion (DEI) and neurodiversity, exist [8].

2.7 SDG 11: Sustainable cities & communities

The creation of sustainable cities and communities requires that those environments foster our health and wellbeing, that which we know is affected by our acoustic environments.

2.8 SDG 14 & 15: Life below water & on land

Environmental noise is, perhaps, one of the largest sectors of the acoustical industry. There is much literature documenting interest and impacts of noise on communities and cities, people, wildlife [9]. There is ongoing research seeking to develop advanced conceptual frameworks to characterize the acoustical experience in these natural environments (e.g., national parks) with the intention of conserving and preserving the soundscape (i.e., the sensorial experience).

3 ESG Pillars

Philosophically, we believe the purpose of ESG frameworks is for an altruistic outcome. For this, it is necessary to study our 'acoustical ecology': the ways in which we connect and interact with our acoustical environments. For this reason, we have repeatedly stated our priority about centering the needs of the 'being.' But topics of acoustics extend beyond the apparent connection with Social pillar with the greatest opportunity existing with Governance. Agencies may, notably where precedents (or guidelines) have been set, to define policies addressing acoustics in and around the built environments and in nature. There is, however, a continuing need to refine our acoustical vocabulary and our metrics [4].

To facilitate the introduction of acoustical principles into ESG frameworks, we proposed adoption of SDGs. SDGs relevant to environmental, social and governance may be {7, 8, 9 and 11}, {3, 4, 10, 11, 14 and 15} and {3, 4, 7, 8, 10, 11, 14 and 15}, respectively.

4 Conclusion

An in-depth study of a company's sustainability and ethical objectives is critical to establishing its identity. ESG provides a universal vocabular connecting professionals to the wider community. Just as we emphasize the role of acoustics and noise control in planning, performance, and policymaking.

References

[1] Principles for Responsible Investment (PRI), "A blueprint for responsible investment," [Online]. Available: https://www.unpri.org/about-us/a-blueprint-for-responsible-investment. [Accessed 15 07 2023].

[2] United Nations (UN), "Sustainable Design Goals," [Online]. Available: https://www.undp.org/sustainable-development-goals. [Accessed 15 07 2023].

[3] United Nations, "The 17 Goals," 2015. [Online]. Available: https://sdgs.un.org/goals. [Accessed 15 06 2023].

[4] E. Bourdeau and V. Koukounian, "The role of acoustical privacy in a hierarchical framework for acoustical satisfaction: Past, present and future," in Inter-noise 2022, Glasgow, UK, 2022.

[5] V. Koukounian and N. Moeller, "In Pursuit of Acoustical Equity," *The Construction Specifier,* no. May, pp. 10-19, 2021

[6] N. Ildiri, H. Bazille, et al., "Impact of WELL certification on occupant satisfaction and perceived health, well-being, and productivity: A multi-office pre- versus post-occupancy evaluation," Building and Environment, vol. 224, pp. 1-18, 2022.

[7] W. E. Morrison, E. C. Haas, et al., "Noise, stress, and annoyance in a pediatric intensive care unit," Critical Care Medicine, vol. 31, no. 1, pp. 113-119, 2003.

[8] M. M. Haines, S. A. Stansfeld, et al., "Chronic aircraft noise exposure, stress responses, mental health and cognitive performance in school children," Psychological Medicine, vol. 31, pp. 265-277, 2001.

[9] HOK Group, Inc., "Designing a neurodiverse workplace," 2019.

[10] A. C. M. Kok, B. W. Kerhout, et al., "How chronic anthropogenic noise can affet wildlife communities," Fontiers in Ecology and Evolution, pp. 1-10, 2023.

IMPACT OF SPEED AND THROTTLE ADJUSTMENT ON FTA NOISE MODEL IN TRANSIT RAIL ANALYSIS INCLUDING CASE STUDY

Ian Matthew*[1], Anthony Amarra †[1]
[1]Valcoustics Canada Ltd, Richmond Hill, Ontario, Canada

1 Introduction

This paper provides a comparison of results using the US Federal Transit Authority (FTA) Detailed Noise Modelling method [1] for calculating the noise impact from railway for various speeds and throttle settings.

2 FTA Model – Locomotive and Rolling Noise

2.1 Dependence on Speed

The FTA Detailed Noise Modelling method accounts for the noise generated by various sub-sources, including the locomotive engine, rail car ("wheel-rail interaction" or "rolling noise"), and noise from whistles. For the purpose of this study, only locomotive and rolling noise are considered.

In diesel-locomotive trains, locomotive noise is dominated by the diesel engine, which emits a steady noise at a given throttle setting. The equivalent continuous sound level (L_{eq}) at a point of reception is therefore affected by the exposure time to the source. As such, a locomotive travelling at a faster speed will result in a lower L_{eq} at a point of reception than a locomotive travelling at slower speeds at that same point.

Rolling noise, on the other hand, is generated by the vibrations of the track and wheel due to surface roughness [2]. The radiated noise from the wheel/track vibrations is therefore modelled as increasing with increasing speed.

Figure 1 shows the 1-hour equivalent sound levels ($L_{eq,\ 1hr}$) from a single locomotive and a single rail car at 15 m (50 ft), illustrating the increasing and decreasing sound levels as a function of speed for rolling noise and locomotive noise (respectively).

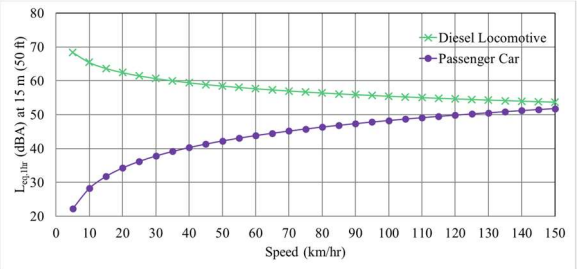

Figure 1: Diesel-Electric Locomotive and Rolling Noise as a function of Speed

2.2 Contribution from Locomotive Throttle

Locomotive sound emissions are also affected by the throttle setting. At low throttle (notch 5 or lower), the FTA model uses an adjustment of 0 dBA to the locomotive emission level. At notch 8, a +6 dBA correction is added.

Table 1 shows a comparison of the calculated $L_{eq,\ 1hr}$ at a receptor 15 m (50 ft) from the railway line at a height of 1.5 m (5 ft) above grade using the FTA method for three different speeds. The values are presented for one locomotive (notch 1 and 8), one rail car, as well as a sample train consisting of two locomotives and twelve cars.

The results indicate that the worst-case results are calculated for the trains operating at lower speeds and full throttle.

Table 1: FTA Sound Levels for Varying Speed and Throttle.

Speed (km/hr)	$L_{eq,\ 1hr}$ (dBA) at 15 m				
	Locomotive		Rolling Noise	Sample Train	
	Notch 1	Notch 8		Notch 1	Notch 8
20	62.4	68.4	34.3	65.5	71.5
70	57.0	63.0	45.2	61.5	66.4
120	54.7	60.7	49.9	62.4	65.4

3 Case Study

3.1 Description

In order to further illustrate the above concepts, consider a commuter train having 12 cars and 2 locomotives travelling along a railway line 15 m from the closest façade of a proposed noise-sensitive development. The site is also in the vicinity of a train station where commuter trains decelerate, stop, and accelerate. Typically, locomotives run at full throttle (notch 8) when accelerating, and low throttle when decelerating or travelling at speed [3].

A noise assessment is to be performed in order to determine requirements for the proposed development's façade construction (i.e., walls and windows) such that the indoor acoustical environment is acceptable for the intended use. Note that while this example may apply broadly, the example is typical for a GO Transit commuter train (Greater Toronto Area of Ontario).

When using the Ontario Ministry of the Environment model (Sound from Trains Environmental Analysis Method, STEAM [4]), a conservative assumption regarding speed (that is, the modelled speed that would result in the highest predicted sound level) would be the maximum allowable speed through a corridor. It should be noted that STEAM does not account for variations in throttle and generally produces an increasing predicted sound level (combined wheel-rail and locomotive noise) with increasing speed above 30 km/hr.

3.2 Assessment Scenarios

The case study compares three different scenarios, each using the FTA Detailed Noise Analysis method.

* ian@valcoustics.com
† anthony@valcoustics.com

- Design Speed Without Accounting for Accelerating/Decelerating Trains
- Design Speed Accounting for Accelerating/Decelerating Trains
- Actual Speed Accounting for Accelerating/Decelerating Trains

In each case, the following parameters are used in the assessment:

- 8 trains in an hour (half are decelerating toward the station and half are accelerating from the station)
- 2 locomotives and 12 cars per train
- Locomotives at notch 8 for accelerating trains and notch 1 for decelerating trains (where applicable). Note that where acceleration/deceleration is not considered in a scenario, it is assumed that all locomotives operate at notch 1
- Design speed of 120 km/hr, and actual speed in the vicinity of the proposed development is 35 km/hr

3.3 Results

Based on the above operating parameters, Table 2 provides the predicted $L_{eq,\ 1hr}$ at the receptor point 15 m from the railway at a height of 1.5 m above grade. Note that varying the setback distance, intervening ground characteristics, and receptor height would affect the results for each of the scenarios by the same amount.

3.4 Discussion

It is clear from the results in Table 2 that using the FTA model with the assumption that trains are operating at track design speed does not predict the most conservative sound levels at the receptor. In this example, the predicted sound level at the receptor location is 4.7 dB lower for the "Design Speed" assessment (ignoring the impact of acceleration/deceleration) when compared to the "Actual Speed" assessment (which accounts for acceleration and deceleration). This is a significant difference.

Furthermore, it's shown that even when acceleration/ deceleration is included in both assessment scenarios, the "Design Speed" assessment still predicts a sound level that is 2.9 dB lower than the assessment which assumes trains are operating at "Actual Speed" (where the speed is largely dictated by proximity to the station). This under-prediction is again significant and could result in a development design that may not sufficiently protect the development from railway noise.

For context, it should be noted that based on GO Transit acceleration deceleration data [3], a speed of 35 km/hr (either accelerating or decelerating) extends approximately 200m from the stopping point of the locomotive. It should also be noted that the under-prediction using the design speed applies in this example at almost all speeds, though the difference is reduced at higher "Actual Speeds" (further from the station).

Taking a wider view of the phenomenon, Figure 2 provides the speed/sound level relationship for the theoretical train operation including for acceleration/deceleration.

It is clear from the figure that although the speed/sound level relationship does exhibit a point of inflection (in this case at approximately 100 km/hr), the increase in sound level at higher speeds is much less significant than the increase in sound level with decreasing speed below the point of inflection.

Table 2: Predicted Sound Levels for Three Scenarios

	$L_{eq,1\ hr}$ (dBA)		
	Accel	Decel	Total
Design Speed – No Accel/Decel	68.4	68.4	71.4
Design Speed – Incl Accel/Decel	71.4	68.4	73.2
Actual Speed – Incl Accel/Decel	75.1	69.2	76.1

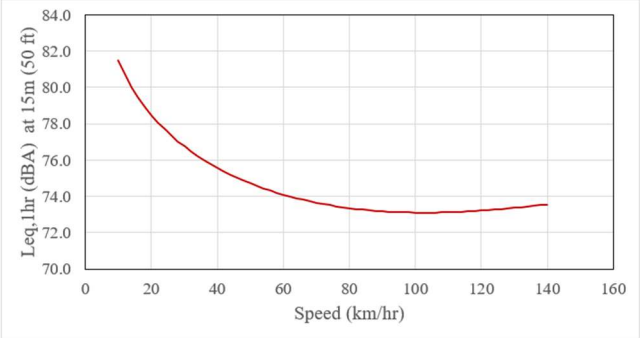

Figure 2: Sound Emission as a Function of Speed – Sample Train Scenario

4 Conclusion

The study provides a comparison of the emitted sound levels from diesel locomotives and rail cars as functions of speed using the FTA Detailed Noise Assessment Method. The results show that modelling trains travelling at lower speeds and full throttle provides higher predicted sound levels than trains travelling at higher speeds and low throttle.

Based on the Case Study, it is proposed that a suitably conservative approach to predicting sound levels at proposed noise sensitive receptor locations would be to use actual speeds of trains at the location of the proposed noise sensitive use as opposed to assumed design speeds that would yield lower predicted sound levels for the train operation.

References

[1] A. Quagliata et al., Transit Noise and Vibration Impact Assessment Manual, FTA Report No. 0123, September 2018.

[2] Thompson, D.J., Railway noise and Vibration: The Use of Appropriate Models to Solve Practical Problems, 21st International Congress on Sound and Vibration, July 2014.

[3] GO Railway Network Electrification TPAP – Final Noise and Vibration Modelling Report – Barrie Corridor, Gannett Fleming Report No. 060277, September 2017.

[4] V. Schroter, Sound from Trains Environmental Analysis Method, July 1990.

SIGN LANGUAGE HANDSHAPES, SIMILARLY TO SPEECH SOUNDS, EXPLOIT BIOMECHANICAL ENDPOINTS

Oksana Tkachman[1*], Shannon Hsu[1†], Maria Samarskaya[1‡], Cindy Zhao[1], Bryan Gick[1, 2‡‡]**
[1]Department of Linguistics, University of British Columbia, Vancouver, Canada
[2]Haskins Laboratories, New Haven, Connecticut, USA

1 Introduction

Speech motor control approaches have argued that the dimensionality problem can be handled by exploiting endpoints, a type of biomechanical quantal region [1, 2], where a stable output can be obtained regardless of the starting position or variable muscle activation of the articulators [3]. Endpoints involve a contact between two articulators or an active articulator and a passive articulator. One advantage endpoints offer is in preventing overshoot. In spoken languages, endpoints are maximally exploited in plosive sounds, the most frequent type of consonants occurring in all known spoken languages [4]. In signed languages, endpoints are exploited in signs where two hands make contact with each other, or where a hand(s) makes contact with the signer's body [5]. For example, in signs produced with body contact, variable arm muscle activation does not lead to variable place of articulation [6]. In this study, we extend research on sign-language endpoints by investigating handshape-internal endpoints, which is a state of a finger/joint where it is maximally extended or flexed, or where the fingers and/or thumb make a contact with each other and/or the palm. We annotated handshape inventories from three genetically distinct sign languages (Icelandic Sign Language, Turkish Sign Language, and Taiwan Sign Language) to determine the extent to which phonemic handshapes in the inventory exploit handshape-internal endpoints. These results support the view that the biomechanical quantal regions previously observed for speech are general to communicative control systems.

2 Methods

2.1 Data

Phonemic handshape inventories from three genetically unrelated sign languages have been chosen for annotation and analysis: Icelandic Sign Language (ISL) [7], Turkish Sign Language (TID) [8], and Taiwan Sign language (TSL) [9]. The ISL inventory consisted of 33 handshapes, the TID inventory of 32 handshapes, and the TSL inventory of 60 handshapes.

2.2 Annotation and analysis

The handshape inventories have been annotated following a modified version of the Sign Language Phonetic Annotation (SLPA) system proposed by Johnson and Liddell [10, 11]. SLPA is probably the most phonetically comprehensive sign annotation system proposed to date; each handshape requires 23-34 symbols of annotation. It focuses on four subcomponents of the handshape: (1) the configuration of the four fingers, including extension/flexion of each joint and abduction/adduction of adjoint fingers; (2) the presence and manner of a contact between the thumb and finger(s); (3) the thumb configuration, including extension/flexion of each joint and abduction/adduction/opposition to the palm; and (4) extension to the forearm (for cases where a forearm forms a part of the sign). In this project, we focus exclusively on handshape-internal endpoints, and therefore no annotation for the handshape extension (4) has been included.

In addition, following Tkachman et al. [12], we use fewer labels for degrees of flexion. SLPA uses six labels for indicating different degrees of flexion for each finger joint: fully extended *E* (0°), partially extended *e* (+30° for proximal joints, +10° for distal joints), partially flexed *f* (+60° for proximal joints, +20° for distal joints), fully flexed *F* (+90° to 100° for proximal joints, +45° to 80° for distal joints), and two degrees of hyperextension, *h* and *H*, where the joint extension goes beyond *E*. Some of these distinctions have been argued to be impossible to distinguish, especially in distal joints. Following [12], we do not differentiate between *h* and *H* (that is, all hyperextension cases are treated the same). Similarly, we adopt *I* (intermediate) instead of *e* and *f*, for all cases of partial extension/flexion of the joints. Thus, we only use 4 labels for join flexion: *E, I, F,* and *H*.

Each inventory was annotated by two coders. In cases of disagreement between coders, a third coder made the judgment as to which annotation to use. The number of endpoints was calculated for each handshape individually. There are three types of handshape-internal endpoints: one pertaining to joints (when a finger/thumb joint is either maximally extended/hyperextended or maximally flexed), one pertaining to contact (contact between fingers, contact between finger(s) and the thumb, and contact between fingers/thumb and the palm of the hand), and one pertaining to maximum abduction (when the fingers and/or thumb are maximally abducted from each other). Thus, a single handshape can have up to 14 joint endpoints (3 for each finger and 2 for thumb), up to 9 contact endpoints (3 between fingers, 1 between the thumb and fingers/palm, and 4 between fingers and the palm), and up to 5 abduction endpoints (4 for fingers and 1 for thumb). Accounting for the fact that a handshape cannot have a maximum amount of adduction and abduction endpoints simultaneously, the maximum number of endpoints per handshape therefore is 23 for handshapes with all fingers abducted (14 joint endpoints + 4 contact with the palm endpoints + 5

[*]o.tkachman@alumni.ubc.ca
[†] chsu02@student.ubc.ca
[‡] samarsky98@gmail.com
[**]cindyzhao325@gmail.com
[‡‡] bryan.gick@ubc.ca

abduction endpoints, but excluding 4 adduction endpoints) or 22 for handshapes with all fingers adducted (because there are only 4 adduction endpoints). Note that it is possible for a handshape not to have any endpoints (e.g., in a relaxed hand all joints are intermediate, and fingers and the thumb are neither adducted nor fully abducted). Thus, each handshape was assigned an endpoint number between 0 and 23, based on its annotation.

3 Results

The ISL handshape inventory has an average of 17.15 endpoints per handshape (range 9-23); the TID inventory has an average of 17.125 endpoints per handshape (range 2-22); and the TSL inventory has an average of 15.88 endpoints per handshape (range 4-22).

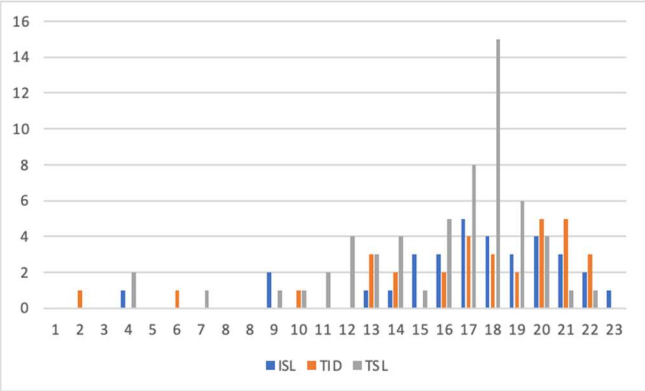

Figure 1: The distribution of endpoint values across handshape inventories (ISL: Icelandic Sign Language; TID: Turkish Sign Language; TSL: Taiwan Sign Language).

Results indicate that all three sign languages heavily exploit handshape-internal endpoints in their handshape inventories. Those handshapes with fewer endpoints do occur, most handshapes in all three sign languages exploit multiple endpoints of various types (see Figure 1).

4 Discussion

Human hands allow for an incredible intricacy; each hand has about 25-30 degrees of freedom [13, 14]. However, sign languages do not exploit the whole range of possible handshapes; only a limited number of phonemic handshapes get conventionalized. Phonemic handshapes have been argued to maximally distinctive/perceptually salient; however, articulatory factors undoubtedly also play a role in shaping handshape inventories. In this preliminary study, we explored the possibility that phonemic handshapes in sign languages exploit biomechanical endpoints, which at least for spoken languages have been argued to be a type of quantal region [1, 2]. Even though this is just a preliminary study, the fact that three unrelated sign languages heavily exploit endpoints just like spoken languages do suggest that biomechanical quantal regions are general to communicative control systems. Theories of speech motor control need to incorporate evidence from both spoken and signed languages to fully account for cross-modal tendencies exploited by articulatory systems of natural human languages.

References

[1] Moisik, S. R., & Gick, B. (2017). The quantal larynx: The stable regions of laryngeal biomechanics and implications for speech production. *Journal of Speech, Language, and Hearing Research*, *60*(3), 540-560.

[2] Gick, B., Mayer, C., Chiu, C., Widing, E., Roewer-Després, F., Fels, S., & Stavness, I. (2020). Quantal biomechanical effects in speech postures of the lips. *Journal of neurophysiology*, *124*(3), 833-843.

[3] Moisik, S., & Gick, B. (2013, June). The quantal larynx revisited. In *Proceedings of Meetings on Acoustics*, 19(1). AIP Publishing.

[4] Maddieson, I. (1984). *Patterns of sounds*. Cambridge: Cambridge University Press.

[5] Tkachman, O. (2022). *Embodiment and emergent phonology in the visual-manual modality: factors enabling sublexical componentiality* (Doctoral dissertation, University of British Columbia).

[6] Goyal, H., Venkata, P. S., Tkachman, O., & Gick, B. (2019). Simulating Biomechanical Endpoints in Sign Language Movements. Paper presented at *the Language Sciences Undergraduate Research Conference (LSURC),* Vancouver, Canada.

[7] Ivanova, N., Sverrisdóttir, R., & Björk Þorvaldsdóttir, G. (2022). Raising Handshape Awareness: The Handshape Inventory for Icelandic Sign Language (ÍTM) in Early Intervention and Teaching of ÍTM. *Hrvatska revija za rehabilitacijska istraživanja*, *58*(Special Issue), 27-51.

[8] Kubuş, O. (2008). *An analysis of Turkish Sign Language (TİD) phonology and morphology* (Master's thesis, Middle East Technical University).

[9] Tsay, J., & Myers, J. (2009). The morphology and phonology of Taiwan Sign Language. *Taiwan sign language and beyond*, 83-130.

[10] Johnson, R. E., & Liddell, S. K. (2011). Toward a phonetic representation of hand configuration: the fingers. Sign Language Studies, 12(1), 5-45.

[11] Johnson, R. E., & Liddell, S. K. (2012). Toward a Phonetic Representation of Hand Configuration: The Thumb. Sign Language Studies, 12(2), 316-333.

[12] Tkachman, O., Hall, K. C., Xavier, A., & Gick, B. (2016). Sign Language Phonetic Annotation meets Phonological CorpusTools: Towards a sign language toolset for phonetic notation and phonological analysis. In *Proceedings of the annual meetings on phonology*, 3.

[13] Flanagan, J. R., & Johansson, R. S. (2002). Hand movements. Encyclopedia of the human brain, 2, 399-414.

[14] van Duinen, H., & Gandevia, S. C. (2011). Constraints for control of the human hand. The Journal of physiology, 589(23), 5583-5593.

Abstracts for Presentations without Proceedings Paper
Résumés des communications sans article

How Does Interpretation Of Acoustic Features Affect Perceived Musical Emotion?

Cameron Anderson, Jamie Ling, Michael Schutz

Music communicates emotion through structural and interpretive acoustic cues—including pitch, timing information, and amplitude. Structural cues for musical emotion remain invariant across different performances and include the discrete pitch information making up a melody. Conversely, interpretive cues vary across different performances of a musical work, including the amplitude and timing of individual pitches in a performance. To clarify how structural and interpretive cues affect perceived emotion, past work compared emotional responses to performed single-line melodies against responses to computerized renditions lacking performance expression. These studies reveal structural cues largely communicate music's perceived valence (negative–positive emotional quality), whereas interpretive cues affect its arousal (low–high emotional intensity). However, no study to our knowledge has explored the effects of expression on valence and arousal in complex works with several concurrent voices—or how these effects vary across different levels of pitch, timing, and amplitude. To discern the effect of performance in naturalistic music, we conducted four listening experiments—each with a distinct combination of music composer (Bach/Chopin) and performance condition (expressive/deadpan). In each experiment, 30 different participants rated 24 musical excerpts along emotion scales of valence and arousal. The deadpan renditions used the same average timing and amplitude information as matched performances in the expressive condition but lacked interpretive cues. Our results reveal highly consistent emotion ratings between expressive and deadpan conditions—however, arousal ratings differed significantly between conditions, consistent with previous work. Post-hoc regression analyses revealed fast timing, high amplitude, and low pitch elicited larger differences between arousal ratings in expressive and deadpan conditions. Together, these outcomes suggest that structural cues are generally sufficient for communicating emotion, but interpretive cues strengthen perceived emotional intensity—especially for slow, soft, and high pitched music. These outcomes provide novel insight into how interpretation of acoustic cues can evoke diverse emotions in listeners.

Acoustic Properties Of Cork Fiber Reinforced Micro-Perforated Panel Made With Polylactic Acid Through Additive Manufacturing

Umberto Berardi

The present study investigated the acoustic performance of biodegradable MPP absorbers made of natural fiber-reinforced composites (NFRC) using 3D printing. The FDM technique was used to fabricate test samples utilizing the PLA/corkwood composite. Using an impedance tube device with two microphones, the acoustic absorption coefficients of MPPs with different perforation diameters, thicknesses, and perforation rates were measured. Maa's analytical model was used to predict the acoustic absorption performance. Moreover, considering the average sound absorption and total cost of fabricating the samples, RSM-CCD was employed to optimize these samples. In the end, the parallel arrangement of MPP double layer and the combination of MPP with kenaf porous material were tested in order to improve the sound absorption performance. The results showed that the average sound absorption coefficient of the NFRC-MPP sound absorber is 25% more than that of conventional MPP sound absorbers. The sample with a perforation diameter of 0.70 mm, a panel thickness of 0.90 mm, and an 8 mm distance between the perforations was selected as the optimal sound absorber. The measurement and model data for NFRC-MPP panels do not correspond well. The parallel arrangement of two layers of MPP and the addition of an optimized kenaf layer behind the MPP significantly improved the sound absorption performance in the intended frequency range. When compared to traditional manufacturing methods like manual preparation and pressing, the use of contemporary 3D printing technology in the development of acoustic absorbers allows us to quickly and simply produce absorbers with greater sound absorption performance.

Challenges Of Road Noise Prediction Methods In Canada

Petr Chocensky

Computer assisted prediction methods have been used extensively over the past 40 years as a cost effective and practical way of determining traffic sound levels in the urban environment. In Canada, the acoustical community is familiar with the United States Federal Highway Administration's traffic noise model (TNM) or STAMSON, a model developed in 1989 by the Ontario Ministry of the Environment. Some provinces, such as Quebec, have not yet officially adopted any prediction methods and rely on physical noise measurements for the purposes of

evaluating environmental traffic noise. Based on results collected via extensive acoustical consulting practice, the author evaluated the precision of the prediction methods used in Canada and identified several important shortcomings. This paper provides rationale for the need of either developing an updated prediction method or adopting one from another jurisdiction. In either case, it is imperative that any method used in Canada produces results that mirror direct measurements as close as practical.

Robust Continous Health Monitoring And Occupational Safety With Hearables

Alexandre Petrosky, Jérémie Voix, Rachel Bouserhal

Wearables are becoming more common in various industrial sectors. They can take various forms including that of a watch, an earpiece, or a piece of clothing. Hearables, or in-ear wearables, have gained particular attention in recent years. This is because the ear can serve as a nest for a variety of signals generated from important bodily functions such as the heart beating, pressure from local blood vessels, and brain activity making them a useful and essential tool for continuous health monitoring. This presentation includes a literature review pertaining to the various applications of hearables focusing on three main aspects of health monitoring: diagnosis, prevention, and rehabilitation. This review shows the impact that vital signal monitoring has on the development of new applications in the field but also its importance for helping diagnose early diseases. This in turn contributes to the prevention and rehabilitation of affected users.

AEROACOUSTICS - AÉROACOUSTIQUE

HIGH-FIDELITY ACOUSTIC SIMULATION OF A RECORDER USING POWERFLOW

Elissa El Hajj [*1], Davide De Cicco [†1], Annie Ross [‡1], and David Vidal [#1]
Laboratory for Acoustics and Vibration Analysis (LAVA), Polytechnique Montréal, Montréal, Québec, Canada

1 Introduction

Computational acoustics is a rapidly evolving field of study that relies on a variety of simulation and analysis methods to model the acoustic behavior of different systems, including musical instruments.

Among them, SOLIDWORKS Flow Simulation and ANSYS Fluent employ the finite volume method (FVM) and Unsteady Reynolds Averaged Navier-Stokes (URANS) equations, coupled with the Lighthill acoustic analogy, to simulate acoustics [1, 2]. Although ANSYS Fluent could also use the Ffowcs Williams and Hawkings (FWH) equation, this method requires an additional step to describe the acoustic field. On the other hand, PowerFLOW uses the Lattice Boltzmann Method (LBM) with the Very Large Eddy Simulation (VLES) method [3]. Fundamentally LBM solves the unsteady flow field in small time steps. Its low numerical dissipation and high accuracy make it an ideal choice for aeroacoustic simulations.

This study aims to highlight the precision and robustness of PowerFLOW simulation software to simulate the acoustics of a Turkish treble recorder. This woodwind music instrument is chosen for its modeling simplicity, serving as an optimal case study for the comparison of various simulation techniques.

2 Methodology

Airflow behavior in the Turkish treble recorder was initially characterized by Celik *et al.* [1], both experimentally and numerically, using SOLIDWORKS Flow Simulation, thus establishing a baseline for the current study. The referenced work examined the initial four tones produced from the head of the recorder when played in a closed position, assuming no leakage in the closed holes, under four distinct blowing speeds of 2, 4, 5.5, and 10 m/s. The numerical values of air velocity, pressure, and acoustic power level in the simulation domain were then determined.

The same recorder was simulated in ANSYS Fluent, with a Cartesian-based meshing technique used for the fluid region, with an element size of 0.001 m. The default k-epsilon model constant were chosen [4]. The less-computational expensive broadband noise source model [2] was used instead of the FWH equation.

Finally, the recorder was also simulated in PowerFLOW. The boundary conditions were defined similarly to the one used for SOLIDWORKS Flow Simulation. The computational domain was divided into nine virtual regions (VR) of progressively higher resolution, as shown in Figure 1, resulting in an effective number of voxels of around 10.9 million and a time step (dependent on the finest resolution) of 1.04 μs.

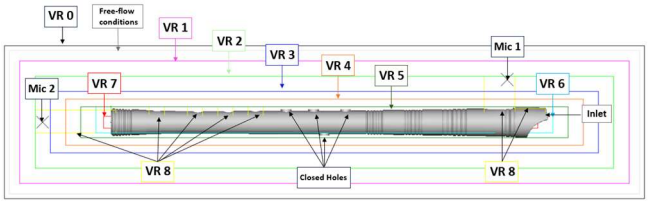

Figure 1: Side view of the simulation set-up.

The precise probe location of the experimental measurements was not specified in [1]. A simulation probe (Mic 1) was assumed to be placed 20 mm above the jet opening of the recorder and another probe (Mic 2) was placed 45 mm from the recorder's exit. The maximum simulated sound pressure level of Mic 1 was compared to the experimental measurements from [1], the SOLIDWORKS Flow Simulation results, and the ANSYS Fluent results. Additionally, the peak values recorded by Mic 2 were analyzed alongside measurements taken experimentally with an anemometer in the referenced work.

3 Results and discussion

PowerFLOW simulation, using LBM, demonstrated more distinct vortex formation, attributable to its microscopic, particle-based approach which excels in acoustic studies. Unlike the macroscopic URANS approach, LBM's time-stepping technique accurately captures complex flow physics and transient details, making it superior in resolving small vortices as shown in Figure 2.

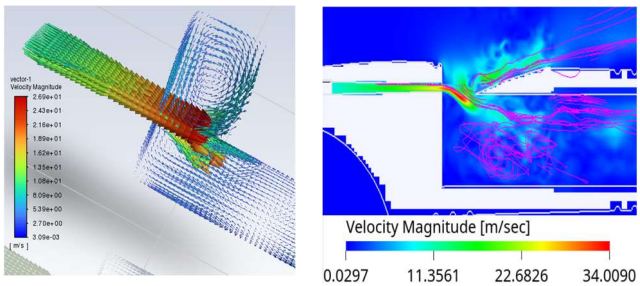

(a) (b)

Figure 2: Velocity magnitude around the jet opening for an inlet speed of 10 m/s: (a) ANSYS simulation and (b) PowerFLOW simulation.

Moreover, the λ_2 parameter, which is a non-dimensional parameter representing turbulence, could only be obtained directly with PowerFLOW and reveals intricate vortex

[*] elissa.el-hajj@polymtl.ca
[†] davide.de-cicco@polymtl.ca
[‡] annie.ross@polymtl.ca
[#] david.vidal@polymtl.ca

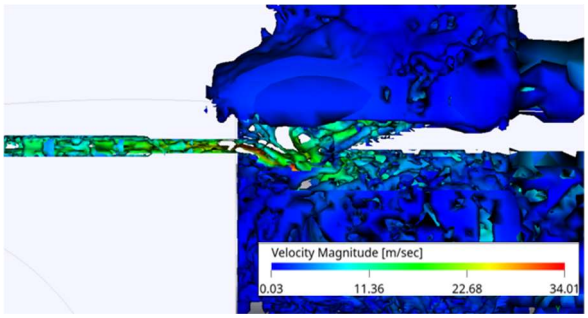

Figure 3: λ_2 criterion applied to the recorder.

structures within the instrument. These structures were color-mapped according to their velocity, as illustrated in Figure 3.

PowerFLOW is also used to extract the sound pressure level spectrum, an advantage not available with the other simulation methods, as illustrated in Figure 4. The maximum sound pressure level at Mic 1 is identified and compared with the values provided in the referenced article.

The results in Table 1, showing the maximum sound pressure levels at the four inflow rates, further help highlighting the superiority of PowerFLOW. Overall, the difference between the experimental and numerical results is the lowest with PowerFLOW. A comparison with ANSYS FLUENT indicates larger relative deviations from the experimental results, consistent with Oberkampf's assertion of a potential 35% error for the employed k-ε model [5]. While ANSYS Fluent shares a similar methodology to SOLIDWORKS Flow Simulation, its unique implementation of boundary conditions has resulted in diminished accuracy.

Upon examination of Table 2, it can be noted that the dominant tone frequencies simulated by PowerFLOW display a maximum difference of only 4.5% from those measured experimentally in [1]. While the referenced article did not provide a numerical comparison of the frequencies derived experimentally, this study successfully bridged this gap using PowerFLOW. This further confirms that PowerFLOW accurately replicates the recorder's note better than the other two software.

4 Conclusion

This research explored the application of computational acoustics, specifically the use of PowerFLOW simulation software, to model the acoustics of a Turkish treble recorder. The study highlighted the software precision and robustness, benefiting from its use of LBM and the VLES method. These findings underscore the importance of precise experimental measurements in future work to further validate the performance of LBM in accurately simulating acoustic phenomena.

Acknowledgments

Gratitude is expressed for the substantial support received from NSERC, CRIAQ, Bell Textron, and Hutchinson. Appreciation is extended to Dr. H.K. Celik for providing the CAD file and to Dr. S. Cyr and 3DS team for their invaluable training assistance.

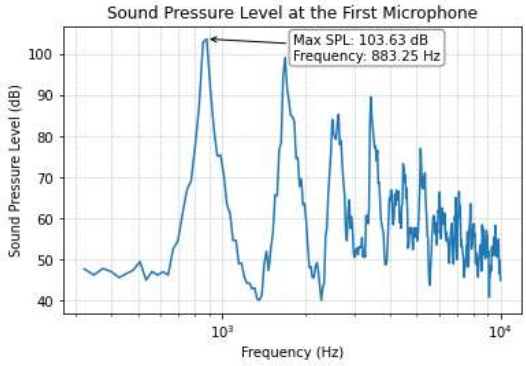

Figure 4: Sound pressure level for an inlet speed of 10 m/s.

Table 1: Comparison between experimental and simulated acoustic power levels at various inlet airflow rates. For conciseness, only the relative difference with respect to the experimental value is reported.

Inlet speed	Experim.	SolidWorks	ANSYS	PowerFLOW
2 m/s	62.9 dB	11.8%	42.1%	2.8%
4 m/s	81.6 dB	7.1%	29.1%	7.2%
5.5 m/s	98.1 dB	12.7%	38.0%	1.6%
10 m/s	102.6 dB	13.3%	30.8%	1.0%

Table 2: Comparison between experimental and PowerFLOW-simulated dominant tone frequencies, measured at Mic 2, for various inlet speeds.

Inlet speed	Experimental	PowerFLOW	Relative diff.
2 m/s	879.4 Hz	862.4 Hz	1.9%
4 m/s	1759.7 Hz	1686.3 Hz	4.2%
5.5 m/s	2634.8 Hz	2516.2 Hz	4.5%
10 m/s	3514.2 Hz	3426.3 Hz	2.5%

References

[1] H. K. Celik *et al.* CFD Simulation of Air Flow Behaviour at Different Flow Rates in a Turkish Woodwind Instrument (Turkish Treble Recorder). *OJA*, 1-16, 2021.

[2] Y. Wang *et al.* A fast and storage-saving method for direct volumetric integration of FWH acoustic analogy. *Ocean Engineering*, 2022.

[3] R. Schäfer and M. Böhle. Validation of the Lattice Boltzmann Method for Simulation of Aerodynamics and Aeroacoustics in a Centrifugal Fan. *Acoustics*, 735-752, 2020.

[4] M. Shirzadi *et al.* Improvement of k-epsilon turbulence model for CFD simulation of atmospheric boundary layer around a high-rise building using stochastic optimization and Monte Carlo Sampling technique. *J. Wind Eng. Ind. Aerodyn.*, 366-379, 2017.

[5] W. L. Oberkampf and M. F. Barone. Measures of agreement between computation and experiment: Validation metrics. *J. Comput. Phys*., 5-36, 2006.

A New Empirical Model Derivation for the Estimation of Turbulent Boundary Layer Power Spectral Density Aircraft Using Machine Learning Regression

Zachary Huffman *[1] and Joana Rocha †[1]
[1]Department of Mechanical and Aerospace Engineering, Carleton University, Ottawa, ON

1 Introduction

At cruise conditions, the most significant source of aircraft cabin noise are wall-pressure fluctuations induced by the turbulent boundary layer (TBL). This noise is often significant and has been associated with an elevated risk of cardiovascular disease, hearing loss, and sleep deprivation in flight crews [1, 2]. Therefore, the development of an accurate empirical model that predicts noise generated from TBLs is an important ongoing research topic. Early models, such as those from Lowson and Robertson, were primarily derived by simplifying and solving the Reynolds-averaged Navier-Stokes equations for the pressure fluctuation term and adding length and velocity scales to best match experimental data. Subsequent models were derived by applying statistical and mathematical techniques to simplify earlier models, or via modifications that addressed apparent shortcomings. Past research has had varying success. Most models are accurate only near their design Mach and Reynolds numbers [3]. Only recently was the possibility of using machine learning techniques explored by Dominique, who produced a highly accurate TBL model via an artificial neural network [4]. This paper extends Dominique's work by applying a different machine learning technique, nonlinear least squares regression (NLS).

2 Method

The model was derived in five steps, as outlined in [5]. First, an exploratory data analysis (EDA) was performed, which sought to identify data sources and possible candidate variables. In total, 14 data sources were available, consisting of wind tunnel data procured at Carleton University. 12 experimental runs were placed in the training dataset, which had an average airspeed of 10.6 m/s and Reynolds number of approximately 850,000; while the testing dataset had an average airspeed of 8.92 m/s and Reynolds number of 650,000. Additionally, a total 23 candidate variables were to be considered –most were selected based on their appearance in previous TBL noise models, but some other common dimensionless fluid dynamic parameters were also considered.

The second step was dimensional analysis, which sought to establish a priori knowledge on the final form of the model via consideration of the dimensions. Specifically, the since the PSD of pressure fluctuations in the TBL has units of [Pa^2/Hz], Equation 1 represented a highly simplified model that could theoretically predict the PSD:

$$\emptyset(f) = \frac{A[P]^2}{1/t} \tag{1}$$

where P is any candidate variable in units of Pa, $1/t$ is any candidate variable in units of Hz, and A is some coefficient to be fit to the model.

While dimensional analysis made it theoretically possible to create candidate models and iteratively add complexity (via the addition of terms), it left two unanswered problems: how to fit coefficients/exponents and how to identify the performance of each model. These problems were solved via the third and fourth steps, model development and testing, respectively. For the third step, the NLS algorithm was implemented in R to fit the model against all possible candidate variable combinations. Next, model testing was performed via a combination of its Akaike Information Criterion (AIC), Bayesian Information Criterion (BIC), and Mean Squared Prediction Error (MSPE). After the optimum form of any given candidate model was selected, its shortcomings were identified, a new model form was proposed, and steps three and four were repeated. This process stopped only when it became clear that added complexity failed to yield a superior model. At this point, the final selected model underwent validation, which sought to assess model accuracy against outside data. However, due to the limited availability of outside data, only freestream velocities from 7.20 m/s to 27.1 m/s and Reynolds numbers from approximately 530,000 to 6,200,000 could be considered [6].

3 Results

In total, iterative model generation procedure allowed for 186 unique model forms to be tested. The best performing model, per the statistical tests, is presented in Equation 2 below:

$$\emptyset(f) = \frac{(0.39031)M^{2.6241}q^2}{\left({}^{U_\tau}/_{\delta}\right)\left[(0.019972)St^{5.2179} + Re_T^{1.3968}\right]} \tag{2}$$

where M is the Mach number, q is the dynamic pressure, U_τ is the friction velocity, δ is the boundary layer thickness, St is the Strouhal number, and Re_T is the turbulence Reynolds number. Figures 1-3 show plots of Equation 2 against internal training data, testing data, and validation data, respectively. Additionally, note that the iterative procedure itself provided several useful insights into the nature of TBL modelling. First, the optimum candidate variables to use in the velocity/time term in the denominator has been a source of disagreement amongst researchers; however, the algorithm repeatedly suggested that either U_τ/δ or U_∞/δ^* (freestream velocity and displacement boundary layer thickness) were the optimum options. Second, the optimum Reynolds number in

* zacharyhuffman@cmail.carleton.ca
† joana.rocha@carleton.ca

the denominator has been disputed, but this paper suggests Re_T is optimum; and finally, concerning pressure in the numerator, this paper suggests q is optimal.

4 Discussion and Conclusion

Overall, Equation 2 showed a better agreement with all three plots, albeit with a tendency to underestimate PSD in the medium-to-high frequency regions. Furthermore, while less apparent in the plots, the model tended to lose accuracy against validation data if it was at higher airspeed and Reynolds number. However, given the limited number of cases covered in validation datasets, this should not be seen as an absolute conclusion. Possible causes of this discrepancy include the limited number of unique parameters in the training dataset leading to low data over-fitting issues; the noisiness of the training datasets at low and high frequencies necessitating cleansing; compilation issues with the NLS algorithm, reducing the number of available candidate models to choose from; the inability of statistical tests to filter out frequencies that were less important to human hearing; limited validation data; and the highly negative exponent on St leading to the PSD roll-off occurring at too low of a frequency.

This technique offered several advantages that were not present in earlier TBL modelling techniques. First, it permitted 186 unique model forms to be tested. This is unmatched in prior literature, except by Dominique. However, the use of the neural networks in the Dominque model did not permit the same number of statistics, plots, and visual analysis to be performed/calculated on each model [4]. Second, the openness of the NLS technique allowed unanswered TBL-modelling questions to be answered, such as the optimum candidate variables to use in the numerator and denominator. Finally, as the model generation technique did not rely on TBL-specific physics, it can be generally applied to other engineering applications. Overall, the performance of the model presented and advantages demonstrate that future researchers may consider extending these techniques to novel problems and datasets.

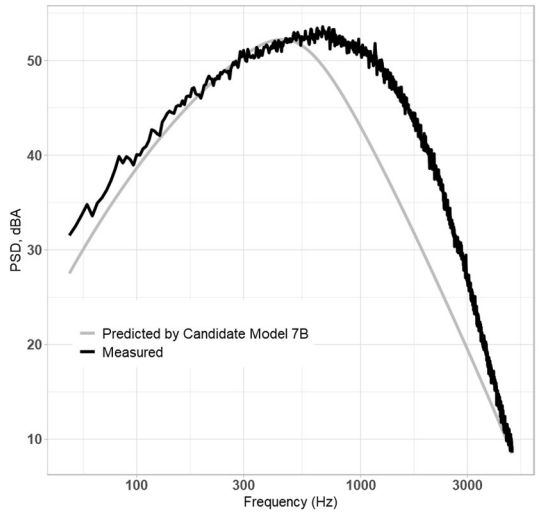

Figure 1: Plot of Equation 2 against selected training data.

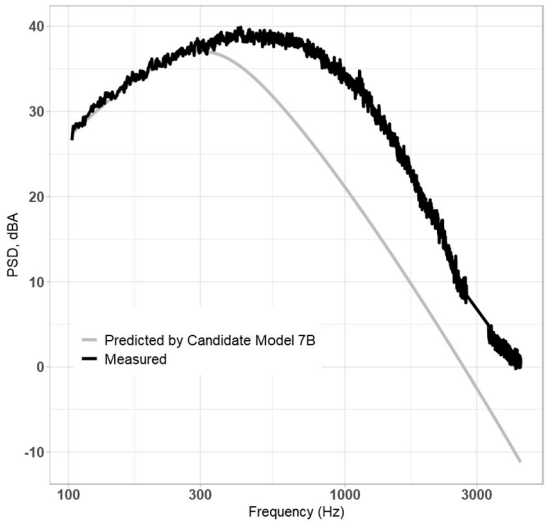

Figure 2: Plot of Equation 2 against selected testing data.

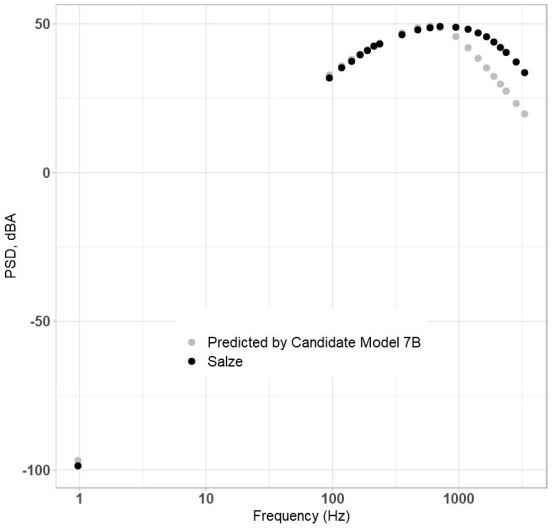

Figure 3: Plot of Equation 2 against selected validation data.

References

[1] C. D. Zevitas et al., "Assessment of noise in the airplane cabin environment," *Journal of Exposure Science and Environmental Epidemiology*, vol. 28, p. 568–578, Mar. 2018.

[2] J. E. Robertson, "Prediction of in-flight fluctuating pressure environments including protuberance induced flow," Wyatt Laboratories, Huntsville, AL, Tech. Report, WR 71-10, Mar. 1971.

[3] J. B. Blitterswyk and J. Rocha, "An experimental study of the wall-pressure fluctuations beneath low Reynolds number turbulent boundary layers," *The Journal of the Acoustical Society of America*, vol. 141, pp. 1257-1268, Feb. 2017.

[4] J. Dominique et al., "Artificial Neural Networks Modelling of Wall Pressure Spectra Beneath Turbulent Boundary Layers," *Physics of Fluids*, vol. 34, no. 3, Mar. 2022.

[5] C. Chatfield, *Problem Solving: A Statisticians Game*. Chatfield, UK: Chapman & Hall, 1988.

[6] N. Thompson and J. Rocha, "Comparison of Semi-Empirical Single Point Wall Pressure Spectrum Models with Experimental Data," *Fluids*, vol. 6, no. 270, Jul. 2021.

TURBULENCE DISTORTION EFFECT ON LEADING EDGE NOISE FROM WIND TURBINE BLADES

Vasishta Bhargava Nukala *[1], Chinmaya Prasad Padhy †[1]
[1]Department of mechanical engineering, GITAM (Deemed to be) University, Hyderabad, Telangana, India

1 Introduction

Turbulence distortions is a potential source for production of flow induced noise and rely on the turbulence properties of aerodynamic flow field. Particularly in wind energy applications, the broadband leading-edge noise from rotating blades becomes significant when the turbulence intensity (TI) and integral length scale factors vary with mean flow velocity and rms velocity fluctuations. The noise radiated at leading edge of blade varies significantly with turbulence characteristics of velocity spectrum that describes the turbulent kinetic energy envelope. In this work, leading edge noise predicted by modified rapid turbulence distortion (RDT) model proposed by [1] is applied and compared with noise levels predicted by Grosveld, Moriarty and Lowson turbulent inflow models for a 2MW model wind turbine blade. For low frequencies in sound spectra, 50 Hz < f < 200 Hz the sound power predicted by both models agreed within 2-5% with experiment data of a SWT 2.3 MW wind turbine blade which has tip speed of ~83 m/s. However, for mid-band frequencies 250 Hz < f < 1 kHz, the modified rapid distortion model scales the turbulence properties in velocity spectrum more accurately leading to better estimation of noise levels. The modified RDT model has been computed for different turbulence intensities and found that as turbulence intensity increased the standard error for noise was reduced by at least 1 dB in low frequency region of sound spectrum. This trend is not observed with other models and on contrary it was found to increase.

2 Method

2.1 Modified rapid distortion theory (RDT)

To understand sudden changes to turbulence characteristics in flow field, rapid distortion theory (RDT) model developed by [2] provides an insight on how turbulence velocity or pressure fluctuations in homogeneous isotropic incompressible flows. It essentially uses a wavenumber analysis to calculate the surface pressure fluctuation to approximate the smaller scale of eddies which distorts the flow field relative to mean velocity field with changing boundary conditions under homogeneous isotropic turbulence. According to [3] in order to obtain rapidly distorted turbulent velocity spectra by applying RDT method, following conditions are necessary:

- Turbulence intensity in atmosphere must be very negligible compared to normalized local turbulence values in flow field.
- The integral length scales need to be smaller compared to length scale of eddies developed in the turbulent boundary layer.
- Reynolds number associated with turbulent flow velocity field is significantly large compared to mean flow velocity.

For unsteady incompressible flows, the leading edge noise is affected by the strength of turbulence or distortion in turbulence field which can be measured by velocity gradients in leading edge of boundary layer on aerofoil. [4, 5] studied the effect of angle of attack and different aerofoil geometry specifications, e.g. thickness, LE radius and camber on the leading edge turbulence interaction noise based on [6] noise prediction model. They found that model overpredicts the far field leading edge noise at high frequencies with respect to measured noise due to small thickness assumption for aerofoil and ignores the turbulence distortion effects. Hence the corrected model for velocity spectrum takes account of velocity perturbations that cause turbulence distortion near LE boundary layer, even at higher wave numbers and thus predicted the LE turbulence interaction noise more accurately. Later, [1] has done further modifications related to length scale proposed by [3, 7] to study the local turbulence properties and derived the improved rapidly distorted turbulent energy spectra, ϕ_{ww} for velocity field as given by Eq. (1):

$$\phi_{ww}(k_x,k_y) = \frac{91}{36\pi}\frac{\overline{u^2}}{k_e^2}\frac{\left(\frac{k_x}{k_e}\right)^2+\left(\frac{k_y}{k_e}\right)^2}{\left(1+\left(\frac{k_x}{k_e}\right)^2+\left(\frac{k_y}{k_e}\right)^2\right)^{\frac{19}{6}}}. \quad (1)$$

The expression obtained by Eq. (1) is substituted in the modified turbulent inflow noise model proposed by Lowson method for sound pressure. The final expression for sound pressure estimation derived by [1] in his validation study resulted in change of the empirical constant from 78.4 to 89.95 and given by Eq. (2):

$$SPL_{1/3} = 10\cdot\log\left(\frac{\rho^2c^2lL}{2r_e^2}\frac{M^3U^2I^2\left(\frac{k_x}{k_e}\right)^3\bar{D}_L}{\left(1+\left(\frac{k_x}{k_e}\right)^2\right)^{\frac{19}{6}}}\right)+85.95, \quad (2)$$

where k_x and k_y are the wave numbers of turbulent velocity fluctuations along blade chord and span directions respectively. k_e is the wave number corresponding to energy containing turbulent eddies in velocity spectra. $\overline{u^2}$ is the *rms* value of turbulent velocity fluctuations in energy spectra.

* vasishtab@gmail.com
† cpadhy@gitam.edu

3 Results

Fig. 1 illustrates the comparison of sound power predicted by modified RDT, Grosveld, Lowson and Moriarty models for a wind speed of 12 m/s at turbulence intensity of 10%. It can be noted that for frequencies, $f < 60$ Hz, the Grosveld model showed a less conservative prediction for L_w with a maximum value of 110 dB and closely agrees the trend predicted by modified RDT model. However, for $f > 60$ Hz, the noise outputs agree better with Moriarty & Migliore and Lowson noise models. Also, sound levels predicted by Moriarty & Migliore and Lowson models show a difference of ~3 dB between 20 Hz $< f <$ 60 Hz. For frequencies between 100 Hz and 1 kHz in the noise spectra, the slope of curves for Grosveld, Lowson and Moriarty models show a similar trend and agree strongly with each other. However, the RDT model shows a steeper slope for noise curve in that region. Also, the validation of turbulent inflow noise predicted by four semi empirical models has been done with experiment noise data of Siemens SWT 2.3 MW – 93. For low frequencies, $f < 100$ Hz, the standard Lowson, Moriarty & Migliore, and RDT model showed strong agreement with experiment data, but the Grosveld model deviated by 3 dB because the turbulent velocity energy spectra for Moriarty & Migliore and RDT models was modified based on standard Lowson method and was not implemented in Grosveld model. Further, it can be seen that experiment data shows a sound power peak near f~1 kHz which is due to the trailing edge noise from blade. So, for subsonic turbulent flows, the turbulent inflow noise exhibits M^6 dependence and radiates sound as a dipole in rotor plane.

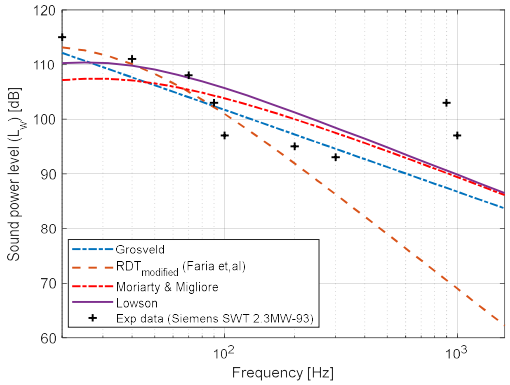

Figure 1: Comparison of the turbulent inflow noise predicted from the Grosveld, Moriarty, Lowson, and modified RDT models at mean wind speed of 12 m/s, at turbulence intensity of 10%, and validated with experiment data of Siemens SWT 2.3 MW-93 model.

4 Discussion

The sound power, L_w for turbulent inflow noise computed by all four models shows relative difference in low frequency part of spectra, at different turbulent intensity levels. For this reason, standard error for sound power, L_w has been evaluated for each of TI levels used in the study. Table 1 show that the standard error for L_w in the frequency range, 20 Hz $< f <$ 315 Hz is reduced with increasing values of TI at mean wind speed of 10 m/s. This suggests that all four models predict similar trends for TI noise levels and agree with experiment data shown in Fig 1.

Table 1: Comparison of standard error in sound power level, L_w predicted at different turbulent intensities for mean wind speed of 10m/s

TI, %	1/3rd octave frequency, [Hz]							
	20	31.5	63	80	125	160	200	250
6.0	2.35	1.71	1.29	1.36	1.76	2.08	2.41	2.75
8.0	1.88	1.24	0.79	0.90	1.39	1.75	2.09	2.45
10.0	1.55	0.94	0.50	0.65	1.21	1.58	1.93	2.29
12.0	1.32	0.80	0.48	0.63	1.17	1.52	1.86	2.22
14.0	1.18	0.79	0.63	0.76	1.21	1.54	1.86	2.20

5 Conclusion

The present study investigated the turbulence distortion effect based on the modified RDT model to predict turbulent inflow noise for wind turbine blades. The modified RDT model predicted the turbulent inflow noise curve more accurately in the low frequency region of sound spectra and agreed well with experiment data, compared to Moriarty and Migliore, Grosveld and Lowson models. The mechanism for broadband turbulence interaction noise at leading edge of turbine blade is thus dependent on turbulence velocity spectra characteristics considered in each of model. Model comparisons also show that maximum standard error for sound power is ~2.8 dB at 250 Hz in sound spectra.

Acknowledgments

Authors thank GITAM (Deemed to be) university for their continuous motivational support in this work.

Reference

[1] Faria, M. A., Saab, J. Y., Rodriguez, S., Pimenta, M. M., A rapid distortion theory based airfoil turbulent inflow noise prediction method, *Journal of Brazilian society of mechanical sciences and engineering*, 42: 397, 2020

[2] Hunt, J. C., A theory of turbulent flow round two-dimensional bluff bodies, *Journal of fluid mechanics*, 61(4), 625-706, 1973

[3] Goldstein, M.E., Afsar M.Z., Leib, S.J., Nonhomogeneous rapid distortion theory on transversely sheared mean flows, *Journal of fluid mechanics,* 736: pp, 532-569, 2013

[4] Moreau, S., and Roger M., Effect of angle of attack and airfoil shape on turbulence-interaction noise, *11th AIAA/CEAS aeroacoustics conference*, 2005

[5] dos Santos, F.L., Botero-Bolivar, L., Venner, C., and de Santana, L. D., Modelling the turbulence spectrum dissipation range for leading edge noise prediction, *AIAA Journal*, 2022

[6] Amiet, R., Acoustic radiation from an airfoil in turbulent stream, *Journal of sound and vibration.* 41: 407-420, 1975

[7] Christophe, J., Application of hybrid methods to high frequency aero-acoustics, *Dissertation, Von Karman institute for Fluid dynamics*, 2011

Abstracts for Presentations without Proceedings Paper
Résumés des communications sans article

Evaluation Of Wall Pressure Spectrum Models For Fan Noise Prediction

Marlene Sanjose, Natacha Galand, Teddy Garnier, Stéphane Moreau

As new concepts for rotating machines in applications ranging from unmanned aerial vehicles to small wind turbines for urban areas emerge as possible future innovations, it is important to consider noise levels when evaluating the acceptability of such concepts. At the design stage, it is important to be able to rely on rapid predictions of noise for rotating machines. The current work focuses on low cost broadband noise prediction for low speed rotating machines. The main focus is on the rotor self-noise caused by the scattering of turbulent eddies at the trailing edge of the rotor blades. The objective is to improve noise predictions based on the Amiet approach, which is informed by Reynolds Averaged Navier-Stokes results. With this approach, advanced Wall Pressure Spectrum (WPS) models are essential when the rotor is operated under high load conditions. In the present work, several empirically based wall pressure spectrum models are evaluated. The performance of the models is highly dependent on whether they are tested in their training domain of boundary layer parameters. The models have been calibrated on flat plate or airfoil flows.In the present work, the models are evaluated on three low speed axial fans. Fan applications present several challenges related to three-dimensional boundary layers and secondary flows. The first fan is a fan used in automotive engine cooling systems, the second is typical of ventilation systems that are essential in any passenger compartment, and the third is characteristic of drone propellers for recreational and localized use. First, the boundary layer near the trailing edge of the fan blades is characterized and compared with the training range of the models. Then, the far-field sound power levels obtained with Amiet's approach and the WPS models are compared with experimental measurements from published databases.

Interaction Noise For A Rotor-Stator Assembly In A Short Duct

Marlene Sanjose, Baahirham Shanthalingam

Aeroacoustic noise emission is an area of extensive research in turbomachinery, helicopters, and airplanes. The helicopter tail rotor can be a significant source of noise during takeoff, landing, and flight maneuvers. In the present work, the aeroacoustic noise sources in a high-thrust ducted fan system, typically designed for an electrically driven anti-torque system, are investigated.The rotor-stator fan system is first studied using Reynolds Averaged Navier-Stokes (RANS) simulations, and noise predictions have been computed using classical analytical approaches based on empirical and statistical modeling of the noise sources. The noise sources investigated are multiple in such a compact assembly, including both broadband and tonal noise sources at the leading and trailing edges of the rotor blades and stator vanes. These evaluations have shown limited accuracy when compared to experiments. The present work focuses on the analysis of Unsteady RANS (URANS) simulations to provide a better understanding of the rotor-stator interaction noise. In this work, the URANS simulation is performed using the ANSYS CFX software. The domain is limited to half of the machine with rotational periodicity and includes the casing and hub geometric features of the complete fan assembly in a large domain to capture the fan wake evolution in free field. Simulations were performed over 30 revolutions. Both the periodic wake and the blade tip vortex generated by the rotor are studied to better capture their interactions with the stator vanes. The analytical approaches for noise prediction are compared with the far-field noise calculated by an acoustic analogy using the pressure fluctuations recorded during the simulation. Both free field and infinite duct Green functions are considered to evaluate potential shielding effects from the casing.

ARCHITECTURAL AND BUILDING ACOUSTICS - ACOUSTIQUE ARCHITECTURALE ET DU BATÎMENT

INCIDENCE DES MENEAUX D'UN MUR-RIDEAU SUR L'INDICE ASTC DE CLOISONS INTÉRIEURES

Julien Fenninger [*1] **et Alexandre Couture** [†1]
[1]SNC-Lavalin, 85 Rue J-A Bombardier, Boucherville, QC, Canada

1 Introduction

De nos jours, le mur-rideau est un revêtement extérieur de plus en plus utilisé dans l'architecture moderne. Ceci est vrai pour beaucoup de bâtiments de types commerciaux et résidentiels, tels que des hôpitaux, écoles, centres commerciaux ou tours d'habitation. Ce type de revêtement implique que certaines cloisons intérieures séparant deux locaux soient directement reliées à un meneau en aluminium issu du mur-rideau. Cette particularité peut amener une voie de flanquement importante et réduire la performance acoustique de la cloison intérieure initialement visée.

Sachant que l'isolement acoustique d'un espace demeure une priorité et ce, particulièrement pour des environnements où des informations de type confidentielles sont transmises, par exemple, dans les hôpitaux, il est important d'avoir une isolation sonore de qualité et de limiter les voies de flanquement afin de respecter la confidentialité. Le présent article a pour but de déterminer à l'aide de mesures de bruit *in situ*, l'effet que peut avoir un meneau sur l'indice ASTC d'une cloison séparant deux espaces sensibles. Dans un premier temps, une mise en contexte ainsi que la méthodologie utilisée pour effectuer les mesures seront présentées. Ensuite, les résultats des différentes séries de mesures seront discutés. Le tout sera suivi d'une conclusion afin de connaitre l'incidence que peuvent avoir les meneaux sur l'indice ASTC.

2 Méthode

Les mesures ont été réalisées en 2020 à Montréal lors de la construction d'un nouveau bâtiment ayant un mur-rideau comme revêtement extérieur. Les tests ont été réalisés en s'accordant avec la procédure du standard ASTM E336-14 intitulé " *Standard Test Method for Measurement of Airborne Sound Attenuation between Rooms in Buildings* ".

Pour ce faire, une source sonore a été placée dans la salle émettrice. Lorsque la source était en fonction, les niveaux sonores ont été mesurés dans la salle émettrice (LpS) et dans la salle réceptrice (LpR) et ce, à au moins six (6) points de mesures dans chacune des pièces. Ensuite, les niveaux de bruit ambiant (BG) ont été mesurés à ces mêmes positions dans la salle réceptrice lorsque la source sonore été arrêtée. La durée de chacun des échantillons sonores prélevés était d'au moins 20 secondes ($L_{Zeq,20s}$).

De plus, l'absorption sonore de la salle réceptrice a été déterminée à l'aide de mesures de temps de réverbération. Celles-ci ont été réalisées à chacune des positions de mesures utilisées précédemment et au nombre de trois mesures par position. Les prescriptions du standard ASTM E2235-04 intitulé " *Standard Test Method for Determination of Decay Rates for Use in Sound Insulation Test Methods.*" ont été suivies pour effectuer les mesures de temps de réverbération.

Finalement, l'ensemble des mesures a permis d'établir la réduction sonore (NR : Noise Reduction), la réduction sonore normalisée (NNR : Normalized Noise Reduction) et l'affaiblissement sonore apparent (ATL : Apparent Transmission Loss) procurés par la cloison mitoyenne située entre la salle émettrice et la salle réceptrice. Ces résultats ont permis à l'aide du standard ASTM E413-10 intitulé "*Classification for Rating Sound Insulation*" de déterminer l'indice de transmission sonore apparent (ASTC : Apparent Sound Transmission Class). L'indice de transmission sonore apparent (ASTC) ainsi mesuré est celui que l'on compare généralement aux normes et critères applicables.

3 Description de l'assemblage testé

Plusieurs variantes de la cloison mitoyenne ont été testées afin de vérifier et de quantifier l'influence du meneau sur la performance acoustique du mur. Selon les informations reçues, la composition de la cloison mitoyenne testée était comme suit :

- 2 panneaux de gypse ignifuge de 16 mm ;
- Colombage métallique de 92 mm, calibre 20 @ 600 mm c/c ;
- Isolant phonique (12 à 45 kg/m^3) remplissant la cavité entre les colombages ;
- 2 panneaux de gypse ignifuge de 16 mm

En principe, un STC 48 est attendu pour une cloison de ce type. Cette cloison vient se buter à un meneau simple provenant du mur-rideau.

Il est à noter que les pièces où les essais ont été effectués étaient inoccupées et non meublées. Les murs étaient composés d'une fenestration abondante et de gypse. Les planchers étaient acoustiquement réfléchissants et les plafonds, en tuiles acoustiques.

Selon les informations reçues lors de la réalisation des mesures, l'intérieur du meneau possédait un revêtement viscoélastique d'environ 3,15 mm d'épaisseur mais ne possédait aucun isolant acoustique (laine).

Afin de déterminer l'impact du meneau sur la performance de la cloison mitoyenne, plusieurs configurations ont été testées :

- Test 1 : Aucun ajustement, la composition initiale telle que décrite plus haut est testée ;
- Test 2 : Une cornière en aluminium est placée sur l'intersection meneau/cloison dans la salle émettrice ainsi que dans la salle réceptrice ;
- Test 3 : Ajout d'une plaque d'aluminium de 1,59

∗. julien.fenninger@snclavalin.com
†. alexandre.couture@snclavalin.com

mm d'épaisseur sur l'un des côtés du meneau. Les cornières sont toujours présentes ;
— Test 4 : Ajout d'une plaque d'aluminium de 1,59 mm d'épaisseur sur les deux côtés du meneau. Les cornières sont toujours présentes ;
— Test 5 : Ajout d'une plaque d'aluminium de 1,59 mm d'épaisseur sur l'un des côtés du meneau et de deux plaques de l'autre côté du meneau. Les cornières sont toujours présentes ;
— Test 6 : Le meneau est temporairement encoffré par du gypse sur chacun des côtés.

4 Résultats

Les résultats des mesures sont présentés sous forme graphique à la Figure 1. L'affaiblissement sonore apparent (ATL) par bande de fréquence ainsi que l'indice de transmission des bruits aériens apparents (ASTC) y sont présentés.

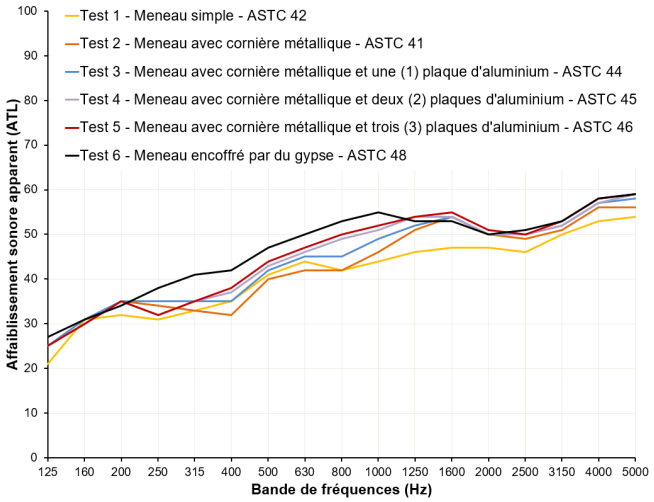

FIGURE 1 – Résultats de l'affaiblissement sonore apparent (ATL) pour les différentes compositions testées

Lors des essais, des voies de flanquement ont été subjectivement observées et pour la majorité des situations testées, celles-ci étaient localisées au niveau du meneau simple du mur-rideau. Pour le test 6, aucune voie de flanquement n'a été observée.

5 Discussion

Les mesures acoustiques effectuées ont permis d'établir l'indice ASTC pour plusieurs variantes d'un assemblage ayant une condition d'intersection typique entre une cloison intérieure et un mur-rideau. Les résultats ont permis de tirer différentes constatations et conclusions sur l'influence d'un meneau simple sur la performance acoustique d'une cloison mitoyenne.

La valeur STC (rationalisée) attendue pour une cloison sèche telle que présentée ci-dessus (excluant le meneau) est de STC 48.

L'essai effectué avec le meneau temporairement isolé avec du gypse respectait la valeur attendue en affichant un résultat de ASTC 48. L'essai effectué sur la composition initiale (sans correctif) sur le meneau affiche un résultat de ASTC 42, soit une différence de 6 points par rapport à la performance désirée. Cette différence montre que le meneau est une voie de flanquement et qu'il a bel et bien un impact sur la performance attendue de l'assemblage testé.

L'essai réalisé avec les cornières avait pour but de valider si la voie de flanquement provenait de l'ensemble du meneau ou de la jonction entre le meneau et la cloison sèche. Le résultat obtenu pour cet essai (ASTC 41) montre que la voie de flanquement ne provient pas de la jonction. La différence de un (1) point entre l'essai avec cornières et sans cornières entre dans la marge d'erreur envisageable.

Finalement, les résultats des essais avec l'ajout d'une ou de plusieurs plaques d'aluminium de 1,59 mm ayant pour but d'ajouter de la masse au meneau montrent une amélioration de l'indice ASTC. Les résultats varient entre ASTC 44 et 46 dépendamment du nombre de plaques utilisées.

6 Conclusions

Les résultats de ces essais montrent bel est bien qu'un meneau simple issu d'un mur-rideau directement relié à une cloison sèche intérieure peut avoir une influence importante sur la performance acoustique de celle-ci. Une réduction de l'indice ASTC allant jusqu'à six (6) points peut être envisagée si la cloison est jumelée à un meneau simple possédant une membrane viscoélastique. Ainsi, il est important de prendre en compte la présence ou non d'un meneau lors de l'analyse de performance d'une cloison mitoyenne. Si le meneau n'est pas acoustiquement traité, il sera peut-être nécessaire de rajouter de la masse aux alentours du meneau dans le but de limiter son impact sur la performance acoustique.

Remerciements

Nos remerciements vont à l'équipe ayant participé aux différentes sessions de mesures nocturnes et à l'analyse des résultats.

Références

[1] Gouvernement du Québec. Règlement concernant la valorisation de matières résiduelles. 2021.

[2] KV Horoshenkov and MJ Swift. The effect of consolidation on the acoustic properties of (...). *App. Acoust.*, 62, 2001.

[3] NN Voronina and KV Horoshenkov. A new empirical model for the acoustic properties of loose granular media. *App. Acoust.*, 64, 2003.

[4] Vu Viet Dung and coll. Prediction of effective properties and sound absorption of (...). *J. Acoust. Soc. Am.*, 145, 2019.

RECENT EXPERIENCE IN THE DESIGN OF MUSIC RECITAL HALLS

William J. Gastmeier *[1], and Mandy Chan †[1]
[1]HGC Engineering, Mississauga, Ontario, Canada.

1 Introduction

Recital Halls are essential teaching/performance spaces at educational facilities for the performing arts. They provide flexible space for the creative training of musicians, performers, technicians and theatre staff; they encourage the development of new musical compositions; and they function as concert venues for education and fundraising to support programmes.

HGC Engineering recently assisted the project team during design, construction and commissioning of the 145 Seat Armouries' Performance Hall at the University of Windsor and the 350 Seat McMaster Concert Hall at McMaster University. The architect in both cases was CS&P Architects Inc. in Toronto.

This article deals with acoustical design elements, primarily the acoustical treatment required to achieve optimum levels of reverberation. Extensive consideration was also given to sound isolation and the control background HVAC noise and those could be the subject of future article.

2 Reverberation Considerations

ANSI S12.60-2010 American National Standard, "Acoustical Performance Criteria, Design Requirements, and Guidelines for Schools" [1] provides guidelines for the design of teaching spaces. A recital hall is a teaching space and reverberation must be controlled to enhance speech intelligibility, music quality and sound system performance.

Reverberation is measured by the time it takes sound to die away in the space, using a quantity known as the reverberation time (RT500) measured in the mid-frequency (500 Hz) octave band.

A lack of early reflections and the excessive use of absorptive treatments result in low levels of reverberation (a 'dead' space).

Excessive levels of reverberation cause the space to sound noisy or boomy for some activities, limiting speech intelligibility and sound system functionality.

For concert halls, the reverberation requirements depend strongly on the music performance itself as can be seen in Table 1. HGC Engineering used and adapted reverberation criteria from several sources; Beranek L.L (2004) "Concert Halls and Opera Houses" [2] and Egan, D.M. (1988) "Architectural Acoustics" [3] to develop the design goal for theses spaces. Reverberation times approaching 2 seconds constrain the effective functioning of sound reinforcement systems and result in low levels of speech intelligibility.

In the subject halls the requirement was to place more emphasis on multiuse capability with less emphasis on symphonic repertoire. To reinforce this requirement L.R. Wilson planners suggested that the space be designed to as much as possible duplicate the acoustics of a successful multipurpose music venue, the Stockie Centre in Parry Sound. Measurements of reverberation were conducted there to serve as a benchmark and are reported below.

Table 1: Target Reverberation Criteria

Music Classification	RT500 (Seconds)
Traditional Organ Music or Choir Performance	2.5 to 5.0
Symphonic Repertoire	1.8 – 2.1
Chamber Music Including Secular and Religious Baroque	1.2 – 1.8
Modern/Popular/Band	1.1 – 1.7
Electronic or Amplified Music or Rock Concerts	0.8 to 1.2

3 Design Considerations

Both spaces were to be provided with upholstered theatre seating which is a sound absorbing element which functions to control the acoustics under varying degrees of occupancy. Both incorporated retractable theatre curtains to provide additional acoustical control for the varied uses. Based on all these considerations, a reverberation target approaching 1.5 seconds (500 Hz) was adopted so that the stage curtains could reduce it further towards 1 second when deployed. Another important consideration was the provision of diffusion to enhance a sense of spaciousness avoid defects such as echo and acoustic glare.

Our role in the design process was to direct the creative architectural designs to incorporate absorptive and diffusing elements in appropriate locations and amounts to achieve the goals. Diffusion was provided by multi-angled surfaces and surface textures as can be seen in the pictures in Figures 1 and 2.

Absorption was provided by placing acoustically absorptive treatments behind appropriate areas of perforated or slotted wood features and the ceiling.

Where possible surfaces were oriented to provide early reflections to the audience to enhance the sense of intimacy, enhance inter-musician audibility and clarity remembering that the angle of reflection equals the angle of incidence.

* bgastmeier@hgcengineering.com
† machan@hgcengineering.com

Figure 1: Armories Performance Hall, U of Windsor [4].

Figure 2: McMaster Concert Hall McMaster University [5].

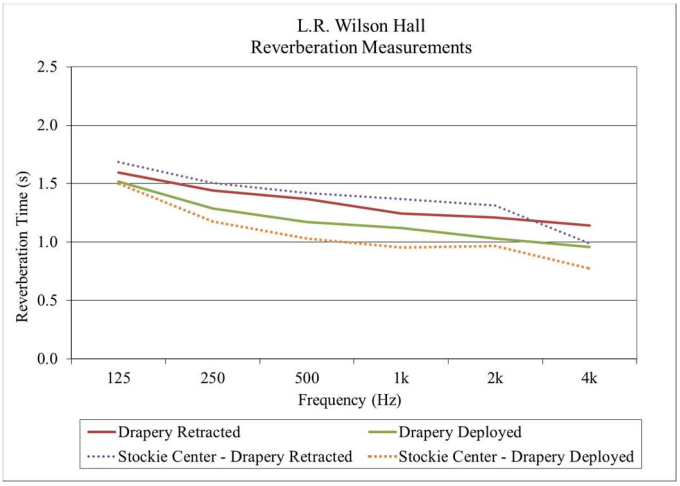

Figure 3: Reverberation Measurements

4 Conclusions

Measurements taken at the Stockie Centre during Design Development and at L.R. Wilson Hall during commissioning are reported in Figure 3 below. The results indicate that the design goals in terms of reverberation were largely met. audience and owner feedback from both the subject halls reports a satisfying experience.

References

[1] American National Standard, “Acoustical Performance Criteria, Design Requirements, and Guidelines for Schools”, ANSI/ASA S12.60-2010 (Revision of ANSI/ASA S12.60-2002)

[2] Beranek, L.L. (2004). Concert halls and opera houses. New York: Springer-Verlag.

[3] Egan, M.D. "Architectural Acoustics" J. Ross Publishing, Originally Published by McGraw Hill Book Co., 1988

[4] Photography by Shai Gill

[5] Photography by Tom Arban

EFFECT OF ACOUSTIC TREATMENT AND TABLE DIVIDERS ON DINERS' EXPERIENCE IN A MONTRÉAL RESTAURANT

Cynthia Tarlao [*1,2], Edda Bild [†1,2] et Catherine Guastavino [‡1,2]
[1]School of Information Studies, McGill University, Montréal, Québec, Canada
[2] Centre for Interdisciplinary Research in Music Media and Technology, Montreal, Québec, Canada

1 Introduction

Acoustic comfort in dining spaces has recently received increased attention (see [1] for a review). It is often characterized through acoustic measurements of the dining room and sometimes using self-reported measures of diners' experience and behavioural intentions. However, there are large variations in operationalization across studies. In addition, given that the main activities in restaurants are eating and communicating, diners' experience can be studied using an audiology framework with a focus on listening effort and vocal effort.

We bring together these different approaches to investigate the effect of acoustic treatment in an upscale restaurant located within ITHQ (Institut de Tourisme et d'Hôtellerie du Québec) in Montréal, Canada. A questionnaire was administered to a total of 225 diners before (N = 140) and after (N = 85) the installation of acoustic panels on the ceiling of the dining room. Participants were asked to rate their overall experience, the soundscape of the restaurant, as well as their vocal and listening effort. Additionally, as this work was conducted during the COVID-19 pandemic, we explored the effect of transparent dividers on tables.

2 Methods

2.1 Restaurant and conditions

The restaurant has high ceilings (4.80 m), large windowpanes, wooden walls and floor (reverberation time of 1.2 s pre-treatment). Wooden tables were covered with heavy tablecloths and chairs with thick leather cushions.

The study was conducted in two phases, during which questionnaires were distributed at the dinner service on weekdays and weekends: the phase before the installation of acoustic treatment in December 2020 (N = 140 over 9 evenings), hereafter referred to as the Before condition, the phase after the installation of acoustic treatment in April and May 2021 (N = 85 over 9 evenings), hereafter referred to as the After condition. The acoustic treatment consisted in Decoustics panels covering about 1/3 of the ceiling surface.

Additionally, in the context of the COVID-19 pandemic, transparent acrylic (i.e., Plexiglas®) dividers were installed on tables to separate and protect diners. Three types of configurations were used: no divider, flat divider for 2 people, and complex configurations for more than 2 people. Under the hypothesis that this would likely influence sound propagation and the ability of diners to communicate, dividers conditions were added (None, Flat, Complex). To control for background music, the same playlist was played at the same volume setting in both conditions.

2.2 Procedure

Due to COVID-19-related health restrictions, data collection was carried out by waiting staff of the restaurant, trained to distribute the questionnaires to diners. The staff approached diners after their meal, inviting them, in English or French, to fill in a short questionnaire about their restaurant experience. Due to health restrictions, the only diners allowed in the restaurant were employees and staff of the ITHQ. Participation was voluntary and diners were first asked if they had filled out the questionnaire before, and completed it only if they had not done so before.

The questionnaire was based on previous research done on restaurant soundscapes [1] and audiology. It included 26 5-point Likert scales grouped into 4 sections on 1) overall experience and satisfaction, 2) sound experience and soundscape evaluation, 3) vocal and listening effort, 4) person-related (e.g., demographics) and situational factors (e.g. number of diners at the table).

Tablets were used for data collection and respondents filled out their answers digitally. The survey took 5-10 minutes to complete. To track the duration of the dining experience and the consumption pattern, we relied on contextual information collected by the waiting staff, namely when diners seated, when they paid their bill, and the amount spent.

2.3 Analysis

The five-point Likert scales (from strongly disagree to strongly agree) were converted to numerical values (from 1 to 5, respectively, no missing data), and MANOVAs and follow-up ANOVAs were conducted to compare scale ratings between Before and After, as well as across the three types of dividers (using a .05 significance level).

3 Results

3.1 Effect of acoustic treatment

The installation of acoustic treatment had a significant effect on overall satisfaction, soundscape evaluations, and vocal and listening effort.

First, the MANOVA on overall ratings shows a significant effect of acoustic treatment ($F(3,221) = 3.06$, $p = 0.029$). The effect is positive with a significant increase in

[*]cynthia.tarlao@mail.mcgill.ca
[†]edda.bild@gmail.com
[‡] catherine.guastavino@mcgill.ca

satisfaction ($F(1,223) = 8.52$, $p = 0.004$), but no effect on conviviality ($F(1,223) = 1.35$, $p = 0.246$) or visual pleasantness ($F(1,223) = 0.37$, $p = 0.545$).

Second, the MANOVA on the general and musical sound experience (i.e. perceived overall level, music attention, perceived music level) shows no significant effect of acoustic treatment ($F(5,219) = 1.11$, $p = 0.36$).

Third, the MANOVA on soundscape evaluations shows a significant effect of acoustic treatment ($F(8,216) = 2.71$, $p = 0.007$). Specifically, acoustic treatment (see Figure 1) significant increases pleasantness ($F(1,223) = 9.28$, $p = 0.003$), eventfulness ($F(1,223) = 5.35$, $p = 0.022$), and vibrancy ($F(1,223) = 1.35$, $p = 0.015$).

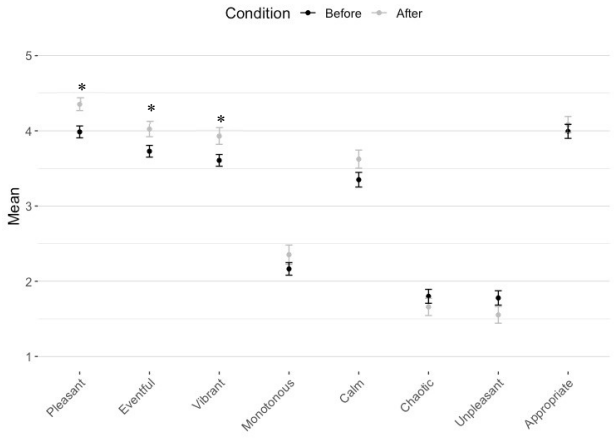

Figure 1: Mean and standard error for soundscape ratings before and after acoustic treatment. * for significant differences

Finally, the MANOVA on conversational effort shows a significant effect of acoustic treatment ($F(6,218) = 3.26$, $p = 0.004$). The effect (see Figure 2) is positive, reducing significant the difficulty to be heard ($F(1,223) = 11.21$, $p < 0.001$), the need to raise the voice ($F(1,223) = 16.87$, $p < 0.001$), the difficulty to understand ($F(1,223) = 13.25$, $p < 0.001$) and to hear ($F(1,223) = 14.54$, $p < 0.001$), but there is no effect on distraction, either from other people's conversations ($F(1,223) = 0.63$, $p = 0.428$) or the overall noise ($F(1,223) = 0.15$, $p = 0.695$).

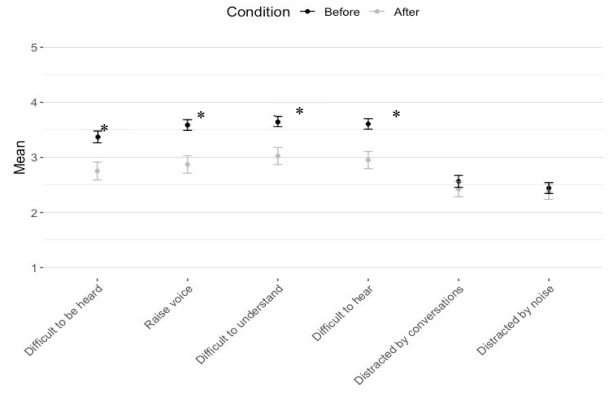

Figure 2: Mean and standard error for vocal and listening effort ratings before and after acoustic treatment. * for significant differences.

Effect of table dividers

The installation of table dividers had a significant effect on vocal and listening effort ($F(12,436) = 2.87$, $p < 0.001$), but not on overall ratings ($F(6,442) = 1.89$, $p = 0.080$), general and musical sound experience ($F(10,438) = 1.48$, $p = 0.144$), or soundscape evaluations ($F(16,432) = 0.91$, $p = 0.556$). Separate ANOVA on vocal and listening effort shows a significant negative effect of table dividers on difficulty to be heard ($F(2,222) = 9.75$, $p < 0.001$), raising voice ($F(2,222) = 9,13$, $p < 0.001$), difficulty to understand ($F(2,222) = 15.53$, $p < 0.001$), and difficulty to hear ($F(2,222) = 15.34$, $p < 0.001$), but not distraction, either from other people's conversations ($F(2,222) = 1.92$, $p = 0.149$) or the overall noise ($F(2,222) = 1.08$, $p = 0.343$).

4 Discussion

We observed significant effects of both interventions on vocal and listening effort, as well as a significant effect of acoustic treatment on satisfaction and soundscape judgments. Specifically, in the presence of acoustic treatment, participants were more satisfied and found the soundscape more pleasant, eventful, and vibrant. They found it easier to be heard, understand, and hear, and had to raise their voice less, all this, with no decrease in visual pleasantness. Additionally, the presence of table dividers resulted in increased vocal and listening effort.

However, due to COVID restrictions, only employees and students from ITHQ were allowed in the restaurant, which might affect the generalizability of the findings. Additionally, the groups in the divider conditions were highly unbalanced.

In the future, we will explore the effect of personal-related factors (e.g. demographics, noise sensitivity) [2], situational factors (weekdays vs. weekends, number of diners at the table) and the interaction between acoustic treatment and dividers.

5 Conclusion

By comparing diner's experience in a restaurant before and after acoustic treatment, our results highlight the benefits of acoustic treatment on diners' experience as well as the detrimental effect of table dividers. On methodological grounds, the proposed questionnaire could be used to assess acoustic interventions from the user perspective in a wide range of settings.

Acknowledgments

The authors would like to thank Cédric Camier, Sylvain Berger, Pauline Fernandez, and ITHQ. This work was supported by Saint-Gobain Recherche.

References

[1] C. Tarlao, P. Fernandez, I. Frissen, and C. Guastavino, Influence of sound level on diners' perceptions and behavior in a Montreal restaurant. Appl. Acous., 174:107772, 2021.

THE ACOUSTICAL CHALLENGES FOR MODULAR BUILDINGS USED FOR RESIDENTIAL PURPOSES

David Stepanavicius [*1] and Paul E. Marks [†1]
[1]BKL Consultants Ltd., Burnaby, British Columbia, Canada.

1 Background

As the need for affordable housing increases throughout Canada, modular buildings, which were traditionally used for temporary construction trailers or portable classrooms, have now been adopted as a solution for permanent housing in both remote and urban locations. Modular buildings offer a cost-effective alternate to "*stick-built*" construction, that enables a rapid mobilization due to off-site pre-fabrication, with a flexible and ease-of-use approach to the spaces that can be readily adapted to both residential or ancillary support uses.

However, while the typical interior modular assemblies are well rehearsed for non-residential uses, there are currently no directly comparable assemblies contained within the Building Code, and published formal acoustical performance data of such assemblies is scarce which can lead to some ambiguities in the expected acoustical performances.

2 Building Code

The latest iteration of the National Building Code[1] (the Code), not only relies on objective sound isolation standards for separating assemblies but, along with many other provincial Housing Design Guidelines and Construction Standards, places much greater emphasis on the control of flanking sound within multi-family occupancy buildings.

Within Article 9.11.1.4, the Code requires that the adjoining constructions (i.e., flanking wall, floor and ceiling assemblies) end or be interrupted at the junction of the separating element. It also presents compliance options for the construction of assemblies with flanking elements, which are typical of stick-built buildings. However, these compliance options do not necessarily reflect the design construction of modular building elements.

Since modular wall and floor-ceiling systems are fabricated off-site as single contained units, and then shipped and assembled on-site, maintaining structural integrity is a key design element. To maintain the structural integrity of modular buildings, the interior wall systems often include additional sheathing layers on the inner side(s) of separating stud walls, and the flooring systems often include continuous flooring layer(s) across the two rows of the separated party-wall studs. Breaks in the flanking constructions generally only occur at the perimeter edge of the individual modules.

Since the modular units, some of which may be partially open, are often stacked, the longitudinal walls are typically load-bearing (with end walls only providing stability), and, therefore, bracing is required for multiple storeys. This bracing can present s

ome conflict with the design intent of Article 9.11.1.4.

3 Acoustical Challenges

3.1 Initial Field Testing

In 2018, BKL Consultants Ltd were invited to perform in-situ sound transmission testing in a number of a standard modular constructed units being used for residential purposes. The field measurements were generally conducted in accordance with ASTM E336-17[2], except noting that the available room volumes were less than 40 m^3 but greater than 25 m^3.

It was found that in general floor assemblies were able to maintain Apparent Sound Transmission Class (or ASTC) ratings consistent with the Code requirements. However, for the wall assemblies, constructions that were broadly similar to assemblies with tested acoustical performance ratings, demonstrated a wider range of ASTC ratings. In some cases, ASTC ratings were as much as 10 points lower than the published Sound Transmission Class (or STC) ratings due to the flanking conditions, while in others greater consistency with published laboratory data was achieved.

3.2 Structural Bracing

The assemblies listed within the "Fire and Sound Resistance Tables" of the Code do not include systems with structural (and seismic) loading, crush plates, or bracing (as needed in modular assemblies). The absence of reliable and laboratory tested acoustical data for various modular constructions introduces challenges in demonstrating compliance with the Code Sound Transmission Class (STC) requirements.

The post-construction field measurements of modular units established that the sound isolation ratings for separating floors and walls were commensurate with somewhat similar double stud (or joist) row assemblies in low rise buildings, where OSB sheathing or bracing is not being used.

However, where longitudinal walls include "fully sheathed" layers for structural bracing (thus forming a 2 or, in some cases, 3 cavity assembly arrangement), the effects of the "*mass-air-mass resonance*" appeared to significantly reduce the expected sound isolation rating, with reductions of 5 to 10 ratings points being found.

The challenge of providing structural bracing, particularly for seismic purposes, while not compromising the acoustical properties has meant that working actively with the manufacturing teams is encouraged. In some cases, the use of intermittent bracing panels is acceptable in lieu of the fully sheathed systems, although some recent developments have included the greater use of "*stud-packs*", (i.e., laminations of

[*] stepanavicius@bkl.ca
[†] marks@bkl.ca

timber studs grouped together), 75 mm (3") O.C. nail spacing on fastening walls or overlapping headers as an alternate approach without any overly detrimental effects to the sound isolation properties.

3.3 Within Module Separating Walls

While scaling through repetitive module construction is economically beneficial, many designers want to explore the spatial options on the units to increase floor space or room uses. In some cases, this has meant that a wall assembly separating two dwelling units is contained within a single modular unit to offer greater occupancy options. However, these arrangements result in a conflict with the need to have discontinuous or interrupted junctions with the adjoining constructions.

The structural stability of the flanking wall, floor and ceiling elements rely on them remaining continuous across separating junctions. Now while this is a common occurrence with timber floors where structural subfloors are often continuous in stick-built constructions, then an additional layer (having a mass of no less than 8 kg/m^2 per Article 9.11.1.4) is laid over the subfloor. The off-site construction of each unit means that there is sometimes an unpredictable floor height at the module edge, meaning a mismatch at the junction of the additional floor layers.

Early field measurements of "in-unit" separating bedroom walls found that that sound isolation ratings were not able to consistently achieve ASTC 47 ratings even for enhanced wall assemblies due to the contribution from the flanking sound paths. To some extent the smaller room volumes (i.e., $\leq$ 40 m^3) associated with the module sizing did appear to influence the measured noise reductions at the 125 Hz and 160 Hz one-third octave centre band frequencies.

However, greater success in achieving ASTC ratings of at least 47 were achieved with ad-hoc treatments, such as additional floor layers over elastomeric or foam interlayers, additional or "checker-boarding" gypsum board layers to flanking walls and ceiling boards on resilient bars to minimize the effects of flanking sound transmission between the units. Nevertheless, these are relatively labor intensive and costly fixes at the assembly stage, which off-set some of the cost benefits of modular construction.

3.4 Service Penetrations

Through experience, the acoustic treatment of building service penetrations and riser shafts within modular buildings has been generally poor. Common services, such as piping or waste water lines, kitchen or bathroom exhaust ducts and Packaged Terminal Air Conditioners (PTAC) gas lines have historically been located within overly large dimensioned shafts that can accommodate a wide variety of services. It is often overlooked that all riser shafts separating dwellings from other parts of the same building require a minimum STC 50 rating, with adjoining constructions that conform to the control of flanking sound.

In one instance, a common open building services shaft was found to be located within a utility cupboard in the stacked kitchen-dining rooms of a residential building, meaning each the neighboring families could hear even normal dinner table speech from each unit. In fact, it was possible to conduct 2-way conversations from the utility cupboard to neighbours some floors away.

The acoustical detailing requirements of riser shafts and common penetrations through separating assemblies is the responsibility of the assembly team, but checking and enhancing the acoustical detailing during the early design is critical to achieving the necessary airborne sound isolation. While space constraints inhibit airborne sound testing of services shafts, typically, the best practice for reducing flanking sound transmission can include enclosing the riser shafts with materials having a mass per unit area of at least 15 kg/m^2 lining the shaft with unfaced mineral fibre and packing openings.

4 Conclusion

The design of established modular constructed buildings has been found to require architectural enhancements in order to demonstrate consistency with the requirements of the Code. The need for structural stability both within individual modules and stacked modules creates flanking sound transmission paths that, unless adequately treated, provides conflict with both the need for discontinuous junctions at the perimeter of separating elements and the objective field-tested sound isolation ratings set out in the Code.

Project experience has found that measures to mitigate the effects of flanking sound transmission will need to be commensurate with the design intent of the Code and, moreover, be included at an early stage of the module design in collaboration with the structural team of the manufacturers.

The use of additional materials or layers, along with upgraded or amended assemblies can be targeted to optimize the sound isolation qualities of the separating assemblies, and has been found to achieve ratings consistent with those required by the Building Code in Canada when tested in the field.

References

[1] Canadian Commission on Building and Fire Codes National Research Council of Canada. National Building Code of Canada Volume 2, 2020.

[2] ASTM International. Designation: E-336-17 Standard Test Method for Measurement of Airborne Sound Attenuation between Rooms in Buildings, 2017.

AIRBORNE SOUND TRANSMISSION IN CROSS-LAMINATED TIMBER BUILDINGS: THE INFLUENCE OF BUILDING HEIGHT

Erik Nilsson *[1], Sylvain Ménard †[1] and Delphine Bard ‡[2]
[1] Department of Applied Sciences, University of Québec at Chicoutimi, Chicoutimi, Québec, Canada
[2] Department of Physics and Astronomy, Katholieke Universiteit Leuven, Belgium

1 Introduction

Buildings with cross-laminated timber (CLT) has gained growing popularity in several countries. In addition, buildings constructed with CLT are increasing in building height, which increases the load on the junctions and structural building elements lower down in the buildings. These increasing loads could have an impact on the elasticity of junctions and thus affect the sound transmission between apartments on different stories as suggested by Ref. [1]. Moreover, Ref. [2] focused on airborne sound transmission measurements in a lightweight wooden frame building and found that the sound insulation was better higher up in the building. However, it was suggested that the results were due to a mismatch between load and elastic strip stiffness, rather than the load itself. Ref. [3] measured in a real CLT building and found that the vibration reduction index reduces with increased load for the path wall to wall. The authors of Ref. [1] investigated vibrations induced by a tapping machine in a multi-family wooden frame building and concluded that junctions attenuated vibrations better higher up in the building.

Previous studies, mentioned above, have investigated how the number of stories, or the load, affects the sound insulation or the vibration reduction index between apartments or different building elements. However, the actual difference in airborne sound insulation with increasing load is not thoroughly investigated in previous research. The purpose of this paper is to show the effect of the building height, and thereby the load, on the vertical airborne sound insulation between apartments on different stories in different CLT buildings which is a summary of Ref. [4].

2 Method

2.1 Project description

Airborne sound insulation measurements took place in three different projects at different locations in Sweden before people had moved in which are described as projects A, B, and C. The same floor plan is used over the different stories per building in the evaluations. Moreover, vertical measurements were conducted and compared between the same type of rooms over the different stories to minimize the number of affecting parameters. To sum up, the surface dividing area, the volume and the construction elements were the same and the rooms had no furniture in them. Thus, the main parameter that is different between measurements over different stories is the load on the junctions and the stiffness of the resilient interlayers dependent on the load.

Measurements in project A took place in two separate buildings, building 1 with twelve stories, and building 2 with ten stories. The building system in project A is built up with CLT, a suspended gypsum ceiling, concrete above an impact sound insulation board and 6 mm resilient interlayers in the junctions in building 2 but none in building 1. The difference in number of stories was in project A: six in building 1 and five in building 2. Project B consist of 6 stories and measurements were conducted between stories 2–3 and 4–5. The building system in project B is built up with CLT, a suspended gypsum ceiling, a raised resilient floor and 25 mm resilient interlayers in the junctions. Project C is constructed with eight stories and measurements were conducted between stories 3–4 and 7–8. The building system in project C is built up with volume modules of CLT, with a raised resilient floor and resilient interlayers between the volume modules.

2.2 Evaluation description

Evaluation of the measurements are done separately for each building by subtracting the differences in vertical airborne sound insulation between low and high stories accordingly: $D_{nT,high} - D_{nT,low}$. Identical floor plans are used where measurements took place in each building. Thus, the only main difference in the evaluation is the load on the junction. Moreover, for Project A – Building 2, Project B and Project C, the stiffness of the resilient interlayers is different depending on the load on the junctions.

3 Results

Over the three different projects, with in total four buildings, 58 vertical airborne sound insulation measurements were conducted. Each project consisted of varying junctions, different dividing elements and a varying total number of stories. The result from the projects and buildings are displayed in Fig. 1 were the mean values over the frequency range for each project is compared and evaluated. Measurement data show that there is an overall positive difference in vertical airborne sound insulation between high and low stories. This result indicate that the vertical airborne sound insulation decreases lower down in the building with increasing load on the junctions. However, the results are spread with several decibels over the frequency range, and there is no clear correlation between the reduction in sound insulation and the different buildings.

* erik.nilsson@uqac.ca
† sylvain_menard@uqac.ca
‡ delphine.bardhagberg@kuleuven.be

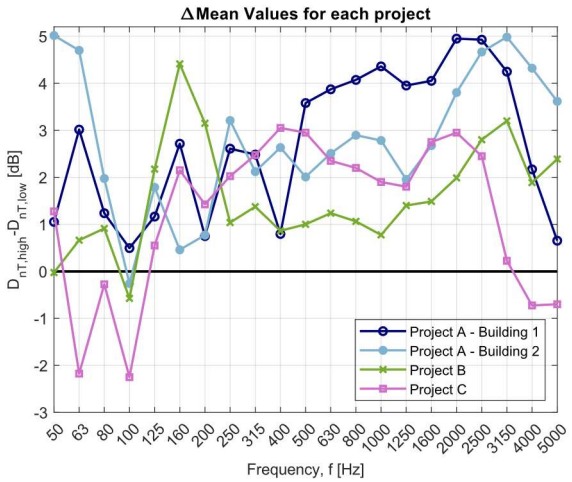

Figure 1: Mean values of the difference in vertical airborne sound insulation between high and low stories for each building and project.

4 Discussion

The number of stories in each project differs where measurements took place, from two to six stories depending on the project and the building. The result in Fig. 1 is therefore divided with the difference in the number of stories for each measurement in each building and the result is presented in Fig. 2. This approach results in a good agreement between the difference in vertical airborne sound insulation per story for each building for frequencies between 250 and 2000 Hz with a linear correlation. The improvement in sound insulation higher up in the building is vaguely apparent in low frequencies which is likely caused by the effect of the direct sound transmission. Yet, the improvement is clearly apparent in mid-frequencies, which is typically around the critical frequency region of CLT panels. Above 2000 Hz, the mean values are spread and reduced which is likely due to the background noise. The black dashed line is a mean value curve for the data in Fig. 2. However, the mean value curve is modified to not include values between 125 and 200 Hz from project B since it is suggested in Ref. [4] that it is related to the specific design system of the project.

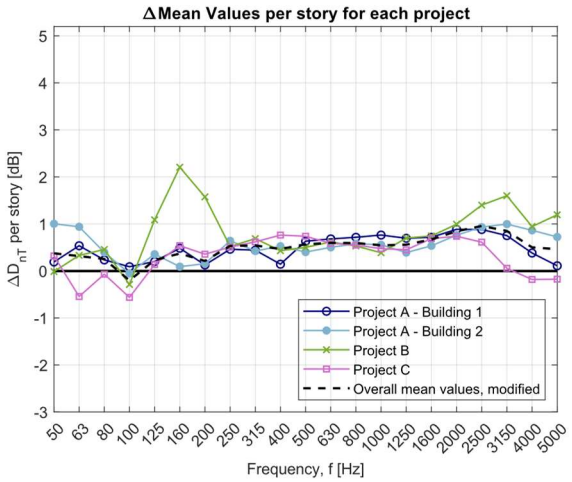

Figure 2: Mean values of the difference in vertical airborne sound insulation between high and low stories, per story, for each building and project with a mean value curve modified between 125 and 200 Hz.

This measurement data indicates that the stiffness of the resilient interlayers has less effect on the difference in vertical airborne sound transmission between stories at high and low levels in buildings. The result also shows that the primary dependent factor for the difference is the load, with or without resilient interlayers, in cross-laminated timber junctions.

The difference in the result is related to the difference in load on the junctions and the flanking sound transmission. If flanking paths are suppressed to greater extent in a building, the same result is not expected to be visible. Moreover, flanking sound transmission is typically more dependent in wooden buildings compared to concrete buildings. Consequently, the same result presented here cannot be expected in a concrete building, and specifically in a building with low-flanking sound transmission. To evaluate the result further, vibration reduction index measurements are required.

5 Conclusion

Measurements from several projects with various building systems suggests that increasing load on junctions results in a worse vertical airborne sound insulation (lower down in the buildings). Measurements also indicate that the effect is similar regardless of the presence of resilient interlayers in the junctions. With or without resilient interlayers, increasing load results in a higher sound transmission between apartments and, therefore, lower sound insulation.

The result further suggest that the vertical airborne sound insulation have a mean difference per story over the measured frequency range of 0.5 dB. Although 0.5 dB is a low number, a 6-story difference in a CLT building is expected to have a mean difference of 3 dB and the effect is expected to increase further with more stories. Therefore, with increasing building height in high-rise CLT buildings, the load on the junction should be considered and specifically at lower levels to choose the right treatments and to ensure good sound insulation performance.

References

[1] D. Bard, P. Davidsson, P.-A. Wernberg, Sound and Vibrations Investigations in a Multi-Family Wooden Frame Building, International Congress on Acoustics, Sydney, Australia, 2010. August 23-27.

[2] R. Öqvist, F. Ljunggren, A. Ågren, Variations in sound insulation in nominally identical prefabricated lightweight timber constructions, Building Acoustic 17 (2) (2010) 91–103, https://doi.org/10.1260/1351-010x.17.2.91.

[3] J. Hörnmark, Acoustic Performance of Junctions in Cross Laminated Timber Constructions, Department of Architecture and Civil Engineering, Chalmers University of Technology, Gothenburg, Sweden, 2019.

[4] E. Nilsson, S. Ménard, D. Bard, K. Hagberg, Effects of building height on the sound transmission in cross-laminated timber buildings – Airborne sound insulation, Building and Environment 229 (2023), https://doi.org/10.1016/j.buildenv.2023.109985.

AIIC Testing of Various Roof Terrace Assemblies and Evaluating the Need for Additional Mitigation

Jessica Tsang [*1]
Valcoustics Canada Ltd., Richmond Hill, Ontario, Canada.

1 Introduction

Common amenity and private rooftop terraces, overtop of other residential spaces, are common in mid and high-rise multi-family buildings. As these multi-family residences continue to be constructed, it is becoming more apparent that noise from footfalls and other objects impacting the structure can cause significant annoyance. The Ontario Building Code (OBC) has no requirements with respect to impact sound isolation, and there is limited laboratory or field test data available for the Impact Insulation Class (IIC) ratings for rooftop terrace assemblies.

This paper presents the results of the Apparent Impact Insulation Class (AIIC) field tests done on various rooftop assemblies in concrete multi-family buildings. This research aims to contribute field test data to the existing body of knowledge on typical roof terrace assemblies and help determine if or when additional mitigation is beneficial. The test results provide an indication of the acoustical performance of typical terrace assemblies that are used. The findings point to the benefit of exploring and conducting further testing of other assemblies with different floor finishes, supports, and underlayments.

2 Background

2.1 Impact Sound Isolation – Floor Systems

Structure-borne noise generated from activities such as footfalls or dragging furniture across a floor can be a significant cause of noise complaints. IIC ratings indicate a floor boundary's resistance to structure-borne noise transfer. The higher the IIC rating, the better the floor boundary will be at insulating impact noise.

The main components that make up a rooftop terrace are the floor finish and supports/underlayment. In concrete multi-family buildings, the floor finish is typically modular concrete pavers.

2.2 Building Code Requirements

The Ontario Building Code (OBC) has no requirements with respect to impact sound isolation. Appendix A, Volume 2 of the OBC does provide some information about impact noise: "Footstep and other impacts can cause severe annoyance in multi-family residences" [1]. However, Appendix A of the OBC is for information only, and is not part of the OBC requirements.

3 Method

Field tests to determine AIIC ratings were completed on two different roof terrace assemblies in concrete multi-family buildings. The test procedure involved the generation of floor impact noise using a standardized tapping source, adhering to the specifications of ASTM E1007-21. Sound levels were measured in the receiver space below the tapping machine using a calibrated sound level meter. The microphone was moved through each receiver space using a "slow sweep" technique to obtain the space-time sound energy average.

The roof terrace assemblies selected for testing were typical configurations used in concrete multi-family buildings. The different configurations that were tested were constructed on two different sites. In both tests, the assemblies were constructed on top of 200 mm thick cast-in-place concrete slabs.

The construction for the roof terrace assembly for Assembly A is:

- 50 mm thick 600 mm x 600 mm concrete pavers
- 50 mm thick extruded polystyrene rigid insulation paver supports (2 layers of 25 mm thick pieces)
- 50 mm thick extruded polystyrene rigid insulation (2 layers of 25 mm thick sheets)
- Roof membrane

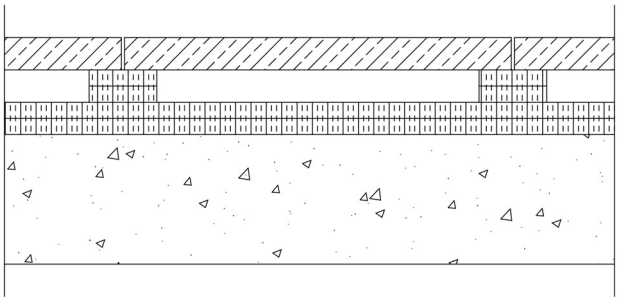

Figure 1: Roof terrace for Assembly A

The construction for Assembly B is:

- 50 mm thick 600 mm x 600 mm concrete pavers
- 100 mm thick bedding (gravel) substrate
- 100 mm thick extruded polystyrene rigid insulation
- Roof membrane

4 Results

Assembly A achieved a rating of AIIC 76, and Assembly B achieved a rating of AIIC 74. The normalized impact sound pressure level and AIIC curves for Assembly A and B are shown as Figures 3 and 4, respectively.

[*] jtsang@valcoustics.com

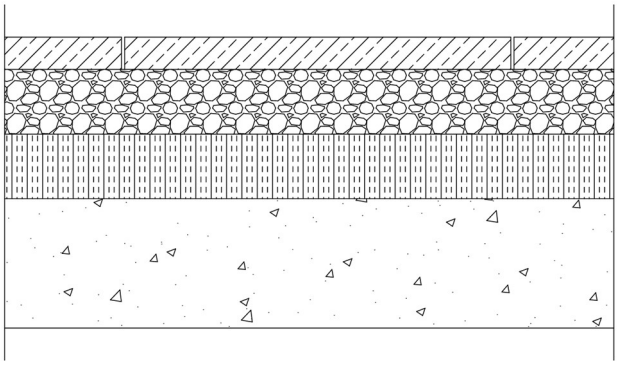

Figure 2: Roof terrace for Assembly B

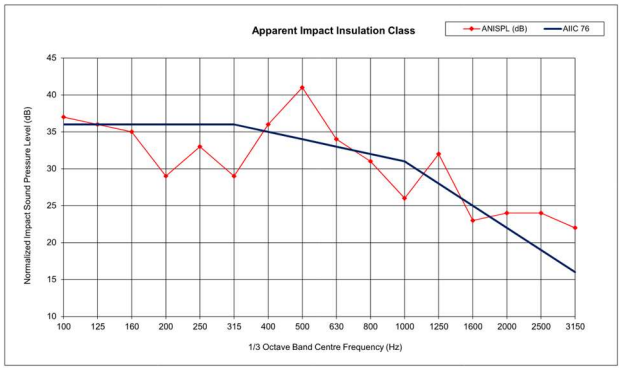

Figure 3: Measured impact sound pressure level for Assembly A

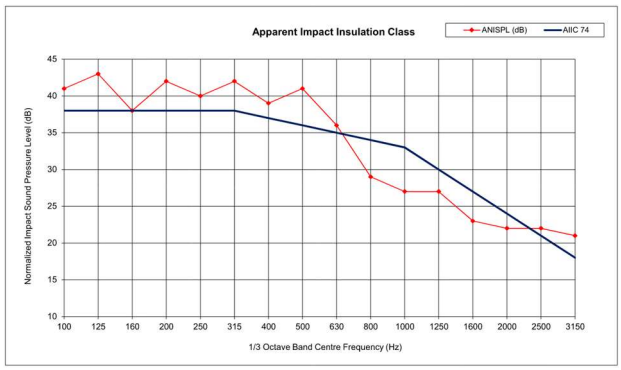

Figure 4: Measured impact sound pressure level for Assembly B

Subjectively, the tapping machine was observed to have a faint tapping noise that was barely audible in both receiver spaces below.

5 Discussion

Figure 3 shows that the overall AIIC rating of Assembly A is limited by the "8 dB" rule at the 500 Hz octave band, whereas in Figure 4 the overall AIIC rating of Assembly B is limited by the "sum of 32 dB" rule at the low and mid frequency bands (particularly between 100 to 630 Hz).

Field AIIC testing has a number of limitations, including the quality of construction and the differences between the buildings and receiver spaces. Variability between the material size, air space depth, and uniformity of substrate thickness, may also affect the performance of these as-built assemblies.

Due to the limited available opportunities to test these outdoor terrace assemblies, the conditions of the tests did not fully conform to the test standard due to the receiver room volumes being less than 40 m^3. This limitation should be considered when interpreting the results.

Based on the test results, typical roof terrace assemblies that include concrete pavers and extruded polystyrene rigid insulation appear to provide adequate impact sound isolation. However, this only applies to concrete structures, whereas the results would be different with wood structures which have a propensity to exacerbate low frequency sound.

Therefore, in general, additional mitigation measures to improve the impact sound isolation performance of these assemblies may not be necessary but may still be needed in cases where higher isolation is desirable.

The building industry would benefit if further research was conducted for these types of assemblies, and by exploring the use of different types of floor finishes and supports. It would be beneficial to examine if and/or how the performance of typical assemblies can be improved with the use of different underlayments between the floor finish and supports, and between the supports and the building structure.

Laboratory test data can establish the IIC ratings of typical assemblies that are used in these types of buildings, and examine how the variability of air space, and material size and depth can influence the IIC performance.

6 Conclusion

The AIIC test results presented in this paper indicate that typical roof terrace assemblies that include concrete pavers and extruded polystyrene rigid insulation in the assembly are sufficient in providing adequate impact sound isolation. Further independent laboratory and field testing should be explored to confirm how variables within these assemblies influence the acoustical performance of these assemblies. Further research of the impact sound isolation of different types of floor finishes, supports, and underlayments should also be explored.

References

[1] *Appendix A,* 2012 Building Code Compendium Volume 2, 2022.

Abstracts for Presentations without Proceedings Paper
Résumés des communications sans article

Acoustic Design Of Floor Ceiling Assemblies In High Seismic Zones

Aedan Callaghan, William Thrall

In the updated 2020 National Building Code of Canada (NBC), one notable change was the increase in seismic design requirements across many geographic areas. Previous work by Popvski et al. investigated the benefits associated with light wood frame and engineered wood structures for their reduction of seismic inertial forces. However, the shift to lighter weight structures presents a challenge for applying traditional concrete toppings to these wood structures. The added cost and bracing requirements of these concrete toppings often make them impractical or impossible, in high seismic zones. The utilization of concrete toppings has long been the standard approach to add mass and help improve the low frequency performance of wood frame structures. For this reason, alternative floor ceiling assemblies, without the reliance on the mass of these toppings are necessary. This paper investigates acoustic solutions for wood structures that do not utilize concrete toppings. It examines a number of strategies to maintain the airborne and structure-borne sound isolation without concrete toppings, while using isolated ceilings and decoupled dry floor linings and reviews specific floor ceiling assemblies implemented on projects in high seismic zones.

Acoustique D'un Établissement Hospitalier – L'agrandissement Du Centre Hospitalier De L'université De Montréal (Chum)

Vincent Chavand

Le présent article décrit le processus de gestion de la problématique acoustique du projet d'agrandissement du centre hospitalier de l'Université de Montréal (CHUM) de la phase de conception jusqu'à la phase de vérification des travaux. On retrouve sur ce projet plusieurs des grands thèmes de l'acoustique architecturale : le traitement de l'enveloppe du bâtiment, les cloisonnements intérieurs, le contrôle de la réverbération et la qualité d'écoute, ainsi que la maîtrise du bruit de ventilation, le tout pour une grande diversité de situations particulières aux établissements de soin. Cet article passe dans un premier temps en revue les critères acoustiques retenus pour le projet et décrit les enjeux associés. Ensuite, les divers choix techniques de traitement de l'acoustique sont discutés selon les situations rencontrées, du point de vue des contraintes liées au milieu médical, de la sensibilité des espaces concernés et des approches méthodologiques retenues. Sans s'y limiter, les enjeux discutés incluent les assemblages plancher-plafond et les séparatifs entre espaces sensibles, le traitement des façades et des réseaux de ventilation ainsi que le choix des finis. L'article s'intéresse également au cas particulier de l'amphithéâtre, qui se trouve directement sous une importante salle mécanique, créant une sensibilité acoustique toute particulière au-delà du travail sur les finitions. Enfin, le programme de vérification de la performance acoustique du projet est présenté en termes de méthodologie et de résultats par rapport aux cibles applicables. Notamment, l'application des normes de mesure de l'affaiblissement acoustiques dans les grands volumes est décrite ainsi que les enjeux rencontrés.

Novel Method For Reverberation Time Measurements In Natatoriums

Adam Collins

Nataorium's pose unique challenges for reverberation time measurements due to the presence of water and elevated background noise. A novel method utilizing a bicycle tire burst was investigated as a substitution for the interrupted source method in this environment. Preliminary results indicate the bicycle tire burst may offer an alternative to established methods and warrants further investigation.

Acoustic Properties Of High-Rise Wood Residential Buildings

Raphaël Duée, Hugo Vasseur

High-rise wood buildings are becoming more and more popular. These buildings, much more ecological than conventional concrete or steel buildings, also have many other advantages such as their aesthetics or their short construction time. However, it is necessary to pay particular attention to acoustics because a wooden structure is much more subject to vibration transmission and less effective for sound attenuation. Considering the variety of high-rise wood construction types, each of them has their own acoustic challenges and induces specific solutions. This paper highlights the various problems present in a residential high-rise building with a wood structure associated with the structure type. Thus, measures can be taken to create a harmonious assembly responding to

acoustic, thermal, structural, etc. problems. A bibliographic study was conducted at first to list the emblematic projects and different solutions associated in past studies all over the world. The paper then highlights the various problems present in a high-rise residential building with a wood structure and Canada available solutions in regard with typical acoustic isolation performance thresholds. The final objective is to create an acoustic guidebook to help residential building developers and professionals designing their wood residential structures.

Amplifying Change For Music Venues In Montreal: Rethinking The Technical Regulatory Framework Towards Harmonious And Sustainable Nightlife

Romain Dumoulin

Montreal has emerged as a prominent nightlife destination in Canada, largely due to its vibrant bars, nightclubs, and venues. Over the past twenty-five years, a large-scale transformation of previously quiet taverns or restaurants into nightclubs or music venues has contributed to the high urban density and mixed-use development that characterizes Montreal's central neighborhoods. Consequently, there has been a rise in noise complaints from residents. In the past decade, numerous live music establishments in the city center have faced the threat of closure due to mounting noise complaints and associated fines. Notable venues like Le Divan Orange in Plateau-Mont-Royal eventually succumbed to financial instability and closed in 2018, while more recently, the La Tulipe venue finds itself entangled in noise complaint disputes that have escalated to legal proceedings at both the municipal and provincial court levels. In 2022, the City of Montreal launched a $1.4 million subsidy program to help small alternative music venues improve their sound/noise management and reduce their impact on their neighbors. Soft dB was mandated to define the acoustical/technical requirements and conditions for this program. This paper presents Montreal's existing regulatory framework and the current shortcomings in regulation enforcement and application that have led to a problematic and unsustainable status quo. Furthermore, it provides an overview of the subsidy program's technical specifications and highlights the lessons learned and best practices identified from Soft dB's acoustic studies conducted for five venues participating in the program. Lastly, the paper explores the feasibility of implementing the Agent of Change principle, discussing short-, medium-, and long-term solutions to effectively address the issue.

Contextualizing Speech Privacy Criteria In Well/leed Guidelines

Dorsa Fardaei

Speech privacy is an integral aspect of acoustic design which is consistently highlighted by users of offices, institutional buildings, and healthcare facilities. WELL and LEED guidelines are accessible resources in quantifying speech privacy and as such, often form the basis for user requirements or project agreements for these sectors. However, the absence of contextual information within these guidelines can result in a misguided approach in the design for speech privacy. The applicability and feasibility of speech privacy criteria presented in these guidelines is often overlooked among those with limited background in acoustics. This presentation is intended to bridge the gap between sustainability guidelines and practical design for speech privacy, while critically evaluating the suitability of the speech privacy metrics presented in these guidelines. First, the universality of speech privacy criteria presented in these guidelines will be explored. Furthermore, the feasibility of achieving these speech privacy criteria will be discussed using sample field measurements of partition assemblies and room front systems typically used in offices. Finally, the reliability of the speech privacy metric used in these guidelines will be critically examined to consider its effectiveness in guiding design decisions for speech privacy in office buildings.

Physical And Perceptual Comparison Between Single And Multiple Diffraction For Thick Edge

Clément Girin, Alain Berry, Philippe-Aubert Gauthier, Louis-Xavier Buffoni

Diffraction is an important acoustic propagation phenomenon for accurate sound environment modeling. In auralization software, diffraction is often ignored or modeled using statistical approximations. Yet diffraction is essential, particularly in interactive applications, as it enables us to hear what we cannot see directly. In addition, the development of real-time acoustic modeling software raises the question of the compromise between physical fidelity, perceptual realism and real-time computation. Approaches must be developed to achieve this compromise by optimizing the modeling of propagation phenomena, diffraction being one example. A cost-efficient method is to consider a diffracting object as a single edge and to use the Uniform Theory of Diffraction. This method is based on geometrical acoustics and is for an infinite simple edge. However, in many cases, the obstacle is not a single knife edge, but an edge of finite thickness: a double diffraction is formed. For such scenarios, the multiple diffraction method for obstacles of finite thickness can be used. The case study, in this paper, is a double edge

with variable thickness. This study focuses on comparing different diffraction modeling methods to determine the threshold thickness, at which the single diffraction method should be replaced by multiple diffraction methods for more perceptually accurate predictions. To achieve this, objective comparisons are used to quantify the differences between these two modeling methods. Subsequently, perceptual tests are conducted to understand if a perceptual difference exists between these approaches, and then determine a threshold thickness from which it is necessary to switch modeling methods.

Characterization And Sustainable Acoustic Correction Of The Mosque. Case Study Of Two Mosques In Constantine, Algeria.

Zohra Bemaghsoula Hammou

Nowadays, faced with the global issue of climate change, sustainable construction seeks to provide solutions focused on sustainable construction processes and ecological materials. Thus, the use of bio-based materials helps address energy efficiency challenges for buildings that meet all levels of thermal, acoustic, and lighting comfort. In this regard, sustainable design of acoustic environments refers to the sustainable approach in creating architectural environments that integrate effective acoustic solutions, including the selection of sustainable materials. The use of bio-based materials enables the pursuit of sustainable acoustics, both for sound insulation and room acoustics. Despite the growing interest in the study of soundscapes and the significant role that mosques play in our societies, research on the acoustic quality of mosques is very limited. The few studies conducted on this subject have concluded that the architectural aspects of mosques are inadequacy for their function as listening spaces. With this in mind, this study aims to make a meaningful contribution to this research field by characterizing and implementing sustainable acoustic corrections in mosques using bio-based materials. This research employs an experimental approach using numerical simulation to characterize the acoustic comfort of two mosques with different volumes and propose sustainable acoustic corrections using bio-based materials in the form of straw panels. The evaluation was carried out by calculating two objective criteria: Sabine's reverberation time and the C50 clarity criterion. The acoustic simulation will be performed using the EASE4.4 software, distributed by AFMG and owned by Constantine 3 University. The acoustic simulation allowed us to establish a detailed acoustic diagnosis of the two mosques. The obtained results reveal a highly reverberant space. Based on these results, we installed straw acoustic wall panels on the back wall and the dome. In conclusion, the results obtained after the corrections yielded satisfactory outcomes for both mosques. In the case of the smaller mosque, we achieved listening comfort without relying on electroacoustic assistance, which will lead to energy savings and reduced expenses. bio-based materials sustainable acoustics; numerical simulation.

Case Study: Variation In Astc Ratings With Loudspeaker Position When Using Directional Loudspeakers

Anil Joshi

Field experience indicates that there can be significant variation in measured Apparent Sound Transmission Class (ASTC) ratings when re-testing assemblies in-situ. ASTM standard E336 notes that, when using directional loudspeakers as the sound source, variability in ASTC results can be reduced by using multiple loudspeaker positions. This presentation will examine the variability of ASTC ratings with speaker position through several case studies where ASTC was measured using directional loudspeakers and multiple speaker locations.

Evaluating Ambient Noise And Reverberation In Classrooms: A Case Study Of A Native School

Daniel Paromov, Victoria Duda, Julie Mcintyre, Phaedra Royle, Adriana Lacerda

This study aimed to analyze the ambient noise levels in nine classrooms of a Native School, using a collaborative approach with the community and the School of Speech Therapy and Audiology at the University of Montreal. The acoustic environments were measured given their potential to impact students' speech comprehension and academic performance. The measurements were taken using an integrating sound level meter and the ClapReverb app. Results show that the noise levels ranged from 37.6 to 50.2 dBA and the reverberation time ranged from 0.73 to 1.27 seconds across the classrooms, exceeding the ANSI/ASA S12.60.2010 standard (35 dBA, and 0.6 s for reverberation for rooms less than 10,000 ft3) for all of the classrooms. These findings point to a clear need for interventions to reduce noise and improve acoustic conditions. Indeed, despite its relatively new construction, the school significantly deviates from established acoustic norms with its high noise levels and reverberation times. This reveals a critical oversight in prioritizing acoustics during the design and construction process, which may negatively affect the learning environment. It also underscores the necessity of integrating acoustical considerations

early in the design of educational facilities to ensure optimal learning conditions.

Speech Level Variations By Office Type And Work Environments

Rewan Toubar, Roderick Mackenzie, Joonhee Lee

Standardized speech levels and spectra presented in ASTM or ISO standards allow for the prediction of speech privacy or intelligibility. Mostly, these data were obtained in anechoic chambers, with participants who were guided to speak in scripted scenarios. However, previous research has shown that the speech levels and spectra change significantly depending on parameters such as room size, absorption, and distance between talker and listener. This paper aims to identify the speech levels used by over 70 workers in different office room types and workstation types. The paper also looks at differences in speech levels used between in-person and video-conferencing communication, as well as the language of communication. The participant's speech spectra and levels were obtained with different office environment and types of speech contexts (in-person/online meetings) in real offices in Quebec, Canada. The obtained data can be used to better inform the standardized speech levels used in ASTM and ISO standards for different office locations. This research offers new insights into the speech patterns of office workers in diverse work environments and highlights the influence of communication medium and language on speech levels.

Comparison Of Predicted And Measured Astc In A Mass Timber Structure

Sarah Mackel

While mass timber construction has become an important part of reducing the carbon footprint of the built environment, it continues to present challenges in meeting the sound isolation required by NBC 2015 when used in multi-family residential construction. While there is often a desire to keep the timber structure exposed within the units, there is limited data available which describes the effect of structure-borne sound flanking through this condition. This presentation will give an overview of measurements taken in a two-storey mock up of a modular mass timber building system. Most timber in the mock-up structure was encapsulated, with the exception of the timber beams and the interior face of the mass timber façade panels. Measurements were taken of the structure-borne sound flanking path through the exposed timber façade panels (Kij) as well as the ASTC between floors. A comparison will be made between the measured ASTC (ASTM E336) and the ASTC predicted using the measured Kij values and the ISO 12354 method.

Quantifying The Reduction In Sound Insulation And Speech Privacy In Offices Due To Typical Design And Workmanship Errors

Roderick Kt Mackenzie

This paper presents an updated series of case studies demonstrating the expected sound insulation and speech privacy performance reductions attributable to individual and combined weaknesses that result from design and/or workmanship errors. Over 20 separate studies of ASTC, NIC and SPC measurements in a variety of offices are used to examine the effect of common acoustical airborne leakages or flanking through connected elements. Weaknesses, ranked in order of the severity of impact on performance found in these case studies, include: lack of or ineffective door seals, continuous heating elements, ventilation duct crosstalk, door closure pressure against seals, open ceiling plenums, lack of acoustical sealant on modular and GWB partitions, façade mullions and transoms, interior windows and their frames, lack of raised door threshold, continuous metal door frames, uninterrupted gypsum on side walls, and thin continuous floor toppings

Adding Layers Of Gypsum Board Inside The Cavity Of Double Stud Walls. A Sound Idea?

Jeffrey Mahn, Sabrina Skoda, Markus Müller-Trapet, Iara Cunha

New high rise residential buildings are popular in hot real estate markets in Canada and most of these are being constructed with lightweight party walls. A party wall that is frequently being specified in the Toronto market is a double steel stud walls with one or more sheets of gypsum board installed in the cavity between the rows of studs. While locating the gypsum board inside the cavity between the rows of studs may not affect the fire rating nor the STC rating of the wall, locating the gypsum board in the wall cavity can sharply decrease the transmission loss on the order of 13 dB or more below the 200 Hz one-third octave band. The transmission loss of typical double steel stud walls which are being specified in Toronto will be presented as well as testing data to counter many of the arguments being made for locating the gypsum board between the rows of studs of double stud walls.

Publication Of A New Guide From The Gouvernement Du Québec About Noise Protection Of Dwellings

Jean-Philippe Migneron, Jean-Gabriel Migneron, André Potvin

After a few years of collaboration between the provincial authorities and the research team at Laval University's School of Architecture, the new guide titled "Insonorisation de l'habitation pour la protection contre les bruits extérieurs – guide des bonnes pratiques" is finally available online since April 2023. The project was initiated by the concerned ministries after the adoption of the Health Prevention policy by the provincial government of Québec, first to review the literature on noise protection strategies for residential development, and then to suggest existing ideas to architects, urban planners, builders, or owners. This presentation aims to share some examples of solutions and technical information that can be found in the new document. Comments will also be added on the value of educating all stakeholders on appropriate soundproofing of residential facades and roofing as a community health prevention action plan suitable for all Canadians exposed to significant levels of environmental noise.

Noise And Sleep Quality Of Aging Adults – An Open Question

Iara B Cunha, Ashley Nixon, Jennifer A Veitch, Hiroshi Sato, Jeffrey Mahn, Markus Müller-Trapet, Sabrina Skoda

Indoor environmental quality is directly related to the health and well-being of building occupants. Noise exposure, for example, is established as a risk factor for the development of cardiovascular disease and is a cause of sleep disturbance. As people age, it is possible that they become more sensitive to the adverse effects of those environmental conditions, yet most studies and guidance are based on research with young or working-age adults. As part of a broader research focused on establishing guidance for suitable interior conditions for adults as they age, the National Research Council of Canada in partnership with the National Institute of Advanced Industrial Science and Technology of Japan are jointly investigating the effects of noise on the quality of sleep of older adults. The methodology for a laboratory sleep study, focusing on older adults, will be presented. The future results of this study will be part of a set of guidance for both new-build and retrofit scenarios of dwellings for aging in place.

Critical Importance Of Acoustical Design In New Developments

Zoe Razavi

The significance of acoustics in ensuring comfortable living is frequently overlooked in new developments, despite its importance. Multifamily housing developments are rapidly increasing nationwide. The Canada Mortgage and Housing Corporation (CMHC) mandates that noise from roads and railways be limited within habitable spaces. The British Columbia Building Codes (BCBC) align with the National Building Codes by requiring noise reduction between dwellings. However, acousticians are often not consulted to ensure the satisfaction of these requirements, leading to poor acoustical design and significantly impacting occupant comfort. As housing density rises, it becomes crucial to incorporate effective acoustical design during the planning phase of development. Attempting to mitigate noise or rectify poor acoustical design post-construction is often more difficult or even impossible, resulting in increased costs for all parties involved. This not only impacts occupant comfort but also affects the developers' reputation. One of the signs of poor acoustical design is the increase in Civil Resolution Tribunal (CRT) cases due to noise complaints within urban housing. This presentation will showcase case studies and propose solutions for sound mitigation after development, emphasizing the importance of incorporating sound design principles during the planning phase.

Repeatability And Reproducibility Of Apparent Sound Transmission Class (Astc) Measurements

Henning Schlechtriem

The evaluation of the partition sound isolation performance within buildings plays a crucial role in ensuring acoustic comfort and privacy. The Apparent Sound Transmission Class (ASTC) is a widely adopted metric used to quantify the sound transmission properties of building elements. However, reproducible measurements for the sound transmission of partitions, particularly at lower frequencies, remains a challenge. This presentation focuses on the repeatability and reproducibility of measurement results for ASTC ratings, with a specific emphasis on the transmission loss at lower frequencies. In this context, the impact of the room volume on the measurement precision will be examined, highlighting the challenges faced in rooms with smaller volumes, often due to non-diffuse room conditions, resulting in inconsistent ASTC ratings. The presentation will showcase comprehensive measurement results, presenting graphs that depict the measured sound transmission at third-octave frequency bands between

125 Hz to 4 kHz, relevant for the derivation of ASTC ratings. Comparisons will be provided for test results of the same partitions tested in rooms with varying volumes, exploring the influence of room size on ASTC ratings. Furthermore, the presentation will discuss the evolution of the minimum room volume requirements as defined in the measurement standard ASTM E 336, with the material changes to the standard and their potential impact on measurement accuracy identified. This presentation aims to enhance the understanding of the challenges involved in accurately assessing the sound isolation performance of building partitions by addressing issues with the repeatability and reproducibility aspects of ASTC measurements and their correlation with room volume.

Online Evaluation Of Floor Impact Sounds: Who Is More Likely To Be Annoyed? Canadians, Germans Or Koreans?

Sabrina Skoda, Markus Müller-Trapet, Young-Ji Choi, Iara Batista Da Cunha, Jeffrey Mahn

Impact sounds can be a source of annoyance in multi-residential buildings. To improve the acoustic conditions for building occupants and to support the inclusion of limits on impact noise in future editions of the National Building Code of Canada, the National Research Council of Canada has been evaluating the perceived annoyance from different types of impact sound. Listening experiments to link subjective annoyance ratings to different single number metrics were implemented in Canada, Korea and Germany. Early results indicated that test participants in the three countries agreed on relative annoyance rankings between different types of impact sources, but the absolute levels of annoyance differed among countries. To further investigate the possible multicultural aspects of impact noise perception, an additional online listening test was implemented on a global scale. The results of the online listening test indicate that annoyance ratings from Canada were higher in average than in other countries. The results of the global listening test will be presented and the ultimate question of who is most annoyed will be answered in this presentation.

Apparent Transmission Loss Through Stud Walls With Mass Timber Flanking Assemblies

Jeremy Thorbahn

The prevalance of mass timber in residential, commercial and institutional building construction in North America is steadily increasing. Airborne and impact sound transmission between rooms in buildings constructed using mass timber elements is an important and frequently discussed issue for building owners, designers and acoustical practitioners. The currently available laboratory and field test data for airborne sound transmission loss in mass timber buildings is often limited to direct sound transmission through a specific construction assembly, or in some cases flanking sound transmission for specific combinations of assemblies where both the walls and floor-ceilings are mass timber. There is limited information published on the effect of mass timber on flanking sound transmission when the direct sound path is not mass timber. Here we present recent field test data for airborne transmission loss through gypsum board and stud walls with a Cross-Laminated Timber (CLT) ceiling as a flanking assembly. Results with and without gypsum board linings applied to the underside of the CLT ceiling are presented.

ARTIFICIAL INTELLIGENCE IN ACOUSTICS - INTELLIGENCE ARTIFICIELLE EN ACOUSTIQUE

WALL-PRESSURE SPECTRUM MODEL BASED ON ARTIFICIAL NEURAL NETWORKS PREDICTIONS

Andrea Arroyo Ramo[*1,2], **Michaël Bauerheim** [†2], **and Stéphane Moreau** [‡1]
[1]Faculté de Génie, Université de Sherbrooke, Sherbrooke, Canada
[2]Département Aérodynamique, Énergetique et Propulsion, ISAE-Supaero, Toulouse, France

1 Introduction

The wall-pressure fluctuations induced by a turbulent boundary layer (TBL) are of interest in multiple applications, among them the aeronautical sector, wind energy generation, ground transportation and general use machines with rotating components. Under clean, laminar flow, the minimum noise level produced by rotating machines comes from the interaction between the turbulent boundary layer developing on the wall and the airfoil trailing edge. Moreover, these wall-pressure fluctuations may induce fluid-structural coupling and vibro-acoustic transmission. So, there is a special interest in finding simplified models that relate the wall-pressure fluctuations –or their spectrum (WPS)– to the main characteristics of the TBL.

Several semi-empirical models have been proposed in the past. All of them relating the WPS to boundary layer statistical parameters such as inner or outer layer scaling variables, e.g. BL thickness, external velocity or friction velocity. The empirical model of Chase-Howe was modified by Goody to account for Reynolds number effects. Then, further extensions were introduced by Kamruzzaman *et al.* , Rozenberg *et al.* , Hu or Lee to account for pressure gradient effects on the boundary layer development. The main drawback of such models is that they were generated *ad-hoc* for the specific dataset used to tune the model, or they are valid only within specific ranges of pressure gradient or flow conditions.

Deep Learning has been considered as an alternative to find complex dependencies between the TBL physical parameters [1]. The use of Artificial Neural Networks (ANN) as universal function approximator may permit to find a relationship between the BL and the WPS.

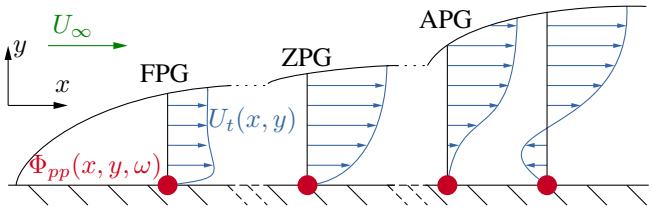

Figure 1: Boundary layer development on a flat plate. Forward, zero and adverse pressure gradient effects.

The proposed approach, differently from previous studies, uses the complete boundary layer profile. With that, the information of the flow evolution is retained in the model i.e. there is no *a-priori* choice of TBL parameters nor potential loss of relevant characteristics of the flow. The ANN training and analysis is performed on data coming from Large Eddy Simulations (LES) of a Controlled Diffusion (CD) airfoil produced by the European SCONE project [2]. The set of data includes zero and adverse pressure gradient effects, comprising flows experiencing strong adverse pressure gradients at various Mach and Reynolds numbers, which provides a large variety of flow conditions over the airfoil surface.

[*]andrea.arroyo.ramo@usherbrooke.ca
[†]michael.bauerheim@isae-supaero.fr
[‡]stephane.moreau@usherbrooke.ca

2 Boundary layer and wall-pressure spectrum

The boundary layer development over a flat plate is represented in Fig. 1. The thickness of the boundary layer increases as the pressure gradient becomes more negative. To find boundary layer thickness $\delta(x)$, the recovery of the 99% of the stagnation pressure is used: $p_{tot} = p + 1/2\rho U^2$. Velocity profile in the normal direction of the airfoil suction side is collected and normalized with the free-stream velocity U_∞.

The semi-empirical WPS models mentioned in the introduction can be collected in the Universal WPS (Eq. (1)). The constants a-h, FS and SS have different definitions for each one of the models, for instance Goody, Rozenberg and Lee [3]. These definitions rely on the use of inner and/or outer boundary layer parameters. The presence of pressure gradient effects and their strength is crucial in the formulation of such models and their range of application.

$$\phi_{pp}(\omega)SS = \frac{a\left(\omega FS\right)^b}{\left[i\left(\omega FS\right)^c + d\right]^e + \left[\left(fR_T^g\right)\left(\omega FS\right)\right]^h} \qquad (1)$$

3 Numerical datasets

The dataset employed in the current study contains the numerical LES data of SCONE project [2] on the flow over a controlled diffusion (CD) airfoil. The seven LES computations are collected in Tab. 1, where the flow conditions (Mach, Reynolds and angle of attack) are specified for each one.

The data points are split in three different groups: training, validation and testing. The case C32 is reserved for testing, and the remaining cases are used for training (80%) and validation (20%). The validation dataset is used only to evaluate the training.

Table 1: Flow parameters covered by the dataset

Case	Mach [-]	Reynolds [-]	AoA [°]
C11 | C12	0.3	8.30×10^5	4 | 7
C21	0.3	2.40×10^6	7
C31 | C32 | C33	0.5	2.29×10^6	4 | 5 | 6
C41	0.7	2.40×10^6	1
N pts. per case:	119	Total data:	833

4 Artificial Neural Network (ANN)

A 1D ANN structure is developed for the prediction of wall-pressure fluctuations on the CD airfoil. The structure of such a network, sketched in Fig. 2, contains two main parts. First, an autoencoder (Fig. 2, bottom) is used to compress the boundary layer profile into a reduced latent space, to avoid *ad hoc* parametrization. Second, this latent space, which contains all the information to reconstruct the boundary layer, is used as an input, together with the flow and position input data, into the WPS prediction ANN (Fig. 2, top). In this architecture, three fully connected layers have been employed. Each neuron computes a weighted sum of the input components $\mathbf{X}$, adding a bias $\mathbf{b}$, and applying an nonlinear activation function σ. The output of the fully connected layer l is input into the following one: $\mathbf{y}^{(l+1)} = \sigma^{(l+1)}\left(\mathbf{w}^{(l)}\mathbf{y}^{(l)} + \mathbf{b}^{(l+1)}\right)$. The training uses the NAdam optmizer (stochastic gradient descent) and the mean-squared error as loss function.

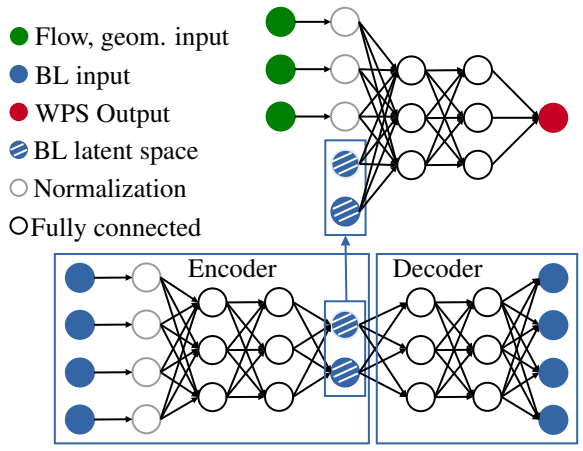

Figure 2: ANN schematic. Use of encoder as ANN input.

5 Results

The boundary layer autoencoder is used to compress the data of the velocity profile into its minimum expression. A parametric study has been performed in order to evaluate the minimal dimension of the latent space required to reconstruct the input boundary layer profile. It has been found that a three-dimensional latent space is sufficient to reconstruct accurately the velocity profile. Fig. 3 shows the reconstruction in three locations over the airfoil suction side on case C32, unseen by the autoencoder. The locations are characterized by FPG, ZPG and APG effects.

The prediction of the WPS under strong APG effects is shown in Fig. 4, as it is the regime which presents the most difficulties for the semi-empirical models. The ANN provides a good agreement with the numerical LES data available. There is an overall offset with the reference data lower than 5 dB, whereas the semi-empirical models produce, in the best case, offsets of about 10 dB. Furthermore, the trends in the low, mid and high frequency range are observed satisfactorily. It is not the case of the slopes provided by Goody, Rozenberg and Lee semi-empirical models.

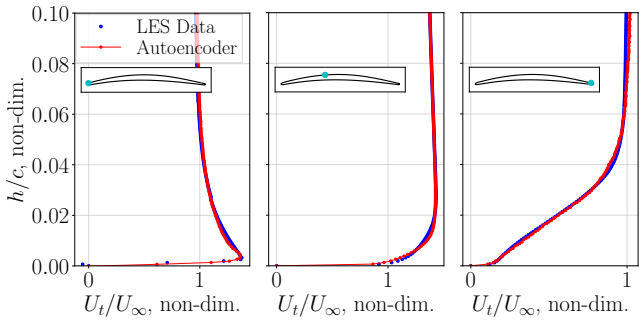

(a) FPG. **(b)** ZPG. **(c)** APG.

Figure 3: Boundary layer reconstruction from autoencoder on case C32, unseen during training. Encoder with 3 latent spaces.

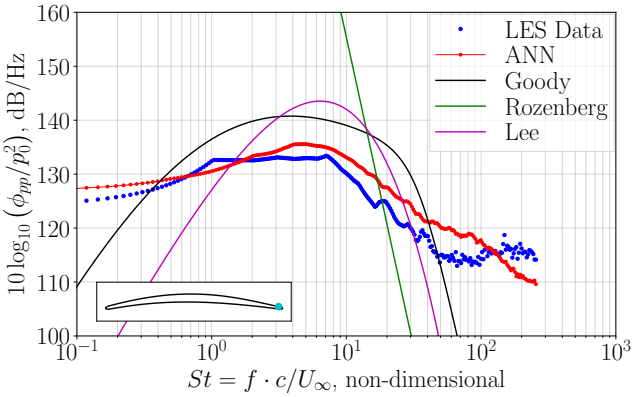

Figure 4: Prediction of the ANN, and compared to semi-empirical models. Testing on APG data of case C32, unseen during training.

6 Conclusions

The existing semi-empirical models fail to predict WPS when evaluated in cases of strong APG driving the boundary layer on a CD airfoil. ANNs have been proven to be an alternative for such predictions. It is first able to reduce the BL velocity profile into its minimum expression and then to use the latter to predict the WPS with lower error compared to semi-empirical models.

Acknowledgments

This work was partly supported by EUR-TSAE and NSERC. The Digital Research Alliance of Canada provided the computational resources.

References

[1] Joachim Dominique, J Van Den Berghe., Christophe Schram, and M A Mendez. Artificial neural networks modeling of wall pressure spectra beneath turbulent boundary layers. *Physics of Fluids*, 34(3), 2022.

[2] Radouan Boukharfane, Matteo Parsani, and Julien Bodart. Characterization of pressure fluctuations within a controlled-diffusion blade boundary layer using the equilibrium wall-modelled LES. *Scientific Reports*, 10(1):1–19, March 2020.

[3] Seongkyu Lee. Empirical wall-pressure spectral modeling for zero and adverse pressure gradient flows. *AIAA Journal*, 56:1–12, 01 2018.

MODELING OF FIELD SOUND INSULATION FOR MULTI-LAYERED CLT FLOOR ASSEMBLIES USING ARTIFICIAL NEURAL NETWORKS

Mohamad Bader Eddin[*1], Sylvain Ménard[†1], Delphine Bard Hagberg[‡2], and Jean-Luc Kouyoumji[§3]
[1]Department of Applied Sciences, University of Quebec at Chicoutimi, Quebec, Canada
[2]Katholieke Universiteit Leuven, Belgium
[3]Technological Institute FCBA, France

1 Introduction

Despite the advantages of wood as a constructional material, it has a lower subjective quality of sound insulation, due to its relatively low stiffness and mass, compared with heavy structural materials, such as concrete [1]. The sound insulation measurements are cost and time-demanding due to the large construction efforts of full-size assemblies. In addition, the acoustic performance of tested structures is sometimes varied between laboratory to on-site measurements. This paper aims to develop a prediction model based on the ANN approach to estimate the field sound insulation of multi-layered CLT-based floor systems.

2 Method

2.1 On-site sound insulation measurements

The database collection comprises 104 acoustic field measurements implemented on multi-layered CLT-based floor systems for different buildings in Europe that are reported in one-third-octave bands (50 Hz − 5 kHz). Fifty-one of them are airborne insulation measurements, and fifty-three are impact curves. Measurements were carried out according to ISO 16283 (Part 1 & 2) [2, 3] and ISO 717 (Part 1 & 2) [4, 5]. The database includes several structural parameters of each measured floor, such as linked walls and specific information about junctions (T or X-junction, the thickness of visco-elastic interlayer). For each acoustic measurement, the structural materials of each floor and wall and their installation orders, thickness, densities, floor construction system, and wall type are considered in the modeling. In addition, each test floor's area and the receiving room's volume are included in the classification.

2.2 Artificial neural networks modeling

This study developed a multi-layer perceptron ANN model with three hidden layers. Cross-validation and dropout techniques were employed to avoid overfitting and validate the network model. LeakyReLU (Leaky Rectified Linear Unit) is used as an activation function for the three hidden layers. The data is split into three subsets: training, validation, and testing set with percentages of 80%, 10%, and 10%, respectively. The root-mean-square error (RMSE) function is used as the cost function to calculate the difference between each measured and predicted curve in one-third-octave bands from 50 Hz to 5 kHz. The same model is used to predict the acoustic performance of floors by using each measurement type separately (airborne, impact insulation curves).

3 Results

3.1 Prediction of airborne and impact sound insulation

Five measurements related to different buildings are used to test the model's accuracy. Figure 1 shows each test floor's plan view and construction material. Errors are viewed for each measured curve against its prediction in each 1/3-octave band. Figure 2 shows the five test floor systems' measured and predicted insulation curves. The gray area in the background of each sub-figure represents the mean and standard deviation values used to train the network model. The single number quantities and RMSE values for each acoustic curve are presented in Tables 1 and 2.

Table 1: Predicted and measured weighted standardized level differences of test floors (in dB).

Floor no.	RMSE	D_{nTw}	$D_{nTwPred}$
1	3.44	54	54
2	3.56	58	58
3	2.97	51	51
4	2.90	54	55
5	3.34	60	60

Table 2: Predicted and measured weighted standardized impact sound pressure level of test floors (in dB).

Floor no.	RMSE	L'_{nTw}	$L'_{nTwPred}$
1	4.58	45	47
2	1.61	51	52
3	2.90	53	55
4	2.26	50	49
5	3.34	54	53

4 Discussion

The estimations for both airborne and impact sound were found to be close to measured ones; see Figure 2. Compared to other study [6], a good agreement was found in estimations near both the fundamental (below 200 Hz) and critical frequencies (1.25 - 3 kHz). This is likely due to multiple measurements on the same floor composition but with different connected walls, floor surfaces (and therefore room volume), and junctions, allowing the model to capture the structure's

[*]Mohamad.Bader-Eddin1@uqac.ca
[†]S2menard@uqac.ca
[‡]Delphine.Bard@acouwood.com
[§]Jean-Luc.Kouyoumji@fcba.fr

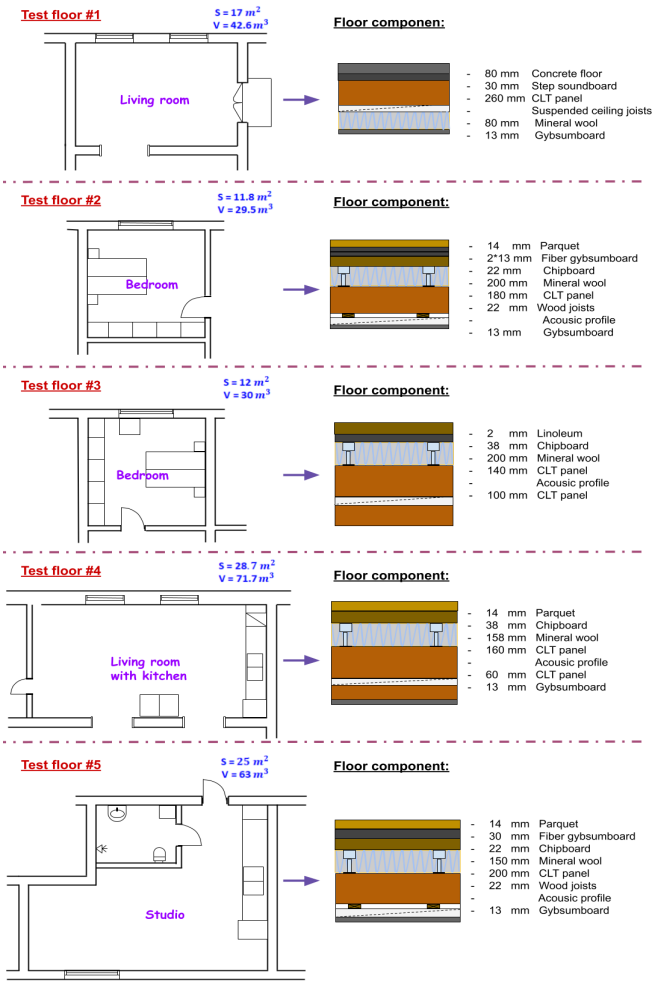

Figure 1: A schematic layout and section drawing of each test floor assembly.

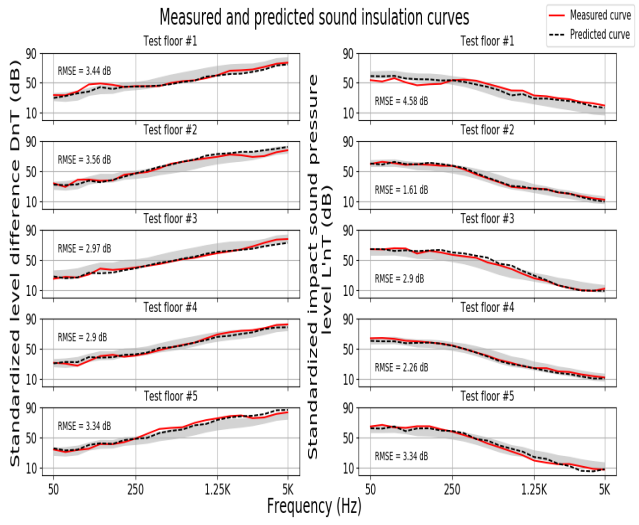

Figure 2: Airborne and impact sound insulation predictions.

insulation behavior around these frequencies accurately. In certain cases, discrepancies are observed between the predicted and measured curves at mid and high frequencies. The latter can be explained due to sound flanking transmission paths, which usually exist in those ranges in field measurements. The highest discrepancy in the prediction of D_{nTw} (Table 1) was 1 dB (test floor #4). However, it is 2 dB in the prediction of L'_{nTw} (test floor #1 and #3).

5 Conclusions

The present publication reveals a potential means of predicting on-site acoustic insulation curves for CLT-based floor systems using an ANN approach. The network model is developed using various structural parameters for 104 field acoustic insulation curves. The highest deviation is 1 dB in the estimation of weighted standardized level differences D_{nTw}, while it is 2 dB for weighted standardized impact pressure level L'_{nTw}. The results encourage acoustic designers to adapt the network model in practical engineering works, especially differences up to 2 dB are less than noticeable human differences in noise level.

Acknowledgments

This research Is funded by the Natural Sciences and Engineering Research Council (NSERC) of Canada through its IRC and CRD programs (IRCPJ 461745-18 and RD-CPJ 524504-18), the Region Nouvelle-Aquitaine (ref. 2017-1R10223) and the industrial partners of the NSERC industrial chair on eco-responsible wood construction (CIRCERB).

References

[1] Rasmussen B, Machimbarrena M. *Building Acoustics throughout Europe Volume 1: Towards a Common Framework in Building Acoustics throughout Europe*; DiScript Preimpresion, S.L.: Madrid, Spain, 2014.

[2] *ISO.16283-1*; Acoustics–Field measurement of sound insulation in buildings and of building elements—-Part 1: Airborne sound insulation. International Organization for Standardization: Geneva, Switzerland, 2014.

[3] *ISO.16283-2*; Acoustics–Field measurement of sound insulation in buildings and of building elements—Part 2: Impact sound insulation. International Organization for Standardization: Geneva, Switzerland, 2015.

[4] *ISO.717-1*; Acoustics–Rating of Sound Insulation in Buildings and of Buildings Elements—Part 1: Airborne Sound Insulation. International Organization for Standardization: Geneva, Switzerland, 2013.

[5] *ISO.717-2*; Acoustics–Rating of sound insulation in buildings and of building elements—Part 2: Impact sound insulation International Organization for Standardization: Geneva, Switzerland, 2013.

[6] Bader Eddin M, Ménard S, Bard Hagberg D, Kouyoumji J-L. Vardaxis, N.-G. Prediction of Sound Insulation Using Artificial Neural Networks—Part I: Lightweight Wooden Floor Structures. *Acoustics* 2022, 4, 203–226. https://doi.org/10.3390/acoustics4010013.

[7] Vigran, T.E. *Building Acoustics*. CRC Press: Boca Raton, FL, USA, 2014. https://doi.org/10.1201/9781482266016.

USE OF LOGISTIC REGRESSION MODELS AS A SUPERVISED LEARNING ALGORITHM TO IDENTIFY IMPULSIVE SOUNDS IN MONITORED SOUND DATA

Harry Ao Cai *[1]
[1]HGC Engineering, Mississauga, Ontario, Canada

1 Introduction

Impulsive sounds, characterized by their transient nature, often pose challenges in sound monitoring applications such as environmental noise assessments. Noise emission regulations, such as those given in NPC-300 of the Ontario Ministry of Environment, Conservation and Parks[1], and specific project needs can require impulsive sounds to be identified and processed separately from other impulsive and non-impulsive sounds. This paper investigates the use of logistic regression models, implemented as a supervised learning algorithm, to identify impulsive sounds from monitored sound data and to calculate their logarithmic mean impulse sound level (LLM).

2 Background and Existing Methods

Several methods exist to identify impulsive sounds, such as by listening to recorded audio or manual examination of the logged frequency-spectral data. These methods can be time-consuming for long-term monitoring projects. Methods that automatically tag or identify segments of the data based on a trigger criterion still requires manual a review of each segment.

Recent advances in data science have also introduced various audio classification machine learning algorithms. These methods can involve large volumes of audio recording files and require extensive computing power. The presented method aims to automate some of the analysis procedure required for handling large volumes of spectral data involving impulsive sounds without processing audio files.

3 Methodology

3.1 Data Source

Logged spectral sound pressure data, in the form of raw third-octave impulsive sound pressure levels (LISPL) and equivalent sound pressure level (LEQ), measured in 1 second windows from 6.3 Hz to 20 kHz, from sound level meters were used as input.

The data source for this paper came from sound pressure level data measured at four locations around a facility containing a pulse jet dust collector system. In this case, the targeted impulsive sound are the short bursts of pressurized air from the dust collectors, which were observed to emit an impulsive sound with similar amplitude. Four datasets were assessed, each containing around 40 minutes of data at each monitoring location.

3.2 Logistic Regression Model

A logistic regression model was constructed as a supervised machine learning algorithm to classify each 1-second window of frequency-spectral data, with each second being a data point. Logistic regression is a statistic model, which is similar to linear regression such that it predicts the probability of an event based on several independent variables, used to predict discrete categorical values.

The model presented herein outputs a binary prediction; an output of "1" if a data point is predicted to be an instance of the targeted impulsive sound and a "0" if otherwise. Raw LISPL and LEQ data were processed to create two sets of custom variables that mirror the manual method of identifying impulsive sounds; the arithmetic difference in LISPL between two data points, and the arithmetic difference between LISPL and LEQ.

3.3 Training and Evaluation

The model was constructed using Python, using pandas libraries to store and manipulate data and SciPy libraries to construct the logistic regression model. Approximately 20% of each dataset was labelled manually for the targeted impulsive sound and was used train the model. The logistic regression then assigns parameters of different weights to the custom variables, which ideally would capture the determinant characteristics of the targeted impulsive sound.

A logistic regression model was created for each dataset, since the frequency content of the impulsive sound can vary from measurement location to location. The same model, constructed for the first dataset, was also used to predict impulsive sounds in the other three datasets to investigate the feasibility of reusing the same model for different measurement locations.

4 Results

4.1 Sound Identification

The model was validated by splitting the training dataset into a "learning" and "validation" subset, such that the parameters of the regression model were developed on the "learning" subset and tested on the "validation" subset. The confusion matrix below, which is a measurement of machine learning classification, shows the performance of the first dataset (for the first measurement location), yielding a total accuracy of 97 %. It is also noted that the performance of the model was noticeably improved with custom features instead of relying on raw LFISPL and LEQ data. It is noted that the models are more prone to making false-positive predictions than false-

* hcai@hgcengineering.com

negatives. This makes intuitive sense as the learning data contains far more negatives than positives.

Figure 2 below is a time-history plot of A-weighted LISPL values of dataset 1, with the impulsive sounds of interest marked in orange, shown for datapoints around the cut-off between labelled datapoints and the unlabeled data.

4.2 Determining LLM

After the model has predicted the impulsive sounds, LLMs were calculated for the manually labelled impulsive sounds and for the predicted impulsive sounds. Table 1 shows the labelled data LLM and predicted LLM for each dataset. Ideally, the predicted and the labelled LLM would be similar, assuming that the targeted impulsive sound and the soundscape at the measurement location remained do not significantly change throughout the duration.

5 Discussion

The results show that for monitoring locations where the general soundscape remained the same, the impulsive sounds identified by the model matches very closely to the manually labelled data, implying that the model was able to identify impulsive sounds accurately. However, in cases where the soundscape varied throughout the monitoring duration, such as in the case of dataset 4 with numerous helicopter pass-bys, the model can over-predict and result in a much higher LLM than the labelled data. Since the helicopter pass-bys were not present in the training data, the frequency-spectra data of helicopter sounds can resemble the characteristics of the targeted impulsive sound, triggering false-positives.

The use of one prediction model for multiple datasets was investigated since the targeted sound is expected to have similar spectral characteristics at different locations. This approach would only require one training dataset, reducing the amount of work required to manually label data. The results also show that the model tends to over-predict and when presented with new transient and intrusive, more so than using dataset-specific models. This suggests that dataset-specific models are required for each monitoring location, to account for different soundscapes.

6 Conclusion

The supervised learning model can identify targeted impulsive sounds in scenarios where the training dataset can sufficiently represent the soundscape at the measurement location. However, variations in their soundscape can greatly reduce the accuracy of the learning model. Changes in background levels or the presence of sounds that were not described in the training dataset can trigger false-positive predictions, which can over-predict the LLM. Further work should be conducted to isolate the background sound and the non-impulsive sounds from the targeted impulsive sound. Another limitation of this model is the inability to identifying impulsive sounds when the targeted impulsive sound levels are lower than the background sound level, which could introduce a bias such that only the louder instances of the targeted sound are identified.

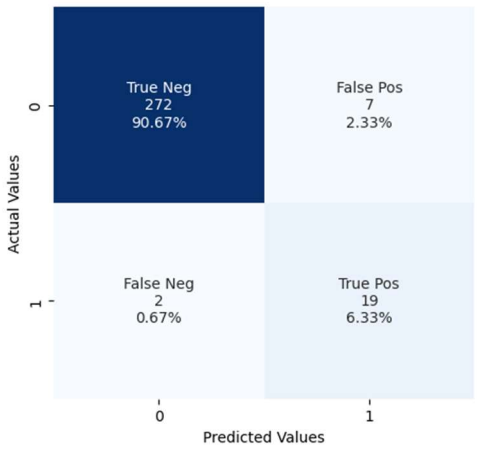

Figure 1: Confusion Table of Dataset 1 Model

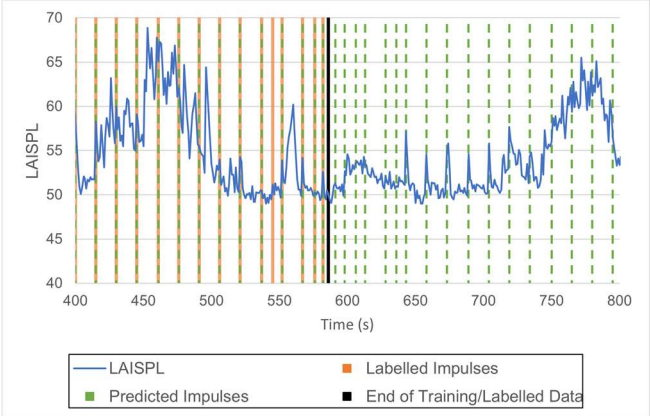

Figure 2: Identified Impulses over Time

Table 1: Model Results

		LLM [dBAI]			
Dataset	Acc.	Manually Labelled Data	Predicted using dataset-Specific Model	Predicted using Dataset 1 Model	Qualitative Notes Over Duration of Dataset
1	97%	58.2	58.2	58.2	No significant variations
2	98%	55.5	57.4	61.5	Increasing intrusive sounds
3	94%	57.0	57.1	57.6	No significant variations
4	96%	58.4	64.0	65.1	Helicopter pass-bys & intrusive sounds

References

[1] Ontario Ministry of the Environment. (August 2013). *NPC-300, Environmental Noise Guideline Stationary and Transportation Sources - Approval and Planning.* Retrieved from https://www.ontario.ca/page/environmental-noise-guideline-stationary-and-transportation-sources-approval-and-planning

ENHANCING ENVIRONMENTAL NOISE MANAGEMENT THROUGH SIAMESE CONVOLUTIONAL NEURAL NETWORK WITH TRIPLET LOST FUNCTION FOR IDENTIFICATION OF PRINCIPAL SOUND SOURCES

Jean-Pierre Côté *[1], Marc-André Gaudreau †[1] et Sousso Kelouwani ‡[1]
[1]Département de Génie mécanique, Université du Québec à Trois-Rivières

1 Introduction

In the realm of industrial environmental noise management, correctly identifying the source of the disturbance is paramount. This initial step not only sets the foundation for subsequent noise mitigation strategies but also aids in preventing further escalation of the noise problem. Furthermore, to optimize effectiveness and reduce costs, this process of identifying the noise source should be automated [1].

In a multi-source environment, a major obstacle in identifying primary noise sources is the convergence of multiple sound sources from inside as well as outside of the industrial zone, coupled with the degradation of acoustic signals over distance. Additionally, sources can be mobile, which adds to the intricacy of identifying the dominant noise sources from a distant field where the disturbance is measured.

This research aims to automatically link noise sources to environmental measurements from distant fields, providing a proof of concept for this complex task. While our larger project focuses on real-time feedback (Figure 1), this paper details our algorithm's development, results, and their significance.

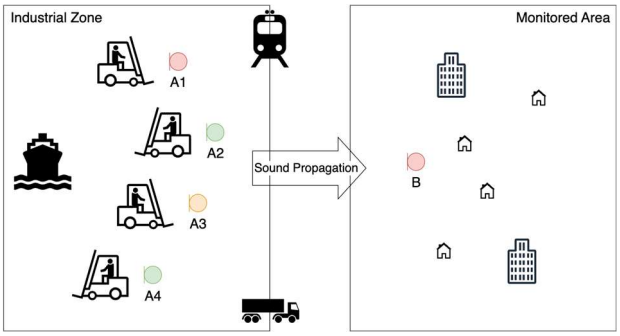

Figure 1: Schematic diagram of the studied scenario. A1-4 represents sound captures from potentially noisy mobile equipment. B is an environmental monitoring station. Colors at A indicate feedback to the user as to which source triggers B to surpass regulatory levels.

2 Method

The experiment we describe below involves the use of in the field recorded data to simulate real-time captures of close and far field versions of sounds. Those simulations are fed to an Artificial Neural Network (ANN) for machine learning.

* Jean.Pierre.Cote@uqtr.ca
† Marc-Andre.Gaudreau@uqtr.ca
‡ Sousso.Kelouwani@uqtr.ca

2.1 Database

Our research project is sponsored and commissioned by a medium-sized port on the Saint-Lawrence River, active in the bulk and general cargo sector. At this port, 3 noise monitoring stations are set up to automatically capture 20-second sound clips when a specified noise level is exceeded. Over the past three years, these stations have recorded over 150,000 sound snippets, each stored in WAV file format. After an automatic processing to isolate loudest parts and eliminate irrelevancy, we randomly selected 5000, 2-second snippets from those files to serve as instances of sound A. The sounds, predominantly created by the movement of large metal beams and plates by lift trucks in an open space, are marked by metallic impacts, scrapes, intermittent backup alarms, engine noise, and passing trains. The database can be considered as varied.

2.2 Simulations

In order to train the ANN, we also require far-field captures (B) to be compared with the original sounds (A). We simulate these captures by generating new audio files that blend three original sounds with pink noise. While A1 is the reference, A2 and A3 are selected randomly for each twin set. For each of the individual source extracts, we generate 20 positive and 20 negative twin pairs. In positive twins, A1 is dominant, while in negative twins, A2 or A3 dominates.

2.3 Network

We propose a Siamese Convolutional Neural Network (SCNN) with triplet lost function, as described below (Figure 2).

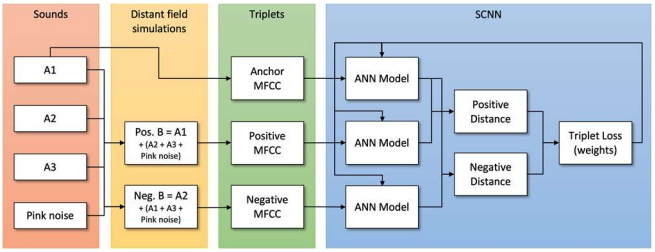

Figure 2: Schematic diagram of the learning process using a SCNN with triplet lost function.

Feature extraction

Based on its successes in automatic Environmental Sound Classification (ESC) [2], we use Mel Frequency Cepstral Coefficients (MFCCs) for feature extraction. The 2 second sound extracts are applied a 512 FFT pt (Hamming) with

hop size = 256 pt on 32 Mel filters to generate 20 - 1 cepstral coefficients, which produce a matrix of dimension 19 × 171 for each instance to feed the network.

Convolutional Neural Network model

Convolutional Neural Networks (CNNs) are a class of deep neural networks specifically tailored to process grid-like data where local patterns matter and there is a natural notion of translation invariance [3]. A key benefit of using CNNs in our research is their ability to identify the attributes of a sound notwithstanding the level of asychnonicity between A and B. The ANN architecture that we use is adapted from the SEnv-Net CNN model [4] that was developed and optimized for ESC (Figure 3).

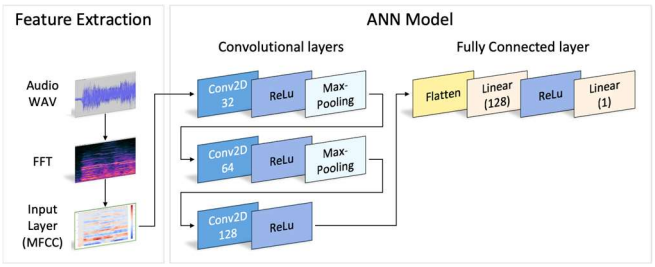

Figure 3: Schematic diagram of the ANN model which uses 3 convolutional layers and 2 linear layers.

Siamese network

For this research, sound A1 needs to be matched to sound B, while also being a component of sound B when another sound, A2 or A3, is the correct match. Therefore, straightforward classification is not the goal; discrimination is.

Siamese networks are a special type of neural network architecture used primarily in tasks involving the comparison of two distinct inputs [5]. They are used to match pairs of data and are a solution when the number of classes is very large and unknown during training, as is our case. The purpose of a Siamese network is to judge how similar the inputs are, rather than classify inputs independently of each other.

The key characteristic of Siamese networks is that they have identical subnetworks, which means they share the exact same parameters and weights. Each of these subnetworks processes one of the inputs. The subnetworks are joined at the top by a layer (or several layers) that combine the outputs of the subnetworks and compute a final output.

Triplet lost function

An extension of the Siamese network is the triplet loss, where a third input (a negative sample) is used along the anchor and the positive sample to improve the discrimination power of the network [6].

The use of the triplet loss function enables the neural network to process triplets of data in which sound A1 serves as the anchor that is compared with a positive instance of sound B and a negative instance of sound B. The goal of the function is to calculate and minimize the distance with positive B and maximize the distance with negative B.

3 Results and Discussion

Performance measured on the test set yield 70% precision for S/N = 0 dB, up to 84% for S/N = 10 dB.

Table 1: Accuracy of the correct identification achieved over signal-to-noise ratios.

S/N (dB)	Accuracy (%)
10	84.29
6	81.20
0	69.68
-6	54.19

The increase in precision with the rise in the signal-to-noise ratio suggests that the algorithm successfully identifies principal individual sounds in simulations of far-field complex signals.

4 Conclusion

Our ongoing research suggests a promising pathway towards balancing the need for maximizing production with adherence to environmental noise standards. If our method proves successful, it could contribute to the automatic identification of the principal sound source in a noisy and desynchronized complex signal. This tool could become useful in different situations and fields.

Acknowledgments

This work was supported by Mitacs through the Mitacs Accelerate program. It is commissioned and sponsored by the Administration du Port de Trois-Rivières and Logistec, with the help of the Cégep de Drummondville.

References

[1] Murovec, J., et al. (2023). Automated identification and assessment of environmental noise sources. Heliyon, 9(1).

[2] This subject is addressed in numerous studies, one of which is Jin, S., et al. (2021). Evaluation and modeling of automotive transmission whine noise quality based on MFCC and CNN. Applied Acoustics, 172, 107562.

[3] A fundamental paper on this topic is LeCun, Y., et al. (1998). Gradient-based learning applied to document recognition. Proceedings of the IEEE, 86(11), 2278-2324.

[4] Al-Hattab, Y. A., et al. (2021). Rethinking environmental sound classification using convolutional neural networks: optimized parameter tuning of single feature extraction. Neural Computing and Applications, 33(21), 14495-14506.

[5] A fundamental paper on this topic is Chopra, S., et al. (2005, June). Learning a similarity metric discriminatively, with application to face verification. In 2005 IEEE computer society conference on computer vision and pattern recognition (CVPR'05) (Vol. 1, pp. 539-546). IEEE.

[6] A fundamental paper on this topic is Schroff, F., et al. (2015). Facenet: A unified embedding for face recognition and clustering. In Proceedings of the IEEE conference on computer vision and pattern recognition (pp. 815-823).

DEEP LEARNING-BASED APPROACH FOR ACOUSTIC SOURCE LOCALIZATION IN TURBULENT FLOWS

Arnav Joshi [*1] **and Jean-Pierre Hickey** [†1]
[1]Mechanical and Mechatronics Engineering, University of Waterloo

1 Introduction

Detection of acoustic sources in turbulent flows forms an important part of the study of aeroacoustic noise. Passive Acoustic Source Localization uses the pressure fluctuations recorded by a microphone array to triangulate the location of the source, an application of this is the detection of aircraft wakes. Aircraft wakes are responsible for causing wake turbulence, and thus airports have to factor in the conventional time it takes for the wakes to dissipate. These wakes are characterized by wake vortices that are formed on the wing tips and have been shown to emit characteristic noise that generally lies in the low-frequency range (100-500 Hz). Accurate detection of these wakes is critical and could lead to an increase in airport efficiency and throughput. The low-frequency nature of the noise causes traditional methods such as Acoustic Beamforming to fail. Thus in this work, we tackle the problem of low-frequency, Passive Acoustic Source Localization (ASL) using a Deep Learning-based approach. The ability of deep learning algorithms to extract features from data in any shape or form provides a lot of scope for their application in ASL. Building a robust framework for ASL involves identifying the right input features and selecting the appropriate architecture. We developed various test cases to study the viability of different input features and architectures. Ultimately, a Convolutional Neural Network (CNN) using the input feature best suited to that case was employed. The test cases include two-dimensional ASL for detecting sources on the horizon or on a scanning plane parallel to the microphone array plane, three-dimensional ASL, and moving source localization. Section 2 gives a brief description of all the simulated test cases. Section 3 provides results that testify to the approach's viability followed by Discussion and Conclusion.

2 Method

The method is summed up in Figure 1. Acoustic pressure data is obtained using a microphone array. The data is then processed to generate an input feature which is then fed to the CNN.

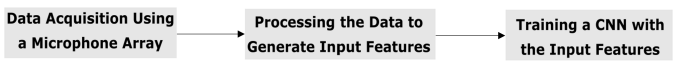

FIGURE 1 – Flow of Information in the Method

2.1 Microphone Array and Source Simulation

A virtual microphone array and two types of sources with different levels of complexity are simulated for all cases. Source 1 is a traditional, analytically defined monopole that oscillates at a fixed frequency f. The expression $P_s(m)$ [1] shows the acoustic pressure due to a monopole s as detected by a microphone m located at a distance r_s from the source. Here, c_0 is the speed of sound in air. $\mathrm{P}_s(m) = \frac{e^{-j2\pi f r_s/c_o}}{4\pi|r_s|}$ The second type of source, Source 2, is also an analytical source however unlike the monopole, it is represented by a time-domain sinusoidal signal of amplitude A, frequency f, and phase difference ϕ, polluted with noise : $P(t) = \mathrm{A}sin(2\pi ft + \phi) + Noise$. It is computationally more expensive than the monopole source as it has to be processed. The monopole source allows us to test the model rapidly while Source 2 provides scope for the application of signal processing techniques, a procedure we would have to do when working with real signals.

2.2 Case 1 : Stationary Source Localization on a Scanning Plane

This case is based on validating the work done by Xu et al. [1]. A 64-microphone array in the shape of a logarithmic spiral was simulated. To generate the training dataset, S monopole sources were randomly distributed across the plane, and the acoustic pressure of all the sources was calculated at all the microphones (M) to form the combined pressure vector P given as $P = \left[\sum_{s=1}^{S} P_s(1), \sum_{s=1}^{S} P_s(2), \sum_{s=1}^{S} P_s(3), , \sum_{s=1}^{S} P_s(M)\right]$. This, in turn, was used to get the Cross-Spectral Matrix (CSM) as $CSM = PP^H$, where P^H is the conjugate transpose of P. The CSM was used as an input feature to the CNN that was trained against the ground truth to predict the strength and location of the sources.

2.3 Case 2 and 3 : Two-Dimensional ASL on the Horizon and Three-Dimensional ASL

A classification-based approach was used for these two cases. This focuses on determining the Direction of Arrival (DoA) of the acoustic signal from the source. For locating sources on the horizon, only the azimuth angle (θ) has to be determined, whereas, for 3D ASL, both the azimuth and the elevation (α) angles have to be determined simultaneously. The range of possible values of θ (0-180°) and α (0-90°) is discretized into classes and the output of the network is the probability distribution of all the classes. To generate the training set, a monopole is placed at a random angle from the center of the 4-microphone array at a fixed radial distance r. The CSM is calculated and used as an input feature. The setups of the two cases are shown in Figures 2 and 3 respectively. For Source 2, the Generalized Cross Correlation (GCC) algorithm was applied to microphone pairs, and the resulting GCC vector was

∗. a5joshi@uwaterloo.ca
†. j6hickey@uwaterloo.ca

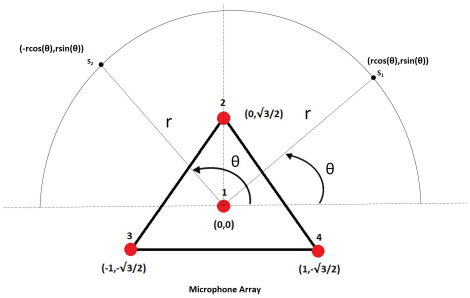

FIGURE 2 – Case 2 : Two-Dimensional ASL on the Horizon

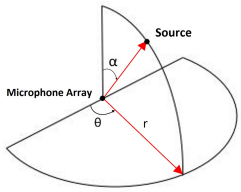

FIGURE 3 – Case 3 : Three-Dimensional ASL

reshaped and fed to the CNN. GCC is a Time Delay of Arrival (TDOA) approach and is known to be robust to noise and reverberation. Figure 4 shows the GCC pattern obtained using a pair of microphone signals that are polluted with correlated and uncorrelated noise sources.

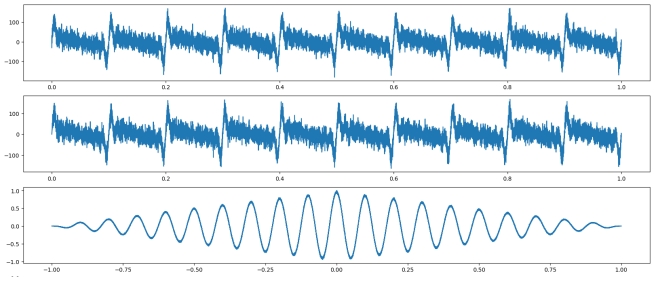

FIGURE 4 – GCC Pattern for a Pair of Microphone Signals

2.4 Case 4 : Moving Source Localization

The moving source localization problem is the most expensive and complicated case as the amplitude, frequency by virtue of the Doppler effect, and phase of the source change at every instant. The Short-Time Fourier Transform (STFT) of the signal gives the time variation of frequency as sensed by the microphone and is used as input to the model. We defined a Source 2 signal at 100 Hz moving in a straight line away from a single microphone and used the STFT calculated over a given time interval to predict the initial and final coordinates of the source.

3 Results

A result for source localization on a plane parallel to the array plane (Case 1) is shown in Figure 5. The model was trained to detect 6 monopole sources at 300 Hz, spread randomly across a 12x12 scanning grid plane.

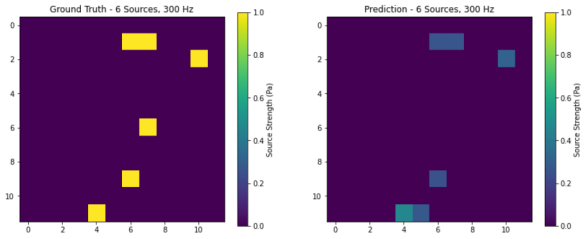

FIGURE 5 – Case 1 : ASL on a Scanning Plane

Tables 1 and 2 show the prediction accuracies for the monopole source and Source 2 at 100 Hz in classification-based cases (Cases 2 and 3) respectively.

TABLE 1 – Prediction Accuracy for a Monopole Source.

Case	θ	α
2D ASL	98%	-
3D ASL	88%	78%

TABLE 2 – Prediction Accuracy for Source 2 with GCC Input in 2D ASL.

No. of Classes	Accuracy
90 (2°class size)	$\approx 40\%$
60 (3°class size)	$\approx 52\%$

Table 3 shows the prediction of source coordinates for a moving source (Case 4).

TABLE 3 – Prediction for Position of a Moving Source (Initial and Final Coordinate.

Sr. No.	Ground Truth	Model Prediction
1	(72.794, 91.381)	(72.305, 91.696)
2	(16.008, 76.569)	(16.401, 76.287)

4 Discussion and Conclusion

It can be seen from Figure 5 that for ASL on a scanning place, the model was able to capture the source distribution reasonably well. For Source 2 detection on the horizon (Table 2), an accuracy greater than 50% for 60 classes in the presence of noise shows the robustness and reliability of GCC as an input feature.

Overall, this work managed to test out the various aspects of Acoustic Source Localization using a Deep Learning-based Approach. The results are testimony to the viability of the approach and it is expected that with more data and deeper networks, a robust framework for ASL can be built and successfully applied to the detection of acoustic sources in turbulent flows.

References

[1] Pengwei Xu, Elias JG Arcondoulis, and Yu Liu. Acoustic source imaging using densely connected convolutional networks. *Mechanical Systems and Signal Processing*, 151 :107370, 2021.

ENHANCING AUTOMATIC SPEECH RECOGNITION OF A REGIONAL DIALECT: A PILOT STUDY WITH QUÉBÉCOIS FRENCH

Xinyi Zhang[*1], **Lucia Eve Berger**[†2], **Duc-Hoa Tran**[‡1], **and Rachel E. Bouserhal**[§1]
[1]École de technologie supérieure, Université du Québec, Canada
[2]MILA, Université de Montréal, Canada

1 Introduction

Automatic speech recognition (ASR) systems have been significantly improved by the implementation of deep neural networks (DNN) in natural language processing. However, the performance of these DNN-based systems largely depends on the amount of training data available [1]. When speech patterns deviate from the norm, they may not be sufficiently represented in the training data, which leads to lower performance in such cases. Therefore, making ASR systems more robust – not only to noise in the environment but also to the *implicit noise* within speech – is becoming more and more important [2]. This study examines such robustness in a state-of-the-art (SOTA) ASR system, Whisper, for the regional dialect of French spoken in Québec, Canada.

1.1 Whisper

Whisper is a multilingual and multitask ASR system developed by Radford et al. [3] with large-scale weak supervision. It uses sequence-to-sequence learning, which directly takes a sequence (in this case, audio) and outputs another sequence (in this case, text). After scaling its training data to 680k hours, Whisper was able to achieve robust zero-shot performance, approaching human-level robustness. Moreover, this excellent performance was attained without using self-supervision and self-training techniques, which are more complex but currently trending in the field.

Whisper is constructed with a transformer encoder-decoder architecture, where the encoder encodes the audio and the decoder decodes the output of the encoder into text. Within each transformer encoder block, there is a self-attention mechanism and multi-layer perceptron; it is also the case for the transformer decoder blocks, except additionally, there is a cross-attention mechanism between the encoder and the decoder.

1.2 Québécois French

Phonological, lexical, and syntactic differences are observed between Québécois French (QF) and Metropolitan French (MF). Reviewed in [4], QF and MF share the same consonant and glide inventories, although differences are seen in the realization of ”r”, the affrication of alveolar plosive before high vowels, and more. For vowels, QF has four more vowels than MF, resulting in fewer homophones. In addition, there is a phenomenon called the diphthongization of long vowels in QF. These movements are easily captured in a spectrogram, which is a time-frequency representation of speech and is usually given as input to neural networks.

In Canada, more than 7 million people speak French natively, and most of them speak QF. A strong demand for a speech-to-text model of QF arises in social services, second language learning for immigrants, smartphone applications, and so on. Despite the existing demand, there needs to be more research in this area. In 2020, Lancien et al. adapted the existing French lexicon, developed a QF-specific pronunciation dictionary, and created an acoustic model [4]. Other efforts made for this task include Gagnon et al. (2008), where a decision-based audiovisual fusion model was created for large-vocabulary speech recognition of French Canadian speech [5]. It is worth exploring the SOTA end-to-end deep neural network for the task of QF recognition.

2 Method

2.1 Data preparation

We searched for publicly available YouTube videos with human-transcribed closed-captioning and selected twelve videos that featured a diverse group of speakers (N = 83) with various sub-regional accents of QF and covered a variety of common topics. The selected videos consisted of casual conversations, interviews, scripted speech, and noises like music and background noise. See Table 1 for detailed statistics.

The audio files were converted into mono WAV format and down-sampled to 16 kHz. The VVT transcripts underwent preprocessing and then were used to extract plain text and timestamps. We used Montreal Forced Aligner (MFA) [6] to obtain precise, word-by-word timestamps. The audio files were then segmented into 5-sec chunks based on word-start and word-end timestamps. Since MFA's output was normalized, the text transcription of each segment was generated by matching MFA's pseudo-truth to the original text.

Table 1: Descriptive statistics of the QF data set videos

	Mean	SD	Sum
Duration (s)	1355.2	501.4	8809.0
Speech ratio	73.0%	2.8%	-
Speaker (F;M)	7.1 (2.4;4.7)	4.0 (1.5;3.8)	83 (29;54)

The audio segments were transformed into 80-channel log-Mel spectrograms that were computed on a 25-millisecond window with a stride of 10 milliseconds, and the text segments were tokenized in French and padded to the same length. We obtained 1568 segments, which were randomly split into three sets: 80% for the training set, 10% for the validation set, and 10% for the testing set.

[*]xinyi.zhang.1@ens.etsmtl.ca
[†]lucia.eve.berger@umontreal.ca
[‡]duc-hoa.tran.1@ens.etsmtl.ca
[§]rachel.bouserhal@etsmtl.ca

2.2 Model Training and Evaluation

We fine-tuned the pre-trained Whisper model of the base and small versions to investigate the impact of model size on the zero-shot and fine-tuned performance. To avoid the potential of overfitting as the training data is limited, we maintained most of the pre-trained weights and only retrained a certain group of layers. We froze the encoder blocks and re-trained the decoder layers. In fine-tuning the base model, there were 52 M trainable parameters and 19.8 M non-trainable parameters. In fine-tuning the small model, there were 153 M trainable parameters and 87 M non-trainable parameters.

We used a learning scheduler, where after a warm-up period, the scheduler linearly decreases the learning rate to zero. We also AdamW optimizer [7] for weight decay regularization and a learning rate finder from Tune [8] to find the optimal initial learning rate. Every model was trained for 10 epochs. We used Python and PyTorch Lightning for our model implementation.

We used Word Error Rate (WER) as our performance evaluation metric, and the performance difference between zero-shot and fine-tuned is denoted as R-WER. Each fine-tuning experiment was run 10 times, each with a different random split of the data set. Means and standard deviations are reported.

3 Results

Table 2: Whisper's WER (%) on benchmarks reported in [3]

	base size	**small size**
Multilingual LibriSpeech	26.6	16.2
Common Voice 9	37.3	22.7
VoxPopuli	24.9	15.7
Fleurs	28.5	15.0
Mean	**29.3**	**17.4**

As shown in Table 2, Whisper's French transcription WER on four benchmarks was averaged to be 29.3% for the base size and 17.4% for the small size [3]. The zero-shot and fine-tuned performances for QF are shown in Table 3. After fine-tuning, the WER is reduced by 13.9% for the base version and 42.9% for the small version.

Table 3: WER (%) of the zero-shot and fine-tuned Whisper models transcribing QF

	zero-shot	**fine-tune**	**R-WER**
base - Mean (SD)	51.3 (6.9)	37.4 (5.5)	13.9 (5.6)
small - Mean (SD)	62.4 (6.8)	19.5 (2.8)	42.9 (8.5)

4 Discussion and Conclusion

There is a clear performance reduction of Whisper when transcribing QF in the zero-shot setting as compared to benchmarks that mostly consist of MF, motivating the need to fine-tune the Whisper model for this regional dialect. The QF zero-shot WER was almost twice as high as reported with MF, demonstrating the effect of the differences between QF and MF. Surprisingly, a higher WER was observed for the small model (62.4%) than the base model (51.3%). This unexpected result is unlikely to be attributed to the limited trial runs as the standard deviation was small and similar for both model sizes, but an explanation for it has not been found. Our fine-tuning reduced the WER by 13.9% for the base model and 42.9% for the small model, approaching Whisper's performance on benchmarks, especially the small model.

In conclusion, our study demonstrated that Whisper has the capability to be adapted for a regional dialect even with limited resources, and it could serve as a pre-trained model to enhance inclusivity and accessibility in voice-based technologies.

Acknowledgments

The authors would like to thank Yimei Yang for her contribution. We acknowledge financial support from the Natural Sciences and Engineering Research Council of Canada as well as the Fonds de recherche du Québec.

References

[1] Hardik B. Sailer, Ankur T. Patil, and Hemant A. Patil. Advances in low resource asr: A deep learning perspective. 2018.

[2] Meredith Moore. Speech Recognition for Individuals with Voice Disorders. In Troy McDaniel and Xueliang Liu, editors, *Multimedia for Accessible Human Computer Interfaces*, pages 115–144. Springer International Publishing, Cham, 2021.

[3] Alec Radford, Jong Wook Kim, Tao Xu, Greg Brockman, Christine McLeavey, and Ilya Sutskever. Robust speech recognition via large-scale weak supervision. Technical report, Tech. Rep., Technical report, OpenAI, 2022.

[4] Mélanie Lancien, Marie-Hélène Côté, and Brigitte Bigi. Developing resources for automated speech processing of quebec french. In *12th Language Resources and Evaluation Conference*, pages 5323–5328. European Language Resources Association, 2020.

[5] L Gagnon, S Foucher, F Laliberte, and G Boulianne. A simplified audiovisual fusion model with application to large-vocabulary recognition of french canadian speech. *Canadian Journal of Electrical and Computer Engineering*, 33(2):109–119, 2008.

[6] Michael McAuliffe, Michaela Socolof, Sarah Mihuc, Michael Wagner, and Morgan Sonderegger. Montreal Forced Aligner: Trainable Text-Speech Alignment Using Kaldi. In *Proc. Interspeech 2017*, pages 498–502, 2017.

[7] Ilya Loshchilov and Frank Hutter. Decoupled Weight Decay Regularization. 2017. Publisher: arXiv Version Number: 3.

[8] Richard Liaw, Eric Liang, Robert Nishihara, Philipp Moritz, Joseph E Gonzalez, and Ion Stoica. Tune: A research platform for distributed model selection and training. *arXiv preprint arXiv:1807.05118*, 2018.

[9] Yu Zhang, Daniel S Park, Wei Han, James Qin, Anmol Gulati, Joel Shor, Aren Jansen, Yuanzhong Xu, Yanping Huang, Shibo Wang, et al. Bigssl: Exploring the frontier of large-scale semi-supervised learning for automatic speech recognition. *IEEE Journal of Selected Topics in Signal Processing*, 16(6):1519–1532, 2022.

ACCURACIES IN ALGORITHMIC PREDICTORS OF MUSICAL EMOTION

Jackie Zhou [*1], Cameron Anderson [†1], Michael Schutz [‡1,2]
[1]*Department of Psychology, Neuroscience & Behaviour*; McMaster University, Hamilton, Ontario, Canada
[2]*School of the Arts*; McMaster University, Hamilton, Ontario, Canada

1 Introduction

Music Information Retrieval (MIR) is an interdisciplinary domain where researchers develop and deploy algorithms to shed light on musical structure. Notable applications include analyzing features in expansive music databases, computational composition, and categorizing tracks' genres, artists, and instrumentation. To automate musical analyses, MIR studies often employ diverse audio feature extraction. MIRToolbox is perhaps the most widely used, having received over 1300 citations in academic publications [1]. Past research has used MIRToolbox to extract features in diverse musical works [2-3]. This includes perceptual work using MIRToolbox to evaluate features' effects. For example, one study used MIRToolbox functions to assess how mode (specific grouping of notes that contribute an emotional aspect in music), and tempo affected perceived emotion in Western classical melodies [2]. Yet, despite its wide use, the accuracy of MIRToolbox algorithms remain underexplored. According to previous work [3], only one study has directly assessed the reliability of MIRToolbox feature extraction algorithms [4]. We address this gap by comparing automated analyses of timing and mode from MIRToolbox with manual analyses of classical works.

2 Methods

2.1 Stimulus Preparation

To evaluate algorithmic consistency in analyses of major and minor excerpts, we analyzed excerpts from Chopin's *Préludes* [5], which includes 12 major and 12 minor pieces. Chopin composed all pieces for piano, providing some level of timbal consistency across different interpretations. The corpus includes performances by prominent pianists, such as Friedrich Gulda, Vladimir Ashkenazy, Martha Argerich, and Pietro de Maria—enabling comparisons of multiple interpretations. We prepared musical excerpts with Amadeus Lite, capturing the first eight full measures of each prelude performance (appending partial lead-in measures where necessary) and included a two-second fade-out.

2.2 Feature Extraction and Comparison

We analyzed timing and mode in the initial eight measures of each excerpt, excluding the two-second fade-out. We followed methods outlined in [6], codifying timing features in attacks per second (i.e., attack rate). To assess mode, we consulted the respective scores.

We used functions from MIRToolbox and assessed mode and timing using default parameters. To evaluate mode and key, we encoded information from *mirkey*, and *mirmode*. *Mirkey* estimated the tonal center of each piece, using the highest coefficient from a key strength graph. *Mirmode* predicts mode as a number between -1 and +1 (positive values identify major keys and negative values minor keys). We calculated attack rate with two functions: *mironsets* estimates the number of note attacks in the given audio input; *mirlength* evaluates the duration in seconds of each eight-measure excerpt. We calculated the predicted attack rate by dividing the number of onsets in an excerpt by its duration in seconds.

We assessed algorithmic consistency by comparing manual analyses of mode and attack rate with MIRToolbox estimates. We compared multiple interpretations of each piece to assess reliability, clarifying predictions' resilience across variation in recording quality, performance environment and timbre.

3 Results

We compared attack rate to information previously tabulated by our team for related projects [7] and compared computed estimates of mode and key to the nominal information coded in the score (i.e., the notated key).

3.1 Mode

Figure 1 depicts where predictions of key and mode align with the nominal key and mode. Green points indicate predictions consistent with both nominal mode and key. Purple points indicate predictions aligning with the nominal *mode*, but not key (e.g., a prediction of "f# minor" for pieces nominally in "eb minor"). Orange points indicate predictions consistent with neither nominal mode nor nominal key. Across the four performers, 62.5% (60/96) of key predictions were consistent with the nominal key (Argerich: 15/24=62.5%; Ashkenazy: 17/24=70.8%; De Maria: 15/24=62.5%; Gulda: 13/24=54.2%).

Notably, across all four performance interpretations, three preludes—C, E, and F minor—were incorrectly predicted to be in different keys. This was the case for almost all unaligned key predictions except one. Chopin's A minor prelude was predicted as G major across all four interpretations. This was the only piece where the algorithm consistently predicted *the same incorrect key* across all interpretations.
Although only 62.5% of predictions were consistent with the nominal key, 84.4% of mode predictions aligned with the manually analyzed major/minor mode. Mode predictions of Argerich and Ashkenazy's performances were 88% accurate, whereas predictions of de Maria's performances were 83% accurate, and Gulda's 79% accurate. For each performer, the

[*] zhouz109@mcmaster.ca
[†] andersoc@mcmaster.ca
[‡] schutzm@mcmaster.ca

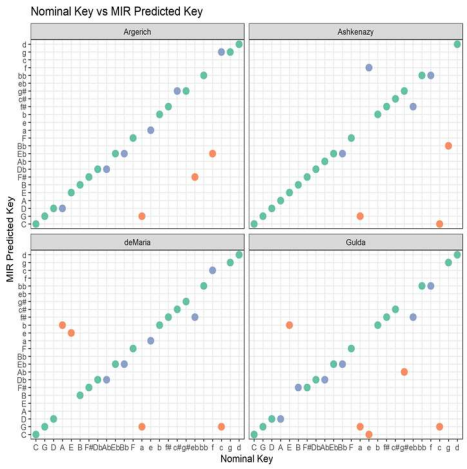

Figure 1: Mode and Key Comparison

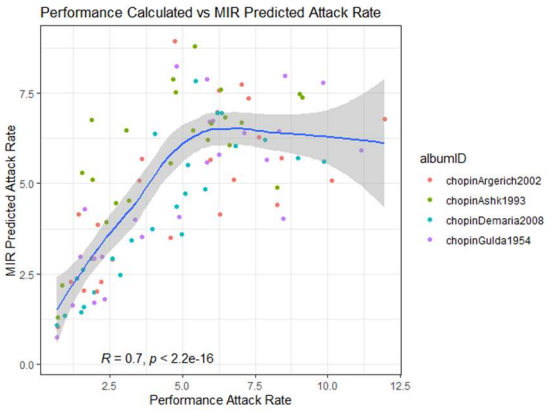

Figure 2: Attack Rate Comparison

algorithm incorrectly predicted mode in at least three, and at most five, excerpts out of 24.

3.2 Attack Rate

Figure 2 plots MIR attack rate predictions against previously extracted values. A Locally Estimated Scatterplot Smoothing curve shows MIR-predicted values begin to level off at higher attack rates, indicating worse estimation of timing in faster pieces. Despite this, automated and manual analyses of timing correlated strongly ($R = 0.7$, $p < 0.01$).

4 Discussion

Inconsistencies regarding timing information represent a technical challenge (i.e., a need for better onset detection), rather than a conceptual one. Consequently, we focus our discussion on discrepancies in mode estimates which raise numerous issues both technical and theoretical. Specifically, they raise questions regarding why multiple interpretations of the same performances differ in their assessment with *mir-mode*. Although different performers will often use different tempi, a piece's modality is not generally thought to vary as a function of interpretation. Therefore, these results showing variable estimates of key and mode for different performances of the same composition suggest extraneous factors may affect the accuracy of estimates widely used in the music cognition literature as ground-truth (i.e., information assumed to be true) for perceptual experiments.

5 Conclusion

Ensuring accurate and consistent MIR algorithms is crucial as their convenience might not fully capture audio performance nuances in automated music analyses. We offer a new method for exploring tools which are widely used within the field of music cognition—yet may not be as accurate as would be assumed given their prominence.

Acknowledgments

We are grateful to Konrad Swierczek for his module which inspired part of this project. This work was supported by the Social Sciences and Humanities Research Council of Canada (SSHRC) and the Canada Foundation for Innovation.

References

[1] Lartillot, O., Toiviainen, P., & Eerola, T. (2008). A Matlab toolbox for music information retrieval. *Data Analysis, Machine Learning and Applications: Proceedings of the 31st Annual Conference of the Gesellschaft Für Klassifikation EV, Albert-Ludwigs-Universität Freiburg, March 7–9, 2007*, 261–268.

[2] Quinto, L., & Thompson, W. F. (2013). Composers and performers have different capacities to manipulate arousal and valence. *Psychomusicology: Music, Mind & Brain,* **23**(3), 137–137.

[3] Lange, E. B., & Frieler, K. (2018). Challenges and opportunities of predicting musical emotions with perceptual and automatized features. *Music Perception: An Interdisciplinary Journal*, **36**(2), 217-242.

[4] Kumar, N., Kumar, R., & Bhattacharya, S. (2015, February). Testing reliability of Mirtoolbox. In *2015 2nd International Conference on Electronics and Communication Systems (ICECS)* (pp. 710-717). IEEE.

[5] Chopin, F. (1839). *Preludes op. 28* (R. Pugno, Ed.). Schlesinger'sche Buch-und Musikhandlung.

[6] Poon, M., & Schutz, M. (2015). Cueing musical emotions: An empirical analysis of 24-piece sets by Bach and Chopin documents parallels with emotional speech. *Frontiers in Psychology*, **6**(November), 1–13.

[7] Anderson, C. J., & Schutz, M. (2022). Exploring Historic Changes in Musical Communication: Deconstructing Emotional Cues in Preludes by Bach and Chopin. *Psychology of Music*, **50**(5), 1424–1442.

Abstracts for Presentations without Proceedings Paper
Résumés des communications sans article

Detecting Ringed Seal Vocalizations Using Deep Learning

Karlee Zammit, William Halliday, Fabio Frazao, Stan Dosso

Climate change is causing the sea ice in the Canadian Arctic to thin and form later each year, creating more extensive areas of open water. Completely ice-free summer conditions are projected by 2050, which will make passage through proposed shipping corridors in the Arctic possible. Increased shipping will increase anthropogenic sound levels in a historically acoustically pristine environment, which can cause behavioural disturbance, hearing damage, and persistent stress in marine animals. Passive acoustic monitoring (PAM) is used to explore marine soundscapes and acoustically detect marine mammals. Acoustic detections can aid in the creation of conservation regulations to protect marine species. Employing a human expert to manually analyze these very large (multi-year) data sets is time-consuming and costly, which has motivated the development of automated analysis methods. Deep learning methods, specifically convolutional neural network architectures, have previously been successfully applied to detect a variety of marine species vocalizations within PAM data. Ringed seals, a species of Arctic seal, were listed as a species of special concern in Canada in 2019, but to date no practical acoustic detector exists for this species. In this work, state-of-the-art deep learning architectures are applied to terabytes of PAM data containing ringed seal vocalizations to create the first practical and reliable ringed seal vocalization detector. The ringed seal detector is part of a long-term goal to create a single acoustic detector for multiple Arctic marine species. The trained detector will be available as an open-source tool for researchers to use as the basis for further development of new automated detectors.

BIOMEDICAL ACOUSTICS AND ULTRASONICS - ACOUSTIQUE ULTRASONIQUE ET BIOMÉDICALE

Characterization of Noise Produced During Continuous and Sparse Sampling Functional Magnetic Resonance Imaging

Olivier Robin [*1], **Félix Le Moigne-Le Dem** [†1], **Pascal Tétreault** [‡2], **Dominique Lorrain** [§3], **and Vivien Staehle** [¶4]
[1]Centre de Recherche Acoustique-Signal-Humain, Université de Sherbrooke, Canada.
[2]Faculté de médecine et des sciences de la santé, Département d'anesthésiologie, Université de Sherbrooke, Canada.
[3]Faculté des lettres et sciences humaines, Département de psychologie, Université de Sherbrooke, Canada.
[4]Phonoptics, 8 Rue Jean Mermoz, 91080 Courcouronnes, France

1 Introduction

Noise is generated during magnetic resonance imaging (MRI) and comes from the gradient magnetic field (Lorentz forces acting on the gradient coils) and radiofrequency pulses used to generate sequences for scanning [1–3]. Characterizing this noise is complicated by the fact that sensors without any metal parts must be used, given the intense magnetic fields present in MRI. Also, the typical continuous acquisition scheme that generates continuous noise is hardly compatible with auditory-related experiments. To avoid or reduce noise during stimulus presentation, the use of headphones, sound absorbing material or even active noise cancellation have been considered. Another approach to decrease the level of the interfering noise is the implementation of less noisy MRI sequences. Sparse sampling functional MRI [4] has been suggested and involve the acquisition of imaging volumes interspersed with silent periods (i.e. no acquisition periods). This communication describes the use of optical fiber microphones to characterize the noise produced during continuous and sparse sampling functional MRI sequences. The instrumentation chain is described, along with the preliminary results obtained in terms of overall sound pressure level and time-frequency content.

2 Magnetic Resonance Imaging

MRI is a noninvasive medical imaging test that can produce highly detailed images of almost every internal structure in a living body (this can include organs, bones, muscles and even blood vessels) and help to establish diagnostics. No ionizing radiation is produced during a MRI tests (unlike X-rays), since MRI scanners create images of the body using radio waves and a large magnet (magnetic flux densities from 1.5 Tesla up to 10 Tesla are typically used). The scanner uses the effect of nuclear magnetic resonance and the differences in relaxation processes between different tissues to generate an image contrast. In parallel, functional MRI (fMRI) allows measuring brain activity since neuronal activation and cerebral blood flow are coupled (an increase in neuronal activity is followed by an increase in the flow of oxygenated blood, therefore the term Blood-Oxygen Level Dependent - BOLD - response is used). Combining functional and structural images allows linking physiological processes to the anatomical structures of the human brain and exploring neural activity with a spatial resolution of a few millimetres and a temporal resolution of several seconds (electrophysiological methods like electroencephalograms - EEG - provide on their side a poor spatial resolution, in the order of several centimeters, but a fine temporal resolution in the order of few milliseconds). MRI comes with some limitations that are linked to the noise but also the strong electromagnetic field it generates, that exclude people having metallic implants or cardiac pacemakers but also the use of sensors using ferromagnetic materials.

3 Instrumentation, data acquisition and measurements

To measure noise in a MRI, a remote microphone using a tube can be used, but this requires the use of a correction transfer function [5]. Microphones that do not include ferromagnetic parts like fiber optic microphone are also a possible solution that is here evaluated, in order to be able to perform *in situ* (and not remote) measurements. The two considered microphones are manufactured by Phonoptics and depicted in Figure 1. The Alpheus microphone has a 3 mm diameter with a 15 mm length, and a sensitivity of 0.3 mV/Pa, while the Evotis microphone has a 10 mm diameter, a 23 mm length and a sensitivity of 10 mV/Pa. The patented technology follows a

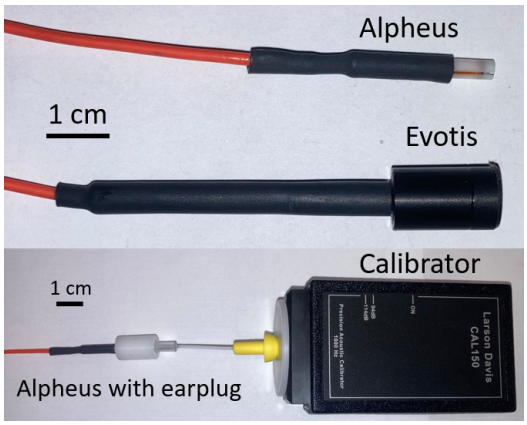

Figure 1 – Pictures of the optical fiber microphones.

a light intensity modulation principle and relies on a single optical fiber with an associated conditioning unit that provides the one light source, one photo-detector and one splitter. It also features 3-level signal amplification, headphone and BNC AC outputs, SMA DC output for sensor integrity monitoring and a USB 44 kHz, 16 bit, digital output. In order

*. olivier.robin@usherbrooke.ca
†. Felix.Le.Moigne-Le.Dem@USherbrooke.ca
‡. Pascal.Tetreault@USherbrooke.ca
§. Dominique.Lorrain@USherbrooke.ca
¶. vivien.staehle@phonoptics.fr

to be able to perform noise measurements as close as possible to the eardrum, adaptors were 3D-printed to link microphones with 3M™ E-A-R™ UltraFit™ probed test earplugs. A data acquisition program was developed to perform measurements using the direct output from the conditioning unit as a sound device. The program includes a frequency-calibration step, the acquisition and visualization of signals (as a function of time, frequency and time-frequency) and the calculation of equivalent sound levels (L_{eq}). It can be run through the Matlab interface, but a standalone version was also created. To validate the whole measurement chain, a comparison with a Bruel&Kjaer half-inch microphone connected to a Bruel&Kjaer Connect data acquisition system was performed in hemi-anechoic conditions.

4 Results

The presented results were generated using measurements made with the Evotis microphone. The acquisition computer was placed in the control room (out of the magnetic field), the microphone was calibrated in the same room and then positioned at 1 meter from the MRI coil's center. Since the optical fiber involves negligible losses, a 20-meter fiber is used and allows a convenient connection between the control room and the MRI, while preventing mechanical stress and excessive curvature on the fiber. The background noise was first measured and the estimated 1-second L_{eq} was 70 dB (re. 2e-5 Pa), and mostly linked the MRI cooling system functioning. The MRI noise was then characterized in standard acquisition mode, see Figure 2 in which raw time signal, spectrogram and $L_{eq,1s}$ are provided. As the noise generated by MRI is cyclic (see Figure 2(a)), measurement results are only shown over 3 seconds. According to the spectrogram (see Figure 2 (b)), a time-modulated harmonic and tonal high-level noise is generated. The mean L_{eq} equals 102.1 dB (re. 2e-5 Pa). MRI noise during compressed (or sparse) acquisition is finally characterized, see Figure 3. The MRI now only generate noise during 1 second at 3-second intervals. The results show that the measured L_{eq} reaches the background noise level between acquisition steps, leading to an effective 30 dB difference.

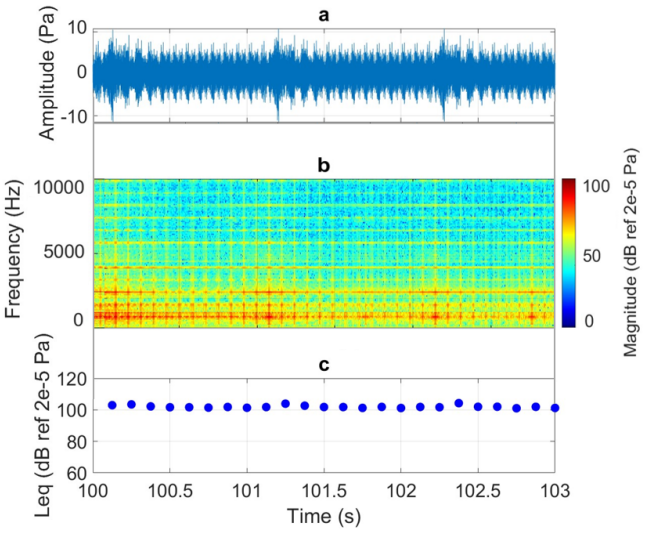

FIGURE 2 – FRMI with continuous acquisition - (a) Raw time signal ; (b) Spectrogram ; (c) 1/8-second Leq.

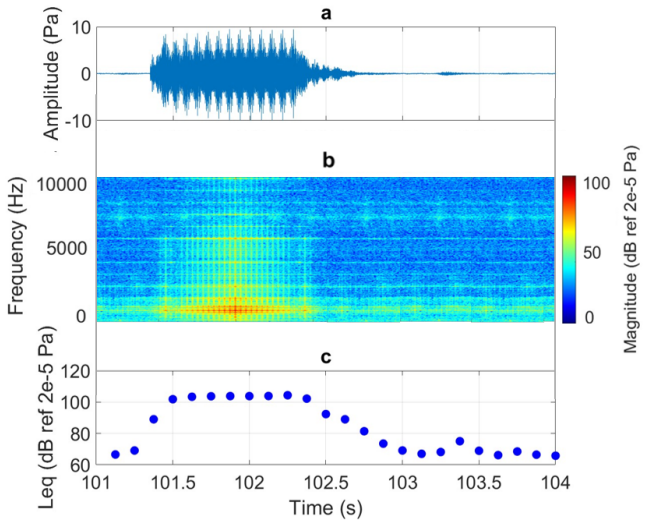

FIGURE 3 – FRMI with sparse acquisition - (a) Raw time signal ; (b) Spectrogram ; (c) 1/8-second Leq.

5 Conclusion and perspectives

The use of optical fiber microphones for noise measurements during MRI together and the development of a tool for convenient acquisition and processing of signals were both validated. Future works will include the presentation of various acoustic stimuli during fMRI but also using EEG, and the analysis of corresponding neuroimages and recordings to enlarge our knowledge of the auditory processes. An improved understanding of the perception of sound alarms in order to improve their design is an underlying goal.

Acknowledgments

This research was funded by the *Programme d'appel à projets pour la recherche interdisciplinaire et interfacultaire*, from Université de Sherbrooke.

References

[1] S .M. Jacobs et al. Image quality and subject experience of quiet T1-weighted 7-T brain imaging using a silent gradient coil. *European Radiology Experimental*, 6(36) :337–346, 2022.

[2] D. Price et al. Investigation of acoustic noise on 15 MRI scanners from 0.2 T to 3 T. *Journal of Magnetic Resonance Imaging*, 13(2) :288–293, 2001.

[3] M. McJury. Acoustic noise and magnetic resonance imaging : A narrative/descriptive review. *Journal of Magnetic Resonance Imaging*, 55(2) :337–346, 2022.

[4] S. Uppenkamp. Functional neuroimaging in hearing research and audiology. *Zeitschrift für Medizinische Physik*, 31(3) :289–304, 2021. Special Issue : Audiology.

[5] S. Benacchio et al. Use of magnetic resonance image registration to estimate displacement in the human earcanal due to the insertion of in-ear devices. *The Journal of the Acoustical Society of America*, 146(4) :2452–2465, 10 2019.

MINIATURIZED ACOUSTIC CONCENTRATORS FOR LOCAL GENERATION OF ULTRASONIC WAVES

Ibrahima Touré [*1] **and Nicolas Quaegebeur** [†1]
[1]CRASH-UdeS - Dept of Mechanical Engineering, Université de Sherbrooke, Québec.

1 Introduction

3D ultrasound imaging is an essential medical imaging technique used for diagnosing and monitoring diseases. It is based on the use of ultrasonic waves to create real-time, non-invasive images of soft tissues [1]. To form these images, virtual sources are usually used as emitters, enabling the creation of diverging or planar ultrasonic beams from different virtual positions. This approach offers greater flexibility in exploring the region of interest and reach high frame rates up to 10 kHz [1]. Research has been conducted to optimize the use of these virtual sources and improve the quality of the obtained images [2]. However, there are challenges related to a low sensitivity of the virtual sources, their positioning, and the complexity of multiplexing. To overcome these obstacles, the use of miniaturized concentrators based on cylindrical waveguides is emerging as a promising solution. The approach adopted is described in Figure 1 and opens up new possibilities in the field of 3D ultrafast imaging.

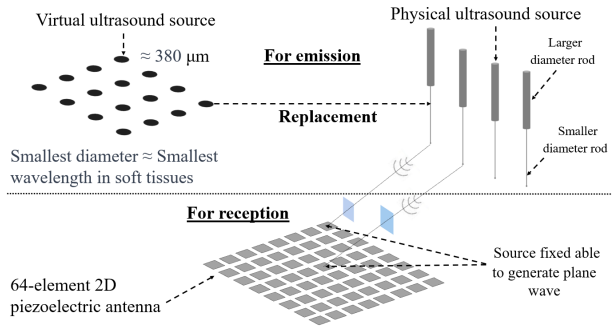

Figure 1: Transition from virtual ultrasound sources to physical ultrasound sources based on waveguides for ultrafast 3D imaging.

2 Transmission and Reflection in Axisymmetric Waveguides

2.1 Propagation of Axisymmetric Longitudinal Waves in a Cylindrical Waveguide

The propagation of axisymmetric longitudinal waves in a cylindrical rod with a uniform cross-section are theoretically described by the Pochhammer-Chree equations [3]. The elastic properties of the rod are taken into account. The frequencies of interest for this study range from 20 kHz to 2 MHz. The axisymmetric longitudinal modes are characterized by the radial displacement (u) and axial displacement (w) in the cylinder. Eq.1 describes the relationship between the wavenumbers (k and q) and the frequency (f) of the axisymmetric longitudinal modes in the cylinder.

$$\frac{2p}{a}(q^2+k^2)J_1(pa)J_1(qa) - (q^2-k^2)^2 J_0(pa)J_1(qa)... \\ -4k^2pqJ_1(pa)J_0(qa) = 0 \quad (1)$$

Where a represents the radius for a given rod, p and q are related to the wavenumber. This dispersion curve $k(f)$ is obtained by numerically solving the Pochhammer-Chree equation and allows the determination of the allowed propagation modes in the cylindrical rod.

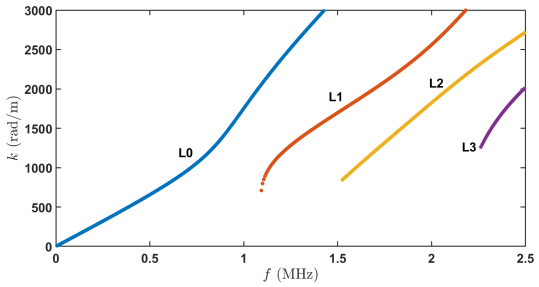

Figure 2: Dispersion curve of axisymmetric longitudinal modes in the rod: wavenumber (k) as a function of frequency (f).

2.2 Transmission and Reflection of Axisymmetric Longitudinal Waves in a Variable Cross-Section Guide

The propagation of modes in a waveguide with a variable cross-section is illustrated by the diagram in Figure 3. This guide allows the transmission of a mode from a large-diameter cylindrical rod (D_1) to a small-diameter cylindrical rod (D_2). The study is conducted in the frequency domain by considering a 2D axisymmetric FEM model in COMSOL Multiphysics 6.0 with MATLAB. The model parameters, such as the material (stainless steel), waveguide length, maximum phase velocity, maximum and minimum wavelengths, as well as the PML length and mesh element size are taken into account. The modes are normalized with respect to the incident energy to determine the transmission and reflection coefficients.

2.3 Numerical Results

At $f = 1$ MHz, only the L0 mode propagates effectively in the guide. For low diameter ratios $D_2/D_1 < 0.75$, the

[*]ibrahima.toure@usherbrooke.ca
[†]nicolas.quaegebeur@usherbrooke.ca

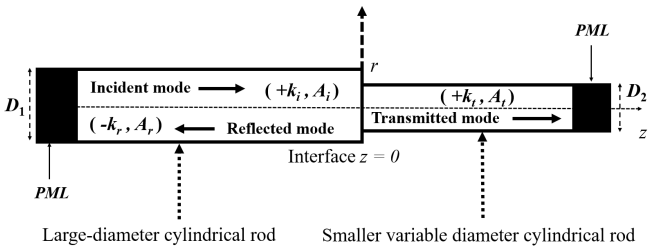

Figure 3: Transmission of a mode in a guide with a variable cross-section.

energy transmission is below 80 %. However, for ratios $D_2/D_1 \geq 0.75$, the energy transmission is complete. This relationship between the diameter ratio and energy transmission is illustrated in Figure 4. This analysis demonstrates the

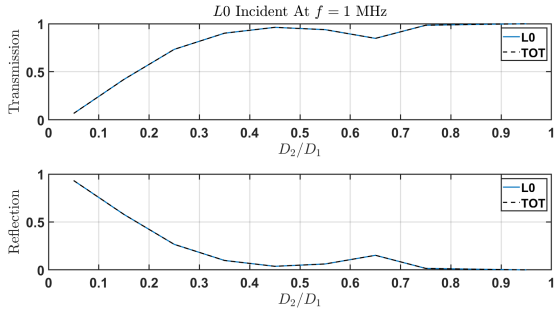

Figure 4: Energy transmission and reflection for the incidence of an L0 propagating mode at a frequency of 1 MHz as a function of the diameter ratio D_2/D_1 between the reducer and the base waveguide.

influence of the diameter ratio on energy transmission and reflection in a variable cross-section waveguide, highlighting the conditions favorable for efficient transmission of ultrasonic waves.

3 Preliminary Experimental Study

The experimental setup used is illustrated in Figure 5. In this

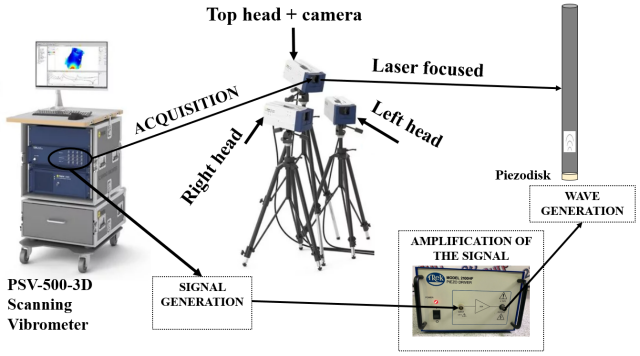

Figure 5: Experimental setup.

experiment, a 3D laser vibrometer is used to measure the vibrations of the cylindrical rod. The generation of ultrasound is performed using a 5A-type piezodisk, with a diameter of 5 mm and a thickness of 0.5 mm. For vibration measurements, a single 3D laser Doppler vibrometer head is used, consisting of an upper head and a camera. A stainless steel cylindrical rod is used. It has a length of 1.2 m and a diameter of 6.3 mm. The piezodisk is attached to the base of the rod using epoxy glue. A pseudo-random input signal amplified with a piezo amplifier is used to excite the piezodisk. Post-processing of the data is performed using a 2D FFT method to convert from the spatial domain (x, t) to the wavenumber-frequency domain (k, f). Figure 6 shows the longitudinal and flexural modes that propagate in the guide. The matrix pencil method is then used to extract only the longitudinal modes, characterized by their amplitudes and wavenumbers.

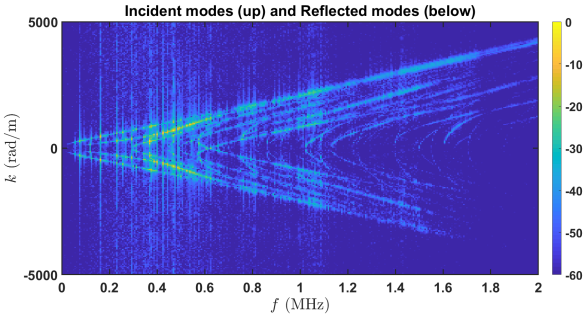

Figure 6: Incident and reflected modes obtained experimentally using 2D FFT for the steel rod.

4 Conclusions

Numerical simulations were used to determine the optimal diameters of a reducer (D_2) used in the imaging domain. The performance of the reducer was evaluated through preliminary simulations, which selected a minimum diameter of 0.381 mm to ensure efficient operation. In parallel, experimental results obtained using a 3D LDV will be used as a reference to measure the longitudinal modes in different variable cross-section guide models. The goal is to detect and characterize these modes. These two types of results, from numerical simulations and experiments, play an essential role in understanding the performance and characteristics of reducers and variable cross-section guides. They will serve as a basis for future studies, improvement of designs, and exploration of new applications in the fields of imaging and acoustic technologies.

References

[1] Jean Provost, Clement Papadacci, Juan Esteban Arango, Marion Imbault, Mathias Fink, Jean-Luc Gennisson, Mickael Tanter, and Mathieu Pernot. 3d ultrafast ultrasound imaging in vivo. *Physics in Medicine & Biology*, 59(19):L1, 2014.

[2] Goulven Le Moign, Nicolas Quaegebeur, Patrice Masson, Olivier Basset, Marc Robini, and Hervé Liebgott. Optimization of virtual sources distribution in 3d echography. In *2019 IEEE International Ultrasonics Symposium (IUS)*, pages 904–907. IEEE, 2019.

[3] J. D. Achenbach. *Wave propagation in elastic solids*. Number v. 16 in North-Holland series in applied mathematics and mechanics. North-Holland Pub. Co. American Elsevier Pub. Co, Amsterdam New York, 1973.

NUMERICAL ANALYSIS OF ENERGY DENSITY DISTRIBUTION IN THE HUMAN LUNGS UNDER LOW-FREQUENCY ACOUSTIC EXCITATION

Arife Uzundurukan [*1,2], Sébastien Poncet [¶1,2], Daria Camilla Boffito[†3], and Philippe Micheau[‡1,2]

[1] Department of Mechanical Engineering, Université de Sherbrooke, Sherbrooke, Québec, Canada

[2] Centre de Recherche Acoustique-Signal-Humain de l'Université de Sherbrooke, Sherbrooke, Québec, Canada

[3] Department of Chemical Engineering, Polytechnique Montréal, Montréal, Québec, Canada

1 Introduction

The standard treatment for chest physiotherapy is clapping, which causes vibrations on the chest surface. It affects the viscoelastic, shear-thinning, and thixotropic properties of bronchial mucus, liquefying it to ease expectoration. Acoustic airway clearance devices (AACD) could be up to 1.8 times more effective than the standard treatment [1]. Therefore, with the help of such acoustic medical devices, high-frequency chest compression (HFCC) therapy is currently the most common way to relieve excessive mucus accumulation.

Despite the fact that HFCC therapy has been shown to improve lung function and mucociliary clearance, further research is necessary to optimize the AACD used [1,2,3]. For that reason, computed tomography-based numerical finite element analysis (CT/FEA) is necessary to obtain accurate results for the kinetic and elastic energy densities of the lungs under the frequency domain [2,4].

In a previous study, the average kinetic energy density and the strain energy density under 5-100 Hz have already been examined [2]. Nevertheless, no work has yet to be done so far to examine the influence of acoustic harmonic excitation in the low-frequency range on the interior of 3D lungs. This study aims at investigating the human lungs under AACD with a 3D-validated realistic CT/FEA of the human thorax using COMSOL 6.1 Multiphysics®.

2 Method

2.1 CT Thorax Model and Material Properties

In order to achieve accurate results from a 3D CT/FEA, image processing is deemed necessary for having realistic geometries [4]. The physical properties of the human thorax depend from one person to another in terms of weight, height, and chest size. For that reason, in this study, we use a validated CT based human thorax data [5] in order to overcome the effects of the different extreme physical features of the human and represent the average results.

Each internal organ, trachea and bronchioles, lungs, rib cage, and soft tissues are displayed in Figure 1 before assembling the thorax. They were created by using image processing of the CT data.

*arife.uzundurukan@usherbrooke.ca

¶sebastien.poncet@usherbrooke.ca

†daria-camilla.boffito@polymtl.ca

‡philippe.micheau@usherbrooke.ca

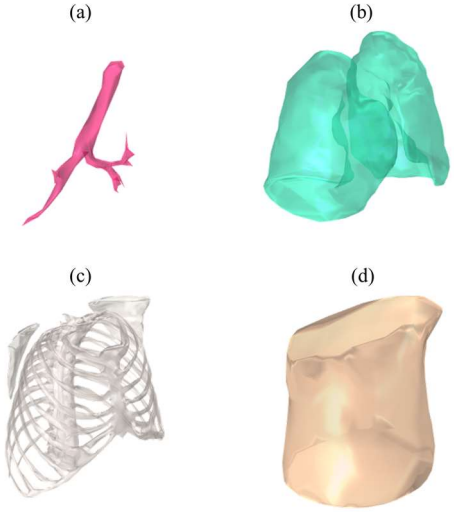

Figure 1: CT based realistic modelling of (a) trachea and bronchioles, (b) lungs, (c) rib cage, and (d) soft tissues for human thorax modelling

To represent the essential characteristics of the human internal organs, the complex material properties of the thorax are handled. Moreover, to simplify the representation of micropore structure and viscoelasticity, different models are used. For example, the Voight model is particularly useful for osseous and soft tissue regions. The material properties of the lungs have been improved by using the Biot's theory [2]. To homogenize the heterogeneous, fully saturated material features of the lungs, this theory is used to calculate the complex fast compression waves and slow compression waves as well as shear wave speeds [2].

2.2 CT-Lung Frequency Domain Analysis

The final geometry is decomposed into 14 domains, and gathers 10k boundaries, 15k edges, and 5k vertices. The complete mesh comprises 292k tetrahedra, 53k triangles, 33k edge elements and 5k vertex elements. It leads to a good mesh quality, with an average skewness quality of 0.58.

For gentle drainage of the mucus in the lungs, numerical acoustic studies selected the low-frequency range to be applied to the human chest wall under harmonic excitation. The acoustic harmonic excitation is investigated here by using a 28 mm radius cylinder as an effect of AACD with 146 dB_{SPL}. The result took about 2 h 30 min with the processor Intel(R) Core (TM) i7-9700 CPU @ 3.00 GHz with 16 GB RAM memory.

3 CT/FEA Acoustic Analysis Results

3.1 Kinetic Energy Density

The kinetic energy density distributions for the lungs under 30 Hz and 41 Hz are displayed in Figure 2. It could be deduced that the kinetic energy density of the lungs under 30 Hz excitation is accumulated mainly on the sternum and the lung part near the sternum; however, at 41 Hz, the middle region of the lungs seems to be more affected.

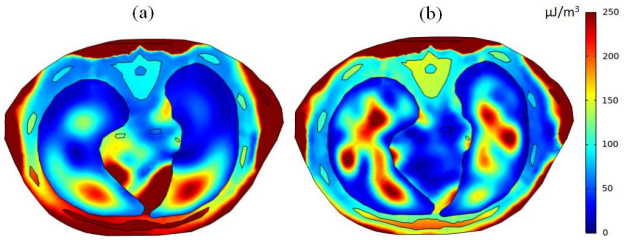

Figure 2: Kinetic energy density results of the human thorax at (a) 30 Hz and (b) 41 Hz

3.2 Elastic Strain Energy Density

The elastic energy density distribution results for the lungs under 32 Hz and 42 Hz are illustrated in Figure 3. Even though the average values are the same and match the results from the literature [2], the distributions in the lungs are different from one case to the other.

Moreover, as they are the most rigid materials in the human thorax, the highest strain energy density appears to be stored in the osseous region, such as the rib cage and scapula, as expected.

4 Discussion

The kinetic energy density in the low-frequency range appeared very sensitive to the applied frequency between 30 and 41 Hz, especially in the softer materials, like soft tissues and lungs. On the other hand, it is obvious that the strain energy density in the osseous region is higher than that of the lungs. This is mainly due to the material properties of the lungs, which are the softest material among the other biomaterials.

Despite the fact that two different frequencies have been applied to the human chest surfaces, the average values remain the same as 180 μJ/m^3 at both 32 Hz and 42 Hz, as indicated in Table 1 [2]. In this study, notwithstanding, it is revealed that their effects on the lungs differ from each other. Therefore, in order to decide the optimum frequency range in HFCC therapy, more numerical studies are needed. Owing to the fact that the characteristic size of the mucus layer is infinitely small compared to the dimensions of the human thorax, the mucus properties are not considered in this study.

5 Conclusion

In this study, the internal effects of HFCC on the lungs under an AACT device are clarified by numerical simulations. This paper revealed the kinetic and elastic strain energy density distributions on the human lungs using CT/FEA at four different peak frequencies. Though similar average values are obtained for two different frequencies, an insight into the local distributions shows that frequencies around 41 Hz lead to more homogeneous kinetic and elastic strain energy density distribution in the lungs.

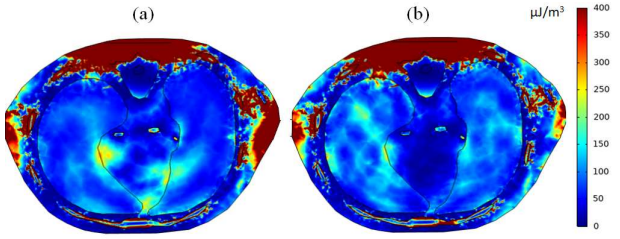

Figure 3: Elastic strain energy density results of the human thorax at (a) 32 Hz and (b) 42 Hz

Table 1: Comparison of the analysis results with respect to average peak values [2]

Average Feature	Peak Value (μJ/m^3)	Frequency (Hz)
Kinetic Energy Density	56	30
	46	41
Elastic Strain Energy Density	180	32
	180	42

As a future study, a set of new numerical simulations coupling acoustics and computational fluid dynamics are planned to imply the mucus properties. The objective will be to identify the frequency of optimizing the mucus transport in the lungs.

References

[1] L. G. Hansen, and W. J. Warwick, "High-frequency chest compression system to aid in clearance of mucus from the lung," Biomedical Instrumentation & Technology, 24(4), pp. 289-294, 1990.

[2] A. Uzundurukan, S. Poncet, D. C. Boffito, and P. Micheau, "Examination of the Behaviour of Lungs under High-frequency Chest Compression Airway Clearance Therapy," CSME/CFD Canada 2023 International Congress, Sherbrooke, Canada, pp. 1-4, in press, 2023.

[3] D. Schieppati, R. Germon, F. Galli, M.G. Rigamonti, M. Stucchi, and D.C. Boffito, "Influence of frequency and amplitude on the mucus viscoelasticity of the novel mechano-acoustic Frequencer™," Respiratory Medicine, 153, pp. 52-59, 2019.

[4] S. M. B. Netto, A.C. Silva, R. A. Nunes and M. Gattass, "Automatic segmentation of lung nodules with growing neural gas and support vector machine," Computers in Biology and Medicine, vol. 42, no 11, pp. 1110-1121, 2012.

[5] A. Uzundurukan, S. Poncet, D. C. Boffito, and P. Micheau, "Computed Tomography-Based Finite Element Model of the Human Thorax for High-Frequency Chest Compression Therapy," Proceedings of the 10th International Conference on Biomedical Engineering and Systems (ICBES 2023), London, United Kingdom, in press, 2023.

Abstracts for Presentations without Proceedings Paper
Résumés des communications sans article

Printing Beyond Barriers Using Ultrasound In Direct Sound Printing

Mohsen Habibi, Shervin Foroughi, Muthukumaran Packirisamy

Direct sound printing (DSP) is a new class of additive manufacturing processes in which chemical reactions during the 3D printing process are driven by sonochemical route using cavitation bubbles induced by focused ultrasound waves. The present paper aims at elaborating on the remote distance printing (RDP) aspect of this approach and consequent applications. RDP is a new paradigm introduced by DSP method in which the printing location is not accessible by common energy sources like light or heat. In this situation, ultrasound could penetrate optically opaque materials and conduct printing without direct access to the printing location. This concept opens a wide variety of applications in engineering or medical fields. The focus of this paper is the application of DSP-RDP in biomedical application to print objects inside body without open surgery in a non-invasive manner. Ultrasound penetrates skin and tissues in DSP and is focused on the printing location inside body where the printing material is injected. This work explains DSP in detail and the interaction of the sound with the printing material and how the material is transformed from liquid to solid. The process is demonstrated using a test study conducted using tissue phantoms and also real porcine tissue. The polymerization progress is characterized using Fourier transform infrared measurements of Si-H bands of the printed material. This work opens new applications to 3D print with ultrasound where no other 3D printing approaches can achieve.

EDUCATION IN ACOUSTICS - ÉDUCATION ET ACOUSTIQUE

UNDERSTANDING THE SKILL GAP OF POST-SECONDARY GRADUATES ENTERING THE ACOUSTIC CONSULTING PROFESSION

Abigail Farkas*[1]
[1]Stantec Consulting Ltd, Mississauga, Ontario, Canada

1 Introduction

The acoustic consulting profession in Canada is comprised of consultants with a diverse range of technical backgrounds as formal acoustics-based education programs remain limited in provinces and territories. As a result, currently, post-secondary graduates lack the necessary skillsets to meet the needs of consulting firms that would benefit from these employees entering the workforce.

This skills gap between post-secondary education and the acoustic consultant industry is investigated through a survey of practicing acoustic consultants. Results from the survey are summarized to assess the most in-demand skills for the next generation of acoustic professionals with a focus on educational program development. The results of this survey may also give valuable insight to new graduates on how they can educate themselves on these critical skills to give them an advantage as they start a career in acoustic consulting.

2 Methodology

2.1 Creating the survey

A literature review was conducted on similar past studies and publications, which served as a resource of what type of questions would be asked in such a survey. One referenced study was conducted in India, which focused on the employability of newly graduated engineers with no particular specialization [1].

Based on this review, a 25-question survey was created to gather opinions and anecdotes from working acoustic consultants on the topics of demographics, hiring, job skills, and education. The survey is a combination of multi-select and write-in answers which were summarized to determine trends and commonalities.

Participants

This survey was sent to actively working acoustic consultants in firms of varying size and specialties. There were 28 Canadian participants located in Ontario, Quebec, and Nova Scotia and 15 international participants from the United States, United Kingdom, and Australia.

This survey was voluntary for all participants, who were informed of the purpose of the survey and what their answers would be used for. They were also informed that the survey was anonymous.

Although this study is conducted with the focus on the lack of Canadian post-secondary education in acoustics, international opinions are of particular interest as there is more awareness and opportunities for acoustics-focused formal education globally.

2.2 Validation of the survey

Both quantitative and qualitative methods were employed in order to establish the validity of the survey. The survey was expert reviewed to determine the face validity and content validity in relevance to the topic at hand. Potential biases or ambiguity stemming from the wording or ordering of questions were discussed and minimized. Pre-testing was conducted with a small sample of respondents who filled out the survey in the presence of the survey conductor in order to gather their immediate thoughts on the clarity and ease of answering the survey.

For quantitative validation, the answers to the multi-select questions were analyzed using Cronbach's Alpha [2]. This determines the consistency of responses across questions. In a range of 0 to 1, 0.7 is considered the minimally acceptable benchmark value for internal consistency. The Cronbach's Alpha for the collected dataset of this survey was calculated to be 0.87, therefore validating the multi-select questions.

3 Results

3.1 Education

When asked what they would consider to be the ideal diploma held by a potential new hire, 75.0% of Canadian consultants answered a Bachelor of Engineering of varying specialties. 17.8% responded with a B.Sc or B.A.Sc in relevant disciplines such as physics and architecture, and 7.2% answered with an international Bachelor's in Acoustics.

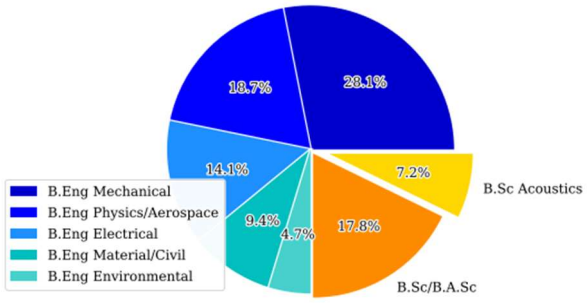

Figure 1: Ideal diploma for Hire Candidates According to Canadian Acoustic Consultants.

In comparison, two-thirds of international consultants answered that they considered a degree in acoustics to be the ideal diploma.

*abigail.farkas@stantec.com

In response to what knowledge and skills needed for acoustic consulting, regardless of degree and nationality, consultants believed to be missing from post-secondary education, answers could be sorted into three main categories: in-depth acoustical theory, applied multidisciplinary acoustics concepts, and practical consultancy skills. Within the category of theoretical acoustics, consultants specified in which specializations they believed more education was needed: vibrations and waves through solid state material, and reflections and propagation of sound in buildings. Practical consultancy skills included mentions of technical report writing, client interfacing, and project procedure.

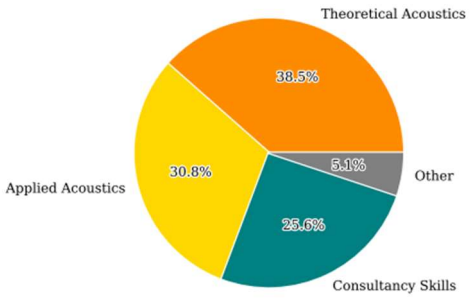

Figure 2: Critical Acoustic Consulting Education Missing from Post-Secondary Programs, According to Participant Consultants.

3.2 Employment

The consultants were asked what they looked for the most when reviewing resumés of candidates for hiring. Responses fell into three main categories: soft skills and culture fit; fundamental math, physics, or acoustic skills; consultancy skills.

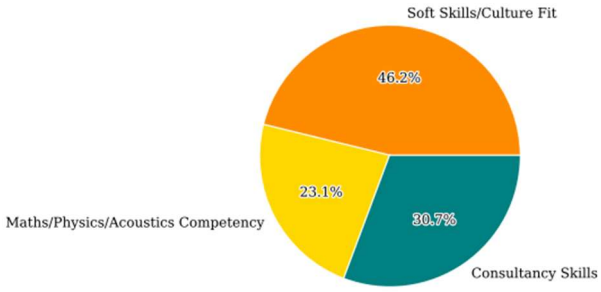

Figure 3: Most Important Qualifications of Potential Hires, According to Participant Consultants.

When asked what the biggest challenge they faced in hiring new team members, 60% of consultants answered that they're having trouble simply finding people who are interested and have the right competencies. 26% of consultants answered that they have trouble finding qualified candidates with industry skills and background. 14% indicated other difficulties, such as getting candidates up to speed on projects.

4 Discussion

Almost one-third of all consultants answered that a degree in Mechanical Engineering was most ideal for new candidates, while there is more spread for other engineering specialties. It can be stated that specialties in which a consultant works is the largest influence on which diploma they believe would benefit a candidate the most; all participant consultants have experience in a combination of environmental acoustics, architectural acoustics, and/or vibration, with experience in other specializations such as aeroacoustics and psychoacoustics to lesser degrees.

Regardless of degree, consultants have expressed that they believe there to be a lack of education in the critical areas which compose the work of acoustic consulting. Even so, soft skills such as eagerness to learn and ability to communicate ideas are stated to be of almost equal importance when considering a candidate to hire.

From the consultants' perspectives on the difficulty of hiring, only approximately 30% of consultants use external resources such as job boards and university databases to find candidates. This implies that consultants aren't reaching a wider audience of potential candidates, and candidates aren't aware that these job opportunities exist for them to aim for.

However, in contrast to the idea that the lack of Canadian post-secondary education in acoustics is negatively affecting the employment rates of new graduates, 85% of consultants answered that they were at least "very likely" to hire a new graduate within the next 10 years, and 20% said they had active plans to hire a new graduate within the next 5 years.

5 Conclusion

With the focus on educational program development for the purposes of preparing graduates for a potential career in acoustic consulting, the first step is promoting awareness of the field to the student bodies of relevant faculties. Courses could be offered that teach acoustics from a multidisciplinary/multispecialty perspective such as environmental attenuation, propagation through buildings, and solid matter vibration.

When it comes to finding employment, graduates have very positive prospects if they take the initiative to educate themselves in these areas that their degree failed to cover, and to personally connect with working acoustic consultants to express their interest in the field.

Acknowledgments

This study would not have been possible without the support of Stantec Consulting Ltd.

References

[1] A. Blom, H. Saeki. Employability and Skill Set of Newly Graduated Engineers in India. The World Bank South Asia Region Education Team (2011).

[2] L.J. Cronbach. Coefficient Alpha and the Internal Structure of Tests. Springer Science and Business Media LLC (1951).

TEACHING CONCEPTS OF ACOUSTICAL WAVES IN AIR, PART 2

William J. Gastmeier,
HGC Engineering, Mississauga, Ontario, Canada

1 Introduction

This paper has been written to participate in the "Teaching Acoustics" session at the 2023 Acoustics Week in Canada. It builds on Part 1 which was presented at the 2022 Acoustics week in Canada and contains materials from 30 years of teaching Architects at the University of Waterloo and Dalhousie University. The goal is to provide teachers with practical demonstrations to enhance learning. "Hands on" teaching methods can engage multiple senses to be effective using sight and sound as well as written material.

Part 1 dealt primarily with sound propagation in air and the concepts of longitudinal wave motion, speed, frequency and wavelength and related effects which relate to what we perceive as pitch. Part 2 expands on those concepts by discussing superposition, identifying the concept of source path and receiver, and introducing the definition of sound pressure, decibels and the decibel scale which correlate with loudness. If time permits, or perhaps in a third installment, we will examine the hearing mechanism to discern how we physically perceive pitch and loudness.

2 Principle of Superposition

While waves do interfere (combine their pressure) at a point in space, they successfully pass through each other without changing. That is why a sound maintains its character in the presence of other sounds as in Figure 1.

Figure 1: Principle of Superposition [1].

3 Source, Path and Receiver

An acoustical situation comprises three basic éléments as shown in Figure 2. If a sound is desirable, favourable conditions are provided for its production, transmission and reception and the listener relieved of distractions like competing noise.

If sound is undesirable, unfavourable conditions are provided for its the production, transmission and reception. These measures belong to the realm of noise control.

* bill@gastmeier.ca

Figure 2: Source, Path, Receiver [2].

4 Sound Pressure

Of all the quantities which could be used to characterize the "strength" of a sound wave (particle velocity, displacement, intensity, power, etc) the most amenable to measurement is sound pressure.

The variation in pressure caused by speech, music or noise is shown in the following figure. Most sounds in the everyday world are complex (Figure 3) consisting of a variety of pressures of different frequencies which vary with time.

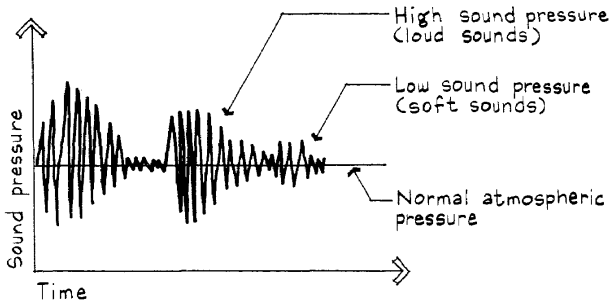

Figure 3: Complex Sounds [2].

The range of audible sound pressures is 20 micro-Pascals to 100 Pascals. Atmospheric pressure is approximately 100,000 Pascals. The quietest sound a normal hearing individual can hear is approximately 20 µPascals (0.00002 Pascals).

5 The Decibel Scale

The decibel scale is a logarithmic scale used to describe sound levels. It was named after its inventor, Alexander Graham Bell. We define the Sound Pressure Level (SPL) in decibels (tenths of a Bell) to be:

$$\mathrm{SPL} = 20\log_{10}(p/p_{\mathrm{ref}}) \quad (\mathrm{dB}), \qquad (1)$$

where the reference pressure is

$$p_{\mathrm{ref}} = 20\mu\ \mathrm{Pa} = 20\cdot 10^{-6}\ \mathrm{Pa} = 2\cdot 10^{-5}\ \mathrm{Pa}. \qquad (2)$$

The range of audible sound pressures (20 µ Pascals to 100 Pascals) is a ratio of 5 million to one. If a bathroom scale had the same sensitivity range as the human ear, it would be able to weigh both a human hair and a building. The decibel scale compresses this range of audible sound pressures into a

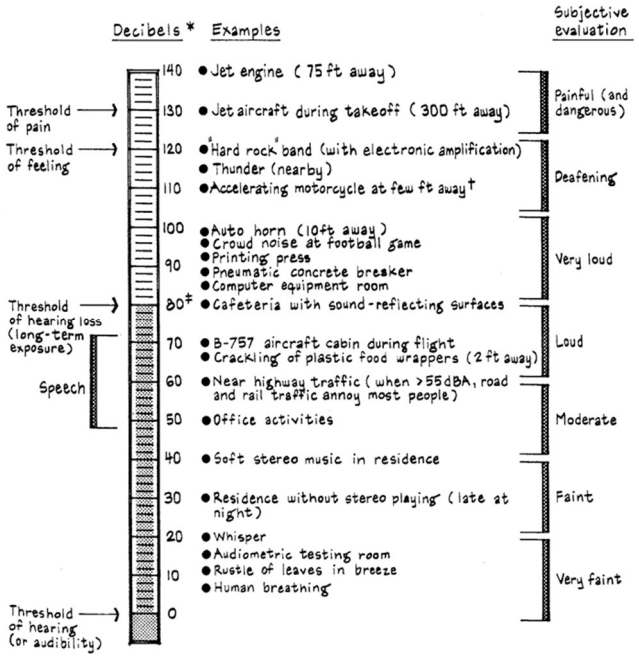

Figure 4: The Decibel Scale [2]

more intuitively understandable scale which correlates well with our perception of loudness.

The ear hears logarithmically, not arithmetically. That is why a logarithmic scale correlates closely with our perception of loudness. In other words, the ear judges louness of sounds by the ratio of their pressures, not by arithmetic addition.

1. A 1 decibel change in sound level is not perceptible to most individuals.
2. A 3 dB increase is "just perceptible".
3. A 5 dB increase is "clearly perceptible".
4. A 10 dB increase is regarded as twice as loud.
5. "0 dB" is not an absence of sound, it is a sound level equal to the reference level which was chosen to be the average threshold of hearing.
6. Decibels do not add arithmetically. They add logarithmically (Figure 5). 60 dB + 60 dB is not = 120 dB, 60 dB + 60 dB = 63 dB

$$\mathrm{SPL_{TOT}\,(dB)} = \mathrm{SPL_1(dB)} + 10\log_{10}(N) \qquad (1)$$

where N = # of sources of equal magnitude.

6 Audio Demonstrations

A set of Audio Demonstrations is available from the Acoustical Society of America for use in demonstrating the above concepts and related psychoacoustic phenomena. [3].

7 The Sound Level Meter

Sound levels are measured with a sound level meter compliant with IEC 61672-1:2002 consisting of:

1. A good quality microphone
2. A linear amplifier
3. An attenuator

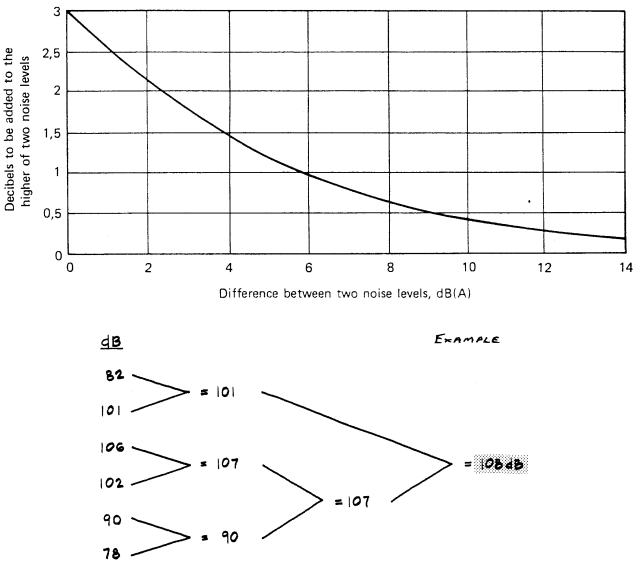

Figure 5: Decibel Addition [1, 2].

4. An indicating meter or digital display
5. A set of weighting networks to make the meter readings correspond closely to either physical pressure or perceived loudness since the ear is not equally sensitive at all frequencies.

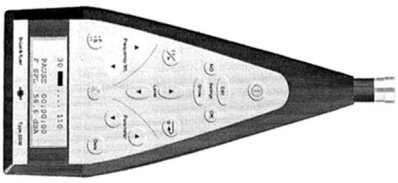

Figure 6: The Sound Level Meter [1].

8 Conclusion

Presenting visual and audible examples and demonstrations can be helpful to teachers of acoustics. Providing this kind of baseline knowledge to our communities is important as acoustical fundamentals may not always be taught in our public schools.

References

[1] Files and company seminars of HGC Engineering, Mississauga, Ontario

[2] Egan, M.D. "Architectural Acoustics" J. Ross Publishing, Originally Published by McGraw Hill Book Co., 1988

[3] "Acoustical Demonstrations – The Decibel Scale" Acoustical Society of America.

Abstracts for Presentations without Proceedings Paper
Résumés des communications sans article

Improving Audiology Student Training By Clinical Simulation Of Tinnitus: A Glimpse Of Tinnitus Lived Experience

Pierre H Bourez, Guillaume T Vallet, Philippe Fournier

Purpose: Student audiology training in tinnitus evaluation and management is heterogeneous and has been found to be insufficient. To encourage better training in this field, we have designed a new clinical simulation laboratory for training students on psychoacoustic measures of tinnitus: one student plays the role of the tinnitus patient wearing a device producing a sound similar to tinnitus on one ear while another student plays the role of the audiologist evaluating his condition. The objective of the study was to test this new clinical simulation laboratory of tinnitus from the perspective of the students and make the protocol available to the audiology community. Method: Twenty-one audiology students participated in this laboratory. All students played the role of the clinician and the patient, alternatively. At the end of the laboratory, they had to fill out a questionnaire about their experience of being the audiologist and the simulated patient. Results: The qualitative analysis revealed three main themes: "Benefits of the laboratory on future practice", "Barriers and facilitators of the psychoacoustic assessment", and "Awareness of living with tinnitus". Overall, they reported that this laboratory will have a positive impact on their ability to manage a tinnitus patient in their future career. Conclusions: This fast, cheap, and effective clinical simulation method could be used by audiology educators and other healthcare educators to strengthen students' skills and confidence in tinnitus evaluation and management. The protocol is made available to all interested parties.

Noise Evaluation At The École De Technologie Supérieure Campus In Montréal: A Student Project

Olivier Doutres, Maël Lopez, Kévin Rouard, Louis-Philippe Campagna, Titouan Cougoulic, Anthony Jutras, David Lauzon, Pierre-Luc Pépin-Pagé, Alexis Purson

University campuses situated in urban areas often face significant noise levels, which can negatively impact students' learning, the performance of faculty and staff, and the overall quality of life for nearby residents. Within the framework of the "Industrial Acoustics" course (MEC636) at École de technologie supérieure (ÉTS), a class undertook a semester project focused on conducting a comprehensive noise study of the ÉTS campus. The objective was to contribute to enhancing the acoustic environment and thereby improving the overall quality of life for the community. The project consisted of several steps. Firstly, the students investigated the outdoor noise levels across the ÉTS campus. Subsequently, they proceeded to characterize the sound environments in various rooms located in different buildings on campus, including the auditorium, classrooms, cafeteria, offices, and library. The aim was to assess the acoustic quality of these spaces. The project specifically targeted stationary noise sources related to building operations, such as ventilation systems, mechanical equipment, and computer servers. Additionally, the students were tasked with identifying the primary sources of noise within the buildings, including electrical and mechanical rooms. As a final component, they were required to design an acoustic metamaterial to enclose electrical transformers and mitigate their potential impact on neighboring rooms. In addition to serving as a pedagogical exercise to apply the theoretical and practical knowledge gained throughout the course, the project aimed to inspire the students to actively engage and learn. They were aware of the significant impact their efforts would have on the health, safety, and well-being of their community, which further motivated them in their work.

Teaching Architectural Acoustics Using Project-Based Learning With Real-World Building Projects

Christoph Hoeller, Adrian Bloedt

As part of the master program in civil engineering, students at OTH Regensburg University of Applied Sciences can take an elective course on advanced building physics to deepen their knowledge of heat and moisture performance, energy efficiency of buildings, and architectural acoustics. In previous years, this course was offered as a lecture-based course, with weekly lectures presented by the two authors of this contribution. It was noticed that student attendance and student motivation were not satisfactory. Therefore, the course was redesigned during the last year to focus on group work and to include project-based learning with real-world building projects. For the architectural acoustics part, a recently constructed multi-family dwelling was used as the basis for the project tasks. Students were divided into five groups, each dealing with one aspect of the acoustical planning process: airborne and impact sound insulation; room acoustics; façade sound insulation; noise from building service equipment; and

environmental noise. Each group task was carefully designed to include calculations and measurement aspects. Students were supported by selected lectures, small-group tutoring, and during a final "day of measurements". At the end of the semester, each group presented the methods used for the project tasks and the results. First feedback from students has been positive. Student engagement with the module has noticeably increased. The practice-oriented approach also meant that students experienced real problems in the planning process, for example unknown data, difficult measurement equipment, faulty measurement data, or complex regulations, and how to deal with these problems. This contribution will present details of the project and the positive and negative experiences gained so far.

HEARING PROTECTION - PROTECTION AUDITIVE

EFFECTS OF THE HARDNESS OF ACOUSTIC TEST FIXTURES' EARS ON THE EVALUATION OF EARPLUG'S DIRECT TRANSMISSIONS FACING HIGH-LEVEL IMPULSE NOISES.

Cyril Blondé-Weinmann [*1], **Pascal Hamery** [†1], **Thomas Joubaud** [‡1], **and Véronique Zimpfer** [§1]
[1]Acoustic and Soldier Protection (APC), French-German Research Institut of Saint-Louis (ISL).

1 Introduction

The performance of hearing protectors is limited by both (i) indirect transmissions through the outer ear tissues and (ii) direct transmissions through the protector. In the case of high-level impulse noises, it has been shown that these direct transmissions can induce displacements of the protector in the auditory canal axis that are proportional to the acoustic pressure measured at the eardrum [1]. These displacements can result from (i) inertial effects, where the plug moves like a rigid body, and (ii) deformation effects resulting from structural deformations of the protection [2, 3]. For ethical reasons, the performance evaluation of protectors facing high-level impulse noises requires using an Acoustic Test Fixture (ATF). Nevertheless, it doesn't fully reflect the behavior of a human ear. Therefore, a posteriori correction based on continuous noise measurements is used to account for tissue conduction. Nevertheless, there is no correction for impulse noise nor the ATF's effects on the direct transmissions. A new experimental study is performed to understand the role of the ATF ear's material hardness on the protector's direct transmissions.

2 Method

Impulse noises of various levels were generated using explosive charges to stimulate a medium-hardness (shore 95A) earplug built in our laboratory. Table 1 lists the impulse wave characteristics (peak amplitude and A-duration) obtained from the weapons and charges.

Table 1: Charge type and corresponding impulse wave characteristics at 7 meters.

impulse peak level	charge type	impulse A-duration
[dB]	[-]	[ms]
156	detonator	0.8
167	17g relay	1.8
177	220g C4	2.5
180	400g C4	2.9

The earplug was inserted in the canal of an ATF with two ears of different hardness (low and medium). The employed ATF has been developed at the ISL to comply with the ANSI/ASA S12.42-2010 requirements. The ear canal is cylindrical and mechanically independent of the rest of the ear. The earplug velocity was measured with an OPTOMET SWIR Laser Doppler Vibrometer (LDV). The laser beam orthogonally targeted the exterior earplug base, and the sampling frequency was 51.2 kHz. The sensor's dynamic range was refined for each measurement to record the signal variations best. The measures follow an experimental protocol already used and validated with a high-speed camera in the past [4]. It bases on the temporal decomposition of the measured velocity to separate the useful signal (earplug velocity) from the perturbations 1 and 2 (respectively, laser beam and laser-vibrometer body). Then LDV, the ATF, and the source respect a precise arrangement specified by Figure 1. The values of distance d_i in Figure 1, approximate related propagation duration $T(d_i)$, and approximate perturbation duration T_{Pi} are given in Table 2.

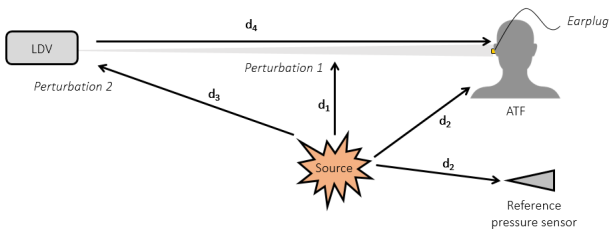

Figure 1: Positioning of the source, ATF, and sensors.

Table 2: Estimated distance d_i and related propagation duration $T(d_i)$ for the sensor positioning. A propagation speed in the air of 343 m/s is used. Durations T_{P1} and T_{P2} of the perturbations 1 and 2 arise from previous estimations measured in Blondé-Weinmann et al. (2022) [4].

i	d_i [m]	$T(d_i)$ [ms]	T_{Pi} [ms]
1	2.0	6	10
2	7.0	20	10
3	14.1	41	?
4	20.7	-	-

For each impulse level, the earplug's velocity was evaluated with the LDV, the closed ear canal acoustic pressure was measured with the ATF microphone, and the stimulating pressure was estimated with a pressure reference sensor manufactured at the ISL from a KISTLER-6031 quartz sensor. Each level was measured twice to detect an unexpected variability that could occur from a defect in impulse generation. If this happened, a third measurement was made to keep two iterations with equivalent characteristics to achieve an average. Then, the earplug's maximal displacement and ear canal peak acoustic pressure for the three stimulation levels were compared for the two ATF ears' hardness.

[*]cyril.blonde-weinmann@isl.eu
[†]pascal.hamery@isl.eu
[‡]veronique.zimpfer@isl.eu
[§]thomas.joubaud@isl.eu

3 Results

Figures 2a and 2b show, respectively, the relationships between the maximum peak pressures in the occluded ear canal and the maximum insertion displacements of the plug in the two ATF ear canals (of low and medium-hardness material) for the four peak impulse levels.

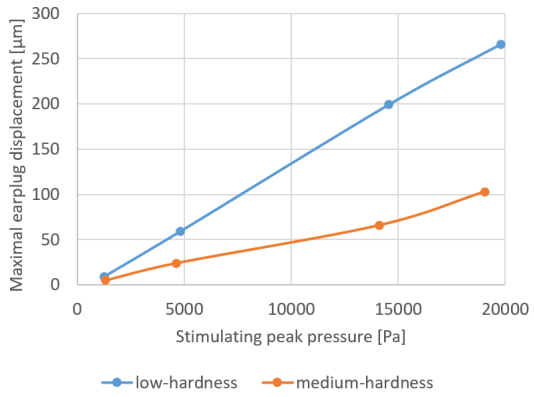

(a) Maximal earplug displacement as a function of the peak amplitude of the incident impulse wave.

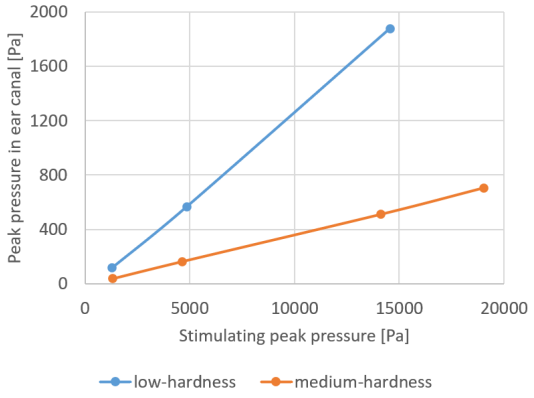

(b) Peak pressure in the ear canal as a function of the peak amplitude of the incident impulse wave. The 180 dB measurement for the soft ear was removed as it exceeded the dynamic range of the artificial head microphone.

Figure 2: Effect of ATF ear hardness on the maximum displacement of an earplug and resulting ear canal peak pressure.

Each curve has a proportional relationship to the peak stimulation pressure. This proportionality is given by β, the ratio between the peak pressure in the ear canal and the maximum displacement of the protection in the canal. The values for β and related peak Noise Reduction (pNR) are given in Table 3.

Table 3: Pressure increase in the occluded ear canal following a micrometer displacement of the outer lateral face of the protection (β) and related pNR.

hardness	β [Pa/μ]	pNR [dB]
soft	10.7	19
medium	7.2	29

A low-hardness ear induces more displacement of the plug and a higher peak sound pressure in the canal during high-level impulse noise. Moreover, the soft material also generates a higher peak pressure in the ear canal for the same displacement.

4 Discussion

Direct transmissions induced by earplug displacements are greater for a low-hardness ear than a medium-hardness ear. Given the properties of the human ear, it may be that soft material is more representative of reality. So, depending on the material, the evaluation of the protector's performance can be greatly altered. This effect results in a pNR highly dependent on the ear material used for the ATF ear. In the case of a medium-hardness ear, the average pNR is 29 dB for all measurements, compared with 19 dB for a low-hardness ear. This raises the question of the representativeness of ATFs for evaluating the performance of protectors facing high-level impulse noise. It also raises questions about the materials used for the protectors themselves. It is conceivable that, for an ear with a given hardness, a protector of different hardness will induce direct transmissions of different significance and pNR of different values. As demonstrated in [1], the value of β is inversely linked to the pNR, indicating a relation between the earplug displacement and the earplug performances. It seems that earplugs made of the hardest materials are better able to move among the soft tissues of the outer ear by compressing the outer ear tissues in the direction of the canal, thanks to a Poisson effect. It may be advisable to work on the materials used for protectors to limit this effect.

5 Conclusions

Using a LDV and an ATF equipped with different ears, it has been shown that direct transmissions through the same protector depend on the ear's hardness. These results call for further improvements in the materials used in ATFs to get as close as possible to human ear tissues.

References

[1] Cyril Blondé-Weinmann. *Description et caractérisation des phénomènes impliqués dans la limitation des protections auditives lors d'impulsions de fort niveau*. PhD thesis, UTBM, 2023.

[2] Joel T Kalb. An electroacoustic hearing protector simulator that accurately predicts pressure levels in the ear based on standard performance metrics. Technical report, A.R.L., Aberdeen P.G., Hum. Res. and Eng., 2013.

[3] Franck Sgard, Hugues Nélisse, Marc-André Gaudreau, Jérôme Boutin, Jérémie Voix, and Frédéric Laville. Étude de la transmission sonore à travers les protecteurs auditifs et application d'une méthode pour évaluer leur efficacité en milieu de travail: partie 2: étude préliminaire d'une modélisation par éléments finis. 2011.

[4] Cyril Blondé-Weinmann, Thomas Joubaud, Pascal Hamery, Sébastien De Mezzo, Véronique Zimpfer, and Sébastien Roth. Experimental evaluation of earplug behavior in front of high-level impulse noises. *Baltic-Nordic Acoust. Meet.(Aalborg)*, 2022.

MEASUREMENTS IN THE OPEN AND CLOSED EAR CANAL: COMPARISON BETWEEN DIFFERENT ARTIFICIAL HEAD CONCEPTS

Véronique Zimpfer [*1], Cyril Blondé-Weinmann [†1], Pascal Hamery [‡1], Thomas Joubaud [#1] and Franck Sgard [♦2]
[1] French-German Research Institute of Saint-Louis (ISL), St Louis France
[2]Institut de recherche Robert-Sauvé en santé et en sécurité du travail (IRSST), Montréal, Québec, Canada

1 Introduction

The use of Acoustic Test Fixtures (ATF) in the field of hearing protection has become essential for assessing the performances of hearing protectors facing high-level impulse noises. However, using this tool can be limited and, under certain conditions, does not reflect the actual behavior observed in subjects. As part of Huiyang Xu's thesis work [1], the IRSST designed a new and more realistic artificial head. This results from a desire to consider tissue or bone conduction to obtain a realistic occlusion effect compared with measurements on subjects. It integrates both the morphological characteristics of a subject's head, using medical imaging studies (MRI), and the physical characteristics of the head's constituent materials. This difference in comparison to commercially available ATF (or the ISL ATF) is interesting because, to date, measurements with ATF still require post-measurement compensations based on empirical results to take tissue or bone conduction into account [2].

In the context of joint discussions with the IRSST, this study aims to carry out various characterizations of this head and compare them with those obtained with other ATF in the ISL laboratory.

This paper evaluates the characteristics of solid transmission of acoustic waves from bone conduction transducer to the ear canal. The measurements are carried out simultaneously on the IRSST artificial head, on one ISL ATF equipped with two different external ears, and on three subjects to compare existing tools and the actual human response.

2 Material and method

Solid transmission of acoustic waves is assessed by:

- measuring the occlusion effect: sound pressure difference between the open and occluded ear canal;
- measuring the transmission delay in the same configuration.

2.1 Material

The ISL ATF used to compare measurements has two different types of external ear:

- One ear with a homogeneous pina and ear canal made of a flexible silicone-type material with a realistic morphology (noted ATF1).
- Another ear with a simplified pina made of a rigid silicone-type material and decoupled from the silicone ear canal (noted ATF2 and referenced in standard S12.42 [2]).

The three subjects (two men and one woman) participating in the experiment were laboratory members, trained to wear hearing protection and with different morphology. The performed measurements did not affect the hearing system, and the subjects were informed of the protocol before each measurement. Although the ISL ATF is instrumented to measure the acoustic pressure in the ear canal, a microphone probe, shown in Figure 1, had to be used due to the absence of a technical solution for similar measurements using the IRSST head and on the subjects. This figure also shows the two earpieces to hold the microphone, used to realize measurements either in the open ear or in the occluded ear.

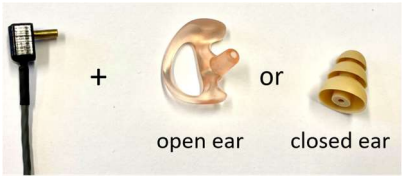

Figure 1: Microphone probe used for measurements, and earpieces used to hold it in the ear canal, depending on the type of measurement (open or closed ear).

Figure 2 shows a schematic diagram of the measuring device and a photograph of the system installed on the IRSST head. The transducer is of the electrodynamic type, designed for stealthy military headgear and has already been used in Blondé-Weinmann et al. (2021) [3].

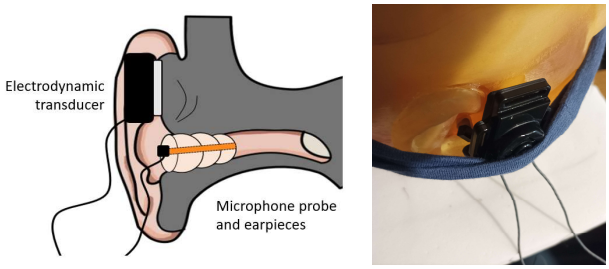

Figure 2: Experimental evaluation of the solid transmission (schematic illustration and photograph).

2.2 Measurement of the occlusion effect

The objective is to estimate the transfer function between the transducer input and the sound pressure in the ear canal measured by the probe microphone. The signal used is a sine sweep between 80 Hz and 8 kHz. The transfer function is determined when the ear is open (TF_{open}) and when the ear is closed (TF_{closed}). Three transfer function measurements are

[*] veronique.zimpfer@isl.eu
[†] cyril.blonde-weinmann@isl.eu
[‡] pascal.hamery@isl.eu
[#] thomas.joubaud@isl.eu
[♦] Franck.Sgard@irsst.qc.ca

performed for each configuration. Between each measurement, the transducer is repositioned close to the tragus. The occlusion effect (OE) corresponds to the difference between these two averaged log-magnitude transfer functions:

$$OE = TF_{closed} - TF_{open} . \quad (1)$$

2.3 Measurement of the transmission delay

The goal is to estimate the transmission delay of a wave delivered by the electrodynamic transducer positioned on the tragus and propagated to the ear canal. The method employed is based on the minimum-phase method [4]. That is, to consider the global system G($j\omega$) as the superposition of a pure delay τ and a minimum-phase function $H(j\omega)$ of phase θ as follows:

$$G(j\omega) = e^{-j\omega\tau}.|H(jw)|e^{-j\omega\theta} . \quad (2)$$

The transfer function G($j\omega$), is measured using a series of 10 Gaussian pulses, with 1 ms duration, transmitted by the transducer for each configuration. Using Equation 2, the delay τ is estimated.

3 Results

3.1 Occlusion Effect

The transfer functions (TF_{open} and TF_{closed}) were used to deduce the average occlusion effect induced by transducer stimulation. Figure 3 shows the average OE depending on the head used. Only the average over the three subjects is shown in this figure.

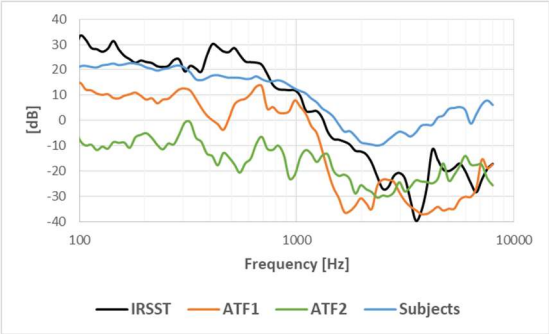

Figure 3: The occlusion effect determined by Equation 1.

In the low-frequency range (< 2 kHz), we observe:

- ATF1 (soft silicone ear) has a slight occlusion effect (about 10 dB).
- ATF2 (with the rigid silicone pina decoupled from the canal) shows no occlusion effect.
- The IRSST head has an occlusion effect of 25 dB, in line with measurements on subjects.

3.2 The transmission delay

Figure 4 shows the transmission delays of the wave delivered by the transducer, deduced from the recording of the probe microphone for an "open" and "closed" ear canal. The results obtained on the three subjects have been averaged.

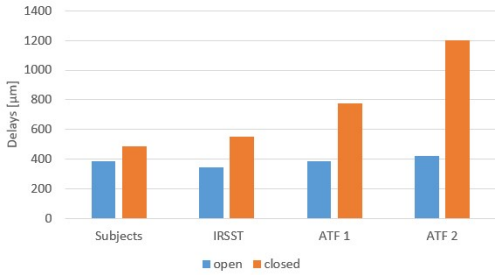

Figure 4: Transmission delays of wave delivered by an electrodynamic transducer for the open and closed ear canal

The transmission delay for the open ear canal is approximately 400 µs for all heads, with the smallest value for the IRSST head. The transmission delay for the closed ear canal is very different depending on the head, with very long delays for both ATFs. The delay on the IRSST head is of the same magnitude as the delay obtained on the subjects.

4 Discussion & conclusion

The IRSST has developed an innovative artificial head to consider tissue and bone conduction. This head corroborates subject measurements for the objective occlusion effect in the low-frequency range (<2 kHz), unlike traditional ATF. Given the transmission delays from cutaneous stimulation to the air in the ear canal, the IRSST head stands out for transmission paths close to those of a real ear and marks a break with other ATF. Other measurements, not described in this paper, have been carried out, such as the performance of hearing protection and the Transfer Function in Open Ear (TFOE), this time using air sound waves.

References

[1] Huiyang XU, « A finite element model of a human head and a corresponding acoustic test fixture to assess the objective occlusion effect induced by earplugs under bone-conducted stimulation » (2022). PhD Thesis, Montréal, École de technologie supérieure, https://espace.etsmtl.ca/id/eprint/3168/.

[2] Berger E., Standard ANSI/ASA/S12.42 2010. American National Standard Methods for the Measurement of Insertion Loss of Hearing Protection Devices in Continuous or Impulsive Noise Using Microphone-in-Real-Ear or Acoustic Test Fixture Procedures. New York, American National Standards Institute.

[3] Blondé-Weinmann C., Zimpfer V., Joubaud T., Hamery P., Roth S., "Characterization of cartilage implication in protected hearing perception during direct vibro-acoustic stimulation at various locations." Applied Acoustics 179 (2021): 108074

[4] Blondé-Weinmann C., Zimpfer V., Joubaud T., Hamery P., Roth S., "Numerical and experimental investigation of the sound transmission delay from a skin vibration to the occluded ear canal." Journal of Sound and Vibration (2022): 117345

BINAURAL BEAMFORMER: AN EARLY PROOF OF CONCEPT FOR WEARABLES AUDIO DEVICES

Stéphane Dedieu[*1], **Thomas Padois**[†2], **and Jérémie Voix**[‡2]
[1]Bloo Audio Inc, Ottawa (ON), Canada
[2]ÉTS, Université du Québec, Montréal (QC), Canada

1 Introduction

Binaural Beamforming, using signals from microphone arrays from both ears and respecting 3D localization, is a promising approach to improve speech intelligibility in the presence of interfering sound sources for all wearable audio devices. Despite the imposed small size of the microphone arrays, it offers strong interfering noise reduction potential due to the large inter-array distance and the natural attenuation provided by the head. This study is a proof of concept conducted in 2015, for a technology that several commercial products now casually feature (hearing aids, digital hearing protectors, hearables, etc.)

2 Method

A pair of small identical 3-microphone arrays is designed for a "Behind The Ear (BTE)" headset. The array geometry is visible in Figure 1. In one simple implementation of binaural beamforming, where left and right arrays are connected (through wired or wireless link), the monaural beamformer output is filtered with Head-Related Transfer Functions (HRTFs) to preserve binaural localization cues. The monaural beamforming is based on a fixed Minimum Variance Distortionless Response (MVDR) algorithm for robustness.

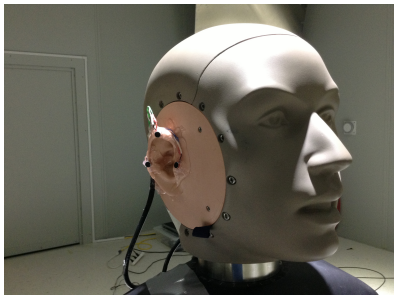

Figure 1: Microphone array on artificial head's right ear

2.1 MVDR beamformer

MVDR minimum-variance distortion-less response beamformer is built in the frequency range of [150-7000] Hz and a set of direction of interests: "look directions" from -90 to 90 degrees, with 30 degree increments. Assuming that $d_0(\omega)$ is the look direction defined by an acoustic monopole at 1 m in the simulation, filters $w(\omega)$ are found by solving the following optimization problem (dependency on the circular frequency ω is omitted for clarity) [1]:

$$min_w \; w^H \Gamma_{\nu\nu} w \;\; \text{subject to} \;\; w^H d_0 = 1 \tag{1}$$

$\Gamma_{\nu\nu}$ is the noise covariance matrix that is generally ill-conditioned at low frequencies and requires a regularization. The constraint guarantees a constant gain in the look direction d_0. The optimum weight vector w_{opt} is defined by:

$$w_{opt} = \frac{\Gamma_{\nu\nu}^{-1} d_0}{d_0^H \Gamma_{\nu\nu}^{-1} d_0} \tag{2}$$

$\Gamma_{\nu\nu}$ can easily be built in free-field, assuming isotropic 3D or back-to-front noise fields. Here, the arrays are adjacent to a large rigid obstacle made from the head structure. Therefore the computation of optimal beamforming filters requires the use of Boundary Element Method (BEM) implemented with FEMAP Finite Element Modeling and Postprocessing software (Simcenter Femap/NASTRAN XaaS) for characterizing the acoustic field surrounding the head for noise and speech sources. Such approach is more effective than traditional binaural beamforming implementations [2]. In this investigation, the beamformer is designed and validated with the 45CB artificial head (GRAS, Holte, Denmark). The BEM mesh model is illustrated in Figure 2.

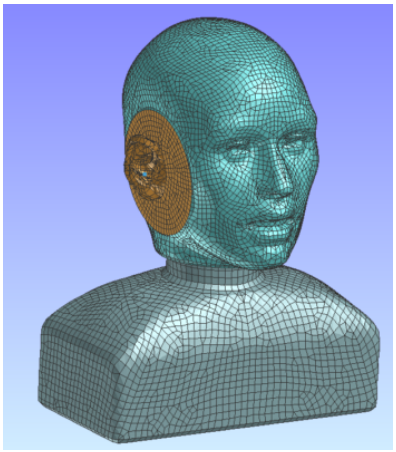

Figure 2: BEM mesh model of GRAS 45CB artificial head

2.2 Simulations

Simulations consists of determining optimal complex filters $w(\omega)$, Directivity Index (DI), White Noise Gain (WNG), and producing 3D beam patterns. DI varies from 5 dB around

[*]stephane.dedieu@bloo-audio.com
[†]thomas.padois@etsmtl.ca
[‡]jeremie.voix@etsmtl.ca

200 Hz to a maximum of 9 dB around 3 - 4 kHz. Maximum WNG degradation is limited, around 10-15 dB at low frequencies.

2.3 Validations

Validation took place in a 100 m^3 anechoic room, with source at 1 m from the center of the artificial head, at all azimuths, in the 150-7,000 Hz frequency range.

Figure 3: Test set-up in the anechoic room

In the horizontal plane, the agreement is excellent for all frequencies of interest, at all azimuths. An example is shown in Figure 4.

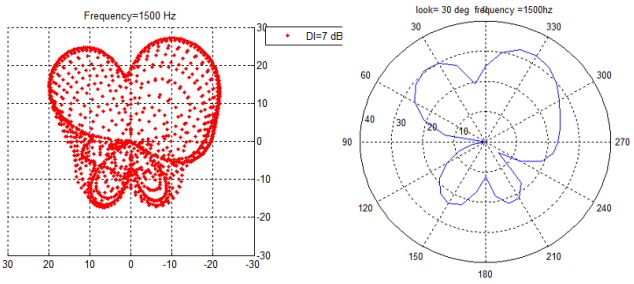

Figure 4: Validation - Horizontal plane - 30 deg. azimuth - 1500 Hz

If a larger array is an advantage when rejecting ambient noise at low frequencies, 1,500 Hz is an interesting frequency because with an inter-array distance of $\sim$ 16 cm, spatial aliasing starts to take place for all "look directions" angles.

2.4 Binaural GSC implementation

There are several approaches to handle such edge case. One can work with individual Left & Right small arrays, but this would make steering at 30 deg. and 60 deg. relatively inefficient. In this study, we implement (1) a Binaural strategy based on the monaural beamformer output, filtered with HRTFs and (2) a simple realization of a General Sidelobe Canceller (GSC) [1], by adding a "noise channel". The "noise channel", equivalent to the usual GSC blocking matrix, is built by filtering all microphones' outputs. Optimal filters are determined by steering a null in the look direction $d_0(\omega)$ using equation 1 and a proper set of constraints. Their definition is not unique. The noise channel signal is then used for implementing a Noise Reduction algorithm at the output of the main beamformer, based on a modified Wiener gain. The method is tested with recordings in the next section.

3 Results

Tests are performed in a large reverberant room. Four large loudspeakers at each corner generate the interfering noise field. Speech samples taken from the HINT database [3] are played from a smaller loudspeaker placed 1 m away from the head, in the plane of the arrays.

Recordings and array processing are performed in 4 different conditions: in Silence, and with different background noises (White noise, Industrial noise, Cocktail party noise). In the present demo, the sound source is located at 60 deg. on the right. The binaural beamformer properly positions the speech source at 60 deg., but the residual noise is also located at 60 deg. which sounds a bit unnatural. The waveform of the right channel signal of the binaural beamformer is shown in Figure 5. The MVDR beamformer improves reverberations and reduces the white noise, overall by about 4 to 8 dB. The General Sidelobe Canceler (GSC) strategy with a modified Wiener gain further attenuates reverberations, and reduces white noise by about 9 to 12 dB. Speech sounds a bit "dry" and distorted, but it is clear and intelligible.

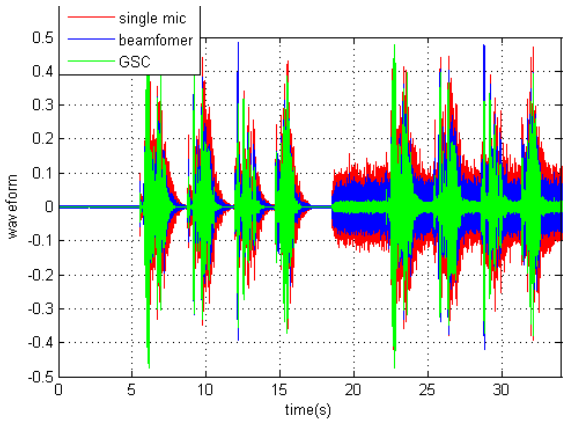

Figure 5: Right channel audio waveforms in various conditions

Acknowledgments

The authors acknowledge the technical support received from the NSERC-EERS Industrial Research Chair in In-Ear Technologies (CRITIAS) and from ICAR laboratories (Infrastructure commune en acoustique pour la recherche ÉTS-IRSST).

References

[1] Michael Brandstein, Darren Ward: "Microphone Array", Springer-Verlag, 2001

[2] Zhengwei Luo, "Beamforming for binaural hearing aids", Master Thesis, Univ. of Ottawa, 2009

[3] Nilsson M, Soli SD, Sullivan JA. Development of the Hearing in Noise Test for the measurement of speech reception thresholds in quiet and in noise. J Acoust Soc. Am. 1994 Feb;95(2):1085–1099

TOWARDS ADJUSTABLE LOUDNESS COMPENSATION IN HEARING PROTECTORS FOR MUSICIANS

Elliot Drees[*1,3], **Eugénie Segers**[†1], **Caroline Traube**[‡2,3], **and Jérémie Voix**[§1,3]
[1]ÉTS – École de technologie supérieure, Université du Québec, Montréal (QC)
[2]Faculté de musique, Université de Montréal, Montréal (QC)
[3]CIRMMT – Center for Interdisciplinary Research in Music, Media and Technology

1 Introduction

Working in a noisy environment is, in certain cases, unavoidable. To prevent noise-induced hearing loss (NIHL), wearing hearing protection devices (HPDs) is something necessary. However, due to the certain barriers to their use, HPDs are not always worn [1]. In this article, we will be focusing on the acoustic comfort of hearing protectors, which depends on two factors: the isolation effect on external sounds and the occlusion effect on internal sounds [2]. This paper solely focuses on the isolation effect, which corresponds to the unnatural sensation of being isolated from a given sound environment and can be caused by wearing HPDs that do not compensate for psychoacoustical factors and therefore alter the wearer's auditory perception.

Musicians belong to a population particularly affected NIHL [3]. High fidelity active HPDs are now available on the market and seemingly have better acceptance compared to passive protection [4], as they gives more flexibility in filtering and equalisation. For this project, we wish to investigate the integration in active HPDs of loudness compensation algorithms [5] [6] to minimize the isolation effect. For this purpose, two experiments were conducted to assess the effectiveness of various loudness compensators in the context of hearing protection, with a dBA level constraint.

2 Method

2.1 Participants

For both experiments, participants needed to have some significant experience with music, either as amateur musicians, professional musicians, or experience with mixing or recording. A pre-study questionnaire allowed to assess their eligibility. Those with an ear surgery history, current ear infection, physical hypersensitivity of the ear canal, or a hearing loss of more than 25 dBHL hearing loss were excluded from the study. Additionally, an otoscopic examination was performed to verify that the ear was not blocked.

For the first experiment, 21 participated, with one abandoning. For the second experiment, 17 participated, with one being excluded for being over the hearing level threshold. Each participant was offered ETY-Plugs ER20 (Etymotic Research, Elk Grove Village, IL, USA) as compensation. The research project was submitted to and approved by the ÉTS research ethics committee (reference H20210503).

[*]edrees@critias.ca
[†]esegers@critias.ca
[‡]caroline.traube@umontreal.ca
[§]jeremie.voix@etsmtl.ca

2.2 Design, materials and procedure

Both experiments controlled identical parameters, however, the participant's control over them varied. In both cases, the participant had to listen to samples with varying sound pressure levels: a reference sound at 80 dB, to be compared in timbre with other versions of this sound at a lower level (70 dB or 60 dB), processed by different loudness compensators.

The sample sets was composed of 5 musical excerpts and 1 speech in noise excerpt, all of 10 second duration, in 24 bit/48 kHz lossless format. The musical excerpts are: (1) Peer Gynt, Suite No. 1 Op. 46, Morning Mood, (2) Pink Floyd, Breathe In The Air, (3) Nile Rodgers/Daft punk, Get Lucky, (4) Sylvain Barou/Kevin's Reel, The Session, (5) Paolo Fresu, I Was an American Boy.

Although the computer used for the experiment varied, both experiments used an OCTA-CAPTURE (Roland, Hosoecho Nakagawa, Japan) as a sound source. For experiment 1, the samples were played on a Beridynamic DT 770 (Heilbronn, Germany) headphones while experiment 2 used Shure SE 215 earphones (Niles, Illinois, U.S.) to be closer to the type of HPDs musician use in a rehearsal or stage performance situation.

Experiment 1: Four filtering conditions were tested: (1) Adaptative Loudness Compensation [5], (2) Approximate Spectral Balance Compensation [5], (3) Moore & Glasberg based compensation (developed in-house), and (4) no filtering at all. For each excerpt, the original reference sound at 80 dB was presented with four versions of this sound at a lower level. To collect the participants' ratings on each loudness compensation algorithm in this subtle timbre comparison task, a listening test was designed on the basis of the Multiple Stimulus with Hidden Reference and Anchor (MUSHRA) protocol using an existing framework [7]. The experiment consisted in 3 parts with 8 timbre evaluations each, the first part being a training phase. Open questions were also included to inquire about the participant's confidence.

Experiment 2: The participant listened to three version of a same sample, the reference at 80 dB, an attenuated at 70 dB and a filtered version at 70 dB. they had control over the parameters of the filter during each adjustment task. The user interface was made from scratch using Python language and Tkinter library. Filters more similar to the ones used in audio mastering were used this time: (1) a loudness filter using the equal-loudness contours, (2) a low-high filter, and (3) an 8-band EQ. An additional dBA constraint was added on top of

these filters. The participant's task was to adjust the filter to make the timbre of the lower-level sound match the timbre of the reference sound at 80 dB. The adjusted filter parameters were recorded and saved. As a training phase, 3 adjustment tasks were presented, then 3 filtering methods were evaluated in a random sequential order with 3 samples being evaluated 3 times for each filter. Additionally, participants had to rate each filter on a 5-point Likert scale in terms of ease of use, quality, and their desire to use such a filter in a protector.

All testing was done in silent rooms to mitigate the impact of external sounds: either a semi anechoic room within CIRMMT, or a laboratory at the U. of Montreal's Faculty of Music, or an audiometric booth at CRITIAS. Additionally, to reduce participants fatigue, several breaks were imposed during the experiment.

3 Results

In both experiments, participants overwhelmingly shared the desire to be able to adjust HPDs, with all participants in experiment 1, and 14 out of the 16 participants for experiment 2 expressing the need for HPD adjustment, the remaining two expressing uncertainty about it.

Experiment 1: The original sample was always preferred with a higher median compared to the other compensators. When considering t-tests between the distributions of the original sample and the other compensators (c) in the context of the sound pressure level (l) and compensator interaction $l \cdot c$, statistically significant difference were found for the MGCL: $p = 3.32 \cdot 10^{-6}$ at $l = 70$ dB and $p = 3.32 \cdot 10^{-6}$ at $l = 70$ dB, and for the ALC at $l = 70$ dB: $p = 9.28 \cdot 10^{-3}$.

Experiment 2: Although the results are preliminary, the Likert scale testing in figure 1 shows that the low high setting is preferred when it comes to all three categories, with the 8-band filter being the less intuitive.

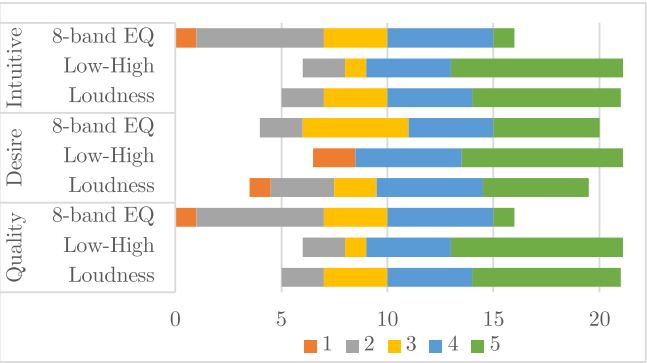

Figure 1: Diverging stack bars representing the responses to the Likert rating question for experiment 2. Intuitiveness, quality and desire to be used are grouped for ease of comparison.

4 Discussion

These two studies evaluated the use of loudness compensation in the use of HPDs as well as possible control schemes to adjust their frequency response.

Although loudness compensators in the literature had been tested on human subjects, the results in our first study does not favor existing loudness compensator. A hypothesis explaining this result is that loudness compensators increase the overall level of the sound by affecting the lower and higher frequency, making the timbre more similar. This effect could be mitigated by our dBA constraint.

In experiment 2, participants preferred simple control schemes (loudness, low-high) over more complete and complex ones (8-band). This can be explained by the need for simple controls while adjusting hearing protector in a live setting.

In both experiments, ideal HPD conditions were simulated by varying the volume of predetermined sounds. Additional studies focused on HPD adjustment in live situations are necessary.

Acknowledgments

The authors would like to acknowledge the financial support received from NSERC Alliance (ALLRP 566678-2021), MITACS IT26677 (SUBV-2021-168) and PROMPT (#164_Voix-EERS 2021.06), for the ÉTS-EERS Industrial research chair in ear technologies, sponsored by EERS Global Technologies Inc.

References

[1] Olivier Doutres, Franck Sgard, Jonathan Terroir, Nellie Perrin, Caroline Jolly, Chantal Gauvin, and Alessia Negrini. A critical review of the literature on comfort of hearing protection devices: Definition of comfort and identification of its main attributes for earplug types. *International Journal of Audiology*, 58(12):824–833, December 2019.

[2] Antoine Bernier and Jérémie Voix. Active musician's hearing protection device for enhanced perceptual comfort. In *Euronoise 2015, the 10th European Congress and Exposition on Noise Control Engineering*, Maastrich, The Netherlands, 2015. EAA-NAG-ABAV.

[3] Arianna Di Stadio, Laura Dipietro, Giampietro Ricci, Antonio Della Volpe, Antonio Minni, Antonio Greco, Marco de Vincentiis, and Massimo Ralli. Hearing Loss, Tinnitus, Hyperacusis, and Diplacusis in Professional Musicians: A Systematic Review. *International Journal of Environmental Research and Public Health*, 15(10):2120, September 2018.

[4] Ian O'Brien, Tim Driscoll, Warwick Williams, and Bronwen Ackermann. A Clinical Trial of Active Hearing Protection for Orchestral Musicians. *Journal of Occupational and Environmental Hygiene*, 11(7):450–459, July 2014.

[5] Leonardo Fierro, Jussi Rämö, and Vesa Välimäki. Adaptive Loudness Compensation in Music Listening. May 2019.

[6] Oliver Hawker and Yonghao Wang. A Method of Equal Loudness Compensation for Uncalibrated Listening Systems. In *Audio Engineering Society Convention 139*. Audio Engineering Society, October 2015.

[7] Michael Schoeffler, Sarah Bartoschek, Fabian-Robert Stöter, Marlene Roess, Susanne Westphal, Bernd Edler, and Jürgen Herre. webMUSHRA — A Comprehensive Framework for Web-based Listening Tests. *Journal of Open Research Software*, 6(1):8, February 2018.

DEVELOPMENT OF THE SUBJECTIVE EVALUATION METHOD OF HEARING PROTECTORS

Farhad Forouharmajd [*1], Adrian Fuente [†2], Hadi Asady [‡1], Siamak Pourabdian [‡1]
[1]Department of Occupational Health Engineering, School of Health, Isfahan University of Medical Sciences, Isfahan, Iran,
[2]École d'orthophonie et d'audiologie, Faculté de médecine, Université de Montréal, Montréal, Quebec, Canada

1 Introduction

Exposure to high sound levels causes hearing loss [1]. Using hearing protection devices is one of the ways to prevent exposure to loud noises, reduce noise-induced hearing loss and prevent other problems such as cardiovascular disorders, blood pressure or noise annoyance. This study was conducted due to the prevalence increase of hearing loss in industries, despite the outspread in hearing protection programs. One of these reasons in increasing noise-induced hearing loss can be related to the inefficiency of hearing protector evaluation methods. Hearing Protective tools are not evaluated at actual levels and therefore may perform differently when used in the field than in laboratory conditions. There are various methods in order to evaluate the reduction of the noise in ear protectors, which are divided into two general subjective and objective categories [2].

As the current subjective method of evaluation of the ear protector, ISO standard 4869-1, is not based on industrial noise and in the field, a suggested way is developed for the evaluation of hearing protectors based on the subjective feedback of the volunteers [3]. In fact, the instructions for obtaining a feedback are completely subjective, and after extracting the results, these qualitative values are converted into quantitative values. In this method, one step is completed by using the person's subjective response to the received sound before and after using the ear protector. This part is developed by defining the subjective perception of people and their feelings towards understanding the sound and scoring the answers and then converting it into decibel values of the sound. This research is somehow aimed at developing of subjective method for the measurement of sound attenuation-based ISO standard 4869-1. This method makes it possible to evaluate hearing protectors completely subjectively.

2 Method

2.1 Exposed to 85 dB (A) noise

This experimental study was conducted on 64 students between the ages of 18 and 25. The measurements were carried out in semi-free field conditions. In this study, pink noise as well as pure noise at frequencies of 500, 1000, 2000 and 4000 have been used. First, people were talked about the testing process and how to be exposed to sound and how to respond were explained [4].

First, the person sat in a chair in a quiet room and listened to the sound played at a level of 85 dB (A). The sound of 85 dB was played for at least 1 minute for the volunteer to remember this sound level. Subjects were asked to listen carefully to the produced sound after hearing it. The volunteers were not aware of the level of sound produced. They only tried to remember based on what they heard in this stage (without protection) and remembered for the next stage (by using ear protectors).

2.2 Exposed from 85 dB (A) noise while using hearing protection

In the second stage after using earmuff, ear plug or both, the sound level of 85 dB was played again for at least 1 minute for the volunteer. The volunteers were asked to announce when they felt the same sound level as they heard in the first stage. As a matter of fact, they were asked to remember the noise level of the sound that they heard before by recalling the level of the sensed sound.

In this stage, because the goal is to determine the amount of reduction of the protectors in a subjective method, the sound level started from 85 dB and increased until the candidate feels the same sound level as the first stage. The difference between the level of 85 and the maximum level declared by the person indicates the amount of reduction of the noise.

3 Results

3.1 Subjective responses of individuals before and after using hearing protectors

People's responses were collected after receiving their hints. Pointing people indicates the same level of level received in the first stage. It is obvious that the feeling of the person after using the protection is expressed at higher levels. At the time of pointing candidates, the levels of the sound played have been recorded.

3.2 Evaluated noise reduction between objective and subjective method

In this step, we compare the recorded sound levels according to people's feelings with the sound level of 85 dB and obtain their difference. The noise reduction values of the ear protectors have been extracted and given in a subjective and objective way separately in Figure 2.

In fact, the ability of efficiency of ear protectors to reduce noise has been evaluated in two quantitative and qualitative ways. Then two methods have been compared in terms of accuracy and efficiency. As the results show, the subjective method is reported with a slight difference compared to the objective method. Using earmuff and ear plug simultane ously has demonstrated more reduction noise. And this

[*] forouhar@hlth.mui.ac.ir
[†] adrian.fuente@umontreal.ca
[‡] asadyhadi60@gmail.com
[†] pourabdian@hlth.mui.ac.ir

reduction is shown in the subjective method as well as the objective method.

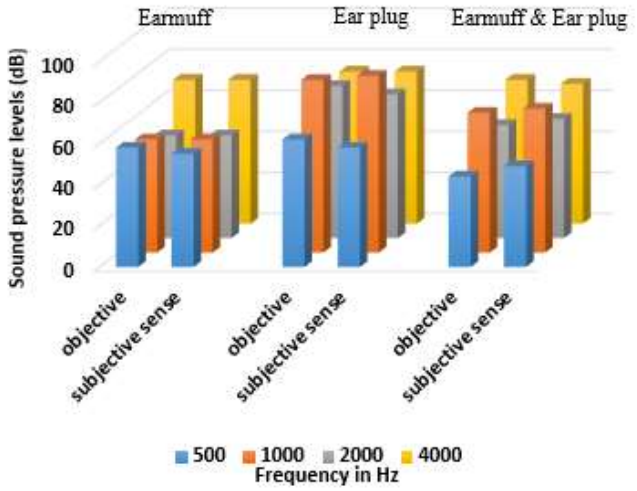

Figure 1: Comparison of two subjective and objective evaluation method of ear protectors

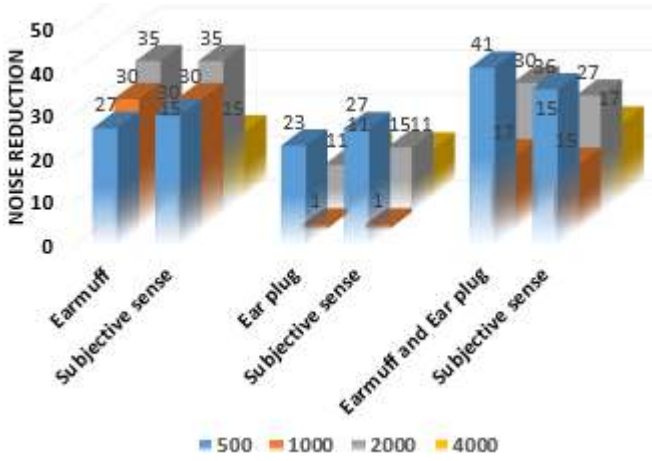

Figure 2: Evaluation method of ear protectors in noise reduction

4 Discussion

In Figure 1, based on the results, the proposed method has been compared with the objective method. To increase accuracy, measurements have been made separately for earmuff, ear plug and their combined use. It is clear that in all three cases the difference between the obtained values is very small. It means that the subjective method performed has an acceptable accuracy. The results of pink and sinusoidal sound were similar to each other.

This section is developed by defining the subjective perceptions of individuals and their feelings with respect to the sound comprehension, the score of responses, and then converting them into level amounts of the sound. A number of students between the ages of 18 and 25 were selected. First, a hearing test was performed on their ear to determine their hearing threshold. They were then confronted with a distinct sound level. When using the ear protector and without using it, they were asked how they felt about the amount of sound received. This qualitative feeling was converted into level amounts and compared with a quantitative method. Of course, more candidates are needed to improve the accuracy of the test results.

5 Conclusion

To have better results, it is necessary to perform subjective methods to test hearing protectors and compare them with other techniques with a greater number of samples to reach a result as Figure 2. As a result of the laboratory evaluation of ear protectors, it is possible not to justify the proficiency of ear protectors in a subjective method. The method is suggested by using the individual's subjective response before and after using the ear protector. This method is based on the subjective perceptions of individuals and their feelings with respect to the sound comprehension, in an acceptable noise level for occupational and environmental fields.

Acknowledgments

The protocol of this study was approved by the Research Ethics Committees of Isfahan University of Medical Sciences and Health Services with IR.MUI.REC.1396.1.162. This article is prepared by the results of a research work with number of 196162 at Isfahan University of Medical Sciences. The authors like to express their gratitude to the volunteers and the lab of the noise and vibration of Isfahan University of Medical Sciences School of Health.

References

[1] Hong O, Kerr MJ, Poling GL, Dhār S. Understanding and preventing noise‐induced hearing loss. Dis Mon 2013;59:110‐8.

[2] European Standard. Hearing protectors Testing Physical test methods. EN13819-1-2002.

[3] ISO 4869‐1:2018 Acoustics — Hearing protectors — Part 1: Subjective method for the measurement of sound attenuation.

[4] Farhad Forouharmajd, Kamyar Nazaryan, Adrian Fuente, Siamak Pourabdian, Hadi Asady. The Efficiency of Hearing Protective Devices against Occupational Low Frequency Noise in Comparison to the New Subjective Suggested Method. Int J Prev. Med 13 (1), 143-149, November 2022.

TIME-DOMAIN NUMERICAL INVESTIGATION TO ASSESS NOISE REDUCTION ALLOWED BY A NON-LINEAR PASSIVE EARPLUG FACING IMPULSE NOISES.

Christophe Ruzyla [*1,2], Pascal Hamery [†1], Cyril Blondé-Weinmann [‡1], and Sébastien Roth [♦2]
[1] Acoustics and Soldier Protection, French-German Research Institute of Saint-Louis (ISL), Saint-Louis, France.
[2] Laboratoire Interdisciplinaire Carnot de Bourgogne, site UTBM, UMR 6303 CNRS / UBFC, France.

1 Introduction

On the battlefield, soldiers are regularly exposed to high-level impulse noises. These noises are characterized by a rapid and spontaneous acoustic pressure evolution. In order to allow communication between military personnel and situational awareness, Non-Linear Passive Earplugs (NLPE) were developed [1]. These devices provide an attenuation that increases with the impulse level. In this work, a NLPE integrating a filter composed of two perforates patented by the ISL in the 90s will be studied. This filter is present in protectors now widely used by several armed forces. To better integrate these filters in new earplugs' configurations (e.g., molded plug), the consequences on the protection's effectiveness of modifying the plug and filter geometry (length and diameters), material as well as the filter position in the protector are needed. In this context, numerical modeling appears to be a valuable tool. In this work, a time-domain finite-elements model of the acoustic phenomena resulting from high-level impulses on NLPE will be carried out with the software COMSOL Multiphysics 6.1 (© COMSOL Inc).

2 Finite Element Model

The model aims to simulate the non-linear effects arising from a high-level impulse noise propagating through the perforates of a NLPE inserted into an ear canal and the resulting acoustic pressure attenuation. Given the system's geometry, an axisymmetric approach was considered as a first approximation. The wave equation in the time domain was solved at each point of the discretized air domain. Thermo-viscous acoustic equations were also considered in the earplug and the ear canal, where viscous losses and dissipation due to thermal conduction become important. It allows to compute the transient evolution of acoustic pressure variations, velocity, and temperature, as well as non-linear effects as a function of time. To consider the reflection and absorption of acoustic waves at the interface of solid material parts (plug body, non-linear filter, deformable silicone plug, ear canal, and eardrum), impedance conditions were applied. The values were deduced from the considered material's sound velocity and density. The material properties used are summarized in Table 1.

An artificial air volume of 2 cm3 was added behind the plug to induce a compliance equivalent to the eardrum [2].

[*] Christophe.RUZYLA@isl.eu
[†] PASCAL.HAMERY@isl.eu
[‡] sebastien.roth@utbm.fr
[♦] cyril.BLONDE-WEINMANN@isl.eu

As an input for the model, the acoustic pressure measured during previous experimental campaigns at the ear canal entrance [3] was applied as an incident plane wave of 110 dB-peak and 150 dB-peak at the inlet. These levels were chosen to compare a situation where non-linear effects are negligible with one where they are significant. The resulting 2D axisymmetric model composed of 6 components is represented in Figure 1.

Table 1: Properties of the solid materials used in the model.

	Density (kg/m^3)	Sound velocity (m/s)
Silicone	1250	1485
Acrylic plastic	1030	2230
Skin	1100	1400
Eardrum	1200	1400

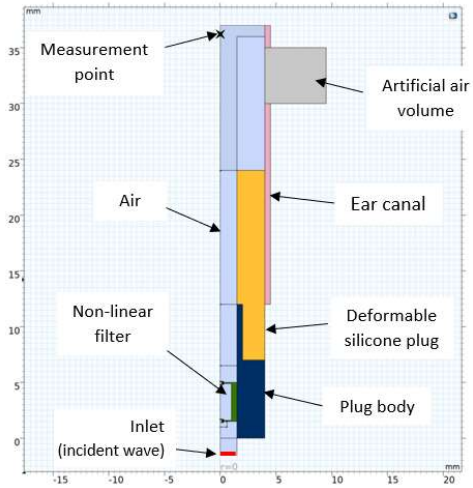

Figure 1: Geometry of the NLPE model.

The maximal resolution frequency was set to 15 kHz. Then, the mesh was built to have sufficient spacial discretization according to the minimum wavelength considered (at least five elements each). Local mesh refinements were made in areas where strong pressure gradients appear. To take into account boundary layers, a dedicated mesh refinement was applied on the orifice's surfaces. Thus, for each pressure level, a dedicated mesh was built. Finally, for 110 dB-peak and 150 dB-peak, the model has 50977 and 157753 degrees of freedom, respectively. The solver used was the generalized-α method with a maximal time step of 1.1 µs to respect the Courant–Friedrichs–Lewy condition. This method was chosen for its good accuracy and low numerical damping.

3 Results

The acoustic pressure history close to the eardrum (0.5 mm upstream) for a 110 and 150 dB-peak are shown in Figure 2. A comparison with results obtained with an Acoustic Test Fixture (ATF) from previous experimental campaigns is performed [1].

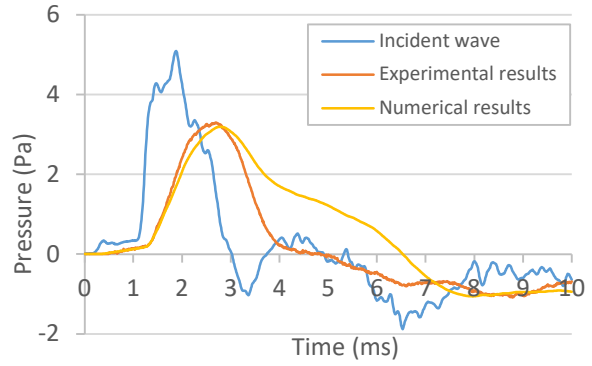

(a) 110 dB-peak

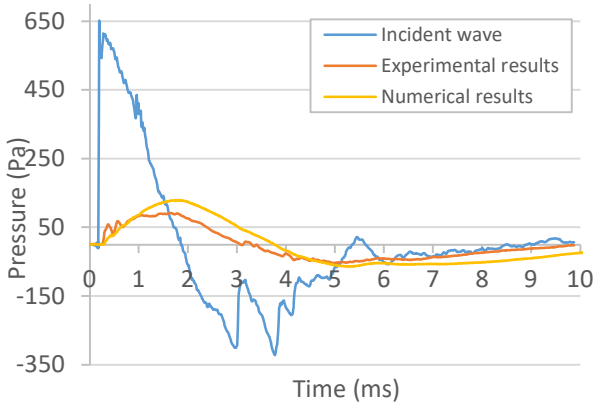

(b) 150 dB-peak

Figure 2: Comparison of numerical and experimental acoustic pressure measured at the eardrum when the NLPE faces high-level impulse wave of 110 and 150 dB-peak.

For an excitation of 110dB-peak, a good correlation of the peak pressure level can be observed. The pressure decay estimated numerically between 3.5 and 6.5ms is slower than by the experiment. For an excitation of 150 dB-peak, the duration of the positive phase and rising times are similar numerically and experimentally. The resulting Peak Noise Reductions (PNR), estimated from the difference between the stimulation peak pressure and the resulting peak pressure close to the eardrum, are listed in Table 2.

Table 2: Noise reduction estimated numerically and experimentally.

Impulse level	Exp. PNR	Numerical PNR
110 dB-peak	3.8 dB	4.0 dB
150 dB-peak	16.5 dB	13.5 dB

The perforates-induced vortex rings induced by the non-linear effects are illustrated in Figure 3 for a 150 dB-peak impulse wave.

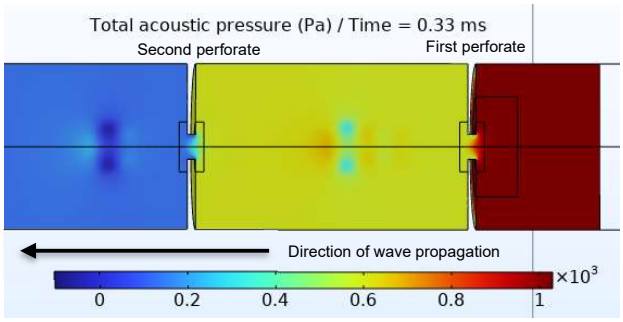

Figure 3: Illustration of the vortex rings induced by the perforates for a 150 dB-peak impulse.

4 Discussion

The numerical acoustic pressure at the eardrum is overall in good agreement with experimental measurements. The differences observed might result from the model simplifications. First, although the added equivalent compliance corresponds to an effective first approximation of the eardrum, it may underestimate its effects. Second, as the mechanical properties of ATFs are still unknown, it was decided to use the actual acoustic properties of the ear canal skin lining, which may therefore differ. Lastly, the plug inertial effects and ear canal compression arising from high-level impulse noises were not modeled. These phenomena could explain the acoustic pressure oscillations during the positive phase of the 150 dB-peak experimental measurements.

5 Conclusion

In this work, a simplified model of a non-linear filter earplug inserted in the ear canal was built in COMSOL Multiphysics 6.1 (© COMSOL Inc). It enabled us to evaluate the noise reduction behind the earplug for two excitation levels and observe the non-linear effects arising from the perforates. The numerical solutions obtained for 110 dB-peak and 150 dB-peak have shown a good correlation with experimental results obtained with an ATF. More excitation levels should be considered in future studies to extend these results. Finally, this work provides new perspectives to integrate non-linear filters in new configurations of earplugs while enhancing their performances.

References

[1] A. Dancer, P. Hamery, 1998, "A New Nonlinear Earplug for Use in High Level Impulse Noise Environment ", The Journal of the Acoustical Society of America 103, 2878; https://doi.org-/10.1121/1.421756

[2] International Electrotechnical Commission, 2010, "Electro-acoustics - Simulators of human head and ear - Part 4: Occluded-ear simulator for the measurement of earphones coupled to the ear by means of ear inserts", ISBN 978-2-88910-121-4

[3] P. Hamery, V. Zimpfer, K. Buck, S. De Mezzo, 2015, "Very high-level impulse noises and hearing protection ", Euronoise 2015, French-German Research Institute of Saint-Louis, Saint-Louis, France.

On the Use of Wide Dynamic Range Compression and Other Algorithms to Improve Hearing Protection of Workers with Hearing Impairment: A Preliminary Study on Speech Intelligibility.

Solenn Ollivier[*1], **Hugues Nélisse**[†2], **and Jérémie Voix**[‡1]
[1]ÉTS, Université du Québec, Montréal (QC)
[2]Institut de recherche Robert-Sauvé en santé et en sécurité du travail (IRSST)

In Canada, noise-exposed workers are more likely to experience hearing difficulties. This population, who either works or have worked in noisy environment, represents 43% of Canadians [1]. While workers with hearing loss in such environment stand as a substantial part of workers in need of hearing protection, hearing conservationists have not yet come to an agreement on the safest and most efficient way to protect their residual hearing. Common practices of those workers include wearing hearing aids, either turned off or on underneath earmuffs. Hardly any research have explored the potential benefits or dangers of such practice [2].

One solution, based on Leroux et al.' recommendation, is to develop a device for suitable research that incorporates features from both hearing aid devices and Hearing Protection Devices (HPDs). Such device requires the implementation of different signal processing algorithms. One algorithm, popular in hearing aids, is multichannel wide dynamic range compression (WDRC) which allows to amplify while protecting. Different parameters can be used to adjust the amplification/protection to a person's specific needs. Despite numerous research for daily-life applications, the effect of WDRC on speech intelligibility in typical workplace noise has barely been explored. Moreover, research has shown that the use of different WDRC parameters impact speech intelligibility in many ways depending on several factors, including the noise environment and use of WDRC in combination with other algorithms (e.g. noise reduction).

This research first introduces the algorithms to be implemented in the platform for research. Then, a proposed methodology to explore their potential benefits on speech intelligibility in a typical factory noise is presented.

1 Hearing device algorithms

Modulation Based Digital Noise Reduction (MBDNR)

A noise reduction algorithm is used to improve the signal-to-noise ratio (SNR) before compression, thus to increase comfort and speech intelligibility. In this study, the algorithm is adapted from Lezzoum et al.' MBDNR algorithm [3]. After filtering the signal into subbands, the signal envelope is extracted and, based on its modulation frequency, a gain is applied to attenuate the noisy portion of the signal.

WDRC and gain prescription

Wide dynamic range compression is used to decrease the amplitude of a signal using a certain compression ratio (CR) when a defined compression threshold (CT) is reached. Two key constants are used to smooth the signal: the attack time (AT) and the release time (RT). Below the CT, a gain can be applied to the signal. In hearing aids, the gains are usually prescribed by prescription algorithms that typically use hearing loss profile of the wearer. Here the gain computation is based on NAL-RP prescription [4]. The obtained target gains are applied at 65 dB SPL [5]. The compression threshold is chosen as $CT = 50$ dB SPL. To ensure there is no amplification above a certain input level, an anchor point is defined such that $A_{in} = A_{out} = 90$ dB SPL. The CR and gain below threshold can then be computed. As the aforementioned levels are overall levels, the corresponding band-levels were computed using speech-shaped noise processed through the multiband filter. The influence of different time constants on speech intelligibility vary in different noise environments. The AT is often short, below 10 ms, to protect from a sudden increase of loud sounds, although such AT may induce distortions. Longer RT have been reported to be more beneficial in noise for individuals with hearing impairment. In this research, the influence of different AT and RT will be assessed using three AT/RT combinations presented in table 1. WDRC can be applied in different frequency bands to adapt to the user's HTs in different frequency regions. Five-channel WDRC allows for a good individualization of amplification without increasing too much algorithm complexity and latency. The cut-off frequencies [450;900;1800;3600] Hz are chosen such that each band contains the same proportion, approximately 20%, of band importance function for short text passages according to the Speech Intelligibility Index standard (ANSI/ASA S3.5).

Compression Limiting

A compression limiting algorithm is finally used at the output to protect from very loud noise. Thus, more aggressive parameters are used: $CT_{lim} = 90$ dB SPL, $CR_{lim} = 10$, $AT_{lim}/RT_{lim} = 5/50$ ms.

2 Proposed methodology

Participants

Participants' eligibility and hearing thresholds (HTs) were assessed through otoscopic examination and pure tone audiometry. Their pure tone audiogram enabled to classify the participants in 2 groups: the No Hearing Loss (NHL) group and the Hearing Loss (HL) group for participants with mild to moderate hearing loss. All participants were adults and either native speakers of English or French (including French Canadian).

Hardware

The Auditory Research Platform Virtuose (ARPV) is used

[*]sollivier@critias.ca
[†]hugues.nelisse@irsst.qc.ca
[‡]jeremie.voix@etsmtl.ca

as a soundcard connected to a computer. It consists in two earplugs, each with an outer-ear microphone, an in-ear microphone (IEM) and an in-ear loudspeaker (IELS). In this experiment only the IEM and IELS were used.

Speech intelligibility test and software

Speech intelligibility was assessed through measuring differences in speech reception thresholds (SRTs) using a variation of the Hearing in Noise Test (HINT). The HINT consists in presenting a list of sentences mixed with noise with varying SNR to the participant. The participant is asked repeat each sentence. If the repeated sentence matches the original one, the SNR of the next presented stimuli is lower, otherwise the SNR is higher. Once the list of sentences is over, the SRT is obtained. The stimuli used are standardized list of sentences [6, 7], mixed with a factory noise. The **Matlab Speech Test Environment (MSTE)** [8] was used to automate the HINT. This Matlab platform developed by Ellaham et al. at University of Ottawa enables to perform the HINT procedure while allowing to simulate hearing devices. The experimenter inputs the participant's information including HTs. Then test paradigms can be chosen, including the simulation of a hearing device. If simulation of a hearing device is chosen, the stimuli are processed through the implemented algorithm before being played by the IELS. For each subject the HINT was administered for the 5 conditions presented in in table 1. In the table "whole" refers to the combination of the three aforementioned algorithm, and "WDRC" to WDRC only. The order of testing between conditions was randomized and organized in a double-blinded study.

Table 1: Different testing conditions

Condition	Simulated device	WDRC AT/RT (ms)
1	None: unaided	/
2A	Whole	10/800
2B	Whole	100/800
2C	Whole	10/1,500
3	WDRC	10/800

Response time and clarity ratings

Response time is a measure of the benefit of amplification by being indicative of listening effort [9]. The response time is defined as the time between the end of the presented stimuli and the start of the sentence repeated by the participant and was computed for each sentence in the post-processing phase. To assess user preference, five sentences mixed with noise at a fixed SNR and processed for each condition were then presented to the participant who repeated the sentence and rated its clarity on a scale from 1 to 5 (1 being very unclear and 5 being very clear).

Test procedure

After their HTs were obtained, the participants performed the five HINT tests in a semi-anechoic room. The participants wore both ARPV earplugs which were connected to the computer, the IELS playing the stimuli of the automated HINT using MSTE. After repeating a sentence, its understanding was rated by the experimenter on MSTE until an SRT value was achieved. The participants were then presented noisy speech mixtures, had to repeat the sentence and rate its clarity. The whole experiment was both audio and video recorded to later compute the response times, and evaluate the corresponding presentation SNR, for each sentence.

3 Conclusions

The impact of different hearing device configurations with WDRC on speech intelligibility in workplace noise are explored. Differences in SRTs and assessment of listening effort are evaluated to select the best configuration. The selected algorithms will then be implemented on the ARPV, as an embedded platform, allowing further research in more realistic working conditions.

Acknowledgments

The authors would like to acknowledge the financial support received from the IRSST, from the ÉTS-EERS Industrial research chair in in-ear technologies, sponsored by EERS Global Technologies Inc, and from Fonds de Recherche du Québec - Nature et Technologies for the Merit-Based Scolarship for Foreign students. They would also like to thank Valentin Pintat for his assistance with the prototyping of the experimental prototypes and Prof. Christian Giguère for providing knowledge and expertise.

References

[1] Pamela Ramage-Morin and Marc Gosselin. Canadians vulnerable to workplace noise. *Health reports*, 29:9–17, August 2018.

[2] Tony Leroux, Chantal Laroche, Christian Giguère, and Jérémie Voix. Hearing Aid Use in Noisy Workplaces. *Institut de recherche Robert-Sauvé en santé et en sécurité du travail, Studies and Research Projects*, page 117, 2018.

[3] Narimene Lezzoum, Ghyslain Gagnon, and Jérémie Voix. Noise reduction of speech signals using time-varying and multi-band adaptive gain control for smart digital hearing protectors. *Applied Acoustics*, 109:37–43, August 2016.

[4] Denis Byrne, Aaron Parkinson, and Philip Newall. Hearing Aid Gain and Frequency Response Requirements for the Severely/Profoundly Hearing Impaired:. *Ear and Hearing*, 11(1):40–49, February 1990.

[5] Harvey Dillon. *Hearing Aids*. Thieme, Sydney, 2 edition edition, June 2012.

[6] Michael Nilsson, Sigfrid Soli, and Jean Sullivan. Development of the Hearing In Noise Test (HINT) for the measurement of speech reception thresholds in quiet and in noise. *The Journal of the Acoustical Society of America*, 95:1085–99, March 1994.

[7] Véronique Vaillancourt, Chantal Laroche, Chantal Mayer, Cynthia Basque, Madeleine Nali, Alice Eriks-Brophy, Sigfrid Soli, and Christian Giguère. Adaptation of the HINT (hearing in noise test) for adult Canadian Francophone populations. *International journal of audiology*, 44:358–69, July 2005.

[8] Nicolas N. Ellaham, Christian Giguère, and Wail Gueaieb. A new research environment for speech testing using hearing-device processing algorithms. *Canadian Acoustics*, 42(3), August 2014. Number: 3.

[9] Rolph Houben, Maaike van Doorn-Bierman, and Wouter A. Dreschler. Using response time to speech as a measure for listening effort. *International Journal of Audiology*, 52(11):753–761, November 2013. Publisher: Taylor & Francis _eprint: https://doi.org/10.3109/14992027.2013.832415.

FUNCTIONAL DISCOMFORT OF EARPLUGS AND ITS INFLUENCING VARIABLES

Bastien Poissenot-Arrigoni [*1], Alessia Negrini [†2], Djamal Berbiche [‡3], Franck Sgard [♦2] and Olivier Doutres[#1]
[1]École de Technologie Supérieure, Montréal, Québec, Canada.
[2]IRSST, Montréal, Québec, Canada.
[3]Université de Sherbrooke, Longueuil, Québec, Canada.

1 Introduction

Earplugs are widely used to prevent noise-induced hearing loss. Their effectiveness depends on both attenuation and wearing time, which are affected among other factors by (dis)comfort aspects. Discomforts experienced by the wearer can make him/her deteriorate intentionally the fit quality or remove the protector which causes a drastic reduction in protection. The comfort is a multidimensional construct, and in the context of earplug use, four dimensions of earplug (dis)comfort have been proposed [1]. The 'functional' dimension of interest in this work, corresponds to the practical acceptability of earplugs and refers to the usability, efficiency and usefulness concepts. The (dis)comfort results from the complex interactions between the triad constituted of the person wearing the earplugs (wearer), his/her earplug, and his/her work environment. The triad components (wearer / earplug / environment) can be described by many physical and psychosocial characteristics which may have an impact on the (dis)comfort [2]. As examples, physical characteristics of the triad include person ear morphology and hand dominance, earplug shape and mechanical properties or work environment temperature. Psychosocial characteristics of the triad include for example the person gender and previous experience with earplugs, earplugs discreetness or aesthetic design and environment type of work or physical activity (e.g., body, head or jaw movements). A better knowledge of the characteristics of the triad promoting comfort, and thus effectiveness of the earplugs, could allow (i) manufacturers to design earplugs taking into physical and psychosocial characteristics and (ii) preventionists to propose to workers the most adapted earplugs fitting to their needs and characteristics, as well as to those of their work environment.

Following previous studies [3], the objective of this contribution is to identify the characteristics of the triad that significantly influence the general attribute of the functional comfort dimension and an attribute specifically related to earplugs "efficiency" (other attributes will be the subject of a future publication). The acoustic and psychological dimensions of comfort will be the subject of future publications.

2 Method

This study uses data of morphologic descriptions of the participants' earcanals and field survey on earplug comfort approved by the ethical committee of the École de Technologie Supérieure (ethics certificate H20171101).

2.1 Earplugs comfort assessment in the field

Nine earplug models among the most used in North America were tested as follows: three roll-down-foam four push-to-fit (one premolded and 3 push-to-fit-foam), and two custom earplugs. A total of 173 persons (84% of men) working in three different companies in Quebec (Canada) participated in this field study.

Participants first filled out the questionnaire "User Profile Questionnaire (UPQ)" and a custom earplugs manufacturer molded participants' earcanals.

Over seven weeks, participants tested an earplug from each of the earplug's families in their workplace. For both the roll-down foam and push-to-fit foam earplugs, the participant wore the same earplug model for one week, then wore it for another week, two weeks apart. A typical test week was as follows. At the beginning of the week, an individual training on earplugs insertion and use was offered to each participant by an audiologist. At the end of the individual training, if the earplug provided a safe attenuation for the participant, the test week could start. At the end of the week, participants completed the "Comfort of hearing protection devices – North America Questionnaire" (COPROD-NAQ) to express their opinion about the four dimensions of earplug comfort (i.e., physical, functional, acoustical and psychological).

To answer to the objective of this contribution, the functional dimension of comfort was evaluated with one general item (i.e., corresponding to the general attribute "functionality") and one explanatory item "efficiency" (i.e., a specific attribute "efficiency"). Specifically, these two attributes were measured by the two questions "*Generally speaking, these earplugs are functional (efficiency, good fit, intuitive installation...)*" and "*These earplugs are useful considering: your work environment*" to which participants answered on a five points Likert scale ranging from 1 "Totally disagree" to 5 "Totally agree".

2.2 Assessment of the triad characteristics

The triad characteristics considered in this study for the "person" component are the following: morphology of the external earcanal (girth and shape of 3 cross-sections, length and conicity), hearing loss, hand dominance, age, education and experience with HPD use. The characteristics of the work environment include the perception of exposition of high noise levels, possibility of changing departments, team work, work duration, shift and physical activity (body, head or jaw movements).

[*] bastien.poissenot.1@ens.etsmtl.ca
[†] alessia.negrini@irsst.qc.ca
[‡] djamal.berbiche@usherbrooke.ca
[♦] franck.sgard@irsst.qc.ca
[#] olivier.doutres@etsmtl.ca

The characteristics of the "earplug" component included the earplugs shapes which were described with a dichotomous variable to characterize earplugs conicity (conical/cylindrical) and the presence of a stem (yes/no). Earplugs masses were measured in grams on a scale and their diameter were assessed using a caliper placed at the position corresponding to the first bend of the earcanal.

The mechanical characteristics of the earplugs were assessed using two "comfort testers" described below. The J-Crimp™ Station (figure 1 (a)) enabled to measure the total radial force exerted by an earplug inserted in a rigid cylindrical earcanal, at different compression rates. The second comfort tester (see figure 1(b)) enabled to measure the force required to extract an earplug inserted inside a rigid cylinder of 9 mm diameter (the diameter was chosen based on earcanals morphologic data). The ratio between the extraction force and the radial force at 9 mm compression diameters was used to compute a static friction coefficient for each earplug.

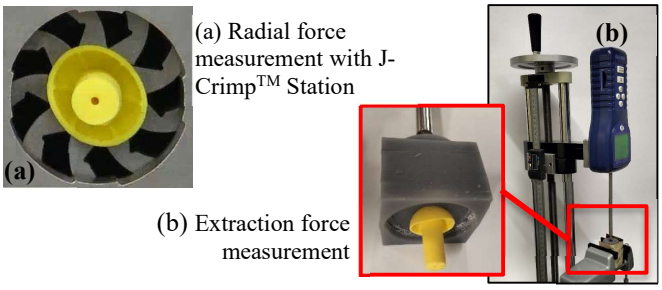

(a) Radial force measurement with J-Crimp™ Station

(b) Extraction force measurement

Figure 1: Two comfort testers: (a) J-Crimp™ Station (©Blockwise, USA). (b) Extraction force measurement setup: the earplug is pushed out of the grey sample holder by a rigid rod connected to a Newtonmeter.

Linear mixed effect modeling was used to find relationships between triad characteristics and the two attributes of the functional comfort. Given the large number of variables characterizing the triad (around 50) in relation to the number of participants, an iterative procedure was carried out to sort out the variables of each component of the triad that influence significantly functional comfort (see more details about statistical analyses in [3]).

3 Results

The analyses mostly showed that the characteristics of the person influenced significantly the "Functionality": being use to wear earplugs from the same family (roll-down foam, push-to-fit foam or premolded) as the one tested and having a small earcanal entrance make participants feel earplugs more functional. The influence of the size of the earcanal entrance on functional comfort is not easy to interpret, as the general element of functional comfort encompasses several different concepts linked, for example, to earplug maintaining in position or ease of insertion or removal. The fact that participants preferred (in term of functional comfort) the earplugs that they were used to wearing could be in line with the literature, which points out that habituation (or acclimatization) enhances comfort [4]. "Efficiency" was also influenced by the habits of the worker wearing the earplugs: being use to wear earplugs from the same family as the one tested make participant feels earplugs more useful. Moreover, participants found their earplugs more useful if they didn't interfere with their other work equipment (which are a characteristic of the triad that describes the work environment). This last finding underlines the importance of choosing earplugs that are adapted not only to the individual, but also to the working environment, which is characterized by the worker's other protective equipment.

The functional comfort of earplugs encompasses several concepts related to the practical acceptability of earplugs such as usability, efficiency and usefulness. Evaluating all these concepts using a very limited number of items is not very conducive to finding the characteristics of the triad that influence earplugs comfort. Consequently, other explanatory items measuring other attributes of the functional comfort (e.g., stay in position, easy to use/to insert/to remove) will be used in an attempt to gain a more exhaustive view of the characteristics of the triad that influence the functional comfort of earplugs, and will be the subject of a future publication.

4 Conclusion

Functional comfort evaluated through its attributes "Functionality" and "Efficiency" is mainly governed by characteristics of the wearer: his/her previous experience with earplugs, his/her earcanal girth and a characteristic of the work environment: the interference of the earplug with other protective equipment. However, functional dimension of comfort refers to several other attributes and further analyses (which will be the subject of a future publication) are needed to better understand functional comfort influencing variables.

Acknowledgments

The authors acknowledge the support of the Institut de Recherche Robert-Sauvé en Santé et en Sécurité du Travail (IRSST) (Funding Ref. No. 2015-0014) and the MITACS Accelerate program (Funding Ref. No. IT10643).

References

[1] Doutres, O., Sgard, F., Terroir, J., Perrin, N., Jolly, C., Gauvin, C., & Negrini, A. (2019). A critical review of the literature on comfort of hearing protection devices: Definition of comfort and identification of its main attributes for earplug types. International journal of audiology, 58(12), 824-833.

[2] Doutres, O., Terroir, J., Jolly, C., Gauvin, C., Martin, L., & Negrini, A. (2022). Towards a holistic model explaining hearing protection device use among workers. International Journal of Environmental Research and Public Health, 19(9), 5578.

[3] Poissenot-Arrigoni, B., Negrini, A., Berbiche, D., Sgard, F. and Doutres, O. (2023). Analysis of the physical discomfort of earplugs experienced by a population of Canadian workers and identification of the influencing variables. Article under review in the International journal of industrial ergonomics.

[4] Doutres, O., Sgard, F., Terroir, J., Perrin, N., Jolly, C., Gauvin, C., & Negrini, A. (2022). A critical review of the literature on comfort of hearing protection devices: Analysis of the comfort measurement variability. International Journal of Occupational Safety and Ergonomics, 28(1), 447-458.

Abstracts for Presentations without Proceedings Paper
Résumés des communications sans article

Providing Focused Hear-Through On Active Hearing Protection Devices Using Dipole And Omnidirectional Outer-Ear Microphones.

Hugo Besnard

Active hearing protection devices (HPD) equipped with an outer-ear microphones (OEM) and an in-ear loudspeaker allow users to hear their environment at unity gain when ambient conditions are quiet. This active hear-through can enable natural face-to-face communication without removing the HPD. In moderately noisy conditions, however, users can feel overwhelmed by the active hear-through which, due to omni-directional OEM, does not discriminate the source of interest from the background noise, achieving poor signal-to-noise ratio (SNR). Through the addition of a second miniature OEM that exhibits a dipole pickup pattern, an overall cardioid or hyper-cardioid pattern can be obtained through signal processing and focused towards the direction where the user looks, effectively improving the SNR of the face-to-face conversation during active hear-through. This work presents the design, prototyping and preliminary validation of an earpiece enabling focused active hear-through. Preliminary objective results indicate SNR improvement in the range of 15dB at 250Hz and 17dB at 1kHz, relative to omni-directional pickup, while preliminary subjective impressions are favorable.

Evaluating Mechanical Comfort Of Ear Tips: An Experimental-Computational Approach

Amir J Bidhendi, Katrin Braun, Jacob Bouchard-Roy, Farshid Ghezelbash

The mechanical comfort of in-ear devices is integral to their usability. Particularly for hearing protection devices intended for long-term wear, discomfort can lead to inconsistent or improper use, thus undermining their purpose. We have tested a three-pronged approach for evaluating ear tip comfort: the utilization of 3D ear canal data to create ear canal surrogates, the development of finite element models of ear canals, and the collection of user feedback. In our trial, 3D printed models of ear canals, obtained from 3D scan of ear impressions, were used as surrogates. Equipped with load cells, these surrogates measured forces generated from the insertion of commercially available ear tips. For instance, we observed that, while similar in foam stiffness, the ear tip with a larger and more rigid sound bore exerted nearly twice the force on the ear canal surrogate. In blind trials for a period of 2 hours, 60% of the participants (n=7) deemed the same ear tip as less comfortable for long-term wear. However, feedback varied widely, likely due to individual differences in ear canal geometry and tissue mechanics. Notably, most users did not favor any of the tested tips for extended wear periods, highlighting the need for design improvement. Finite element simulations enabled an in-depth investigation of the deformation behavior of ear tips and the identification of the pressure hotspots within the ear canal depending on the characteristics of the ear canal and tip such as material, geometry, and sound bore dimensions. Further, the simulations proved capable of detecting folding that affects some types of ear tips. By integrating computational mechanics, mechanical testing, and 3D-printed ear canal surrogates, our platform quantifies the user experience and allows parametric ear tip design to optimize comfort. Our next steps include expanding our user population and improving our understanding of ear tissue biomechanics.

3d Printed Meta-Earplug For Minimizing The Occlusion Effect

Kévin Carillo, Franck Sgard, Olivier Dazel, Olivier Doutres

Passive earplugs are commonly associated with the occlusion effect, which refers to the increased perception of one's own physiological noise at low frequencies. This effect poses a significant challenge as it leads to acoustic discomfort, thus limiting the usability and effectiveness of earplugs. To address this issue, we developed a novel design of a 3D printed meta-earplug composed of four Helmholtz resonators arranged in series. The meta-earplug design is optimize to achieve near-zero occlusion effect in a broadband frequency range from 300 Hz to 1 kHz, as verified through comprehensive measurements conducted on an artificial ear adapted to bone-conducted stimulation. The optimization of the meta-earplug geometry was carried out using an analytical model of the occlusion effect that includes the acoustic impedance of the meta-earplug medial surface. Due to the simplified geometry of the prototype, the acoustic impedance of the meta-earplug was modeled using a transfer matrix model. Results show that the optimized input impedance of the meta-earplug medial surface approximately matches the input impedance of the open earcanal weighted by the ratio of volume velocity imposed by the earcanal wall to the earcanal cavity between open and occluded cases. Furthermore, we demonstrate that the acoustic properties of the meta-earplug yield significant improvements in the sound attenuation measured on artificial test fixture, particularly at the piston-like mode of the system. Hence, our findings highlight the potential of this innovative

meta-earplug design to overcome the occlusion effect and enhance the sound attenuation for individuals using earplugs.

The Effect Of Training Material On The Personal Attenuation Rating Achieved By An Initially Untrained Population

Lucas Carneiro, Lydia Behtani, Antoine Bernier

The actual amount of protection offered by a given hearing protection device (HPD) in the field is subject to great variations. Aside from the HPD itself, the amount and the format of the training material can influence the personal attenuation rating (PAR) that user obtain in the field. An active HPD equipped with an outer-ear microphone (OEM) and an in-ear microphone (IEM), can perform a measurement derived from the field microphone in real-ear (FMIRE) method to quickly estimate a personal attenuation rating (PAR) as per ANSI S12.71-2018. This method was used to characterize the PAR achieved by a population of 23 untrained participants of mean age 50 with an advanced hearing protection device, as well as characterize the effect of progressively more involved training material. The training material included three phases: written instructions with images, a training video, and personalized one-on-one training administered by the experimenter. The first phase training yielded an average PAR of 22 dB, with 78% of participant achieving a PAR of 20 dB or more and 9% achieving a PAR of 30 dB or more. The final phase training yielded an average PAR of 28 dB, with 96% of participant achieving a PAR of 20 dB or more and 48% achieving a PAR of 30 dB or more. This research enables insight into realistic levels of protection that an advanced HPD can provide in the field and allows to statistically predict the noise exposure of the population in specific environments. It also highlights the importance of providing proper education and training on the use of HPD and the value of measuring PAR in the field.

Development Of A Realistic Artificial Ear Dedicated To Earplugs Attenuation Measurements

Said Ezzaf, Luiz Melo, Bastien Poissenot-Arrigoni, Hugo Saint-Gaudens, Alain Berry, Franck Sgard, Olivier Doutres

"One size fits the most" disposable or reusable earplugs currently manufactured are not adapted to the diversity of human ear canal morphologies. According to the standard ASA/ANSI S12.42, an objective method for designing earplugs is to use acoustical test fixtures (ATFs) comprising cylindrical ear canals of a signe size. Consequently, this ATF is unable to fully capture the inter-individual and the intra-individual variability when testing earplug attenuation and may therefore not be suitable for properly designing "One size fits the most" earplugs. Several more realistic artificial outer ears mainly intended for evaluating the occlusion effect have been developed in the past by the ÉTS/IRSST research team, but have not been able to correctly reproduce the attenuation measured on a reference human participant (from which the artificial outer ears were designed). These discrepancies can be partly attributed to (i) the realism of the synthetic materials, (ii) defects due to the manufacturing process (presence of air bubbles in the final part representing the soft tissue of the outer ear) and (iii) its self-insertion loss which may not have been important enough and could not have been measured properly due to the small size of the outer ears. The objective of this work is to develop a realistic artificial ear dedicated to acoustical attenuation measurements of earplugs and allowing for capturing the intra-variability due to fit and the measurement of its self-insertion loss. This ear is reverse-engineered from magnetic resonance imaging (MRI) images of the human head of a living participant. The cartilage and bone parts of the artificial ear are manufactured using 3D printing whereas a molding technique is used for soft tissues. Synthetic materials are chosen to have mechanical properties close to those of biological tissues. The ability of the artificial ear at measuring the sound attenuation of three families of earplugs (roll-down foam, push-to-fit, pre-molded earplugs) is evaluated by comparison with experimental data obtained in a diffuse field carried out on the participant whose head was imaged. The next step will be to make a total of three artificial ears with three different ear canal morphologies (small, regular, large) to cover a larger part of the population and capture the inter-variability.

Statistical Shape Modeling Of The Human Ear Canal For Designing Hearing Protection Devices And Auditory Wearables

Farshid Ghezelbash, Katrin Braun, Amir Jafari Bidhendi, Jacob Bouchard-Roy

Current in-ear device designs rely mostly on a limited number of sizes or a 'one-size-fits-all' approach, based on basic shapes such as cones, circles, and/or ellipses. Moreover, the choice of size is often based on the linear scaling of an average design, leading to issues including insufficient or excessive contact pressure, improper device fit, and inferior acoustic performance. An understanding of ear shape is crucial for the acoustic performance of the

in-ear device and for all-day wearability. To address this challenge, we present a method for generating statistical ear shapes for designing devices that are reflective of ear canal morphology. First, we collected ear impressions from 86 subjects, which were digitized using a 3D scanner. A novel landmarking algorithm was developed to reliably and automatically identify key features of the canal (i.e., entry plane and first/second bend). 3D parametric shapes of the canal were then created from these landmarks. Principal shape modes were identified using principal component analysis. k-means algorithm was utilized to identify clusters within the dataset based on relevant data features. The clustering process was conducted on the centroid axis, selected 2D cross-sections, and the 3D shape of the ear canal. Despite considerable variation within the dataset, the landmarking algorithm proved to be robust by performing well across all subjects. Using our parametric shapes, we calculated the average shape of the ear canal across the population. The first and second shape modes corresponded to overall size changes, and variations at the entry plane, respectively. After analyzing the data, we generated 4-5 clusters for centroid axis, cross-sections, and 3D shapes. The shapes derived from our analysis capture all ear canal morphologies, and offer a blueprint for innovative design of sound bores, flanges, and ear plugs tailored to fit the canal, thus, opening up new avenues in auditory equipment design.

Source-Separated Dosimetry In An Active Hearing Protection Device

Max Henry

Active hearing protection devices, when equipped with an outer-ear microphone, inner-ear microphone, and in-ear loudspeaker, can allow for two-way communication, music listening and ambient hear-through audio, while affording a baseline level of noise protection from ambient sounds. Each sound source contributes separately to user total sound exposure; knowledge of the contribution of each source is valuable, as it can enable data-driven, actionable recommendations to reduce overexposure.While the signal at the inner-ear microphone can be used to measure the level under the protective earplug, this method cannot identify the contribution of each individual sound source. This approach is all-the-more challenging due to wearer-induced disturbances, such as speaking or coughing, which pollute the in-ear noise exposure measurements.This work details a novel system for personal dosimetry that can separate dose by sound source, by modeling the transfer function of the earpiece, and the media playback from the in-ear loudspeaker. The models are updated opportunistically—allowing the system to compensate for changes in wearer fit—when favorable measurement conditions are detected.The proposed system uses these models to estimate of the portion of in-ear level attributable to ambient sounds, communication and media playback signals. When subtracted from the total in-ear level, these estimates yield a residual value, attributable to wearer-induced disturbances.Preliminary validation using a scenario of simultaneous music playback (in-ear level of 82–89 dB(A)) and ambient noise (90 dB(A)) through a highly attenuative earpiece (20–45 dB), shows that in-ear playback heavily dominates noise exposure. In a small study (N=3), the proposed system correctly attributes the majority of in-ear level to media playback, while correctly estimating the contribution of ambient sound as attenuated under the earplug (ranging 45-70 dB (A)).

Finite Element Simulation Of The Ear Canal Wall Vibrations

Simon Kersten, Chalotorn Möhlmann, Michael Vorländer

When the ear canal is occluded by devices such as earplugs or hearing aids, the perception of bone conducted sounds is increased, which results, e.g., in an alteration of one's own voice perception. This is denoted as occlusion effect. It contributes to the discomfort of workers wearing hearing protection, and reduces the acceptance of hearing aids among their users. The effect is caused by a vibration of the ear canal wall that induces a sound pressure at the eardrum. In this study, finite element simulations are conducted to investigate the vibration. The model is based on an anatomical outer ear geometry with the ear canal surrounded by soft tissue, cartilage, and bone. The results indicate the spatial distribution of the vibration of the ear canal wall to potentially vary with frequency due to the ear canal's complex geometry and the material composition of the surroundings. A decomposition of the imposed volume velocity quantifies the different boundaries' contributions. Knowing the characteristics of the ear canal wall vibration could help with the design of earplugs, and to improve measures to reduce the occlusion effect. This work is funded by the Deutsche Forschungsgemeinschaft (DFG, German Research Foundation) ¬ Project-ID 352015383 ¬ SFB 1330 A4.

Experimental Investigation Of The Static Mechanical Pressure Induced By Roll-Down Foam Earplugs

Luiz G. C. Melo, Ahmed Dalaq, Franck Sgard, Olivier Doutres, Éric Wagnac

Roll-down foam earplugs are a popular choice for hearing protection in North America. They are made of a soft,

malleable foam that is compressed (rolled) into a small cylinder shape for proper insertion into the earcanal. Once inserted, the earplug expands, conforming to the shape of the earcanal, creating an acoustic seal that blocks out potentially harmful external noise. After full expansion, the static mechanical pressure (SMP) exerted by the earplug on the earcanal walls can cause physical annoyance or pain. In this work, we experimentally investigate the SMP of a PVC roll-down foam earplug by using a commercial radial force tester, commonly employed for assessing the mechanical properties of stent grafts. It is found that the degree of pre-compression (before expansion) plays an important role in the observed SMP, that is, the more compressed the earplug, the lower the SMP. This is mainly due to viscoelastic effects and damage mechanisms within the foam under excessive compression. These results suggest that users could adjust the SMP and fit of the earplug by varying the roll-down technique leading to improved physical comfort and better protection.

Design Considerations To Optimize Occlusion Effect Mitigation With Acoustic Noise Cancelling Hearing Protection

Vincent Nadon

Earpiece designs for optimal active noise canceling (ANC) require multiple loudspeakers for minimal saturation for occlusion effect compensation. Such multi-loudspeaker design for feedback ANC is facilitated through lumped elements electro-acoustical modeling and key design guidelines. In this work, the authors review key concepts of lumped element modeling, review desirable characteristics, present earpieces design archetypes of earpieces destined for feedback ANC and detail one chosen design. Acoustical validation of a maximal gain of 18dB at 250Hz in the feedback loop and measured Total Harmonic Distortion (THD) of 10% at approximately 122dB at 125Hz plus the limitations of the design are discussed along with the perceptual effects of feedback ANC provides.

Effect Of Aging On The Ear Canal Morphology : A Large Scale Study

Pierre Buyssens, Robin Petit, Gwenolé Nexer

Performances of custom molded earplugs are among the best ear protection devices since they are designed to perfectly fit an ear canal and to guarantee a high quality sealing. Evolution of the ear morphology is then a crucial element when designing such earplugs. This paper proposes a large scale study of the evolution through time of the external ear morphology, and especially the evolution of the ear canal. The dataset used for this study is composed of more than 388K pairs of ear scan, each pair capturing the morphology of a single ear at different times. The gap between scan varies from 1 to 120 months. To our knowledge, this is the first study on such a large dataset.Given this amount of data, any manual action is prohibited, hence the whole process has been automated and acts in three steps:First, several algorithms that extract some morphological features have been designed. A particular focus has been made on the robustness to achieve a high success rate on many external ear morphologies.Second, the old and recent canals have been aligned using a coarse to fine approach : the morphological features are first used to get a good guess for a classical Iterative Closest Point refinement.Finally, several algorithms have been used to measure the morphological differences between scans.This process allows us to exhibit general tendencies of the evolution of the external human ear through time (dilation/contraction) but also sketch correlations between evolution tendancies and the ages of the scans.

Effect Of Aging On The Ear Canal Morphology : Measurements On Human Subjects

Robin Petit, Pierre Buyssens, Gwenolé Nexer

Hearing Protection Devices (HPD) must be used by workers when the noise level value exceeds 85dB(A) for reducing the effect of high noise and sound on the hearing health. HPD are generally available in two main forms: earmuffs and earplugs. Earplugs are designed to be inserted into the ear canal or to cover the ear canal entrance and three main types exist on the market:the pre-shaped earplugs often come with different sizes,User-formable earplugs are made from compressible materials that the user forms before inserting them into the ear canal,For the custom molded earplugs, they are directly manufactured from an ear print.Even if the performance depends on several parameters such as the training, motivation, general aspect, the attenuation is guaranteed when the earplug is well fitted to the ear which avoids air leaks and a drop off in low frequencies.A problem appears when the geometry of the ear is evolving through the age and the protection is no longer adapted to the original shape becoming potentially dangerous for the users.This work is focused on the evolution of the ear canal and won't consider some parameters that is difficult to obtain like weight, medical operation, injuries ...For this study, 24 people were selected and several custom molded earplugs with a different geometry of the part placed inside the ear canal were tested. This article will describe the protocol and the measurements done for observing changes (in channel geometry and size) and their influence on sealing and protection of the users.

Assessment Of The Effect Of Earplug Type, Insertion Depth And Background Noise Level On The Occlusion Effect In Laboratory Conditions

Hugo Saint-Gaudens, Hugues Nélisse, Franck Sgard, Olivier Doutres

Inserting an earplug in the earcanal's entrance can lead to various discomforts, one being the occlusion effect (OE), typically described as a distorted perception of one's own voice. This discomfort can lead to users misusing or removing their earplugs, significantly lowering their efficiency. Therefore, it is critical to reduce the OE generated by earplugs to enhance user comfort. However, the influence of factors such as earplug type, insertion depth and background noise level on the OE remains poorly understood. Consequently, this ongoing research aims to identify the underlying factors contributing to the discomfort generated by the OE during speech. To achieve this, tests are conducted in laboratory conditions with 33 normal hearing participants with varying levels of experience in daily earplug use for work or personal activities. The OE is assessed subjectively using a user comfort questionnaire focused on the perceived and experienced OE, and objectively using surrogate earplugs for in-ear microphonic measurements. Multiple combinations of earplugs, insertion depths and background noise levels are tested to obtain a ranking of the conditions generating more or less OE, and to identify the factors contributing to the discomfort. The improved understanding of the OE resulting from this study will allow manufacturers to develop more comfortable and, as a result, more efficient earplugs.

Bandwidth Extension Of In-Ear Speech Through Machine Learning-Based Dynamic Equalization

Ajin Tom, Antoine Bernier

In-ear voice pickup, using an Inner-Ear Microphone (IEM) within a communication-equipped hearing protection device, improves signal-to-noise ratio for better intelligibility in high noise. To enhance the perceived quality of IEM speech which otherwise sounds muffled or 'boomy', signal processing techniques like fixed filtering, whitening filter, and bandwidth extension algorithms based on harmonic regeneration and machine learning have been developed. Traditional machine learning techniques have shown impressive results but are computationally expensive for embedded systems. On the other hand, traditional signal processing techniques are suitable for embedded systems but lag behind air-conducted reference (REF) speech in perceived quality.This research combines machine learning and traditional signal processing by training a model to dynamically adjust a filter in real-time based on speech content. The model considers the spectral differences between IEM and REF speech to filter and denoise IEM speech, matching air-conducted speech captured by a REF microphone.A particular implementation of the system involves preconditioning the IEM using an established denoising technique and decomposing it into four audio buses using a filter bank. Simultaneously, temporal and spectral features are extracted from the full bandwidth IEM signal in a frame-wise manner. These features are utilized by the model to determine corrective gains (CG) for each sub-band for each frame, which are applied to the audio buses before recombining them to obtain the processed full bandwidth signal. The model is trained using a database of 20 subjects speaking phonetically balanced sentences. The ground truth CG is the instantaneous energy difference between IEM and REF for each sub-band.After data augmentation, feature selection, and further tuning, the models generally achieve an average Rsquared value of 0.7. Interestingly, the technique can also perform denoising if the model is trained to map synthesized noisy IEM speech to clean REF speech.

MATERIALS FOR NOISE AND VIBRATION CONTROL - MATÉRIAUX ACOUSTIQUES

DEVELOPMENT OF AN ECO-ACOUSTIC ABSORBER BASED ON LOCAL RE-CYCLED GRANULAR MATERIALS

Islam Ben Amara [*1], Raymond Panneton [†1], and Richard Gagne´ [‡1]
[1]Centre de recherche acoustique-signal-humain de l'Université de Sherbrooke, Sherbrooke, Québec, Canada

1 Introduction

Nowadays, noise pollution is causing significant socio-environmental problems, impacting both humans and the planet. It is crucial to address the detrimental effects of noise and find effective solutions. Traditional sound absorbers such as foams and mineral wools are commonly used indoors and outdoors to attenuate sound waves. However, the Earth is facing a severe shortage of raw materials due to high consumption and extraction rates. Consequently, massive amounts of materials are wasted. In response, Quebec government is working to establish new regulations to value various types of residual waste [1]. This presents an opportunity to explore sustainable alternatives that address both acoustic and material concerns. Previous research has shown that granular materials can be a suitable substitute for conventional applications. Several researchers have studied the acoustic performance of porous granular absorb-ers. Empirical and numerical approaches have been employed to predict the acoustical performance of these materials, identifying mechanical and structural parameters which can improve their acoustic response [2–4]. Additionally, the recycling of granular waste can contribute to sustainable development.

This study aims to investigate the potential of polydisperse granular recycled materials through experimental methods to enhance acoustic absorption across a broad range of frequencies. Furthermore, the antiresonant behaviors will be examined, based on combinations between transport properties, particle size, and the dosage of cementitious binders.

2 Recycled granular materials

The selection of granular materials is based on three primary criteria: sustainability, local availability, and affordability. Evaluation and determination of physical parameters, including particle size, shape, and diameter range, are also performed. Two types of granular waste, namely expanded glass beads and perlite, are characterized within a fixed diameter range of 250 µm to 2 mm. Acoustic and nonacoustic parameters are investigated through testing various recipes, including monodisperse, bidisperse, and polydisperse configurations. The main objective is to identify and analyze the acoustic absorption potential of these granular blends.

3 Experimental methods and results

3.1 Granulometry

Considering the improvement of acoustic absorption potential using granular wastes necessitates a comprehensive understanding of the material granulometry. The significant variation in particle sizes, coupled with the compaction level and the addition of a cementitious binder for consolidation purposes, can influence the dynamic porosity and, specifically, the open porosity crucial for attenuating acoustic waves. In the case of expanded glass beads, their granular size is already predetermined, ranging from 250 µm to 2 mm. However, for perlite, a granulometry test was conducted to analyze the distribution of particles, considering its low resistance and tendency to fracture when subjected to blending. Throughout the mixing process, the particle size of perlite gradually decreased within a timeframe of less than 5 minutes. To compare the particle size before and after the mixing phase, two portions were tested: the raw material and the crushed granules. The sieves utilized ranged from 0.08 to 10 mm. The results can be interpreted as follows: the grinding process predominantly affected the larger perlite beads, resulting in their fragmentation and the generation of a variety of smaller beads, primarily distributed within the 1.25 to 5 mm sieves. Concerning the smaller beads, a correlation was observed between the results obtained before and after the grinding process.

3.2 Porosity and resistivity

To characterize the samples, both monodisperse and polydisperse, measurements of open porosity and airflow resistivity are carried out. These two parameters are important as they are part of the transport properties essential for subsequent acoustic simulations. The experimental measurements were conducted using porosity and resistivity meters on cylindrical specimens of 44 mm diameter and 120 mm long.

Perlite

The perlite specimens have variable dosages of cement binder of 500 g/L, 600 g/L and 700 g/L, which enabled us to study the influence of the binder content on the properties of the granular soundabsorbent material. The binder dosage is defined as the sum of the masses of water and cement divided by the volume of the granular material in the dry state. The results of the measurements are given in Table 1. The results revealed that as binder content increases, the porosity decreas. Specifically, for a binder content of 700 g/L, the porosity is 49.5%. In contrast, for a lower binder content of 500 g/L, the porosity rises to 74%. Also, it appears from the measurements that the resistivity varies with the binder content. Specifically, blends with a higher proportion of binder exhibit the highest resistivity values.

[*] islam.ben.amara@usherbrooke.ca
[†] raymond.panneton@usherbrooke.ca
[‡] richard.gagne@usherbrooke.ca

Table 1: Porosity and resistivity of perlite samples

Binder (g/L)	Porosity (%)	Density (kg/m³)	Resistivity (Pa·s/m²)
500	74	509	2 423 ± 52
600	64	676	3 557 ± 71
700	50	967	17 720 ± 354

Table 2: Porosity and resistivity of expanded glass beads at binder dosage of 500 g/L and different mixtures of small (0.25-0.5 mm) and large (1-2 mm) beads.

Mixture (small vs large)	Porosity (%)	Density (kg/m³)	Resistivity (Pa·s/m²)
100 – 0%	56	652	112 403 ± 2 250
70 – 30%	47	654	58 413 ± 1 077
50 – 50%	54	613	53 673 ± 1 070
30 – 70%	55	594	19 473 ± 759
0 – 100%	52	663	37 940 ± 390

Expanded glass beads

The experimental methodology employed for the expanded glass beads samples followed a similar approach. Five blends, with the same binder dosage of 500 g/L, were prepared by varying the mixture of beads to create bimodal samples. Small beads (0.25–0.5 mm in diameter) and large beads (1-2 mm in diameter) were used. Additionally, monodispersed specimens were examined to facilitate a comparative analysis of their performance with that of the bimodal samples. The results of the measurements are given in Table 2. The porosity values exhibit a relatively consistent behavior across the blends, except for a slight decrease observed in the 70 30% bimodal mixture. Regarding the resistivity results, the influence of polydisperse properties is noticeable. Despite the consistent binder quantity maintained across all blends, the impact of particle size becomes apparent. Specifically, as the particle diameter increases, the resistivity proportionally decreases going down from 112 403 for the 100 0% mixture to 19 473 for the 30 70% bidispersed mixture. Regarding the resistivity results presented in Table 2, the influence of polydisperse properties is noticeable. Despite the consistent binder quantity maintained across all blends (500 g/L), the impact of particle size becomes apparent. Specifically, as the averaged particle diameter increases, the resistivity proportionally decreases.

3.3 Sound absorption coefficient

According to the ASTM E1050-12 standard, the sound absorption coefficients of the samples were measured using a 44.4 mm impedance tube. The chosen materials, perlite and expanded glass beads, are tested using cylindrical samples (44 mm diameter, 120 mm long). To ensure airtightness, a layer of" cellophane wrap" is applied on the contour of the samples. Measurements are taken on both sides of the specimens to assess symmetry of the samples in the frequency range 100-4500 Hz. The results are given in Figures 1 and 2. One can note that samples containing a significant proportion of larger particles exhibit oscillating curves and resonant dips, particularly at lower frequencies. These observations highlight the link between acoustic absorption, particle size, and mixture. This knowledge will be useful in our future work with the aim of optimizing the sound absorption of an acoustic absorber made from recycled granules.

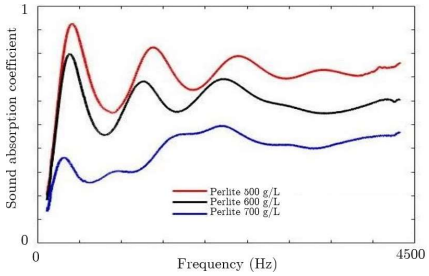

Figure 1: Absorption coefficient of granular perlite samples.

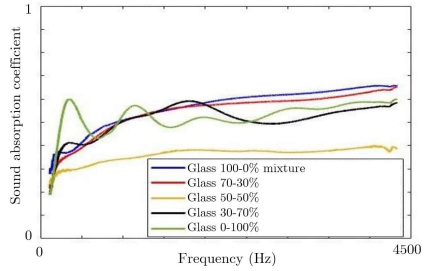

Figure 2: Absorption coefficient of expanded glass bead samples.

4 Conclusion

Revalorizing local granular wastes is a conscious and efficient approach to improve acoustics while considering environmental and economic factors. By optimizing both acoustic and non-acoustic parameters, granular absorbents have shown promising results in terms of sound absorption, comparable to conventional materials. However, it is essential to address constraints like binder quantities, polydiversity in particule diameters, and compaction to ensure the efficiency and durability of these acoustic materials.

Acknowledgments

Authors acknowledge the support of the Natural Sciences and Engineering Research Council of Canada (NSERC). Special thanks to Mecanum Inc for making their characterization laboratory available to us.

References

[1] Gouvernement du Québec. Règlement concernant la valorisation de matières résiduelles. 2021.

[2] KV Horoshenkov and MJ Swift. The effect of consolidation on the acoustic properties of (...). App. Acoust., 62, 2001.

[3] Vu Viet Dung and coll. Prediction of effective properties and sound absorption of (...). J. Acoust. Soc. Am., 145, 2019.

[4] NN Voronina and KV Horoshenkov. A new empirical model for the acoustic properties of loose granular media. App. Acoust., 64, 2003.

CFD Simulations of the Static Airflow Resistivity of a Perforated Solid: Effects of Size and Flow Velocity

Alla Eddine Benchikh Le Hocine [*1], **Tenon Charly Kone** [†2], **Maël Lopez** [‡3], **Raymond Panneton** [§1], **Thomas Dupont** [¶3], **and Kévin Verdière** [‖4]

[1]Centre de recherche acoustique-signal-humain de l'Université de Sherbrooke (CRASH-UdeS), QC, Canada
[2]National Research Council Canada, Flight Research Laboratory, ON, Canada
[3]Department of Mechanical Engineering, École de Technologie Supérieure, QC, Canada
[4]Mecanum Inc., QC, Canada

1 Introduction

For acoustic absorbers, the airflow resistivity is the parameter which has the greatest impact on their acoustic absorption coefficient. Therefore, its measurement according to standard ISO 9053-1 :2018 (or ASTM C522) should be done with care. This ISO standard gives specifications on the size and mounting of specimens, their location in the measuring cell, minimum and maximum flow velocities, calibration specimens and the measurement procedure. An important constraint is to ensure a stable linear flow so that the resistance is independent of the velocity. Additionally, it specifies the use of a calibration test specimen to ensure proper operation of hardware and software. The suggested calibration specimen consists of straight cylindrical pores whose value can be calculated theoretically. However, no other specification is given for designing the calibration specimen. Since the airflow resistivity of a perforated low porosity solid can behave nonlinearly with velocity, it is important to present some additional guidelines for their design. This work presents experimental results and CFD simulations on the flow resistivity of a cylindrical solid containing a single perforation subjected to an air flow velocity ranging from 0.5 mm/s to 10 mm/s. The simulations replicate a commercial airflow resistivity meter. The results of the simulations are compared with the theoretical formula and the experimental measurements. The results show the importance of the size of the perforation and the flow velocity so that the measurement corresponds to the theoretical value.

2 Materials and methods

The material considered here is a calibrated test specimen (CTS) as specified in the ISO standard to "ensure the proper functioning of the hardware and software of the measurement system". A CTS may consist of a solid cylinder containing straight circular perforations. The value measured on the CTS must not deviate by more than 10% from the theoretical value. ISO standard recalls the theoretical formula for the specific resistance to airflow (R_s) of a solid sample perforated with circular perforations : $R_s = 32L\eta/(\phi d^2)$, where L is the thickness of the material, η the dynamic viscosity of air, ϕ the perforation rate, and d the perforation diameter. ISO standard does not specify the number and rate of perforations, nor the thickness, nor the diameter of the CTS. However, it specifies that the lateral dimension of a porous sample must contain at least 10 pores, fibers or granules for respectively foams, fibrous materials and granular materials. Also, it specifies that the thickness must allow a measurement of the head loss. From these details, the simplest CTS is studied here. It is made of a perforated solid containing only one circular perforation. To better fulfill the criterion on the lateral dimension of the specimens, the CTS should contain at least 10 perforations. To the knowledge of the authors, this criterion aims only to ensure the statistical representativeness (homogenization) of the specimen. In the case of CTS, fine manufacturing tolerances are used and adding additional perforations would only lead to greater uncertainty effects. Therefore, as no other information is given in the standard, only one perforation is used. Two different diameters are tested : 2.10 mm for CTS#1, and 4.10 mm for CTS#2. Both CTS have a thickness of 30 mm. The fabrication tolerance is ± 0.03 mm. Figure 1(a) presents the CAD of the CTS mounted on the measurement cell.

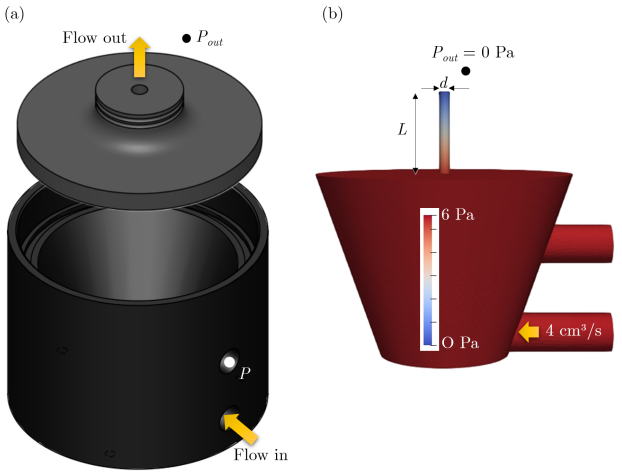

Figure 1 – (a) Calibrated test specimen on measurement cell. (b) CFD results on CTS#1.

The measurement procedure is applied according to the ISO standard using a Mecanum's Airflow Resistance Meter with Sigma-X software. Sigma-X adjusts flow velocity to ensure a measurable pressure drop. The first speed is always the lowest allowing a measurable pressure drop. Then the speed is increased step-wise. The measurement cell is shown

*. alla.eddine.benchikh.lehocine@usherbrooke.ca
†. tenoncharly.kone@nrc-cnrc.gc.ca
‡. mael.lopez.1@ens.etsmtl.ca
§. raymond.panneton@usherbrooke.ca
¶. thomas.dupont@etsmtl.ca
‖. kevin.verdiere@mecanum.coml.ca

in Figure 1(a). Its reference surface for velocity calculation is $D = 100$ mm in diameter. The CTS sits on the cell and an O-ring eliminates air leaks. The airflow comes through the lowest side inlet and is generated by a mass flow controller. The pressure before the specimen is measured at the upper side hole. A differential pressure gauge measures the pressure drop between this inlet point and the atmospheric pressure at the outlet of the sample. One condition imposed by the ISO standard is that the measurement must be made within a certain range of linear flow velocities. If pressure drop in this range is not measurable, the flow velocity can be increased step-wise without exceeding a velocity of 15 mm/s. In this case, we proceed to a second order regression on the pressure drop data (ΔP) versus velocity (U). The y-intercept is fixed at 0. The linear term is then the specific resistance.

To validate measurements with the hardware and software used, and further understand the results, CFD simulations are performed in the same conditions and geometry of the experimental measurement procedure. The mesh is generated with Salome on the air volume of the CAD shown in Figure 1(a). A RANS calculation is performed using OpenCFD OpenFOAM. A typical CFD model with results for CTS#1 is shown in Figure 1(b).

3 Results

Figure 2 shows the pressure drop in function of the volumetric flow rate for the small (CTS#1) and large (CTS#2) perforations. It is clear that both specimens have a non linear behavior. The small perforation is more resistive to airflow. This helps to have a measurable pressure drop at lower flow rates. On the contrary, the measuring equipment needs to increase the flow to have better measurements for the large perforation. ISO standard indicates that the flow velocity should not exceed 15 mm/s. It is not specified if this velocity is the macroscopic one (in front of the specimen) or the microscopic one (in the specimen). If the reference diameter is the one of the measurement cell ($\approx$ 100 mm), the velocity ranges from 0.5 mm/s to 1.5 mm/s for CTS#1, and from 0.5 mm/s to 10 mm/s. For conventional porous material, since porosity ϕ is close to one, the velocities at macro and micro-scales are similar. However, for perforated samples, the microscopic velocity can be much larger. For the studied CTS, the microscopic velocity ranges from 1130 to 3401 mm/s for CTS#1, and 296 to 5747 mm/s for CTS#2.

To be more related to flow conditions, it would be better to add a limit in terms of Reynolds number (Re) instead of flow velocity. Since the ISO standard states that the specific resistance can be obtained from second-order regression, the standard indirectly assumes the existence of nonlinear behavior. Therefore, why limit the flow velocity to 15 mm/s. The authors understand that this limit is more related to the nonlinear acoustic response of certain materials (notably microperforated plates) typically starting at 110 dB-re20μPa (which corresponds to an acoustic velocity of 15 mm/s). Since in a pipe the transition from laminar to turbulent flow takes place at Reynolds numbers around 2300, one could imagine that the approach would work for $Re < 2300$.

If we perform a regression of order 2 on the points of the figure, our results on the 30-mm thick specimens show that we obtain a good correspondence with the theoretical value if the regression is limited to $Re < 500$, see Table 1. If all points are taken for CTS#2, the obtained resistance is near 50% away from the theoretical one. We believe that in addition to the laminar/turbulent transition, the entrance length to establish developed flow in the perforation reduces this limit. This entrance length is proportional to the Reynolds number.

Further analyses are ongoing with CFD to better establish a flow criterion that could complement the ISO standard and to give additional recommendations for the calibration specimen. Some of these additional developments will be presented at the conference.

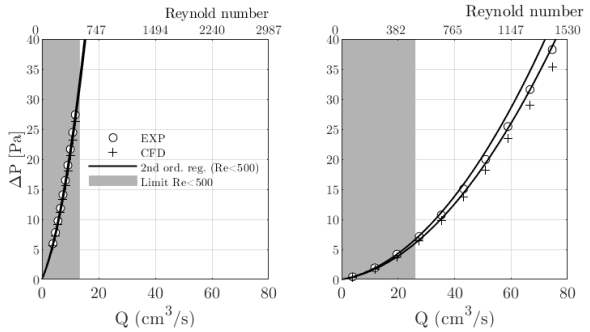

FIGURE 2 – Pressure drop versus volumetric flow rate of (a) CTS#1 and (b) CTS#2

TABLE 1 – Results of specific airflow resistance of two CTS. Values are scaled to the perforation ($\phi = 1$). Values in parentheses represent absolute deviations from theoretical values. Calculations on the regression is limited to data points with $Re < 500$.

CTS#	Theoretical (Pa*s/m)	Experimental (Pa*s/m)	CFD (Pa*s/m)
1	4.02 ± 0.23	4.00(0.48%)	3.61(7.67%)
2	1.05 ± 0.03	1.13(6.03%)	1.01(3.22%)

Conclusion

CFD and experimental results were obtained on perforated solids to emphasize limits of the ISO 9053 standard when measuring on a calibration sample. It has been shown that the speed limit of 15 mm/s specified by the standard can be misunderstood and constraining for the design and validation of a calibration specimen. It has been suggested that the limitation should be in terms of the Reynolds number. Preliminary tests have shown that the second-order extrapolation of specific resistance should be limited to Reynolds numbers less than 500 in the perforation of a 30 mm thick specimen. Further tests are needed to validate this proposition and give additional details to help in the design of the calibration specimen.

Acknowledgments

Authors acknowledge the support of the Natural Sciences and Engineering Research Council of Canada (NSERC).

ASSESSMENT OF ACOUSTIC PROPERTIES OF MYCELIUM-BASED COMPOSITES MATERIALS

Alexis Boisvert [*1,2], Saïd Elkoun [†1,2], Olivier Robin [‡1,2] et Félix-Antoine Bérubé-Simard [♦3]
[1]Centre de Recherche Acoustique-Signal-Humain de l'Université de Sherbrooke, Sherbrooke, Québec, Canada.
[2]Department of Mechanical Engineering, Université de Sherbrooke, Sherbrooke, Québec, Canada.
[3]CCTT Biopterre, La Pocatière, Québec, Canada.

1 Introduction

Nowadays, the increasing concern for the environmental impact of plastic or petroleum-based materials has led to a growing interest in biomaterials. Mycelium-based composites are self-grown materials, based on agricultural residue fibers that are inoculated with fungi mycelium. The mycelium forms an interwoven 3-dimensional filamentous network, binding every fiber particle together to create a rigid, lightweight composite material with no additional energy input and no extra waste or residue production [1]. Mycelium-based composites could replace current products in the packaging industry, as well as in construction (e.g., materials for thermal and acoustic insulation) [2]. Many physical properties can be adjusted by controlling the fungal species, the growth conditions and the post-growth processes [3]. To evaluate the sound absorption properties of mycelium-based composites made from residual hemp fiber and Ganoderma lucidum fungi, sound absorption tests were conducted in a small reverberant chamber and in an impedance tube.

2 Materials and experimental procedure

2.1 Materials

The most predominant criterion when working with mycelium-based composite are the selection of fiber residue used for the growth of the fungi species. Thus, hemp fiber, generally used for livestock litter, was chosen as the feeding material for the growth a white-rot fungi, well known by the name of *Ganoderma Lucidum* and its strong filamentous mycelium network (figure 1). Mycelium-based composite fabrication
The fabrication of mycelium-based composite requires first a sterilization of the hemp fiber in a polyethylene bag to ensure no microbial activity other than the one of the fungi mycelium species. This sterilization step is carried out in an autoclave operating at 121°C and 15 psi for about 20 minutes. Subsequently, the fibers are cooled down to approximately 40°C and hydrated with water at about 60% by weight. Then, the resulting substrate is inoculated with the fungi mycelium with a maximum 30% proportion of the total mass. The inoculated substrate is then placed in an incubation chamber for a minimum of 7 days at a temperature between 20 and 30°C and a minimum relative humidity of 60%. During this incubation period, the mycelium develops and colonizes the whole bagged hemp fibers, resulting to firmly joined interwoven 3-dimensional filamentous network. To form mycelium based composite panels, the inoculated substrate is set in a 210 x 210 x 15 mm^3 mold and put back into the incubation chamber for another week. Finally, the square panel is unmolded and placed in an oven at 90°C for, at least, 4 h to stop fungi mycelium growth.

a) Residual hemp fibers b) Ganoderma lucidum mycelium

Figure 1: Mycelium-based composites: a) hemp fiber residues (feeding material) and b) Ganoderma lucidum mycelium.

a) Conventional mineral fiber-based acoustic ceiling tile b) Mycelium-based composite panel

Figure 2: Pictures of tested materials.

2.2 Sound absorption measurements

Reverberant chamber

A small reverberant chamber of 4 m^3 volume was used to perform reverberation tests following ASTM C423 standard. Six mycelium-based composite square panels were assembled to reach a 0,26 m^2 area. An equivalent area of conventional mineral fiber-based acoustic ceiling tiles were used for comparison purpose [4]. The side length of both specimens was not covered for these comparative tests, and not considered in sound absorption calculation which could bring some uncertainties on the estimated sound absorption coefficient.

[*] alexis.boisvert2@usherbrooke.ca
[†] said.elkoun@usherbrooke.ca
[‡] olivier.robin@usherbrooke.ca
[♦] felix-antoine.simard@biopterre.com

Impedance tube

Absorption coefficient was measured by means of a 100 mm diameter impedance tube following the standard method ASTM E1050 using two microphones [5]. All tests were performed on 100 mm diameter mycelium-based composite samples, laser cut from the 15 mm thick panels and compared with same size conventional mineral fiber ceiling tiles. Given the 100 mm diameter, the high frequency limit of analysis is approximately 1900 Hz. The 5 cm spacing of the microphone puts a theoretical low-frequency limit at approximately 70 Hz.

3 Preliminary results

Figures 3 and 4 show the sound absorption coefficient as a function of frequency for the selected materials in an impedance tube and reverberant chamber respectively. As can be seen, mycelium-based composites exhibit similar absorption coefficients to conventional mineral fiber acoustic ceiling tiles over the whole range of frequency. Consequently, one can, reasonably, expect that, if compactness of this material is increased, sound absorption coefficient of this material would be, at least, comparable to that of the conventional acoustic ceiling tile or even better [6].

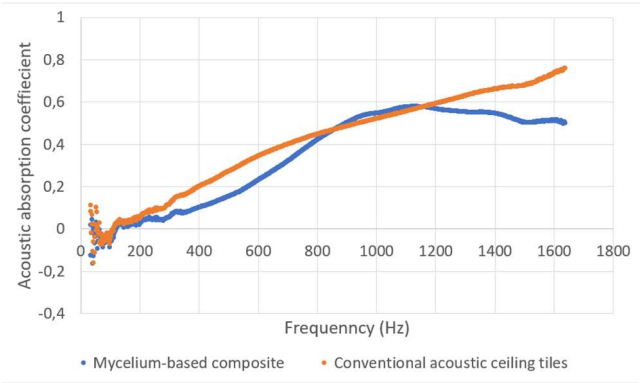

Figure 3: Sound absorption coefficients of mycelium-based composite and conventional acoustic ceiling tiles measured in impedance tube.

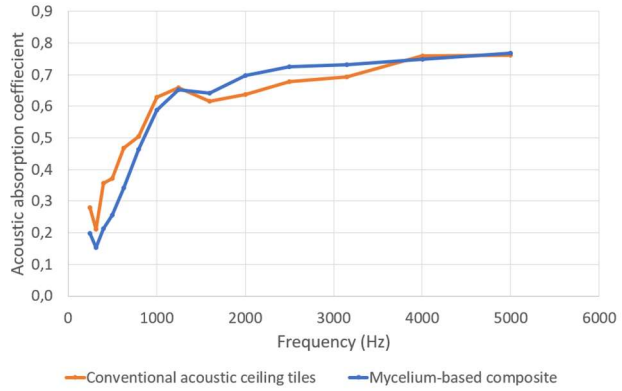

Figure 4: Sound absorption coefficients of mycelium-based composite and conventional mineral fiber acoustic ceiling tiles measured in reverberant chamber.

4 Concluding remarks

In this paper sound absorption efficiency of mycelium-based composite was investigated. It was shown that the selected residual hemp fiber and Ganoderma Lucidum fungi species, created mycelium-based composite panels with comparable sound absorption performance to conventional mineral fiber-based acoustic ceiling tiles. Since the tested mycelium-based panels were preliminary prototypes, the fabrication process requires further optimization to reach improved sound absorption performance.

Acknowledgments

The authors would like to thank Biopterre, Centre Collégial de Transfert de Technologie, for providing technical support in the fabrication of the mycelium-based composite panels as well as the Centre de Recherche acoustique-signal-humain de l'UdeS, CRASH, for financial support from the Aide Agile d'Amorçage internal grant program.

References

[1] E. Elsacker, S. Vandelook, J. Bracart, E. Peeters, and L. De Laet, "Mechanical, physical and chemical characterization of mycelium-based composites with different types of lignocellulosic substrates," PLOS ONE 14(7), e0213954(2019), doi: 10.1371/journal.pone.0213954

[2] M. Jones, A. Mautner, S. Luenco, A. Bismarck, and S. John, "Engineered mycelium composite construction materials from fungal biorefineries: A critical review," Materials & Design187, p. 108397 (2020). doi:10.1016/j.matdes.2019.108397

[3] M. Jones, T. Huynh, C. Dekiwadia, F. Daver, and S. John, "Mycelium Composites: A Review of Engineering Characteristics and Growth Kinetics," J. Bionanoscience, vol. 11, no. 4, pp. 241–257, Aug. 2017, doi: 10.1166/jbns.2017.1440.

[4] ASTM C423-22 - Test method for sound absorption and sound absorption coefficients by the Reverberation Room Method, ASTM International (2022). doi:10.1520/c0423-22

[5] ASTM E1050-19 - Test method for impedance and absorption of acoustical materials using a tube, two microphones and a digital frequency analysis system, ASTM International. doi:10.1520/e1050-19

[6] M. G. Pelletier et al., "An evaluation study of pressure-compressed acoustic absorbers grown on agricultural by-products," Industrial Crops and Products 95, 342–347 (2017). doi: 10.1016/j.indcrop.2016.10.042.

On the Use of Condensation Models for Describing Highly Damped Multilayered Structures

Rafael da Silva Raqueti[*1,2], **Noureddine Atalla**[†1], **Morvan Ouisse**[‡2], **and Emeline Sadoulet-Reboul**[§3]
[1]Université de Sherbrooke, Centre de recherche acoustique-signal-humain (CRASH-UdeS), 2500 boul. de l'Université, Sherbrooke (Québec), J1K 2R1, Canada
[2]SUPMICROTECH, Université de Franche-Comté, CNRS, Institut FEMTO-ST, F-25000 Besançon, France
[3]Université de Franche-Comté, CNRS, Institut FEMTO-ST, F-25000 Besançon, France

1 Introduction

Multilayered composite structures are of interest to many industries, such as aeronautics, aerospace and automotive, because of their high specific modulus. Nevertheless, reinforcement materials have low damping and improving the dynamic behavior of multilayered structures is an ongoing research area. Constrained layer damping treatment is a solution that increases damping and dissipates energy through shearing motion in the added viscoelastic layer. This method is suitable for high frequencies, but is not efficient at low frequencies and also lacks adaptability.

In [1], a shape memory polymer (SMP) was used as viscoelastic core of a sandwich structure. The mechanical properties of this SMP depend on frequency and temperature. It also exhibits excellent damping capacity over a wide frequency range at temperatures close to its glass transition temperature. The structure becomes adaptive, and can be "programmed" to reduce vibrations by controlling the temperature inside the core. However, the stiffness of the sandwich structure is compromised by the increase in temperature.

The combination of surface temperature fields enables the sandwich structure to maintain stiffness while reducing vibrations. In [2], heaters were distributed on a skin of a sandwich structure with SMP core. They can be controlled independently and many combinations of temperatures fields are possible. The selection of specific combinations was based on the evaluation of static and dynamic criteria, which were obtained from a finite element model (solid, 3D). While this strategy is suitable for small structures, it may become unfeasible for large structures due to the high computation time involved. This approach may also be inappropriate for reevaluating in short time the configurations according to different criteria. Instead of using the finite element model (solid, 3D) approach, reduced-order models based on plate theory are required to reduce computational time. However, the selection of a condensation model capable of determining the effective properties of highly damped structures remains a challenge.

2 Materials and methods

2.1 A sandwich structure with SMP core

A symmetrical sandwich structure with aluminum (Al) skins and SMP core is considered. The length is 0.7 m and width 0.5 m. All edges are simply supported and a point excitation is applied at its center. Table 1 contains the properties values. The loss factor $\tan(\delta)$ of the SMP depends on angular frequency ω and temperature. Figure 1 shows the frequency and temperature evolution of $\tan(\delta)$. Sandwich structures with SMP core have controllable properties, and some configurations are highly damped.

Table 1: Properties of the sandwich structure (SI units).

	h	ρ	ν	E	η
Al	0.0005	2700	0.33	$7 \cdot 10^{10}$	0.001
SMP	0.0022	990	0.37	$E'(\omega)$	$\tan(\delta(\omega))$

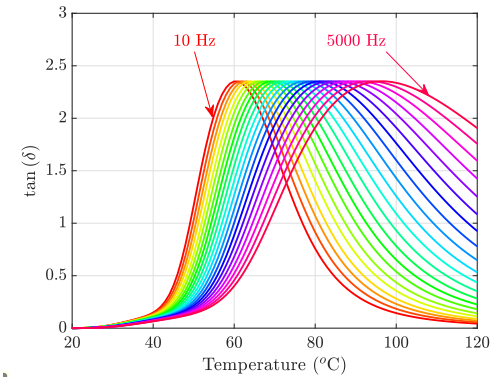

Figure 1: SMP loss factor $\tan(\delta)$. The SMP storage modulus E' is also affected by frequency and temperature (see [1] for details).

2.2 Calculation of effective properties

The bending (c_B), shear (c_T) and longitudinal (c_L) waves velocities propagating in a homogeneous and isotropic plate are related to the plate properties (thickness, density, Poisson's ratio and Young's modulus). The respective wavenumbers are $k_B = \omega/c_B$, $k_T = \omega/c_T$ and $k_L = \omega/c_L$. Dispersion relations can be determined with the General Laminate Model (GLM) [3]. The GLM considers rotational inertia and transversal shearing, membrane and bending deformations in composite plates with orthotropic orientation. The GLM also considers the frequency dependency of viscoelastic layers.

Table 2 gives the formulas used to calculate the effective properties of an equivalent (homogeneous and isotropic) plate. The effective properties are used in a Discrete-Kirchhoff plate finite element formulation [4]. The condensed finite element model intends to describe the dynamic behavior of the sandwich structure with reduced computational cost.

[*]rafael.da.silva.raqueti@usherbrooke.ca
[†]noureddine.atalla@usherbrooke.ca
[‡]morvan.ouisse@femto-st.fr
[§]emeline.sadoulet-reboul@univ-fcomte.fr

Table 2: Effective properties of an equivalent (homogeneous and isotropic) plate that preserves bending, shear and extension wavenumbers.

Equivalent thickness	Equivalent density	Equivalent Poisson's ratio	Equivalent Young's modulus
$h_{eq} = \sqrt{12}\frac{k_L}{k_B^2}$	$\rho_{eq} = \sum_{i=1}^{3} \frac{\rho_i h_i}{h_{eq}}$	$\nu_{eq} = 1 - 2\left(\frac{k_L}{k_T}\right)^2$	$E_{eq} = \frac{12\rho_{eq}\omega^2\left(1-\nu_{eq}^2\right)}{h_{eq}^2 k_B^4}$

2.3 Damping estimation

Two techniques are used to estimate the structural damping loss factor η. In the first, the GLM is used to estimate damping by energy balance considering the characteristics of main propagating wave [3]. In the second, the Power Input Method (PIM) is used to compute the structural loss factor from dissipated power Π_d, kinetic energy E_c and strain energy E_d):

$$\eta = \frac{\Pi_d}{\omega\left(E_c + E_d\right)}. \tag{1}$$

The latter method is also used to obtain a reference solution using a full 3D solid element based model of the sandwich structure. Obtaining this solution is computationally intensive as a direct forced response is used and an average over several excitation locations is needed.

3 Results and discussion

Two high damping configurations (80°C and 65°C) are studied. In both cases, compared to the reference solution, the energy balance considering the main wave overestimates the structural loss factor, except at low frequencies, as shown in Figure 2. A much better correlation is obtained using the GLM computed forced response.

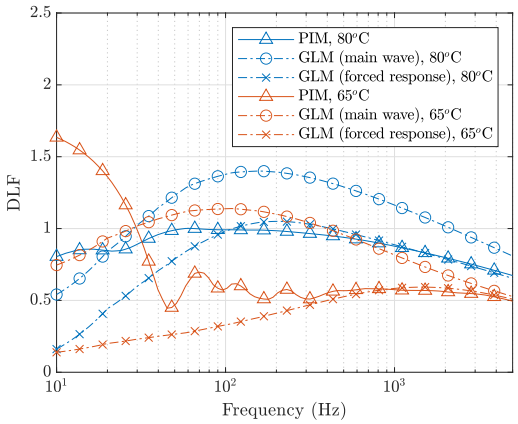

Figure 2: Structural damping loss factor (DLF) estimation: Power Input Method (PIM); GLM (energy balance, main wave) and GLM (forced response).

Systematic comparisons are presented between a reference finite element model (TET10 elements) of the sandwich structure and the equivalent plate (TRIA3). Figure 3 shows that for moderate damping the equivalent properties model is able to capture the response of the structure. However, it starts failing for the extremely damped configurations.

4 Conclusions

An equivalent plate model that preserves the dispersion relations of a highly damped sandwich structure with controllable properties is described. Estimating the structural damping loss factor for highly damped structures is an open research topic. For these cases, preliminary results indicate that the GLM can be used to adequately estimate the damping from the forced response. Overall, the equivalent plate model describes the dynamic behavior of the sandwich structure, but the discrepancies are still significant compared to a full 3D finite element model. By this approach, there is an important reduction in the computational cost (by one order of magnitude approximately). An accurate equivalent plate model allows to (re)evaluate in reduced time the configurations of the sandwich structure with SMP core for vibration control while maintaining stiffness.

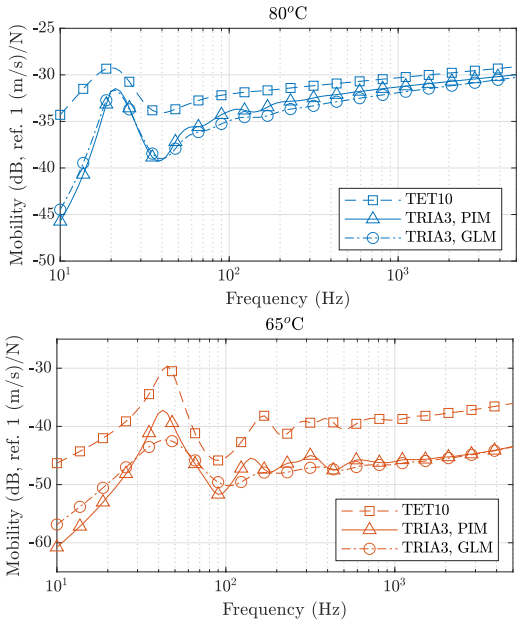

Figure 3: Point mobility: full 3D finite element model (TET10); and equivalent plate model (TRIA3) considering the effective properties and both damping estimates (PIM and GLM, main wave).

Acknowledgments

The authors would like to thank ISITE-BFC (ANR-15-IDEX-0003), EUR EIPHI (ANR-17-EURE-0002) and the Natural Sciences and Engineering Research Council of Canada (NSERC) for their financial support.

References

[1] P. Butaud, E. Foltête, and M. Ouisse. Sandwich structures with tunable damping properties: On the use of Shape Memory Polymer as viscoelastic core. *Composite Structures*, 153:401–408, 2016.

[2] P. Butaud, D. Renault, B. Verdin, M. Ouisse, and G. Chevallier. In-core heat distribution control for adaptive damping and stiffness tuning of composite structures. *Smart Materials and Structures*, 29(6):065002, 2020.

[3] S. Ghinet and N. Atalla. Modeling thick composite laminate and sandwich structures with linear viscoelastic damping. *Computers & Structures*, 89(15-16):1547–1561, 2011.

[4] J.-L. Batoz and G. Dhatt. *Modélisation des structures par éléments finis*, volume 2. Presses Université Laval, 1990.

IN-SITU MEASUREMENT OF ACOUSTIC IMPEDANCE IN PRESENCE OF GRAZING FLOW

Xukun Feng [*1], **Zacharie Laly** [†1], **and Noureddine Atalla** [‡1]
[1]Université de Sherbrooke, Sherbrooke, Québec, Canada

1 Introduction

Perforated plates are used in many engineering applications for noise reduction. The high sound pressure level (SPL) and the airflow have considerable impacts on their acoustic performances. Numerical, experimental and theoretical methods have been used to characterize perforated plates [1-6]. Lee et al. [1] proposed an empirical impedance model of perforated plate under grazing flow using nonlinear regression analysis. The model was validated by comparison with experiments. Goldman et al. [2] studied the acoustic impedance of an orifice under a turbulent boundary layer. They observed a significant interaction that depends on the frequency and friction velocity between the acoustic and turbulent motions. Shah et al. [4] used an experimental three-port technique to study the transfer impedance of a perforated plate with and without the presence of grazing flow and analyzed the effect of acoustic incidence relative to the flow directions.

In this paper, a direct in-situ method is implemented and used to investigate experimentally the grazing airflow and higher SPL effects on the acoustic impedance of perforated plates. The measurements are validated by comparison with theoretical models and the effects of the grazing airflow and high SPL on the acoustic resistance are demonstrated.

2 Description and results of the in-situ measurement method with airflow

Figure 1 shows the experimental set up of the in-situ measurement method under grazing airflow. High sound pressure speakers capable of delivering a high SPL up to 145 dB are used and the airflow through the duct is generated by a compressor. One temperature probe OMEGA HX94C is mounted in the tube with a static pressure sensor MEAS U5244-000005-030PA to determine the environmental condition parameters during the measurement. An anechoic termination is mounted at one end of the tube to minimize the acoustic wave reflection. A controlled flow meter measures the airflow rate. The sample holder consists of two cavities of 9 mm deep that are separated by a rigid wall. The lateral dimensions of each cavity are 50.8 mm x 20 mm. Four 1/4'' microphones PCB 378A14 denoted by M_1 to M_4 are mounted flush with the inner wall of the tube. One microphone is mounted flush in the bottom of each cavity and two microphones are flush mounted in the tube just above the sample as shown in Fig. 1. All the signals acquisitions are done by a NI Compact DAQ system.

A phase and amplitude calibrations are performed to minimize the error measurement of the microphones. From

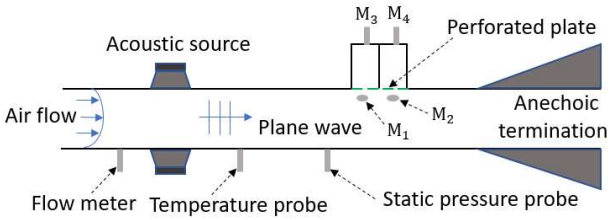

Figure 1: In-situ measurement set up.

the acoustic pressures P_1 to P_4 that are measured by the 4 microphones, the normalized acoustic impedance of the perforated plate is determined using the following relation

$$Z_n = (H_{ij} - \cos kD) / (j \sin kD), \quad (1)$$

where H_{ij} is the transfer function, k the wavenumber and D the cavity depth that is 9 mm. For the first cavity, the impedance Z_1 was calculated using in Eq. (1) $H_{31} = P_1/P_3$ and for the second cavity Z_2 is calculated using $H_{42} = P_2/P_4$ and the impedance Z of the tested sample is obtained by averaging Z_1 and Z_2.

Figure 2 shows the normalized flow induced resistance of a micro perforated panel (MPP) with a thickness of 1 mm, a perforation diameter of 1 mm and a perforation open area of 5%. The measurement is perforated at 140 dB with airflow Mach number M of 0.15. The resistance in Fig. 2 is obtained by subtracting the resistance without flow from the resistance with Mach 0.15. A frequency-dependent contribution of grazing flow is obvious. The result correlates fairly with the theoretical model proposed by Lee et al. [1]. The dip around 2700 Hz should be caused by the interaction between the nonlinear and grazing flow effects [2]. The presence of grazing flow can partially reduce the nonlinearity. Therefore, when subtracting the resistance without flow, an extra part is subtracted and the dip appears.

The normalized resistance and reactance of the previous micro perforated panel at 140 dB are presented in Figs. 3 and 4 for different airflow Mach numbers. The grazing flow increases the resistance and this effect is decreasing with respect to the frequency until a critical frequency, after which the flow effect can be neglected (therefore the higher frequency part of the curve will superpose on the one without flow). The critical frequency is found to be proportional to the Mach number [1]. In Figure 3, for different Mach numbers of 0.0.3, 0.09 and 0.15, the critical frequency corresponds respectively to 700 Hz, 2100 Hz and 3500 Hz. In Figure 4, for frequency f >1000 Hz, the reactance decreases with the Mach number and the slope remains almost the same.

The impact of the high SPL on the normalized acoustic impedance of the previous MPP is illustrated in Fig. 5. The measurement is performed at different SPL without airflow. The nonlinear effect is observed with the increase of the SPL, especially around the Helmholtz resonance (2700 Hz), where

[*] xukun.feng@usherbrooke.ca
[†] zacharie.laly@usherbrooke.ca
[‡] noureddine.atalla@usherbrooke.ca

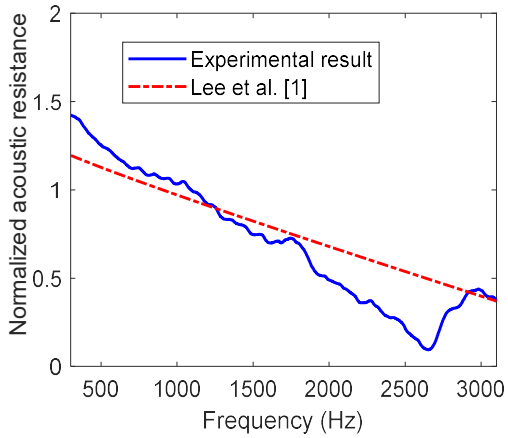

Figure 2: Resistance introduced by the airflow.

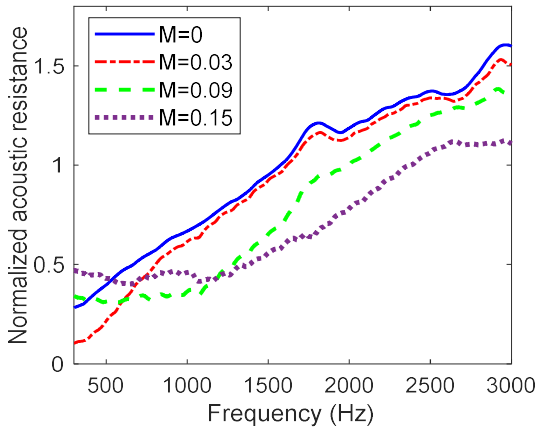

Figure 4: Effect of grazing airflow on the acoustic reactance.

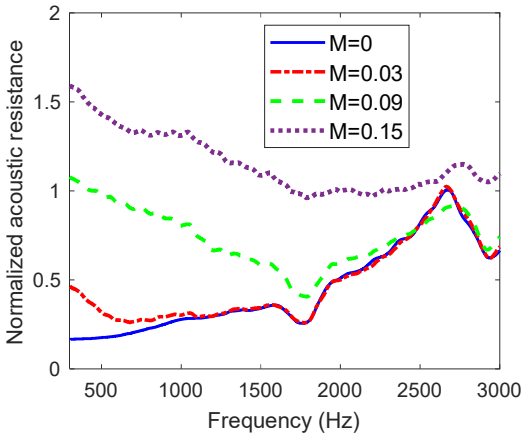

Figure 3: Effect of grazing airflow on the acoustic resistance.

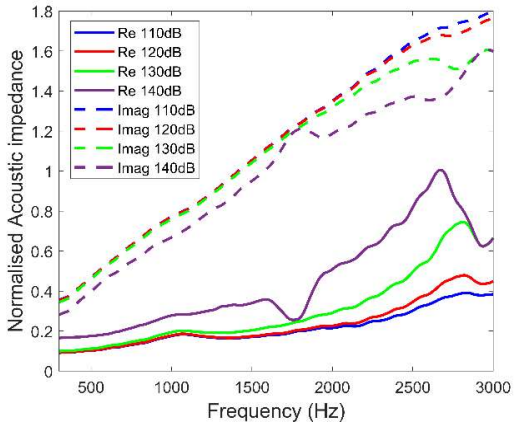

Figure 5: Effect of High SPL on the acoustic impedance.

the acoustic velocity in the perforation reaches its maximum. At higher SPL, the jet formation and vortex at the exit of the orifices increase the resistance and reduce the orifice end correction, which induces a decrease of the reactance [5].

The grazing flow and the high SPL have a significant impact on the acoustic impedance of the micro perforated plates as illustrated in figures 3 to 5. The in-situ method used in this work can help to investigate the acoustic performance of these perforated plates.

3 Conclusions

An in-situ measurement method is presented and used to investigate the impacts of the grazing flow and high SPL on the acoustic impedance of micro perforated plates. The theoretical result shows generally good correlation with the measurement. It is demonstrated that the high SPL and grazing airflow increase the acoustic resistance of micro perforated plates while the reactance is reduced. This in-situ method can be used to identify the acoustic properties of macro perforated plates and others materials with airflow at high SPL.

Acknowledgments

This study was performed under the framework of the dXBel project, funded by the Natural Sciences and Engineering Research Council of Canada (NSERC) and Bombardier Research Recreational Products (BRP).

References

[1] S-H. Lee, J-G. Ih. Empirical model of the acoustic impedance of a circular orifice in grazing mean flow. J. Acoust. Soc. Am. 114 (1), 98-103, 2003.

[2] A. L. Goldman, R. L. Panton. Measurement of the acoustic impedance of an orifice under a turbulent boundary layer. J. Acoust. Soc. Am. 60 (6), 1397-1405, 1976.

[3] P. D. Dean. An in situ method of wall acoustic impedance measurement in flow ducts. Journal of Sound and Vibration, 34(1), 97-130, 1974.

[4] S. Shah, H. Bodén, S. Boij, M. D'Elia. Three-port measurements for determination of the effect of flow on the acoustic properties of perforates. Proceedings of the AIAA AVIATION Forum, 2 – 6 August 2021.

[5] Z. Laly, N. Atalla, S-A. Meslioui. Acoustical modeling of micro-perforated panel at high sound pressure levels using equivalent fluid approach. Journal of Sound and Vibration **427**, 134-158 (2018).

[6] Z. Chen, Z. Ji, H. Huang. Acoustic impedance of perforated plates in the presence of fully developed grazing flow. Journal of Sound and Vibration 485, 115547, 2020.

ADDED VISCOUS DAMPING IN MICROPERFORATED PLATES WITHIN A NONLINEAR ACOUSTIC REGIME

Lucie Gallerand[*1], Mathias Legrand [†2], Thomas Dupont [‡1], Raymond Panneton [§3], and Philippe Leclaire [¶4]
[1]Department of Mechanical Engineering, École de Technologie Supérieure, Montréal, Canada
[2]Department of Mechanical Engineering, McGill University, Montréal, Canada
[3]Department of Mechanical Engineering, Université de Sherbrooke, Sherbrooke, Canada
[4]DRIVE EA1859, Université de Bourgogne, ISAT, Nevers, France

1 Introduction

Microperforated plates (MPPs) are simple systems conventionally used as sound absorbers. In the linear acoustic regime, models characterizing MPP acoustic absorption based on (i) the work by Champoux and Stinson [1] and the Johnson-Champoux-Allard model applied to perforated plates [2] along with (ii) the Kirchhoff equations [3] have been proposed. Extensions to a nonlinear acoustic regime were performed using the Forchheimer law [4] and showed a maximum acoustic absorption for a specific value of fluid velocity. Recent works by the authors in the context of linear dynamics have demonstrated MPP added damping capacities in the low frequency range [5]. The added damping results from the dissipation of energy by viscous friction mechanisms in the boundary layers of the microperforations. MPPs are also susceptible to be implemented in hostile environments with strong fluid displacements in the perforations. The present contribution proposes to extend the MPP linear *vibration* model to the nonlinear framework involving the nonlinear acoustic Forchheimer law.

2 Linear MPP model

2.1 Governing equations

The investigated MPP of dimension $L_x \times L_y \times h$ is oriented in the xy plane and excited by an external periodic driving force $f_{\text{ext}}(x, y, t)$. Using an alternative form of Biot's theory, the model developed in the framework of porous plates in [6] is adapted to an MPP. An *ad hoc* homogenization procedure is performed, leading to two coupled partial differential equations (PDEs) presented in Equation (1) that govern the dynamics of a structural plate and a virtual fluid plate. Obtained by identifying the MPP with a porous plate [2], they account for the vibratory behavior of the MPP and read:

$$h(\rho\ddot{w}_{\text{s}} + \rho_{\text{f}}\ddot{w}) + D\nabla^4 w_{\text{s}} = f_{\text{ext}}, \tag{1a}$$

$$\rho_{\text{f}}\ddot{w}_{\text{s}} + \frac{\rho_{\text{f}}\alpha_\infty}{\phi}\ddot{w} + \sigma_0\dot{w} + \alpha M_{\text{f}}\nabla^2 w_{\text{s}} = 0, \tag{1b}$$

where $w_{\text{s}}(x, y, t)$ is the solid motion and $w(x, y, t)$ corresponds to the relative fluid-solid motion. The density of the fluid-solid mixture $\rho = (1-\phi)\rho_{\text{s}} + \phi\rho_{\text{f}}$ where ρ_{s} and ρ_{f} are the densities of solid and fluid, respectively, depends on the perforation ratio ϕ. Equation (1a) represents the elastic response of the homogeneous solid plate while Equation (1b) describes the relative fluid-solid motion. The parameters α and M_{f} are elastic coefficients defined by Biot [7]. The coefficient D is the bending stiffness. In order to consider the influence of the microperforations in the MPP stiffness, it becomes

$$D = \frac{Eh^3}{12(1-\nu^2)}\frac{(1-\phi)^2}{1+(2-3\nu)\phi}. \tag{2}$$

All Johnson-Champoux-Allard (JCA) parameters defined for a porous medium can be rewritten for an MPP as functions depending on ϕ and the diameter of the perforations d. For instance, the resistivity and the tortuosity are defined by

$$\sigma_0 = \frac{32\mu_{\text{f}}}{\phi d^2} \quad \text{and} \quad \alpha_\infty = 1 + \frac{2\epsilon}{h} \tag{3}$$

with μ_{f} the fluid dynamic viscosity and $\epsilon = 0.24\sqrt{\pi d^2}(1 - 1.14\sqrt{\phi})$ [2] is a correction factor used to consider the interaction between the perforations and the distortion of the flow at the perforation orifices.

2.2 Added damping

For an MPP, the existence of a substantial added damping in the low frequency range could be exhibited [5]. The added damping reaches a maximum at the characteristic frequency

$$f_{\text{c}}(d) = \frac{32\mu_{\text{f}}}{2\pi\alpha_\infty\rho_{\text{f}}d^2} \tag{4}$$

defined from the Biot frequency for porous materials [6]. In Equation (4), $f_{\text{c}}(d)$ depends on fluid parameter, μ_{f} and ρ_{f} and on d, which can be tuned to induce maximum added damping at the resonance frequency, i.e. to make $f_{\text{c}}(d)$ coincide with a resonance frequency of the microperforated plate.

3 Nonlinear MPP model

3.1 Governing equations

When the fluid velocity in the microperforations becomes sufficiently large, the inertial effects occurring in the microperforations become significant. It is then necessary to consider them by using the Forchheimer law $\sigma = \sigma_0(1 + \varepsilon|\dot{w}_{\text{f}}|)$, where ε is the Forchheimer coefficient and $|\dot{w}_{\text{f}}(x, y, t)|$ is the absolute value of the fluid velocity. This law was used for rigid MPPs with a high fluid flow in microperforations [4]. In the context of a vibrating microperforated plate, the relative fluid-solid velocity corresponds to the fluid velocity for a rigid

[*]lucie.gallerand.1@ens.etsmtl.ca
[†]mathias.legrand@mcgill.ca
[‡]thomas.dupont@etsmtl.ca
[§]Raymond.Panneton@USherbrooke.ca
[¶]Philippe.Leclaire@u-bourgogne.fr

MPP. Accordingly, the resistivity is expressed as a function of $\dot{w}(x,y,t) = \phi(\dot{w}_\mathrm{f}(x,y,t) - \dot{w}_\mathrm{s}(x,y,t))$

$$\sigma(\dot{w}(x,y,t)) = \sigma_0(1 + \varepsilon|\dot{w}(x,y,t)|). \tag{5}$$

Inserting Equation (5) in Equation (1) provides the following nonlinear system with a quadratic damping term:

$$h(\rho\ddot{w}_\mathrm{s} + \rho_\mathrm{f}\ddot{w}) + D\nabla^4 w_\mathrm{s} = f_\mathrm{ext}, \tag{6a}$$

$$\rho_\mathrm{f}\ddot{w}_\mathrm{s} + \frac{\rho_\mathrm{f}\alpha_\infty}{\phi}\ddot{w} + \sigma_0\dot{w} + \sigma_0\varepsilon\dot{w}|\dot{w}| + \alpha M_\mathrm{f}\nabla^2 w_\mathrm{s} = 0. \tag{6b}$$

The resulting nonlinear governing equations are space semi-discretized and projected onto the non-perforated plate mode. The solid motion is expanded as

$$w_\mathrm{s}(x,y,t) = \sum_i^N w_i^\mathrm{s}(t)\Psi_i(x,y), \tag{7}$$

where $w_i^\mathrm{s}(t)$ represents the generalized coordinate of eigenmode i of shape $\Psi_i(x,y)$; N is the number of degrees-of-freedom in the plate spacial discretization. A similar formulation is used for $w(x,y,t)$. After spacial discretization, Equation (6) is solved in the steady state regime by using the Harmonic Balance Method, which consists in the use of truncated Fourier series to describe the problem's unknowns.

3.2 Results

The model is used to study the vibratory behavior of a simply supported MPP in the nonlinear acoustic regime. An MPP of dimension $490\,\mathrm{mm} \times 570\,\mathrm{mm} \times 1\,\mathrm{mm}$ with $d = 2.2\,\mathrm{mm}$ and $\phi = 10\,\%$ is excited at one point by an external force of magnitude F_ext. The corresponding mobility of the plate, *i.e.* displacement divided by F_ext, is plotted as a function of dimensionless forcing frequency for three values of F_ext in Figure 1. The frequencies f_0 and f correspond respectively to

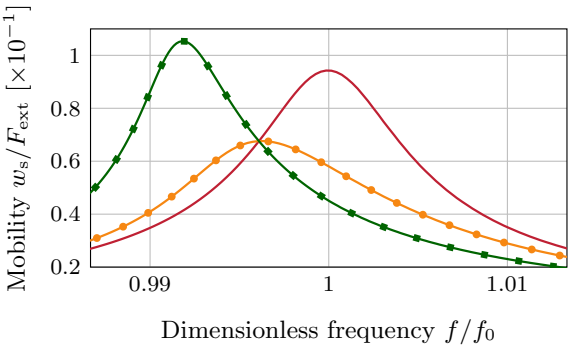

Figure 1: Mobility of the first linear microperforated plate mode for three magnitudes of external excitation: (——) $F_\mathrm{ext} = 0.5\,\mathrm{mN}$; (—●—) $F_\mathrm{ext} = 20\,\mathrm{mN}$; (—■—) $F_\mathrm{ext} = 110\,\mathrm{mN}$.

the resonance frequency obtained in the linear case and to the forcing frequency. The Forchheimer nonlinearity parameter $\varepsilon = 0.8\,\mathrm{s/m}$ is obtained by experimental measurement. It can be observed that increasing the nonlinearity softens the system and that the added damping reaches a maximum for a specific value of F_ext, *i.e.* for a characteristic value of the magnitude

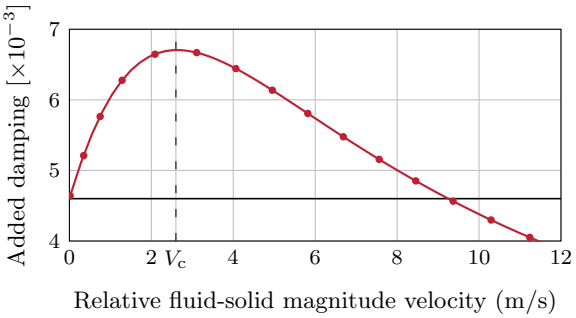

Figure 2: Added damping for the first linear MPP mode: (—●—) the nonlinear case; (——) the constant value of the linear case.

of the relative fluid-solid velocity as shown in Figure 2. A theoretical development provides an expression for a critical relative fluid-solid velocity

$$V_\mathrm{c} = \frac{I_1^{(3)}}{I_1^{(4)}}\frac{\omega\rho_\mathrm{f}\alpha_\infty - \sigma_0\phi}{\sigma_0\phi\varepsilon} \tag{8}$$

for which the added damping is maximum, where $I_1^{(3)}$ and $I_1^{(4)}$ are spacial integrals associated with the beam functions in the spacial projection of the coupled equations for the first linear plate mode. $I_1^{(4)}$ carries the Forchheimer acoustic nonlinear physical mechanism.

4 Conclusions

The vibratory response of a fluid-saturated MPP in a nonlinear acoustic regime is presented. The inertia effect due to the high velocity of the airflow in the microperforations is captured analytically by the Forchheimer law, which yields a system of coupled PDEs with a nonlinear damping term. The results show that the nonlinear damping introduced by the Forchheimer law softens the system. In addition, a critical relative fluid-solid velocity is found for which the added damping reaches a maximum.

References

[1] Y. Champoux and M.R. Stinson. On acoustical models for sound propagation in rigid frame porous materials and the influence of shape factors. *Journal of the Acoustical Society of America*, 92:1120–1131, 1992. DOI, OA.

[2] N. Atalla and F. Sgard. Modeling of perforated plates and screens using rigid frame porous models. *Journal of Sound and Vibration*, 303:195–208, 2007. DOI, OA.

[3] D.-Y. Maa. Potential of microperforated panel absorber. *Journal of the Acoustical Society of America*, 104:2861, 1997. DOI, OA.

[4] R. Tayong, T. Dupont, and P. Leclaire. On the variations of acoustic absorption peak with particle velocity in micro-perforated panels at high level of excitation. *The Journal of the Acoustical Society of America*, 127(5):2875–2882, 2010. DOI, OA.

[5] L. Gallerand, M. Legrand, T. Dupont, and P. Leclaire. Vibration and damping analysis of a thin finite-size microperforated plate. *Journal of Sound and Vibration*, 541:117295, 2022. DOI, OA.

[6] P. Leclaire, K.V. Horoshenkov, and A. Cummings. Transverse vibration of a thin rectangular porous plate saturated by a fluid. *Journal of Sound and Vibration*, 247(1):1–18, 2001. DOI, OA.

[7] M.A. Biot and D.G. Willis. The elastic coefficients of the theory of consolidation. *Journal of Applied Mechanics*, pages 594–604, 1957. DOI, OA.

METHOD FOR CHARACTERIZING THE ACOUSTIC PROPERTIES OF THIN METAMATERIALS CAPABLE OF ATTENUATING BROADBAND NOISE AT LOW FREQUENCIES.

Tenon Charly Kone*[1], Sebastian Ghinet[†1], Raymond Panneton[‡2] and Anant Grewal[§1]
[1]National Research Council Canada, Flight Research Laboratory, Ottawa, Ontario, Canada.
[2]CRASH, Centre de Recherche Acoustique-Signal-Humain, Université de Sherbrooke, Sherbrooke, Québec, Canada.

1 Introduction

Attenuating noise, especially at low frequencies, poses a persistent and challenging problem across various industries such as transportation, aeronautics, and building sectors. The complexity lies in the design constraints imposed by long acoustic wavelengths associated with low frequencies, necessitating specialized approaches. This challenge becomes particularly significant when addressing noise generated by Unmanned Aerial Systems (UAS). Among the primary sources of UAS noise, the tonal noise emerges as a prominent concern. Although conventional resonators have been commonly used to tackle this issue, their effectiveness is limited by spatial constraints and their ability to attenuate only a single frequency.

In recent works by the authors [1-3], a solution that utilizes thin structuring materials was introduced, to effectively attenuate multiple resonant frequencies that could be combined to broaden the resonant attenuation frequency range of a metamaterial at low frequencies. The present study focuses on configurations comprising two parallel sub-metamaterials embedded within a layer of fiberglass. Each sub-metamaterial consists of a serial assembly of periodical unit cells, contributing to its unique acoustic properties. To evaluate the performance and potential of these metamaterial configurations, COMSOL Multiphysics finite element methods (FEM) was utilized. This approach enabled the prediction of crucial acoustic parameters, such as the normal incidence sound absorption coefficient (SAC) and sound transmission loss (STL), for each metamaterial configuration. Implementing this FEM approach for optimizing design parameters can be challenging but is crucial for accurate assessments.

The primary objective of this article is to characterize the metamaterial configurations proposed by Kone et al. [3]. Transfer matrices (TM) in series and in parallel arrangements were used to thoroughly analyze the effectiveness and applicability of these novel metamaterial designs in noise attenuation applications. Through the preliminary findings in this article, valuable insights into the potential advancements and future directions of research in the field of noise reduction are provided.

2 Materials and Methods

The metamaterial used in this study is constructed by overlaying two axisymmetric sub-metamaterials embedded in a glass wool (GW) layer of thickness t_p and the length $N\ell_{PUC}$.

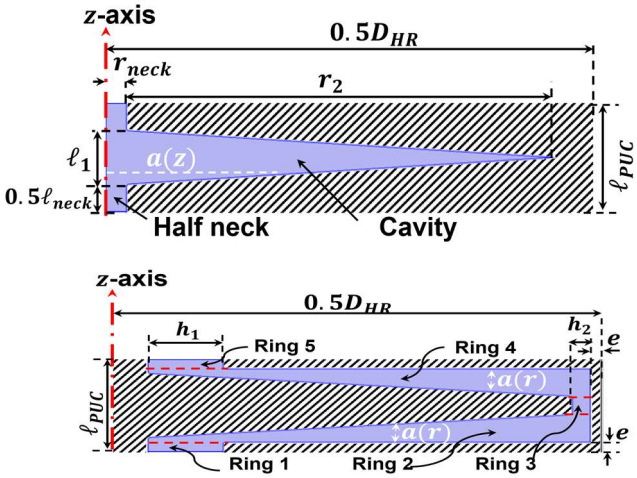

Figure 1: Top image: PUC of first sub-metamaterial. Bottom image: PUC of second sub-metamaterial. 2D-axisymmetric view.

Each sub-metamaterial consists of N periodical unit cells (PUCs).

The first sub-metamaterial's PUC (Fig. 1, top) consists of a cylindrical half neck with a radius r_{neck}, a length $0.5\ell_{nec}$. It also includes an annular cavity in the shape of an isosceles triangle of height r_2 and base $\ell_1 = \ell_{PUC} - \ell_{neck}$. In this configuration, plane wave propagation occurs along the axis of revolution, i.e. the z-axis, of the metamaterial. Therefore, the PUC was discretized perpendicular to the z-axis of revolution with transfer matrices in series. Each cell (i) has a thickness h_i and a height $a(z_i)$. The transfer matrix of cell i is given by

$$\boldsymbol{T_i} = \left[cos(k_i h_i)\ jZ_i sin(k_i h_i);\ \frac{jsin(k_i h_i)}{Z_i}\ cos(k_i h_i)\right],$$

where k_i and Z_i are the wave number and characteristic impedance of the effective fluid, respectively. These parameters are modeled using the Johnson Champoux Allard (JCA) model. Each cell is a cylinder of radius $a(z_i)$. Applying the Transfer Matrix Method (TMM) in series, the transfer matrix of the PUC (T_{PUC}) is obtained as the product of all T_i matrices of the elementary cell ($\boldsymbol{T_{PUC1}} = \prod_{i=1}^{N} \boldsymbol{T_i}$, where N represents the number of discretization elements). Sub-metamaterial 1 is a superposition of N_{PUC} PUCs. Finally, the TM of sub-metamaterial 1 can be expressed as $\boldsymbol{T_{meta1}} = (\boldsymbol{T_{PUC1}})^{N_{PUC}}$.

The second sub-metamaterial's PUC, as shown in Fig. 1 (bottom), was created by combining multiple rings of different geometries: (*i*) Ring 1: This is a simple ring geometry of rectangular cross-section. (*ii*) Ring 2: Following Ring 1, there is a ring with a trapezoidal cross-section. (*iii*) Ring 3: After Ring 2, is another ring of rectangular cross-section. (*iv*) Rings

*TenonCharly.Kone@nrc.gc.ca
† Sebastian.Ghinet@nrc.gc.ca
‡ Raymond.Panneton@USherbrooke.ca
§Anant.Grewal@nrc-cnrc.gc.ca

4 and 5 are the mirror images of the first two rings. According to the propagation of the wave in this sub-metamaterial two types of discretization were used. The first discretization was used for Rings 1, 3 and 5. It was perpendicular to the axis of revolution of the metamaterials as in the first sub-metamaterial. The second discretization concerned Rings 2 and 4 where the plane wave propagates radially. Thus, the type of discretization (radial discretization) used in these two rings was parallel to the axis of revolution of the metamaterials. Whatever the type of axial or radial discretization, the thickness of each cell i had a thickness h_i and a height $a(r)$. The heights $a(r)$ of the discretization of Rings 1, 3 and 5 were constant, while they vary linearly with the radius for Rings 2 and 4. As for the first sub-metamaterial, the TM of each ring j was defined as $\boldsymbol{T_{rg,j}} = \prod_{i=1}^{N} \boldsymbol{T_i}$, where N represents the number of discretization elements of the ring, and T_i the TM of the i^{th} element. Each cell is a slit of radius $a(r_i)$ with JCA effective fluid properties. By considering section-change matrix T_c (for conservation of volumetric flow) between rings, the transfer matrix of the PUC of metamaterial 2 is given by $\boldsymbol{T_{PUC2}} = \boldsymbol{T_{rg,1}}\boldsymbol{T_{C1}}\boldsymbol{T_{rg,2}}\boldsymbol{T_{C2}}\boldsymbol{T_{rg,3}}\boldsymbol{T_{C3}}\boldsymbol{T_{rg,4}}\boldsymbol{T_{C4}}\boldsymbol{T_{rg,5}}$. Finally, the TM of sub-metamaterial 2 can be expressed as $\boldsymbol{T_{meta2}} = (\boldsymbol{T_{PUC2}})^{\boldsymbol{N_{PUC}}}$.

The TM of the glasswool (GW) in which both metamaterials are embedded has been analytically calculated using the JCA equivalent fluid model [4]. The resistivity of the GW was 20709 Pa*s/m^4. Knowing the TMs of each sub-metamaterial and of the GW, the global TM of the metamaterial can be calculated. Since these three elements are in parallel, the parallel transfer matrix method (PTMM) is used for their assembling [1,5].

3 Results

The sound absorption coefficients (SAC) of each sub-metamaterial, as well as the assembled metamaterial, were analyzed using the present approach (TMM-Current Model) and compared with results obtained using COMSOL FEM (Figs. 2-4). The focus was on the first two resonance frequencies. Regarding the sub-metamaterials, the TMM model accurately predicts the first two resonance frequencies, which closely match those obtained from COMSOL simulations. However, the amplitudes of these resonant frequencies are overestimated by the TMM model (Figs. 2 and 3). The present approach using the PTMM to calculate the SAC of the assembled metamaterial is also in good agreement with COMSOL mainly for the first two resonance frequencies. Moreover, as for the results obtained using COMSOL a broadening of the attenuation at the first resonant frequency can be observed (Fig. 4).

4 Conclusion

This study highlights the potential of the transfer matrix method (TMM) in analyzing complex configurations. The TMM model accurately calculated sound absorption resonant frequencies for individual sub-metamaterials, closely matching numerical FEM results with a fraction of computation time (quasi-instantaneous computation time). However, the

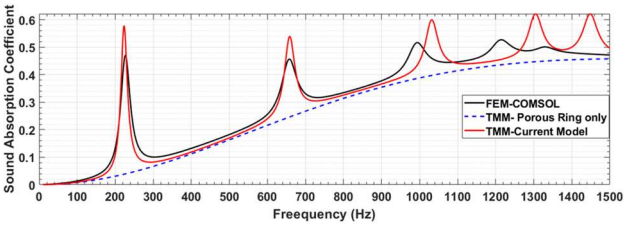

Figure 2: SAC of the first metamaterial embedded in GW layer

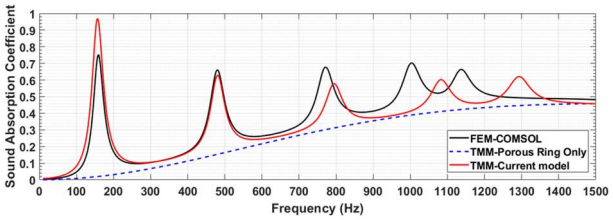

Figure 3: SAC of the second metamaterial embedded in GW layer

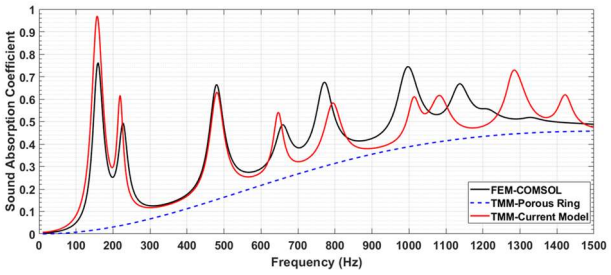

Figure 4: SAC of the metamaterial embedded on the GW layer

results obtained using the present model in terms of sound absorption coefficient of the assembled material demonstrate that some numerical improvements are still required on the proposed TM approach. Ongoing investigations aim to improve the present approach before applying it to sound transmission loss predictions. This research provides a foundation for future advancements in utilizing TMM for complex configurations and improving predictions of absorption and sound transmission properties.

References

[1] T. C. Kone, S. Ghinet, R. Panneton, T. Dupont and A. Grewal. Multi-tonal low frequency noise control using Helmholtz resonators with complex cavity designs for aircraft cabin noise improvement. NTER-NOISE 2021, vol. 263 (2), 1-5 August, Washington, US.

[2] T. C. Kone, S Ghinet, R Panneton, Z Laly, C Mechefske and A. Grewal. Control and broadening of multiple noise frequencies using an assembly of sub-metamaterials connected by membranes for aircraft noise mitigation. IinterNoise 2022, Glasgon, UK.

[3] T. C. Kone, S Ghinet, R Panneton and A. Grewal. Broadband low frequency noise attenuation using thin acoustic metamaterials for aircraft cabin noise mitigation. NTER-NOISE 2023, 20-23 August, ChiBa, Greater Tokyo, Japan.

[4] Y. Champoux and J. Allard. Dynamic tortuosity and bulk modulus in air-saturated porous media, Journal of Applied Physics, 70(4), 1975-1979 (1991).

[5] K. Verdiere, R. Panneton, S. Elkoun, T Dupont, and P. Leclaire. Transfer matrix method ap-plied to the parallel assembly of sound absorbing materials, JASA, 134, 4648-4658 (2013).

FINITE ELEMENT STUDY OF PERFECT SOUND ABSORBING POROUS MATERIAL WITH PERIODIC CONICAL HOLE PROFILE

Zacharie Laly [*3], Noureddine Atalla [†1], Raymond Panneton [‡1], Sebastian Ghinet [♦2], and Christopher Mechefske [♯3]

[1]CRASH, Centre de Recherche Acoustique-Signal-Humain, Université de Sherbrooke, Québec, Canada.
[2]Aerospace, National Research Council Canada, Ottawa, ON K1A 0R6, Canada.
[3]Department of Mechanical and Materials Engineering, Queen's University, Kingston, ON, K7L 3N6, Canada.

1 Introduction

The acoustic performance of porous materials used in several engineering applications for noise reduction is limited at low frequencies. Their sound absorption can be improved at low frequencies by increasing the thickness, however if the thickness is equal to the acoustic penetration depth, the sound absorption reaches its asymptotic limit so that any additional thickness will show no improvement for the absorption coefficient. Laly et al. [1] proposed a design of porous absorbing material with periodic decreasing hole profiles using the finite element method (FEM). They showed excellent sound absorption performance with large frequency band where the limitation of the critical depth was overcome. To increase the sound absorption of the porous materials beyond the asymptotic absorption limit, classical wedge-shape [2] can be used, the concept of double porosity or holes with decreasing profile [3] (see Figure 1) can be used.

In this paper, a porous material design with a periodically distributed conical hole is presented and its acoustic performance is investigated numerically. Multi-layered system made of porous material with embedded periodic conical holes that is combined with other conventional porous materials is studied. It is demonstrated that the sound absorption coefficient of the proposed designs is significantly improved over a large frequency band.

2 Design and investigations of porous material with embedded conical hole

Figure 1(a) shows a porous material (1) containing a set of holes with decreasing profiles (2). Figure 1(b) presents a section of the unit cell (3) with a conical hole, which is approximated by a series of cylindrical holes of decreasing diameter as shown in Fig. 1(c). The thickness of the porous material is denoted by L and H is the length of the conical hole. The radii of the conical hole are denoted by Ra and Rb¬. Figures 2(a) and (b) show the numerical geometry and mesh of the periodic unit cell (PUC) used for the calculations of the acoustic parameters. The pressure acoustics module of Comsol Multiphysics is used to model all the domains in Fig. 2. The porous material is characterized using the Johnson-Champoux-Allard model. A normal incidence plane wave with pressure amplitude of 1 Pa is applied on the inlet plane with plane wave radiation condition. The two microphones transfer function method is used to calculate the reflection and sound absorption coefficients from the surface average acoustic pressures P1 and P2 at planes 1 and 2 positions. The reflection and sound absorption coefficients are given by

$$R = e^{2jk(L_m+s)}(H_{12} - e^{jks})/(e^{jks} - H_{12}), \qquad \alpha = 1 - |R|^2 \qquad (1)$$

with k the wavenumber and H12 the transfer function, s=30mm and Lm=120 mm.Résultats

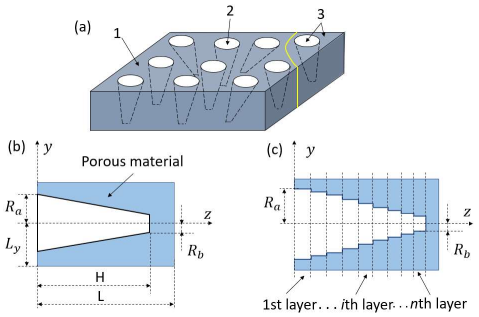

Figure 1: Porous material: (a) with decreasing hole profile (b) conical hole and (c) a series of cylindrical holes.

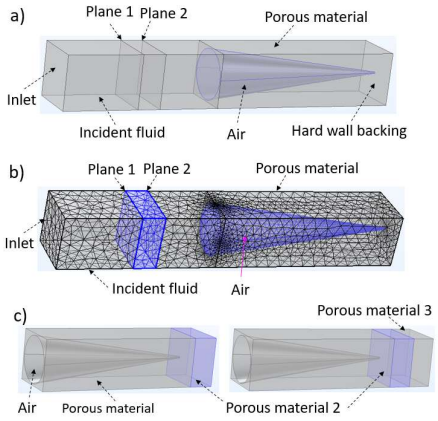

Figure 2: Numerical model: (a) porous layer with conical hole (b) mesh, and (c) multi-layer system.

Figure 3 shows the sound absorption coefficient of the porous material A of Table 1 for different thickness values L, L_y=30 mm, R_a=28 mm and R_b=1 mm. For L=0.254 m (10 inches), H is 0.25 mm and for L=0.381 m (15 inches), H is 0.379 m.

Figure 3 shows that the sound absorption coefficient of the porous material without conical holes does not increase when its thickness L is greater than the critical depth ($\approx 50\ mm$). With the conical hole, a significant improvement of the sound absorption is obtained.

[*] zacharie.laly@usherbrooke.ca
[†] noureddine.atalla@usherbrooke.ca
[‡] raymond.panneton@usherbrooke.ca
[♦] sebastian.ghinet@nrc-cnrc.gc.ca
[♯] chris.mechefske@queensu.ca.

Table 1: Porous material properties.

Materials	φ	σ (N s m^{-4})	α_∞	Λ (μm)	Λ' (μm)
A	0.99	123 170	1	22.25	44.49
B	0.99	17 717	1	58.40	116.8
C	0.99	26 000	1.02	150	300
D	0.99	13 904	1	65.88	131.8

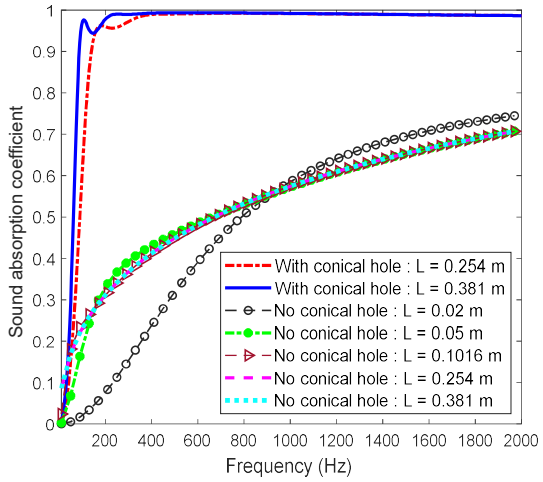

Figure 3: Comparison of the sound absorption coefficient.

The analytical sound absorption coefficient of the porous material with a series of cylindrical holes using the double porosity model is compared with FEM result in Fig. 4. The i^{th} layer is modeled by its transfer matrix T_i [4] and the global matrix T is obtained by multiplying all the matrices of the different layers $T = T_1T_2 \ldots T_i \ldots T_n$ [1]. The comparison in Fig. 4 is presented using the porous material D from Table 1 for n=12 and n=20 material layers with a thickness of 152.4 mm (6 inches), L_y = 15 mm, R_a = 13 mm, R_b = 1 mm; and H=150 mm. The analytical results of the sound absorption coefficient agree well with FEM result. The sound absorption presents a large frequency band.

Figure 5 shows the absorption coefficient of porous material A from Table 1 with periodic conical hole combined with one and two other porous layers (see Fig. 2(c)). Porous materials 2 and 3 in Fig. 2(c) have respectively the same properties as B and C in Table 1 with a thickness of 20 mm, L=0.254 m, H=0.25 m, L_y=*30 mm,* R_a= *28 mm* and R_b=*1 mm*.

The sound absorption coefficient of the multiple layer system containing periodic conical hole in Fig. 5 is significantly improved compared to the multiple layer system without periodic conical hole.

3 Conclusion

A design of porous material with a periodically distributed conical holes was presented and its acoustic performance was studied using the finite element method. It was demonstrated that the sound absorption coefficient of the material design is significantly improved over a large frequency band. An excellent sound absorption performance was obtained at low frequency where conventional porous material presents poor sound absorption. The porous material with periodic conical hole was combined with other conventional porous materials

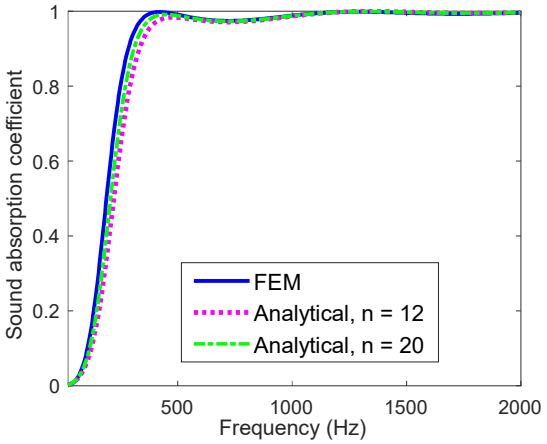

Figure 4: Comparison of FEM with analytical results.

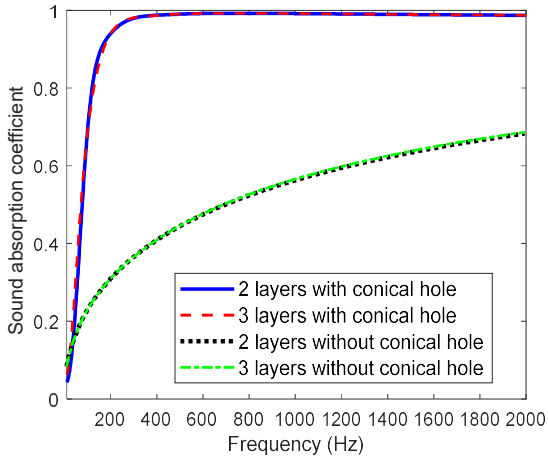

Figure 5: Sound absorption coefficient of multiple layers.

to create multi-layered systems with sound absorption strongly improved compared to classic multi-layered system.

Acknowledgments

The authors would like to thank Ministère de l'Économie, Science et Innovation and Consortium for Aerospace Research and Innovation in Canada for their financial support. We acknowledge the support of the Natural Sciences and Engineering Research Council of Canada (NSERC), [funding reference number RGPIN-2018-06113].

References

[1] Z. Laly, N. Atalla, R. Panneton, S. Ghinet and C. Mechefske. Finite element analysis of sound absorbing material with periodic decreasing hole profiles. Noise Control Engr. J. 71 (2), 75-91, (2023).

[2] P. Bonfiglio and F. Pompoli. Numerical methodologies for optimizing and predicting the low frequency behavior of anechoic chamber. J. Acoust. Soc. Am., 134, 285–291, (2013).

[3] K. Verdière and R. Panneton. Absorbent material containing holes with decreasing profile to improve sound absorption. Proceedings of 26th International Congress on Sound and Vibration (ICSV 2019), Montreal, Canada, July 7–11, 2019.

[4] Z. Laly, R. Panneton and N. Atalla. Characterization and development of periodic acoustic metamaterials using a transfer matrix approach. *Applied Acoustics* 185, 108381 (2022).

INVESTIGATION OF A PERIODIC ACOUSTIC METAMATERIAL FOR MULTI-TONAL NOISE ATTENUATION

Zacharie Laly [*3], Christopher Mechefske [†1], Sebastian Ghinet [‡1], Behnam Ashrafi [♦2], and Charly T. Kone [♯3]
[1]CRASH, Centre de Recherche Acoustique-Signal-Humain, Université de Sherbrooke, Québec, Canada.
[2]Department of Mechanical and Materials Engineering, Queen's University, Kingston, Ontario, Canada.
[3]Aerospace, National Research Council Canada, Ottawa, Ontario, Canada.
[4]Aerospace Manufacturing Technology Center, National Research Council Canada, Montreal, Canada.

1 Introduction

Acoustic metamaterials based on periodic Helmholtz resonators constitute potential solutions for low-frequency noise attenuation. Laly et al. [1,2] used the finite element method (FEM) to study the sound attenuation performance of porous material with embedded periodic Helmholtz resonators which contain damping material in the cavity and multiple transmission loss (TL) peaks were obtained. Abbad et al. [3] investigated a front membrane cavity Helmholtz resonator embedded in a porous matrix and observed that the TL was improved at the Helmholtz resonance with a degradation of the sound absorption.

In this paper, the TL of acoustic metamaterial based on periodic Helmholtz resonators containing a damping material in the cavity to which a small mass is attached is investigated using FEM. The mass that is attached to the membrane is a solid material. The TL of the proposed metamaterial presents multiple resonant peaks while only one peak is obtained using a conventional resonator. It is demonstrated that the resonant frequencies and the number of TL peaks can be controlled by the size and material properties of the added mass.

2 Finite element design and analysis of periodic acoustic metamaterial

Figure 1 shows a Helmholtz resonator with extended neck that contains a damping material in the form of a membrane in the cavity. A small solid mass with cylindrical shape is attached at the center of the membrane. The radius of the added mass is denoted by R and its thickness by H. The resonator is periodically embedded within a porous material. Figure 2 shows the cut-out view of the numerical geometry and the mesh of the periodic unit cell (PUC).

The membrane and the attached solid mass are modeled as linear isotropic materials using the solid mechanics module of COMSOL Multiphysics while the air inside the neck is modeled using the thermo-viscous acoustic module to account for the viscous and thermal dissipation effects. The porous layer with airflow resistivity of 26 kN s m^{-4}, a porosity of 99%, a tortuosity of 1.02, and respective characteristic viscous and thermal lengths of 150 µm and 300 µm is characterized using the Johnson-Champoux-Allard model [4].

[*] zacharie.laly@usherbrooke.ca
[†] chris.mechefske@queensu.ca
[‡] sebastian.ghinet@nrc-cnrc.gc.ca
[♦] behnam.ashrafi@nrc-cnrc.gc.ca
[♯] tenoncharly.kone@nrc-cnrc.gc.net

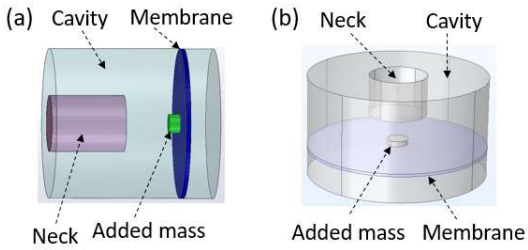

Figure 1: Helmholtz resonator with a membrane in the cavity (a) geometry (b) numerical model.

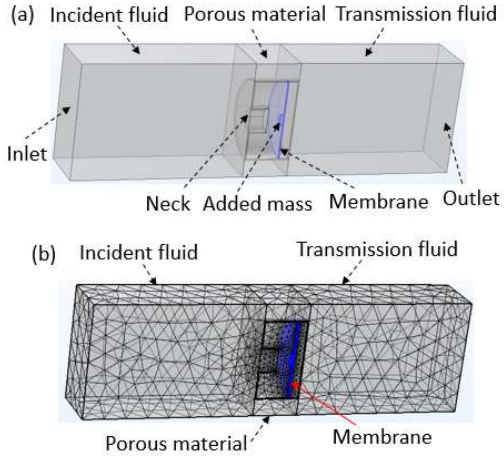

Figure 2: Cut-out view of the acoustic metamaterial (a) geometry of the PUC (b) mesh of the PUC.

The membrane material is ethylene vinyl acetate rubber with a thickness of 1 mm, Young's modulus of 5 MPa, density of 660 kg/m^3 and Poisson's ratio of 0.45. The radius of the neck is set to 15 mm and the diameter of the resonator cavity is 70 mm with a length of 40 mm, which is equal to the thickness of the porous material. Periodic boundary conditions are applied on all parallel planes.

Plane wave radiation conditions were applied on the inlet and outlet planes to minimize the reflection of acoustic waves. A normal incidence plane wave with pressure amplitude of 1 Pa was applied on the inlet and the transmission loss was calculated by the following relation:

$$\mathrm{TL} = 10\log_{10}(W_{in}/W_{out}) \quad (1)$$

where W_{in} and W_{out} are respectively the incoming power at the inlet plane and the outgoing power at the outlet plane. Figure 3 shows the TL of the metamaterial for membrane free and fixed boundary conditions without added mass. The

length of the neck is 15 mm and the membrane is located at 10 mm from the bottom inner wall of the resonator cavity. The TL with a conventional resonator shows one resonant peak of 43 dB at 692 Hz. When a membrane is integrated into the resonator cavity without added mass, the TL shows 2 peaks of 47 dB and 42 dB at 596 Hz and 1044 Hz respectively for membrane free boundary conditions and 5 peaks are observed with membrane fixed boundary conditions.

Figure 4 shows the effect of the added mass size on the TL. The length of the neck is set to 20 mm and the membrane with a thickness of 1 mm is located at 8 mm from the bottom inner wall of the cavity. The added mass is made of steel with a thickness of 2 mm and radius R varying from 1 mm to 6 mm.

With a radius R of 1 mm, the TL resonant frequencies in Fig.4 are 510 Hz, 612 Hz, 884 Hz and 1006 Hz where the TL peaks values are 29 dB, 38 dB, 30 dB and 27 dB respectively. With a radius of 4 mm, the resonant frequencies are 510 Hz, 646 Hz, 956 Hz and 1086 Hz. Apart from the first resonant frequency, the other three resonant frequencies with R= 4 mm have increased compared to R=1 mm. With R=6 mm, 3 resonance frequencies are observed which are respectively higher than the first three resonance frequencies with R=1 mm and R=4 mm. The TL resonance frequencies increase when the radius of the added mass increases. The resonance frequencies can then be controlled by adjusting the radius of the added mass.

Figure 5 illustrates the effect of the added mass material properties on the TL. The distance between the membrane and the bottom wall of the cavity is 8 mm. The length of the neck is 20 mm while R and H are set to 3 mm. The TL in Fig. 5 presents 6 resonant frequencies when the added mass is made of steel and 5 resonant frequencies are observed when the added mass is made of aluminum.

3 Conclusion

The TL of an acoustic metamaterial based on a periodic Helmholtz resonator was investigated using FEM. A membrane was integrated within the resonator cavity to which small solid masses were attached. It was demonstrated that the multiple TL resonant frequencies and peak values generated can be controlled by adjusting the parameters (size and material properties) of the added mass.

Acknowledgments

The authors would like to acknowledge the National Research Council Integrated Aerial Mobility Program for the financial support.

References

[1] Z. Laly, C. Mechefske, S. Ghinet, and C.T. Kone. Numerical modelling of acoustic metamaterial made of periodic Helmholtz resonator containing a damping material in the cavity. In Proceedings of 2022 Inter-national Congress on Noise Control Engineering, INTERNOISE 2022, 21-24 August 2022, Glasgow, UK.

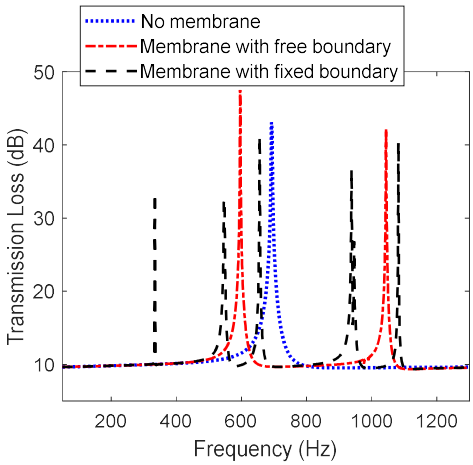

Figure 3: Comparison of the transmission loss.

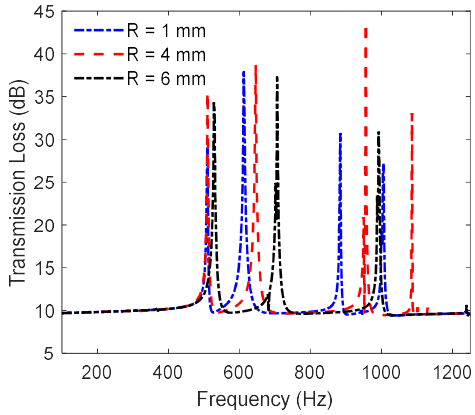

Figure 4: Effect of the added masses on the transmission loss.

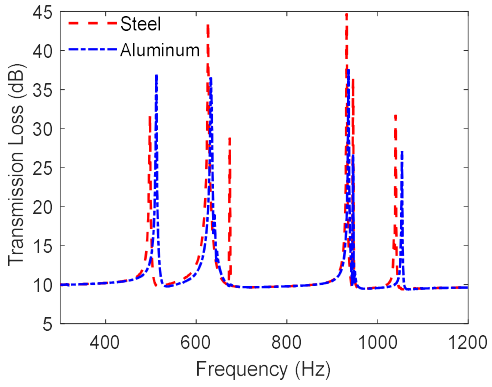

Figure 5: Effect of the added mass material properties on the TL.

[2] Z. Laly, C. Mechefske, S. Ghinet, B. Ashrafi, and C.T. Kone. Finite element design of acoustic metamaterial based on parallel Helmholtz resonators with embedded membranes. Canadian Acoustics Proceedings, 50(3), 20-21, 2022.

[3] A. Abbad, N Atalla, M. Ouisse, and O. Doutres. Numerical and experimental investigations on the acoustic performances of membraned Helmholtz resonators embedded in a porous matrix. *Journal of Sound and Vibration,* 459, 114873, 2019.

[4] J-F. Allard and N. Atalla. Propagation of sound in porous media: modeling sound absorbing materials, 2nd Edition. New York: Elsevier applied sciences, 2009.

AEROACOUSTIC OPTIMIZATION OF A METACAGE TO BLOCK THE NOISE EMITTED BY AN EXHAUST FAN

Marco Lizotte [*1], **Jean-Bernard Piaud** [†2], **Raymond Panneton** [‡3], **Tenon Charly Kone** [§4], **Jean-Christophe Cuillière** [¶5], **and Vincent François** [‖6]

[1]Venmar Ventilation ULC
[2]Independant Ventilation and Acoustic advisor
[3]Université de Sherbrooke
[4]National Research Council of Canada
[5,6]Université du Québec à Trois-Rivières

1 Introduction

The recent pandemic showed the importance of well ventilated areas to preserve safety of the occupants. For that reason, the addition of Heating, Ventilation and Air Conditioning (HVAC) is needed to exchange air. However, these systems can be noisy and have a negative effect on people such as sleep disturbances, cognitive problems or influences on heart diseases [1]. Recent research in acoustics has proven the effectiveness of sonic crystals in blocking some of the ventilation noise without adding too much restriction to the flow [2–4].

The aim of this study is to reduce noise transmitted from an exhaust fan by replacing the conventional grill, shown in Figure 1, by an optimized metagrill (acoustic metacage made from sonic crystals). The original noise level of the fan was measured at 55.2 dBA, at an operation point of 0.1 inH2O at 110 CFM. The objective is to maximise noise reduction while maintaining ventilation performance in the same conditions.

FIGURE 1 – Exhaust fan

2 Method

2.1 Sonic crystals

The strategy here is to implement sonic crystals (SC) inside the grill, between the fan and the air inlet. SC are arrays of scatterers. Ideally, it consists of a unit cell of size H with a scatterer (example solid cylinder of diameter D) in its center. The unit cell is infinitely periodized and the SC shows a band gap where no transmission of sound is possible. The central frequency f_c of the band gap is given by the Bragg condition, $\lambda/H = 2$ or $f_c = c/2H$, where λ is the wavelength, and c is the speed of sound. For a finite number N of periodicity along the wave propagation direction, the sound transmission loss is typically proportional to the filling ratio D/H.

In reality, the SC must fit into the available envelope. In the case of the exhaust fan, the envelope is limited and the scatterers must be distributed radially up to a maximum external radius. In addition, to minimize head losses, the azimuth distance between scatterers should not be too small. Note that the flow of air over a scatterer can generate noise. Thus, the metagrill to be designed must attenuate more noise than it could generate while allowing air to flow with a minimum of pressure drop. This reality therefore forces us to proceed with an optimization of the various design parameters of the metagrill, while adding geometric, acoustic and flow constraints.

2.2 Optimization

The optimization is conducted with open source software. Sandia Dakota®is used to perform a numerical design of experiment (NDOE), EDF Salome®to CAD and mesh, EDF Code_Aster®to simulate, with the finite element method, the acoustics, OpenCFD OpenFOAM®to compute head losses, and development platform ERICCA MAGiC to obtain sound transmission loss (TL).

Due to the limited space, only two rows of scatterers will be used along the radial direction. The parameters to optimize are shown in Figures 2 and 3. The constraints are given in Table 1. The NDOE optimization will use a 25 samples Latin Hypercube Sampling (LHS).

TABLE 1 – NDOE of the metagrill. A 25 samples Latin Hypercube Sampling (LHS) was used.

Parameters	A1/A0 (%)	H1/H0 (ratio)	Entry Height (inches)	Mid Height (inches)	Nb.crystals radially
Lower	0.4	0.5	1	1	20
Upper	0.7	0.8	3	3	28

3 Results and discussion

The result coming out of the LHS was then fed to the Efficient Global Optimization (EGO) to find if there was an optimal solution within the response surface of the LHS. The final metagrill consist of 28 rows of two sonic crystals, with a $H1/H0$ of 0.7, $A1/A0$ of 0.6, an entry height of 1 inch and a

∗. lizottem@venmar.ca
†. piaudjb@gmail.com
‡. raymond.panneton@usherbrooke.ca
§. tenoncharly.kone@nrc-cnrc.gc.ca
¶. jean-christophe.cuilliere@uqtr.ca
‖. vincent.francois@uqtr.ca

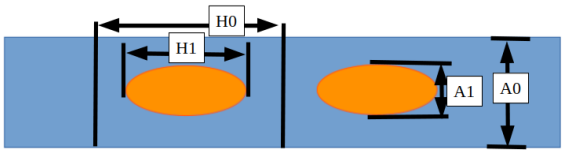

FIGURE 2 – Design parameters for the sonic crystals

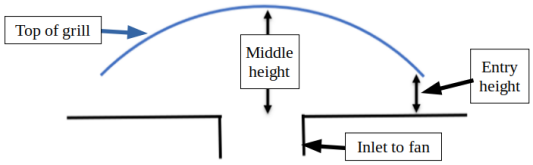

FIGURE 3 – Design parameters for the dome shape of the cover

middle height of 3 inches. A photo of the prototyped optimal metagrill is shown in Figure 4

To validate the prototype, sound and ventilation measurements were taken. The sound measurements were carried out according to the ISO 9614-1 standard at the Venmar Ventilation ULC laboratory on the fan equipped with the conventional grille and the metagrill. The results showed that the overall fan sound power with the metagrill was reduced from 55.2 dBA to 49.7 dBA. Also, to verify the type of attenuation provided by the metagrill, its transmission loss was measured at Mecanum Inc on a small reverberation chamber. Figure 5 shows the measured TL. The result demonstrates the broadband attenuation of the designed metagrill.

For ventilation measurements, ISO 5167-1 was used on the ventilation test bench of Venmar laboratory. The results obtained were similar to the simulated ones. The designed metagrill does not offer more resistance to flow than the original grill.

4 Conclusion

To conclude, a metacage optimization approach, with sonic crystals, was presented as a solution to reduce noise transmitted while keeping good ventilation. The optimized design has achieved a noise reduction of nearly 6 dBA by blocking the transmission of ventilation noise over a wide frequency band.

Acknowledgments

Authors acknowledge the support of the Natural Sciences and Engineering Research Council of Canada (NSERC). Special thanks to Mecanum Inc for making their small reverberating room available to us.

References

[1] Mathias Basner, Wolfgang Babisch, Adrian Davis, Mark Brink, Charlotte Clark, Sabine Janssen, and Stephen Stansfeld. Auditory and non-auditory effects of noise on health. *The lancet*, 383(9925) :1325–1332, 2014.

[2] P Bouché. Elaboration d'une grille de filtration pour hotte de cuisine inspirée des méta-matériaux ayant un maximum d'isolation acoustique. *Université de Sherbrooke, Département de génie mécanique*, 2017.

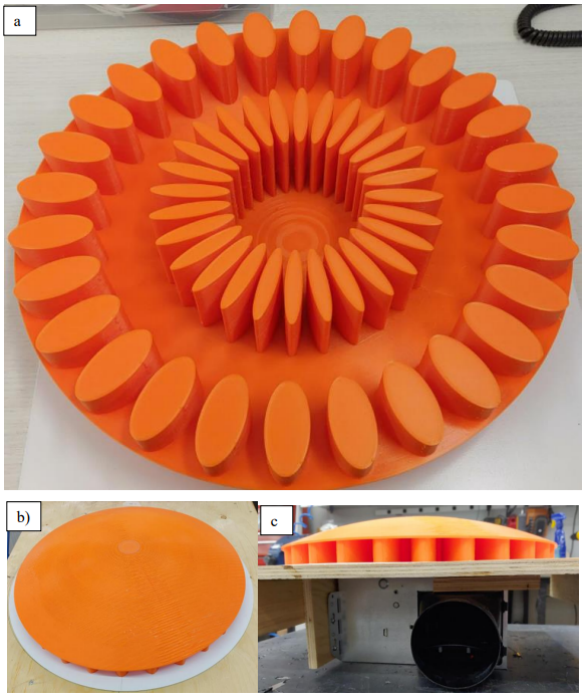

FIGURE 4 – Prototype of the optimized metagrill. a) Inside view. b) Outside view. c) Side view with wood representing the ceiling

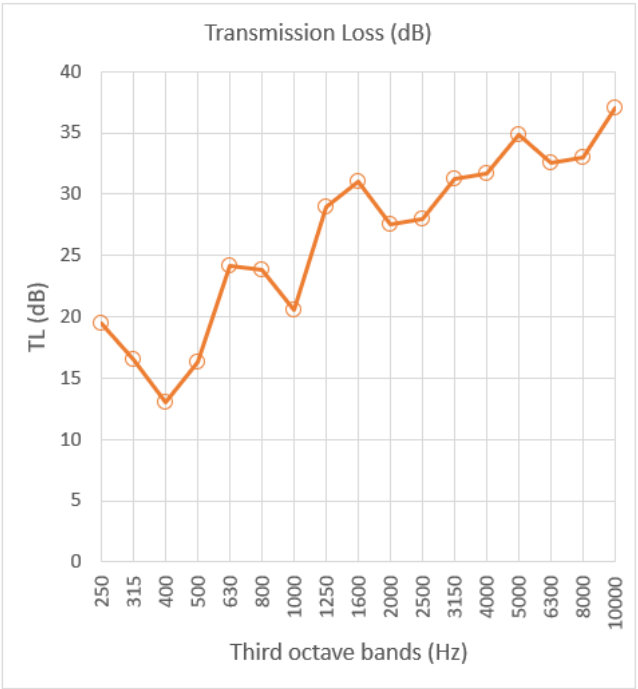

FIGURE 5 – Transmission loss measurements at Mecanum

[3] Antonella Bevilacqua, Gino Iannace, Ilaria Lombardi, and Amelia Trematerra. 2d sonic acoustic barrier composed of multiple-row cylindrical scatterers : Analysis with 1 : 10 scaled wooden models. *Applied Sciences*, 12(13) :6302, 2022.

[4] Chenkai Liu, Jinjie Shi, Wei Zhao, Xiaoxi Zhou, Chu Ma, Ruwen Peng, Mu Wang, Zhi Hong Hang, Xiaozhou Liu, Johan Christensen, et al. Three-dimensional soundproof acoustic metacage. *Physical Review Letters*, 127(8) :084301, 2021.

ENGINEERED MATERIALS FOR ACOUSTICS: METAMATERIALS, SONIC CRYSTALS AND CALCULATED MICROSTRUCTURES

Raymond Panneton *[1]
[1]Centre de recherche acoustique-signal-humain de l'Université de Sherbrooke (CRASH-UdeS)

1 Introduction

For two decades, research on acoustic materials (absorbent and insulating) has largely translated into metamaterials and sonic crystals or, more generally, into engineered acoustic materials. A large number of scientific articles on these unconventional materials appear every week, even every day. While research is moving towards a more in-depth knowledge of these materials and new concepts, their applications are already numerous in several sectors of industry. Through all the research, it is sometimes difficult to fully define what acoustic metamaterials, sound crystals, and engineered acoustic materials really are. This extended summary presents the author's personal definition and classification of these different classes of materials, adding the class of optimized conventional materials (or calculated microstructures), and grouping them under the family of "engineered acoustic materials".

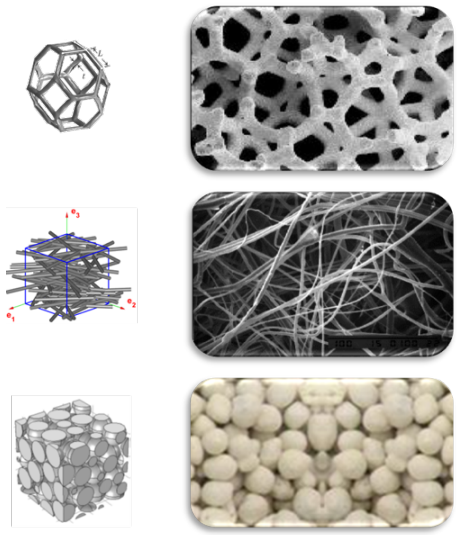

FIGURE 1 – Examples of conventionnal materials

2 Definitions

2.1 Conventionnal materials for acoustics

Conventional acoustic materials are notably foams, fibers and granular media. They are open-cell porous media with interconnected void spaces or pores saturated by air, see examples in Figure 1. They can be represented by a periodic unit cell (PUC) or a representative volume element (RVE) of characteristic size H. At audible frequencies, their characteristic size is much smaller then the wavelength $\lambda : H \ll \lambda$. When the motion of their solid phase is negligible, they are homogeneous equivalent dissipative fluids of effective density ρ_e and bulk modulus K_e. These two latter properties account for thermoviscous dissipation of the sound waves in these fluids. In the harmonic regime, the equation governing wave propagation is the Helmholtz equation $\Delta p + k^2 p = 0$. Here, the wave number is given by $k = 2\pi f/c_e$ and the effective sound speed by $c_e = \sqrt{K_e/\rho_e}$.

Such conventional acoustic materials generally offer low sound transmission loss (TL) per meter (db/m). Their TL is mainly governed by their resistance to airflow. On the other hand, they have good sound absorption coefficients at medium and high frequencies ; however, they exhibit asymptotic absorption. This limit cannot naturally be exceeded with increasing thickness. Moreover, their first absorption does not naturally exceed a wavelength-to-thickness ratio λ/L of 5. Consequently, they are of little use at low frequency in places of limited thickness.

2.2 Engineered materials for acoustics (EMA)

It may sound a little pompous, but while nature aims for energy minima in the manufacture of materials, Man aims for maximums in the performance of materials. Thus, by mastering the physics behind wave propagation and dissipation in air-saturated media, one finds complex optimal geometries that maximize, for example, sound absorption or transmission loss in a given frequency range. This is why such materials are called engineered materials or structured materials. The structuring of the materials may be at different scales : microscopic (much smaller than wavelength), mesoscopic (smaller than wavelength), and macroscopic (comparable to wavelength).

One of the first types of macroscopically structured acoustic materials was non-resonant sonic crystals (SC). A SC is a periodic arrangement of scatterers. They present band gap in the transmission of sound. The central frequency of the first band gap is given by the Bragg condition : $\lambda/H = 2$, where H is the size of the PUC of the SC. Since it requires at least two crystals to introduce Bragg diffraction, the size of the SC is of the order of the wavelength. It is used to block sound transmission and may require large dimensions at low frequencies.

At the mesoscopic scale, one can find materials formed of periodic resonant elements which are added along the path of acoustic propagation. Depending on the type of resonances, acoustic or elastic, they slow down the modulus of the speed of sound by decreasing the effective bulk modulus of air or increasing its density respectively. In this case,

∗. raymond.panneton@usherbrooke.ca

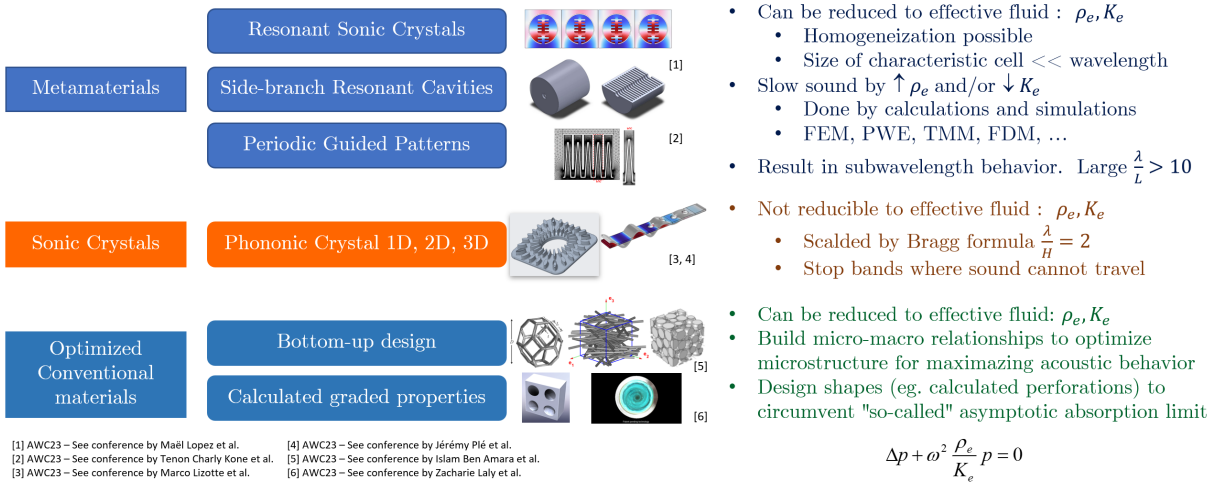

FIGURE 2 – Classification of engineered materials for acoustics.

they are also called sub-wavelength or slow sound materials. Much of the articles in the literature refer to these materials as metamaterials. Therefore, metamaterials shift the acoustic spectrum to lower frequencies and can achieve a wavelength-to-thickness ratio well over 10. Additionally, due to the resonances, their types and periodic arrangement, the wavenumber may be either positive real, imaginary, or negative real. This has the effect of creating band gaps of different natures.

Finally, at the microscale, one can find materials for which their microstructure and transport parameters are optimized by caculations to maximize thermoviscous dissipation. The author calls these materials optimized conventional materials. On the one hand, they may be conventional materials whose microstructure has been optimized by multi-scale calculations (bottom-up approach). For example, sheets of fibers whose angular orientation and polydispersity of fiber diameters have been optimized to obtain the best acoustic absorption at low frequencies. In these cases, wavelength-to-thickness ratios as high as 10, even 20, can be achieved, which is more than twice the ratio of conventional materials. On the other hand, porous materials with graded properties can also be considered. The gradation can be continuous or stepwise.

3 Classification

As described in the previous paragraphs, three distinct classes emerge : sonic crystals (SC), metamaterials (MM), and optimized conventional materials (OCM). Since ”Meta” in metamaterial is a Greek word meaning ”beyond”, for the author, metamaterials refer to materials for which the properties (speed of sound, density, bulk modulus, wave number, refractive index or other characteristic properties) are beyond those typically found in conventional materials. Therefore, according to the author’s definition, SC and OCM should not be considered as metamaterials. However, since the shapes and matter organization of the three (SC, MM, and OCM) come from engineering calculations (whether simple or complex), they are all engineered materials or structured materials. Finally, the MM and the OCM being designed respectively at the mesoscopic and microscopic scales, they can also be homogenized at the macroscopic scale (wavelength scale) as for classical acoustic materials. Therefore, OCM and MM can be represented as equivalent fluids of effective properties for which the Helmholtz equation governs sound propagation.

Based on the previous short definitions, Figure 2 presents the classification proposed by the author. This classification and the underlying definitions are not the result of a consensus of the scientific community in acoustics. The author proposes here a classification that seems consistent with what is found in the literature. It remains to be debated and validated by peers. Its presentation at this conference is only one step.

4 Discussion and conclusion

As shown in Figure 2, the engineered materials for acoustics are divided in three classes : MM, SC and OCM. Note that reality is more complex than this simple classification. Indeed, acoustic solutions may imply combinations of many classes. For instance, a combination of SC with resonant MM elements, such as resonant sonic crystals, or a combination of side-branch resonant cavities embedded in a conventional porous materials. In this classification, the most important thing to keep in mind is the description given on the right side of the figure, or the wavelength-to-thickness ratio that each class can achieve. Based on this, an intelligent decision on the type of noise control elements for a given application can be made by acoustic engineers or architects.

Acknowledgments

Author acknowledges the support of the Natural Sciences and Engineering Research Council of Canada (NSERC).

References

[1] Pierre A Deymier. *Acoustic metamaterials and phononic crystals*, volume 173. Springer Science & Business Media, 2013.

[2] Noé Jiménez and coll. Acoustic waves in periodic structures, metamaterials, and porous media. *Springer International Pub.*

SONIC CRYSTAL ACOUSTIC ATTENUATION APPLIED TO EXHAUST AIR SYSTEMS

Jeremy Plé [*], **Tenon Charly Kone** [†], **Allaeddine Benchikh Lehocine** [‡], **and Raymond Panneton** [§]
Centre de recherche acoustique-signal-humain de l'Université de Sherbrooke (CRASH-UdeS)
& National Research Council Canada, Flight Research Laboratory, Ottawa

1 Introduction

Air quality is a critical aspect of maintaining comfort and good health inside homes or in transportation vehicles. According to the Government of Canada's health website, Canadians spend on average 90% their time indoors. Thus, it is necessary to develop air filtration systems to reduce humidity and impurities caused by stagnant air. The commonly used mechanical ventilation systems in Canada can be noisy and cause discomfort. This study focuses on reducing the noise from these systems.

To solve the noise problem, one approach is to prevent the noise from escaping the system. Another option is to design a more acoustically efficient fan. This study focuses on the former method. Sonic crystals [1] can effectively block ventilation noise while allowing uninterrupted airflow. These crystals can be designed with various geometries, permeability, and thickness. The objective is to create a method to determine the transmission loss of a sonic crystal lattice that is both fast in computation time and simple in design in order to then optimize certain parameters efficiently.

The proposed approach using transfer matrices will be applied to circular sonic crystals subjected to a plane wave at normal incidence. Thermo-viscous losses will be incorporated by assigning effective properties to the air between the crystals. The effective density and bulk modulus will be calculated using the Johnson-Champoux-Allard (JCA) [2] equivalent fluid model. The predictions obtained from this approach will be validated by comparing them to normal-incidence transmission loss measurements in an acoustic tube and finite element simulations conducted in previous studies. A correction in tortuosity is also applied due to the proposed method not seeing changes in inertia due to the changes in geometry brought by the sonic crystals.

2 Methods

2.1 Materials

The solution proposed in this paper is a periodic structure comprised of N rows of sonic crystals, arranged so that the acoustic waves hit the sides of the cylinders. Each periodic unit cell (PUC) can be separated into two segmented crystals of different diameters. This allows us to build the transfer matrix of each diameter separately, and reconstruct the transfer matrix of the PUC using the parallel transfer matrix method (PTMM). Once done, the PUC is periodized in a linear array using the classical TMM to reconstruct the entire crystal network. Figure 1 shows the general methodology.

All crystal segments simplify into a single uniform solid cylinder inside a rectangular cube of air, its PUC can be represented in a 2D plane. The 2D parameters of a global PUC, composed of the parallel assembly of two individual cells, are shown in Figure 1. They are D_i and h_i, the diameter and height of individual cell i, where $i = 1$ or 2, and H_x, H_z, the width and depth of the cell.

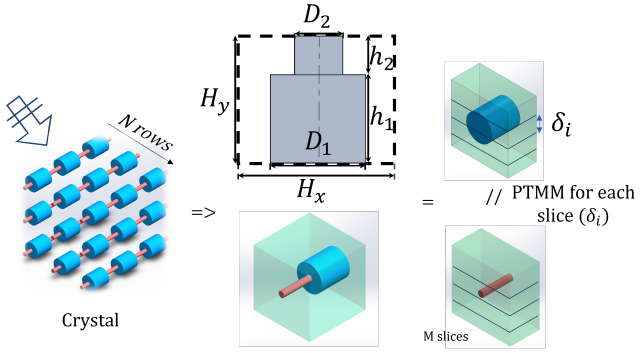

FIGURE 1 – Periodic unit cell (PUC) of the studied sonic crystal : Side view of the parallel assembly of two different sized crystals to form the global PUC.

The experimental samples tested in an impedance tube were made from resin with a SLA 3D printer, and their dimensions are shown in table 1. The parameter h represents the total height of the sonic crystal, also written as H_y.

TABLE 1 – Parameter values for each sonic crystals samples

Sample set ID	H_x (mm)	H_y & H_z (mm)	h_1 (mm)	h_2 (mm)	D_1 (mm)	D_2 (mm)
A	60	38	h	0	31.5	0
B	60	38	$\frac{2}{3}h$	$\frac{1}{3}h$	31.5	9.5

2.2 Discretized PTMM

To model the geometries of the sonic crystals, a discrete transfer matrix (DTMM) approach is proposed. The air domain between crystals is discretized to accommodate their intricate shapes. Each element of width δ_i in the domain will have a transfer matrix that considers local thermo-viscous losses. These element transfer matrices will be combined into a global transfer matrix using the PTMM [3] alongside the surface ratio of air for each element and the classical serial transfer matrix method (TMM) as shown in Figure 1. By applying the proposed approach and Bragg's law to sonic crystals, the sound transmission loss of the crystal network, exhibiting "stop-bands," can be predicted.

*. jeremy.ple@usherbrooke.ca
†. TenonCharly.Kone@nrc-cnrc.gc.ca
‡. Alla.eddine.benchikh.lehocine@usherbrooke.ca
§. raymond.panneton@usherbrooke.ca

3 Results & Discussion

3.1 Sample set A & tortuosity

Figure 2 shows the transmission loss (TL) for sample set A (Table 1) with three 31.5 mm diameter crystals in series distance from each other by 60 mm in reference to their centers. A stop-band appears around a central frequency of 2830 Hz, with a transmission loss peak of 34 ± 1 dB. All methods yield similar TL curves with a variation of around ± 2 dB, except for a small frequency shift observed with the DTMM without correction. This shift is due to the fixed tortuosity of each discrete element, and can be recentered with a correction to the previous tortuosity as the TMM does not consider the inertia from contraction and expansion between elements. This corrected tortuosity, hereby called geometric tortuosity (α_g), is established using the number of discretizations of a single PUC (M) as well as the formula defining the distance between the surface of a crystal and the opposing face of the PUC ($a(x)$). It can then be applied as a corrected thickness written as : $\delta_i' = \delta_i.\alpha_g$. With this correction applied, the DTMM with correction better represents the experimental and numerical models

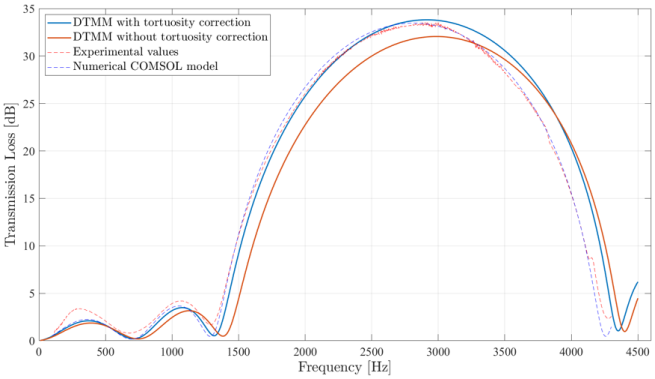

FIGURE 2 – Sound transmission loss obtained with sample set A. Comparison between transfer matrix methods, experimental method and numerical method.

3.2 Sample set B & tortuosity

Figure 3 shows the transmission loss for sample set B (Table 1) made up of the parallel assembly of two diameters (9.5 mm and 31.5 mm). As the distance between the crystals remains unchanged compared to sample set A, the central frequency remains the same, and the level of TL is slightly above half the one of set sample A. The same trend is observed with the DTMM without correction. However when applying the corrected tortuosity, the shift in frequencies is not sufficient enough to be validated by the experimental and numerical models. The authors think this is due to the the corrected tortuosity only considering corrections in a 2D plane and not a 3D one, which is justified for sample set A, but not B. Further research needs to be conducted to implement a more robust corrected tortuosity.

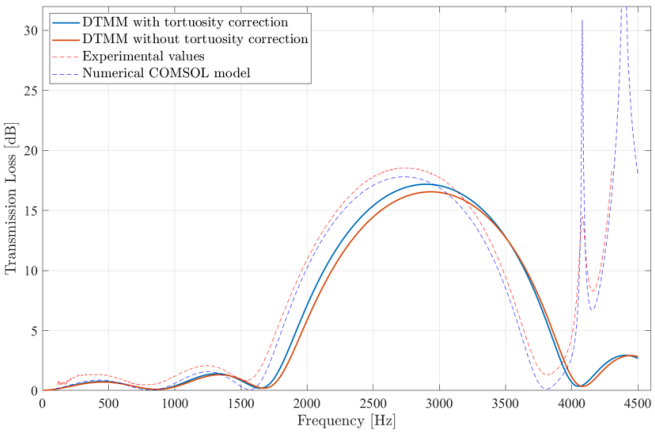

FIGURE 3 – Sound transmission loss obtained with sample set B. Comparison between transfer matrix methods, experimental method and numerical method.

Conclusion

A discrete transfer matrix method (DTMM) has been developed to model a periodic linear array of complex-shaped sonic crystals (SC). The method discretizes the air domain between the crystals into rectangular elements. Each element is characterized by a transfer matrix that accounts for thermoviscous losses. Two different crystals arranged in parallel are combined into a global transfer matrix using the parallel transfer matrix method (PTMM) applied to each element individually. The linear N-periodic lattice of the sonic crystal parallel assembly is constructed using the classical serial transfer matrix method. The transfer matrix of the linear array is then used to predict the transmission loss under normal incidence. This functional method answers the established objective of being both simple, using only 2X2 matrices, and fast in computation time.

However, the tortuosity remains difficult to determine for each element. Even with a global tortuosity correction this is only sufficient for sonic crystals with no variations in diameter along its axis, and further study is needed. An optimization method is underway in order to create the best lattice possible for a given sonic crystal exterior geometry.

Acknowledgments

Authors acknowledge the support of the Natural Sciences and Engineering Research Council of Canada (NSERC). Special thanks to Mecanum Inc for making their square impedance tube available to us.

References

[1] Farzad Zangeneh-Nejad and Romain Fleury. Active times for acoustic metamaterials. *Reviews in Physics*, 4 :100031, 2019.

[2] Yvan Champoux and Jean-F Allard. Dynamic tortuosity and bulk modulus in air-saturated porous media. *J. App. Phys.*, 70(4) :1975–1979, 1991.

[3] Kévin Verdière, Raymond Panneton, Saïd Elkoun, Thomas Dupont, and Philippe Leclaire. Transfer matrix method applied to the parallel assembly of sound absorbing materials. *J. Acoust. Soc. Am.*, 134(6) :4648–4658, 2013.

ACOUSTIC METAMATERIALS FOR LOW-FREQUENCY NOISE REDUCTION: A REVIEW

Niloofar Rastegar [*1], Davide De Cicco [†1], David Vidal [‡1], and Annie Ross [♦1]
Laboratory for Acoustics and Vibration Analysis (LAVA), Department of Mechanical Engineering,
Polytechnique Montreal, Montreal, Canada

1 Introduction

Noise pollution from transportation vehicles is a growing problem in densely populated areas. Among various sources of noise pollution, helicopters are known for their disruptive and intrusive sounds, which can have harmful effects on the health and well-being of nearby residents. The continuous exposure to high levels of noise in urban environments can lead to annoyance, sleep disturbance, and even more severe long-term health problems, including hypertension, stroke, and heart attacks [1].

Conventional porous materials such as foams exhibit favorable sound absorption characteristics. However, very thick layers of such materials are required for absorbing low-frequency sounds, thus making them unpractical in most applications. Moreover, they have limited design tailorability, and they cannot be effectively employed in complex structures [2].

Acoustic metamaterials are innovative materials engineered to manipulate and control the propagation of sound waves in ways that are not possible with traditional materials. These structures typically consist of periodic arrangements of subwavelength unit cells, which interact with sound waves at specific frequencies to achieve desired acoustic effects [3].

The aim of this review is (i) to contribute valuable insights to the field of noise control and its practical implementation in the aviation industry and (ii) to propose a metamaterial design suitable for large-scale manufacturing and capable to address low-frequency noise reduction in helicopters.

2 Metamaterials

2.1 Folded Metaporous Materials

The "folding" technique is an innovative approach used in the design of acoustic metasurfaces to overcome the thickness requirements needed for effective low-frequency absorption with traditional porous materials. Instead of using thick materials, the folding technique involves creating intricate patterns or structures that allow sound waves to traverse through a compact and folded surface. This enables the metasurface to achieve efficient low-frequency sound absorption despite its reduced thickness, making it a promising solution for compact and effective acoustic absorption applications [4].

Boulvert *et al.* [4] proposed a folded metaporous surface for achieving sub-wavelength and broadband perfect sound absorption. As depicted in Fig. 1, the structure consists of four helicoidal cavities filled with porous media - in this case, micro-lattices. The effective thickness and intrinsic losses of each helicoidal cavity can be independently adjusted by varying their macro- and micro-structures. The results show almost perfect absorption over the frequency range 1000 – 2000 Hz that is not achievable with homogeneous porous materials or single helicoidal cavities.

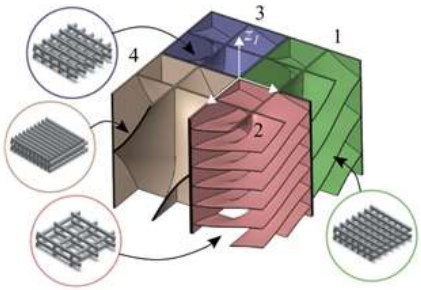

Figure 1. Schematic of parallel assembly of four folded metaporous materials [4].

2.2 Double Porosity Metamaterials

Double porosity metamaterial (DPM) refers to a type of porous material that has two levels of porosity: a meso-scale porosity and a micro-scale porosity.

Zhao *et al.* [5] designed a DPM, incorporating labyrinthine channels for meso-porosity and utilizing melamine foam to achieve microporosity. The DPM exhibits significantly lower frequency sound absorption compared to the homogenous porous materials with equal thickness. The distribution of sound pressure and velocity indicates that the improved sound absorption is brought about by two factors: the resonance of the labyrinthine channel and the hybrid resonance that occurs between the porous layer and the labyrinthine channel. These phenomena contribute to the overall enhancement in sound absorption. Moreover, the DPM offers greater design flexibility to customize the sound absorption spectrum in the desired frequency range.

2.3 Hybrid Acoustic Metamaterials

Costa-Baptista *et al.* [6] designed a multilayered microchannels structure which exhibited effective subwavelength and near-perfect broadband sound absorption. This metamaterial offered a good compromise between effective acoustic properties and useful mechanical properties, making them viable candidates for applications where both sound absorption and structural resistance are required. However, performance drops for frequencies lower than 1000 Hz. Therefore, for providing low-frequency absorption, helical tubes are combined with the multilayered microchannels, as depicted in Fig. 2. This hybrid metamaterial exhibits enhanced acoustic

[*] niloofar.rastegar-dehkordi@polymtl.ca
[†] davide.de-cicco@polymtl.ca
[‡] david.vidal@polymtl.ca
[♦] a.ross@polymtl.ca (corresponding author)

absorption capabilities, both in the low-frequency range and across a broader spectrum. The helical tubes would provide a smooth and continuous pathway for the sound waves to be trapped in and dissipated. Coiling is a highly effective method for compactly containing long tubes within limited volumes. In a subsequent work [7], the authors demonstrated that the helical conformation is the most efficient way to fold a tube to provide compact and structurally stable tubes. Furthermore, increasing the length of the tubes causes the resonance to shift towards lower frequencies, further optimizing the material's performance.

2.4 Acoustic Black Holes

An acoustic black hole (ABH) is a sound-absorbing structure designed to gradually slow down and weaken the sound waves as they travel towards the inner part of the structure. They are often comprised of a series of rings with different radii positioned along the inner wall of a rigid cylindrical tube, forming a conical shape. At the tip, there is an extremely small diameter, causing the sound waves to be reflected back and forth multiple times, resulting in a substantial reduction of sound energy and effective sound absorption [8].

Xiaoqi and Li [9] suggested combining an ABH sound absorber with microperforated panels (MPPs) as a liner covering the inner surface of the rings (Fig. 3). The designed structure demonstrates near perfect absorption performance in a rather low and broad frequency range from 200 Hz to 3000 Hz, with much fewer fluctuations of the absorption coefficient value compared to traditional structures.

MPPs offer high acoustic resistance and low acoustic reactance, which makes them a highly effective sound absorption material. The integration of the MPP with the cavity behind the panel creates a resonant system, facilitating the interaction of sound waves passing through the micro-perforations, thereby enhancing sound absorption within a specific frequency range. Furthermore, the MPP dissipates sound energy through viscous losses and frictional effects, contributing to the overall sound absorption performance of the ABH absorber. Therefore, incorporating the MPP into the ABH absorber significantly improves its sound absorption capabilities across both broadband and low-frequency ranges, making it a more versatile and efficient solution for noise control applications [9].

3 Conclusion

In conclusion, acoustic metamaterials offer innovative solutions for broadband and low-frequency sound absorption. Conventional porous materials, while effective in sound absorption, face limitations in dealing with low-frequency noise and complex structural applications. The studies on folded metaporous materials, double porosity metamaterials, hybrid acoustic metamaterials, and acoustic black holes have shown significant advancements in achieving efficient sound absorption across various frequency ranges. With their ability to overcome traditional material constraints and enhance sound absorption in both low and broadband frequencies, acoustic metamaterials hold great promise in creating quieter and more livable urban environments.

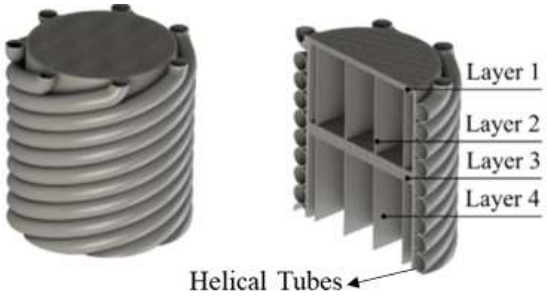

Figure 2. Schematics of hybrid metamaterials [7].

Figure 3. Schematic of acoustic black hole and microperforated panel as a liner [9].

Acknowledgments

This financial support received through Mitacs, CRIAQ and NSERC, as well as through our industrial partner, Hutchinson, is gratefully appreciated.

References

[1] H. J. Jariwala *et al*. Noise Pollution & Human Health: A Review. *Indoor and Built Environment*, 2017

[2] C. Gaulon, et al. Acoustic absorption of solid foams with thin membranes. *Appl. Phys. Lett.,* 112, 2018.

[3] N. Gao *et al*. Design, fabrication, and sound absorption test of composite porous metamaterial with embedding I-plates into porous polyurethane sponge. *Appl. Acoust.,* 175, 2021.

[4] J. Boulvert *et al*. Folded metaporous material for sub-wavelength and broadband perfect sound absorption. *Appl. Phys. Lett*., 117, 2020.

[5] H. Zhao *et al*. A double porosity material for low frequency sound absorption. *Compos. Struct.,* 239, 2020.

[6] J. Costa-Baptista *et al*. Design and fused filament fabrication of multilayered microchannels for subwavelength and broadband sound absorption. *Addit. Manuf.,* 55, 2020.

[7] J. Costa-Baptista *et al*. Hybrid acoustic materials through assembly of tubes and microchannels: design and experimental investigation. *Rapid Prototyp. J.,* 2023.

[8] A. E. Ouahabi, V. Krylov, and D. J. O'Boy. Experimental investigation of the acoustic black hole for sound absorption in air. *22nd International Congress on Sound and Vibration,* 2015.

[9] Z. Xiaoqia and C. Li. Broadband and low frequency sound absorption by Sonic black holes with Micro-perforated boundaries. *J. Sound Vib.*, 512, 2021.

BRAGG BANDS GENERATION IN BEAMS AND PLATES FOR MASS REDUCTION AND VIBROACOUSTIC PERFORMANCE

Olivier Robin[*1], **Vania Gonzalez**[†2], **Nicolas Bohmwald**[‡2], **and Viviana Meruane**[§2]
[1]Centre de Recherche Acoustique-Signal-Humain, Université de Sherbrooke, Sherbrooke, Canada.
[2]Departamento de Ingeniería Mecánica, Universidad de Chile, Santiago, Chile.

1 Introduction

Most of the existing approaches for designing locally resonant metamaterials involve addition or inclusion of elements such as tuned mass dampers or masses following a periodic pattern [1]. Modifications to the geometry can also provide interesting results in the case of beams with corrugations [2] or for plates using periodic structuring [3, 4]. The primary focus of this study is on the generation of band gaps (Bragg bands) in aluminum cantilever beams and plates following a subtraction-based approach. Periodic cells are created by using a simple machining operation, that is periodically removing material in the thickness direction. The goal is to design structures that are lighter than their homogeneous versions, but that can nevertheless exhibit similar or improved vibroacoustic behavior.

2 Band gap generation in beams by periodic material removing

Regarding beams, the effects of the number of periodic cells along length and the thickness removal are studied for a fixed beam length. The upper part of Figure 1 shows the considered problem (the left part of the beam is clamped and the right part of the beam is free). The proposed cantilever beam configurations include a regular pattern that is created by periodic material removal. The beam consists of a base thickness denoted by h_1, with specific regions featuring a reduced thickness of h_2. Each unit cell within the periodic beam has a length of *d*, wherein a cell comprises two halves: the first half has a length of *d/2* with a thickness of h_1, followed by the second half with a length of *d/2* and a thickness of h_2. Several key parameters define the periodic beam, including *n* the number of cells, *L* the overall length of the beam, *w* the beam width and *f* the beam's section on which no material removal is achieved. The tested configurations include aluminum and polylactic acid (PLA) cantilever beams excited close to the clamped side. An automatic modal hammer vImpact-63 was used to apply a transient force with a mean amplitude of 10 N. Vibration velocity measurements are taken along the beam with a multipoint laser Doppler vibrometer (Polytec MPV-800) and processed using the extension Structural Dynamics Toolbox (SDT) from Matlab (simulations are also conducted using this toolbox). Ten consecutive measurements were performed for each beam with 10 seconds of waiting time between each test and *Complex average* was used to average the responses. Eight measurement points are positioned along the beam whose positions respect to the clamped end are indicated in the lower part of Figure 1.

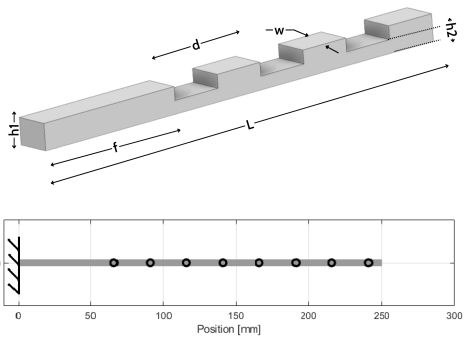

Figure 1: (Upper part) Illustration of the considered beams including discontinuities; (Lower part) Position of response measurement points.

The numerical and experimental results obtained for one of the beams (aluminium, 3 discontinuities, L = 250 mm, w = 20 mm, h1 = 3.2 mm, h2 = 1.6 mm) are provided in Figure 2. The measurement (thick gray line) and simulation (dashed black line) results for the machined beam are in good agreement. When compared with calculations made for a beam of homogeneous thickness (3.2 mm) or a beam of equivalent mass (a uniform beam with a thickness that would provide the same mass), these results also indicate a reduction of the vibration level in the whole frequency range, but especially above a frequency of 4500 Hz.

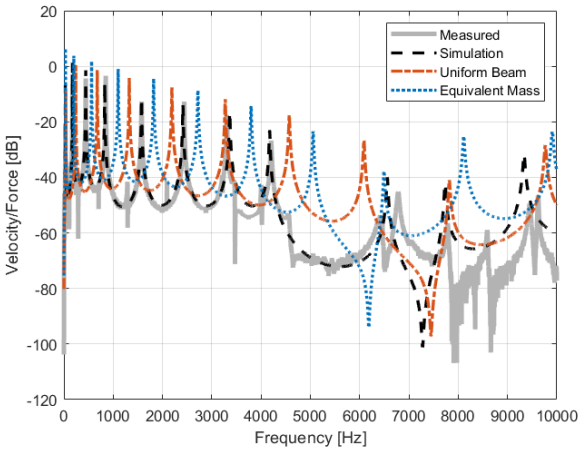

Figure 2: Simulation and measurement results for beam A5 (50 % thickness removal over three periodicities).

[*]olivier.robin@usherbrooke.ca
[†]Vania.Catalina.Gonzalez.Cartes@usherbrooke.ca
[‡]Nicolas.Bohmwald@usherbrooke.ca
[§]vmeruane@uchile.cl

3 Band gap generation in plates by periodic material removing

For plates, the results obtained in terms of sound transmission loss (STL) are provided. STL was evaluated for one homogeneous plate and one plate that includes periodic material removal along the diagonal direction (see Figure 3). The plates dimensions are 480 mm $\times$ 420 mm $\times$ 3.2 mm (length times width times thickness).

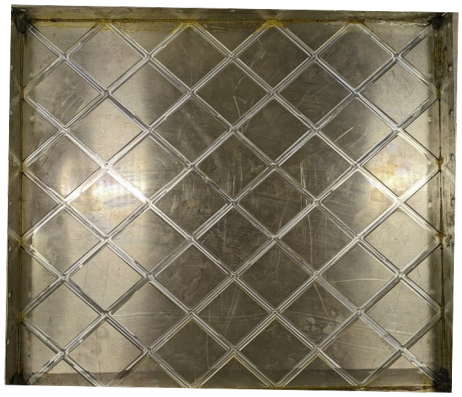

Figure 3: Picture of a panel machined in the diagonal direction.

Simply supported boundary conditions are achieved along the four edges of the panels using a dedicated procedure, and a double wall structure was built around the panel with silicone sealing along the edges to prevent acoustic leaks. The panels were mounted in the test window between coupled reverberant-anechoic rooms using a frame made of plywood with acoustic sealant and subjected to a Diffuse Acoustic Field excitation. Following standards, STL is determined using measurements of the spatially averaged sound pressure level in the source room L_p and of the spatially averaged average sound intensity level L_i over a scanning surface S_m on the receiving side (both in dB), STL $= L_p - L_i - 6 - 10\log_{10}(S_m/S)$ (with S the effective panel area, considered equal to the scanning area S_m so that the last term was neglected). L_p was obtained using a rotating and three fixed quarter-inch PCB microphones on the reverberant room side, while the average radiated sound intensity level L_i was measured in the anechoic room using a Bruel & Kjaer sound intensity probe composed of two half-inch microphones and a 12 mm spacer. Manual scanning was performed at a distance of 5 cm from the panel surface following recommended scan patterns. Results are provided in $1/3$th-octave bands in the 50-5000 Hz frequency range. The obtained results show that :

- The homogeneous panel performs better than the machined one in the 50 Hz and 63 Hz third octave bands (TOB), this being attributed to a reduction of the static stiffness,
- The results are nearly equivalent between the 100 Hz and 200 Hz TOB, a STL reduction is observed for the machined panel at the 250 and 315 Hz TOB and an equivalent STL for both panels in the 400 and 500 Hz TOB,
- From the 630 to the 5000 Hz TOB, the STL values obtained with the machined panel are always larger than its homogeneous equivalent, even in the critical frequency region (acoustic critical frequency $\approx$ 3750 Hz for standard 6061 aluminium).

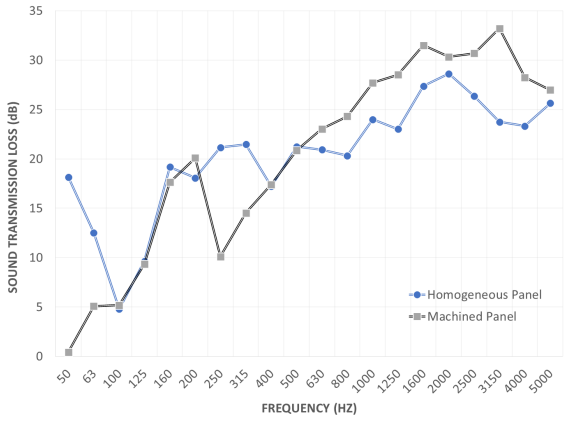

Figure 4: Sound transmission loss measurement results for an homogeneous panel and a machined panel.

4 Conclusion and perspectives

The obtained results generally indicate that periodic material removal using machining operations can be a simple but efficient way for the generation of band gaps in beam-like and plate-like structures. Compared with their homogeneous equivalents, the machined structures lead to an overall mass reduction together with generally improved vibroacoustic behavior.

Acknowledgments

The financial support from the *Appel à projets coopération bilatérale Québec-Chili 2021-2023 – Ministère des Relations internationales et de la Francophonie, Québec* for the project *Métamatériau à compromis énergétique positif pour la réduction du bruit* is here greatly acknowledged. The authors also received financial support provided by the Agencia Nacional de Investigación y Desarrollo (ANID) de Chile through the project FONDECYT 1210442

References

[1] Yong Xiao, Jihong Wen, Gang Wang, and Xisen Wen. Theoretical and Experimental Study of Locally Resonant and Bragg Band Gaps in Flexural Beams Carrying Periodic Arrays of Beam-Like Resonators. *Journal of Vibration and Acoustics*, 135(4):041006, 06 2013.

[2] Adrien Pelat, Thomas Gallot, and François Gautier. On the control of the first bragg band gap in periodic continuously corrugated beam for flexural vibration. *Journal of Sound and Vibration*, 446:249–262, 2019.

[3] Denis Caillerie. Plaques élastiques minces à structure périodique de période et d'épaisseur comparables. *Comptes rendus des séances de l'Académie des sciences*, 294, 1982.

[4] Jarosław Jedrysiak. The effect of the material periodic structure on free vibrations of thin plates with different boundary conditions. *Materials*, 15(16), 2022.

CREATING OPTIMIZED ACOUSTIC STRUCTURE VIA CONCENTRATED EMULSIONS

Mina Saghaei [*1], Annie Ross [†2] and Edith-Roland Fotsing [‡2], Louis Fradette [♦2]
[1]Chemical Engineering Department, Polytechnique Montréal, Québec, Canada
[2]Laboratory for Acoustics and Vibration Analysis (LAVA), Polytechnique Montréal, Québec, Canada

1. Introduction

Recent advancements in polymer foams for sound absorption applications have encountered challenges in achieving precise foam structures with controlled interconnectivity due to uncertainties in the chemical reactions during the foaming process[1]. To address this limitation, a novel method utilizing solid-stabilized emulsions (SSE) with high concentration of the dispersed phase is proposed for acoustic foam production. The technique involves emulsion templating i.e. creating a stable emulsion with more than 75% dispersed phase using micron-sized particles for stabilization. Post-processing this emulsion eliminates the two liquid phases and promotes the sintering of the particles. The result is a solid, porous foam structure.

Pores in the foam and droplets in the SSE are in direct relation. A droplet refers to a oil sphere surrounded by particles that prevent it from coalescing[2, 3]. Additional components can be incorporated into the emulsion to control pore interconnectivity and influence the sound-proofing properties. The study investigates key factors such as rotational speed and emulsification time, which play a vital role in determining droplet and pore size in the acoustic foam.

2. Method

2.1. Materials

The continuous phase of the emulsion contained Polyimide (PI) powder (P84NT, Evonik Fibers GmbH), which was dispersed in distilled water. The oil phase was pure silicone oil (Clearco Products Co. Inc., USA).

2.2. Process

The SSE, highly concentrated, were prepared using a double-helical ribbon impeller. This is known to be highly efficient mixer for viscous materials. Initially, a predetermined quantity of powder was uniformly dispersed in the continuous phase. Afterwards, oil was injected into the tank at a constant flow rate, while agitation continued until the desired time was reached. Various rotational speeds were used. The prepared emulsions were put in the oven to evaporate water and oils, during this step, particles are sintered and create a solid porous material.

2.3. Tests

The droplet size was measured using a Mastersizer 3000 (Malvern Panalytical, UK). The microscopic images were captured using Digital Microscopes (KEYENCE CANADA INC). The sound absorption coefficient was determined using a Kundt's tube (MTTC, France) following standard NF EN ISO 10534-2, with the sample thickness set at 1 cm.

3. Results

3.1. Effect of mixing time on droplet size

Prolonged mixing time not only decreases the droplet size but also reduces the uniformity number. The uniformity number is based on the distance of each droplet size (D_i) to the average $\overline{D}$ size. The lower the uniformity number, the more homogeneous the emulsion is. This number can be calculated using the following equation [4]:

$$uniformity = \frac{\sum v_i * (abs(\overline{D} - D_i))}{\overline{D} * \sum v_i}. \quad (1)$$

Here, "i" indicates droplet size class, v_i is the volume percentage for this droplet size class.

Figure 1 (a) illustrates the emulsions prepared at mixing times ranging from 6 to 24 minutes, with a fixed formulation and 100 RPM. Figure 1 (b) shows the evolution of droplet size over time. Longer mixing times lead to more droplet breakage and result in smaller stabilized droplets. The decrease in the uniformity number represents a narrower size distribution of droplets. The slight increase after 20 minutes might be due to the larger decrease in the average size compared to the width of the size distribution graph.

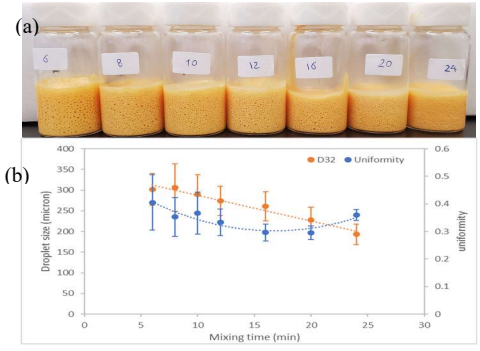

Figure 1. (a) Image of emulsion prepared at different mixing times. (b) Evolution of droplet size and uniformity over time.

3.2. Consistency of droplet and pore size

The most significant advantage of this process is that during the post-process step, when the two liquid phases are evaporated in a controlled manner, the resulting porous solid retains its structure without the droplets shrinking or coalescing into larger ones. Figure 2 (a) illustrates the size distribution in the

[*] mina.saghaei@polymtl.ca
[†] a.ross@polymtl.ca (corresponding author)
[‡] e-r.fotsing@polymtl.ca
[♦] louis.fradette@polymtl.ca

emulsion, and Figures 2 (b) show the porous structure of the same sample after the oil and water have evaporated. Table 1 summarizes the average sizes and the range between the smallest and largest droplet and pore sizes. Based on these results, it can be concluded that the pore size and droplet size in an emulsion belong to the same distribution class. Thus, the desired pore size in the porous structure can be achieved by manipulating the droplet size in the emulsion.

Table 1: Comparison of droplet and pore size (micron).

sample	Average	Range
Emulsion	800	400-1200
Porous structure	857	400-1200

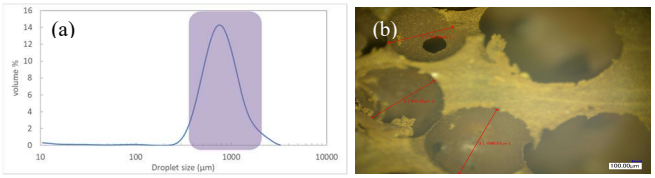

Figure 2. (a) distribution of droplet size in emulsion prepared at 100 rpm and 8 minutes. (b) microscopic images of the final porous material from the same emulsion.

3.3. Effect of process condition on the droplet size and final sound absorption

The prolonged mixing time reduces the droplet size and has a direct impact on sound absorption. Figure 3 illustrates the correlation between pore size and acoustic performance. As the pore size decreases due to longer emulsification time (Figure 3 (a)), the first peak in sound absorption coefficient shifts to a smaller frequency (Figure 3 (b)). The highest sound absorption was obtained with samples prepared with an 8-minute mixing time, which resulted in an average droplet size of around 800 microns.

Faster rotational mixing breaks droplets into smaller ones (Figure 4 (a)), leading to the formation of finer pore sizes in the porous structure. Consequently, at 150 rpm, the sound absorption first peak shifts to a smaller frequency. Moreover, for frequencies above 2000 Hz, lower sound absorption was obtained compared to the results at 100 rpm.

4. Discussion

We investigated the two main variables acting on the final structure of a concentrated SSE: time and rotational speed. This work reveals the potential application of sound absorption using porous material obtained from concentrated emulsions. By employing a longer process duration or faster rotational speed, smaller droplets and pore sizes were achieved, resulting in higher sound absorption at frequencies below 2000 Hz and lower sound absorption at frequencies above 2000 Hz. Hence, depending on the desired frequency range for absorption, the pore size can be tailored by manipulating the process conditions.

It is worth mentioning that although the acoustic results were obtained with samples having a thickness of 1 cm, which is one-third smaller than the size we typically study, they still exhibit similar absorption levels compared to previous work[5]. This performance, despite needing validation, might be attributed to the higher interconnectivity and tortuosity resulting from the sintering of the solid particles.

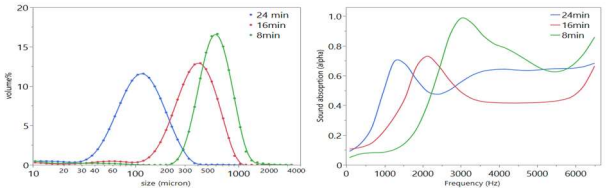

Figure 3. (a) size distribution of droplets at different mixing times; (b) sound absorption of samples

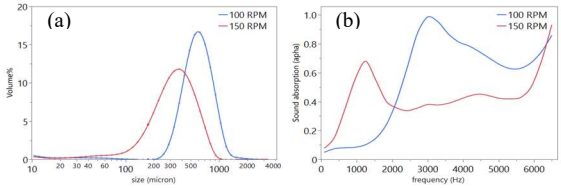

Figure 4. (a) size distribution of droplets at different rotational speeds and constant rotation number; (b) sound absorption

5. Conclusion

We showed that process conditions are able to control the droplet sizes while producing a highly concentrated, solid-stabilized emulsion. This methodology offers potentially strong solution for tailoring the pore size in an acoustic structure. The proposed process, with low energy consumption and the absence of complex and harmful formulations, promises great opportunities for finely tailored microstructure for acoustic applications.

Acknowledgments

The authors are grateful to the Natural Sciences and Engineering Research Council of Canada (NSERC) and CREATE program for funding and supporting this work.

References

[1] K. Gao, J. A. W. van Dommelen, and M. G. D. Geers, "Microstructure characterization and homogenization of acoustic polyurethane foams: Measurements and simulations," *Int. J. Solids Struct.*, vol. 100–101, pp. 536–546, Dec. 2016, doi: 10.1016/j.ijsolstr.2016.09.024.

[2] È. Tsabet and L. Fradette, "Effect of the properties of oil, particles, and water on the production of Pickering emulsions," *Chem. Eng. Res. Des.*, vol. 97, pp. 9–17, May 2015, doi: 10.1016/j.cherd.2015.02.016.

[3] B. Wan, E. Tsabet, and L. Fradette, "Impact of Particles on Breakage and Coalescence Processes during the Preparation of Solid-Stabilized Emulsions," *Ind. Eng. Chem. Res.*, vol. 58, no. 14, pp. 5631–5639, Apr. 2019, doi: 10.1021/acs.iecr.8b05900.

[4] N. J. Edward L, Paul (Merck & Co., Inc. Rahway, M. Victor A, Atiemo-Obeng (The Dow Chemical Company Midland, and C. Suzanne M, Kresta (University of Alberta Edmonton, Eds., *HANDBOOK OF INDUSTRIAL MIXING*, vol. 1. John Wiley & Sons, Inc.: New Jersey, 2004.

[5] S. Butler, E. R. Fotsing, and A. Ross, "Acoustic thermoset open-cell foams produced by particulate leaching process," *J. Mater. Sci.*, vol. 54, no. 19, pp. 12553–12572, Oct. 2019.

Abstracts for Presentations without Proceedings Paper
Résumés des communications sans article

Predicting Acoustic Absorption In Additively Manufactured Porous Microlattices: A Sensitivity Analysis Approach

Ayoub Ait Aariba

The study explores the use of sensitivity analysis based on surrogate modeling to predict the absorption coefficient of porous microlattices fabricated through additive manufacturing. Unlike conventional analytical or numerical models, the proposed approach considers the impact of additive manufacturing imprecision on acoustic parameters, which is often overlooked when discrepancies between models and experimental results arise. Additive manufacturing, while offering unparalleled design flexibility, introduces non-trivial defects in the microlattice structures. The manufacturing process typically leads to three main types of defects: elliptical filament sections, filament section shrinkage, and surface roughness. These imperfections can significantly influence the acoustic properties of the porous material, leading to deviations from the idealized geometry assumed in conventional modeling approaches. In this work, sensitivity analysis using Morris and Sobol indices is employed to identify the most influential manufacturing defects affecting the absorption coefficient of the porous microlattice. To address the challenges posed by additive manufacturing imprecision, a metamodel is developed, which efficiently combines the experimental data obtained from fabricated samples with numerical simulations accounting for various defect scenarios. The metamodel serves as a powerful tool for cost-effective and accurate prediction of acoustic properties, even for untested configurations. The sensitivity analysis identifies critical manufacturing parameters and offers valuable insights into the dominant sources of variability. The approach offers a comprehensive framework for quantifying the impact of each additive manufacturing defect on the acoustic performance of porous microlattices, thus prioritizing improvement efforts in the manufacturing process. The scientific outcomes contribute to understanding how additive manufacturing influences the acoustic behavior of porous materials, facilitating the development of more accurate predictive models and informed design choices. The proposed methodology can have significant implications in diverse applications, including acoustic insulation, sound absorption, and noise control in various engineering and architectural fields.

On The Use Of Weakly Coupled Absorber For Low Frequency Sound Absorption

Mohamed Amin Ben Lassoued, Edith Roland Fotsing, Annie Ross

Weakly coupled systems have promising potential in the design of low-frequency sound absorption systems. Traditional sound absorption techniques often struggle to effectively address both low-frequency sounds and a large frequency band. However, weakly coupled systems can utilize a combination of various sub wavelength resonant absorber to mitigate this challenge. By incorporating elements such as multiple layers and air gaps, these systems can be coupled to achieve enhanced absorption of low-frequency sounds. One key advantage of weakly coupled systems is their ability to exploit the phenomenon of mode veering. By strategically designing the dimensions and materials of the subsystem, multiple resonance can be induced at the target low-frequency range. Due to non-symmetry between the modes, a condition of non-superposition of modes is created. At optimal geometrical and material parameters the system have multiple absorption peaks at near identical frequencies creating an absorption plateau. Furthermore, weakly coupled systems offer flexibility in customization. Designers can fine-tune the system's parameters to match specific low-frequency requirements, making them suitable for various applications such as architectural acoustics, automotive noise control, and industrial noise reduction. Additionally, advancements in computational modeling and optimization techniques enable the optimization of weakly coupled systems for improved absorption performance. As research and development in this field continue to progress, weakly coupled systems hold great promise for addressing the challenging task of low-frequency sound absorption and creating quieter environments in a wide range of settings.

Mass-Spring Model For A Resonant Metamaterial At High Sound Pressure Level

Maël Lopez, Alla Eddine Benchikh Le Hocine, Charly Tenon Kone, Thomas Dupont, Raymond Panneton

Metamaterial composed of array of resonators, called here resonant metamaterial, are efficient and compact solutions to achieve high sound absorption at low frequencies. The studied resonant metamaterial is composed of a compact linear periodic array of thin air cavities spaced by small air pores. Recently, a mass spring model was developed to study this acoustic metamaterial. The pores are modelled by a mass and the thin cavities by springs. Thermoviscous losses in the metamaterial are considered following an effective fluid approach. This model has

shown good agreement with impedance tube measurements in linear regime (sound pressure levels up to 100dB). For concrete applications (such as aircraft engines), the studied metamaterial could be used under high levels of acoustic excitation. For sound pressure level greater than 100dB acoustic nonlinear effects appear at orifices. Acoustic resistance of orifice increases with the amplitude of acoustic velocity. At high sound pressure levels, the orifice fluid regime changes and vortex forms at both sides of the orifice, leading to an increase of losses. The air flow resistivity of the pores becomes a linear function of the amplitude of the acoustic velocity (Forchheimer's law). The air flow resistivity coefficients are determined by curve fitting over the entire geometry, based on experimental airflow results and computational fluid dynamics calculations at different flow rates. The different approaches show good agreements with each other. The airflow resistivity function is then included in the mass-spring model. This adapted model allows to predict normal incidence sound absorption coefficient at high sound pressure level. The results of the model are compared with experimental measurements made in an impedance tube at different sound pressure levels.

Waste Corn Husk Fibers For Sound Absorption Applications

Umberto Berardi

In the last decade, noise pollution and global warming and their effects on human health and the environment have received much attention. Building sectors are one of the most important areas for potential improvements. To this end, sound-absorbing and thermal insulation construction materials are being used effectively. Recently, a great deal of interest has arisen in using various natural fibers as sound-absorbing and/or thermal insulation materials. In line with these studies, this work investigates the acoustic absorption and thermal insulation characteristics of corn husk fiber (CHF). The results showed that the samples enjoy excellent noise reduction coefficients of 0.36-60. The Dunn and Davern (DD) model and a modified model of DD based on the Nelder-Mead simplex algorithm were also used to predict the acoustic behavior of the samples. It was found that the proposed model provides very excellent prediction accuracy.

Novel Acoustic Materials Made From Wood Processing Residues

Suzhou Yin

Wood processing residues, such as shaving, chips, sawdust, wool, bark, present interesting sound absorption properties et have a great potential in the manufacturing of bio-based acoustic materials. Panels were made from shaving, wood wool and grinded bark, with 10% polyvinyl acetate resin as adhesive. The dimensions of the panels were 700 x 700 x 25 or 50 mm and their density varied from 150 to 225 kg/m3. The sound absorption coefficients at 1/3 octave frequencies were measured using an acoustic cabin (Mecanum) between 250 and 10000Hz. Based on the coefficients at four or twelve specific frequencies, the NRC (noise reduction coefficient) and SAA (sound absorption average) were estimated according to ASTM C423. It is shown that the density has an important effect on the NRC and the SAA. In general, panels with a density of 175 to 200 kg/m3 present the best sound absorption performance and good mechanical properties for handling. For panels made with shaving and having a thickness of 25 mm, the NRC varies between 0.70-0.80 and the SAA between 0.60-0.75. By doubling the thickness to 50 mm, the NRC and the SAA increased to 0.95 and 0.93, respectively. The panels made with wool and bark of cedar demonstrate similar or even better sound absorption properties. The manufactured panels were also used as core material in a sandwich system composed of a gypsum board and an oriented strand board (wood) as envelope to improve its sound insulation properties. The STC (sound transmission class) of such a system, for a total thickness of 100 mm, are equal or higher than 50 (minimum requirement for walls and floors between dwellings in the building code). The results of this study suggests that the novel panels are a promising alternative to traditional non-renewable acoustic materials.

NOISE CONTROL - CONTRÔLE DU BRUIT

VALUE ENGINEERING 'ACOUSTICS' INTO PROJECTS

Michael Bolduc *[1], Viken Koukounian †[1]
[1]Parklane Mechanical Acoustics, Oakville, Ontario, Canada

1 Introduction

It can be said that 'cost' is the most significant constraint in the construction or remediation of buildings. More specifically, a project's budget is regularly overrun by its expenses—negatively impacting its [the project] health, as well as its various stakeholders (e.g., building professionals, engineering specialties, trades, and subcontractors). This is often the case in remediation efforts, where seemingly simple acoustical solutions, such as barriers and silencers, require complex engineering.

The 'hidden' costs associated with these critical multi-disciplinary engineering challenges are not usually apparent during the initial estimating stage and can exceed the estimates for the acoustical scope. This unknown cost risk is further amplified in large scale complex retrofit noise mitigation projects where the abatement plan may cover multiple years and involve dozens of sources. However, the determination of these unknown costs can be uncovered quickly and efficiently during an initial feasibility design study. By uncovering these costs sooner, projects can be completed more efficiently allowing plant management to properly plan and allocate capital financing more accurately for the project.

This paper characterizes types of projects where there is an intrinsic benefit to conducting an initial design feasibility study to determine the required scope of work prior to the commencement of a project. In these examples, the implications of unknown or unforeseen costs are detailed, demonstrating the financial risks.

2 Initial Design Study and Project Benefits

An initial engineering design study is intended to confirm solution feasibility while dramatically reducing unknown cost risk (i.e. within 25% of construction) associated with complicated large-scale projects.

Three types of projects that benefit most from such a study are described and detailed within this paper. These include:

- Retrofit involving multi-discipline engineering and sub-trades,
- Facility-wide noise mitigation with unknown site-specific challenges,
- Noise abatement projects exceeding 'normal' scale.

2.1 Retrofits involving multi-disciplinary parties

As the number of independent parties involved in a job increases (i.e., consultants, engineering specialties, trades, and sub-contractors) so too does the complexity and unknown cost risk associated with the job. The earlier the coordination and communication between these separate parties can occur, the earlier any unforeseen expenses can be captured, and a more accurate estimation can be provided.

The modelled enclosure detailed in Figure 1 presents a project where an initial noncompliance with provincial sound level limits resulted in a complex engineering design study involving various multi-disciplinary engineers and trades. This project consists of newly proposed residential development overlooking the mechanical rooftop equipment of a grocery store and restaurant. Due to the proximity of the windows of this new development to this equipment, the noise abatement option was to acoustically enclose and replace the entirety of the mechanical equipment on the roof.

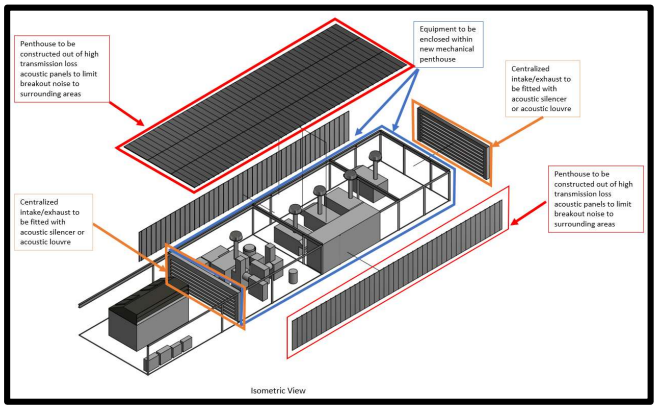

Figure 1: Mechanical Penthouse Enclosure intended to reduce noise emissions to adjacent residential development.

To reduce the risk of interruptions to impacted persons, a detailed investigation of the required cooling capacities of each of the tenants was conducted for proper selection of equipment and phasing of the noise abatement install. Mechanical design consisted of reselection of mechanical equipment, determination of proper air ventilation and cooling capabilities to each of the tenants.

This work was conducted concurrently with a structural assessment of the base building, and acoustic modelling of sound levels from the new equipment on the adjacent development. The acoustic modelling at each of the noise sensitive receptors fed into both the mechanical selection and any additional noise abatement required at the outlets of the enclosure.

2.2 Facility-wide noise mitigation with unknown site-specific challenges

Site-specific constraints or limitations that are unknown at the initial estimating phase of a project can result in a significant increase in cost and delays during project implementation. The extent of these costs and delays become significant

*michael@parklanemechanical.com
†viken@parklanemechanical.com

in multi-year facility-wide noise abatement projects that often include many sources of noise. Uncovering these limitations on the onset allows plant management to effectively plan and secure capital financing prior and during the project lifecycle.

An example of a large facility-wide noise abatement project is shown in Figure 2. This project consisted of an older industrial facility requiring noise mitigation on dozens of exhaust fans located on its various roofs. Due to the elevation of these fans, additional dead load was required to counteract the high wind loads imposed on the new silencers. As a part of the initial feasibility study of the project a structural review determined that the existing roofing structure required a significant amount of structural reinforcement prior to the installation of any noise abatement on the exhaust fans on each of the facility's five roofs).

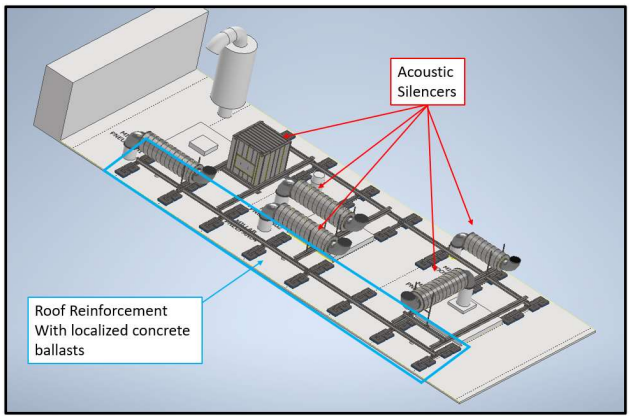

Figure 2: CAD model detailing extent of structural reinforcement with acoustical mitigation for facility-wide mitigation project.

Figure 2 illustrates the complexity of the structural framing and distribution of weight of noise control solutions. The feasibility study ensured the financial wellbeing of the client, and, therefore, the project. It also reduced the time required for design and avoided delays to the project. The feasibility study empowered the client with the information necessary to better plan, budget and manage their project.

2.3 Noise abatement projects exceeding 'normal' scale

The benefits of a preliminary engineering study become more evident as projects grow (in size) and complexity. Atypical engineering needs, constraints and/or limitations are threats to the completion of the project. A detailed engineering review by an experienced and specialized team can reduce the number and extent of uncertainties to allow for better planning of costs, milestones and deadlines. Figure 3 is a photograph taken during the install an acoustic barrier that is 10 m in height and 90 m in length. The intent of the acoustic barrier was to shield facility trucking noise from an adjacent condominium.

More specifically, a detailed engineering design study was conducted to establish costs and timelines for the proposed acoustic barrier solution. Because of the significant height of the barrier, as well as other onsite conditions, it was determined that the foundations for the posts needed to be significantly deeper than typical recommendations; thereby impacting their cost. This also affected the design and cost of the barrier. More specifically, the lengths of the structural steel columns needed to be longer—to coincide with the deeper foundations. Additional optimizations were required to properly overlay over any deflections.

Figure 3: Photograph taken during the install of a large 10 m acoustic barrier.

In addition to cost, a design study allowed a more accurate prediction of project timelines. Detailed breakdowns of lead times were critical for scheduling of permitting (with the local municipality) as well as installation of the foundation to occur prior to the winter months. Careful coordination with the client, acoustical consultant, and various contractors were needed to properly layout the barrier in relation to existing site conditions while ensuring the acoustic performance of the barrier was accurate to what included in the acoustic consultant's model.

3 Conclusion

Through the implementation of an initial feasibility design study, 'hidden' costs and unknown site-specific challenges can be uncovered in a timely manner for large scale noise abatement projects. In some projects, these costs can be of comparable scale to the actual supply of the noise abatement product. By uncovering these costs sooner, projects can be completed in a more efficient manner allowing plant management to properly plan and allocate capital financing more accurately.

PRELIMINARY NUMERICAL AND EXPERIMENTAL STUDIES OF ACTIVE ACOUSTIC CONTROL OF DOUBLE-GLAZED PARTITION WALLS

Jonathan Mifundu Nzengi[*1], **Pierre Grandjean**[†1], **Alain Berry**[‡1], **and Philippe Micheau**[§1]
[1]Centre for Research in Acoustics-Signal-Human of the Université de Sherbrooke, Sherbrooke, Québec, Canada

1 Introduction

In open-space work areas, glazed partitions are sometimes used to delimit work zones while maintaining a certain transparency. To improve their acoustic insulation, these partitions are composed of double-glazed units separated by an air space. However, such double partitions offer low insulation at low frequencies. Double partitions have a breathing mode, and cavity modes attenuate the level of insulation. The breathing mode is a mass-air-mass resonance observable at low frequencies, where the two partitions vibrate in antiphase and transmit a very large proportion of the incident acoustic wave [1].

The aim of this study is to implement an active system to improve the low-frequency sound insulation of double glazing. This study presents the level of acoustic insulation achievable with an active system for the case of a double-glazed unit submitted to an acoustic wave in normal incidence. First, the method is presented in section 2, followed by the results in section 3. The results are then discussed and a conclusion drawn.

2 Controller synthesis

The study is based on the assumption that minimizing the acoustic pressure in the cavity formed by the two glass partitions (or cavity in the following), will minimize the partition-air-partition coupling and thus increase the acoustic insulation of the double glazing. This approach will be compared with the optimal strategy of directly reducing sound pressure in the receiving environment, i.e. downstream of the double glazing. The study is limited to a waveguide configuration and a sample of small size.

2.1 Numerical method

The numerical model of the double-glazed unit is composed of two identical, square, tempered glass partitions 30.48 cm aside, 6 mm thick and 60 mm separated. This tempered glass has a young's modulus $E = 48.5$ GPa, a density $\rho = 2500\ \mathrm{kg\,m^{-3}}$, a Poisson coefficient $\nu = 0.24$ and a structural loss factor $\eta = 0.01$. The structural loss factor is chosen to be large enough to create an unfavorable condition. The double glazing has free boundary conditions and is placed in a waveguide with a cut-off frequency of 562 Hz. The cut-off frequency of a waveguide is the frequency above which the waves in the guide are no longer plane. Four microphones are placed upstream and downstream of the double glazing to calculate its transmission loss. To form the active system, an error microphone and a secondary loudspeaker are placed in the cavity. The loudspeaker is modelled by a surface on which a normal velocity is imposed. To compare with the minimization of transmitted wave strategy, sixteen error microphones are placed downstream of the double glazing, and their distances from the double partition are randomly chosen between 28.11 cm and 34.11 cm.

The numerical study is carried out to understand the effect of the active system on the pressure distribution in the cavity and the vibratory velocity field of the glazing. The COMSOL acoustic module is used to simulate vibroacoustic phenomena, and Matlab is used to calculate the optimal control of the secondary source. The study is conducted in the frequency domain. To obtain the optimal input of the secondary source, the contribution D of the primary source is first obtained by evaluating the pressure at the error microphone. Then, the complex gain H of the transfer function between secondary source and the error microphone is obtained by evaluating the pressure at the error microphone for a unitary control of the secondary source. The optimal control is calculated by $U_{opt} = -H^* D$. Where * represents the inverse or pseudo-inverse depending on whether H is invertible or not. The primary and secondary fields are then superimposed in COMSOL to obtain the effect of the active control. The same method is used to minimize the transmitted wave.

2.2 Experimental method

Experimental tests are carried out for harmonic disturbances at normal incidence on the double-glazing. A test bench equivalent to the numerical model is set up as shown in Fig. 1. To test the strategy of minimizing the pressure downstream of the double glazing, two microphones are used as error sensors, those used to estimate the sound transmission loss. Data acquisition and control signal generation are performed using a Speedgoat real-time computer. Harmonic disturbances are in the frequency range of 50 to 550 kHz to satisfy the plane-wave condition, and are sampled at 10 kHz.

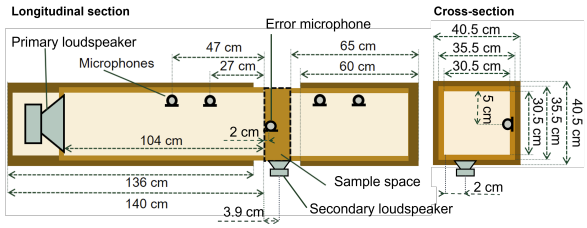

Figure 1: Schematic diagram of the experimental set-up for measuring the transmission loss of active double glazing in a waveguide.

Since the disturbance to be cancelled is harmonic, it can

[*]jonathan.mifundu.nzengi@usherbrooke.ca
[†]Pierre.Grandjean@USherbrooke.ca
[‡]Alain.Berry@USherbrooke.ca
[§]Philippe.Micheau@USherbrooke.ca

be represented by a complex envelope [2]. The controller can then easily adjust the phase and amplitude of the anti-noise. Newton's algorithm is used to minimize the square of the modulus of the pressure phasor at the error microphone. To obtain the error phasor, the microphone signal is demodulated by $e^{-j\omega t}$, where w the disturbance frequency, and then filtered by a 4th-order low-pass filter with a cut-off frequency of 10 Hz. The control phasor is then adapted according to the Eq. 1 and modulated by $e^{j\omega t}$ to obtain the time signal to be applied to the secondary source.

$$U[k+1] = U[k] - \mu H^* Y[k], \tag{1}$$

where U is the control input phasor, k the iteration, μ the convergence coefficient, Y the pressure phasor at the error microphone. The same method is used to minimize the transmitted wave.

3 Results

The numerical study shows that minimizing the pressure at the error microphone creates zero pressure at the error microphone, while minimizing the transmitted wave means imposing almost zero pressure on a line passing through the middle of the upstream glazing Fig. 2.

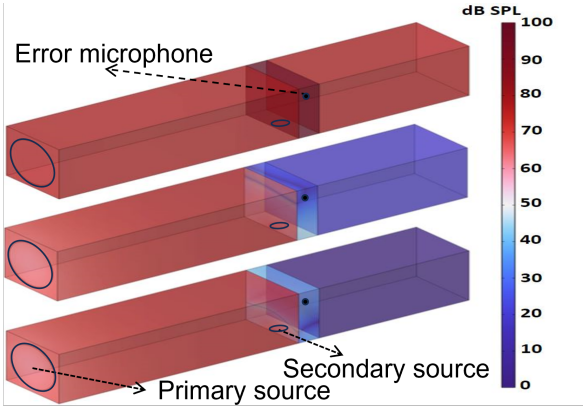

Figure 2: Pressure level at 74 Hz (breathing mode). From top to bottom: without control, minimization of cavity pressure, minimization of transmitted wave.

Minimizing the transmitted wave therefore leads to better acoustic insulation, as it tends to impose a dipolar vibration pattern of the upstream glazing, that inefficiently couples with the inter-glazing cavity and the receiving acoustic domain. The drop in transmission loss observed around 250 Hz seems to correspond to the breathing mode Fig. 3. In addition, the experimental average transmission attenuation between 50 and 550 Hz is 14 dB when the transmitted wave is minimised, while it is 2 dB when the acoustic pressure in the cavity is minimised. The low average insulation when minimizing cavity pressure is due to the fact that it is only effective up to 250 Hz.

4 Discussion

Simulations and experiments have shown that controlling low-frequency sound pressure in the double-glazed cavity is

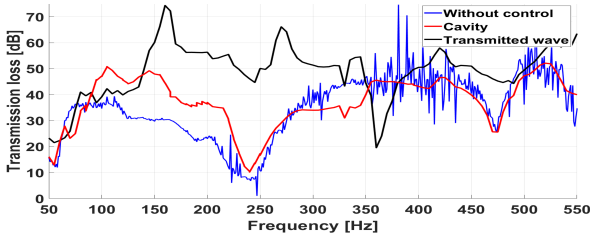

Figure 3: Experimental sound transmission loss

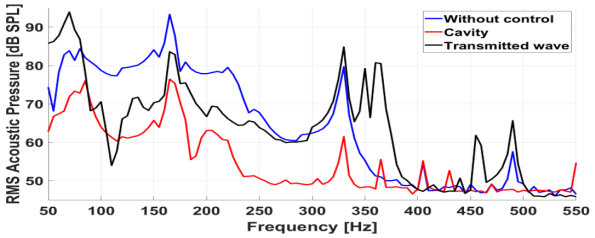

Figure 4: Experimental pressure level in the cavity

an acceptable, but not optimal, approach. The transmitted wave minimization strategy does not imply zero pressure at the error microphone in the cavity Fig. 4. The inefficiency of improving insulation beyond 250 Hz when minimizing cavity pressure is due to the inefficient pressure distribution it imposes, and not a lack of control sources, since minimizing the transmitted wave improves insulation beyond 250 Hz. The experimental results show an improvement in transmission loss in the breathing mode only when the transmitted wave is minimized.

5 Conclusions

Minimizing the acoustic pressure in the cavity improves the insulation of the double glazing, but this improvement is less significant than when minimizing the transmitted wave, which leaves a residual pressure at the error microphone. Since minimizing the pressure in the cavity is not an optimal strategy, the controller must impose a residual pressure to achieve optimal insulation. Such a sound pressure compensation strategy has been developed by Drant et al. [3] and will be the subject of future work. Multi-loudspeaker and multi-microphone configurations will also be tested.

Acknowledgements

The authors would like to thank Moderco, Mitacs and NSERC for their financial support.

References

[1] Frank Fahy. *Sound and structural vibration: radiation, transmission, and response*. Academic Press, 1985.

[2] Leon W. Couch. *Digital and analog communication systems*. Pearson, 8th ed edition, 2013. OCLC: ocn755904467.

[3] Julien Drant, Philippe Micheau, and Alain Berry. Active noise control of higher modes in a duct using near field compensation and a ring of harmonic acoustic pneumatic sources. *Applied Acoustics*, 188:108583, 2022.

DYNAMICS OF HARMONIC ACTIVE SOUND CONTROL WITH A HARMONIC ACOUSTIC PNEUMATIC SOURCE

Alexandre Schiavini [*1,2], **Philippe Micheau** [†1], **Pierre Grandjean** [‡1], **and Gwénaël Gabard** [§2]
[1]CRASH-UdeS, Mechanical Eng. Dpt, Université de Sherbrooke, Sherbrooke, Canada
[2]LAUM, Université du Mans, Le Mans, France

1 Introduction

During takeoff, the harmonic noise of the turbofan is the main acoustic nuisance for people near airports. Much research has been done on the topic of active reduction of turbofan noise [1]. Loudspeakers used as secondary sources present the disadvantage of being fragile and requiring a high power consumption to produce the required sound intensity. In this context, an alternative solution, called the Harmonic Acoustic Pneumatic Source (HAPS), has been designed to generate a high harmonic noise level controllable in amplitude, phase and frequency. Previous studies on the subject have demonstrated the possibility to perform active noise control with a ring of HAPS in a cylindrical duct, but the convergence time of the controller was about several seconds [2]. The dynamics of the controller is thus a limiting factor for active noise control applications. The objective of this study is to address this problem by characterizing and designing a controller with a short response time, typically less than a second. In Sec. 2, the HAPS and its dynamics is presented. Then a controller is designed and simulated in Sec. 3. Finally, the experimental setup for future noise control measurements is presented in Sec. 4.

2 Dynamics of the Harmonic Acoustic Pneumatic Source

2.1 HAPS presentation

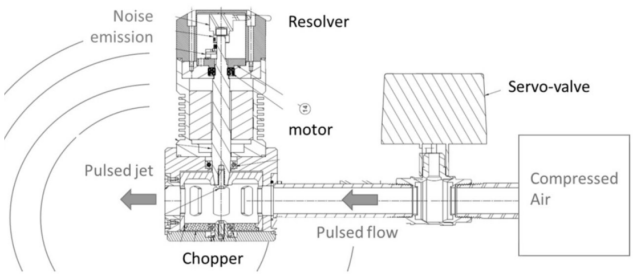

FIGURE 1 – Section view of the acoustic pneumatic source.

The two mechanical components of a HAPS, presented in Fig. 1, are a valve for flow regulation and a flow chopper using a rotating perforated cage. The flow chopper and the valve are equivalent to a variable throat orifice between a plenum of high pressure and the exhaust at the atmospheric pressure [3]. The time variation of the orifice due to the rotation of the chopper generates a pulsed flow. The phase of the pulsed flow is controlled by the rotation angle of the flow chopper. The amplitude of the pulsed flow is controlled by the valve opening. This pulsed flow generates a periodic pressure fluctuation perfectly controlled in amplitude and phase by two signals ($|U|$ and $\angle U$ respectively) in order to physically perform a complex-amplitude modulation of the generated anti-noise. For the following, the complex signal $U(t) = |U(t)|e^{j\angle U(t)}$ is the command for the complex amplitude of the anti-noise first harmonic.

2.2 Dynamics of the HAPS

The HAPS performs a mechanical complex amplitude modulation at a given frequency f_0 controlled by the complex command $U(t)$. However, the time response of the HAPS is not instantaneous, mainly due to the dynamics of the Phase Locked Loop (PLL) algorithm controlling the flow chopper. The PLL is used to synchronize the measured instantaneous angle of the chopper $\theta(t)$ with the reference angle of the anti-noise phase command $\angle U$. An experimental campaign in a semi-anechoic chamber is performed in order to characterize the dynamics of the PLL. A microphone is placed at one meter distance and at an angle of $45°$ from the HAPS mouth. The reference frequency is $400\,\mathrm{Hz}$. A phase step is used to experimentally evaluate the characteristic time response of the HAPS. The reference phase is initially 0 and jumps to $\frac{\pi}{2}$ at $t = 10\,\mathrm{s}$. The result is shown in Fig. 2. The cage phase is following the reference and the convergence time is $\tau = 0.3\,\mathrm{s}$. Active noise control on a non-stationary primary tone is therefore possible as long as the phase of this primary excitation changes at a slower rate than τ. The signal measured by the microphone indicates a good match with 8 times the phase of the cage, which is a consistent result since there are 8 holes on the cage.

3 Controller design

Knowing the dynamics of the HAPS, a controller is designed. A classical configuration for active noise control experiments including a rectangular duct, a primary loudspeaker, a HAPS and an error microphone, illustrated in Fig. 3, is considered. The unmeasured state of the system is composed of the real and imaginary parts of the acoustic mass flow rate $Q(t)$ at the HAPS mouth. The only measured output is the complex pressure $P(t)$ obtained after demodulation at f_0 of the pressure signal at the microphone $p(t)$. It is the sum of the pressure generated by the HAPS and the perturbation due to the primary source. The dynamics between the command $U(t)$ of the HAPS and the state variable $Q(t)$ is modeled with a first order system with a constant time of $0.3\,\mathrm{s}$, according to the

*. Alexandre.Schiavini@usherbrooke.ca
†. Philippe.Micheau@usherbrooke.ca
‡. Pierre.Grandjean@usherbrooke.ca
§. gwenael.gabard@univ-lemans.fr

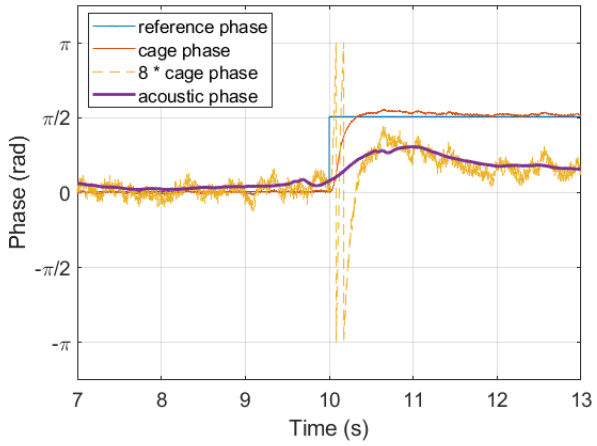

FIGURE 2 – Chopper cage phase and acoustic phase measurement for a step in reference phase.

results about the PLL in Sec. 2.2. The relation between the mass flow rate at the HAPS mouth and the pressure at the microphone is given by the transfer functions extracted from an analytical model of the acoustic propagation in duct. A linear quadratic regulator controller with integral action is designed to minimize the pressure at the microphone. It is complemented with a Kalman observer estimating an augmented state of the system containing the unmeasured state, i.e. the acoustic mass air flow $Q(t)$ and the pressure due to the primary source.

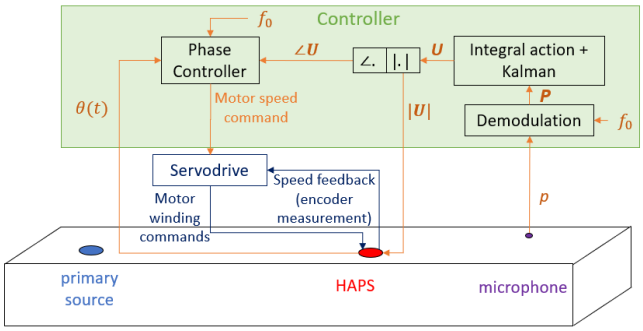

FIGURE 3 – Illustration of the experimental configuration for active noise control.

3.1 Controller simulations

The dynamics of the controller is simulated for a primary sound frequency $f_0 = 300\,\mathrm{Hz}$. The initial state of the system is set to 0, meaning that the HAPS is not activated. The Kalman observer is also initialized at 0, including its estimation of the system state and the primary perturbation. As shown in Fig. 4, the amplitude of the pressure at the microphone is converging to $0\,\mathrm{Pa}$, meaning that the secondary source is canceling the primary sound. An attenuation of $20\,\mathrm{dB}$ is reached in about $1.3\,\mathrm{s}$. The output of the observer is initially zero but it is converging very fast to the system output, in less than $0.03\,\mathrm{s}$, adapting itself to a correct estimation of the primary pressure.

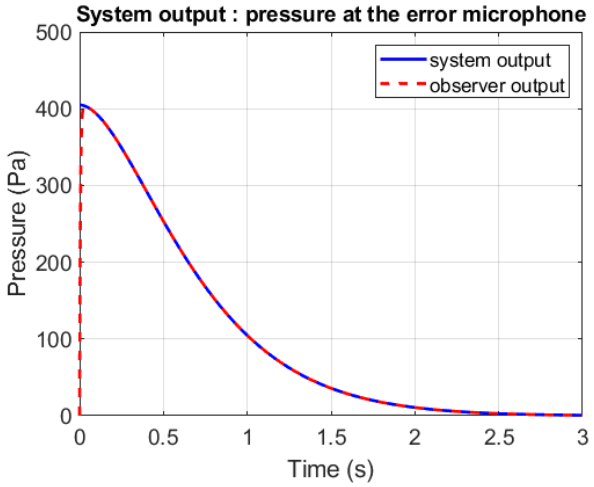

FIGURE 4 – Numerical simulation of the time response of the acoustic pressure modulus $|P|$ at the error microphone. $t = 0$ corresponds to the activation of the secondary source.

4 Noise reduction measurement

In order to validate the control strategy, an experimental setup was designed. It is composed of a duct section with a loudspeaker, a HAPS and a microphone placed on the top side (Fig. 3). It is planned to realize an experimental campaign to perform active noise control. The controller described in Sec. 3 will be implemented using a Speedgoat real-time computer. The measurement of the acoustic attenuation induced by the HAPS at the microphone will be compared to simulations.

5 Conclusions

Measurements of the dynamics of the PLL used to control the flow chopper have been carried out and allowed to measure the characteristic time of the HAPS, $\tau = 0.3\,\mathrm{s}$. Simulations of a controller designed for active noise control in a duct with a HAPS have also been performed. They showed a convergence time of $1.3\,\mathrm{s}$ for the controller. Finally, an experimental setup has been designed in order to validate the control strategy. Future experimental results will provide an accurate estimation of the attenuation achievable with the controller.

Acknowledgments

This work is supported by Association Nationale Recherche Technologie (ANRT, France) and Safran Nacelles (Le Havre, France). We gratefully acknowledge Marc Versaevel from Safran Nacelles.

References

[1] Russell H. Thomas, Ricardo A. Burdisso, Christopher R. Fuller, and Walter F. O'Brien. Active control of fan noise from a turbofan engine. *AIAA Journal*, 32(1) :23–30, January 1994.

[2] Julien Drant, Philippe Micheau, and Alain Berry. Active noise control in duct with a harmonic acoustic pneumatic source. *Applied Acoustics*, 176 :107860, May 2021.

[3] A. Allard, N. Atalla, and P. Micheau. Theoretical, numerical and experimental analysis of a high level electropneumatic sound source, 2020.

Abstracts for Presentations without Proceedings Paper
Résumés des communications sans article

Predicting The Noise Impact Of Large-Scale Battery Storage Sites In Ontario

Hillary Fung

Initiative to develop battery storage sites in Ontario has grown recently, driven by the IESO's long term procurement of 4000 MW in energy storage and generation. Due to the nature of these systems, most battery storage sites will be stationed in unenclosed spaces in rural areas. Much of the equipment on the sites – batteries, inverters, and transformers – require substantial cooling. As a result, noise from these cooling units has become a significant constraint and consideration during the design of the sites, impacting the site capacity and need for costly mitigation measures. Since this scale of battery storage has not been seen in Ontario, the predictions are heavily based on manufacturer test data and lack the benefit of validation with similar pre-existing sites. This presentation will outline the challenges faced in modelling the impact of these sites and how these predictive models have been refined.

OCCUPATIONAL AND ENVIRONMENTAL NOISE - BRUIT ENVIRONNEMENTAL ET AU TRAVAIL

MANUFACTURERS' SOUND DATA – APPLICATION EXPERIENCES

Pier-Gui Lalonde*[1] and Gregory E. Clunis[1]
[1]Integral DX Engineering, Ottawa, Ontario, Canada

1 Introduction

In our practice we are regularly asked to validate environmental noise impacts at noise-sensitive receptors, due to proposed new noise-generating equipment. Following validation, we are frequently able to perform sound pressure level measurements of the installed equipment, as a commissioning activity. This paper provides an overview and discussion of the practical challenges at each step of the validation and commissioning processes: input manufacturer sound data; field measurements; and use of acoustic modelling software. Finally, manufacturer equipment sound power levels are compared to those calculated from commissioning measurements.

2 Sound Data from Manufacturers

The quality of noise emissions data available from manufacturers of outdoor equipment varies significantly between manufacturers and equipment models. While claims of "quiet" or "low noise" performance are commonly found in marketing materials, it is not always the case that noise emissions data are available to back up those claims.

Equipment manufacturers can obtain high quality environmental noise emissions data by following an industry standard such as ISO 3744[1] or AHRI 270[2]. The process of then incorporating the resulting octave band (or one-third octave band) sound power levels into environmental noise modelling software is straightforward.

Noise data are often provided as sound pressure levels measured at one or more defined positions around the equipment. Additional calculations are then needed to determine the sound power level. Typically, there are fewer measurement points than would be required per the above-noted standards.

In some cases, noise data are not available for the proposed equipment as a whole, but data are available for its individual noise-generating components, such as condenser fans, blowers, and compressors. The resulting sound power radiated to the outdoor environment will take several paths (including intake/exhaust openings, cabinet breakout noise, or the direct path for condenser fans). The total radiated sound power calculation becomes complex with significant uncertainties, and thus can only be considered an estimate.

Packaged HVAC equipment which may operate in several different modes (e.g. providing both heating and cooling) add further complications to the application of manufacturer sound level data, as the operating conditions represented by the data are not always clarified. A further challenge occurs when key information are missing, such as the type of data (sound power or sound pressure), whether the data are A-weighted, or the distance and spreading conditions of sound pressure level measurements. This is especially common when the data are provided by a third-party vendor rather than the manufacturer – vendors may not accurately replicate all relevant sound information into their documentation.

3 Field Measurements

Field measurements provide significant value in terms of verifying whether newly installed equipment produce the expected level of noise. Significant challenges are nonetheless encountered.

An ideal case would be to measure equipment noise in accordance with ISO 3744, which would produce one-third-octave band sound power levels complete with directivity information. In practice, these measurements are time-consuming, and could be significantly impacted by background noise. In fact, background noise is a primary limitation for field measurement of outdoor equipment. Typical sources of background include other equipment and transportation sources (surface and airborne).

We use multiple strategies to deal with the challenge of background noise. Often, other nearby equipment must be turned off, which can require significant coordination for manufacturing facilities with many outdoor noise sources and full-time production requirements. In some cases, background noise levels can be measured separately, allowing the source measurements to be adjusted accordingly. Finally, we typically take measurements at relatively short distances from noise sources, to maximize the signal-to-noise ratio for the source we are measuring. For packaged HVAC equipment, we typically treat the individual noise-generating components (condenser fans, condenser grills, compressors, air intake and exhaust openings) as separate noise sources: we measure sound levels near the various noise-generating components as needed to determine individual radiated sound power levels.

Where possible, additional verification measurements are taken at a greater distance from the equipment. Those measurements can then be compared to predictions from environmental noise modelling software.

A further challenge for measurement collection is ensuring that the equipment is operating at the representative condition (or conditions) as needed for the environmental compliance assessment. For units that provide both heating and cooling, it is often only practical to measure each mode in the appropriate season.

4 Environmental Noise Modelling

We use CadnaA noise modelling software by DataKustik GmbH, with the calculations completed as per its implement-

* pier-gui@integraldxengineering.ca
† greg@integraldxengineering.ca

tation of ISO 9613 [3].

Validation of a proposed new noise source starts with implementing the available sound level information from the manufacturer. Typically, a single point source with the reported radiated sound power data is added to the model. When the available sound level data include individual components (e.g. condenser fans), this might be modelled separately (one point source per fan), with the equipment cabinet also incorporated as a screening object.

Following field measurements of the equipment, it will typically be modelled in more detail, including the equipment cabinet, point sources for components such as condenser fans and compressors, and large air openings modelled as area sources. If equipment casing breakout noise is significant, this too is modelled as multiple area sources.

Where field measurements at a distance from the equipment are available, a verification process can be used to confirm that noise emissions in the model match those measurement points. This means adding a receptor object in the model at the location of each measurement position. Often, the acoustic model configuration must also be set differently to ensure an accurate comparison. For instance, the Ontario Ministry of the Environment, Conservation and Parks environmental noise guideline [4] requires a +5 dB penalty for noise characteristics that are expected to increase disturbance, such as tonal noise – this penalty needs to be removed for the model verification process. It must also be checked that the calculation configuration doesn't exclude significant reflections that would have been present during measurements.

5 Sound Power Comparisons

Our environmental noise validation and commissioning processes provide an opportunity to compare manufacturer-reported sound data with measurement data of the equipment once installed. For 22 individual pieces of equipment, Figure 1 compares the sound power level determined by measurement, relative to the sound power level provided by the manufacturer (or calculated from manufacturer-provided sound pressure levels). A positive value in Figure 1 indicates that the sound power determined by measurement was higher than expected given the manufacturer sound data. This data set is limited to equipment with relatively high-quality manufacturer data, with no additional calculations needed for duct losses or breakout noise.

Comparing overall dBA ratings, most equipment are within +/- 4 dB of the manufacturer-reported level. Outliers as far as – 6 dB and +12 dB are found. Even greater variability is found in individual octave band data per Figure 1.

There are many possible explanations for significant differences in the measured vs expected sound power ratings. The specific equipment configuration and operating conditions could differ from those represented by the manufacturer data (e.g. differences in air flow conditions can have a considerable impact on noise emissions). Some of the field measurements were performed many years after the equipment was installed, inviting the possibility that sound levels had changed as a result of equipment wear and tear. There are also several possibilities for measurement error, given the above-noted challenges with measurement collection.

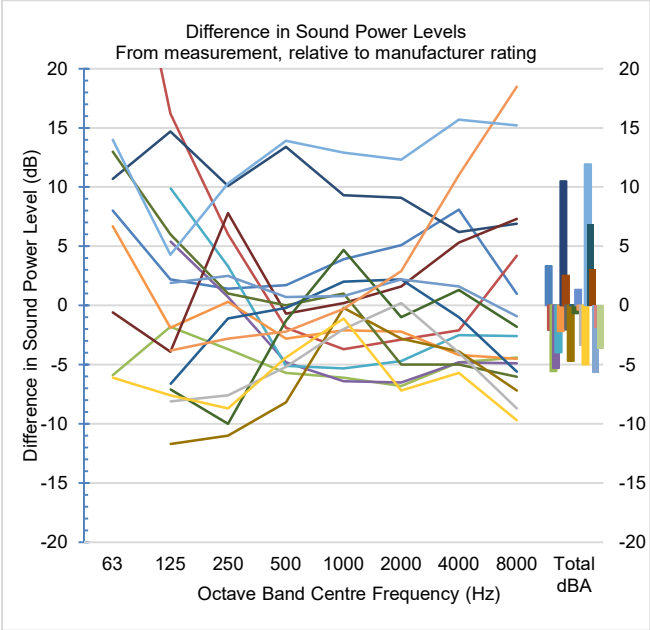

Figure 1: Sound power levels calculated from measurements, relative to sound power levels obtained from manufacturer data.

6 Future Work

Further study into the specific factors affecting the correlation between reported and measured sound power levels could be done by performing a statistical analysis with more input data. This could include tracking the "repeatability" of reported sound power ratings based on the equipment type, model, or manufacturer. Finally, a detailed analysis of the outliers may provide a better understanding of the causes for those discrepancies.

Acknowledgments

The authors would like to recognize Canadian Bank Note Company, Limited, for allowing use of measurements gathered at their facilities as the primary data source for this paper.

References

[1] ISO 3744:2010 Acoustics – Determination of sound power levels and sound energy levels of noise sources using sound pressure – Engineering methods for an essentially free field over a reflecting plane

[2] AHRI 270-2015: Standard for Sound Performance Rating of Outdoor Unitary Equipment

[3] ISO 9613-2:1996 Acoustics – Attenuation of sound during propagation outdoors – Part 2: General method of calculation

[4] Ontario MECP Publication NPC-300 Environmental Noise Guideline – Stationary and Transportation Sources – Approval and Planning

DIGITAL EARPLUG FEATURING COMBINED NOISE DOSIMETRY AND ELECTROCOCHLEOGRAPHY: A PROOF OF CONCEPT.

Adélaïde Douchet[*1], Alexis Pinsonnault-Skvarenina[†1,2], Gabrielle Crétot-Richert[‡1], Malo Richard[§1], Valentin Pintat[¶1,2], and Jérémie Voix[‖1,2]

[1]Université du Québec (ÉTS), Montréal, Québec, Canada

[2]Centre for Interdisciplinary Research in Music Media and Technology, McGill University, Montréal, Québec, Canada

1 Introduction

Noise-induced hearing loss (NIHL) refers to a type of hearing loss caused by prolonged exposure to loud sounds, as is the case for persons evolving in noisy work environments. Continuous exposure to high noise levels can damage structures within the cochlea, specifically the inner ear hair cells, leading to a gradual and irreversible loss of hearing sensitivity. However, NIHL is preventable when using appropriate hearing protection devices and implementing proper safety measures to reduce exposure to loud sounds.

In recent studies [1, 2], electrocochleography (ECochG) has demonstrated the capability to detect auditory nerve damage associated with impaired speech perception that might result from excessive noise exposure. ECochG, an electrophysiological measure, records inner ear electrical potentials generated in response to acoustic stimulation, providing valuable insights into the impact of noise on the auditory system. In-ear noise dosimetry is a developed technique [3] which measures with precision the effective amount of noise a person has been exposed to throughout the day. To enhance hearing conservation practices in work environments, an approach integrating individual measures of noise exposure and early auditory nerve damage (through ECochG) could be used to detect degradation of hearing much sooner. This paper presents a proof of concept for an earpiece, dubbed eCoGeers, featuring concurrent noise dosimetry and ECochG.

2 Methods

The proposed method is based on the study from Pinsonnault-Skvarenina et al. (2023) [4]. The purpose is to ensure the quality of the data capture made possible with the eCoGeers Hardware and Software, which was designed and developed by the co-authors. To this aim, electrocochleography responses have been measured using a clinical gold standard system. The capability of the eCoGeers to detect this signal was assessed.

2.1 Experimental measurement of ECochG in clinical settings

Following the approach presented in [4], the clinical ECochG measures were recorded using a Smart EP Intelligent Hearing System (IHS, Miami, FL, USA) on one subject. ER-3A earphones transmitted 100 μs clicks at a presentation rate of 11.1 Hz and alternating polarity at 85 dBnHL, via silicone tubing. A 3.3 Hz–5,000 Hz passband filter was used, and the gain was adjusted to 100 000. Six trials containing 2,000 responses each were performed to obtain a grand average waveform. From the peak of the waveform, the pre-synaptic summating potential (SP) and wave I (AP) amplitudes were recorded and correlated with the pre-stimulus baseline. While the AP peak was recognized as the highest point between 1 and 2 msec after stimulus onset, the SP peak was defined as the highest point around 1 msec following stimulus onset. Additionally, latencies for the SP and AP were obtained.

2.2 eCoGeers Hardware & Software Acquisition System Design

eCoGeers Hardware

In order to measure the electrophysiological responses, the prototype eCoGeers was developed. The device is based on a prior hardware platform named CochlEEG and developed at the *ÉTS-EERS Industrial Research Chair in In-Ear Technologies* (CRITIAS) laboratories. The CochlEEG unit features a low-Noise, 8-channel, 24-Bit Analog-to-Digital Converter (ADC) for biopotential measurements and integrates the ADS1299 (Texas Instruments, Dallas, TX, USA) chip. The eCoGeers' device features a Teensy4.1 (PJRC, Portland, Oregon, USA) microcontroller unit (MCU). The MCU retrieves electrical potentials from the ADS1299 ADC and transmits them to the UART serial port. To the electronic hardware, a pair of earpiece is wired where each one features a foam eartip with an embedded gold-plated foil electrode and a circum-aural Ag/Ag-Cl reference electrode. By incorporating two audio shields equipped with an SGTL5000 (NXP, Eindhoven, Netherlands) 16-bit audio ADC/DAC, the eCoGeers hardware has the capability to record four channels. These channels are set aside for future audio functionalities, such as generating audio click stimuli for ECochG measurements performed on participants.

eCoGeers Software

The Teensyduino library, an open-source framework based on the Teensy MCU platform, served as the engine for the eCoGeers software. It is used to make the Teensy 4.1 microcontroller unit easier to control when high-level programming in C++ is used. The MCU reads the electrophysiological data from the ADS1299 ADC via the serial connection at an 8kHz sampling rate on 6 channels. The Universal Serial Bus (USB) protocol, which enables dependable data transfer and simple

[*]adouchet@critias.ca
[†]apinsonnault@critias.ca
[‡]gcretot@critias.ca
[§]mrichard@critias.ca
[¶]vpintat@critias.ca
[‖]jeremie.voix@etsmtl.ca

connection to a computer, is used by Teensyduino to simplify serial communication.

2.3 Signal acquisition and analysis

The signal that was sent to eCoGeers was generated using the grand average waveform of Section 2.1. The signal was upsampled to 48 kHz in order to be transmitted through the sound card to the device. 40 ms segments were created and looped over 600 times. The signal was transmitted at the same amplitude as it was recorded 0.55 microVolts. The eCoGeers device recorded the signal with a samping rate of 8 kHz. Continuous data was epoched every 40 ms corresponding precisely to the beginning of each new loop. Epochs were baselined at t0. Epochs that were dominated by noise were eliminated if there maximal amplitude was above 8 standard deviation, about 8 percent of the epochs were rejected. Data was then band pass filtered between 60 and 2000 kHz. The grand average waveform was the computed.

3 Results

Figure 1 shows the grand average waveform recorded by eCoGeers of a signal characteristic of an ECochG potential emitted at the low amplitude of ± 0.55 microvolts. After processing and averaging, the waveform recorded is clear enough to identify the relevant potentials for ECochG measurements. The SP and AP peaks were found at the same latencies as the original signal.

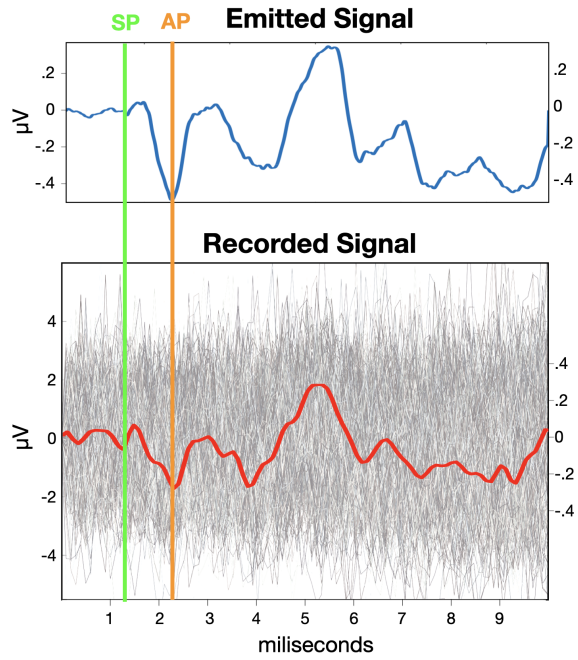

Figure 1: Recordings of the ECochG. Top plot is what was sent to eCoGeers, bottom plot is what the eCoGeers recorded (right axis refers to the red trace representing the average of 400 trials)

4 Discussion

The corresponding responses between the ECochG template and the eCoGeers recorded signal at 0.55μV shows that the device can successfully extract low-level voltage of an ECochG response from the electrical noise floor when extracting grand average waveforms.

Electrocochleography combined with in-ear dosimetry holds a great promise as an effective approach for hearing loss prevention. In a previous study [3], instrumentation and algorithms have been developed for measuring in-ear noise exposure. This method is important in order to precisely quantify noise exposure instead of approximating noise levels delivered to the cochlea with hearing protection. Added to electrocochleography, this new approach could lead to a better understanding of auditory damages, as we could correlate data of in-ear noise exposure throughout the day with auditory impairment.

Further research is needed to ensure the eCoGeers's autonomy and ready to use state. We anticipate that limits of the electric floor noise could be potential challenges in the future.

5 Conclusions

The results obtained on the eCoGeers device demonstrate the capacity of this device to record electrocochleography and dosimetry. The eCoGeers device could ultimately be used to detect damage to auditory nerve fibers following noise exposure with electrocochleography after necessary further advancements and real-world validation studies. Together this hearable technology could be used to protect the wearer against loud sounds, monitor real-time noise exposure and detect auditory damage. The wearer could then be alterted to this hearing degradation and react accordingly, thereby effectively improving occupational noise-induced hearing loss prevention programs.

6 Acknowledgments

The authors would like to acknowledge the financial support received from NSERC Alliance (ALLRP 566678-2021), MITACS IT26677 (SUBV-2021-168) and PROMPT (#164_Voix-EERS 2021.06), for the ÉTS-EERS Industrial research chair in in ear technologies, sponsored by EERS Global Technologies Inc

References

[1] Viacheslav Vasilkov, M Charles Liberman, and Stéphane F Maison. Isolating auditory-nerve contributions to electrocochleography by high-pass filtering: A better biomarker for cochlear nerve degeneration? *JASA Express Letters*, 3(2), 2023.

[2] Kenneth E Hancock, Bennett O'Brien, Rosamaria Santarelli, M Charles Liberman, and Stéphane F Maison. The summating potential in human electrocochleography: Gaussian models and fourier analysis. *The Journal of the Acoustical Society of America*, 150(4):2492–2502, 2021.

[3] Marcos Nogarolli Jérémie Voix Hugues Nélisse, Fabien Bonnet. *Développement d'une méthode de mesure de l'exposition sonore effective intraauriculaire pour une utilisation en milieu de travail*. IRSST, 2021.

[4] Alexis Pinsonnault-Skvarenina, Pierre Claret, Adélaïde Douchet, Gabrielle Crétot-Richert, Valentin Pintat, and Jérémie Voix. Digital hearing protector featuring electrocochleography: a proof of concept. *ICSV29*, 2023.

URBAN NOISE OBSERVATORY AND MANAGEMENT TOOL – APPLICATION TO QUEBEC CASE

Raphaël Duée *[1], Paul Otis-Bouchart D'Orval †[1] and Djesone Gomis ‡[1]
[1]Atelier 7hz, Acoustic and Vibration Engineering, Montréal, Québec Canada

1 Abstract

Despite the densification of cities and the resident exposure to high noise levels, no centralized data of the noise evolution is currently available in Quebec. This makes it difficult to assess the impacts of urban noise on the population. This study seeks to take stock of the methods of observation and management of urban environmental noise around the world. Indirect methods of urban noise management such as the introduction of noise policies, planning practices and the development of quiet zones are first presented. Ways of organizing existing noise observatories around the world are then described, it is discussed how it would be possible to observe the evolution of urban noise in a Quebec context.

2 Data collection method

The data analyzed were collected using three different methods: a bibliographic study, a web-based question form, and interviews with specialists in the field. The questionnaires included around fifteen questions related to urban noise management. Approximately 25 responses to the online questionnaire were received from specialists from Canada, France, UAE, The Netherlands, New Zealand, Hong Kong, China, Slovenia and Switzerland. Ten interviews were also conducted.

3 Noise management good practices

3.1 Legislation

Noise management and control can be done through regulations, planning and incentive schemes. The WHO has defined noise emission limits in order to prevent public health risks [1] and the European directive 2002/49/ EC is a good example of regulation [2]. It sets out three actions:

- Map exposure to environmental noise,
- Be transparent with the public about the impacts of noise,
- Adopt action plans based on the mapping.

Noise control measures are often corrective and not preventive. Noise planning and prevention are good habits to adopt when carrying out an urban development. Incentives can be financial or political in nature. In Brussels, victims of noise pollution have access to subsidies to finance the sound insulation of their homes. Also reporting of noise levels during real estate transactions could be mandatory. Builders would thus be encouraged not to build new buildings in areas with high noise levels [3].

3.2 Urban planning practices

The main sources of urban noise are related to transport. Road traffic noise levels are reduced by decreasing the road fleet density, by traffic management, by appropriate regulatory measures, by lowering speeds and by incentive schemes to reduce noise at source. The road fleet density can be reduced by promoting the development of active and collective transport (London or Paris action plans for example) and by limiting the place of the solo car in urban planning. Limiting noise induced by vehicles at source (Jacob brakes prohibited in certain areas in New Zealand) or prohibiting vehicles at certain times (Hong Kong) are also effective solutions.

Reducing railway noise is generally the responsibility of railway companies and often requires regulations and strict acoustic criteria for the infrastructure conception. Air traffic noise is also complex to control because it involves a large number of different actors. A good solution to reduce it is to apply operating restrictions and operational procedures. The management of airborne noise in Brussels is a good example. The airport is monitored by a network of stations making it possible to initiate proceedings against operators.

3.3 Quiet zones

In Montreal, INRS identified 2266 quiet zones corresponding in majority to green or residential spaces. The beneficial effects of green spaces are well known. For example, they promote psychological restoration, whether affective, cognitive or physiological, which promotes the alleviation of stress. An issue of environmental equity is also associated with the distribution of quiet areas. Quiet areas can also provide economic benefits. The direct economic effect related to noise reduction estimates an increase in property value of approximately 0.5% per decibel.

ISO 12913-2 Acoustics-Soundscape makes it easier to compare results between several studies. This method proposes to evaluate all the sounds perceived in a sound environment in all its complexity. The studies will therefore use different data collection techniques related to human perception, the acoustic environment and the context. This data collection can be done by guided interview, questionnaires, mobile applications, etc. The population survey provides information related to psychoacoustics such as human perception of the sound environment.

4 Observation of noise evolution

4.1 Existing observation structures

It appears that few different countries are equipped with this type of structure and the structures identified are quite variable. Non-profit associations are very present in France

* raphael.duee@atelier7hz.com
† paul.otis-bouchart@atelier7hz.com
‡ djesone.gomis@atelier7hz.com

through *BruitParif* and *Acoucité*. They include a large number of members: state enterprises, associations, communities and activities. These associations are the largest observatories met in this study but it's possible that some of them weren't found because on the cultural distance (Asia for example). Noise observatories can be developed by governmental institutions. For example, In India, the Ministry of Environment has started a program to develop a noise measurement network. There are currently 70 measurement sites in operation spread over 7 different cities [4] with a target of 160 stations in 25 cities. Aéroport de Montréal took the private initiative to make the WebTrak online tool available to the public. This allows aircraft trajectories to be consulted and the associated noise levels to be known. The Worldwide Aircraft Noise Services website (mainly used in Germany) offers citizens' committees to install a network of measurement stations in order to demonstrate that airborne noise levels exceed thresholds.

4.2 Noise mapping

Noise mappings are useful for visually representing the noise levels caused. To date, very few maps have been produced in Quebec Different simulation methods exist. The physical models are based on modelling the physical phenomena of aerial sound propagation. These are the ones most commonly used. Statistical models are based on regression equations describing the relationship between a pollutant and its environment (Land Use Regression model). The modelling is built from a series of sound level measurements, detailed GIS input data and several regression equations. This method has been used for example for Shanghai [5], Vancouver, Toronto, Halifax and Montreal [6]. It is also possible to use an artificial neural network in addition. These statistical models are limited because they don't take into account precisely the built environment, but they make it relatively easy to assess statistical criteria of noise exposure.

4.3 Observation by measurement network

The use of a network of permanent noise measurement stations is common around the world. For example, Station 7hz network is a light, robust and reliable system allowing the display of data measured in real time on an easy-to-use and modular web interface and an automatic detection of sound events (artificial intelligence training).

Noise observation can also be done using mobile measurement networks. These networks consist, for example, in the citizen use of mobile noise measurement applications (NoiseCapture app is an example) or the use of bicycles or vehicles equipped with sound level meters.

5 Quebec context

5.1 Current noise management in Quebec

Noise has been considered a contaminant since the adoption of the Environmental Quality Act, but no regulations govern its monitoring or exposure, whether inside or outside a building. The university community also develops projects that address urban noise. The *Sound City* project, for example, aims to develop knowledge on the management of urban noise. The *Vivre en Ville* organization aims to encourage the development of viable communities across Quebec and provides the public with documentary resources related to environmental noise.

5.2 Prerequisites for a Quebec noise observatory

A noise observatory cannot operate with total autonomy. This must work in cooperation with the technical services of the state, the university network and the data producers. The creation of an urban noise observatory in cities such as Quebec and Montreal is possible, but requires the following elements:

- Raising awareness among the population and decision-makers of the challenges of urban noise,
- evolution of the legislation to induce the development of noise observation and management tools,
- Cooperation to share know-how in this field,
- Stable funding.

6 Conclusion

Legislation must, as best as it can, harmonize the methods for assessing urban noise and clearly determine the noise thresholds to be respected. This must also allow the authorities to intervene effectively in noise issues. These issues require the expertise and coordination of several distinct areas. The creation of a noise observatory in the form of an association would generate this coordination and would bring together in one entity the knowledge acquired in the observation and management of urban noise. Such an observatory could thus be maintained thanks to membership fees and thanks to funding that could be included in legislation or come from the government. A more detailed report is available on demand.

Remerciements/Acknowledgments

We would like to thank all those who helped carry out this study by answering our online questionnaire, our questions via video conference or *de visu*. Special thanks to Bruno Vincent, Patricio Munoz, Marie Poupé, Deborah Delaunay, Maryse Lavoie, Pamela Echeverria and Pierre E Lachapelle.

References

[1] WHO. Burden of Disease from Environmental Noise. 2011

[2] Parlement Européen. Directive 2002/49/CE du Parlement Européen et du Conseil du 25 juin 2002 relative à l'évaluation et à la gestion du bruit dans l'environnement.

[3] Smargiassi et Al. Avis de santé publique sur les risques sanitaires associés au bruit des mouvements aériens à l'Aéroport international PierreElliott-Trudeau. 2014

[4] Jamir et Al. Community noise pollution in urban India: Need for public health action, 2014

[5] Xueyi Xu et Al. Application of land use regression to map environmental noise in Shanghai, China. 2022

[6] Liu et Al. Comparison of Land Use Regression and Random Forests Models on Estimating Noise Levels in Five Canadian Cities. Environmental Pollution, 2019.

NOISEMONITOR : A PYTHON PACKAGE FOR SOUND LEVEL MONITOR ANALYSIS

Valérian Fraisse[*1, 2, 3]
[1]Schulich School of Music, McGill University, Montreal, Canada
[2]STMS Ircam-CNRS-SU, Paris, France
[3]Centre for Interdisciplinary Research in Music Media and Technology, Montreal, Canada

1 Introduction

Noise pollution represents a significant environmental threat that grows with increasing urbanization. In 2011, in the western part of Europe only, at least one million healthy life years were estimated to be lost each year from noise exposure [1]. To evaluate appropriate noise abatement strategies and/or soundscape interventions, the analysis and measurement of acoustic and psychoacoustic indicators through short-term and long-term noise monitoring is required. A large variety of noise indicators have been proposed in an attempt to encompass the complexity of human hearing and subjective assessment of noise (see [2] for a review). In this paper, we present `noisemonitor` (`https://pypi.org/project/noisemonitor/`), an easy-to-use Python package for short and long-term sound level monitor data analysis. In a few lines of code, the package allows to compute standard noise indicators such as proposed in the ISO 1996-1 :2016 standard [3] from short-term or long-term sound level meter data.

2 Noise Indicators

We present in this section a brief description of the noise indicators provided in the package. For a detailed description, please refer to [4].

2.1 Equivalent Sound Pressure Level

The equivalent sound pressure level is probably the most common type of noise indicator. It is an energy-based indicator and represents the total amount of acoustic energy over a specified time period. It is defined as :

$$L_{Eq,T} = 10\log_{10}\frac{1}{T}\int_0^T \left(\frac{p}{p_0}\right)^2 [dB],$$

where T is the time period over which measurements occur, $p(t)$ the instantaneous acoustic pressure and p_0 the reference sound pressure level ($20\mu Pa$).

2.2 Statistical Indicators

Statistical indicators can be used to report on the level of noise exceeded for a certain percentage of the measurement time. The most common are L_{10} (high noise levels) and L_{90} (background noise), representing the noise levels exceeded for respectively 10% and 90% of the time [4]. For instance, an $L_{90,1h}$ of 52 dB means that for 54 minutes in that hour (90% of the time), the sound pressure level exceeded 52 dB. The median sound level, L_{50}, is also known to have a good correlation with perceived sound intensity and pleasantness [2].

2.3 A-weightings

The human ear does not respond equally to sound at different frequencies and sounds at lower and higher frequencies are perceived to have a lower intensity [4]. To account for this a frequency-dependant weighting system (the A-weighting curve) is often applied on environmental noise measurements and provides an acceptable correlation to human response to different noise sources [4], though its relevance is still being questioned [2].

2.4 Day, evening, night sound level

Initially developed in the European Union Directive 2002/49/EC [5], the L_{DEN} (Day, Evening, Night equivalent sound level) is derived from the A-weighted equivalent level indicator and accounts for the fact that noise exposure during evening and night period are generally more problematic for public health than during daytime with the addition of penalties during these periods (+5 dBA for evening and +10 dBA for night, see [5]).

3 Description of the Package and Examples

In this section, we provide an overview of the package's main functionalities. To get more information on how to use the package, a tutorial is available in `https://pypi.org/project/noisemonitor/`. The package takes as input data sheets (`.csv`, `.txt`, `.xlsx` or `.xls` formats are accepted) directly extracted from sound level monitor stations such as the *NoiseSentry Mk4* or the *RION NL-52*. The package's output indicators may be A-weighted, depending on the type of data collected by the sound level meter. This section is illustrated with examples from analyses performed on week-long measurements with `noisemonitor` as part of a field study in Montreal, Canada [6]. The analyzed data consists of $L_{Aeq,5s}$ measurements taken every 5 seconds in seven outdoor positions in a mixed industrial/residential area during a week in August 2022 by engineering company *SNC-Lavalin*.

3.1 Discrete indicators

The `noisemonitor` package allows to get average, discrete indicators computed over long periods of time including L_{eq}, L_{10}, L_{90}, L_{50}, L_{DEN} as well as the individual day, evening, and night levels. These indicators can be computed at specific times of the day and days of the week as shown in Table 1.

*. valerian.fraisse@mail.mcgill.ca

TABLE 1 – $L_{Aeq,24h}$ and L_{DEN} values computed with noisemonitor on weekdays and weekends at positions 1 to 5 [6].

	Weekday		Weekend	
Position	$L_{Aeq,24h}$	L_{DEN}	$L_{Aeq,24h}$	L_{DEN}
1	55.42	59.73	52.51	57.4
2	52.53	56.12	51.0	55.12
3	55.01	59.67	52.81	57.91
4	55.82	59.18	54.38	57.31
5	50.59	55.39	47.95	52.54

3.2 Rolling averages

In addition to discrete indicators, the `noisemonitor` package can perform overall and daily rolling averages on either L_{eq}, L_{10}, L_{90}, or L_{50} values, with the option of choosing window and step sizes. The result can be plotted with a dedicated function, as shown in the next figures. The analysis can be performed on all data (see Figure 1), but also at specific days of the week and times of the day (see Figures 2 and 3).

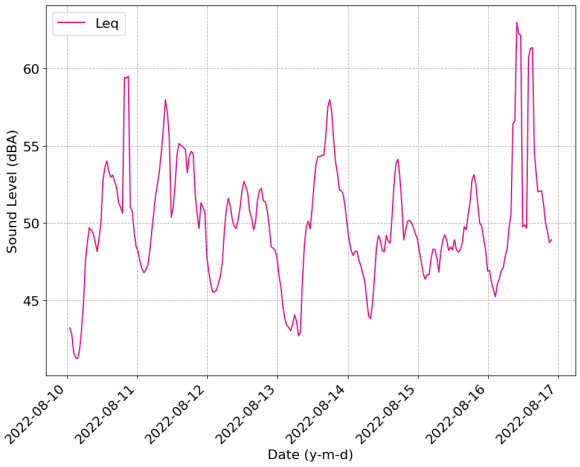

FIGURE 1 – $LAeq, 2h$: rolling average on all data (window size : 2h ; step size : 40min). Output from the noisemonitor package at position two [6].

4 Conclusion

We believe this package can be useful for Professionals of the Built Environment as well as Public Professionals that do not necessarily have the expertise to compute noise indicators from sound level meter data. In addition, the rolling averages provided by this package including daily and weekly profiles allow for the identification of recurrent patterns of noisy activities and/or space use and should help to address them in a tailored way. The package is currently in its early stage of development and will be further updated to include more indicators such as personalized statistical indicators, and to allow for a more versatile use. Any feedback on the package would be highly appreciated, and users are welcome to contact the main author or to create an issue in the GitHub repository (`https://github.com/valerianF/noisemonitor/issues`).

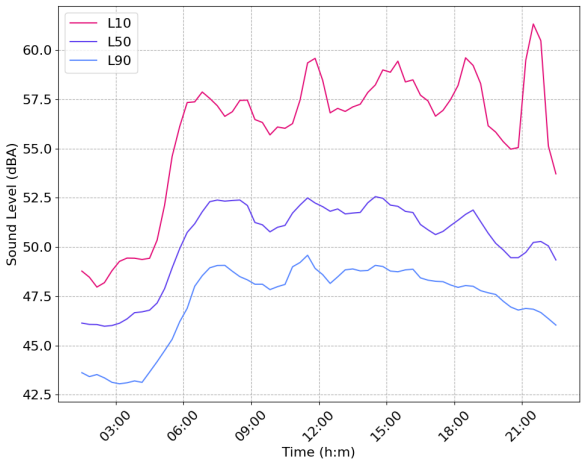

FIGURE 2 – Statistical indicators : daily rolling averages weekdays from 2am to 10pm (window size : 1h ; step size : 20min). Output from the noisemonitor package at position one [6].

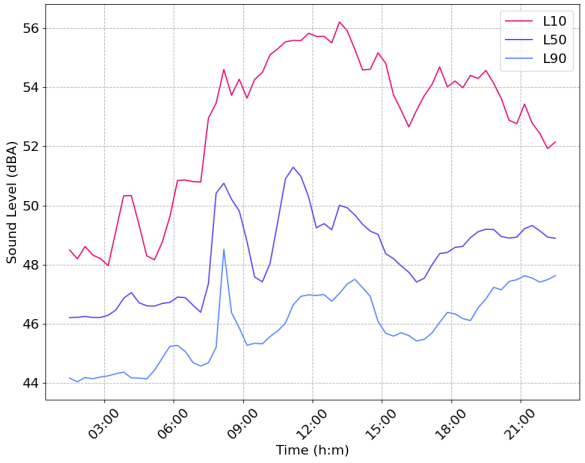

FIGURE 3 – Statistical indicators : daily rolling averages on weekends from 2am to 10pm (window size : 1h ; step size : 20min). Output from the noisemonitor package at position one [6].

References

[1] World Health Organization. Burden of disease from environmental noise. *The WHO European Centre for Environment and Health*, 2011.

[2] Arnaud Can, Pierre Aumond, Sven Michel, Bert De Coensel, Carlos Ribeiro, Dick Botteldooren, and Catherine LAVANDIER. Comparison of noise indicators in an urban context. In *Inter-Noise 2016*, Hambourg, Germany, August 2016.

[3] ISO. 1996-1 :2016 - Acoustics — Description, measurement and assessment of environmental noise, 2016.

[4] Enda Murphy and Eoin King. *Environmental Noise Pollution : Noise Mapping, Public Health, and Policy*. Elsevier Science Publishing Co Inc, Amsterdam ; Boston, 2014.

[5] EUR-Lex. Directive 2002/49/EC of the European Parliament and of the Council of 25 June 2002 relating to the assessment and management of environmental noise., 2002.

[6] Edda Bild, Valérian Fraisse, and Catherine Guastavino. MITACS project : Integrating sound considerations into the Montreal nightlife policy. Terrain 2 : Assomption Sud-Longue-Pointe, 2023.

AURALISATION: A VALUABLE CONSULTATION AND ENGAGEMENT TOOL FOR INFRASTRUCTURE PROJECTS – CASE STUDY OF AIRSPACE CHANGE FOR A REGIONAL AIRPORT

Vincent Jurdic [*1], Calum Sharp [†2], David Hiller [‡2], Ryan Biziorek [♦3] and Caroline Harvey [♯1]
[1]Arup Canada Inc., Montréal, Québec, Canada.
[2]Ove Arup & Partners Limited, London, United Kingdom
[3]Arup US, Chicago, Ilinois, USA

1 Introduction

Since the late 1990s, Arup has developed and used an auralisation capability to inform the design of some of the world's best arts and culture venues. Through Arup SoundLabs around the world, clients, designers, major stakeholders and the general public have been able to take informed decisions by experiencing the acoustic implications of designs as they are developed. More recently, auralisation technology has been developed to simulate sound generation and propagation during planning and design for a broad range of infrastructure projects, such as the High Speed 2 railway, A66 highway and Heathrow airspace change and expansion in the UK; Texas Central High Speed railway and LADoT Advanced Air Mobility (AAM) policy in the US; and a wind farm development in Tasmania.

The aviation industry is currently introducing new disruptive technologies principally to improve its sustainability performance. The introduction of electric aircraft and Advanced Air Mobility (AAM) vehicles is likely to revolutionize regional airspace, creating new opportunities for regional airports. Although it is possible to achieve lower noise levels for these new vehicles compared to traditional light aircraft, the sound characteristics (for example, tonality and high pitch due to electric motors) and their potential for higher traffic, could give rise to concerns about noise being more noticeable and disturbing to local communities than the current situation.

Through a series of sound demonstrations, members of the public and stakeholders could experience and judge for themselves the impacts of the proposed airspace and infrastructure changes, such as new types of aircraft, modification of flight paths and increased air traffic.

2 Auralisation Method

Arup's rigorous methodology has been developed and refined over the years to create representative sound demonstrations of infrastructure projects. The methodology is scalable, covering the needs, requirements, and constraints of the project. It has beensuccessfully applied, for example, to a regional UK airport to address public concerns and assist in the local authority planning process for the airport development masterplan.

Arup's sound demonstrations are created by recording the existing soundscape of the communities surrounding the airport, as shown in Figure 1. By recording the ambient and aircraft flight sounds, the listeners are immersed in a virtual soundscape environment with which they are familiar and can relate to.

Airspace changes are synthetized by combining ambient sound recordings with the sound expected for the new flight conditions.

Figure 1: Ambient sound and existing flight recordings in surrounding communities.

Our methodology relies on recordings as much as possible, captured through a thorough process. As shown in Figure 2, field recordings are performed with:

- ambisonics microphone, to capture the 3-dimension sound field, enabling the reproduction of moving sources.
- calibrated sound level meter, to ensure the recorded sound field can be reproduced at the correct sound level.
- video camera (360° or not) can also be included to provided visual support or create, when required, fully immersive Virtual Reality (VR) demonstrations.

To represent the different airspace changes (e.g., flight paths, flight operation or aircraft), the sound of aircraft operating in similar conditions is recorded. When necessary, these recording are corrected to represent specific flight conditions, for example by adjusting the sound propagation attenuation.

Upcoming hybrid/electric aircrafts and AAM vehicles have the potential to revolutionise regional people and goods transportation. These vehicles are still in development and sound recordings are not widely available at this stage. However, to assess the public perception and potential impact on

[*] vincent.jurdic@arup.com
[†] calum.sharp@arup.com
[‡] david.hiller@arup.com
[♦] ryan.biziorek@arup.com
[♯] caroline.harvey@arup.com

Figure 2: Measurement set-up to capture aircraft flyover - from left to right: video camera, ambisonic microphone, sound level meter.

community health and well-being, a few studies [1, 2] have been already undertaken, mostly by using synthesised sounds, created either through a simple model developed by Arup [3] or more advanced software (NASA ANOPPS).

3 Auralisation Reproduction

Arup's sound demonstrations can be delivered through various systems, depending on the requirements of the project.

Traditionally for the UK regional airport, public consultations are undertaken in a community hall, where all aspects of the scheme are presented simultaneously. Such face-to-face public consultations enable direct discussion between stakeholders. However, the event can be relatively noisy: it is essential to avoid nearby discussions contaminating the representativeness of the sound demonstrations. If a dedicated, isolated room is not available in the hall, soundproofed booths can be used to minimise noise cross-contamination. These booths can also include sensors tracking head movements to provide a better immersive experience using a VR set, as shown in Figure 3.

In the last few years, especially due to the COVID travel restrictions, virtual public consultations are becoming more frequent. Through Arup's online platform[1], auralisation can also be included. These online sound demonstrations, such as shown in Figure 4, generally allow the size of the participant pool to be increased and can also be accompanied by an online questionnaire to capture participant opinions and comments on the scheme. The calibrations of online demonstrations are however performed at the discretion of the participants and could be affected by uncontrolled listener environments and reproduction systems. To minimise the variations between users, the calibration process is described and performed at the start of the demonstration. Online demonstrations are also limited to illustrate relative changes between current and future scenarios.

At critical decision stages of the project, sound demonstrations can be performed in one of Arup's worldwide auralisation facilities (m|Lab or SoundLab) to ensure that the sounds are reproduced with high fidelity.

Figure 3: Dedicated soundproofed booth for immersive VR demonstrations.

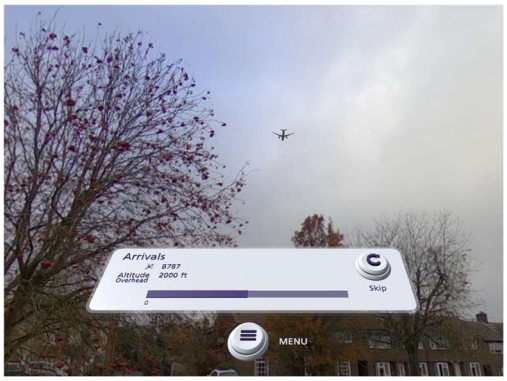

Figure 4: Interactive virtual reality simulation of aircraft passing overhead.

4 Conclusion

Auralisation has proven to be a valuable consultation and engagement tool in many infrastructure projects. Through a rigorous process, complex concepts are made easily accessible. Auralisation has been successfully used to:

- facilitate dialogue on implications for public health and wellbeing from a noise perspective;
- increase transparency on how stakeholders could be affected by a proposed development;
- ensure proposals are inclusive and accessible;
- support data-driven decision making;
- help identify stakeholders' needs and concerns;
- build trust amongst the entities through impartial advice

References

[1] A study on the societal acceptance of Urban Air Mobility in Europe, *EASA,* 2021.

[2] S. Krishnamurthy, S.A. Rizzi, Feasibility study for remote psychoacoustic testing of human response to urban air mobility vehicle noise, *Noise-Con,* 2022.

[3] A.L.P. Maldonado, V. Jurdic, D. Hiller, H. Harris, Auralisation of eVTOL vehicles through empirical assumptions or a simple analytical model, *28th AIAA/CEAS Aeroacoustics Conference*, 2022

[1] https://www.arup.com/services/tools/virtual-engage

LESSONS LEARNED MONITORING NEAR AND FURTHER FROM WIND TURBINES

William K.G. Palmer *[1]
[1]TRI-LEA-EM, Paisley, Ontario, Canada

1 Introduction

Without wind to turn them, wind turbines can be almost a silent neighbour. Yet, when rotating, we ask if what we hear is the wind, the impact of wind on surroundings, or wind on the turbines. Hypotheses have been advanced why some people say they are annoyed by wind turbines [1]. These hypotheses leave unresolved questions why the annoyance is not present at all times.

The intent of this study was to investigate the conditions present when residents report annoyance, to test some existing hypotheses for annoyance, and to determine if an alternative criterion could add to understanding.

2 Méthode/Method

2.1 Acoustic data gathering

A 135-day monitoring program was carried out at a "near" site 537 metres from the nearest wind turbine, with 19 turbines within 3 km. Residents have filed annoyance complaints since the array started operation in 2008. Complaints are often filed when the wind speed at 10 metres is under 6 metres per second.

Acoustic data gathering at the "near" site used a SAM Scribe Mk. II monitoring system with two microphones flat from 1 Hz to 8 kHz, calibrated with an IEC942 Class 2 Lutron SC-941 1000 Hz 94 dB calibrator. 10 minute data files, were recorded on an external hard drive.

The acoustic data was collected during two phases, the first recording 85 days of data, and the second a futher 50 days of data. The second phase used the SAM Scribe, verified by an ACO Pacific microphone, an Earthworks M30BX measurement microphone, and a pair of Superlux ECM999 measurement microphones. The verification microphones used a Scarlett 2i2 interface and a MacBook 5.2 computer running Audacity 2.1.0. All microphones were fitted with 90 mm primary and 450 mm secondary windscreens.

Simultaneous monitoring was conducted over 14-days during Phase 2 at the "near" site and at a second "further" site 6 km from the nearest wind turbine in the same array. Other than for proximity to wind turbines, the two sites were similar. Both are on open terrain, at similar proximity to paved township roads, and are subject to similar environmental conditions. The wind turbines in proximity to the "near" site are visible from the "further" site.

During the initial data gathering at the "near" site, the provincial COVID-19 "stay-home" order was in effect, so microphone calibration could only be checked before beginning data collection and at the end some 6 months later, but were unchanged. During Phase 2, microphone calibrations were checked approximately weekly, and remained unchanged.

Acoustic conditions were processed using the application electroacoustics toolbox version 3.9.10, on an iMac computer. This permitted calculating calibrated values of LA10, LA90, LAeq, LZ10, LZ90, LZeq, as well as charting one-third octave band and FFT analysis.

2.2 Wind turbine output data gathering

The hourly generation of the wind turbine array was collected from the Independent Electrical System Operator (IESO) Generator Output and Capability Reports. This was supplemented by observations of the residents at the "near" site, who recorded times the wind turbines changed operational state. The turbines at this site are constant speed turbines when synchronized to the electrical system.

2.3 Environmental data gathering

The primary source of environmental data for both data collection sites was the Environment Canada hourly record for Saugeen Shores, approximately 16.5 km from the "near" site, and 12.5 km from the "further" site. The record for Saugeen Shores is derived from the attended Environment Canada weather monitoring station at the Wiarton Airport. This weather data was generally close to that seen on a local monitor at the "further" site. Local observations of wind conditions and temperature were also noted at the "near site" when reports were logged with the Ministry.

2.4 Resident annoyance level monitoring

Residents provided a copy of the reports they filed with the Ministry for sample conditions considered annoying. After 14 years of operation, residents do not log every condition of annoyance, but only sample sitiations. With each report, the residents identify an annoyance level ranging from 1 to 9. Although there is no specific criterion level specified by the Ministry, residents have developed their own criterion, from 1 - of no concern, to 9 - of major concern. A 9 generally implies a situation such as when the wind turbine blades are icing and the noise level is very severe. Residents only report conditions ranging from 7 to 9, when the wind turbines are audible above the ambient wind, at an increasing level of annoyance.

3 Résultats/Results

Analysis of microphone recordings near wind turbines showed a correlation between the results and conditions identified as annoying by residents. Annoyance was not necessarily correlated to maximum sound amplitude, but to situations when the difference (LA10-LA90) was $\leq$ 3 dBA while at the same time the difference (LZ10 - LZ90) was $\geq$ 6

* trileaem@bmts.com

dBZ. At these times, sound from the wind turbines was prominent, and dominated noise from the wind, or the wind on the surroundings.

3.1 Initial results – phase 1 Dec. 2020-March 2021

During phase 1 the complaints the residents filed for which data is available are shown in Table 1.

Table 1: Resident complaints filed during phase 1.

Date	Assessment	LZ10-LZ90	LA10-LA90
20-11-28	8/10	13.4	2.3
20-12-05	7/10	7.7	1.8
20-12-09	8/10	13.9	3.0
21-01-23	8/10	9.2	2.5
21-02-20	8/10	13.0	2.5
21-02-24	8/10	15.0	3.1
21-03-01	8/10	13.0	3.0
21-03-06	8/10	8.8	2.3
21-03-09	7/10	13.5	2.6
21-03-26	7/10	7.3	2.6

3.2 Phase 2 results – Jan. 2023 – April 2023

The main emphasis for Phase 2 was to ensure that the annoyance conditions reported and the potential criterion were applicable to sound from the wind turbines, and not just sound from the wind itself. Figures 1 and 2 show the analysis of 5-days of simultaneous monitoring.

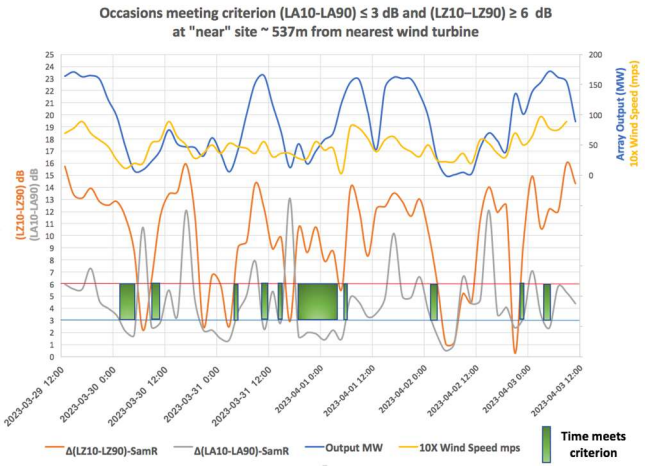

Figure 1: 5-days of data "near" wind turbines

Listening tests confimed that all the times identified as meeting the criterion in Figure 1 for the "near" site exhibited dominant wind turbine sound. Only some of those conditions occured at high turbine output.

Listening tests for the two cases at the "further" site that seemed to meet the criterion in Figure 2, showed they were due a loose microphone rattling inside the windscreen, or rain "drumming". They were not due to wind or wind turbines. Thus none of the "further" cases met the criteron as only due to artifacts.

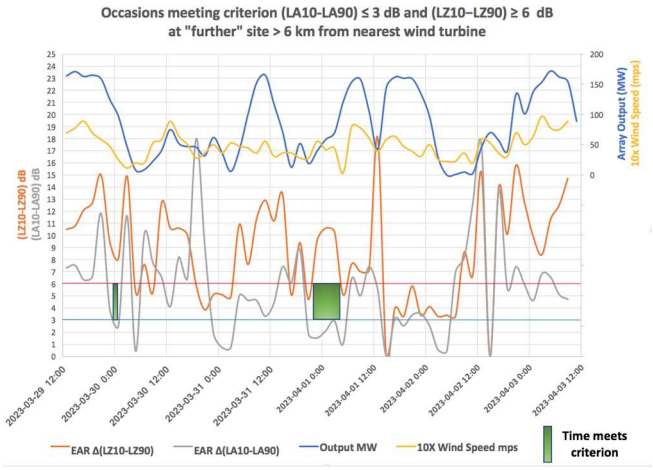

Figure 2: 5-days of data "further" from wind turbines

4 Discussion

It is considered that most people can perceive a change in sound level of > 3 dBA [2]. Thus, a ≤ 3 dBA change between LA10 and LA90, may not be readily perceivable and the sound level may be considered to be unchanged. LA90 represents the background sound level, present over 90% of the time. LA10 represents a higher sound level present less than 10% of the time. However, the annoyance criterion, based on the annoyance reports filed, shows the difference between (LA10-LA90) to be ≤ 3 dBA, and (LZ10-LZ90) to be ≥ 6dBZ. The explanation appears to be that annoyance arises from sound reduced in significance by dBA weighting. When wind speed rises, (LA10-LA90) is > 3 dB, so wind speed is not the reason the criterion is met.

5 Conclusion

The study identified acoustic conditions consistent with reports of annoyance near wind turbines, that did not exist further from wind turbines. They form a screening tool to identify annoyance might occur when (LA10-LA90) is ≤ 3 dBA, and (LZ10-LZ90) is ≥ 6dBZ. This complements, but does not replace criterion based on amplitude alone.

Remerciements/Acknowledgments

The loan of the SAM Scribe Mk-II monitoring system to record acoustic data is acknowledged. Thanks also to the families where the monitoring microphones were installed.

References

[1] T.R. Haac, K. Kalinski and M. Landis, Wind turbine audibility and noise annoyance in a national U.S. survey: Individual perception and influencing factors, Journal of the Acoustical Society of America 146(2), 1124-1141, (2019).

[2] F.Alton Everest, Master Handbook of Acoustics, 5th ed. McGraw Hill, (2009).

RELATIONSHIP BETWEEN COMMUNITY COMPLAINTS AND NOISE LEVEL DURING THE CONSTRUCTION OF A LARGE ROAD INFRASTRUCTURE IN MONTRÉAL

Alexis Pinsonnault-Skvarenina [*1,2], **Véronique Guay** [†1], **Renaud Leblanc-Guindon** [‡1], **Mathieu Carrier** [§3], **and Tony Leroux** [¶1,2]

[1]École d'orthophonie et d'audiologie, Faculté de médecine, Université de Montréal, Montréal, Québec, Canada
[2]Centre de recherche interdisciplinaire en réadaptation du Montréal métropolitain, CIUSSS Centre-Sud-de-l'Île-de-Montréal, Montréal, Québec, Canada
[3]Direction de la planification et de la mobilité durable, Ministère des Transports du Québec, Montréal, Québec, Canada

1 Introduction

Noise has been considered as one of the most important challenges to the quality of life in the last decade by to the World Health Organization [**?**]. While some studies have previously investigated the links between noise annoyance and community complaints related to road and airport transport [**?**], the relationship between construction noise and complaints has been little explored. However, reviewing complaint data could help better understand community annoyance to noise and help plan future major construction work.

The relationship between complaints and noise levels does not seem straightforward. While some researchers have found an association between noise levels and the amount of complaints lodged in a community [**?**], other studies have not found such a clear correlation [**?**, **?**]. Previous work from our research team has found that construction noise level explain only a fraction of annoyance levels (i.e., less than 1%), while psycho-social and contextual factors explained the majority of construction noise annoyance levels (i.e., up to 70%) [**?**].

Therefore, the aim of this study was to investigate the relationship between community complaints to noise and noise levels measured around a large construction worksite. The rehabilitation work of the Turcot interchange, located in Montreal, provided an opportunity to study community annoyance to construction noise.

2 Method

2.1 Complaints

This study was approved by the Ethics Committee of the Centre for Interdisciplinary Research in Rehabilitation of Greater Montreal (CRIR-1236-0317). A total of 1,325 complaints were collected through the complaint management system set up by the Ministère des Transports du Québec (MTQ) between January 6, 2017, and January 11, 2021. Of these, 31 complaints were excluded from the study because they did not concern the rehabilitation work of Turcot (n = 22), were duplicates (n = 5) or no information regarding the nature of the complaint was provided (n = 4). The analyses were conducted on the 1,294 remaining complaints.

[*]alexis.pinsonnault-skvarenina@umontreal.ca
[†]veronique.guay.4@umontreal.ca
[‡]renaud.leblanc-guindon@umontreal.ca
[§]Mathieu.Carrier@transports.gouv.qc.ca
[¶]tony.leroux@umontreal.ca

2.2 Noise levels

Eighteen independent noise stations, consistent with the ISO 1996-1 (2016) standard [**?**], were installed by the MTQ within 50 m of the Turcot complex. They allowed the measurement of multiple noise indicators (i.e., $L_{Aeq.24h}, L_{day}, L_{Evening}, L_{Night}, L_{10}, L_{90}, L_{Max}$) based on $L_{Aeq.1s}$ in 30-minute time averaging. Additional information regarding the localization of noise stations in the study area and the measurement of noise indicators can be found in other publications from our research team [**?**, **?**].

2.3 Statistical analyses

Correlations between noise levels and number of noise complaints were investigated using Pearson's R (SPSS Statistics, 26.0.0.0 version) with a significance level of 5%. Note that a complaint can relate to several sources of noise (i.e., described here has complaint units) and in this case, they were considered independently.

Two approaches were taken to attribute a specific daily noise level to each complaint unit in the correlations. First, the logarithmic average of the sound levels of all active noise stations on the day the complaint was lodged. Second, the noise level at the station with the highest noise level on the day the complaint was lodged. These calculations were applied to all noise indicators.

3 Results

3.1 Noise complaints

Between 2017 and 2021, out of the 1,294 complaints, 457 were related to noise (about 35%). These were the most frequent in 2017 (n = 112), 2018 (n = 187), and 2019 (n = 124). Fewer noise complaints were lodged in 2020 (n = 34), period when most rehabilitation work was completed.

3.2 Correlations between noise complaints and noise levels

Person's correlations between the number of noise complaints units and noise levels were carried for the period between January 2017 and December 2019. Since few noise complaints were lodged in 2020, these were excluded from the analyses.

When using the first approach to attribute a noise level to each complaint unit (i.e., an average of noise levels across all stations on the same day of the com-

plaint), significant correlations between complaint units and noise levels were observed (Table 1): $L_{10}(r(354) = .226, p < .001), L_{Aeq.24h}(r(354) = .192, p < .001)$, and $L_{Max}(r(354) = .158, p = .003)$ for 2017; $L_{10}(r(355) = .160, p = .002)$ for 2018; and $L_{10}(r(331) = .323, p < .001), L_{90}(r(331) = .282, p < .001), L_{Aeq.24}(r(331) = .343, p < .001)$, and $L_{Max}(r(331) = .283, p < .001)$ in 2019.

Table 1: Pearson correlation coefficients between the daily number of complaint units and the daily averaged noise levels across all stations.

	L_{10}	L_{90}	$L_{Aeq.24h}$	L_{Max}
2017	.226***	.074	.192***	.158**
2018	.160**	-.012	.089	-.041
2019	.323***	.282***	.343***	.283***

*$p < .05$; **$p < .01$; ***$p < .001$

When using the second approach, the highest level obtained at a given station on the same day of the complaint, similar results were obtained (Table 2): $L_{10}(r(350) = .193, p < .001), L_{90}(r(350) = .123, p = .022)$, and $L_{Max}(r(354) = .158, p = .001)$ in 2017; and $L_{10}(r(330) = .310, p < .001), L_{90}(r(331) = .213, p < .001), L_{Aeq.24}(r(331) = .268, p < .001)$, and $L_{Max}(r(331) = .282, p < .001)$ in 2019.

Table 2: Pearson correlation coefficients between the daily number of complaint units and the highest daily noise level obtained at a station.

	L_{10}	L_{90}	$L_{Aeq.24h}$	L_{Max}
2017	.193***	.123*	.064	.178**
2018	.040	.034	.008	-.010
2019	.310***	.213***	.268***	.282***

*$p < .05$; **$p < .01$; ***$p < .001$

4 Discussion

In our study, most construction-related complaints regarded noise. We observed that the number of noise complaints were relatively constant over the period of the rehabilitation work, indicating that noise is a major nuisance from the start of construction work until the end.

To better understand the relationship between noise complaints units and noise levels, correlations were computed . Significant correlations were obtained for most noise indicators in 2017 and 2019. However, most of these were poor. It should also be noted that most correlations in 2018 were not significant. This can be explained by the reduced number of active noise stations during that year because construction work was concentrated in two of the five residential areas neighbouring the Turcot structures. Therefore, the noise levels used for the correlations in 2018 might not have been representative of the actual noise levels across the entire worksite. Overall, our results suggest that indeed, the number of complaints lodged during the construction of a large infrastructure can be, in part, associated with noise levels.

Interestingly, the strongest correlations were obtained with the L_{10} noise indicator. The L_{10} is more representative of intermittent sources of noise that can emerge from the ambient noise. These could be more easily perceptible in neighbouring residential areas, which might explain their stronger association with complaints. Intermittent construction noise has also previously been associated with higher levels of construction noise annoyance [**?**].

Our findings are important for government agencies concerned about construction noise. They suggest that, in part, the number of complaints lodged by citizens can be associated with noise levels. Therefore, the use of noise indicators such as the L_{10} to monitor the soundscape and limit annoyance and complaints is supported by our results. However, since correlations between complaints and noise levels were weak, we believe that noise levels alone cannot fully explain why a specific individual decides to file a noise complaint.

5 Conclusions

In our study, we analyzed 1,294 community complaints lodged between 2017 and 2021, in the context of the rehabilitation work of the Turcot interchange in Montreal. Noise remained the nuisance causing the most important number of complaints. Complaint numbers were significantly correlated with various noise indicators, especially those integrating sound levels that emerge from the ambient noise (e.g., L_{10}). Our findings can help guide authorities in managing annoyance to noise and complaints in the community in the context of the construction of a large infrastructure.

References

[1] Chih-Hao Chen, Chii-Yuan Huang, Hsiu-Lien Cheng, Heng-Yu Haley Lin, Yuan-Chia Chu, Chun-Yu Chang, Ying-Hui Lai, Mao-Che Wang, and Yen-Fu Cheng. Comparison of personal sound amplification products and conventional hearing aids for patients with hearing loss: A systematic review with meta-analysis. *EClinicalMedicine*, 46, 2022.

[2] ANSI/ASA S3.22. Specification of hearing aid characteristics. *American National Standards Institute and Acoustical Society of America*, 2014.

[3] ANSI/CTA-2051. Personal sound amplification performance criteria. *American National Standards Institute and Consumer Technology Association*, 2017.

[4] Ibrahim Almufarrij, Kevin J Munro, Piers Dawes, Michael A Stone, and Harvey Dillon. Direct-to-consumer hearing devices: Capabilities, costs, and cosmetics. *Trends in Hearing*, 23:2331216519858301, 2019.

[5] Karina C De Sousa, Vinaya Manchaiah, David R Moore, Marien A Graham, and De Wet Swanepoel. Effectiveness of an over-the-counter self-fitting hearing aid compared with an audiologist-fitted hearing aid: A randomized clinical trial. *JAMA Otolaryngology–Head & Neck Surgery*, 149(6):522–530, 2023.

PSYCHOACOUSTIC PARAMETERS AND EAR CANAL ROLE

Hadi Asady [*1], Siamak Pourabdian [1], Adrian Fuente [2], Mehdi Jalali [3], Ali Ahmadi [1], Fatemeh Ansari [1], and Farhad Forouharmajd [†1]

[1] Department of Occupational Health Engineering, Isfahan University of Medical Sciences, Isfahan, Iran.
[2] École d'orthophonie et d'audiology, Université de Montréal, Montreal, Quebec, Canada.
[3] Department of Occupational Health Engineering, Neyshabur University of Medical Sciences, Neyshabur, Iran.

1 Introduction

According to definition, noise is an unwanted and unpleasant type of sound that could impact human activities and bring them into instability[1]. Exposure to noise associated with the injuries has become a public health issue in recent years. In addition to having adverse impacts on the hearing system, noise may also lead to other harmful health effects on the people, such as sleeping disturbance, impairment of cognitive performance in children, cardiovascular and pulmonary diseases, type 2 diabetes, adverse birth outcomes, and annoyance[2-4]. The effects of noise on humans depend not only on the physical characteristics of the noise, including the sound pressure level, frequency content and etc., but also on the physical, physiological, and psychological body systems reactions[5].

The ear is a sensitive organ of the human body that its structure in the process of the evolution and passing of the many years changed and at this time we can say the design of the human ear is one of nature's engineering marvels[6]. The ear has three regions called the outer, middle, and inner ear. The first two are solely concerned with sound transmission to the inner ear, which houses the transducer called the cochlea that converts fluid motion to action potentials. The auricle (pinna) and the ear canal, located on the outer side of the ear, collect and focus sound waves on the eardrum (tympanic membrane)[6].

Effects of ear canal on the sound pressure levels has been demonstrated by previous studies. Asady and et al. showed that ear canal could increase the level of sound pressure at different frequencies in both genders[5]. Also, Jia-Lin and et al. study showed that the sound pressure level difference between the outlet of external auditory canal and eardrum is different and these differences are more significant in the frequencies <=1500 Hz[7]. Djupesland and et al. study had same findings[8]. In all these studies which were performed in the field of acoustical roles of the human ear's different parts, the sound pressure level was the important parameter but it seems that no study was done on the psychoacoustical roles of the different parts of the human ear until now. The term psychoacoustics is generally defined as the study of listeners' responses to sounds. More specifically, psychoacoustics looks for statistical and causal relationships between certain physical properties of sounds and certain properties of human responses[9]. Same as the physical parameters of sound like sound pressure level(dB) psychoacoustic has its own parameters for calculation and measurements, most practical of them are loudness, sharpness, roughness fluctuation strength and tonality [10, 11].

So, the purpose of this study was to see that the psychoacoustic parameters including loudness, sharpness, roughness and fluctuation strength could changes significantly in the effects of human ear canal and gender had an important role on theses probable changes or not.

2 Method

White and sinusoidal noises each at 3 sound pressure levels (SPLs), including 75, 85, and 95 dBA, were used as the stimulus sound pressure levels (SSPLs). The speakers that were located in front of the participants had a distance of 1.5 meters from them and a height 87 centimeters from the lab ground. Labview software (V 2012), with the data acquisition card (DAQ) made by USA National Instrument Co (model MC-3642), was used for playing and measurement and calculating of the psychoacoustic parameters including loudness(phone), sharpness(acum), roughness(asper) and fluctuation strength(vacil). The psychoacoustic parameters were measured outside (cavum part of the external ear) and inside (at 2.0 cm depths from the entrance to the ear canal) of the right ear of each participant using the Moore method. This measurement was done with using of labview software. A circular-shaped microphone with a 2-millimeter diameter was used for this purpose. The time duration of 10 seconds (10 s) was considered for all the psychoacoustic parameters measurements.

3 Results

Out of 60 participants, 30(50%) was men. Most of them 41(68.3%) were BSc, eighteen (30%) MSc and one (1.7%) subject was PhD level student. The age means and standard deviation (Mean ± SD) of all participants was 22.77 ± 2.60 years old. Also, the mean and standard deviation (Mean ± SD) for height, weight and BMI (Body Mass Index) of all participants were 171.55 ± 9.65 cm, 64.30 ± 11.39 kg, 21.3 ± 2.95 respectively.

Comparison of the psychoacoustic parameters in the situation of the exposure to the different kind of noises and different sound pressure levels between two genders were not statistically significant (all P>0.05).

For sinusoidal noise the mean of all studied psychoacoustic parameters at the different SSPLs were the almost same, these findings were seen for the white noise too. The repeated measures ANOVA test results showed for both sinusoidal noise and the white noise in all three studied

[*] Asadyhadi60@gmail.com
[†] forouhar@hlth.mui.ac.ia

SSPLs the differences of four studied psychoacoustic parameters between outside and inside of participants ear were not statistically significant (all P values>0.05).

4 Discussion

Our findings showed that the human ear canal could not change the psychoacoustic parameters, and the gender had not effective role on this phenomenon in the other words the mean comparison of psychoacoustic parameters between outside and inside ear of both genders was not statistically significant. This finding was against of our hypothesis, that was the human ear canal like the sound pressure level in total or in the different frequencies could change the psychoacoustic parameters but this hypothesis was not supported by this study results. Actually, our hypothesis was according to the other study findings like Park et. al study showed in frequencies 3 kHz, 4 kHz, and 6 kHz and for people older than 30 years, hearing thresholds between both genders are statistically difference while this difference in the 4 kHz frequency was larger than other frequencies[12]. Also gender differences in the association between hearing loss and cognitive function was seen in the Huang and et al. study[13]. This kind of differences was seen in the Wasano and et al. study too[14]. We realized that both gender ear functions in the field of psychoacoustic are same and we can say that gender differences in sound perception is free from external hearing system differences. In other words, external hearing system of the humans dose not have any effects on the perceived sound quality and this parameter are more related to the sound pressure level, loudness, frequency content, level fluctuation, pure-tone components, and impulsiveness[15].

Also, our results showed that the psychoacoustical behaviors of the human ear canal does not change with change in the stimulus sound types and also sound pressure levels. It seems that changes of sound pressure levels at different frequencies in the role of human ear canal [5, 16] are not effective on the psychoacoustic parameters in other words psychoacoustical characteristic of the human ear canal are independent from the sound wave types and pressure levels. We did find the same articles to compare our findings with them.

5 Conclusion

It seems that human ear canal did not have any effects on the psychoacoustic parameters and as far as can be say that noise annoyance that is related to the psychoacoustics parameters[17] does not change in the role of human ear canal. Also, both genders ear canal behaves same in related to the psychoacoustic parameters.

Acknowledgments

The authors would like to thank all students who participated in this study. The study has been reviewed and accepted by the ethics committee at the Isfahan University of medical sciences (No. IR.MUI.MED.REC.1399.771)

References

[1] Nassiri P, Monazam M, Fouladi Dehaghi B, Ibrahimi Ghavam Abadi L, Zakerian SA, Azam K. The effect of noise on human performance: a clinical trial. The international journal of occupational and environmental medicine. 2013;4(2):87-95.

[2] Li X, Dong Q, Wang B, Song H, Wang S, Zhu B. The Influence of Occupational Noise Exposure on Cardiovascular and Hearing Conditions among Industrial Workers. Sci Rep. 2019;9(1):11524.

[3] Bagheri Hosseinabadi M, Khanjani N, Ebrahimi MH, Mirbadie SR, Biganeh J. The effects of industrial noise exposure on lipid peroxidation and antioxidant enzymes among workers. Int Arch Occup Environ Health. 2019;92(7):1041-6.

[4] Basner M, Babisch W, Davis A, Brink M, Clark C, Janssen S, et al. Auditory and non-auditory effects of noise on health. Lancet. 2014;383(9925):1325-32.

[5] Asady H, Fuente A, Pourabdian S, Forouharmajd F, Shokrolahi I. Acoustical role of ear canal in exposure to the typical occupational noise levels. Medical journal of the Islamic Republic of Iran. 2021;35:58.

[6] Sundar PS, Chowdhury C, Kamarthi S. Evaluation of Human Ear Anatomy and Functionality by Axiomatic Design. Biomimetics. 2021;6(2):31.

[7] Liu JL, Qin XL, Wang LH, Liang CY, Jiang T. [Measurement of sound pressure level at outlet of external auditory canal and eardrum]. Zhonghua lao dong wei sheng zhi ye bing za zhi = Zhonghua laodong weisheng zhiyebing zazhi = Chinese journal of industrial hygiene and occupational diseases. 2003;21(5):353-5.

[8] Djupesland G, Zwislocki JJ. Sound Pressure Distribution In The Outer Ear. Acta Oto-Laryngologica. 1973;75(2-6):350-2.

[9] Guski R, Blauert J. Psychoacoustics Without Psychology? Review of General Psychology. 2009;8:265-72.

[10] Poveda-Martínez P, Ramis-Soriano J. A comparison between psychoacoustic parameters and condition indicators for machinery fault diagnosis using vibration signals. Applied Acoustics. 2020;166:107364.

[11] Engel MS, Fiebig A, Pfaffenbach C, Fels J. A Review of the Use of Psychoacoustic Indicators on Soundscape Studies. Current Pollution Reports. 2021;7(3):359-78.

[12] Park YH, Shin S-H, Byun SW, Kim JY. Age- and Gender-Related Mean Hearing Threshold in a Highly-Screened Population: The Korean National Health and Nutrition Examination Survey 2010–2012. PLOS ONE. 2016;11(3):e0150783.

[13] Huang B, Cao G, Duan Y, Yan S, Yan M, Yin P, et al. Gender Differences in the Association Between Hearing Loss and Cognitive Function. American Journal of Alzheimer's Disease & Other Dementias®. 2020;35:1533317519871167.

[14] Wasano K, Kaga K, Ogawa K. Patterns of hearing changes in women and men from denarians to nonagenarians. The Lancet Regional Health - Western Pacific. 2021;9:100131.

[15] Crocker MJ. Handbook of noise and vibration control: John Wiley & Sons; 2007.

[16] Yu JF, Cheng WD. Effect of Canal Depth on Sound Pressure Level Distribution in Human Bilateral Ears. Applied Mechanics and Materials. 2012;145:63-7.

[17] Ellermeier W, Zeitler A, Fastl H, editors. Predicting annoyance judgments from psychoacoustic metrics: identifiable versus neutralized sounds. Proc of 33rd Intern Congress on Noise

A CRITERION BASED ON THE CALCULATION OF A SOLID ANGLE TO ASSESS THE QUALITY OF ACOUSTIC IMAGES OBTAINED WITH A SMA

Kevin Rouard*[1], Julien St-Jacques[1], Franck Sgard[2], Olivier Doutres[1], Hugues Nélisse[2], Loic Boileau[3], Alain Berry[3], Nicolas Quaegebeur[3], François Grondin[3] and Thomas Padois†[2]

[1]École de technologie supérieure (ÉTS), 1100 Rue Notre Dame O., Montréal, QC, H3C 1K3, Canada
[2]Institut de recherche Robert-Sauvé en santé et en sécurité du travail (IRSST), 505 Boulevard de Maisonneuve O., Montréal, QC, H3A 3C2, Canada
[3]Université de Sherbrooke (UdeS), 2500, Boulevard de l'Université, Sherbrooke, QC, J1K 2R1, Canada

1 Introduction

Beamforming algorithm makes it possible to estimate both the direction and the level of the sound sources. Sources are depicted by color spots in an acoustic image. Color spots represent lobes, with the mainlobe identifying the source position, while sidelobes correspond to spurious sources resulting from the array design. Various criteria exist to assess the quality of an acoustic image and, by extension, the efficiency of an array design and the associated algorithm. The level of the source (is indicated by the mainlobe) [1], the level of the mainlobe-to-sidelobe ratio (MSR) [2], and the area ratio of the mainlobe and occasional sidelobes in the acoustic image, known as the spatial resolution [3], are well-established criteria. Several methods are used to calculate the area ratio of the presence of the lobes with respect to the total area of the acoustic image. Mainlobes can be uniform or spread, and sidelobes are scattered, which increases the complexity task. For spherical microphone arrays (SMA), the ellipse area can be used, considering a polar projection of a hemisphere [4] or as an ellipse array ratio [5–7]. The area ratio depends on the array design, the algorithm, and the frequency. This paper proposes to compare the solid angle as a spatial resolution criterion in the field of acoustic imaging.

This paper is organized as follows. Details of the numerical simulation are given first. Then, the covariance ellipse and the solid angle are described. Third, both ellipse area and solid angle as criterion are compared. Finally, Discussion and conclusion are provided in the last section.

2 Methodology

2.1 Numerical simulation

A numerical simulation is conducted in a free-field environment with a rigid SMA and a t-design geometry of 36 microphones [8]. The SMA is located 2 meters away from a monopole that emits a pure tone. In the following, the frequency is represented as kr, a dimensionless number, where k is the wavenumber and r is the radius of the sphere. Several positions of monopoles are considered: directly in front of the SMA ($\theta = 90°, \phi = 0°$), in front of the SMA near the floor ($\theta = 45°, \phi = 0°$) and almost behind the SMA near the floor ($\theta = 45°, \phi = 135°$). Spherical harmonics are used to obtain the sound pressure at each microphone, then the SHB algorithm is used to obtain the acoustic image [6]. The scan zone is a grid of points 90×180, respectively in elevation and azimuth, and is applied at 2 m. The ellipse and the solid angle are calculated at -9 dB to further distinguish the two methods and reach the sidelobes. For acoustic images at $kr = 1$ (low frequency) and $kr = 6$ (high frequency), the truncation order N is equal to 2 and 5, respectively.

2.2 Covariance ellipse

Spatial resolution with the covariance ellipse method to assess the area ratio in the acoustic image consists in computing the area of an ellipse whose radii correspond to the eigenvalues of a covariance matrix from the acoustic image data at a chosen dynamic [3]. The computed surface area is then normalized by the theoretical maximum, that is $\pi \times 90^{\circ} \times 180^{\circ}$ in an arbitrary unit and leads to $\overline{S}$.

2.3 Solid angle

The solid angle is a quantitative method used in various scientific fields to assess the spatial dispersion of light, energy, particles, and the apparent size of celestial objects for instance. For acoustic imaging, the spatial resolution with the proposed solid angle is based on the calculation of the ratio of a portion of the sphere's surface area to the square of the sphere's radius. The infinitesimal solid angle is defined as,

$$\mathrm{d}\Omega = \frac{\mathrm{d}S}{r^2} = |\mathrm{d}(\cos\theta)\mathrm{d}\phi|, \tag{1}$$

where θ is the elevation angle, ϕ the azimuth angle and the total solid angle over a sphere is $\int \mathrm{d}\Omega = 4\pi$ in steradian (sr) [9]. Then, Eq. (2) is decomposed into a sum of finite differences and a normalized solid angle is computed from the acoustic image data at a chosen dynamic given by,

$$\overline{\Omega} = \frac{1}{4\pi}\sum_{i}^{I}(-\cos\theta_{i+1} + \cos\theta_i)(\phi_{i+1} - \phi_i), \tag{2}$$

where (θ_i, ϕ_i) are a set of positions around (θ_l, ϕ_l) positions where $l = 1, ..., L$ is the index of a scan grid and $i = 1, ..., I$ is the index of mid-positions around (θ_l, ϕ_l) of a scan grid. The number of scan grid positions is $L = N_\theta \times N_\phi$ and the number of mid-positions is $I = (N_\theta + 2) \times (N_\phi + 2)$ where N is the number of positions per angle. Attention is given to the continuity of the angular periodicity, *i.e.* $\theta = \pi = 0\,[\pi]$ and $\phi = 2\pi = 0\,[2\pi]$, enabling computation on the whole sphere. Thus, the computation around each position (θ_l, ϕ_l) in the acoustic image represents a fraction of the total solid angle.

3 Results

For $kr = 1$ and for the source directly in front of the SMA, (see in Fig. 1.a), the mainlobe is uniform and both meth-

*kevin.rouard.1@ens.etsmtl.ca
†thomas.padois@irsst.qc.ca

ods provide similar values of area ratio: $\overline{S} = 20\,\%$ and $\overline{\Omega} = 19.1\,\%$. In Fig. 1.b) the source is in front of the SMA near the floor and the mainlobe is spread out towards the south pole due to the spherical plane, although it is the same source as before. The normalized ellipse area increases to $48\,\%$, while the normalized solid angle remains stable at $19.2\,\%$. In Fig. 1.c) the source is almost behind the SMA near the floor, the map is similar, but part of the source shape is transferred to the other side of the acoustic image: $\overline{S} = 82.4\,\%$ is larger and $\overline{\Omega} = 19.2\,\%$ remains unchanged. For $kr = 6$, the source is directly in front of the SMA, (see Fig. 1.d), the mainlobe is smaller and two symmetrical sidelobes appear. In this case $\overline{S} = 28.1\,\%$, which is much larger than the solid angle value $\overline{\Omega} = 7.1\,\%$.

The results for $kr = 1$ show that the solid angle method has a low computational error with respect to the position of the source compared to the ellipse method. The ellipse may exceed the acoustic image frame when the mainlobe is distorted around the poles. The ellipse calculates the lobe area from the radii in a plane, while the solid angle considers the spherical plane, and the solid angle reflects the quality of the acoustic image with a SMA. For $kr = 6$ there are sidelobes and the ellipse surrounding them and exceeding the acoustic image frame, which leads to a high value of the criterion, while the solid angle calculates the sum of the emerging lobes at -9 dB, which leads to a lower value. Sidelobes position affects the value of the ellipse, potentially leading to the misinterpretation of a large mainlobe.

In the literature, the acoustic source is often located in front of the SMA and therefore the source is located at the center of the image. In this case and without sidelobes, similar values are found for both methods. In practice, the source may be close to the ground or ceil (toward a pole) or off-axis of a SMA, and in these cases the solid angle is more suitable than the ellipse.

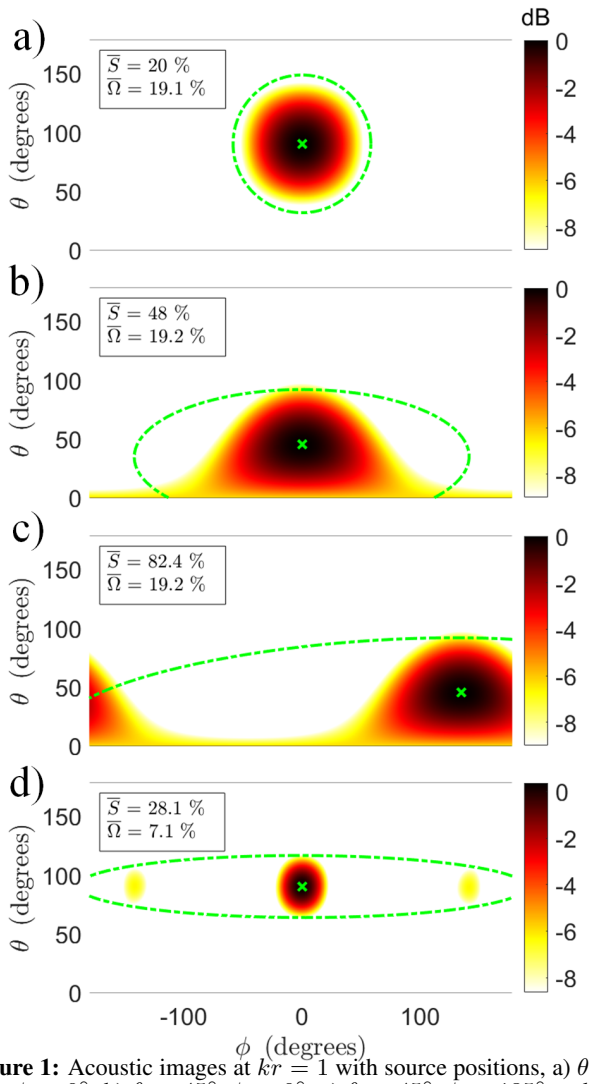

Figure 1: Acoustic images at $kr = 1$ with source positions, a) $\theta = 90°, \phi = 0°$, b) $\theta = 45°, \phi = 0°$, c) $\theta = 45°, \phi = 135°$ and d) at $kr = 6$ with source position $\theta = 90°, \phi = 0°$, the green cross depicted the source position, computed ellipse is depicted in green dashed line and solid angle is computed on displayed colormap.

4 Conclusions

Spatial resolution criteria have been compared, such as the covariance ellipse and the proposed solid angle. Both methods give a similar value when the source is centered in the acoustic image and in low frequency. Differences between these methods occur when the source position is near the edges or when there are sidelobes at high frequency. The values given by the solid angle method, calculated in the spherical plane, are not sensitive to the source position. Therefore, this method is more robust to assess the image quality in the presence of different sources.

References

[1] E. Sarradj. Three-Dimensional Acoustic Source Mapping with Different Beamforming Steering Vector Formulations. *Advances in Acoustics and Vibration*, 2012:1–12, 2012.

[2] P. Chiariotti, M. Martarelli, and P. Castellini. Acoustic Beamforming for Noise Source Localization – Reviews, Methodology and Applications. *MSSP*, 120:422–448, 2019.

[3] T. Padois, J. Fischer, C. Doolan, and O. Doutres. Acoustic Imaging with Conventional Frequency Domain Beamforming and Generalized Cross-correlation: a comparison study. *Applied Acoustics*, 177:107914, 2021.

[4] L. H. Carneiro and A. Berry. Unsupervised Environmental Sound Source Localization and Acoustic Image Analysis of Geometry-Optimized Spherical Microphone Arrays Using the Generalized Cross-Correlation. In *e-Forum Acusticum 2020*, pages 305–312, Lyon, France, 2020. hal-03231913.

[5] T. Padois, J. St-Jacques, K. Rouard, N. Quaegebeur, and al. Acoustic Imaging with Spherical Microphone Array and Kriging. *JASA Express Lett*, 3(4):042801, 2023.

[6] K. Rouard, J. St-Jacques, F. Sgard, H. Nelisse, and al. Numerical Comparison of Acoustic Imaging Algorithms for a Spherical Microphone Array. In *BeBeC*, Berlin, Germany, 2022.

[7] J. St-Jacques, K. Rouard, F. Sgard, H. Nélisse, and al. Effect of the Error on the Sound Speed and Microphone Position on Acoustic Image Obtainde With a Spherical Microphone Array. volume 50-3, page 132, St. John's, Canada, 2022.

[8] R. H. Hardin and N. J. A. Sloane. McLaren's Improved Snub Cube and Other New Spherical Designs in Three Dimensions. *Discrete & Computational Geometry*, 15(4):429–441, 1996.

[9] H. J. Weber and G. B. Arfken. Chap. 2 - Vector Analysis in Curved Coordinates and Tensors. In *Essential Mathematical Methods for Physicists*. Academic, San Diego, 6th edition, 2003.

INFLUENCE OF THE SCATTERING EFFECT ON ACOUSTIC IMAGE OBTAINED WITH A SPHERICAL MICROPHONE ARRAY

Julien St-Jacques [*1], Kevin Rouard [1], Franck Sgard [2], Hugues Nélisse [2], Alain Berry [3], Nicolas Quaegebeur [3], François Grondin [3], Loic Boileau [3], Olivier Doutres [1] and Thomas Padois [†2].

[1]École de technologie supérieure (ÉTS), Montréal, Québec, Canada.

[2]Institut de recherche Robert-Sauvé en santé et en sécurité du travail (IRSST), Montréal, Québec, Canada.

[3]Université de Sherbrooke (UdeS), Sherbrooke, Québec, Canada.

1 Introduction

In Quebec, occupational deafness was the most identified work-related disease representing 89% of the cases from 2015 to 2016 [1]. The most efficient solution is to reduce the noise emitted by the source. To do so, each source must be characterized by their spatial location and contribution. In a workplace, a Spherical Microphone Array (SMA) can be used. When the microphones are held on a wireframe structure or on thin rods, the SMA is considered acoustically transparent and is referred to as open. For open SMAs, the Conventional Beamforming in the Frequency domain (CBF) can be used and does not account for the scattering effect. When the microphones are flush mounted to a rigid sphere, the SMA is referred to as rigid. Rigid SMAs may cause the scattering of the sound field around the sphere. Consequently, frequency dependent errors in the time delays measured by the microphone pairs in the shadowed zone are expected [2]. The aim of this study is to assess the influence of the scattering effect on acoustic images obtained with a rigid SMA using the CBF. First, the microphone signals are obtained numerically and then the acoustic images are generated using the CBF algorithm for the case of a rigid and a transparent SMA. Then, the influence of the scattering effect is assessed using two image quality criteria. Section 2 presents the formulation of the CBF. Section 3 details the SMA design, the simulation parameters, and the image quality criteria. Section 4 presents the numerical results.

2 Convetional Beamforming

In the frequency domain, the acoustic image $\boldsymbol{A}(\omega)$ is provided by

$$\boldsymbol{A}(\omega) = \boldsymbol{W}^*(\omega)\boldsymbol{C}(\omega)\boldsymbol{W}(\omega), \tag{1}$$

where $\boldsymbol{W}(\omega)$ is the steering matrix, $\boldsymbol{C}(\omega)$ is the cross-spectral matrix and $(\cdot)^*$ denotes the complex conjugate transpose operator [3]. Using an SMA of Q microphones and a scan grid of L points, the dimensions of $\boldsymbol{W}(\omega)$ and $\boldsymbol{C}(\omega)$ are $[Q \times L]$ and $[Q \times Q]$ respectively. For the CBF, the steering matrix is obtained
using the free-field Green's function with

$$\boldsymbol{W}(\omega) = \frac{1}{Q}\frac{\boldsymbol{g}(\omega)}{\boldsymbol{g}^*(\omega)\boldsymbol{g}(\omega)}, \tag{2}$$

where one element of the Green's free-field matrix $\boldsymbol{g}(\omega)$ is given by

$$g_{ql} = \frac{1}{4\pi r_{ql}} e^{\frac{i\omega r_{ql}}{c_0}}. \tag{3}$$

In equation (3), c_0 is the sound speed, i is the complex imaginary number and r_{ql} is the distance between the q^{th} microphone and the l^{th} grid point. The cross-spectral matrix is obtained with

$$\boldsymbol{C}(\omega) = \boldsymbol{p}(\omega)\boldsymbol{p}^*(\omega) \tag{4}$$

where $\boldsymbol{p}(\omega)$ is the microphone signal vector of dimension $[Q \times 1]$.

3 Methodology

3.1 Array Design

To assess the influence of the scattering effect, two types of SMA are considered. A rigid array (Figure 1-a) is compared to a theoretical perfectly transparent array (Figure 1-b) referred as the empty SMA. The chosen microphone geometry is based on a commercial SMA commonly used in the literature [4]. The SMA radius is 9.75 cm and has 36 microphones.

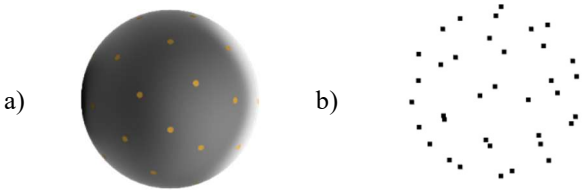

Figure 1: a) Rigid array b) Empty array, 36 microphones geometry, 9.75 cm radius.

3.2 Simulation Parameters

The microphone signals are obtained using a Finite Element Analysis (FEA) model to simulate a point source located at 1 m in front of the SMA. The model is a spherical domain of 1 m in diameter with a perfectly matched layer of 0.1 m to mimic an open infinite domain and avoid reflections. The simulation was done for frequencies ranging from 50 to 4000 Hz.

3.3 Image Quality Criteria

To assess the influence of the scattering effect on the acoustic image, two criteria are used, *i.e.,* the Ellipse Area Ratio

[*] julien.st-jacques.1@ens.etsmtl.ca

[†] thomas.padois@etsmtl.ca

(EAR) and the Mainlobe-to-Sidelobe Ratio (MSR). The EAR is the mainlobe area at -3 dB from the maximum value normalized by the total image area expressed in (%). The mainlobe area is surrounded by an ellipse using the covariance method [5]. A small EAR is preferred to allow for a better localization. The MSR is the level difference between the mainlobe and the highest sidelobe. Since sidelobes are spurious sources, an ideal MSR should be high.

4 Numerical Results

4.1 Ellipse Area Ratio

The EAR results for the rigid and the empty arrays using the CBF algorithm, and the 36-microphones geometry are presented in Figure 2-a. When the EAR criterion is greater than 30%, the image is considered of poor quality, as the mainlobe is too wide (red dashed line). If two sources are to be localized, a mainlobe greater than 30% for both sources would represent more than half of the image, making the localization difficult. The EAR assessed with the rigid array and the CBF is smaller than the ones obtained with the empty SMA for the full frequency range. With the rigid SMA, the source is first considered localized at 670 Hz, while the same result is observed with the empty SMA at 800 Hz. This result could be explained by the time delay between two microphones since the EAR is dependent of the frequency and the SMA radius. Using the CBF, a larger SMA radius will result a smaller mainlobe width for a given frequency. For the empty SMA, the acoustic wave travels through the sphere, therefore the largest distance is the SMA diameter. On the other hand, for the rigid SMA, the acoustic wave is diffracted and travels along the surface of the sphere thus the largest distance is half the perimeter [6].

4.2 Mainlobe-to-Sidelobe Ratio

Figure 2-b presents the MSR measured with the rigid and empty SMA using the CBF for the 36-microphones geometry. The red dashed line represents a -6 dB threshold where the sidelobes are considered too high to properly localize the source. The grey zone delimits the frequency range where no sidelobe are measurable for the rigid SMA since the mainlobe is very large. The MSR assessed with the rigid SMA is higher when compared to the empty SMA for the full frequency range with a maximum difference of 4.75 dB at 2800 Hz. At 3550 Hz, the MSR measured with the rigid SMA reaches a maximum of -6.15 dB, which is barely inside the permitted zone by the threshold. Therefore, the empty SMA provides a better MSR since there is no scattering effect.

5 Conclusion

The aim of this study was to assess the influence of the scattering effect on the acoustic images obtained with a SMA using the CBF. A rigid and an empty SMA with a radius of 9.75 cm and a 36-microphones geometry were considered. The microphone signals were obtained numerically with an FEA model for the case of a single point source in front of the SMA. The acoustic images were generated using the CBF

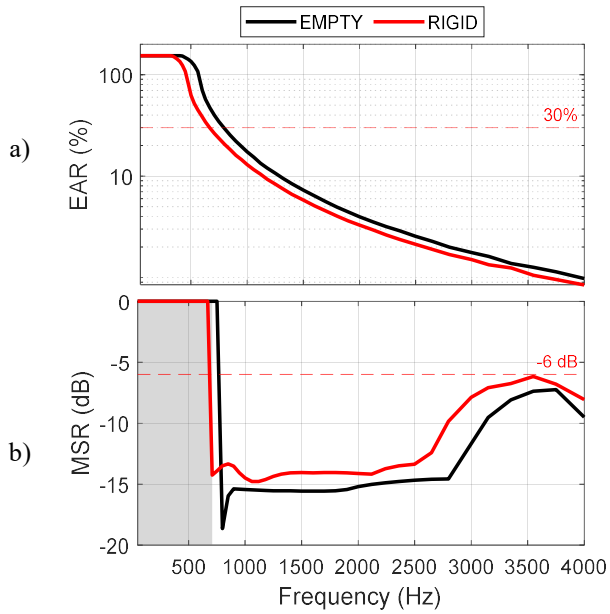

Figure 2: Acoustic images obtained with the CBF algorithm for the rigid and empty SMA of 9.75 cm radius for a point source located at 1 m a) Ellipse Area Ratio b) Mainlobe-to-Sidelobe Ratio. The grey zone delimits the frequency range for which no sidelobe can be measured for the rigid SMA since the mainlobe is too large.

algorithm, which does not account for the scattering of the acoustic waves, for both SMAs. The EAR and the MSR criteria were used to assess the influence of the scattering effect on the image. Results show that the uncorrected scattering effect will provide a smaller mainlobe width. This effect could be related to the time delay between microphone pairs. Also, the scattering effect increases the sidelobes levels, especially in the higher frequencies. The results of this study are valid for the case of a single point source located in front of the SMA. For the case of multiple point sources, different MSR values are expected.

References

[1] Busque, M., Lebeau, M., Tremblay, M., Boucher, A. & Duguay, P. (2022). Portrait statistique des lésions professionnelles indemnisées au Québec en 2015-2016. Montréal: Institut de recherche Robert-Sauvé en santé et en sécurité du travail.

[2] Heilmann, G., Meyer, A. & Döbler, D. (2008). Time-domain beamforming using 3D-microphone arrays. 2nd. Berlin Beamforming Conference.

[3] Padois, T., St-Jacques, J., Rouard, K., Quaegebeur, N., Grondin, F., Berry, A., Nélisse, H., Sgard, F. & Doutres, O. (2023). Acoustic imaging with spherical microphone array and Kriging. JASA Express Lett. 3(4), 042801.

[4] Chu, Z., Zhao, S., Yang, y. & Yang. Y. (2019). Deconvolution using CLEAN-SC for acoustic source identification with spherical microphone arrays. Journal of Sound and Vibration, Volume 440, p.161-173.

[5] Padois T., Fischer J., Doolan, C. & Doutres, O. (2021). Acoustic imaging with conventional frequency domain beamforming and generalized cross correlation: a comparison study. Applied Acoustics, Volume 177, 107914.

[6] Parkins, J.W., Sommerfeldt, S. D. & Tichy, J. (2000). Error analysis of a practical energy density sensor. JASA, 108 (1), p.211–222.

IMPROVING THE DETECTION OF MELODIC SEQUENCES THROUGH THE ADDITION OF INHARMONIC FREQUENCIES

Connor Wessel *[1], Michael Schutz †[1,2]
[1]Department of Psychology, Neuroscience, and Behaviour, McMaster University, Hamilton, Ontario,Canada
[2]School of the Arts, McMaster University, Hamilton, Ontario, Canada

1 Introduction

Our auditory system is continually challenged to extract signals informing us about our environment, filtering out noise and irrelevant signals. Detection and discrimination are two processes that are crucial in this endeavor. The former is our ability to perceive specific sounds, whereas the latter is distinguishing between signals.

Detection can be influenced by perceptual grouping of sounds in our environment. Duplex perception is an example recorded in linguistics literature, in which a 'chirp' presented binaurally alongside a verbal consonant can be simultaneously perceived as contributing to and independent from the consonant [1]. This can also apply to non-verbal sounds and to harmonic tones with a single-mistuned harmonic [2, 3].

Since duplex perception can trigger through mistuning harmonics, this creates a gateway through which to explore its role in detectability. Inharmonicity can be beneficial for grabbing attention, thereby leading to greater detection [4, 5]. Consequently, introducing inharmonic frequencies into otherwise simple harmonic tones could aid detection of these simple tones through the partial perceptual binding established by duplex perception. This study explored the possibility by measuring participants' ability to identify melodic sequences with additional, inharmonic frequencies in noise.

2 Method

2.1 Participants

We recruited sixty students at McMaster University, who received course credit as compensation for their time. Participants completed the study online and received instruction to use a laptop/desktop computer with headphones.

2.2 Materials

We designed three tones for this experiment, each of which contains two components: the harmonically simple 'base' tone, and the complex higher harmonics. The base tones contain three harmonics, including the fundamental, and two overtones along the harmonic series. The higher pitched harmonics contain 10 frequencies, starting at 2000 Hz, and increasing at a rate of 1000 Hz – n x 100 Hz. Each tone lasts 500 ms, starting with a 5 ms linear ramp and ending with a 495 ms exponential decay.

We manipulated three aspects of the sounds, including i) the melodic contour of the higher-pitched harmonics, ii) the direction of the sequence, and iii) the signal-to-noise ratio (SNR). For the first, the tones could either be 'tracking' (follow the same sequence as the base tones), 'stationary' (each tone is the same pitch), or 'absent' (higher harmonics omitted). For the second, we arranged the tones into a three-tone sequence that either ascended or descended. Tracking higher harmonics also ascended and descended at the same frequency interval ratio. Lastly, we presented sequences at six different SNRs, ranging from -20 dB to -30 dB. Figure 1 provides an example of an ascending sequence.

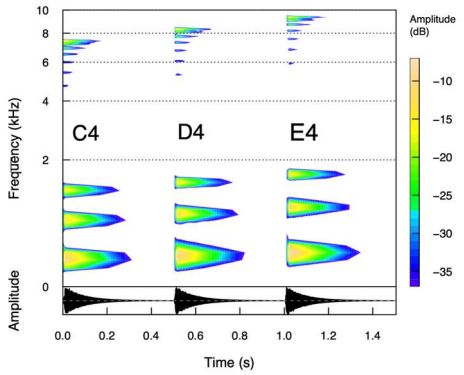

Figure 1: Spectrogram of the three tones within the ascending sequence. The horizontal axis displays time (s), and the vertical axis displays frequency (kHz). The three frequencies at the bottom between 0-2 kHz represent the 'base' sequence, while the frequencies between 4-10 kHz represent the 'higher harmonics.' The labels represent the musical pitch of each tone.

2.3 Procedure

The dependent variables for this experiment include the proportion of correctly identified sequences (ascending or descending) and average reaction times in each trial (ms). This experiment followed a 3 (higher harmonic type) x 2 (sequence) within-subjects design.

We started by presented participants with examples of the stimuli. Participants received instructions to guess the sequence of just the base tones and not the higher harmonics. After completing practice trials, participants underwent 180 experimental trials. This involved presenting the target sound simultaneously with background noise. For 3000 ms afterward, participants received instruction to press 'a' if they heard an ascending sequence, or 'd' if they heard a descending sequence. Failure to respond marked a trial as a miss, leading to its exclusion from analyses.

* wesselc@mcmaster.ca
† schutz@mcmaster.ca

3 Results

3.1 Accuracy

We define accuracy as the average proportion of correctly identified sequences within a given condition. We analysed this data using a two-way within-subjects ANOVA, using Greenhouse-Geiser corrections where required. Figure 2 presents the proportion of correct trials split across the presence of higher harmonics.

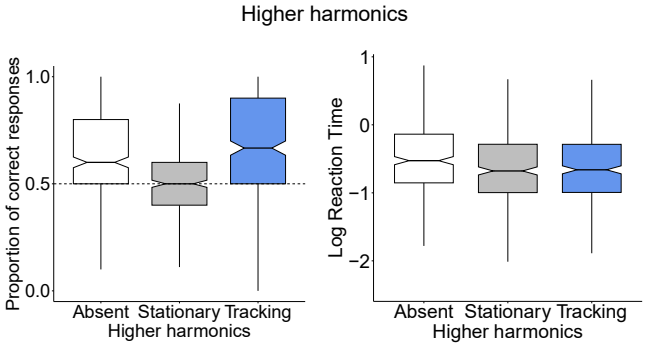

Figure 2: Boxplot displaying the average proportion of correct responses (left) and log reaction time (right) for each type of higher harmonics. The dotted line for proportion represents chance performance (0.5).

We found the presence of higher harmonics significantly affected accuracy, $GG(114) = 0.84$, $p < .001$. Tracking harmonics produced the highest accuracy (M = 0.68, SD = 0.47) and stationary produced the lowest (M = 0.49, SD = 0.50), while their absence falls in the centre (M = .62, SD = .50). A subsequent Tukey test found that comparisons between all types yielded significant differences.

3.2 Response time

We took the average, log-transformed time to press a key in each trial. While we used log transformed values in the analysis, we report raw values for clarity. Figure 2 presents the average response times across the presence of higher harmonics.

We found a significant effect of the presence of higher harmonics, $F(114) = 19.58$, $p < .001$, with lower response times for stationary (M = 566 ms, SD = 528 ms) and tracking (M = 568 ms, SD = 519 ms) vs. absent (M = 667 ms, SD = 546 ms) harmonics. A subsequent Tukey test found that absent sequences yielded significantly different response times from tracking and stationary but tracking and stationary did not differ from each other.

4 Discussion

Adding higher harmonics to a melodic sequence reduced response time and led to context specific effects on accuracy. Specifically, accuracy increased when higher harmonics tracked the melodic sequence of the base tones and decreased when they remained stationary.

Overall, the tracking higher harmonics improve detectability while stationary harmonics reduce it to chance level. This implies that the higher harmonics overwhelm perception of the base tones. Presumably, the tracking higher harmonics lead to better performance as they contain the task-relevant information, whereas the stationary harmonics block it out. This could also be a matter of attention being drawn to the higher harmonics and not to the base tones.

In terms of duplex perception, it is unclear whether the partial perception binding occurred due to the potential overshadowing. This could be addressed by either (1) adjusting the intensity of the higher harmonics relative to the base tones or (2) introducing greater separation between the base tones and higher harmonics by manipulating further parameters of the sound, such as amplitude envelope. If differences in accuracy emerge between different degrees of separation, this can suggest the extent to which higher harmonics bind with the base tones. In terms of duplex perception, we can test the limits on how varied two components of a sound can be to produce dual states of perception.

5 Conclusion

Adding higher harmonics to tones can provide context dependent boosts in detectability. This relies on the higher harmonics containing the information through which participants derive required meaning. While the question of how partial perceptual bindings plays a role will require further exploration, the boost in detectability for tracking higher harmonics is meaningful in practical contexts, such as alert design.

Acknowledgments

This work was supported by Natural Sciences and Engineering Research Council of Canada (NSERC), the Canadian Foundation for Innovation, and the Auditory Performance Division of the US Navy and the Office of Naval Research Grant N00014-22-1-2184.

References

[1] Liberman AM, Isenberg D, Rakerd B. Duplex perception of cues for stop consonants: Evidence for a phonetic mode. *Perception & Psychophysics* 1981; **30**(2): 133–143

[2] Fowler CA, Rosenblum LD. Duplex perception: A compar-ison of monosyllables and slamming doors. Journal of Ex-perimental Psychology: Human Perception and Perfor-mance 1990; 16(4): 742–754

[3] Moore BCJ, Peters RW, Glasberg BR. Thresholds for the detection of inharmonicity in complex tones. The Journal of the Acoustical Society of America 1985; 77(5), 1861–1867

[4] Bonin T, Smilek D. Inharmonic music elicits more negative affect and interferes more with a concurrent cognitive task than does harmonic music. Atten Percept Psychophys 2016; 78(3): 946–959

[5] McPherson MJ, Grace RC, McDermott JH. Harmonicity aids hearing in noise. Atten Percept Psychophys 2022; 84(3): 1016–1042.

Abstracts for Presentations without Proceedings Paper
Résumés des communications sans article

Design And Dissemination Of Environmental Noise Maps: Recommendations For The Province Of Québec

Frédéric Hubert, Jean-Philippe Migneron

Noise is today one the most harmful factors to the population health (sleep disorder, stress, well-being, heart attack). As part of its Health Prevention policy, the Government of the province of Québec has initiated a project on the analysis of noise mapping methods. The goal is to evaluate their applicability for the province of Québec. The objective of our presentation is to describe the main steps of this analysis, realized by a team of researchers from Laval University with varied expertise (acoustic, geography, geomatic). A systematic review was first made to get a better understanding of the applied methods used for noise mapping through the world between 2005 and 2019. Among the results obtained, a typology of these methods was defined. Some methods (i.e., 2D/3D simulation, based on acoustic surveys) were then tested in three locations (Laval University, Montmagny and La Pocatière). An analysis of criteria was carried out to benchmark the added value of such methods. Open-source software or databases for geospatial were also tested to disseminate acoustic data through the Internet: Noise-Planet, NOISE, and the governmental infrastructures IGO, and Territoires. Various recommendations and reflection avenues were finally suggested to the inter-ministerial group of experts on environmental noise (GEIBE) from acoustic and geomatic points of view, such as improving the sharing of acoustic and geospatial data, centralizing road traffic data, studying acoustic models (CNOSSOS, TNM, etc.), creating a technical observatory of environmental noise, and designing a noise monitoring and mitigation infrastructure based on digital twins in an urban environment.

Is Friday The New Saturday? The Impact Of Using Standard Traffic Distribution Models For Friday Traffic Data On Noise Assessment

Kathryn Joanne Katsiroumpas, Morgan Austin

The COVID-19 pandemic has had a prolonged impact on commuter traffic in urban areas as working from home, hybrid work models and flexible office hours continue to remain acceptable alternatives for many workplaces. Examination and comparison of post pandemic traffic to standard traffic distribution models and historical distributions in various Canadian cities have shown that post pandemic changes to the traffic patterns on Fridays remain and are more significant than other days of the week. Universally accepted standards of hourly traffic distributions, from sources such as the ITE, are typically used by acousticians when analysing road traffic noise. Post pandemic traffic distributions and "real-time" traffic congestion data for Fridays in various major Canadian cities were examined and compared to standard hourly traffic distributions for both weekdays and weekends to determine best fit. For acousticians this has implications on sound exposure analysis that is based on road traffic noise prediction modelling and field measurement as well as establishing sound level limits for stationary sources. Regional differences in the applicability of standard traffic distributions to Friday traffic patterns are also discussed.

Effective Methods For Reducing Construction Noise In Densely Populated Environment

Loic Sauvageot

Urban environments are subjected to several noise sources such as construction sites, road traffic, public transportation noise, recreational activities and etc. Those last sources are usually predictable and known, and residents are able to moderate their noise exposure by choosing the area where they live. However, at a time when cities are densifying their population, several construction site are rising for the construction of new dwellings, institutionnal services, city services and expending public transportation. In addition to several disturbances from construction sites, such as trafic deviation, dust, dirty roads, etc, noise is often unpredictable from one day to another and very few city by-laws are regulating construction noise expect moderating construction work hours. The possible high noise levels combined with unpredictable site schedule for the close neighborhood are often a source of stress and annoyance to the close residents of those work sites, especially when projects last more than a few months. After a few years monitoring construction site noise in the Montreal area, efficient noise mitigations were experimented depending on the type of activities on site. Some of the noisiest activities were successfully shouted using simple, affordable and available noise mitigations. The use of noise mitigation programs was one of the clue successfulness of noise reduction by targeting the noisiest activities and the actions required. In addition this article prays for more stringent by-laws to limit noise émission from work sites.

SHOCK AND VIBRATION - CHOCS ET VIBRATIONS

Abstracts for Presentations without Proceedings Paper
Résumés des communications sans article

Vibration Impacts Of Tunneling In Transit Construction

Christopher Bosyj

With the growth in construction of underground public transit systems, it is critical to have a comprehensive understanding of the vibration generated during subgrade construction activities. This study focuses specifically on the vibration impact of tunnel boring machines (TBMs) on surrounding structures and nearby neighborhoods, particularly examining the relationship between observed vibration levels at various distances from tunneling operations. There currently exists very limited literature relating vibration emissions to a variety of tunneling parameters, including TBM size, cutting speed, and geotechnical conditions. This study compares industry standard prediction methods against measured vibration data collected during TBM operations and aims to better define the correlation between these variables.

On The Robustness Of A Decoupling Procedure Used In Conjunction With An Indirect Method To Assess The Full Mobility Of An Aircraft Hydraulic Pump

Simon Prenant, Thomas Padois, Manuel Etchessahar, Olivier Doutres

Structure borne noise caused by small vibrating source is a significant concern for the aircraft manufacturers. Component-Based Transfer Path Analysis with Dynamic Substructuring (CB-TPA-DS) appears as promising methods for aircraft manufacturers to build internal processes to specify and validate the dynamic behavior of the vibrating systems, usually designed by supplier. CB-TPA-DS formulation is based on velocities and mobilities pertaining to the decoupled components of the final assembly (i.e., the vibrating source and its receiving structure) and their performance depends significantly on the accuracy of the substructure characterization. Mobilities and velocities have to be determined to account for rotational degrees of freedom. Indirect methods such as Virtual Point Transformation (VPT) or Equivalent Multi-Point Connection (EMPC) are often employed for this purpose, but they can result in cumbersome experimental setups and increased measurement uncertainties. Their full implementation on freely suspended source to assess its mobility at interface points can be challenging, especially because the sources found in aircraft have small interfaces. To address this issue, the mobility of the source can be assessed using a decoupling procedure, which is an indirect approach to identify the dynamic behavior of a substructure by attaching it to a test bench and characterizing both the test bench and the assembly. The proposed work aims to experimentally validate the applicability of a decoupling procedure used with an indirect method to assess the full mobility of an aircraft hydraulic pump. The mobility of the pump is determined though a decoupling procedure, using a steel plate as a test bench and both VPT and EMPC indirect methods in order to account for all degrees of freedom at the interface points. The robustness of the decoupling procedure is then evaluated by substituting the so obtained mobilities into the CB-TPA-DS's equation in order to predict the vibratory response of the assembly.

Field Measurement And Finite Element Modeling Of Vibration Propagation From Heavy Hard Impacts On Fitness Flooring

Giulio Puglielli, Simon Edwards, Brian Howe

This study presents an investigation into the attenuation of three different types of fitness flooring in response to standard heavy hard impact test conditions. The study aims to provide insights into the dynamic behaviour and modeling vibration propagation of heavy hard impacts above three different types of fitness flooring. Field measurements were conducted with locally-reacting fitness flooring on suspended concrete slabs. Three types of fitness flooring were tested, which varied in thickness, material composition, and physical structure. A 50 lb kettlebell was dropped from 0.5 m high onto the surface of each type of flooring, and accelerometers on the concrete slab measured the vibration at various distances and propagation angle from the impact point. Additional measurements were conducted on a concrete slab-on-grade, with an accelerometer mounted on top of the kettlebell to generate time-dependent forcing functions for use in finite element models. The frequency-dependent vibration responses of each flooring type were derived from these models and examined at frequencies of 500 Hz or below. At the frequency range of interest, the frequency-dependent vibration responses and propagation from these models agreed well with the general form of data from the field testing. This investigation into the methodology of measuring heavy hard impacts and the vibration response of fitness flooring contributes to the field of acoustics by characterizing the flooring performance in a repeatable and comparable way which can be used by consultants

to model effective vibration mitigation solutions in gyms and other environments where dropping heavy objects is a concern.

Rigid Body Motion Of Nail Guns : Modal Analysis And 2d Dynamic Modelling

Maxime Vincent, Marc-André Gaudreau, Thomas Dupont, Pierre Marcotte

In the construction industry, tools with (high amplitude) impulsive vibratory emissions, such as nail guns, can significantly affect the comfort and safety of workers. In order to reduce these hazards, it is necessary to study the dynamic behavior of those tools by generating predictive models that can be also used to enhance tool design. Thus, an experimental modal analysis was performed to get the mode shapes and natural frequencies of a nail gun using an accelerometer and an impact hammer. The rigid body modes were then fed into a 2D rigid body model of the nail gun. This model considers the tool's dimensions, mass, and moment of inertia, and it simulates the translational and rotational motions of the nail gun within a 2D plane. An optimization algorithm was then used to fine-tune certain parameters of the model, with the aim of minimizing differences between experimental and model-based rigid body mode shapes and natural frequencies.

A unique software system for extended acoustic analysis and prediction.

DataKustik is the leading software development company offering state-of-the art solutions in the field of acoustics modeling. Choose from several software solutions including:

– **CadnaA** for the calculation of noise outdoors
– **CadnaB** for the calculation of sound transmission between rooms
– **CadnaR** for the assessment of sound distribution indoors

Although each software is tailored to its specific field of application, they can be connected to form a powerful package for extended calculations from the outside to the inside and vice-versa. For any type of acoustic calculations, from sound propagation outdoors to the assessment of indoor sound, choose DataKustik. For more information about DataKustik products, count on Scantek for expert and responsive sales and support.

For inquiries about DataKustic products in North America contact:

Scantek©
LISTEN – FEEL – SOLVE
A RION COMPANY

800-224-3813
info@scantekinc.com
www.scantekinc.com

SOUNDSCAPE - ENVIRONNEMENTS SONORES

CHARACTERIZATION OF TYPICAL MUSIC ACTIVITIES IN CHINA: IDENTIFICATION, CLASSIFICATION AND QUANTIFICATION

Chang Miao [*1,2], Qi Meng [†1]
[1]School of Architecture, Harbin Institute of Technology, Harbin, China
[2] School of Information Studies, McGill University, Canada

1 Introduction

The impact of music sound in urban open spaces on crowd behavior is substantial. While previous studies have extensively investigated the effects of music sound on walking speed and dwell time, it is crucial to recognize that musical activity and music sound are distinct stimuli. Musical activities offer both visual and auditory experiences, often leading to group congregation. However, there is still a significant research gap concerning the group behavioral characteristics and acoustic environment attributes of musical activities.
Hence, this study commences by categorizing and quantifying characteristic metrics associated with musical events. Subsequently, the focus shifts to identifying behavioral indicator features that influence the acoustic environment during musical activities.

2 Methods

2.1 Selection of musical activities

The musical activities selected for this study were classified into two groups: movement and non-movement activities, based on their metabolic equivalents and intended purpose. Movement music activities, with a metabolic equivalent higher than 3 MET, were primarily designed for exercise, such as square dancing. Conversely, non-movement music activities, with metabolic equivalents below 3 MET, were intended for entertainment purposes, such as instrumental performances.

The inclusion of specific musical activities in the study was guided by two primary criteria. Firstly, the activities had to be regularly conducted on a daily basis, rather than being large-scale organized gatherings like concerts or festivals. Secondly, the selected musical activities needed to involve group behavior, meaning that the number of participants was greater than five.

2.2 Measurement of Sound Environment

To ensure accuracy, SPL measurements were initiated when the number of participants in a musical activity exhibited minimal variation, with no more than five changes observed within a five-minute period after the activities had been underway for some time. In this study, the sound pressure level was measured at a distance of 5 meters from the music loudspeakers. The level meter was set to fast mode and A-weight mode, and readings were recorded at 5-second intervals. A total of 3 minutes of data was collected for each musical event.

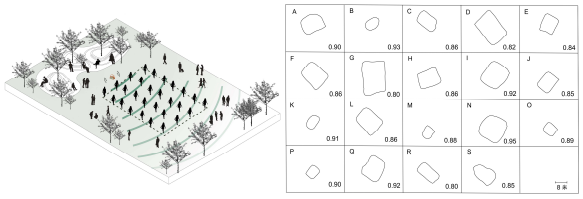

Figure 1: Example of factor form for musical activities

2.3 Observation of Crowd Behaviors

The primary objective of this study was to investigate the characteristics of crowd behavior at musical events. To achieve this, the observational method was employed as the preferred research approach.

For the selection of crowd parameters, we took into consideration previous studies and identified three key indicators: the number of participants, the occupied area, and the shape of the activities. In this study, a novel parameter for quantifying crowd behavior, namely the crowd activity Form Factor, is proposed. When examining the crowd shape aspect, we refer to relevant studies on blade shape quantification in the context of blade vibration [1]. Its formula is $F = 4\pi \mathrm{A}/\mathrm{P}^2$ (F : Form Factor, A:Area, P:Perimeter).

The participation numbers were documented through direct on-site observations. To capture the footprint and perimeter of the event, GPS instrumentation was utilized. The researcher carried the instrument while walking along the boundaries of the event crowd, allowing the instrument to automatically record the path and capture latitude and longitude coordinates.

2.4 Analysis

SPSS 23 was used to establish a database with all the result. In the present study, the power analysis was used to test sample sizes. For data that met normality, an independent samples t-test was employed. G-power test determined that the minimum sample size per group was no less than 30, resulting in a total sample size of 60. For non-normally distributed data, the Mann-Whitney U test was utilized , requiring a minimum sample size of 32 per group and a total sample size of 64. All sample size requirements were met in this study. After careful screening in this study, 91 datasets were chosen for analysis from the initial pool of 105 musical activities. These datasets comprised 51 movement musical activities and 40 none-movement musical activities. In regression analysis, curve fitting was conducted using linear regression.

[*] changmiao0211@gmail.com
[†] mengq@hit.edu.cn

3 Results

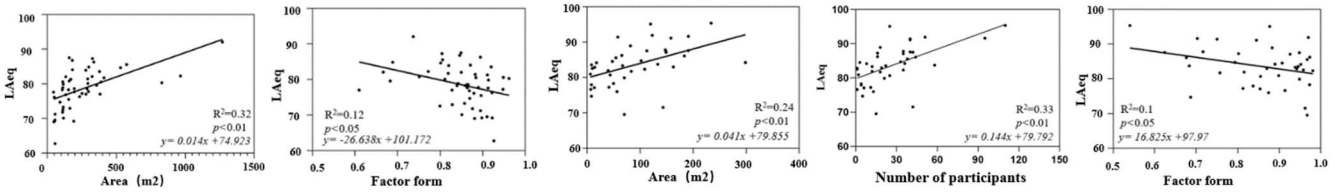

(a) (b) (c) (d) (e)

Figure 2: Effect of behavioral indicators of Movement musical activities on SPL (a ,b movement musical activities; e,f,d none-movement musical activities)

Table 1: Description of musical activities indicators

	LAeq	Lmax	Lmin	Number of Participants	Area	Factor form
A	78.56±5.79	87.86±6.12	63.00±7.42	33.12±27.83	90.86±70.53	0.85±0.07
B	83.58±5.90	93.53±5.64	61.08±7.35	26.30±23.68	258.07±233.6	0.86±0.11
p	0.000**	0.023	0.000**	0.219	0.735	0.000**

(A Movement musical activity; B none-movement musical activities)

3.1 Comparison of movement and none-movement musical activities

The results indicate that the sound pressure level (LAeq and Lmax) during music activities that involve active movement is substantially lower (around 5dB) than during music activities that do not involve movement. The area of movement music activities is 2.84 times larger than non-movement music activities; the number of participants is 1.26 times larger, and the morphology parameters are around 0.86(Table 1).

3.2 Influence of behavioral characteristics of musical activities on acoustic environment

In terms of the correlation between behavioral indicators and LAeq, the LAeq of movement musical activity increases by 1.4 dBA for every 100 square meters of activity area (Fig2a); Its LAeq is not affected by the number of participants. The form factor has a negative correlation with the LAeq, indicating that as the form factor increases, the LAeq decreases. In other words, activities with a more circular shape tend to have lower LAeq (Fig2b).

The LAeq of non-movement music activity increases by 4.1 dBA for every 100 square meters of activity area (Fig2c); the LAeq increases by 1.4dBA for every 10 additional participants(Fig2d). A tendency can be observed where activities with a more circular shape, indicated by larger values of the form factor, correspond to lower sound pressure levels (Fig2e).

4 Discussion

We observed a significant influence of behavioral parameters on the acoustic environment during musical activities. This implies that controlling crowd behavior can effectively reduce the SPL. Among the behavioral parameters, we found that crowd activity area and shape play crucial roles.

However, due to the random nature of crowd behavior during musical activities, our sample was collected from multiple open spaces. This might introduce the influence of spatial morphology on the determination of behavioral boundaries. Therefore, in future research, it would be beneficial to increase the sample size and compare music events within the same space to address this limitation.

This study addresses a crucial gap in the soundscape field by exploring the impact of behavior on the sound environment. The proposed activity factor form enables quantification and graphical characterization of behavior. However, it is worth noting that this study focused solely on the characteristics of the crowd participating in the music activities. In future studies, it would be essential to consider the impact of music events on the perception and behavior of the pedestrian crowd to gain a more comprehensive understanding

5 Conclusion

The LAeq of movement music activities is dominantly correlated to the area of the activity rather than the number of participants and crowd density. Controlling the area of the activity can effectively reduce the ambient sound pressure level of movement music activities. For non-movement music activities, we need to consider both the area of activities and the number of participants to effectively reduce the impact on the acoustic environment. Hence, we can control the scale and shape of the music activity through reasonable planning and division, which could provide guidance to enhance the acoustic experience of urban public space

Acknowledgments

The authors would like to thank Catherine Gustivino(McGill University) and Mengmeng Li.

References

[1] Wang, X. F., Huang, D. S., Du, J. X., & Zhang, G. J. (2006). Feature extraction and recognition for leaf images. Computer Engineerin g and Applications, 3, 190-193.

BRIDGING THE GAP BETWEEN SOUND AND NON-SOUND PROFESSIONALS WITH AURALIZATION TOOLS

Richard Yanaky *[1,2], Catherine Guastavino †[1,2]
[1]Multimodal Interaction Laboratory, School of Information Studies, McGill University
[2]Centre for Interdisciplinary Research in Music Media and Technology

1 Introduction

A soundscape approach to design, despite its long existence as a topic of research, is still radically novel to the public and private sector and remains an untapped resource for most urban sound planning. Current sound planning practices remains dominated by a focus on identifying and limiting sound levels and are performed near-exclusively by specialized sound engineers (e.g. acousticians), supported by relevant sound-level based tools. In contrast, the soundscape approach goes several steps beyond sound levels to focus on the entire auditory experience, in which sound levels play a contributing role. However, uptake of soundscape practices to consider the auditory experience remains a major challenge due to both a lack of tools, *and* professionals trained to consider the auditory experience within the urban planning context. This work presents a new auralization tool, City Ditty, to help bridge this gap between sound and non-sound professionals, and argues in favour of a new profession – an urban sound design facilitator, to act as an intermediary.

1.1 Generating meaningful feedback from stakeholders to support better sounding cities

Urban sound planning is a complex process that, for this context, involves three major groups of stakeholders. First are the acoustic experts who perform the majority of the sound planning; second are the other Professionals of the Built Environment (PBEs) who shape our cities (such as urban planners, designers, and policy makers), but are typically untrained in sound-related planning; and third, city users, who live, work, and play in the city. Currently, acousticians are responsible for the majority of the sound-planning process. Due to the complex and specialized nature of sound, this has typically excluded other PBEs and city users from sound-planning processes, resulting in small groups of people making large decisions that affect large and diverse groups of city users, without understanding how it impacts their daily lives. Furthermore, as PBEs don't typically consider sound in their own work [1], they often engage with acousticians late in the urban planning process, long after decisions have been literally built into the concrete [2], limiting potential sound-intervention possibilities.

To help overcome these issues, a more diverse set of stakeholders should be included in the sound-planning process, at a much earlier time. However, many public consultations can prove problematic, as good intentions with poor methodology for communication and feedback can result in ineffectual token efforts [3]. As current sound planning tools and procedures are sound-level based, this may not generate any meaningful feedback from non-sound experts, and may fail to address the diverse needs of city users or support collaboration with PBEs. It is unreasonable to expect the average city user – or even PBEs – to undergo enough sound training to understand and converse with acousticians at their level. However, discussion of the auditory experience is readily accessible to all – with a little bit of help.

Stakeholders must have a strong understanding of both the situation *and* the implications of proposed designs in order to support meaningful decisions. To facilitate this, simulations are required to demonstrate different design strategies. For example, there are many strategies to reduce unwanted traffic sounds: sound barriers block sounds, but are large, expensive, and can interrupt and/or fragment the urban fabric; installing water features can introduce calming sounds of water that help mask the sounds of traffic; installing quiet pavement or lowering speed limits reduce the sounds of vehicles; or pedestrianizing the area can remove it completely and encourage public space and commercial usage.

1.2 Using City Ditty for rapid development of soundscapes, by non-sound experts

While one-off simulations can be made by specialized experts, simple to use auralization tools can be invaluable to help PBEs to help them engage in early-stage sound planning. City Ditty is a first of its kind auralization tool that was designed through a user-centered design process to help identify the form and functions of such a new tool, as PBEs do not currently engage in sound design [4]. Taking the form of a virtual reality simulator, City Ditty provides a virtual 3D environment of an urban city that enables the user to walk around a virtual environment, listen to the soundscape anywhere in the 3D space, and modify the soundscape both directly and indirectly through simple interactions (Figure 1). Aside from being able to add, move, or remove sound sources from anywhere in the urban space, these interactions focus on giving the user control over different contextual factors (e.g. time of day, season, weather) to help show how soundscapes are always changing, albeit often in predictable ways. City Ditty includes a self-guided sound-awareness session with 36 different tasks, leading users through how to use the software while simultaneously teaching them about foundational principles of soundscape design. A first usability evaluation received positive responses and indicated that users, regardless of their experience, could complete both the learning phase, and implement their own simple soundscape designs in under an hour.

*Richard.Yanaky@mail.mcgill.ca
†Catherine.Guastavino@mcgill.ca

Figure 1: Users can create and listen to their own soundscapes under different contexts (e.g. time of day) with a single design. Software demos and related research can be found at https://www.youtube.com/@MultimodalInteractionLab.

2 Method

The current iteration of City Ditty has enhanced the audio capabilities to binaural output, and include better distance attenuation, sound occlusion, and reverberation, as well as switching from desktop virtual reality to head-mounted virtual reality [5]. Using this version, several usability studies are underway.

First, a usability study using head-mounted VR is underway to explore how to best encourage user engagement with PBEs and how such tools can be integrated into their workflow. This follows previous methodology [4], which invites PBEs from both private and public sector to go through the self-guided sound-awareness session to learn how to both learn to use the software in VR, as well as learn the basics of soundscape design. Questionnaire data on task difficulty, user engagement, and presence is collected, as is click data to perform task performance. These are supported by exit interviews to discuss their experiences and how they foresee potential future usage. This will be followed by an additional usability study which explores how such software can support collaborative designs with multiple users. Data collection is underway.

3 Discussion

Designing towards the auditory experience presents many challenges, amongst multiple stakeholders, which must all be addressed to support future adoption. For example, while City Ditty's first two iterations focus on addressing the needs of PBEs and how to motivate and support them with a soundscape approach to urban sound planning, a broader look at relevant stakeholders indicate further external challenges, outside of most of their control. Economic barriers, for one, may present uncertainty and ambiguity to decision makers who will determine whether or not such a tool as City Ditty is utilized – even if it is free to use [5]. Yanaky et al. discusses this in terms of an emerging technology framework [6] which outlines the pros of soundscape design against the uncertainty of their return on investment, in relation to current market and technology trends.

3.1 Urban sound design facilitators

A crucial question remains: Who will lead urban soundscape designs? A single person cannot speak for a diverse city, although they can facilitate discussion amongst a diverse group. Similarly, while tools like City Ditty can be easy to operate, there must be a knowledgeable person to guide the stakeholders through viable solutions. To perform effectively in this role, an urban sound design facilitator will need a working knowledge of soundscape research, governance and direction by human-centered sound policies and frameworks, accessible tools (like City Ditty) to help create adequate simulations, and continual collaboration and feedback from diverse stakeholders. Research has advanced in these individual topics, but not yet to the point required for integrating them into a proactive sound-planning practice. The pieces have been laid out and await integration for urban sound design facilitators to use. Such skills and experiences would also position these facilitators to be leaders in affecting policy and regulation change.

While this research focuses mainly on the research and development of suitable tools for designing towards an auditory experience, it has also come to understand through its user-centered design process that the 'ideal' user does yet truly exist – at least in a current professional capacity. We suggest that many early career soundscape researchers would make excellent candidates for this role, although expect that many acousticians and PBEs would also make excellent choices for this role as well, with further soundscape training.

Acknowledgments

Continued thank you to the Sounds in the City team, CIRMMT, our collaborators, and our funding agencies for helping to make this research possible.

References

[1] Steele, D., Bridging the gap from soundscape research to urban planning and design practice: how do professionals conceptualize, work with, and seek information about sound?, in Doctoral Dissertation. 2018, School of Information Studies, McGill University.

[2] Steele, D., E. Bild, and C. Guastavino, Moving past the sound-noise dichotomy: How professionals of the built environment approach the sonic dimension. Cities, 2023. **132**: p. 103974.

[3] Arnstein, S.R., A Ladder Of Citizen Participation. Journal of the American Institute of Planners, 1969. **35**(4): p. 216-224.

[4] Yanaky, R., D. Tyler, and C. Guastavino, City Ditty: An Immersive Soundscape Sketchpad for Professionals of the Built Environment. Applied Sciences, 2023. **13**(3): p. 1611.

[5] Yanaky, R., et al. Exploring the use of soundscape sketchpads with professionals. in INTER-NOISE and NOISE-CON Congress and Conference Proceedings. 2023. Chiba, Japan, August 20-23, 2023: Institute of Noise Control Engineering.

[6] Rotolo, D., D. Hicks, and B.R. Martin, What is an emerging technology? Research Policy, 2015. **44**(10): p. 1827-1843.

Abstracts for Presentations without Proceedings Paper
Résumés des communications sans article

Designing And Evaluating Public Space Sound Installations: A Collaborative Research-Creation Approach

Valérian Fraisse, Étienne Legast, Simone D'ambrosio, Catherine Guastavino

We present an interdisciplinary collaboration focusing on the 2-way interactions between researchers from McGill and sound artists from the collective Audiotopie. We report on the iterative process of design, deployment, and evaluation of four different sound installations over two years in a new public square in Montréal, QC.The research team conducted sound level measurement and observations of public space use to identify patterns of use and main activities conducted in the square at different times of day and week. We illustrate how the creative process of the sound artists was informed by these systematic observations, to compose sound installations that "resonate" with the desired ambiances throughout the day. The research team also administered questionnaires to passers-by in the absence and presence of the sound installations. The analysis of questionnaires indicated that public space user experience was enhanced in the presence of all four sound installations, whereby different contents reinforced aspects of the experience. These results highlight the potential of research-creation collaborations to shape urban soundscapes.

SPEECH AND HEARING - PAROLE ET AUDITION

BIOMECHANICAL SIMULATION OF LATERAL ASYMMETRY IN TONGUE BRACING

Jasia Azreen [*1], Connor Mayer [†2], Yadong Liu [‡3], Arian Shamei [♦3], Ian Stavness [♯4], Bryan Gick [♩3]
[1]Department of Electrical and Computer Engineering, University of British Columbia, Canada
[2]Department of Language Science, University of California, Irvine, United States of America
[3]Department of Linguistics, University of British Columbia, Canada
[4]Department of Computer Science, University of Saskatchewan, Canada

1 Introduction

Tongue bracing occurs when the lateral edges of the tongue maintain contact with the palate or upper molars. Bracing is pervasive in speech: previous electropalatogram (EPG) data analysis shows lateral contact is consistently maintained during speech [1]. This research has also indicated the presence of *lateral bias* or *asymmetry* in the tongue: a consistent tendency to release contact more on one side than the other, both in unilateral release and in sequential loss of contact during a bilateral release. The present study explores the muscle activations that underlie asymmetry in lateral tongue bracing through biomechanical simulations. Based on biomechanical simulations [2], certain muscles have been previously identified as *bracing agonists* (e.g., posterior and medial genioglossus (GGP, GGM), mylohyoid (MH), verticalis (VERT), and superior longitudinal (SL)) and *antagonists* (anterior genioglossus (GGA), styloglossus (STY), hyoglossus (HG), transverse (TRANS), and inferior longitudinal (IL)). Agonists tend to raise or widen the tongue and therefore increase the likelihood of bilateral bracing, while antagonists tend to lower or narrow the tongue and decrease the likelihood of bilateral bracing. This paper presents a set of biomechanical simulations using a 3D finite-element model of the vocal tract that explore how unilateral bracing can be achieved by asymmetric activation of agonists, antagonists, or a combination of the two. The results of these simulations suggest that unilateral bracing may be instantiated primarily by contra-lateral muscle activation/deactivation from the side on which bracing contact is maintained, providing a starting point for further exploration of lateral tongue dominance.

2 Materials & Method

To explore the relationship between laterally asymmetrical muscle activation and unilateral tongue bracing, we conducted a series of simulations using the Artisynth biomechanical modeling platform [3]. Artisynth uses a combination of dynamic rigid body and finite-element modeling to simulate the hard and soft structures that make up the vocal tract. Artisynth can perform feedforward simulations where time-varying muscle activations are input to the model, and the resulting kinematic and contact behavior can be observed.

[*] jasia10@student.ubc.ca
[†] cjmayer@uci.edu
[‡] yadong.liu@ubc.ca
[♦] arian.shamei@ubc.ca
[♯] ian.stavness@usask.ca
[♩] gick@mail.ubc.ca

2.1 Data Collection and Processing

For the current simulations[a], we used the model of the tongue, jaw, palate and hyoid complex used in [2] (**Fig. 1**). The model has 96 virtual contact sensors affixed to the hard palate in a similar configuration to the Kay EPG [1]. These sensors can be used to detect tongue-palate contact, including lateral bracing.

The simulations in the present study were based on the simulations from [2], which investigated how laterally symmetrical muscle activation can produce bilateral bracing at different degrees of jaw closure. We used the muscle activations that achieved bilateral bracing with a jaw aperture of 5mm (n=632) as a starting point. For each of these original simulations, we ran four new simulations where we varied the activation of different sets of muscles on the left side of the vocal tract: (1) Agonists and antagonists activated at 100% of the original activation, a replication of the successful bracing simulations in [2]; (2) Agonist activation at 50%; (3) Antagonist activation at 150%; (4) Both 2 and 3.

In all cases, the jaw adductors were activated to reduce midsagittal jaw aperture to 5mm. Lateralized muscle activations were only changed on the left side. Right lateral muscles were kept at the original activations from the simulations in [2]. This approach was based on observations that tongue musculature is symmetrical [4] and so would demonstrate similar behavior if the right side was used instead.

Following [2], we designated GGP, GGM, MH, VERT, SL as bracing agonists, and GGA, STY, HG, TRANS, IL as bracing antagonists. Although SL was also classified as an agonist in [2], it is not lateralized in the Artisynth model, and so its activation level was not varied along with the other agonists.

Each simulation lasted a second. In the first 100 ms, the jaw adductors were linearly activated to produce a 5mm jaw aperture. In the next 700ms, the tongue muscles were linearly activated to their maximum levels. In the final 200ms, the model was left to stabilize and any tongue-palate contact was recorded. The simulations were run using Artisynth's BatchSim tool.

2.2 Data Analysis

Statistical analysis was done using a pair of logistic regression models, which predicted left and right lateral bracing contact respectively. The independent variables in each model were left-side agonist activation (50% or 100%), left-side antagonist activation (100% or 150%) and their interaction. These were normalized to Z scores.

[a] Simulation code and data: https://github.com/connormayer/asymmetrical_bracing

3 Results

Of the 2528 total simulations, 2083 were successful. The remaining 445 simulations failed due to numerical errors.

Results from the simulation study are displayed in **Fig. 2** below. Here, 'Agonists: 1 Antagonists: 1' is the condition with symmetrical muscle activations that reproduces the results from [2], while the other three conditions modify the muscle activations on the left side relative to this condition. These results show that reducing agonist activation on the left side reduces bracing on both sides, but the effect is stronger on the contralateral side. Increasing antagonist muscle activation on the left side has a similar effect, although the asymmetry in bracing contact is not as pronounced.

The model predicting right-side bracing outcomes revealed a significant positive effect of agonist activation (β=2.44, Z=13.135, $p < 0.001$), a significant negative effect of antagonist activation (β=-1.32, Z=-6.879, $p < 0.001$), and a significant negative interaction between the two (β=-1.12, Z=-6.082, $p < 0.001$). The model predicting left-side bracing outcomes showed similar effects of agonist activation (β=1.19, Z=11.166, $p < 0.001$), antagonist activation (β=0.76, Z=-6.815, $p < 0.001$), and their interaction (β=-0.629, Z=-5.973, $p < 0.001$).

These results show that increasing agonist activation on the left side increases the likelihood of a bracing outcome on both sides, while increasing antagonist activation on the left decreases the likelihood of a bracing outcome on both sides. However, the effect is stronger on the contralateral side: increased activation of agonists on the left side causes a greater increase in bracing outcomes on the right side relative to the left, and increasing antagonist activation on the left causes a greater decrease in bracing outcomes on the right side than on the left. The interaction terms suggest a small but significant negative superadditive effect of activating both agonists and antagonists.

4 Discussion & Conclusion

The outcomes of the simulation study have provided insight into the relationship between unilateral bracing and muscle activation patterns. Both reducing agonist activation or increasing antagonist activation on the left while keeping activations constant on the right results in lower tongue-palate contact on the right side. Hence, unilateral release appears to be affected by muscle activations on the opposite side. This can be explained by considering the muscular-hydrostatic properties of the tongue. Activating a muscle unilaterally means contracting it, squeezing that side of the tongue and thus expanding the other side due to the volume-preserving nature of muscular hydrostats [5]. This would cause the opposite side to make more contact with the palate, not the same side, as shown in the tongue diagram in **Fig. 3**. One intriguing inconsistency arises when considering the case where increasing antagonist activation reduces contact on the opposite side. Hydrostatic properties would predict contact to increase, but in this case it may be attributed more to the way in which extrinsic antagonists (e.g. STY, HG) tend to pull the tongue down or move it to the left side rather than affecting volume.

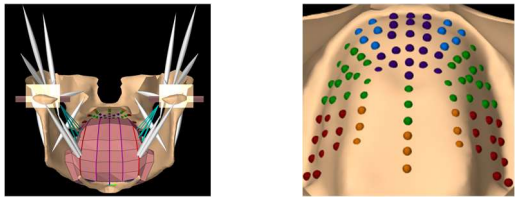

(a) **(b)**

Figure 1: (a) The jaw-tongue-hyoid model in Artisynth; **(b)** the contact sensors locations on the palate

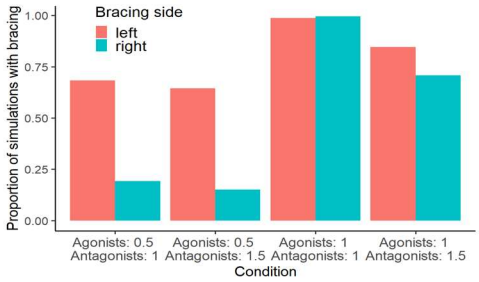

Figure 2: Lateral bracing outcomes for varied agonist/antagonist activation levels on the left side.

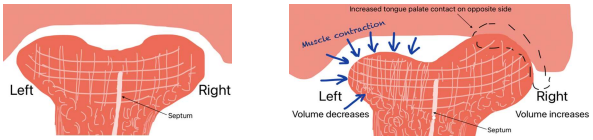

(a) No activations **(b)** Muscle activated on left side

Figure 3: This diagram depicts how simultaneously activating VERT and TRANS displaces tongue volume to the opposite side.

However, further research is necessary to confirm or refute this hypothesis.

Acknowledgments

Research supported by NSERC Discovery grant funding.

References

[1] Gick, B., Allen, B., Roewer-Després, F., & Stavness, I. (2017). Speaking Tongues Are Actively Braced. *Journal of speech, language, and hearing research : JSLHR*, *60*(3), 494–506. https://doi.org/10.1044/2016_JSLHR-S-15-0141

[2] Liu, Y., Luo, S., Łuszczuk, M., Mayer, C., Shamei, A., de Boer, G. & Gick, B. (2022). Robustness of lateral tongue bracing under bite block perturbation. *Phonetica*, *79*(6), 523-549. https://doi.org/10.1515/phon-2022-0001

[3] Lloyd, J.E., Stavness, I., & Fels, S.S. (2012). ArtiSynth: A Fast Interactive Biomechanical Modeling Toolkit Combining Multibody and Finite Element Simulation. *Soft tissue biomechanical modeling for computer assisted surgery,* 355-394. http://dx.doi.org/10.1007/8415_2012_126

[4] Sanders, I., & Mu, L. (2013). A three-dimensional atlas of human tongue muscles. *Anatomical record (Hoboken, N.J.:2007)*, *296*(7),1102–1114. https://doi.org/10.1002/ar.22711

[5] Stavness, I., Lloyd, J. E., & Fels, S. (2012). Automatic prediction of tongue muscle activations using a finite element model. *Journal of biomechanics*, *45*(16), 2841–2848. https://doi.org/10.1016/j.jbiomech.2012.08.031

CREAKY VOICE IN CANADIAN ENGLISH: AN ACOUSTICS-FOCUSED METHOD

Jeanne Brown *[1]
[1] Department of Linguistics, McGill University, Montreal, QC, Canada

1 Introduction

Creaky voice is a voice quality attributed to vocal fold compression without complete glottal closure. Acoustically, prototypical creaky voice is characterized by three key properties: a low pitch, irregular vocal pulses, and decreased transglottal airflow [1].

Previous work provides competing evidence of gender differences with regard to creaky voice in English: some studies find more creak in men's speech [2, 3] whereas more recent studies frequently report increased creakiness among women [4, 5]. Many of these existing sociophonetic studies of creaky voice rely on impressionistic (auditory and/or visual) coding which are vulnerable to important perceptual biases [6, 7]. The present study aims to investigate the often-cited gender differences in creaky voice use by examining Canadian English, crucially quantifying creak by its acoustic correlates.

2 Method

2.1 Speech sample

ICE-Can: A subset of 29 speakers (three girls, seven women and 19 men) from the International Corpus of English – Canada (ICE-Can) [8] were selected for this study. All speakers were born and raised in Canada, across multiple provinces. Speaker ages range from 12 to 77 years old at the time of recording. The speech samples are collected from broadcast events from the early 1990s.

YT Corpus: 21 Canadian speakers make up the YouTube (YT) Corpus: 11 men and 10 women, all aged between 19 and 76 years old (at time of recording) and born in Ontario or Quebec. The audio data contains spontaneous speech from YouTube videos (podcasts, interviews, radio shows and livestreams) recorded within the last 10 years.

2.2 Acoustic analysis

Several acoustic voice quality measurements were extracted from all vowels at the mid-point using PraatSauce [9], a Praat script for spectral measures. A total of 55 315 vowels were analyzed. The acoustic correlates of interest in this paper are pitch (f0), spectral tilt (e.g., H1*-H2*) and Harmonics-to-Noise Ratios (HNRs), specifically Cepstral Peak Prominence (CPP) and HNR between 0-500Hz (HNR05).

Pitch (f0) tracking: Pitch tracking errors in Praat are often caused by irregular voicing which is typical of creaky voice. Therefore, the percentage of tokens (vowels) that have unreliable f0 tracks is interesting for identifying possible creaky voice. Pitch tracks were considered unreliable if Praat returned "undefined" or 0Hz values for more than 50% of the vowel duration.

Spectral tilt: Spectral tilt measures are acoustic indicators of glottal constriction [1, 3]. H1*-H2* is the difference between the amplitudes of the first harmonic and the second harmonic. With a more open glottis (increased airflow), H1 values are boosted, resulting in a higher spectral tilt value. On the other hand, with a more constricted glottis (reduced airflow), H1 values are decreased and/or H2 values are increased, resulting in a lower spectral tilt value which suggests more creakiness [3, 10].

Harmonic-to-Noise Ratios (HNRs): HNRs such as CPP or HNR05 measure waveform periodicity and symmetry, both indicators of noise [1, 3]. As the name suggests, they are ratios between the levels of harmonics and noise. High HNR values indicate a very periodic vibration with strong harmonics and little noise and conversely low HNR values indicate either weak harmonics or aperiodic vibration (typically caused by noise like aspiration or creakiness) [10]. HNR calculated in the frequencies below 500Hz (HNR05) is a particularly good indicator of noise for creaky voice because aspiration noise will typically occur at higher frequencies, whereas creak noise tends to affect the lower frequency bands [10].

Data cleaning: Due to the direct link between f0 and spectral tilt measures, any H1*-H2* data resulting from unreliable f0 tracks was removed (16% of all H1*-H2* data). As for CPP and HNR05, all data points that fell outside of three standard deviations of the means (by-speaker) were excluded.

2.3 Statistical analysis

Using a script modified from [11], mixed models were conducted in R. Fixed main effects were gender, age, corpus, utterance position, vowel height and stress; only gender effects will be reported here. Random effects included by-speaker random intercepts.

3 Results

3.1 Pitch track

Table 1 shows that the percentage vowels with unreliable pitch tracks is higher for men (19.2%) than for women (12.0%), suggesting more irregular voicing, an acoustic indicator of creak (among others).

3.2 Spectral tilt measures (H1*-H2*)

The spectral tilt measure selected in this paper, H1*-H2*, shows significant differences for the main effect of Gender. Men's vowels have lower H1*-H2* values than women's (GenderM: $\beta = -23.30$dB, $t = -6.01$, $p < 0.05$), which is also

* jeanne.brown@mail.mcgill.ca

observable in Figure 1 below (left panel). These results suggest that men produce their vowels with a more constricted glottis than women, indicating a tendency towards more creakiness.

Table 1: Percentages and number of vowels with unreliable f0 tracks (proportion of vowel f0 tracked < 0.5) by gender.

Gender	% unreliable	n unreliable	n
F	12.0%	2357	19681
M	19.2%	6851	35634
Total	16.6%	9208	55315

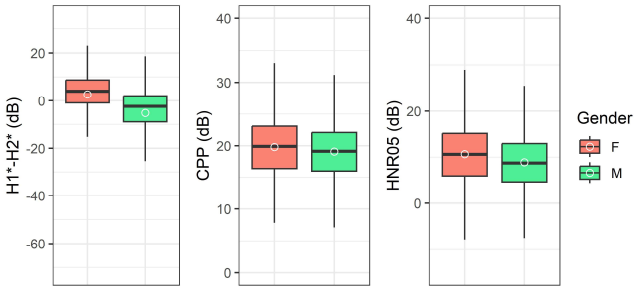

Figure 1: H1*-H2*, CPP and HNR05 values (dB) by gender.

3.3 Harmonics-to Noise-Ratios (HNRs)

Cepstral Peak Prominence (CPP): CPP differences for the main effects of Gender are also significant, men's vowels showing lower CPP values than women's in Figure 1 (middle panel) and in the mixed model summary (GenderM: β = -2.34dB, t = -2.56, p = 0.01). Lower CPP values indicate more noise and/or aperiodicity across all frequency bands, which is indicative of more creakiness.

HNR below 500Hz (HNR05): While Figure 1 (right panel) does seem to show HNR05 differences by Gender, these do not reach statistical significance. The trend does follow previous results for the other acoustic properties of voice quality, with men producing lower HNR05 values than the women (GenderM: β = -1.97dB, t = -1.75, p = 0.09). Low HNR05 values point to more noise in the low frequency band between 0 and 500Hz, which can be attributed to increased creakiness for men compared to women.

4 Discussion

This study presents substantial evidence for more creakiness in men's speech than in women's speech. Men's vowels show less reliable f0 tracks, lower spectral tilt measures (H1*-H2*) and lower HNR measures (CPP and HNR05). Altogether, these acoustic cues indicate more glottal closure and higher levels of noise/aperiodicity, ultimately providing empirical support for more creak among men than women. This result aligns with that of older studies [2, 3] but challenges more recent and well-cited findings [4, 5].

A perceptual explanation for these conflicting findings is that creakiness is much more salient in women's voices because they have higher habitual pitch ranges and often lower their pitch considerably to produce creaky voice. Conversely, men's voices, usually situated at lower pitch ranges, do not require large pitch shifts and as such, creakiness is less perceptually marked. Since most studies examining creaky voice implement impressionistic coding of creaky tokens, a perceptual bias is likely to impact the data. This seems to coincide with work on the interaction of non-modal phonation and pitch [6, 7].

Notable limitations concern the speech sample as well as the data cleaning process and statistical analyses. The current speaker sample is skewed towards men in both quantity of speech and number of speakers. While the precise effect of this gender disbalance is unclear at this time, future work should aim for a more balanced sample. Additionally, the data cleaning and statistical analysis requires more careful consideration to assure that outliers are treated correctly, models are well-calibrated to the data and interactions can be properly interpreted.

Overall, this study highlights the importance of acoustic measures in quantifying creak and provides new insight into the relation between creaky voice and gender.

References

[1] Keating, P., Garellek, M., & Kreiman, J. (2015). Acoustic properties of different kinds of creaky voice. *ICPhS*.

[2] Henton, C., & Bladon, A. (1988). Creak as a sociophonetic marker. In L. Hyman & C. Li (Eds.), Language, speech and mind: Studies in honor of Victoria A. Fromkin (pp. 3–29). London, England: Routledge.

[3] Klatt, D. H., & Klatt, L. C. (1990). Analysis, synthesis, and perception of voice quality variations among female and male talkers. Journal of the Acoustical Society of America, 87(2), 820–857. https://doi.org/10.1121/1.398894

[4] Podesva, R. J. (2013). Gender and the social meaning of non-modal phonation types. In C. Cathcart, I. Chen, G. Finley, S. Kang, C. S. Sandy, & E. Stickles (Eds.), Proceedings of the 37th Annual Meeting of the Berkeley Linguistics Society, pp. 427-448.

[5] Yuasa, I. (2010). Creaky voice: A new feminine voice quality for young urban-oriented upwardly mobile American women? American Speech, 85, 315-337. 10.1215/00031283-2010-018.

[6] Davidson, L. (2020). Contributions of modal and creaky voice to the perception of habitual pitch. Language, 96(1), e22-e37. https://doi.org/10.1353/lan.2020.0013

[7] White, H., Gibson, A., Penney, J., Szakay, A., & Cox, Felicity. (2022). The influence of pitch and speaker sex on the identification of creaky voice by female listeners. In Proceedings of the Eighteenth Australasian International Conference on Speech Science and Technology, ASSTA, 81-85.

[8] Greenbaum, S., & Nelson, G. (1996). The International Corpus of English (ICE project). World Englishes, 15:3–15.

[9] Kirby, J. (2018). Praatsauce: Praat-based tools for spectral analysis. Available at: https://github.com/kirbyj/praatsauce

[10] Keating, P., Kuang, J., Garellek, M., Esposito, C., & Khan, S. (2023). A cross-language acoustic space for vocalic phonation distinctions, Language, 99(2), pp. 351-389. DOI:10.1353/lan.2023.a900607

[11] Brunelle, M., Brown, J. & Thị Thu Hà, P. (2022). Northern Raglai voicing and its relation to Southern Raglai register: evidence for early stages of registrogenesis. Phonetica, 79(2), 151-188. https://doi.org/10.1515/phon-2022-2019

VARIATION IN ARTICULATION RATE IN NEW BRUNSWICK FRENCH

Wladyslaw Cichocki *[1], Luke Hagar †[2] and Yves Perreault ‡[3]
[1]Department of French, University of New Brunswick, Fredericton, New Brunswick, Canada
[2]Department of Statistics and Actuarial Science, University of Waterloo, Waterloo, Ontario, Canada
[3]Université de Moncton, Moncton, Canada

1 Introduction

This study examines articulation rate (AR) in French spoken in five regions of New Brunswick. French is a minority language in this province, and the demographic concentrations of French speakers vary across regions, suggesting that the regions have different degrees of French–English contact. The main research question explored in this paper is how AR varies across the different language contact situations.

Research on contact varieties of various languages – including French [1], Spanish [2], and Swiss German [3] – has found that AR tends to be slower in contact varieties than in majority language varieties. Similarly, ongoing research on varieties of French spoken in Canada [4] has observed that AR is slower in varieties where there is a mid to high degree of language contact and faster in varieties with a low degree of contact.

In the present study, the main predictor factor of AR is region. The degree of language contact is gauged by demographic concentrations of French speakers in each region of New Brunswick; these are as low as 35% in the Moncton-Dieppe urban area and as high as 94% in the NorthWest region [5]. The study includes consideration of other factors that can affect variation in AR: speaker's gender and age, and the length of inter-pause intervals (IPIs).

2 Method

2.1 Speakers and speech materials

Materials are from the RACAD speech corpus of New Brunswick Acadian French, originally designed for speech recognition applications [6]. The corpus consists of recordings by 136 speakers from the five main regions of New Brunswick where there is a sizeable proportion of Francophones. While the corpus is not evenly balanced with respect to region, each region has a reasonably large representation: NorthWest (26 speakers), North (26), NorthEast (39), Moncton-Dieppe (24), SouthEast (21). The sample has a good distribution of gender and age for all five regions. Speakers' ages range from 18 to 69 years.

Each speaker read 12 sentences chosen from a large set of 212 sentences that included two 'calibration' sentences that contain segmental shibboleths. In the present study, we focused analysis on the two calibration sentences because all speakers read both sentences, allowing us to control segmental and syntactic content. The sentences are :

Je viens de lire dans l'Acadie Nouvelle qu'un pêcheur de Caraquet va monter une petite agence de voyage. C'est le même gars qui, l'année passée, a vendu sa maison à cinq Français d'Europe.

2.2 Measurements and statistical analysis

Acoustic analysis and segmentation into phones, syllables, pauses were carried out with Praat. Syllable boundaries were established based on actual pronunciations (and not on orthographic or phonological representations). Pauses were defined as periods of silence longer than 70 msec. Excluded from analysis were filled pauses, false starts, and repetitions. About 25 minutes of continuous speech were examined.

AR was calculated as the number of syllables in an inter-pause interval (IPI) and was measured in syllables per second. This local measure of AR was made for each IPI for each speaker. IPI length was defined as the number of syllables in an IPI.

Linear mixed effects modeling was carried out to assess the relationships between AR and five predictor factors: age and IPI length (both are continuous variables), and region, gender, and sentence (categorical variables). The model was fit using observations with IPI > 2. Age was centered around the median age of 40; IPI values were transformed and the log of IPI was centered around the median value of log(10).

3 Results

3.1 Preliminary descriptive statistics

A summary of mean ARs for the five regions is given in Table 1. Overall mean AR was 4.72 syll/sec (SD = 0.84); the ARs were relatively normally distributed (skewness was 0.09).

Table 1: Mean articulation rate for each region.

NorthWest	North	NorthEast	Moncton-Dieppe	SouthEast
4.74	4.74	4.85	4.58	4.61

Figure 1 is a preliminary plot of the correlation between mean ARs and the demographic concentrations of Francophones in the regions; it shows a direct association between the two. We briefly mention some of the other preliminary observations. There were clear trends between AR and gender, age, logIPI, and sentence. As an example, the plot in Figure 2, which aggregates data from gender and age, shows that average AR is faster for males speakers than female speakers, and that AR decreases with age.

3.2 Modeling for articulation rate

The results of the linear mixed effects modeling indicated

* cicho@unb.ca
† lmhagar@uwaterloo.ca
‡ pyp7450@hotmail.ca

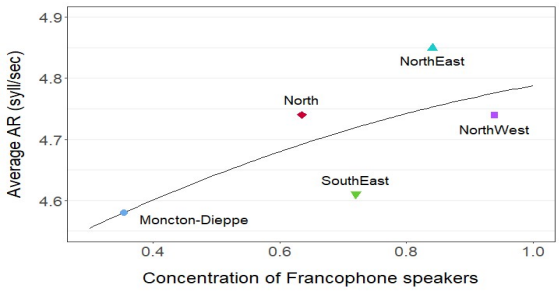

Figure 1: Plot of average AR vs. concentration of Francophone speakers by region.

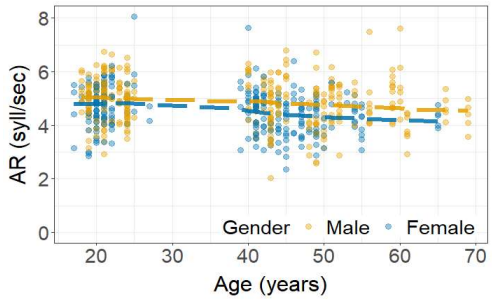

Figure 2: Plot of AR vs. age, grouped by gender.

that there are significant relationships between AR and four of the predictor factors: speaker gender ($p < .001$), age ($p < .001$), log of IPI length ($p < .001$), and sentence ($p < .001$). However, region was not significant ($p = .64$) nor were there any significant interaction effects with region. No interactions among the four predictor factors were significant at the 5% level.

4 Discussion

The goal of this study was to examine variation in AR across five regions of New Brunswick. The main research question asked how ARs vary across the different language contact situations in these regions. A preliminary correlation between average AR and the concentration of French speakers in each region suggested that regions with greater concentrations of Francophones have higher ARs. However, a more formal analysis with linear mixed effects modeling showed that ARs are not significantly different across the regions. Thus, differences in degree of language contact across the five regions – indicated here as demographic concentrations of Francophones – are not related to AR variation in New Brunswick French. This result is comparable with [4]'s findings for other varieties of Canadian French; these authors note that regions in minority situations tend to have similar ARs, regardless of whether the degree of language contact is low or high.

The statistical modeling also showed that the other predictor factors are significant. These effects are generally consistent with patterns established in previous research [4], [7–9]. With respect to gender, many – but not all – studies also find that males have faster ARs than females. As for age, a frequent result is that younger speakers have faster ARs than older speakers. These findings suggest that female and older speakers may be reading more carefully – and thus with a slower AR – than other speakers. The results also confirm the significant role of the log IPI factor: average AR increases as IPI length increases.

An important limitation of this study is the use of sentences in the research design. Several speakers had only one IPI per sentence. This meant that sentence could not be treated as a random effect in the statistical analysis, requiring that the effect of sentence on AR be the same for each speaker. Future research should consider a corpus with several (longer) reading passages. These could be treated as a random effect, which might better account for the variability in AR.

5 Conclusion

The results revealed significant effects of gender, age, and IPI length on AR variation in New Brunswick French. These effects are generally consistent with findings from research on both majority and minority language varieties. However, region is not a significant predictor; that is, ARs do not differ across the different contact situations. Overall, these findings contribute to a description of the temporal properties of varieties of Canadian French, an area that remains relatively under-documented.

Acknowledgments

The RACAD Speech Corpus was developed in collaboration with several colleagues – Sid-Ahmed Selouani, Louise Beaulieu, Mona-Luiza Ungureanu – at the Université de Moncton, Campus de Shippagan, and with generous support from the Canada Foundation for Innovation and the Social Sciences and Humanities Research Council of Canada.

References

[1] M. Avanzi, N. Obin, A. Bardiaux and G. Bordal. Speech prosody in French regional varieties. *Speech Prosody 2012*, 603–606, 2012.

[2] L. García-Amaya, K. Kendro and N. Henrikson. Regional variation, articulation rate, and pausing in three varieties of Spanish. *International Congress of Phonetic Sciences 2023*, 2023.

[3] M.-A. Morand, M. Bruno, S. Schwab and S. Schmid. Syllable rate and speech rhythm in multiethnic Zurich German: A comparison of speaking styles. *Speech Prosody 2022,* 337–341, 2022.

[4] W. Cichocki, S. Kaminskaïa and L. Hagar. Regional variation in articulation rate in French spoken in Canada. *Journal of the International Phonetic Association,* 1–20, 2023. doi:10.1017/S0025100323000154

[5] Statistics Canada. *2006 Community Profiles.* 2006 Census. Statistics Canada Catalogue no. 92-591-XWE. Ottawa. Released March 13, 2007. 2007.

[6] W. Cichocki, S.-A. Selouani and L. Beaulieu. The RACAD speech corpus of New Brunswick Acadian French: Design and applications. *Canadian Acoustics* 36, 3–10, 2008.

[7] E. Jacewicz, R.A. Fox, C. O'Neill and J. Salmons. Articulation rate across dialect, age and gender. *Language Variation and Change* 21, 233–251, 2009.

[8] F. Grosjean and A. Deschamps. Analyse contrastive des variables temporelles de l'anglais et du français : vitesse de parole et variables composantes, phénomènes d'hésitation. *Phonetica* 31, 144–184, 1975.

[9] S. Schwab and M. Avanzi. Regional variation and articulation rate in French. *Journal of Phonetics* 48, 96–105, 2015.

THE ANALYSIS OF SPEECH PERCEPTION WITH THE USE OF HEARING PROTECTION EARPLUGS USING THE CANADIAN DIGIT TRIPLET TEST

Ahmed El Mawazini *[1], Christian Giguère †[2]
[1]School of Rehabilitation Sciences, University of Ottawa, Ottawa, Canada.

1 Introduction

To prevent noise-induced hearing loss, it is recommended that workers wear hearing protection when the daily exposure exceeds 85 dBA. Choosing the right type of protector depends on the amount of attenuation achieved in relation to the noise level. Labelled attenuation values reported by manufacturers, such as the NRR, have limited accuracy in predicting what an individual worker will achieve in practice [1]. To counter this deficiency, fit-testing measurement systems have been developed that have shown to be a reliable method to determine attenuation for an individual wearing hearing protection [2]. Additionally, workers need to communicate and hear important sounds in their environment. Standards like the CZA Z1007:22 [3] recommend conducting practical tests, but there is currently no recognized efficient methodology or objective tool available to determine if the communication needs of workers are adequately met. The Canadian Digits Triplet Test (CDTT) is an automated screening speech test based on simple digit material that can be administered in about 2-3 minutes and could proved to be a useful tool to determine individual worker's speech perception when wearing hearing protectors.

The objectives of this research are to (1) compare earplug attenuation in individuals with normal hearing and hearing loss based on fitting instructions, and to (2) analyze speech perception with earplugs using the CDTT in individuals with normal hearing and hearing loss, considering the attenuation achieved.

2 Methods

2.1 Participants

A total of 18 adult participants, ranging in age from 19 to 74 years, were recruited for this research project. Among them, 11 participants had normal hearing, while 7 participants had a hearing loss in at least one ear.

2.2 Materials

Hearing thresholds in each ear were measured using the Interacoustics AC40 audiometer in conjunction with the supra-auricular RadioEar DD45 headset. Speech perception was assessed using the Canadian Digit Triplet Test (CDTT) on a portable Windows computer, with sound presented through the circum-auricular RadioEar DD450 headset. Each participant was placed in an acoustically insulated room and tested with and without wearing a pair of 3M E-A-R Classic Earplugs.

2.3 Procedures

Before conducting the experimental tests, preliminary measures were administered to determine the participants' hearing status (normal or impaired) and to ensure the absence of contraindications or safety concerns, such as excessive earwax. These preliminary measures consisted of otoscopy, tympanometry, and bilateral tonal audiometry.

Participants then underwent a series of experimental tests under three different conditions: (1) without wearing earplugs, (2) wearing earplugs without receiving specific instructions on their proper usage, and (3) wearing earplugs with instructions on the correct method of insertion. For each condition, participants completed a speech perception test in quiet using the CDTT, which included different lists, male and female voices, in the participants' preferred language (English or French). Additionally, binaural tonal thresholds were measured in each of the three conditions above at frequencies of 250, 500, 1000, 2000, 4000, and 6000 Hz using the Bekesy method and the Interacoustics AC40 audiometer and circum-auricular RadioEar DD450 headset.

2.4 Data Analysis

Data analysis was performed using Microsoft Excel. The collected data for each participant were entered into the spreadsheet, and calculations were conducted to determine the average, standard deviation, minimum, and maximum values for binaural tonal thresholds and speech perception thresholds. These measures were analyzed for all three testing conditions. Furthermore, the attenuation was calculated by subtracting the tonal thresholds obtained without earplugs from those obtained with earplugs at each frequency. The global attenuation of the CDTT speech signals was also calculated by considering the speech spectrum of the male and female speakers.

3 Results

Speech perception thresholds in silence measured with the CDTT are shown in Figure 1 for male and female voices. When testing with the male voice, most participants had higher speech thresholds with earplugs than without and thresholds generally increased after providing instructions on the proper fitting method. Only participants 9, 14 and 15 had higher thresholds without proper fitting instructions. With the female voice, participants 2, 7, 9, 12, and 14 had higher thresholds without proper fitting instructions. Although some participants had lower thresholds with instructions that without instructions, Figure 2 shows that attenuation with instructions is always higher except for participant 14.

* aelma034@uottawa.ca
† cgiguere@uottawa.ca

Figure 3 demonstrates that when comparing participants with normal hearing to those with a hearing loss, there was no significant difference between attenuation when tested in the same condition.

Data analysis also demonstrated that on average, participants with a hearing loss had speech perception thresholds close to 50dBA and sometimes surpassing 65dBA (which corresponds to a normal vocal effort at close range) when wearing earplugs (see Figure 1).

4 Discussion

This pilot study indicates that CDTT thresholds in silence generally increase with the attenuation of an earplug or with a better fit, sometimes to a level where communication could be compromised in some individuals with hearing loss, especially when considering that more complex speech materials like sentences require higher speech levels than digit tests. According to [4], workers situated at a distance of 1.2 meters reported speaking at a normal voice amidst noise reaching up to 81 dBA and at a raised voice level in 87 dBA of noise when not wearing hearing protectors. When wearing hearing protectors in noise, many studies indicate a decrease in voice levels by the speaker [5].

The CDTT is a straightforward and quick speech assessment that simply requires participants typing in digits heard on a computer or tablet and can assist in determining the minimum voice level for speech recognition by workers wearing hearing protectors.

5 Conclusion

Although preliminary findings suggest that the CDTT can proved to be a useful field test to efficiently assess speech perception for individual workers when wearing their hearing protectors, this research has an important limit. Results were collected in silence, and thus relates to situations of low noise levels or noise interruptions. Further speech testing in noise is necessary to obtain valuable information on the efficacy of the CDTT in assessing speech perception for workers wearing hearing protectors in noise.

6 References

[1] Voix, J., & Berger, E. H. (2022). The Noise Manual, 6th edition, chapter 11, American Industrial Hygiene Association.

[2] Voix, J., Smith, P., & Berger, E. H. (2022). The Noise Manual, 6th edition, chapter 12, American Industrial Hygiene Association.

[3] CSA Group (2022). CZA Z1007:22 Hearing loss prevention program (HLPP) management.

[4] Ferguson, M. A., Tomlinson, K. B., Davis, A. C., & Lutman, M. E. (2019). International Journal of Audiology, Vol 58(7), 450–453.

[5] Vaziri, G., Giguère, C., & Dajani, H. R. (2022). The Journal of the Acoustical Society of America, 152(3), 1528–1538.

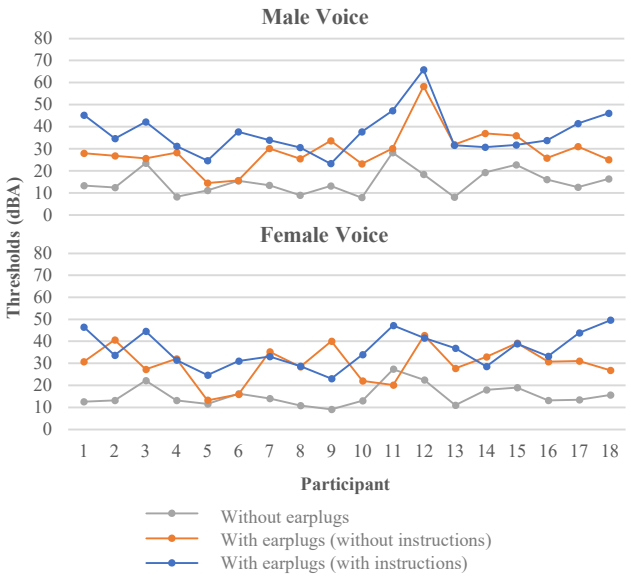

Figure 1: Speech perception thresholds with the use of the Canadian Digits Triplet Test for each Participant.

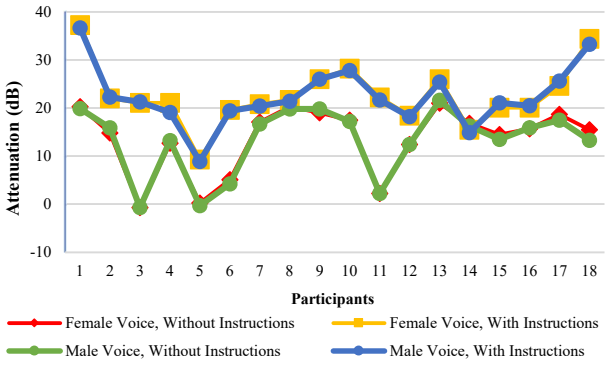

Figure 2: Comparison of global earplug attenuation of the male and female voices for each participant.

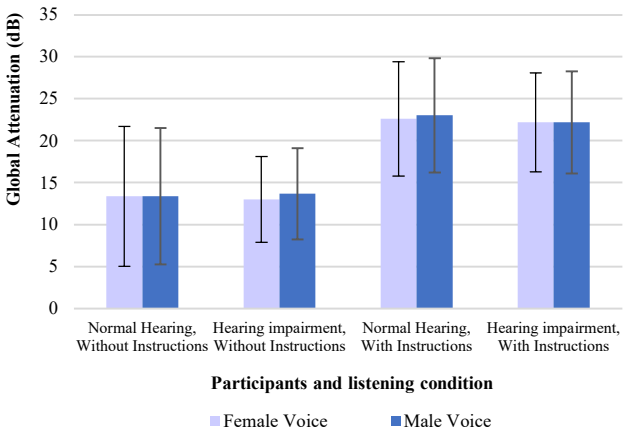

Figure 3: Comparison of global earplug attenuation between normal hearing and hearing-impaired participants.

A 3D Voice-Hearing Simulator Co-Created by Voice Hearers and Researchers: Preliminary Sound Quality Evaluation

Philippe-Aubert Gauthier [*1,2], **Kevin Zemmour**[3], **Sylvain Grignon**[3], **Bálint Demers**[4], **Catherine Lejeune**[1], **Sandrine Rousseau**[5], **Mouloud Boukala**[4], **Sofian Audry**[4], **Sylvio Arriola**[8], **Alain Berry**[6], **and Kevin Whittingstall**[7]

[1]École des arts visuels et médiatiques, UQAM, Montréal, Canada
[2]Centre for Interdisciplinary Research in Music, Media, and Technology (CIRMMT), McGill University, Montréal, Canada
[3]Département de psychiatrie, Faculté de médecine et des sciences de la santé, Université de Sherbrooke, Canada
[4]École des médias, UQAM, Montréal, Canada
[5]Association québécoise pour la réadaptation psychosociale, Québec, Canada
[6]Centre de recherche acoustique-signal-humain de l'Université de Sherbrooke, Université de Sherbrooke, Canada
[7]Département de radiologie diagnostique, Faculté de médecine et des sciences de la santé, Université de Sherbrooke, Canada
[8]École supérieure de Théâtre, UQAM, Montréal, Canada

1 Introduction

Voice hearing (VH) is an auditory hallucination that can touch a wide range of people, not only those with psychosis or schizophrenia. VH can be positive, negative, or anything in between and is distinctive in that the voices do not seem to only come from inside the head but also from the external world, the sound environment, or the body, sometime resulting in a sense of sound externalization. Poor support from professionals of mental health or social work is often reported by voice hearers. Leading to potential issues with service providers lacking proper experiential knowledge of VH. To address this issue, we co-created a 3D voice hearing simulator (3DV) within a participatory research paradigm with a multidisciplinary team of researchers and voice hearers from various fields (acoustics, acting, quantitative methods, neuroimaging, psychiatry, sound art). Several studies have assessed the impact of voice simulator on healthcare professionals, nursing students, etc. [1]. To the authors knowledge, the use of 3D audio or binaural sound and the co-creation approach are not reported in the literature. Since the aim of 3D audio is to recreate the experience of spatial hearing as in natural hearing [2], we explored 3D sound for immersion as described by voice hearers. In this work, since the 3DV should be a portable simulator for *in situ* listening and experiencing, we use basic binaural recording with binaural head or Ambisonics [3] to binaural conversion.

The objective of the project is the creation of an experiential knowledge sharing tool for the training of students in psychiatry or social work, since they both probably have to interact and provide service to voice hearers in their career. We here present our preliminary sound evaluation of the 3DV, including how binaural 3DV performed compared to stereo and to binaural decoding of Ambisonics sound.

2 Methods

2.1 Co-creation of the 3DV simulator

Because of the personal nature of VH, the 3DV should be designed for a specific population. Here, the tested 3DV is aimed at students in social work. It was designed as a pedagogical tool. For six working sessions (3 to 4 hours each), the team (including researchers and two students representing social work) and the voice-hearers have been defining script, keywords, rhythm, style, spatial composition, etc. We explored different VH: positive, negative, neutral, and command voices. These working sessions were non-structured in order to naturally discuss and elucidate the VH experience. We also used an iterative approach : from session to session, the actors/writers were proposing new scripts or demos for iterative validation with and feedback from the voice-hearers. These working sessions were gathering: (1) a recurring group of 2 to 5 voice hearers that freely discussed; (2) actors (one senior, two juniors directed by the senior); (3) researchers (acoustics, psychiatry, sound arts, etc.).

After these sessions, based on the validated 3DV script, the team conducted recordings at the CIRMMT (Fig. 1). For comparison purposes, multi-channel and synchronized records included: binaural with Numan artificial head, stereophonic with a cardioid pair, third-order Ambisonics with Zylia microphone. Next, these recording were cleaned to remove noises and assembled according to the script. This first version was then validated with voice hearers that gived feedabck. Modifications were asked, so new recording were done and combined to the first version. This second version was approved by all our co-researchers and the voice-hearers. The 3DV and working sessions were all done in French.

Figure 1 – Recording of the actors in a semi-anechoic room.

2.2 Participants

Nine social work students from UQAM (Canada) participated to the evaluation (sex: 7 women, 2 men ; gender: 7 women, 1 men, 1 genderqueer). They are considered as "naive listeners" (without experience in audio, confirmed in the form). Participants were informed about the study and provided written consent before participating.

∗. gauthier.philippe-aubert@uqam.ca

2.3 Materials

The 3DV is a 45-minute sound file played on a portable media player using headphones (Sennheiser HD600). The volume was the same for each participant and it was adjusted to represent approximately 80% of perceived sound loudness of a normal discussion, as this was described by the voice hearers.

2.4 Procedure

In a room, participants were invited to complete the agreement form and were informed of the project. Next, they listened to the 3DV while going for a walk and perform their normal student activities (with the 3DV on). After listening, a qualitative evaluation was performed using an interview [4] on their general impression of the 3DV (not covered herein). Next, a quantitative listening test was done. Different versions (binaural, stereo, ambisonics to binaural) of the 3DV where compared and scaled from 0 to 100%. Adjectives (in French) were: sound quality, impact, immersion and envelopment, precision of localisation, externalization, distance, proximity. Each sound sample of 5 seconds for the adjectives were different while focusing on these key features.

3 Results

Preliminary quantitative results are in Tab. 1 with means in percent and standard-type (STD).

-2pt Besides, we had quantitative questions: "Do you see a clear difference between the sound samples ?", "How the rating was difficult ?", etc. From this, 5 from 9 replied that the differentiation was "difficult", one replied "very difficult", 3 replied "nor difficult, nor easy", and none replied "easy". Accordingly, the listening test was judged as a challenge, and therefore results must be interpreted carefully. This is also confirmed by the STD. The trend suggests that Ambisonics to binaural or stereophonic 3DV were the most well rated for all adjectives. Based on this trend, we think that binaural playback based on a binaural render of an Ambisonics microphone (spherical microphone array) is a better a avenue for future versions. Indeed, although it was slightly under-rated with respect to stereophonic sound for few adjectives, Ambisonics recording offer the possibility of spatial recomposition and also rendering for other devices such as Surround, loudspeaker arrays, etc. It would also be more appropriate for interactive binaural rendering using head-tracking for instance.

4 Discussion

Preliminary findings suggest that the 3DV is an effective tool for sharing the VH experience and can be used to increase experiential knowledge of VH among service providers. However, based on quantitative evaluation, the strong nature of the per se 3DV and the words used in the VH scenarios may make it difficult for participants to distinguish between different 3DV versions in terms of audio and immersion quality.

Although these results are limited to 9 participants, we expect more since the evaluation campaign is still active. Preliminary results from interviews suggest that the 3DV was efficient in sharing the VH experience. Still, we here focus on 3D audio and sound quality evaluation using the quantitative form. On this matter, by marked contrast with the qualitative insights, we think that it was difficult for participants to distinguish the sound quality (immersion, etc.) of different 3DV versions due to the strong and impactful nature of the 3DV and the words per se (stressful, annoying, distracting, etc.). Also, this might be explained by the fact, as mentionned, that all participants were self-identified "naive listeners." Besides, we must be careful in our interpretation, since the power of the preliminary data is very limited by its size. We can hardly conclude strongly on this matter from that data.

One limitation of the current data-set is that we only used social work students as participants. We also developed a 3DV for students to become physicians or psychiatrists. This second 3DV should be soon tested twith such students. A further limitation is the number of participants, our target of 30 participants should be reached in the future.

TABLE 1 – Results in terms of rating with respect to adjectives. Green, yellow and red indicate descending rating for each adjective.

	Binaural	**Stereo**	**Ambi to bin**
Quality	47.8% (32.7%)	60.2% (31.0%)	85.6% (19.4%)
Impact	53.4% (35.4%)	46.7% (39.7%)	74.8% (24.7%)
Immersion	51.3% (25.6%)	62.6% (25.2%)	61.1% (32.8%)
Precision	69.3% (35.7%)	66.8% (18.0%)	75.4 % (21.1%)
Externalization	35.0% (37.3%)	59.1% (28.7%)	50.1% (37.2%)
Distance	17.4% (12.7)	35.1% (26.4%)	20.8% (29.3%)
Proximity	56.0% (26.4%)	82.6% (24.2%)	57.1% (22.9%)

5 Conclusion

The co-creation and evaluation of a 3D voice hearing simulator were reported. It is designed to improve experiential knowledge and empathy for VH among service providers. Preliminary results suggested that the 3DV was efficient in sharing the VH experience for both voice hearers and participants. One of the success of the project was in the inclusion of voice hearers as non-traditional research collaborators with experiential knowledge in an horizontal and participatory structure. However, it was difficult for participants to distinguish the sound quality of different technological versions of the 3DV. To improve the immersion, interactive binaural audio with head-tracking or augmented reality may be necessary. For more personalized simulators, interactive and generative 3DV using context-dependent content and augmented reality is a potential avenue. This is planned future work.

Acknowledgments

Support: FRQ Audace. Ethics: UQAM (2023-4194).

References

[1] S. Patterson, N. Goulter, and T. Weaver. Hearing voices simulation : Process and outcomes of training. *J. Mental Health Training, Education and Practice*, 9 :46–58, 04 2014.

[2] J. Blauert. *Spatial Hearing*. MIT Press, 1996.

[3] J. Ahrens. *Analytic Methods of Sound Field Synthesis*. Springer, 2012.

[4] J.C. Kaufmann. L'entretien compréhensif. 1996.

TIMING OF PERIORAL MUSCLE SUPPRESSION IN SMILED SPEECH

Yadong Liu [*1], Kyra Hung [1], Melissa Villasenor [1], Shannon Colcleugh [1], Eunhee Chung [1], Bryan Gick [†1]
Department of Linguistics, University of British Columbia, Vancouver, British Columbia, Canada

1 Introduction

During speech production, temporally overlapping speech and non-speech movements can come into conflict [1]. How such conflicts are resolved remains poorly understood. For instance, during smiled speech, the simultaneous activation of facial-expression and speech-related lip movements can generate oppositions between Zygomaticus Major (ZM) and Orbicularis Oris (OO) muscles; ZM activation pulls the lips apart for the smile, while OO activation pulls the lips together for lip closure and rounding movements [1]. Previous research suggests that this conflict is resolved by suppression of either the smile or the lip closure movement [2]. However, the mechanism by which one or the other movement is selected for suppression, or by which this suppression takes place, remains unknown.

The present study aims to characterize the timing of the interaction that leads to this suppression, as well as the onset and length of suppression of smile when bilabial tokens are produced. Electromyography (EMG) sensors were used to measure ZM and OO activation during speech produced with neutral, smiling and laughing facial postures. Video recordings were processed using a facial tracking tool to corroborate EMG measurements and movement-based Facial Action Units (FAUs). This study seeks to analyze EMG and FAU signals to determine if they exhibit similar trends in muscle activity of the smile and lip closure, with earlier onset of changes observed in EMG signals.

2 Methods

2.1 Participants

Two female undergraduate students between the ages of 21 and 27 (M=24) from the University of British Columbia took part in the study. Both participants were native English speakers of North American English (NAE) as noted in a language background questionnaire

2.2 Experiment

This study's experimental design methodology was similar to Liu et al. [2] Two participants underwent a procedure in which EMG sensors were placed over their OO and ZM nerves.

Following the sensor placement, the participants were provided instructions to read a range of sentences incorporating the intended stimuli under three distinct facial conditions: neutral, smiling, and laughing. Concurrently, video recording was conducted to capture the participants' facial expressions, complementing the EMG recording. To synchronize the two recordings, the EMG recording commenced prior to the video recording, and in order to establish alignment, the sensors were lightly tapped three times in quick succession. This deliberate tapping induced a discernible impulse in the EMG recording, which could be correspondingly correlated with the tapping of the sensor visually captured in the video.

Figure 1: Emg sensor placement on the participant

The stimuli and sentences employed in this study were the same as those used in the study conducted by Liu et al. [2]. Participants were tasked with reading a total of 15 sentences, under three distinct facial conditions: neutral, smiling, and laughing. Each sentence featured a designated target word (see Table 1 in Liu et al. [2]) and was accompanied by an emoji, as illustrated in Figure 2. The sentences were presented to the participants in a random sequence, and they were explicitly instructed to assume the facial expression corresponding to the designated emoji before vocalizing the sentence. This procedure was repeated twice for each participant. Target sounds were annotated and EMG signal and video clip around the target sounds were extracted. Further, video clips were analyzed for facial action unit (FAU) activity using OpenFace 2.0 [3].

Figure 2. Emojis of neutral, smiling, and laughing

2.3 Results

OO activation and lip tightener intensity was measured by taking the normalized mean of all target tokens made by participants. The onset of bilabial closures are indicated by a dotted line in each figure. Sentences, indicated by a dashed line, began approximately seconds prior to bilabial closures in figures. Both neutral and smiling conditions produced OO activation captured by the EMG and FAUs intensity signals. The timing of the activation of the OO was however different among the two conditions being 133ms prior to the closure in the neutral condition and 156ms prior to the closure in the smiled condition. The OO reached a peak of activation at 128ms in the neutral condition and at the smiled condition. Prior to the bilabial closure the lip tightener rose 100ms in the neutral condition and 67 in the smiled condition. The OO peaks for neutral and smiling conditions are observed at 0 se

[*] yadong@alumni.ubc.ca
[†] gick@mail.ubc.ca

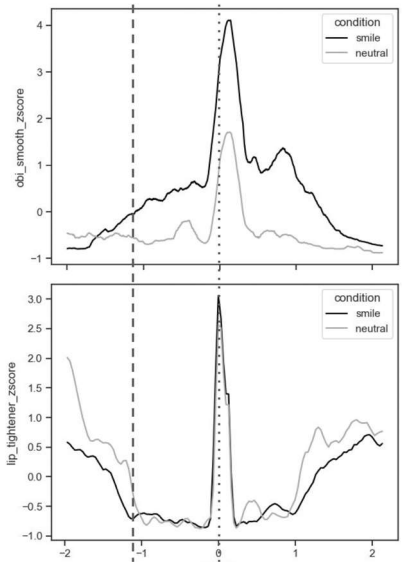

Figure 3: Mean normalized activation of the OO muscle (top) and intensity of the lip tightener FAU (bottom)

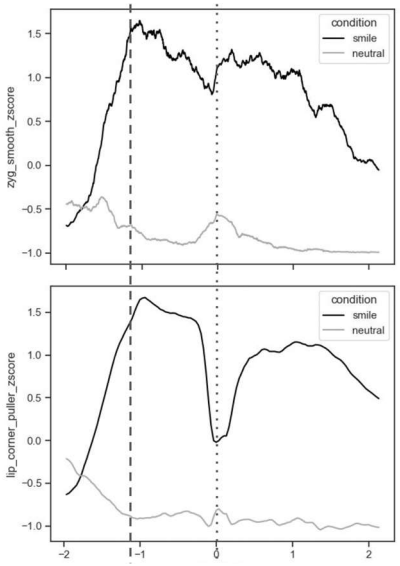

Figure 4: Mean normalized activation of the ZM (top) muscle and the intensity of the lip corner pull FAU (bottom)

In the neutral condition the intensity level reached 2.57 and in the smiled it reached 3.06. ZM activation and lip corner puller intensity was measured by taking the normalized mean of all target tokens made by participants. This is shown in Figure 4. Between the two conditions, neutral and smiled, greater intensity of both the ZM and the lip corner puller FAU intensity is shown in the smiling condition opposed to the neutral. The onset of ZM suppression 452 ms prior to the bilabial closure has an activation level of 1.28. Smiling suppression onset is demonstrated by the lip corner puller at 267ms prior to the closure with an intensity level of 1.4. Peak suppression is seen by the FAU at zero seconds with an intensity level of -0.02.

3 Discussion

Our results show the EMG signals and FAU signals exhibit similar trends in muscle activity of the smile and lip closure, with earlier onset of changes observed in EMG signals as expected. Both the OO activity and the lip tightener. FAU intensity illustrates a rise in lip activity prior to the lip closure in neutral and smile conditions, and an early rising onset is observed in the OO muscle activation. The ZM muscle activation and the lip corner puller FAU intensity present greater smile activity in the smiling condition, and show a suppression of smile occurring prior to the lip closure, with an earlier suppression observed in the ZM muscle activation. Moreover, the onset of such suppression occurs earlier than the onset of lip closure activity, illustrated as 294 ms in the muscle activation and 200 ms in the FAUs intensity, suggesting early planning in suppressing the smile. This finding is consistent with the observation in Liu et al. [2]. The onset of suppression illustrated by the lip corner pull FAU signal is comparable between findings of this study and Hung et al. [4].

The OO activity rises early and to a higher extent when producing bilabials in the smiling condition than the neutral condition, which agrees with findings observed in Sussman and Westbury [5] that earlier and greater activation for /u/ following /i/ than /ɑ/. However, the lip tightener FAU signal only exhibits higher intensity in smiling condition than the neutral, not an earlier rising onset associated with the smile.

Two key limitations were present for this study. First, a small sample size of two speakers were analyzed due to time constraints. Second, our video recording was set at a lower video quality of 30 frames per second (fps). Future research should involve a larger sample size with both male and female demographics and a wider age range when replicating this study. Recordings should also be processed at 60 fps or higher to obtain more accurate timing.

Acknowledgments

This project was funded by an NSERC Discovery grant.

References

[1] Stavness, I., Nazari, M., Perrier, P., Demolin, D., & Payan Y. (2013). A Biomechanical Modeling Study of the Effects of the Orbicularis Oris Muscle and Jaw Posture on Lip Shape. *Journal of Speech, Language, and Hearing Research*, *56*(3), 878-890.

[2] Liu, Y., Chan, T., Purnomo, G., & Gick, B. (2020). Talking while smiling: Suppression in an embodied model of coarticulation. In Proc of 12th International Seminar on Speech Production.

[3] OpenFace 2.0: Facial Behavior Analysis Toolkit Tadas Baltrušaitis, Amir Zadeh, Yao Chong Lim, and Louis-Philippe Morency, *IEEE International Conference on Automatic Face and Gesture Recognition*, 2018

[4] Hung, K., Liu, Y., Purnomo, C., & Gick, B. (2022). Timing of smile suppression during the articulation of labials in smiled speech. *The Journal of the Acoustical Society of America, 152*(4), A287-A287.

[5] Sussman, H. M., & Westbury, J. R. (1981). The effects of antagonistic gestures on temporal and amplitude parameters of anticipatory labial coarticulation. *Journal of Speech, Language, and Hearing Research*, *24*(1), 16-24.

ARTICULATION AND ACOUSTICS OF KOREAN LIQUIDS: A CASE STUDY IN LOANWORD ADAPTATION

Naim Lim *[1], Alexei Kochetov †[1], and Yoonjung Kang ‡[1,2]
[1]University of Toronto, Toronto, Ontario, Canada
[2]University of Toronto Scarborough, Social Sciences Building, Toronto, Ontario, Canada

1 Introduction

This paper presents a case study in phonetic variation in the realization of liquid consonants (laterals and rhotics) in Korean loanwords from English. English has two liquid phonemes, lateral /l/ and approximant /ɹ/. Korean, on the other hand, has a single liquid phoneme, /L/, which is restricted in the native vocabulary to word-medial and word-final positions. Word-medially, it is realized as a tap if single and as a lateral if geminate; in word-final position, it is realized as a lateral [1]. The restriction against word-initial liquids, however, is relaxed in English loanwords, with recent studies observing a range of realizations: with most common variants being taps and laterals, and other variants including approximants, stops, nasals, obstruents, and trills [5,7]. To better understand the details of this variation, we collected electropalatography (EPG) and acoustic data from two native Korean speakers fluent in English. Specifically, we wanted to investigate details of realization of the word-initial liquid in loanwords, as compared to the same phoneme occurring in Korean word-medially and to the English liquids, as produced by the same speakers.

2 Method

2.1 Speakers

The participants were a female and a male native speaker of Korean (KF and KM). Both were in their early forties, originally from Seoul, South Korea, and had been living in Toronto for less than three years. They studied English from the age of 12 and have been speaking it regularly since moving to Canada. Both can be considered intermediate to advanced learners of English.

2.2 Materials

Control items included word-medial singleton /L/ and geminate /LL/ in Korean-native words (n=9; e.g., paLam 바람, 'wind'; taLLi 달리, 'differently') and word-initial and medial /l/ and /ɹ/ in English words (n=38; e.g., lilac; radio). Target items included Korean loanwords corresponding to the English control words (n=38; e.g., LaiLLak 라일락, 'lilac'; Latio 라디오, 'radio'). In loanwords, English /ɹ/ and /l/ are generally adapted as singleton /L/ and geminate /LL/ word-medially, while only a singleton realization is possible word-initially. The loanwords were selected from the *National Academy of the Korean Language* survey ([3]). The stimuli were randomized and produced 6 times each in a language-specific carrier (*이게 또 _ 이다.* /ike t*o _ ita/, 'This another_'; *I saw _ over there*), in separate sessions.

2.3 Articulatory Analysis

We used the WinEPG system [6], which tracks the contact between the tongue and the palate over time (at 100 Hz) using a custom-made acrylic palate with 62 electrodes. This palate, organizing into a grid of 8 rows and 8 columns allows to distinguish among different kinds of liquids: a lateral (a closure at the alveolar ridge and reduced posterior side contact), a tap (a weak postalveolar constriction with some posterior side contact), and an approximant (mainly posterior side contact). A measure of Centre of Gravity (CoG) of linguopalatal contact (higher is more anterior) taken at the consonant midpoint was employed to quantify the anteriority of these categories (lateral > tap > approximant). Additionally, we measured constriction duration, which was expected to be longer for laterals (and Korean /LL/ > English /l/) than the approximant and especially the tap.

2.4 Acoustic Analysis

Word-initial liquids in Korean loanwords and the corresponding English words were extracted from the EPG data, segmented using the Montreal Forced Aligner [4], and classified in Praat [2] following the criteria reported in Yun & Kang [7]. Specifically, taps were defined as sounds with a brief stop-like release burst, and a small abrupt amplitude decrease and increase. Laterals were defined as sounds with a long steady state, with a shorter transition into the next vowel compared to approximants. Approximants were defined to have a longer transition into the next vowel than laterals (although still short) with a gradual increase in amplitude.

3 Results

Articulatory results are summarized in Figure 1, with individual tokens plotted by set/position and speaker. Considering the Korean native control set first (leftmost column), the two word-medial liquids /L/ and /LL/ were clearly distinguished in CoG and duration, reflecting the contrast between a geminate lateral and a tap. In the English control set (last 2 columns), /l/ and /ɹ/ were also clearly distinguished by the speakers, but only by CoG (as would be expected). Turning to the target set (loanwords), we can see two types of liquids being produced word-medially (/L/ vs. /LL/, similarly to the native controls, and corresponding to t he English source), yet no

*naim.lim@mail.utoronto.ca
† al.kochetov@utoronto.ca
‡ yoonjung.kang@utoronto.ca

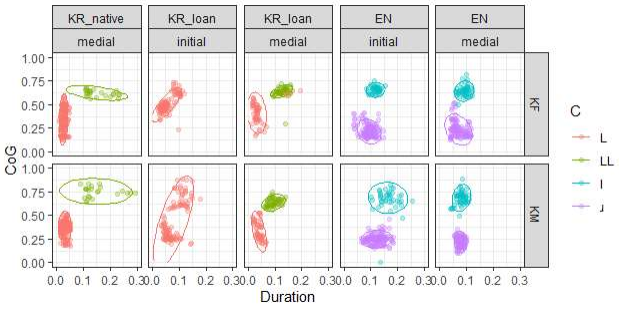

Figure 1: Scatterplots of individual articulatory tokens of liquid phonemes by Centre of Gravity and Duration, separately by set/position and speaker.

clear distinction word-initially. Here, realizations of /L/ show considerable variation, albeit with some separation for KM. Linear Mixed Effects Regression models confirmed significant differences ($p<.05$) among the control items and for the word-medial target items.

Acoustic results showed that for the highly variable word-initial liquid (/L/) in Korean loanwords, the male speaker favoured approximant and lateral realizations (47% and 39%), while the female speaker favoured taps and, to a lesser extent, laterals (68% and 31%). For the English set, productions mostly aligned with the underlying phoneme (Figure 2), as expected, with a lateral-like production for words starting with the underlying phoneme /l/ and an approximant-like production for words starting with /ɹ/, with some exceptions where the female speaker produced a couple of taps.

The logistic regression analyses, performed separately for the proportion of each variant compared to all other variants, tested for effects of language condition, source consonant (English /l/ or /ɹ/), and speaker (cf. [7]). Tests revealed that there were significantly more taps produced in the Korean condition ($p<.001$) and significantly more approximants produced in the English condition ($p<.01$). A significant effect of source consonant was present for approximants when the source consonant was /ɹ/ ($p<.001$), and the effect of speaker was present for taps and approximants, where the female speaker produced more taps, and the male speaker produced more approximants ($p<.001$).

4 Discussion

This study was first to examine variability in the Korean liquid production using both articulatory and acoustic methods. Consistent with observations made in the literature, we saw clear distinctions in the EPG data among liquids in the control sets (Korean native words and English words), as well as for word-medial liquids of Korean loanwords. In word-initial position, which was our main focus, we observed a great amount of variability, also as anticipated. Significant effects of language showed us that speakers were adapting their speech production to the language produced, indicative of some level of mastery of their L2 English. A great amount of individual difference between the two speakers was also observed, which could reflect gender or accentedness levels, although it is difficult to pinpoint exactly which effect given the data from only two speakers. To further explore the cause of variation, we have collected and are currently analyzing acoustic data for 16 new Korean speakers (balanced for gender). Preliminary observations show similar amounts of variability in pronunciations of word-initial /L/ in loanwords, including tap, lateral and approximant realizations.

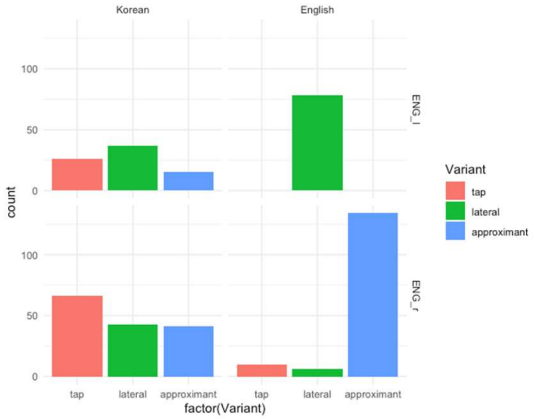

Figure 2: Distribution of counts of word-initial /L/ variants by language condition and source consonant (English /l/ or /ɹ/)

Acknowledgments

Thank you to the participants, as well as to Kelly-Ann Blake, Andrei Munteanu, Fiona Wilson, Jessica Yeung, Zhanao Fu, and Luke Zhou, for contributing to the study design and/or analysis. Funded by an SSHRC Grant to Alexei Kochetov.

References

[1] Ahn, S. W. (2002). The electropalatographic evidence of the Korean flap: An intervocalic Korean liquid sound. Speech Sciences, 9(3), 155-168

[2] Boersma, P., & Weenink, D. (2017). Praat: doing phonetics by computer [Computer program]. Version 6.0.28, retrieved from http://www.praat.org/.

[3] Kwuklipkwukeyenkwuwen [The National Academy of the Korean Language] (1991). Oylaye sayong silthay cosa: 1990 nyento. [Survey of the state of loanword usage: 1990.] Seoul: Kwuklipkwukeyenkwuwen.

[4] McAuliffe, Michael, Michaela Socolof, Sarah Mihuc, Michael Wagner, and Morgan Sonderegger (2017). Montreal Forced Aligner: trainable text-speech alignment using Kaldi. In *Proceedings of the 18th Conference of the International Speech Communication Association*.

[5] Seo, M. (2004). A production-based study of the Korean liquid in onset position. Studies in Phonetics, Phonology and Morphology, 20(2), 257-276

[6] Wrench, A. A., Gibbon, F. E., McNeill, A. M., Wood, S. E. (2002). An EPG therapy protocol for remediation and assessment of articulation disorders. In: Hansen, J. H. L., Pellom, B. (eds), Proc. of the 7th International Conference on Spoken Language Processing, Denver, CO, 965–968.

[7] Yun, S., & Kang, Y. (2019). Variation of the word-initial liquid in north and South Korean dialects under contact. Journal of Phonetics, 77, 100918.

THE ACOUSTICS OF BORROWED /ɚ/ IN QUEBEC FRENCH

Massimo Lipari *[1]
[1]Department of Linguistics, McGill University, Montreal, Quebec

1 Introduction

The English rhotic vowel /ɚ/ (as in soccer, /sɑkɚ/), produced with a bunched or retroflexed tongued and characterized by a uniquely low third formant, is a cross-linguistically rare sound. When a word containing it is borrowed into a language which lacks such a phoneme, some repair must take place to adapt the loanword to the donor language's phonology—a wide variety of strategies are known to be available in such cases, with varying degrees of acoustic fidelity to the original form [1]. Speakers of Quebec French have been claimed to variably employ three methods of adapting English /ɚ/ (cf. [2]). First, the donor language pronunciation may be simply ignored, instead using the orthography and the typical grapheme-to-phoneme mapping of the recipient language (e.g. [sɔk**ɛʁ**] for *soccer*, with different spellings resulting in different vowel qualities). Second, the (phonetically or phonologically/featurally) most similar native phoneme may be substituted for the offending sound (typically /œ/, e.g. [sɔk**œʁ**]). Third, the missing phoneme may be borrowed wholesale (e.g. [sɔkɚ]), creating new (marginal) contrasts.

Despite this claim, loanword /ɚ/ in Quebec French has received little attention in the literature (with the notable exception of [3]). In particular, its acoustics have remained entirely unstudied: the degree of success in emulating the rhoticity (low F3) of the English vowel, as well as the borrowed vowel's relationship to the similar native phonemes /œ/ and /ø/, are unknown. The present paper is a pilot study aimed at addressing these gaps.

2 Data & Methods

The data are from a purpose-built expansion of Milne's *AssNat* corpus [4], a collection of recordings of parliamentary proceedings of the National Assembly of Quebec. For ease of data collection and analysis, all 317 tokens of the loanword vowel—henceforth referred to as X, due to its variable realization—are taken from a single word, *Orford* (a place name of English origin), across 26 speakers. From these same speakers, 797 tokens of /œ/ and 1,157 tokens of /ø/ from the most similar licit phonotactic environment (final syllables closed by a rhotic for the former and final open syllables for the latter) are included for comparison. All formant values are normalized using the *Nearey2* method [5] (albeit using the by-speaker mean of phoneme log means instead of the raw log mean). F1 and F2 are measured at vowel midpoint, whereas F3 is measured at its minimum (capturing the point of greatest rhoticity). Overlap in empirical F1 × F2 × F3 distributions between X and each of the two native phonemes of interest (first averaging all tokens of a given word for /œ/ and /ø/) is calculated using Pillai scores, as per [6, 7].

* massimo.lipari@mail.mcgill.ca

3 Results

3.1 Rhoticity of loanword /ɚ/

Averaging first within then across speakers, mean F3 of X (0.475) is significantly lower than that of /œ/ (0.673, $p < 0.001$) and that of /ø/ (0.595, $p < 0.001$), suggesting that the borrowed vowel often preserves its rhoticity. However, the realization of X is subject to much inter-speaker variability (σ of speaker averages = 0.096)—significantly more so than /œ/ ($\sigma = 0.043$, $p < 0.001$) and /ø/ ($\sigma = 0.048$, $p < 0.001$). This is also shown in **Figure 1**. While most speakers have a sizeable difference in F3 between X and the other vowels, and while the general trend of lower F3 in X than in the other vowels is visible for all but two speakers, a minority have little difference between the categories: for all members of this latter group, F3 of X is particularly high.

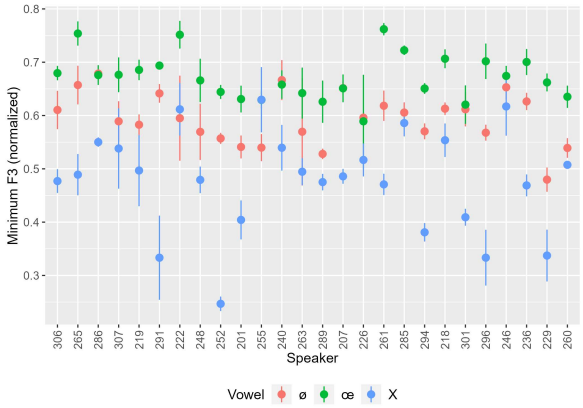

Figure 1: Minimum F3 (μ and σ) by vowel and speaker.

3.2 Relation with /œ/ and /ø/

On average, F2 of X (0.161) is significantly lower than that of /œ/ (0.216, $p < 0.001$) or /ø/ (0.269, $p < 0.001$), indicating a more posterior constriction. Here too, however, X ($\sigma = 0.087$) is significantly more variable than the other vowels: $\sigma = 0.055$ for /œ/ and $\sigma = 0.043$ for /ø/ ($p < 0.001$ in both cases). **Figure 2**, which depicts by-speaker F1 × F2 spaces with 1σ ellipses, shows that the observed variance in F2 is due to a bimodal distribution of speakers, with many producing X with near identical frontness as /œ/ (or even as the slightly fronter /ø/) but some clearly producing a back vowel (consistent with an [ɔ] articulation, which is expected on the orthography-based strategy).

Conversely, in terms of average F1, X (− 0.905) is intermediate between /œ/ (− 0.616) and /ø/ (− 1.12), but significantly different from both ($p < 0.001$ for both tests).

Unlike for F3 and F2, here X is only significantly more variable than /ø/ ($\sigma = 0.12$ vs $\sigma = 0.054$, $p < 0.001$): the difference between X and /œ/ ($\sigma = 0.12$) is negligeable and non-significant ($p = 0.73$). Here (as seen in **Figure 2**), two kinds of speakers can be identified: those who maintain a three-way height distinction between the vowels (the majority) and those who have some degree of overlap between X and /ø/ on the F1 dimension (a minority).

For the average speaker, the F1 × F2 × F3 Pillai score comparing the distributions of X and /ø/ (0.68, $\sigma = 0.17$) is lower than that comparing the distributions of X and /œ/ (0.78, $\sigma = 0.17$), indicating greater overlap between categories in the former case. As seen in **Figure** 3, this holds for most speakers, although a small number exhibit the opposite pattern. In any case, the observed Pillai scores suggest that most speakers maintain a category distinction between X and the other two vowels.

4 Discussion and Conclusions

The present study confirms that the acoustics of English loanword /ɚ/ in Quebec French is subject to much variation across speakers. Nevertheless, the range of variability observed cannot be reduced to the three strategies outlined in Section 1. To be sure, there is evidence for an orthography-based variant (in this case, [ɔ]). A handful of speakers, moreover, show some evidence of substitution of a native phoneme (as reflected in their low Pillai scores)—although interestingly, contrary to traditional descriptions, both [œ] and [ø] are possible variants. Of the remaining speakers, however, the degree of rhoticity observed is variable: while some (e.g., 252) produce X with low F3, others (e.g., 248 and 285) achieve only mild or no rhoticity while still maintaining relatively high distinctness from /œ/ and /ø/ (especially on the F1 dimension). That is, it is possible for speakers to acquire a distinct category for X which does not wholly successfully emulate the acoustic signature of the vowel in the donor language.

While this result is novel and intriguing, further investigation is required to ascertain its robustness. Most notably, more data are needed, with a particular eye to increasing the number of speakers and extending the study beyond the single lexical item *Orford*.

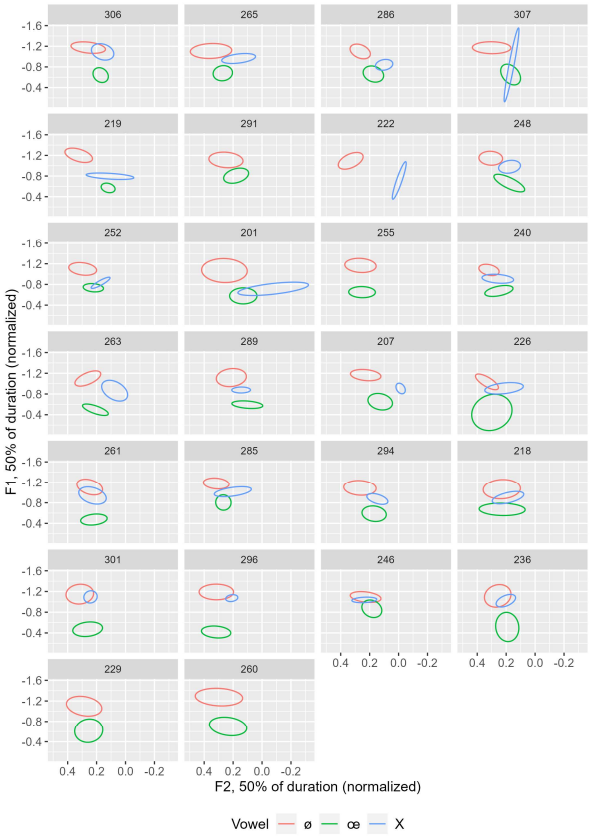

Figure 2: F1× F2 distributions by vowel and speaker.

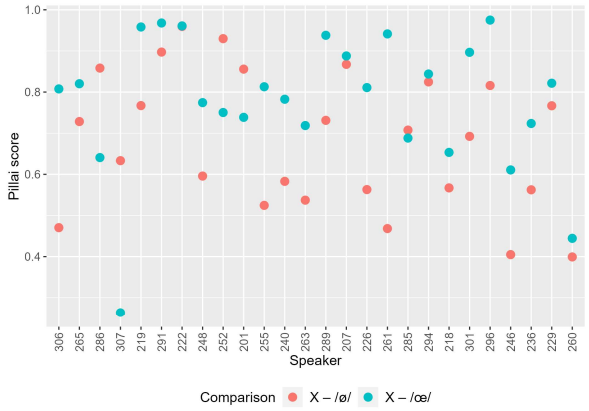

Figure 3: Pillai scores for X – /ø/ and X – /œ/ by speaker.

Acknowledgments

This work was funded by FRQSC B1Z award #321056 to the author, as well as SSHRC grant #435-2017-0925 to Morgan Sonderegger. Many thanks to MS for guidance and insight, and to Irene Smith for comments and support.

References

[1] Y. Kang, 'Loanword Phonology', in The Blackwell Companion to Phonology, John Wiley & Sons, Ltd, 2011, pp. 1–25.

[2] M.-H. Côté, 'L'adaptation des emprunts de l'anglais en français: variation dialectale, phonologie, lexicographie', in L'adaptació de manlleus en català i en altres llengües romàniques, Publicacions i Edicions de la Universitat de Barcelona, 2021, pp. 43–47.

[3] M. L. Friesner, 'The social and linguistic predictors of the outcomes of borrowing in the speech community of Montréal', Ph.D., University of Pennsylvania, 2009.

[4] P. Milne, 'The variable pronunciations of word-final consonant clusters in a force aligned corpus of spoken French', Ph.D., University of Ottawa, 2014.

[5] T. M. Nearey, 'Phonetic feature systems for vowels', Indiana University Linguistics Club, Bloomington, 1978.

[6] J. Hay, P. Warren, and K. Drager, 'Factors influencing speech perception in the context of a merger-in-progress', Journal of Phonetics, vol. 34, no. 4, pp. 458–484, 2006.

[7] J. Nycz and L. Hall-Lew, 'Best practices in measuring vowel merger', Proceedings of Meetings on Acoustics, vol. 20, no. 1, pp. 1–19, 2014.

ACOUSTIC VARIATION IN SPEECH: CONTRASTING INITIAL AND LATER STAGES OF CONVERSATIONS SHOWING OPINION CONVERGENCE AND DIVERGENCE

Charlize Ma [*1], Jahurul Islam [†1], Effie Kao [‡1], Raechel Kitamura [♦1], Stephanie Wang [♯1], Marcell Maitinsky [♩1], and Bryan Gick [♠1]

Department of Linguistics, University of British Columbia, Vancouver, Canada

1 Introduction

The phenomenon of speech accommodation is influenced by various factors, including interlocutor traits, social identity, context, power dynamics, and speech goals [1]. Additionally, a speaker's perception of positive or negative alignment with their interlocutors can also influence speech patterns [2, 3]. The duration of a conversation is another important factor that can impact speech, as individuals may modify their speech patterns as the interaction progresses. Despite extensive research on many of these factors, the effects of speakers' opinion convergence or divergence and the duration of interaction on speech characteristics are relatively new areas of interest [4]. While some studies have explored the impact of duration on speech features (e.g., F0) in human-robot computer games, finding no evidence of accommodation [5], there is a lack of research on how the duration of interaction specifically interacts with the expression of explicit opinion convergence or divergence.

To address this gap, the current study aims to investigate whether the duration of interaction influences the acoustic characteristics of speech produced by individuals during instances of opinion convergence (agreement) or divergence (disagreement) in relation to their interlocutors. By examining this relationship, the study seeks to provide valuable insights into the dynamics of speech accommodation and shed light on how the duration of interaction may shape the expression of opinion alignment or contrast.

2 Methods

2.1 Data

The data came from speakers from a YouTube channel called the *Ellen Fisher Podcast*. Speech from several individuals was extracted from three polarized conversations. The topics included "Plant vs. Animal Regenerative Farming", "Pro-Life vs. Pro-Choice" and "Vegan vs. Animal Foods." The videos did not specify the speaker's language background, but all appeared to be native-level American English speakers (M:4, F:4). Speakers' presumed ages were around 30-60 years, and all speakers were knowledgeable in their respective fields, so they were presumed to have a high education level.

[*] sy.charlize@gmail.com
[†] jahurul.islam@ubc.ca
[‡] effiekao@student.ubc.ca
[♦] raechelk@student.ubc.ca
[♯] smwang@student.ubc.ca
[♩] mlmtnsky@student.ubc.ca
[♠] gick@mail.ubc.ca

The videos had two different discussion structures. In the "Plant vs. Animal Regenerative Farming" video, the four speakers were led by a host to take turns speaking for a few minutes each time. In the other two videos, the two speakers were allowed to speak freely throughout the whole discussion. In each video, the host would encourage turn-taking between interlocutors and guide the conversation by introducing new topics and posing questions.

2.2 Annotation and Processing

From each episode of the selected podcasts, two chunks (each about 20 minutes long) were extracted: the first one was from the initial 30 minutes of the episode while the second one was about one hour into the conversation. Audio was extracted from each video clip and then all the audio clips were transcribed using Praat TextGrids [6]. Next, the phone-level transcriptions were generated using the Montreal Forced Aligner [7]; any errors in the automatic alignment were manually corrected.

Chunks of speech were then manually inspected to identify and code three types of events representing an opinion category: 1) when a speaker expresses an explicit agreement (convergence) with an interlocutor, 2) when a speaker expresses an explicit disagreement (divergence) with an interlocutor, or 3) when a speaker produces a "neutral" statement.

2.3 Analysis

We extracted the fundamental frequency (F0), the first formant (F1) and the second formant (F2) at the midpoint for the monophthongal vowels in the speech using FastTrack [8] which is a Praat-based toolkit for measuring vowel formants in an optimized way. The formant values were normalized in R [9] using the Lobanov method [10]. Statistical analysis of the data was performed using R to investigate the effect of the conversation stage on F0, F1 and F2 within each opinion category.

3 Results

Figures 1, 2 and 3 present the distributions of normalized F0, F1, and F2, respectively, across opinion categories and conversation phases. The x-axis represents whether the data points belong to an event where the talker expressed an agreement ("converged"), a disagreement ("diverged") or neither ("neutral"). Phases of the conversation are marked using colours ("part1" = towards the beginning; "part2" = towards the middle or end).

As Figures 1 and 2 reveal, the distributions of F0 or F1 values across conversational stages are very similar, which is

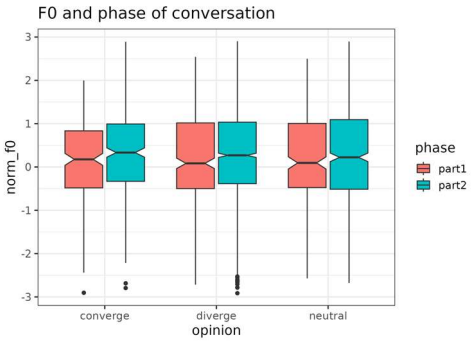

Figure 1: F0 and conversation stage

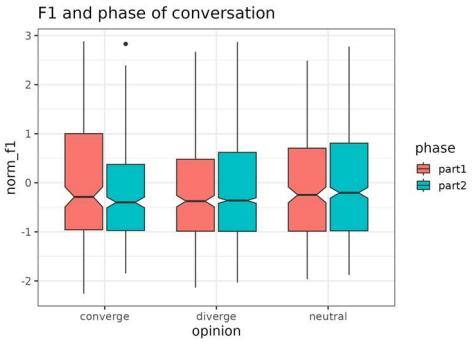

Figure 2: F1 and conversation stage

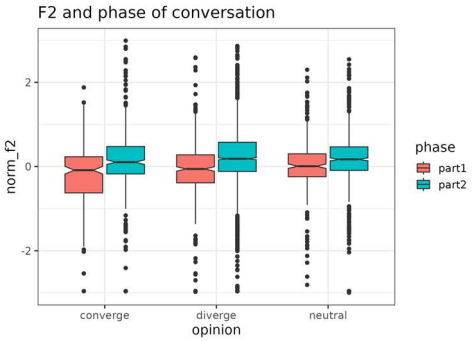

Figure 3: F2 and conversation stage

consistent for the events of both convergence and divergence. This indicates that speakers kept using similar ranges of pitch and vowel heights across the whole conversation and did not vary their pitch or vowel height no matter how far along they are and whether they expressed an opinion or remained neutral in the conversation. Contrarily, Figure 3 reveals that conversational stage. More specifically, vowels in the second phase of the conversations tended to have higher F2 values indicating more fronted vowels.

To investigate the effect on conversational phase on acoustic features within each opinion category, separate linear mixed-effects models were fitted using the R package *lmerTest* [11] for "converge", "diverge", and "neutral" opinion categories. In each model, fixed effects were included for the variables "phase" and "vowel" and random intercepts were included for individual "speakers". P-values were obtained via t-tests using Satterthwaite's method, as provided by the *lmerTest* R package [11].

Results of the linear mixed-effects models revealed a significant effect of conversational phase on F2, both in the events of convergence ($t(387) = 4.35$, $p < 0.001$) and divergence ($t(32) = 4.49$, $p < 0.001$). In both cases, F2 had a significant increase in part 2 of the conversation. Crucially, the effect of phase was not statistically significant in the neutral condition ($t(97) = 1.16$, $p = .25$). No such patterns were observed for F0 and F1.

4 Conclusion

Results of this study revealed that there was a significant effect of the phase of conversation on F2 in the event of convergence or divergence of opinion; similar effect was not confirmed for neutral speech. This suggests that speakers used specific strategies (i.e. making vowels frontier) when they had an opinion to express. For F0, our results are consistent with human-robot interactions [5], showing no accommodations. These results add a new dimension to our understanding of speech accommodation in addition to the affecting factors reported in previous studies (as in [1-3]) by providing evidence that opinion convergence or divergence interacts with the duration of interaction in natural speech.

Acknowledgments

This study was supported by NSERC.

References

[1] Pardo, S., Pellegrino, E., Dellwo, V., & Möbius, B. (2022). Vocal accommodation in speech communication. *J. of Phon.*, *95*.

[2] Babel, M. (2010). Dialect divergence and convergence in New Zealand English. *Language in Society, 39*(4), 437-456.

[3] Babel, M. (2012). Evidence for phonetic and social selectivity in spontaneous phonetic imitation. *J. of Phon.*, *40*(1), 177-189.

[4] Ma, C., Kao, E., Kitamura, R., Wang, S., Islam, J., De Boer, G. & Gick, B. (2023) Relations between Opinion Convergence, Acoustic Convergence and Movement Convergence in Interlocutors. In *Proceedings of the International Symposium on Phonetics & Cognitive Sciences of Language*, 62-63.

[5] Ibrahim, O., Skantze, G., Stoll, S., & Dellwo, V. (2019). Fundamental frequency accommodation in multi-party human-robot game interactions: The effect of winning or losing. *Interspeech*.

[6] Boersma, Paul & Weenink, David (2023). Praat: doing phonetics by computer [Computer program]. Version 6.3.10.

[7] McAuliffe, M., Socolof, M., Mihuc, S., Wagner, M., & Sonderegger, M. (2017). Montreal forced aligner: Trainable text-speech alignment using kaldi. In *Interspeech*.

[8] Barreda, S. (2021). Fast Track: fast (nearly) automatic formant-tracking using Praat. *Linguistics Vanguard*, *7*(1). https://doi.org/10.1515/lingvan-2020-0051

[9] R Core Team (2023). R: A language and environment for statistical computing. R Foundation for Statistical Computing, Vienna, Austria.

[10] Adank, P., Smits, R., & Van Hout, R. (2004). A comparison of vowel normalization procedures for language variation research. *J. of Acou. Soc. of America*, *116*(5), 3099-3107.

[11] Kuznetsova A, Brockhoff PB, & Christensen RHB. (2017). "lmerTest Package: Tests in Linear Mixed Effects Models." *J.of Statistical Software*, *82*(13), 1-26.

VOT Analysis of L1 and L2 Speakers of Itza'

Jack Mahlmann [*1]
[1]Department of Linguistics, University of Toronto, Toronto, Ontario, Canada

1 Introduction

This study explores Voice Onset Time of plain and ejective stops (VOT) in Itza' (ISO 639-3: itz), a critically endangered Mayan language spoken in northern Guatemala. VOT is the amount of time (usually measured in milliseconds) elapsed between the release burst of a stop sound such as /p/ or /t/ and the onset of voicing associated with the following vowel; this measurement can vary for the same phoneme across languages, or within a language according to social or other factors. In addition to the plain stops (/p/, /t/, /k/), Itza' has a series of ejective stops (/p'/, /t'/, /k'/) which are produced with the glottalic ingressive airstream mechanism: upward movement of the larynx compresses the air between the glottal folds and an oral constriction (at the velum, for example, in the case of /k'/), creating the characteristic 'popping' sound of an ejective [1].

Ejectives can be seen as a mark of identity for speakers of languages that have them, especially in the case of endangered languages. Hyper-articulation of particular sounds that are unlike those found in the dominant language (often for the benefit of second-language learners) can result in increased awareness of their connections to the speaker's linguistic identity. In the case of SENĆOŦEN (an endangered Salishan language spoken in the Pacific Northwest), Bird [2] found that L2 teachers produced a "stronger" ejective /t'/ than L1 elders, with a longer VOT. A similar effect may occur in Itza', where there are two main populations of speakers: L2 learners and L1 elders. I hypothesize that if L1 speakers of Itza' have a weaker ejective with a shorter VOT, then L2 speakers will produce a stronger one with a longer VOT. However, if L1 speakers have a strong ejective, then I would not expect the production of L2 speakers to differ because stronger ejectives are more salient and less likely to weaken over time [2].

2 Method

2.1 Participants

Elicitation sessions for this study were carried out in San José, Petén, Guatemala. Participants were recruited through the Itza' Linguistic Community (a community organization associated with the *Academia de Lenguas Mayas de Guatemala*). A total of 8 participants were included in the analysis, 4 L1 (mean age of 72) and 4 L2 speakers (mean age of 45). Each participant was compensated with 50 Guatemalan Quetzales.

2.2 Stimuli

All participants were presented with 12 Itza' words with plain/ejective stops in initial position — 6 initial consonants each followed by /u/ and /a/ — written in the standard orthography. Each word also had an accompanying picture conveying the word intended for elicitation. Words were selected from Hofling & Tesucún's dictionary [3] and approved by a member of the Itza' community. Table 1 shows the full wordlist used.

Table 1: List of Itza' words elicited, with English translations.

Itza'	English
p'ak	*tomato*
p'ul	*smoke*
t'a'	*forehead*
t'ut'	*parrot*
k'ab'	*arm*
k'u'	*nest*
pach	*back*
put	*papaya*
tat	*father*
tup	*earring*
kal	*neck*
kum	*pot*

2.3 Procedure

After signing a consent form, participants self-reported their status as an L1 or L2 speaker of Itza'. They were then instructed to say the name of each item they see using the carrier sentence "Kinwa'lik tech __ ti tech" ("I say __ to you"). During the recorded elicitation session, participants were presented with each word one-by-one, in orthography and with the matching picture at the same time. Once the participant said the word within the provided carrier sentence three times, the stimuli switched to the next word and picture until all 12 words were completed.

2.4 Data analysis

Audio files were analyzed using Praat [4]. VOT for plain and ejective stops in the target words was manually measured from initial release burst of the stop to the onset of voicing for the following vowel. Some tokens were excluded for reasons of audio quality.

The extracted data was analyzed using R [5] to acquire averages and create a mixed-effects model [6] with place of

[*] jack.mahlmann@mail.utoronto.ca

articulation, following vowel, airstream mechanism, and L1/L2 status as fixed effects, and speaker ID as the grouping variable. 216 tokens were included in the analysis: 99 tokens of plain stops and 117 tokens of ejective stops.

3 Results

Figure 1 below shows the distribution of VOT in milliseconds for plain and ejective stops in Itza', separated by L1/L2 status of the speaker and place of articulation.

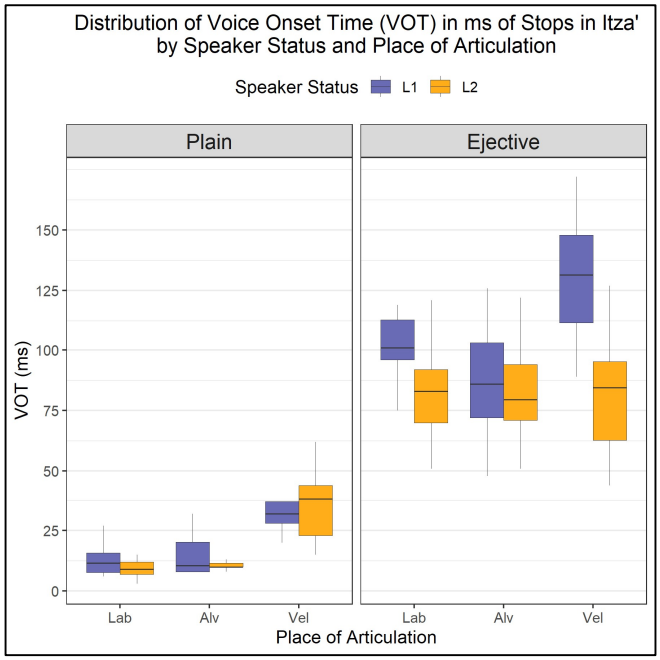

Figure 1: Distribution of VOT (ms) of plain and ejective stops produced by L1 and L2 speakers of Itza' by speaker status and place of articulation.

A higher median value and inter-quartile range can be seen for L1 speakers as opposed to the L2 speakers for the ejectives, particularly at the labial and velar places of articulation. Differences between L1 and L2 speakers in production of plain stops are less prominent.

The mixed-effects model found that L1/L2 status was a significant factor at the $p < 0.01$ level, with the isolated effect being that L1 speakers have a +16 ms higher VOT for stops than L2 speakers. The difference between labial and alveolar places of articulation was not significant, however there was a significant effect ($p < 0.001$) for the velar place of articulation, which is to be expected. Airstream mechanism also had a significant effect at the $p < 0.001$ level; the isolated effect of airstream was that ejectives had a VOT of +72 ms when compared to plain stops. Additionally, the following vowel was also significant at the $p < 0.05$ level. Stops with a following /a/ were found to have a VOT of +5 ms when compared to stops with a following /u/.

4 Discussion

The results of the statistical analysis stand in contrast with the findings of Bird's SENĆOŦEN study [2]. An apparent time interpretation (coupled with the understanding that L1 speakers are few in number and all elderly, and generational transmission will be restarted by L2s) suggests that Itza' ejectives are moving towards the VOT criteria more associated with weaker ejectives. This information could be used to provide Itza' language instructors with advice for L2 students for whom it is a goal to sound as native-like as possible.

5 Conclusion

This study has found that VOT for ejective stops in Itza' is higher in the L1 speakers analyzed than the L2 speakers, while differences in plain stops are less prominent. If one of the goals of the language revitalization efforts is to preserve the way of speaking of the community elders, then Itza' language educators have an opportunity to modify this aspect of their approach to ensure that ejectives are retained in the language in the long-term such as by intentionally hyper-articulating these sounds to increase their salience. While this type of change — the potential loss of a contrasting feature — is natural and doesn't represent a corruption or bastardization of the language in the eyes of linguists, it is important to consider the needs of the language community being served, as determined by members of the community itself.

Acknowledgments

Thank you to José Alfredo Chayax Tesúcun for helping to carry out the elicitation sessions. This study is associated with the University of Toronto's Itza' Revitalization Project, supported by the Connaught Fund.

References

[1] Fallon, P. D. (1998). The Synchronic and Diachronic Phonology of Ejectives [PhD Thesis]. The Ohio State University.

[2] Bird, S. (2020). Pronunciation among adult Indigenous language learners. Journal of Second Language Pronunciation, 6(2), 148–179.

[3] Hofling, C. A., & Tesucún, F. F. (1997). Itzaj Maya-Spanish-English Dictionary. University of Utah Press.

[4] Boersma, P., & Weenink, D. (2022). Praat: Doing phonetics by computer (6.3.02).

[5] R Core Team. (2022). R: A Language and Environment for Statistical Computing. R Foundation for Statistical Computing. https://www.R-project.org/

[6] Bates, D., Mächler, M., Bolker, B., & Walker, S. (2015). Fitting Linear Mixed-Effects Models Using lme4. Journal of Statistical Software, 67(1), 1–48.

TONGUE ADJUSTMENTS IN THE CHEST-HEAD REGISTER TRANSITION OF OPERATIC SINGERS

Grace Bengtson[*], Elena Massing[†], Cindy Zhao[‡], Maria Samarskaya[♦], Jahurul Islam[♯], Bryan Gick[♠]
Department of Linguistics, University of British Columbia, Vancouver, Canada

1 Introduction

The change in register from head to chest voice has been widely associated with laryngeal adjustments, including greater vocal fold adduction [1], longer glottal closed phase [2], and vocal fold thickening [3]. Comparatively little research has looked at supralaryngeal adjustments in singing register. Echternach and colleagues conducted a series of real-time MRI studies investigating the shape of the supraglottal vocal tract between registers [4, 5, 6], and reported that the tongue dorsum was more elevated and farther back in falsetto than in modal voicing for operatic singers [4]. Another study on classical singers and yodellers found the tongue dorsum to be more elevated for higher pitches [5]. These studies showed significant variation across individuals and different vowels [6]. All of these studies, however, measured the tongue at only two points: tongue dorsum/body height and pharynx width.

The present case study aims to provide a qualitative investigation into the specific tongue adjustments made during register shifts. In particular, we will report on overall changes in tongue contour using ultrasound imaging of the midsagittal plane. These measurements will be reported for one trained opera singer producing transitions between chest and head register, across six vowel categories.

2 Methods

2.1 Participants and Procedure

One mezzo-soprano opera singer, age 18, took part in this study and was recruited through word-of-mouth. The participant was enrolled in the opera program at UBC and had eight years of classical voice training, including private voice lessons and choral singing.

The participant was seated in an experiment chair with a stabilizing headrest to prevent unwanted head movement. An ultrasound probe was positioned to view a midsagittal section of the entire tongue length. Ultrasound videos were recorded while the participant sang an ascending and descending one-octave chromatic scale from G3-G4. These notes were chosen because the register transition fell roughly in the middle of the scale, providing ample data for both registers. A chromatic scale was chosen to have a consistent distance between notes to more accurately pinpoint the register transition. One scale was sung for each of the following vowels: /a, e, i, o, u/, and a rhotacized vowel /ɚ /.

2.2 Analysis

Audio was extracted from the ultrasound videos and manually annotated in Praat [7]. A script was then used to identify the midpoints of each note produced, and the corresponding ultrasound image frames were extracted using an R [8] script. These frames were run through EdgeTrak software [9] to find the x,y coordinates of the tongue contour in a two dimensional Cartesian spatial grid. We evaluated the register shape differences for each of the six vowels independently to avoid influence from vowel differences.

3 Results

Figure 1 plots the tongue contours of each token in the scale, for all six vowels, with the tongue tip on the right side. Results show that the presence of noticeable adjustments in tongue shape between registers for this singer is vowel-dependent. Specifically, vowels with constrictions in the inferior and posterior parts of the vocal tract contrast in tongue shape between head and chest voice. Low and mid-back vowels /a/ and /o/, as well as the rhotic vowel /ɚ/, show the most prominent adjustments. Conversely, the mid-front vowel /e/ exhibits minimal adjustments, and no observable adjustments are present for high vowels /i/ and /u/.

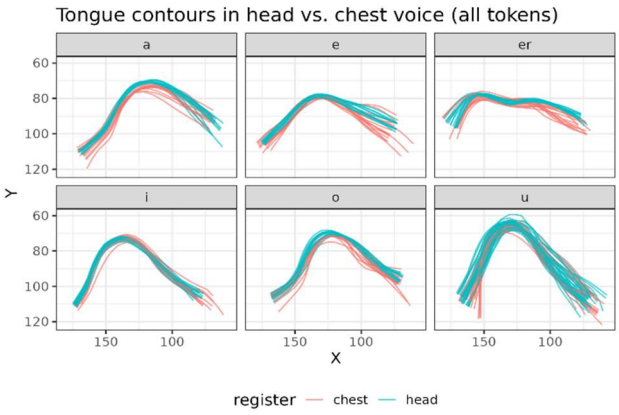

Figure 1. Individual tongue contours. Tokens sung in chest voice are in red, and tokens sung in head voice are in blue. /ɚ / is labeled "er" in this chart.

Figure 2 shows the smoothed contours of both registers for each of the six vowels, obtained via GAM method using ggplot's [10] *geom_smooth()* functionality. In general, for vowels where registers differ in tongue shape, the tongue dorsum is more elevated in head voice than in chest voice. The

[*] graceb14@student.ubc.ca
[†] elenasofiamusic@gmail.com
[‡] cindyzhao325@gmail.com
[♦] samarsky98@gmail.com
[♯] jahurul.islam@ubc.ca
[♠] gick@mail.ubc.ca

tongue root is also positioned higher in head voice than in chest voice, although this adjustment is to a lesser degree, as tongue root position shows some overlap between the registers for all vowels. The tongue tip is more elevated in head voice than chest voice for the vowels /o/, /e/, and /ɚ /, but shows no difference for /a/.

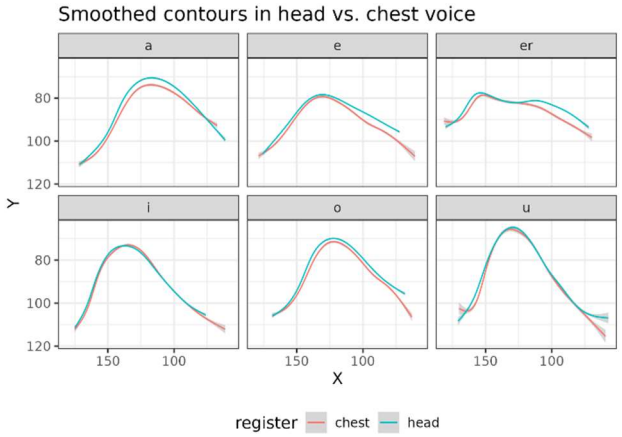

Figure 2. Smoothed contours. Tokens sung in chest voice are in red, and tokens sung in head voice are in blue. The shaded grey regions show the 95% confidence intervals. /ɚ / is labeled "er" in this chart.

4 Discussion

This qualitative case study provides a comprehensive examination of tongue adjustment during register transitions in operatic singing, focusing on tongue elevation and overall change in tongue contour. The obtained results demonstrate the role that supralaryngeal modifications play during vocal register transitions. These transformations in tongue contour emerged as being notably vowel dependent.

In alignment with the findings of Echternach et al. [4], we observed a distinctive variance in tongue position between the head and chest voices. Specifically, we identified an elevation in tongue positioning within the head register across all vowels.

Our analysis further underscores the influence of vowels on the adjustments made in tongue shape and position during register changes. Vowels with constrictions located closer to the posterior corner of the vocal tract exhibited greater differentiation in tongue shape between registers. This pattern indicates a potential link between the phonetic properties of a vowel and the degree of supralaryngeal adjustment during register transitions, meriting further investigation.

While this study offers valuable insights into the subject, we acknowledge the need for a larger participant pool for a more comprehensive analysis. The data presented here is from a single opera singer, limiting the generalizability of the findings. Future research should incorporate a larger participant pool and a wider range of voice types to explore the universality or specificity of these findings.

Acknowledgments

This project was funded by an NSERC Discovery grant.

References

[1] Thalén, M., & Sundberg, J. (2009). Describing different styles of singing: A comparison of a female singer's voice in "classical," "pop," "jazz" and "blues." *Logopedics Phoniatrics Vocology, 26*(2), 82-93. https://doi.org/10.1080/140154301753207458

[2] Henrich, D. N. (2006). Mirroring the voice from Garcia to the present day: Some insights into singing voice registers. *Logopedics Phoniatrics Vocology, 31*(1), 3-14.

[3] Herbst, C. T., Ternström, S., & Švec, J. G. (2009). Investigation of four distinct glottal configurations in classical singing—A pilot study. *The Journal of the Acoustical Society of America, 125*(3), EL104–EL109. https://doi.org/10.1121/1.3057860

[4] Echternach, M., Traser, L., Markl, M., & Richter, B. (2011a). Vocal tract configurations in male alto register functions. *Journal of Voice, 25*(6), 670-677.

[5] Echternach, M., Markl, M., & Richter, B. (2011b). Vocal tract configurations in yodelling—prospective comparison of two Swiss yodeller and two non-yodeller subjects. *Logopedics Phoniatrics Vocology, 36*(3), 109-113.

[6] Echternach, M., Traser, L., & Richter, B. (2014). Vocal tract configurations in tenors' passaggio in different vowel conditions—a real-time magnetic resonance imaging study. *Journal of Voice, 28*(2), 262-e1.

[7] Boersma, P. & Weenink, D. (2023). Praat: doing phonetics by computer [Computer program]. Version 6.3.10, retrieved 3 May 2023 from http://www.praat.org/

[8] R Core Team (2023). R: A language and environment for statistical computing. R Foundation for Statistical Computing, Vienna, Austria. URL https://www.R-project.org/.

[9] Li, M., Kambhamettu, C., & Stone, M. (2005). Automatic contour tracking in ultrasound images. *Clinical Linguistics & Phonetics*, 19(6-7), 545-554.

[10] H. Wickham. *ggplot2: Elegant Graphics for Data Analysis*. Springer-Verlag New York, 2016.

HEARING HEALTH IN REMOTE QUEBEC: A CASE STUDY FROM A NATIVE SCHOOL

Daniel Paromov [*1,2], Victoria Duda [†1,3], Julie McIntyre [‡1], Phaedra Royle [♦1,4,5] and Adriana Lacerda [♯1,2]

[1] École d'orthophonie et d'audiologie, Université de Montréal, Montréal, Québec, Canada.

[2] Centre de recherche de l'Institut universitaire de gériatrie de Montréal – CIUSSS Centre-Sud-de-l'Île-de-Montréal, Canada.

[3] Centre de recherche interdisciplinaire en réadaptation du Montréal métropolitain, Montréal, Québec, Canada.

[4] Centre for Research on Brain, Language and Music, McGill University, Montréal, Québec, Canada

[5] Centre Interdisciplinaire de Recherche sur le Cerveau et l'Apprentissage, Montréal, Québec, Canada.

1 Introduction

In remote regions of Quebec, audiology services remain critical yet challenging to access due to geographic distance. Many rural and indigenous communities are located several hours away from urban areas, where most audiology clinics and hearing health professionals are concentrated. Thus, for individuals residing in these distant regions, accessing audiology services can be difficult, often requiring significant time, resources, and logistical coordination. These barriers are also exacerbated by the nature of audiological intervention. Indeed, hearing tests and hearing aid fittings may require a significant number of visits to the practitioner's clinic or hospital. More specifically for the Abitibi-Témiscamingue region, audiology services are mainly offered through the "Centre intégré de santé et de services sociaux de l'Abitibi-Témiscamingue" with service points in the cities of Rouyn-Noranda and Val-d'Or, and several privately owned audiology clinics which may still require significant travelling.

Currently, in Quebec, there are no major hearing health-specific awareness or screening programs that are established targetting school-age children. The only government-established program is the "The Universal Newborn Hearing Screening Program" which aims to identify infants at risk of hearing loss as early as possible, often within the first few days of their lives, ensuring prompt intervention. This program currently reaches 53% of all newborns in the province, with growing numbers of centers joining the program [1].

Indigenous communities experience higher rates of hearing health problems than the general population. Several studies suggest that Indigenous people, especially children, are more susceptible to persisting otitis media, a leading cause of hearing loss [2]. For children, this early-onset hearing loss can lead to significant developmental challenges, impacting their communication, education, and overall quality of life [3]. While the exact prevalence varies across different communities in Quebec, some studies suggest that it could reach up to 46% of children in some populations, notably northern Inuit communities [4] but it is still high in southern communities (~25% of children surveyed in a Nova Scotia First Nations elementary [2]).

Here we present the results of a visit to an indigenous community from the Abitibi-Témiscamingue region that was accomplished through a collaboration between the University of Montreal's School of Speech-Language Pathology and Audiology, the First Nations Education Council, and an Algonquin community school and community health center.

2 Method

The collaboration between the university and the community took place over a period of 4 years (2019-2023) which included both virtual and in-person visits to the community. Referral reasons for a hearing screening included parental concern, school's staff concern, speech-language pathologists concern or as an update following previous interventions or screenings. During the in-person visits, both audiologists and audiology students performed hearing screenings using otoscopy, tympanometry (*SENTIERO DESKTOP Tympanometer*), transient evoked Otoacoustic emissions (*Otodynamics Echoport IL O292 USB-I*), and air conduction audiometry (*MAICO MA-40 audiometer and TDH-39 earphones*) based on the children's age and profile.

The hearing screenings were performed in an office assigned by the school administration with noise levels slightly exceeding the ANSI/ASA S3.1. standards for the use of supra-aural earphones (mean value = 41.0 dB SPL) when testing up to the 0 dB HL threshold. To account for the ambient noise, the passing criteria for air conduction audiometry was set to 30 dB HL.

3 Results

A total of 29 children were screened at the school during the 2023 visit, with their ages ranging from 4 to 13 years old. The children assessed from pre-kindergarten and kindergarten represented the majority of the participants (6/7 and 8/11). The main findings included hearing loss, middle ear pathology, and significant earwax buildup.

Before any screening was performed, written consent was obtained from the parent or legal guardian. All the results and referral reasons were communicated both to the school administration, the community health and wellness center, and the legal guardians. Probable hearing loss was detected in only 3 children, all with signs of otitis media and in some cases significant wax buildup. All references were made to the region's hospital with pediatric audiology services available, and a follow-up was offered through the community center and medical transportation services available on-site.

[*] daniel.paromov@umontreal.ca
[†] victoria.duda@umontreal.ca
[‡] julie.mc.intyre@umontreal.ca
[♦] phaedra.royle@umontreal.ca
[♯] adriana.lacerda@umontreal.ca

Table 1: Number of hearing screenings performed for each grade.

Grade	Number of Screenings
Daycare	1
Pre-Kindergarten	6
Kindergarten	8
1st Grade	3
2nd Grade	4
3rd Grade	2
4th – 8th Grade	5

Table 2: Hearing screening Results and Referral Reasons (2023).

Result	Treatment or Referral reason	Number of children	Total
Normal	No Treatment	10	23
	Cerumen removal	6	
	Mineral Oil	7	
Need for Referral	Otitis Media	4	6
	Known HL	1	
	Cerumen occlusion	1	

Discussion

Children with hearing loss can face difficulties with speech and language acquisition, academic achievement, and social interaction. Speech and language are central to the learning process, enabling children to follow the teacher's instructions, participate in class discussions, and interact with their peers [5]. Early identification of hearing problems through hearing screenings is thus essential in preventing these adverse outcomes [5], but the long travel distance to specialized health services remains a significant barrier for access to these.

Considering the challenges faced, it appears that a community-based approach [6-8] is the most realistic and accessible option for the promotion of hearing health. Indeed, we show that there is a need for hearing screenings in school-aged children, and that most of the findings are treatable in a timely manner with medical referral required only for a small number of the children tested. It must also be noted that in cases where only otitis media is found, interventions would be possible directly within the community, depending on the availability of medical services and professionals.

Recent advances in tele-audiology appear to be another option for these communities [9]. With little training, members of the community would be able to assist the children in the use of mobile screening applications or devices. This type of intervention would still not account for middle-ear pathologies and ear wax accumulation but would act as a first line of testing prior to more specific interventions. Indeed, we found that there is interest in offering these services by the school nurse and the health center, which would reduce challenges in navigating the health system.

4 Conclusion

We emphasize the pressing need for accessible audiology services in remote Quebec regions, particularly for indigenous communities. Findings from the collaborative initiative between the University of Montreal's School of Speech-Language Pathology and Audiology, the First Nations Education Council, and an Algonquin First-Nations community highlights a high prevalence of treatable hearing conditions in the tested children. We advocate for a community-based approach and the adoption of tele-audiology as viable solutions to overcome accessibility barriers. The strategies identified can serve as a model for other remote communities.

Acknowledgments

We would like to thank all the community members who participated in the organization of the visit, including the First Nations Education Council, the Interdisciplinary Center for Brain and Learning (CIRCA), the school board, the community council, and the community health clinic.

References

[1] *Dépistage de la surdité chez les Nouveau-Nés : Un retard inexcusable pour l'ooaq et l'aqepa*. OOAQ. (2022). https://www.ooaq.qc.ca/decouvrir/actualites/depistage-surdite-nouveau-nes-retard-inexcusable-ooaq-aqepa/

[2] Langan, L. A., Sockalingam, R., Caissie, R., & Corsten, G. (2007). Occurrence of otitis media and hearing loss among First Nations elementary school children. *Canadian Journal of Speech-Language Pathology and Audiology, 31*(4), 178-185.

[3] Williams, C. J., & Jacobs, A. M. (2009). The impact of otitis media on cognitive and educational outcomes. *Medical Journal of Australia*, *191*(S9), S69-S72.

[4] De Wals, P., Lemeur, J. B., Ayukawa, H., & Proulx, J. F. (2019). Middle ear abnormalities at age 5 years in relation with early onset otitis media and number of episodes, in the Inuit population of Nunavik, Quebec, Canada. *International Journal of Circumpolar Health*, *78*(1), 1599269.

[5] WHO. *World Report on Hearing.* (2021). available: https://www.who.int/publications/i/item/world-report-on-hearing.

[6] Kettner, P. M., Daley, J. M., & Nichols, A. W. (1985). *Initiating change in organizations and communities: A macro practice model.*

[7] Suen, J. J., Marrone, N., Han, H. R., Lin, F. R., & Nieman, C. L. (2019, February). Novel Approaches to Fostering Hearing Loss Self-Management in Adults: Translating Public Health Practices: Community-Based Approaches for Addressing Hearing Health Care Disparities. In *Seminars in Hearing* (Vol. 40, No. 1, p. 37). Thieme Medical Publishers.

[8] Marrone, N., Nieman, C., & Coco, L. (2022). Community-based participatory research and human-centered design principles to advance hearing health equity. *Ear and hearing, 43*(Suppl 1), 33S.

[9] Govender, S. M., & Mars, M. (2017). The use of telehealth services to facilitate audiological management for children: A scoping review and content analysis. *Journal of Telemedicine and Telecare, 23*(3), 392-401.

DEVELOPMENT OF A METHOD TO ASSESS IN-EAR SPEECH INTELLIGIBILITY THROUGH LISTENING EFFORT

Alexis Pinsonnault-Skvarenina[*1,2], **Philippe Chabot** [†3], **Ajin Tom** [‡3], **and Antoine Bernier** [§3]
[1] Université du Québec (ÉTS), Montréal, Québec, Canada
[2] Centre for Interdisciplinary Research in Music Media and Technology, McGill University, Montréal, Québec, Canada
[3]EERS Global Technologies Inc., Montréal, Québec, Canada

1 Introduction

Active hearing protection devices equipped with an in-ear microphone (IEM) enable in-ear voice pickup which presents better signal-to-noise ratio over ambient microphones in highly noisy conditions. To improve its intelligibility, in-ear speech requires processing which can take many forms, from fixed filtering to spectral domain processing based on machine learning. Objectively comparing these processing strategies can be difficult. In the authors' experience, objective intelligibility assessment techniques have not provided the necessary resolution to compare various processed in-ear speech. They have also failed to capture a concept of listening effort, which intuitively seemed to increase with in-ear speech over reference speech when recorded in silence.

This work presents the development and preliminary validation of a technique that objectively measures intelligibility of in-ear speech material and its associated listening effort. The technique is based on a dual task paradigm, where a primary task measures intelligibility directly. Performance on a secondary task, performed at the same time, provides a measure correlated with listening effort [1]. Dual-task paradigms are commonly used in audiology such as to evaluate the effectiveness of noise reduction algorithms in hearing aids [2, 3].

2 Method

2.1 Participants

Eleven adults participated in this pilot study. All participants self-reported normal hearing sensitivity.

2.2 Procedures

Primary task: word repetition task

Participants were asked to repeat as many words as they could after hearing recordings of 5-word sentences through Sennheiser HD280 Pro headphones. The material of the American English Matrix test [4] was used to create nine lists of ten random sentences of similar syntax. The sentences were recorded for four conditions to be evaluated: noisy reference speech (microphone in front of mouth while subjected to 85 dB(A) and 80 dB(A) noise), IEM speech without any processing, and IEM speech with BWE processing.

Secondary task: visual-motor task

The chosen visual motor task was a computer game adaptation of the Tower of London test [5]. The goal of the game is to move colored beads on a virtual board to match a given configuration displayed as a target. Colored beads are placed in three stacks on the board, arranged in different patterns and must be moved using a computer mouse.

Subjective speech intelligibility

Subjective speech intelligibility was assessed by asking participants to rate, on a scale of 0 (Bad) to 10 (Excellent), how well they could understand the words.

Procedures

The testing took place in a quiet room. First, after receiving instructions, participants underwent a five sequences familiarization phase for the secondary task. Second, participants were asked to read each of the words of the Matrix. A practice session was then conducted in the dual-task paradigm (word repetition and visual motor concomitantly). Participants were instructed that the primary task (word repetition) should be prioritized. Finally, participants completed the test sessions in single- and dual-task paradigms in random order. After each single-task paradigm involving the word repetition task, subjective speech intelligibility was assessed.

2.3 Analyses

Single-task accuracy was subtracted from dual-task accuracy to obtain two dual-task cost (DTC) scores: DTC Word accuracy and DTC Visual-motor accuracy.

3 Results

3.1 Dual tasks results

Dual-task costs were calculated (Figure 1). No differences in DTC Word were observed amongst conditions. The highest DTC Visual-Motor was observed in the reference speech with 85 dB(A) noise condition ($29\% \pm 17\%$), followed by the 80 dB(A) noise condition ($20\% \pm 13\%$). Both IEM and BWE conditions presented with the similar DTC Visual-Motor (respectively $13\% \pm 12\%$ and $13\% \pm 15\%$).

3.2 Subjective ratings results

Results for the subjective speech intelligibility ratings are presented in Figure 2. Worse subjective intelligibility ratings were obtained with reference speech with 85 dB(A) noise ($2, 7 \pm 1, 1$). Reference speech with 80 dB(A) noise and IEM

[*]alexis.pinsonnault-skvarenina@etsmtl.ca
[†]pchabot@eers.ca
[‡]atom@eers.ca
[§]abernier@eers.ca

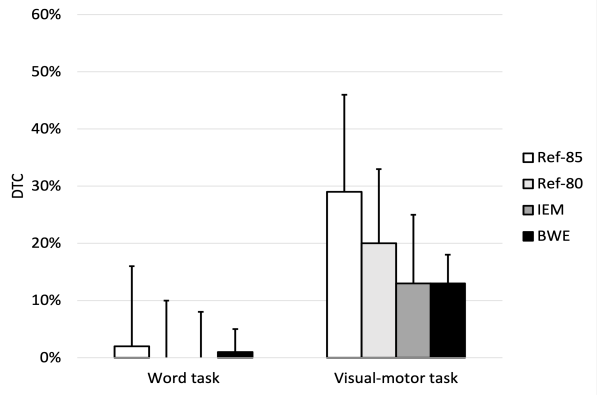

Figure 1: Word and visual-motor task DTC accuracy results for reference speech with 85 dB(A) noise, reference speech with 80 dB(A) noise, IEM, and BWE. Bars represent standard deviations.

speech obtained similar intelligibility ratings ($6, 4 \pm 1, 4$ and $5, 8 \pm 1, 3$ respectively). BWE processing obtained the best intelligibility ratings ($7, 5 \pm 1, 1$).

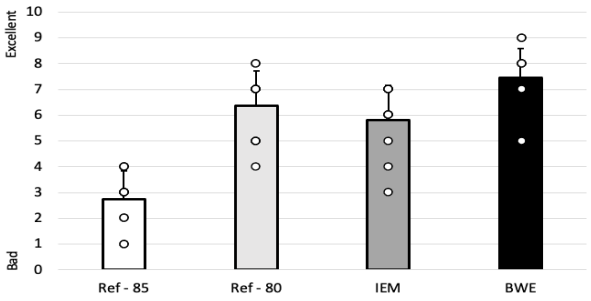

Figure 2: Subjective speech intelligibility ratings for reference speech with 85 dB(A) noise, reference speech with 80 dB(A) noise, IEM , and BWE. White dots represent individual scores. Bars represent standard deviations.

4 Discussion

4.1 Listening effort with in-ear speech

Our preliminary data suggests that a dual-task paradigm can capture nuances an objective intelligibility test alone cannot. According to the DTCs for the visual-motor task, more listening effort is required to understand noisy reference speech than IEM speech (either raw or with BWE processing). This is also supported by participants' subjective evaluation, rating IEM speech with BWE processing to be subjectively the most intelligible over noisy reference speech or raw IEM speech. However, unintuitively, the BWE processing did not improve listening effort over raw IEM speech, despite being subjectively rated as better and having the least performance variability of all the conditions.

Taken together, our results suggest that using a measure of listening effort (i.e., a dual-task paradigm) can be informative when assessing in-ear speech intelligibility. This is supported by previous research that found listening effort to be a better indicator of speech perception than intelligibility accuracy scores [1, 6].

4.2 Limitation and future research

Potential limitation of this preliminary study may have reduced our ability to accurately measure listening effort. First, hearing sensitivity was not objectively measured. It is believed that individuals with hearing loss can present with increased listening effort to understand speech-in-noise [6]. Therefore, if some of our participants did present with a hearing loss, this could have introduced additional variability in our results, which might have affected our ability to measure differences in listening effort across conditions. Second, previous research has suggested that an 80% performance criterion on both word and visual-motor single tasks could improve the potential of a dual-task paradigm to measure listening effort. Since the performances of our participants for the single tasks were very high (nearly 100%), it is unclear how this might have affected the sensitivity of our experimental paradigm. Third, more participants would be needed to achieve statistical significance between the objective scores.

Future development of our test paradigm should seek to refine the secondary task and integrate a time response variable, which might be more suited to evaluate listening effort [1, 6].

5 Conclusions

Our results suggest that a dual-task paradigm to measure listening effort can be a good approach to behaviorally evaluate in-ear speech. Our pilot study supports the use of in-ear speech to improve communication in noisy settings while quantifying its potential for further improvements.

Acknowledgments

The authors would like to acknowledge the financial support received from MITACS IT26677 (SUBV-2021-168) for the ÉTS-EERS Industrial research chair in in ear technologies, sponsored by EERS Global Technologies Inc.

References

[1] Jean-Pierre Gagne, Jana Besser, and Ulrike Lemke. Behavioral assessment of listening effort using a dual-task paradigm: A review. *Trends in hearing*, 21:2331216516687287, 2017.

[2] Brent Edwards. The future of hearing aid technology. *Trends in amplification*, 11(1):31–45, 2007.

[3] Anastasios Sarampalis, Sridhar Kalluri, Brent Edwards, and Ervin Hafter. Objective measures of listening effort: Effects of background noise and noise reduction. 2009.

[4] B Kreisman, R Carroll, M Zokoll, A Warzybok, P Allen, P Folkeard, K Wagener, and B Kollmeier. Design, optimization and evaluation of an american english matrix sentence test in noise. In *American Academy of Audiology Conference*, 2013.

[5] Timothy Shallice. Specific impairments of planning. *Philosophical Transactions of the Royal Society of London. B, Biological Sciences*, 298(1089):199–209, 1982.

[6] Penny Anderson Gosselin and Jean-Pierre Gagné. Use of a dual-task paradigm to measure listening effort utilisation d'un paradigme de double tâche pour mesurer l'attention auditive. *Revue canadienne d'orthophonie et d'audiologie-Vol*, 34(1), 2010.

PERFORMANCES OF ALTERNATIVE LISTENING DEVICES: CANDIDATES FOR INDIVIDUALS WITH MILD TO MODERATE HEARING LOSS?

Alexis Pinsonnault-Skvarenina [*1,2], **Fabien Bonnet** [†1,3], **Mathieu Hotton** [‡4,5], **Hugues Nélisse** [§1,3], **and Jérémie Voix**[¶1,2]
[1] Université du Québec (ÉTS), Montréal, Canada
[2] Centre for Interdisciplinary Research in Music Media and Technology, McGill University, Montréal, Canada
[3]Institut de recherche Robert-Sauvé en santé et sécurité du travail, Montréal, Canada
[4]École des sciences de la réadaptation, Faculté de médecine, Université Laval, Québec, Canada
[5]Centre interdisciplinaire de recherche en réadaptation et intégration sociale, CIUSSS Capitale-Nationale, Québec, Canada

1 Introduction

The past few years have seen a meteoric rise in technological advancements in the hearing health industry. Advances in connectivity, miniaturization and artificial intelligence enable many increasingly sophisticated and diverse features within multifunctional in-ear devices. Such alternative listening devices, often referred to as "hearables", aim to become real "bionic ears" offering hearing protection, amplification, monitoring and biodetection functionalities. With the recent approval of the "Over-the-Counter Hearing Aid Act" in the United States and the introduction of "Over-the-Counter" ("OTC") hearing aids, these devices now have the potential to revolutionize the world of traditional auditory amplification. Recently, a systematic review of scientific literature has concluded that given their availability and affordability, these alternative listening devices could be considered for patients with mild to moderate hearing loss [1].

The aim of this paper is to present a research initiative on hearables and OTC hearing aids, launched within the ÉTS-EERS Industrial Research Chair in In-Ear Technologies (CRITIAS) at the École de technologie supérieure facility. To this end, electroacoustic and acoustic performances of alternative listening devices are explored.

2 Method

2.1 Electroacoustic performances

Alternative listening devices' electroacoustic performances were evaluated according to ANSI S3.22 [2] and ANSI/CTA-2051 [3]. The following characteristics were assessed: 1) OSPL90 Max, 2) Frequency response, 3) Equivalent internal noise (EIN), and 5) Total harmonic distortion (THD). These analyses were either conducted with SoundCheck (Listen Inc., Boston, MA, USA) or with a Verifit 2 real-ear hearing aid analyzer (Audioscan, Dorchester, ON, CA).

2.2 Acoustic performances

Head-related transfer function (HRTF) measurements were performed in an anechoic room, equipped with an automated arm which can move from -45° to 60° on elevation and from 0° to 360° on azimuth. A loudspeaker was installed at one end of the automated arm. For each set of measurements, a total of 72 points were evaluated: from 0° to 360° on the horizontal plane (with 15° steps) and at -40°, 0°, and +45° on the vertical plane. The movement of the automated arm and data collection were fully managed by LabVIEW™ (National Instruments, Austin, TX, USA). At each position, a white noise was generated by the loudspeaker and the acoustic pressure was measured at the two coupler microphones of a 45CB Artifial Text Fixture (G.R.A.S, Holte, Danemark) (Figure 1) with and without the devices in place (on the ATF's ears). For each ear and each position, the device's effect on the corresponding HRTF was then assessed as the pressure ratio between the open-ear and ear-with-device conditions. To evaluate the acoustic performance of the listening devices, these were set into their more transparent mode (i.e., the setting in which -based on the manufacturer's saying- their influence on HRTFs should be minimal).

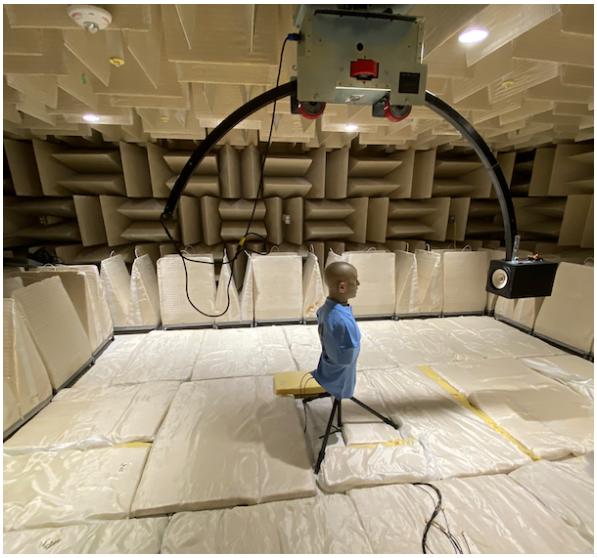

Figure 1: Picture of the anechoic room setup with the ATF and the automated arm holding the loudspeaker.

3 Results

3.1 Electroacoustic performances

Preliminary electroacoustic performance results obtained on two alternative listening devices (Britzgo Optio Hearing Aid Amplifier and AidPods Pro-2nd generation) are presented in Table 1. The two devices were within the tolerance limits regarding OSPL90 Max ($<$ 120 dB SPL) and frequency range

[*]apinsonnault@critias.ca
[†]Fabien.Bonnet@irsst.qc.ca
[‡]mathieu.hotton@fmed.ulaval.ca
[§]nelisse.hugues@irsst.qc.ca
[¶]jeremie.voix@etsmtl.ca

(250–6,000 Hz). Both devices showed higher EIN than the prescribed tolerance ($>$ 28 dB SPL). Finally, for THD, performances for the AirPods Pro were withing the tolerance limits, while the Britzgo Optio showed less satisfactory results, generating a value of 3% at 500 and 800 Hz.

Table 1: Preliminary electroacoustic analysis of two alternative listening devices.

	Britzgo Optio	Air Pods Pro
OSPL90 Max (dB SPL)	113.0	102.0
Frequency response (Hz)	200-5,000	200-6,300
EIN (dB SPL)	30.0	37.0
THD @500 Hz (%)	3.0	0.0
THD @800 Hz (%)	3.0	0.0
THD @1600 Hz (%)	1.0	0.0

3.2 Acoustic performances

Two listening edevices that include a transparency mode were assessed (i.e., Apple AirPods Pro-2nd generation and Nuheara IQbuds 2 MAX). Figure 2 presents the effects of these two listening devices on the 72 assessed HRTFs. While the IQ Buds give satisfactory results, especially for low frequencies, surprisingly, the AirPods' performances do not differ from that achieved when the earbuds are turned off.

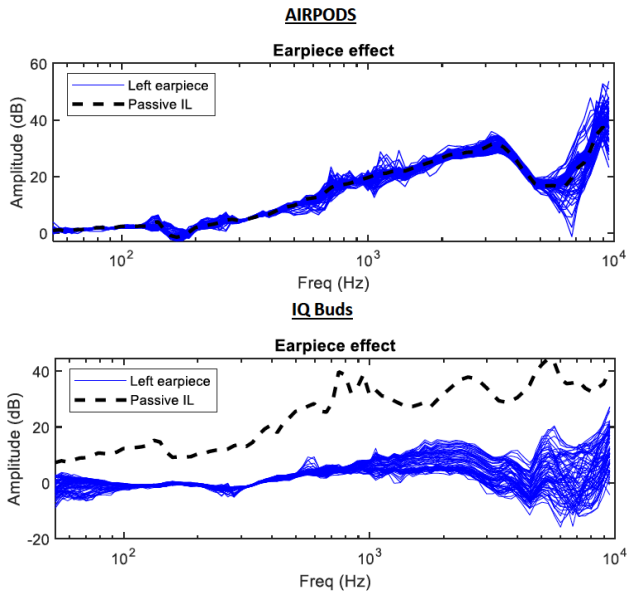

Figure 2: Effects on HRTFs of two alternative listening devices. The black dashed line corresponds to the effect measured when the device was turned off.

4 Discussion

Our preliminary results show that some alternative devices can present with electroacoustic performances that respect current standards ANSI S3.22 [2] and ANSI/CTA-2051 [3]. However, in some cases, these performances are insufficient. For example, while the AirPods Pro present an OSPL90 Max and THD comparable to traditional hearing aids, they also show high EIN and a narrower range of frequency response. Such irregularities could be problematic for users with mild to moderate hearing loss. Current research has shown a wide variety of electroacoustic performances across alternative listening devices [4], similar to those observed in this preliminary study. Future research should aim to investigate the clinical effectiveness of these various devices for individuals with mild to moderate hearing loss. To this regard, some researchers have already obtained promising results [5].

To our knowledge, this research initiative is one of the first to investigate the HRTFs of alternative listening devices to better understand how they can affect localization cues. As for electroacoustic performances, we observed various effects on HRTFs amongst devices. While some devices show promisingly transparent features (e.g., Nuheara IQbuds 2 MAX), others significantly alter the HRTF (e.g., AirPods Pro). Future experiments by our research team will aim to confirm these results and identify what may cause some results to be rather disappointing (e.g.,device malfunction).

5 Conclusions

Our results provide preliminary insight into the electroacoustic and acoustic performances of alternative listening devices. They show that performances can vary from one device to another. Future research should aim to better understand how these devices could be used by individuals with mild to moderate hearing loss.

Acknowledgments

The authors would like to acknowledge the financial support received from NSERC Alliance (ALLRP 566678-2021), MITACS IT26677 (SUBV-2021-168) and PROMPT (#164_Voix-EERS 2021.06) for the ÉTS-EERS Industrial research chair in in ear technologies, and from FRQS Young Researchers Grant 324155 for Université Laval.

References

[1] Chih-Hao Chen, Chii-Yuan Huang, Hsiu-Lien Cheng, Heng-Yu Haley Lin, Yuan-Chia Chu, Chun-Yu Chang, Ying-Hui Lai, Mao-Che Wang, and Yen-Fu Cheng. Comparison of personal sound amplification products and conventional hearing aids for patients with hearing loss: A systematic review with meta-analysis. *EClinicalMedicine*, 46, 2022.

[2] ANSI/ASA S3.22. Specification of hearing aid characteristics. *American National Standards Institute and Acoustical Society of America*, 2014.

[3] ANSI/CTA-2051. Personal sound amplification performance criteria. *American National Standards Institute and Consumer Technology Association*, 2017.

[4] Ibrahim Almufarrij, Kevin J Munro, Piers Dawes, Michael A Stone, and Harvey Dillon. Direct-to-consumer hearing devices: Capabilities, costs, and cosmetics. *Trends in Hearing*, 23:2331216519858301, 2019.

[5] Karina C De Sousa, Vinaya Manchaiah, David R Moore, Marien A Graham, and De Wet Swanepoel. Effectiveness of an over-the-counter self-fitting hearing aid compared with an audiologist-fitted hearing aid: A randomized clinical trial. *JAMA Otolaryngology–Head & Neck Surgery*, 149(6):522–530, 2023.

A Listening Effort Based Comparative Analysis of CROS Hearing Aids and Bone-Anchored Hearing Devices for Single-Sided Deafness Patients

Olivier Valentin[*1,2,3,4,5], **François Prévost**[†1,6], **Don Luong Nguyen**[‡1,2,5,7], **and Alexandre Lehmann**[§1,2,3,4,5]
[1]Laboratory for Brain, Music and Sound Research (BRAMS), Montreal, QC, Canada
[2]Centre for Research on Brain, Language or Music (CRBLM), Montreal, QC, Canada
[3]Centre for interdisciplinary research in music media and technology (CIRMMT), Montreal, QC, Canada
[4]McGill University, Faculty of Medicine, Department of Otolaryngology–Head and Neck Surgery, Montreal, QC, Canada
[5]Research Institute of the McGill University Health Centre (RI-MUHC), Montreal, QC, Canada
[6]McGill University Health Centre (MUHC), Department of Speech Pathology and Audiology, Montreal, QC, Canada
[7]Jewish General Hospital, Department of Audiology and Speech Pathology, Montreal, QC, Canada

1 Introduction

Single-sided deafness (SSD), the near or total loss of hearing in one ear with normal hearing in the contralateral ear, presents significant challenges, including speech-in-noise recognition difficulties, impaired sound localization, and reduced awareness of sounds in the affected auditory hemifield. Current therapeutic approaches aim to improve processing of sounds from the impaired hemifield by rerouting signals to the contralateral non-impaired ear. This can be achieved, for instance, through air conduction using contralateral-routing-of-signal (CROS) hearing aids, or bone conduction using bone-anchored (BA) hearing devices.

While SSD patients report perceived benefits from BA and CROS devices, documenting these benefits using clinical measures has proven challenging. Consequently, the optimal choice between these devices remains uncertain, creating an ongoing dilemma in the clinical management of SSD. The lack of objective assessment regarding the reported reduction in listening effort and differences in funding modalities for each device contribute to a long-standing controversy.

This research project aims to address this long-standing controversy by investigating which device yields superior hearing outcomes for SSD patients. Behavioral (NASA Task Load Index) and pupillometric measurements were used to evaluate the cognitive effort required when SSD patients perform speech-in-noise recognition tasks. The full results presented this year expand upon the preliminary findings reported at the AWC 2023 conference and have the potential to provide the first comprehensive evidence to guide the management of SSD, maximizing patients' benefit, and offering evidence-based justification of funding policies.

2 Material and method

2.1 Participants

Thirteen adult patients (7 men, 6 women) with single-sided sensorineural deafness participated in this study. Single-sided sensorineural deafness was defined as the absence of residual bone conduction hearing and no residual speech recognition in one ear, while the other ear exhibited air conduction audiometric thresholds equal to or better than 25 dB HL between 250 Hz and 4 kHz. All participants were native English speakers without a history of neurological disorders, excessive caffeine intake prior to the measurement session, or any otologic co-morbidity in the unaffected ear. Throughout the study, participants remained seated in a comfortable chair within a double-walled audiometric booth situated in the MUHC Department of Speech Pathology and Audiology. The research protocol was reviewed and approved by the Research Ethics Board (REB) of the MUHC. Prior to their participation in the study, informed consent was obtained from all participants.

2.2 Experimental Procedure

Behavioral performance was evaluated using the Hearing-In-Noise Test (HINT) [1] conducted using the Oticon Medical Experiment Platform (OMEXP) under three different conditions: while wearing a CROS hearing aid (Oticon CROS with OpenSoundNavigator™ 2), while wearing a BA hearing aid (Oticon Medical Ponto™ 4), and without any hearing aid. Twenty sentences were presented in each condition (BA-fitted, CROS-fitted, and unaided), for a total of 60 sentences. Speech signals were presented using a frontal loudspeaker, while white noise was presented using a second loudspeaker placed on the same side as the better ear. The stimulation levels were determined by performing an adaptive HINT prior to the experiment to identify the signal-to-noise ratio (SNR) that corresponded to a 70% speech reception threshold (SRT) without a hearing aid. Participants were instructed to listen to the sentences and repeat them aloud, with no feedback provided.

During the execution of the behavioral task, the Pupil Core eye-tracking platform (Pupil Labs, Berlin, Germany) was used to measure pupil size and location in both eyes. The peak pupil dilation (PPD) was calculated during the time interval between the offset of the sentence and the prompt to repeat it [2], and subsequently averaged across sentences within each condition.

Upon completion of each condition, a subjective assessment of listening effort was conducted using the NASA Task Load Index (NASA-TLX) via a tablet computer. This subjective and multidimensional assessment tool was used to evaluate participants' mental workload level (MWL) during the task of repeating sentences heard in noise.

[*] m.olivier.valentin@gmail.com
[†] francois.prevost@muhc.mcgill.ca
[‡] don.nguyen@mail.mcgill.ca
[§] alexandre.lehmann@muhc.mcgill.ca

3 Results

Results reveal no significant effect of the device on behavioral performance (HINT scores, Fig. 1A), consistent with previous reports [3, 4]. Peak pupil dilation results indicate that both CROS and BA hearing aid conditions require less cognitive effort compared to the unaided (UNAI) condition (Fig. 1B). Subjective effort ratings suggest a diminished perception of cognitive effort among participants when utilizing BA hearing aids during a speech-in-noise task (see Fig. 1C). The higher frustration induced by the requirement of bilateral in-ear devices in CROS hearing aids could explain the differences between the UNAI and BAHA conditions (see Fig. 1C), when considering the subjective assessment of cognitive effort that incorporates evaluations of frustration and physical demand.

4 Conclusion and Future Work

The paradigm presented in this study investigates the integration of objective and subjective methodologies as a valuable tool for selecting appropriate devices in patients with single-sided deafness (SSD). Results confirm a reduced cognitive effort in aided SSD patients, despite no observed behavioral improvement. Each dimension of the MWL assessments will be analyzed to evaluate their impact on participants' perception of cognitive effort. This study constitutes the first step towards a research project aiming to develop an objective biomarker for personalized recommendations and longitudinal tracking of patients' progress in clinical settings.

Acknowledgments

The authors would like to thank the participants for giving their time to take part in this study. This research project received financial support from the William Demant Foundation (Smørum, Denmark). The authors also wish to express their appreciation to the team at Oticon Medical for their feedback and expertise.

References

[1] M. Nilsson, S.D. Soli, and J.A. Sullivan. Development of the hearing in noise test for the measurement of speech reception thresholds in quiet and in noise. *The Journal of the Acoustical Society of America*, 95(2):1085–1099, 1994.

[2] A.A. Zekveld, S.E. Kramer, and J.M. Festen. Cognitive load during speech perception in noise: the influence of age, hearing loss, and cognition on the pupil response. *Ear and Hearing*, 32:498–510, 2011.

[3] J.P. Peters, A.L. Smit, I. Stegeman, and W. Grolman. Review: Bone conduction devices and contralateral routing of sound systems in single-sided deafness. *The Laryngoscope*, 125(1):218–226, 2015.

[4] J. Fogels, R. Jönsson, A. Sadeghi, M. Flynn, and T. Flynn. Single-sided deafness-outcomes of three interventions for pro-found unilateral sensorineural hearing loss: A randomized clinical trial. *Otology & Neurotology*, 41(6):736–744, 2020.

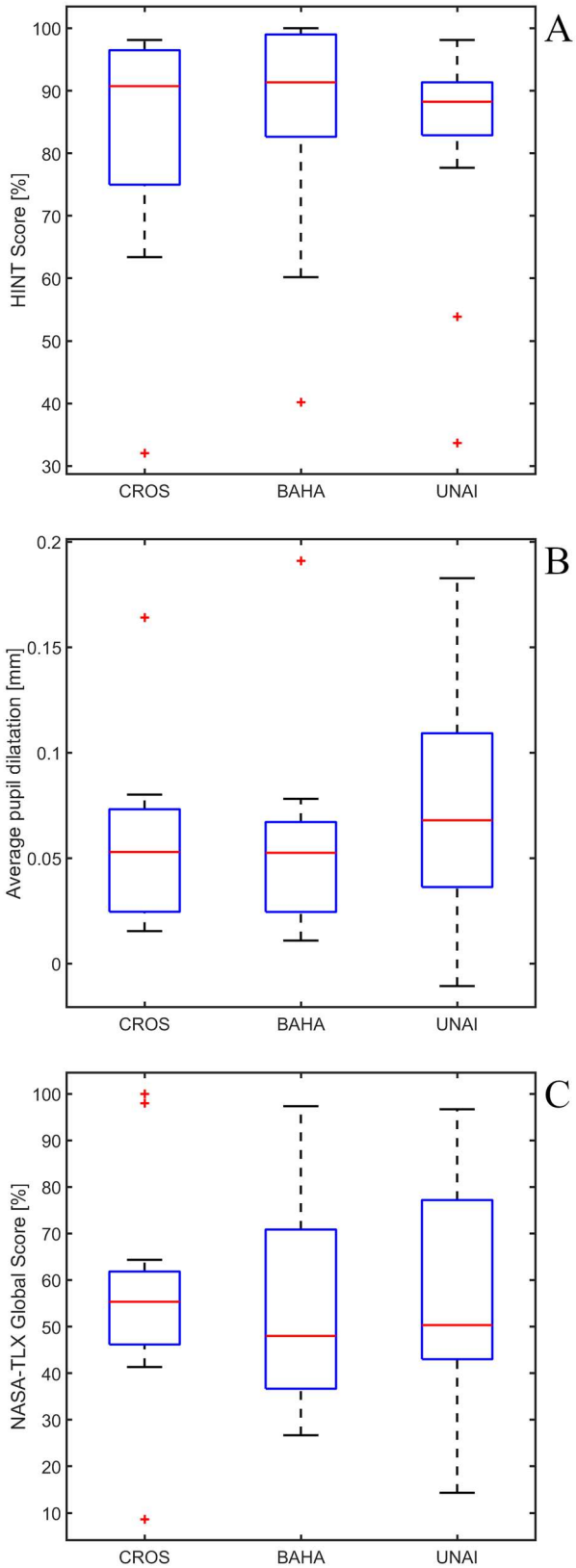

Figure 1: Behavioral (A), objective (B), and subjective (C) results obtained with thirteen SSD patients, with hearing aids (BAHA and CROSS conditions) and without hearing aid (UNAI condition). Medians are indicated by red central marks and outliers are plotted using "+" red markers

Abstracts for Presentations without Proceedings Paper
Résumés des communications sans article

Acoustic Analysis For Automatic Identification And Classification Of Nasality In Simulated Oral-Nasal Balance Conditions Using Only The Nasal Speech Signal

Fatemeh Abnavi, Heather Flowers, Hilmi Dajani, Suzy Ahn, Tim Bressmann

Background: Accurate detection and classification of nasality disorders are important for managing care of children with cleft palate. Detecting and quantifying nasality through acoustic analysis becomes challenging when relying on single microphone recordings, as these recordings capture both nasal and oral signals simultaneously. To address this problem, we aimed to develop an algorithm that could automatically detect and classify four oral-nasal balance conditions (normal, hyper-, hypo-, and mixed) based on exploratory acoustic analyses derived solely from the nasal signal. Methods: Eleven typical female speakers produced a nasal and a non-nasal sentence in their usual voice and also simulated as hyper-, hypo-, and mixed nasality using a nasometer headset. We explored various calculations from a range of acoustic parameters using a linear discriminant analysis (LDA) for various combinations of measures. We anticipated that some parameters might be more robust than others such as mean and standard deviations of intensity for both nasal and non-nasal sentences, as well as the spectral amplitude of 1/3 octave frequency bands at 630Hz and 800Hz collected by the nasal microphone. The latter spectral band variables were entered into the "oralance" formula of the form: (nasal band power for the non-nasal sentence/ (combined nasal band power for the nasal + non-nasal sentences)) * 100, resulting in the oralance 630 and oralance 800 output variables. Results: Among the range of parameter combinations tested in the LDA, six variables (Oralance630, Oralance800, mean nasal intensity, SD nasal intensity, mean non-nasal intensity, and SD non-nasal intensity) detected and classified simulated hyper-, hypo-, mixed and normal nasality with an accuracy of 90.9%. Conclusion: Our exploratory LDA of acoustic parameters based solely on the nasal signal resulted in a highly accurate categorization of the simulated oral-nasal balance conditions. Our next steps involve applying the developed LDA classification algorithm to clinical samples.

Elimination Of Nasality In Typical Speakers Using Forward Voice Focus, Phonetic Replacement, And Biofeedback

Somayah Al-Ees, Tim Bressmann

Background: Nasality disorders, including hypernasality, can impact speech intelligibility and lead to social stigma. However, current speech therapy interventions have limited success in controlling the velopharyngeal sphincter, which regulates nasality. This challenge arises from the limited proprioception of velopharyngeal sphincter movement in speakers, making it difficult to achieve voluntary velopharyngeal closure during speech therapy for individuals with hypernasal speakers (e.g., patients with cleft palate). Previous studies have shown that some individuals were able to reduce their speech nasality using forward voice focus. In this study, a combination of forward voice focus, phonetic replacement, and visual or tactile biofeedback was employed to eliminate nasality in typical speakers' connected speech. Hypothesis: The combined intervention approach involving forward voice focus, phonetic replacement, and biofeedback would lead to a significant reduction in nasality in typical speakers. This reduction would be indicated by a decrease in nasalance scores after the intervention. Methods: Twenty typical speakers were divided into two groups, with one group receiving visual biofeedback and the other group receiving tactile biofeedback. Nasometer was used to measure nasalance scores for sentences containing nasal sounds in various speaking conditions, comparing the baseline and final recordings. Results: Both the visual and tactile biofeedback groups exhibited a significant reduction in nasalance scores after the treatment ($p < 0.001$). The visual biofeedback group's nasalance scores decreased from 59.99 (SD 7.85) at baseline to 28 (SD 14.75) after the treatment. Similarly, the tactile biofeedback group's nasalance scores decreased from 61 (SD 8) at baseline to 32.9 (SD 18.94) after the treatment. Discussion: The study's findings show that combining forward voice focus, phonetic replacement, and biofeedback effectively reduces nasality in typical speakers. The reduction of the nasopharyngeal lumen achieved through forward voice focus may have facilitated voluntary velopharyngeal closure. However, further research is necessary to investigate the effectiveness of this combined intervention approach for individuals with hypernasal speech.

Investigating Gender Differences In The Perception Of Human Infant Vocalizations As A Cuteness Component

M. Fernanda Alonso Arteche, Leatisha Ramloll, Lucie Menard, Linda Polka

Cuteness in human infants, often associated with visual attributes, is known to promote social interaction and

empathy. The auditory dimension of cuteness, however, has remained underexplored. This study examined whether there is a positive association with babies' neutral vowel vocalizations and whether this perception varies based on the perceiver's sex. A total of 40 adults (20 males and 20 females) engaged in four Single Category Implicit Association Tasks (SC-IAT) to discern responses to vocalizations of babies, adults, cats, and kittens. The results revealed a positive implicit association to specific to human babies' vocalizations ($p < 0.05$); other vocalizations showed no significant association. We are currently analyzing the data to determine if there are differences in the perception of infant vocalizations between male and female participants. Insights from this aspect of the study will provide further understanding of whether auditory perception of cuteness in human infants varies by gender.Top of Form These findings introduce an auditory component specific to human infants, in alignment with previous research on visual cuteness and augmenting the concept of an infant schema. The gender differences may add a new perspective to our understanding of the complexity of cuteness as a psychological phenomenon. Future research may explore naturalistic vocalizations or babbling, and specific acoustic characteristics contributing to the perception of cuteness. This study's insights into auditory cuteness enhance our understanding of how cuteness, as a multisensory phenomenon, influences human emotions and behaviors.

A New Individualized, Ecological And Immersive Approach To Measuring Noise-Related Annoyance: Feasibility Study

Pierre H Bourez, Guillaume T Vallet, François Bergeron, Nathalie Gosselin, Philippe Fournier

Hyperacusis is defined as hypersensitivity to loud sounds that can affect people's quality of life. There is no objective diagnostic measure or biomarker for hyperacusis. One assessment method used in clinics called Loudness Discomfort Levels (LDLs) consists in presenting artificial sounds (pure tone or noise) and increasing the level until the patient report discomfort. It has been criticized as it may not reflect adequately everyday experience with sounds. The project aims at validating a new measure of hyperacusis measuring the sound level required to disturb a daily activity (AL) and the level causing discomfort (DL) using different immersive soundscapes. Seven pilot normal-hearing control participants were tested in 5 different sound environments (restaurant, factory, cafeteria, daycare, and babble noise). Participants had to read a book excerpt inside each environment while the level of the soundscape was increased gradually (+2 dB steps) until the participant indicated that he was hindered in his reading (AL). It was then increased further until the participant reported discomfort (DL). The results demonstrated that ALs and DLs can vary considerably from one environment to another. The noise environment with the lowest and highest AL and DL were babble noise (AL and DL, $\bar{x} = 47$, $\bar{x} = 58$ dB Laeq) and factory noise (AL and DL, $\bar{x} = 74$, $\bar{x} = 85$ dB Laeq), respectively. For all environments, AL was lower than DL (mean AL, $\bar{x} = 60$ and mean DL, $\bar{x} = 73$, dB LAeq) with an average difference of 13 dB LAeq. Preliminary results suggest that 1) ALs and DLs may vary for different soundscapes and 2) a level even below the discomfort level may be sufficient to produce annoyance and impact the performance of a day-to-day activity. The complete set of data including controls and hyperacusis patients will be presented at the congress.

Size Of Velopharygeal Opening And Nasality Measurements From Acoustic Features

Jahurul Islam, Bryan Gick

Previous research has explored the relationship between nasality measures obtained from acoustic signals [Chen 1997, JASA 102] and direct measurements such as nasal airflow, highlighting promising outcomes. Carignan [2021, JASA 149; 2023, LabPhon 14] reported that nasality measurements from acoustic features (NAF) using machine learning algorithms like PCA regression and XGBoost highly correlate with airflow data. However, it remains unclear how well acoustic measurements align with the actual size of the velopharyngeal opening (VPO). To address this, the current study examines the correspondence between acoustic measurements of nasality and the size of the VPO. We conducted an investigation using running speech samples produced by 4 Canadian English speakers, obtained from the Université Laval X-ray videofluorography database [Munhall et al. 1995, JASA 98]. Using ImageJ software, we tracked the opening and closing movements of the VPO in both nasal and oral segments. Subsequently, we employed the NAF method [Carignan 2023, LabPhon 14] to measure the degree of nasality in the speech samples. We compared the NAF measurements of nasality with the data obtained from the VPO tracking to assess the degree of correlation between the two measures. The results of our study indicate a positive alignment between nasality measurements derived from acoustic signals and the VPO data. This finding suggests that NAF measurements can be a decent predictor of the actual size of the VPO in nasal speech vs. oral speech segments, indicating a positive relationship between NAF, VPO, and nasal airflow. These results have implications for our understanding of nasality production and contribute to the growing body of research on the relationship between acoustic measurements and physiological aspects of speech production. [Work supported by NIH and NSERC.]

Speech Rate Effects On Length Distinctions In Japanese Vowels And Stops

Hironori Katsuda, Yoonjung Kang

Previous studies have shown that temporal acoustic cues (e.g., VOT, vowel duration) vary as a function of speech rate, and that listeners perceive phonemic contrasts that are signaled by such acoustic cues relative to speech rate (e.g., Miller et al. 1986). However, there has been little research examining how changes in speech rate affect different types of sound categories, such as vowels and consonants, and how the difference, or lack thereof, between them is mirrored in perception. We pursue this issue by comparing vowel- and stop-length contrasts in Japanese.We conducted an experiment consisting of production and perception tasks. A total of 30 native speakers of Japanese participated in a shadowing task in which they produced target words (/ʃokan/, /ʃo:kan/, and /ʃok:an/) embedded in a carrier sentence at fast and slow speech rates. The same participants performed a pair of two-alternative forced choice tasks in which they categorized vowel and stop duration continua embedded in fast and slow speech as phonemically short or long (i.e., vowel: /ʃokan/ or /ʃo:kan/, stop: /ʃokan/ or /ʃok:an/).To quantify the degree of sensitivity to speech rate, we first estimated individual participants' category boundaries for each contrast type at each speech rate in each modality. We then calculated the ratio of fast- to slow-boundary in each modality as a value of speech-rate sensitivity. A linear mixed effects model was fit as a function of type (vowel vs. stop), mode (production vs. perception) and their interaction, with random intercepts for participant and random slopes for type and mode. We found a significant effect of type but did not find a significant interaction effect, suggesting that stops are stretcher than vowels in production, and this difference is reflected in perception.

The Temporal Modulation Of Infant Directed Speech And The Role Of Positive Affect

Samin Moradi, Linda Polka

Speech is structured with different temporal modulations of energy within different spectral regions. A recent study by Leong et al. (2017) comparing the temporal modulation structure of infant-directed (IDS) and adult-directed speech (ADS) revealed differences in the power within isolated modulation rates and in the phase synchronization index (PSI) across these two speech registers. Here, we used the same spectral-amplitude modulation phase hierarchy (S-AMPH) method to analyze and compare the temporal modulation structure across samples of IDS and ADS and across samples of happy and neutral affect ADS. Given that positive affect is a common IDS feature, the later analysis speaks to the potential role of affect in shaping different modulation patterns. For the IDS vs ADS comparison, we used speech samples (English) developed for a large-scale study of infant preference for IDS (Many Babies Consortium, 2020). Our analysis did not uncover any significant power differences within any modulation bands, but we observed similar trends to those reported by Leong et al for the theta-beta PSIs in the lower frequency regions. The short duration of the samples in our analysis likely contribute to this incomplete replication of the Leong et al findings. For the happy vs neutral affect ADS, we selected English sentence materials from a corpus of adult speakers conveying different affective that were validated with perceptual measures (Pell et al 2009). We observed two findings that align with patterns reported previously by Leong et al. for IDS and ADS. First, in the delta modulation band, happy ADS had significantly higher power than neutral ADS. Second, for theta-beta PSI scores, neutral ADS had a higher synchronization in lower frequency regions. These parallels suggest that affect contributes to the observed temporal modulation differences between IDS and ADS observed by Leong et al. (2017).

Classifying Sounds Encountered In Two Million Youtube Videos: Insights For The Future Of Auditory Perception Research

Andrés E. Elizondo López, Michael Schutz

A survey of stimuli from auditory experiments published in top journals indicates roughly 90% of auditory experiments are conducted using simplistic, computer-generated stimuli (Schutz & Gillard, 2020). How does this set of sounds used for assessment of the auditory system compare with what it encounters outside the laboratory? As a truly comprehensive survey of all sounds heard in everyday listening would be prohibitively complex, a classification of audio found in over 2 million YouTube videos into 527 labels by Gemmeke et al. (2017) offers a useful approximation.Two research assistants on our team reviewed 10 representative videos from each of Gemmeke's 527 labels, classifying them according to the categories used by Schutz and Gillard (2020). Our results indicate most sounds (90%) heard in YouTube videos exhibit complex temporal structures. These findings contrast markedly with stimuli used to assess the auditory system, where only 11% exhibit any kind of temporal complexity (Schutz & Gillard, 2020). This disconnect raises important questions about the degree to which theories and models derived from auditory experiments focused on simplistic sounds generalize to auditory processing as it occurs outside the laboratory. It also helps clarify why a small but growing body of experimental work demonstrates that theories derived from experiments using artificial stimuli fail to generalize when assessed with more complex

sounds common outside the laboratory.

Vowel Articulation In Closed-Skull Concussion Patients With No Language Impairment

Arian Shamei, Bryan Gick

Closed-skull traumatic brain injuries (TBIs) refer to brain damage following trauma to the head. Issues with speech and language are common following damage to a variety of cortical and subcortical structures. For example, post-TBI aphasia (impairment of language) and dysarthria (impairment of speech) are well attested in the literature. In many patients, however, speech and language are preserved [Elbourn et al., 2019. Brain Injury]. In neurological disorders such as Alzheimer's Disease and Parkinson's Disease, reduction to vowel space area can be observed even in the absence of perceivable dysarthria or aphasia [Shamei et al., 2023. JASA-EL]. To date, we know of no work that directly compares the articulatory precision of a large cohort of TBI patients with no observable speech or language disorder to a population of healthy controls. Therefore, it remains unknown whether subtle effects to articulatory precision can be observed even in the absence of dysarthria or aphasia. Here, we compare the articulatory precision of vowel articulation across 54 individuals with closed-skull TBI and 50 controls within the TBIbank Coelho dataset [Coelho et al., 2002. Aphasiology]. TBIs are rated as either moderate (duration of coma less than 6 hours) or severe (duration of coma greater than 6 hours) with post-onset time ranging from 1–99 months (mean = 10.5). Mean euclidean distances (ED) for vowel articulations will be reported based on speaker-specific centroids derived from F1 and F2; a linear mixed effect model fitted to the data is used to predict the effect of TBI on euclidean distance with random slopes for vowel, post-onset time, and injury severity. We predict that ED of vowels will be shorter in TBI patients with the magnitude of reduction influenced by injury severity and recency. The implications of these findings for motor control and recovery post-TBI will be discussed.

Prenasal Coarticulation And Allophonic Merger Of /ɪ/ And /ɛ/ Across Dialects Of English

Irene Smith, Morgan Sonderegger

This study examines the effect of prenasal coarticulation on the vowels /I/ and /ɛ/ across a variety of North American and UK dialects of English. /I/ and /ɛ/ are subject to allophonic merger in some North American dialects (specifically, African American English and Southern American English)—the so-called "PIN-PEN" merger. The present study aims to understand the contribution of prenasal coarticulation to this merger, and further to understand cross-dialectal variation in prenasalization. North American English has been shown to have substantial prenasalization on vowels preceding nasal consonants (Solé 2007). The temporal extent of nasalization in North American English is well beyond the "minimum" coarticulatory effect of nasal consonants (Solé 2007) and has been shown to vary sociolinguistically (Tamminga & Zellou 2015). Vowel height and backness are reflected acoustically in F1 and F2, respectively. One acoustic correlate of nasalization is overall compression of the F1 dimension, i.e., high vowels become acoustically lowered and low vowels become acoustically raised relative to their oral counterparts produced with the same tongue position. Thus, nasalization is expected to bring /I/ and /ɛ/ closer together in F1/F2 space, and allophonic merger is expected to cause /I/ and /ɛ/ to overlap completely prenasally. The analysis was carried out using Bayesian mixed-effects models to jointly model F1 and F2. Bhattacharyya affinity between /I/ and /ɛ/ was calculated for each speaker and each corpus, both preorally and prenasally, from the model posteriors. Bhattacharyya affinity quantifies the degree of distributional overlap between /I/ and /ɛ/, indicating how "merged" prenasal vowels are compared to preoral vowels. Results show wide cross-dialectal variation in the degree of prenasal coarticulation, and, within dialects expected to have prenasal merger, a large amount of interspeaker variation in the degree of merger. Additionally, merged dialects show greater difference between prenasal and preoral Bhattacharyya affinity than non-merged dialects.

Perceptual Compensation Of Intrinsic F0 Effects In English Monolingual Speakers

Connie Ting, Meghan Clayards

Previous studies have shown that in production, the pitch (F0) of a vowel varies systematically based on intrinsic properties of the vowel itself and the preceding obstruent. High vowels are associated with higher F0, compared to low vowels, and voiceless obstruents are associated with a higher onset F0 on the following vowel, compared to voiced obstruents. Studies have also shown that these intrinsic F0 effects play a role in perception. For the consonant intrinsic F0 (CF0) effect, listeners have been reported to use onset F0 of a following vowel as a cue to consonant voicing (Whalen et al., 1990, among others). Similarly, for the vowel intrinsic F0 (VF0) effect, other things being equal, perceptual boundaries between different vowels (e.g. /i/ vs. /I/) can shift depending on vowel F0 (Scott 1976, Traunmuller 1981, Di Benedetto 1987). VF0 effects also represent a kind of context effect on voicing

judgements that listeners might need to account for, since any given F0 will be influenced by the vowel quality. It is thus of interest to test whether vowel intrinsic F0 effects can be detected through voicing judgements. In our study, we tested monolingual English speakers' perception of the English voicing contrast. Participants categorized /bi-pi/ and /baj-paj/ syllables manipulated to differ along a VOT continuum, as well as an onset F0 continuum. Overall, our results found that higher onset F0 levels elicited more voiceless responses, in line with the overall production patterns in the literature. However, we also found that given the same onset F0 level, stimuli containing the vowel /aj/ elicited more voiceless responses compared to stimuli containing the vowel /i/. This suggests that listeners perceptually compensate for VF0 patterns in their consonant voicing judgements. This study furthers our understanding of how intrinsic F0 effects interact in perception and, as far as we know, is the first study to show VF0 effects in perception through a voicing judgement.

Tinnitus Residual Inhibition Through Contralateral Acoustic Stimulation

Bérangère Margaux Villatte, Arnaud Norena, Sylvie Hébert

Introduction: Tinnitus is the perception of sound without an external stimulus. Currently, there is no treatment available to completely eliminate it. However, residual inhibition (RI) is a psychoacoustic method that temporarily suppresses tinnitus. The exact mechanisms underlying RI are still not well understood, and the effect of contralateral stimulation has not been explored yet.Objective: This study aims to induce contralateral RI and compare intensity levels with ipsilateral stimulation. RI efficacy is also compared between unilateral tinnitus and bilateral tinnitus with unilateral dominance.Methods: Thirty participants with unilateral or bilateral tinnitus were recruited. Pulsed noise was delivered through headphones, first ipsilaterally and then contralaterally. Tinnitus masking and inhibition levels were measured. Stimulation was performed using narrowband noise centered on the tinnitus frequency and white noise. A mixed ANOVA was conducted to compare levels based on noise type, stimulated side, and tinnitus type.Results: There was no significant difference in intensity between ipsilateral and contralateral stimulations. However, higher inhibition levels were required for bilateral tinnitus than unilateral tinnitus. Contralateral white noise levels were significantly lower for bilateral tinnitus, while contralateral narrowband noise levels were significantly lower for unilateral tinnitus.Discussion/Conclusion: This study demonstrates the feasibility of inducing contralateral RI and characterizes the required intensity levels, which to our knowledge, have not been previously described. Contralateral stimulation appears to induce desynchronization of tinnitus-related activity and seems more effective for strictly unilateral tinnitus. Individuals with single-sided deafness and tinnitus could benefit from contralateral stimulation. However, a better understanding of RI mechanisms and its long-term effectiveness is still needed.

UNDERWATER ACOUSTICS - ACOUSTIQUE SOUS-MARINE

ASSESSMENT OF PROPELLER CAVITATION INCEPTION SPEED BASED ON ONBOARD VIBRATION AND UNDERWATER ACOUSTIC DATA

Kamal Kesour [*1], Paul Camerin [†1], Jean-Christophe Marquis Gauthier [‡1], Cédric Gervaise [♦2]
[1]Innovation maritime, Rimouski, Québec, Canada.
[2]SenseaFR, Grenoble, France.

1 Introduction

The underwater radiated noise (URN) level made by commercial shipping has been steadily rising in recent decades, reaching a point where it is recognized as a significant environmental issue. This increase in noise is related to the growing number and larger sizes of commercial vessels. Adverse effects of underwater noise have been observed in various species, including mammals, fish, and invertebrates. The URN emitted by a ship primarily consists of three types of noise: machinery noise, propeller noise, and hydrodynamic noise. At low speeds, machinery noise is the dominant factor, while at high speeds propeller noise is the main source of noise, particularly when propeller cavitation becomes more pronounced. Estimating the cavitation inception speed (CIS) enables an optimum trade-off between maximizing speed and minimizing noise. Consequently, it is crucial to identify the CIS in order to reduce propeller noise and mitigate its impact on the surrounding marine life.

The propeller's rotation creates a localized under-pressure, forming water vapor bubbles on the hub, blade surfaces, or between the hull and blades. As this depression is localized, the pressure within the fluid is quickly rebalanced, causing the implosion of the bubbles. The implosion of cavities causes damage to the propeller surface in the form of pitting, which can be negligible or considerably deep and lead to rupture. Cavitation also degrades propulsion performance due to water layer delamination. Radiated propeller cavitation noise is a broadband noise whose intensity depends on ship speed, propeller technology, wake and hull hydrodynamic profile.

This paper uses vibrational data in order to detect the occurrence of propeller cavitation as well as to estimate the CIS. The onboard vibration analysis results are validated against underwater acoustic data provided by the Marine Acoustic Research Station (MARS).

2 Methodology

There are several techniques for detecting the presence of propeller cavitation, using sensors installed either on board the ship or externally. Sensors used outside the ship consist mainly of hydrophones. On board ships, various techniques have been developed to characterize the occurrence of cavitation. A distinction can be made between intrusive (e.g. borescope, high-speed camera, pressure sensor) and non-intrusive methods. The latter class is particularly interesting, as it ensures minimal installation costs and preserves the integrity of the ship's hull. The aforementioned approach uses vibration sensors to assess the presence of propeller cavitation. The disadvantage of this type of method is that it requires more sophisticated algorithms to detect propeller cavitation, due to the presence of several potential sources of vibration (engines, pumps, gears, etc.).

By analyzing the vibration and underwater acoustic data generated by the propeller, unique frequency patterns generated by the propeller's cavitation can be identified. In this context, Detection of Envelope Modulation On Noise (DEMON) [1] and Integrated Cyclic Modulation Coherence (ICMC) [2] algorithms are employed. To fully automatize the detection of cavitation, the Fast kurtogram [3] is used to identify the frequency band of demodulation (resp. integration) for DEMON (resp. ICMC). The frequency band with the highest spectral kurtosis is selected from the fast kurtogram.

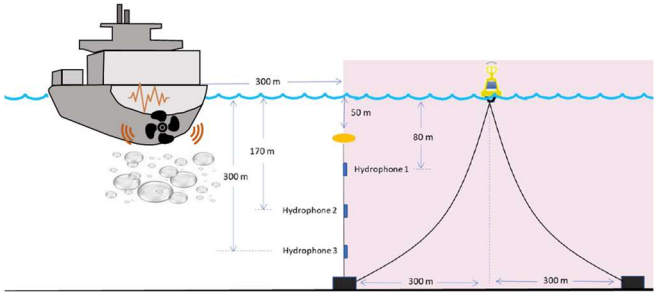

Figure 1: Passage of a vessel through the MARS Station.

The Cavitation generates high-frequency, broadband noise which is modulated by the shaft rotation and propeller blade passage frequencies. The DEMON method involves applying a band-pass filter to extract the modulated signal. The accuracy of the DEMON method is closely linked to the choice of the frequency band of the band-pass filter. Next, the envelope of the modulated signal is obtained by keeping only the low-frequency component (i.e. envelop). Finally, the DEMON spectrum is computed by the fast Fourier transform (FFT) of the envelope.

The ICMC method is based on the principle of cyclostationarity, which provides a rigorous basis for tackling detection problems. First, power spectra are calculated from the measured signal. Then, for each frequency, the power spectrum is calculated over the time axis, leading to a cyclic modulation spectral matrix as a function of frequency and cyclic modulation frequency α. The latter matrix is normalized to form the cyclic modulation coherence (CMC) by dividing it by the frequency spectrum at $\alpha = 0$. Finally, the ICMC is obtained by integrating over the frequency band identified by the fast kurtogram.

[*] kkesour@imar.ca
[†] pcamerin@imar.ca
[‡] jcgmarquis@imar.ca
[♦] cedric.gervaise@senseafr.com

Finally, an analysis of the frequency content of the DEMON or ICMC spectrum of the modulated signal shows whether or not the propeller is in cavitation. The CIS is identified by tracking the maximal amplitude of the propeller shaft rate and its harmonics at different speeds.

3 Results

In this work, the research vessel Coriolis II was instrumented by using accelerometers (PCB 352C33) above the propeller and tachometers to track propeller shaft rotation. The Coriolis II is a 50 m long ship constructed in 1990, equipped with 4-bladed twin screws. Aiming to estimate the CIS, the ship passed through the Marine Acoustic Research Station (MARS) at various speeds (between 2 and 12 knots). Figure 1 shows an antenna of the MARS station composed of three-hydrophone arrays.

3.1 Cavitation detection

Figure 2 shows an example of the obtained ICMC spectrum at a speed of 12 knots. The Shaft rate and its harmonics are clearly identified in the figure which indicates that the propeller was in cavitation at this specific speed.

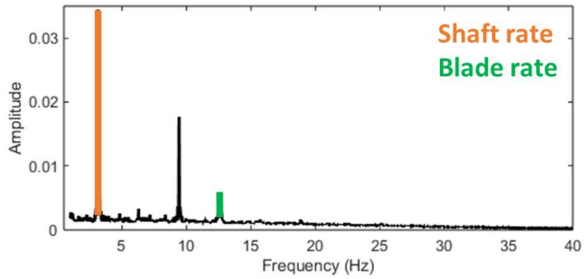

Figure 2: ICMC spectrum using onboard vibration data.

3.2 CIS estimation

In order to estimate the CIS, the maximal amplitude of the shaft rate and its harmonics were tracked over 36 passages of the Coriolis II. Figure 3 shows the results obtained by the ICMC method from vibration data recorded by a sensor placed above the starboard propeller. It's observed that CIS can be estimated around a speed of 8 knots defined by the intersection between the two slopes. The same CIS estimation is obtained by applying the DEMON algorithm to the underwater acoustic data as shown in Figure 4. This result demonstrates that the CIS estimation from onboard data can be a reliable tool, according to the underwater noise analysis.

4 Conclusion

This paper examined the use of onboard vibration data to estimate the CIS and detect its occurrences. In this context, two algorithms were developed and employed to indicate the occurrence of cavitation, namely: the DEMON and ICMC algorithms. The CIS was estimated by tracking the maximal amplitude of the propeller shaft rate and its harmonics at different speeds. The results using on onboard vibration data were validated against the underwater acoustic ones. The results show that the two algorithms of the estimation of the CIS are fairly accurate and reliable. However, more data are required to fully validate the developed methodology. Thereafter, the use of onboard vibration data has the potential to become a standard practice for detecting propeller cavitation, estimating the CIS and potentially reducing underwater noise pollution in the maritime industry.

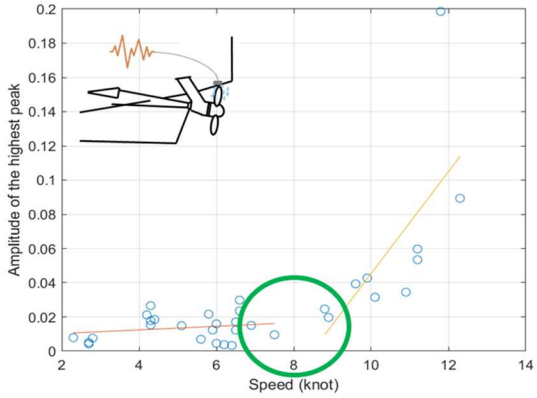

Figure 3: Maximal amplitude of the onboard vibration ICMC spectrum at different vessel speeds.

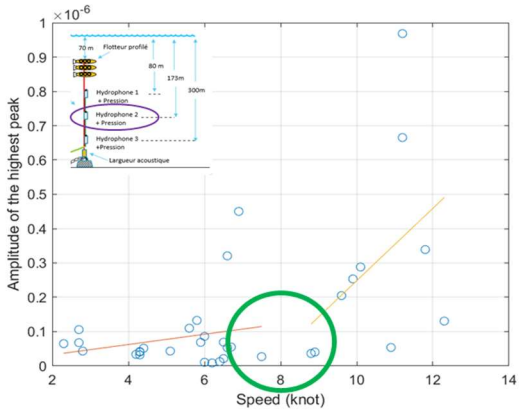

Figure 4: Maximal amplitude of the underwater acoustic DEMON spectrum at different vessel speeds.

Acknowledgments

The authors would like to thank Tranport Canada (TC) and the Ministère de l'Économie, de l'Innovation et de l'Énergie (MEIE) du Québec for their financial support. The authors would like to thank the Réseau Québec maritime (RQM) to have made the Coriolis II available for the measurements.

References

[1] Han, H. S., Lee, K. H., & Park, S. H. (2016). Evaluation of the cavitation inception speed of the ship propeller using acceleration on its adjacent structure. Journal of Mechanical Science and Technology, 30(12), 5423-5431.

[2] Antoni, J., & Hanson, D. (2012). Detection of surface ships from interception of cyclostationary signature with the cyclic modulation coherence. IEEE Journal of Oceanic Engineering, 37(3), 478-493.

[3] Antoni, J. (2007). Fast computation of the kurtogram for the detection of transient faults. Mechanical Systems and Signal Processing, 21(1), 108-124.

MEASUREMENT OF VESSEL UNDERWATER ACOUSTIC SIGNATURE – REPEATABILITY ASSESSED ON THE MARS DATABASE

Pierre Cauchy [*1], Pierre Mercure-Boissonnault [1], Faniry Rabetoandro [1], Cécile Perrier de la Bathie [1], Cédric Gervaise [1,2], Guillaume St-Onge [1] et Sylvain Lafrance [†3]

[1]Institut des sciences de la mer de l'Université du Québec à Rimouski, Rimouski, Québec, Canada

[2]Institut de recherche CHORUS, Grenoble, France

[3]Innovation Maritime, Rimouski, Québec, Canada

1 Introduction

Shipping is the main contributor of anthropogenic noise pollution in the ocean, globally spread and increasing steadily, with adverse effects on marine life. In support for emerging initiatives to reduce shipping noise and mitigate its effects on marine life, the Marine Acoustic Research Station (MARS) applied research project aims to improve measurement, understanding and modeling of underwater noise radiated by ships [1]. A recording station was moored along the St. Lawrence shipping lane during the summer seasons 2021 and 2022. The MARS database contains ~1000 underwater acoustic signatures of ships, representative of the commercial fleet using the St. Lawrence seaway. In this study, we focus on ships that have been measured repeatedly, to demonstrate the reliability of the measurements collected by the MARS station.

2 Method

2.1 The MARS database

The MARS station was specifically designed to collect and process ship noise data following the recommendations of the ANSI/ASA S12.64-2009 [2] and ISO-17208-1 [3] standards, to produce acoustic signatures. Acoustic signatures used in this study are expressed as Monopole Source Level (MSL) on third-octave bands at 1 m. The MSL metric treats the ship's source as a monopole, taking into accounts multiple paths by applying a propagation model [4]. The MARS database consists of about 1000 acoustic signatures measured from 593 individual ships. This database includes a subset of 173 high-quality acoustic signatures from 121 individual ships from participating shipowners, having followed a pre specified measurement protocol to optimize the quality of the acoustic measurement.

2.2 Subset and data analysis

In this study, we focused on the subset of high-quality acoustic signatures. We identified repeated measurements from individual ships, at similar speed, to assess the ability to reproduce the measurement of an acoustic signature.

A preliminary analysis was carried out on four repeated measurements of the same ship, at speeds ranging from 12.6 to 13.7 knots from which we were able to compare the four independent measurements of an acoustic signature.

3 Preliminary observations

The four acoustic signatures collected all share similar features, showing a loud cavitation noise on the 20 – 100 Hz band (Figure 1). The observed spread between the maximum and minimum values of the four signatures is consistent across the 20 – 500 Hz spectrum. For quantification of the spreading between the four acoustic signatures considered and across all the frequency spectrum, we considered the mean signature as the reference for this ship (Figure 1).

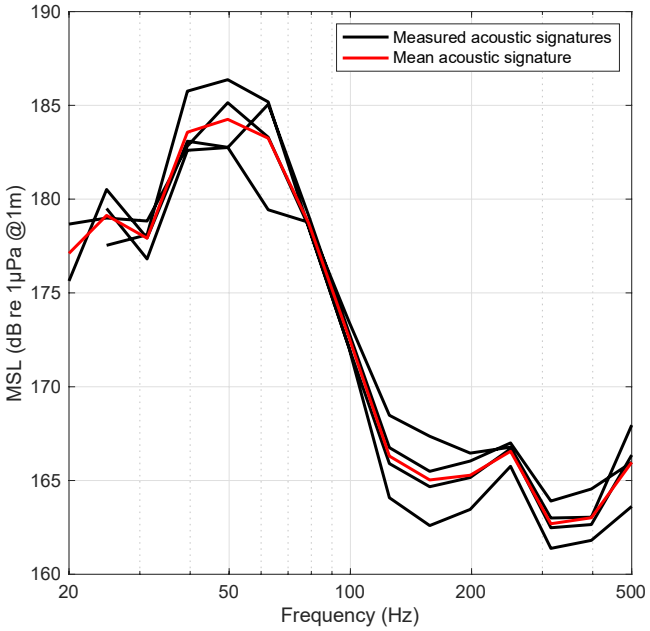

Figure 1: Spectrum of the 4 acoustic signatures collected (black) and mean acoustic signature constructed as a reference (red), expressed in Monopole Source Level (MSL) on third octave bands. Vessel speed ranging from 12.6 to 13.7 knots.

The error was defined as the difference between each acoustic signature and the reference. Analysis of the distribution of the error (Figure 2) shows that 85 % of the observations are within 2 dB from the reference, and the standard deviation of the error is 1.3 dB. Further analysis on an extended dataset including all repeated measurements taken at comparable speed is in progress and will allow to produce robust statistics regarding the expected variability of the acoustic signature measurements taken by the MARS station.

[*] pierre_cauchy@uqar.ca
[†] slafrance@imar.ca

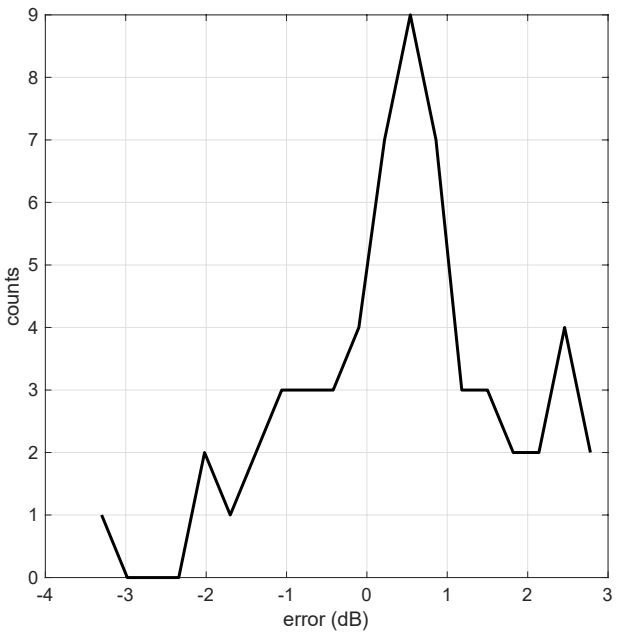

Figure 2: Distribution of the error between each of the 4 acoustic signatures collected and the reference on each third octave bands within 20 – 500 Hz. Associated standard deviation is 1.3 dB.

4 Discussion

The MARS project is building a large dataset of acoustic signatures representative of the underwater noise levels emitted by the St. Lawrence fleet. A significant effort was made to follow the recommendations of the international standards [2,3], and provide high quality acoustic signatures to the scientific community, the industrial actors of the shipping industry, and to the institutions involved in regulation, mitigation, and conservation. The ability to quantify and demonstrate the reliability of our measurements is key to improve acceptability of the decisions based on the MARS database.

This preliminary result is encouraging, regarding the repeatability expected by the ANSI/ASA S12.64-2009 standard [2], of 1.5 dB for the highest grade, and 2 dB and 3 dB for the grades B and C, respectively. Our analysis suggests that 70 % of our observation have an error under 1.5 dB, and 85 % under 2 dB.

It is worth noting that this result was obtained from a ship actively participating in the MARS project, and therefore following a protocol specifically designed to improve accuracy of the measurement. It is expected that data collected from ships being measured without following the protocol will show lower repeatability scores.

5 Conclusion

The design and development of a cutting-edge acoustic recording station, deployed in an ideal environment (bathymetry and proximity from the shipping lane) is a major part of the work carried out by the MARS team. The aim is to collect high-quality measurements and provide the best possible dataset to scientists, industrial partners and regulation and conservation institutions. This preliminary quantification of the repeatability of the measurements suggests that the MARS station will be able to quantify the efficiency of mitigation measures within a 2 dB difference for a ship actively taking part to the measurement process.

Acknowledgments

The MARS project is co-led by the Institut des sciences de la mer (ISMER) of the Université du Québec à Rimouski (UQAR) and Innovation maritime (IMAR), with the support of MTE Instruments and OpDAQ Systems as well as ship owners (Algoma Central Corporation, CSL, Desgagnés and Fednav). The project is financially supported by Transport Canada, the Québec Ministry of Economy and Innovation and the St. Lawrence Economic Development Council (SODES).

References

[1] O. Robin et al. The MARS project: Identifying and reducing underwater noise from ships in the St. Lawrence estuary. *Journal of the Canadian Acoustical Association*, Vol. 50, No. 3, 112-113, 2022.

[2] ANSI/ASA S12.64-2009/Part 1 (R2019): Quantities and procedures for description and measurement of underwater sound from ships - part 1: General requirements, 21 pp, 2019.

[3] ISO 17208-1:2016: Underwater acoustics — Quantities and procedures for description and measurement of underwater sound from ships — Part 1: Requirements for precision measurements in deep water used for comparison purposes.

[4] Y. Simard et al. Analysis and modeling of 255 source levels of merchant ships from an acoustic observatory along St. Lawrence Seaway. *J. Acoust. Soc. Am.*, 140:2002–2018, 2016.

THE MARS DATABASE – SOURCE LEVELS MEASURED FOR THE FLEET NAVIGATING THE ST. LAWRENCE ESTUARY

Pierre Mercure-Boissonnault *[1], Pierre Cauchy [1], Faniry Fitiavana Rabetoandro [1], Cédric Gervaise [1,2], Guillaume St-Onge [1], Jeanne Mérindol [1], Cécile Perrier de la Bathie [1], Hugo Catineau [1] and Sylvain Lafrance †[3]
[1]Institut des sciences de la mer de Rimouski, Université du Québec à Rimouski, Rimouski, Québec, Canada
[2]Institut de recherche CHORUS, Grenoble, France
[3]Innovation Maritime, Rimouski, Québec G5L-4B4, Canada

1 Introduction

Merchant ships can radiate noise underwater over a wide range of frequencies. Those sounds can travel long distances underwater since the sound absorption of water is low at low and medium frequencies [1] and the celerity profiles usually produce a natural waveguide for the sound to travel into. With the increase of the maritime traffic over the last few decades, the shipping noise became a concern for its impact on the marine life.

The MARS (Marine Acoustic Research Station) project [2] (www.projet-mars.ca/en) is designed to improve the knowledge on the shipping noise and to propose reduction methods. Via this project, over 1000 ship acoustic signatures have been measured using hydrophone networks, and a coherent database of ship signatures have been built.

2 Method

2.1 The MARS station

The MARS station consists of 4 vertical arrays of 3 hydrophones that have been deployed near the shipping lanes in the lower St. Lawrence Estuary. They have been placed strategically to allow 2 sets of measurements on port and starboard sides with a minimal trajectory deviation (around 1.2 km in 2021 and 0.4 km in 2022). This way, it allows to produce acoustic signatures in respect to the ANSI/ASA S12.64-2009 [3] and ISO-17208-1 [4] standards without having to make multiple time-consuming passes in front of a single array as the standards suggest.

Five shipowners were partnering with the MARS project to make their ships pass their ships in an optimized trajectory near the station using a set of waypoints.

The arrays have been deployed in 2021 and 2022 with the setup shown in Figure 1. The hydrophones were recording at a sampling frequency of 16kHz.

2.2 Numercal treatment

Ships passing through the station are detected using their position received via AIS (Automatic Identification System) by a ground station in Mont-Joli operated by MTE Instruments. Analysis of the AIS data allows to estimate the time, the distance and the speed at the closest points of approach (CPA) in front of each array.

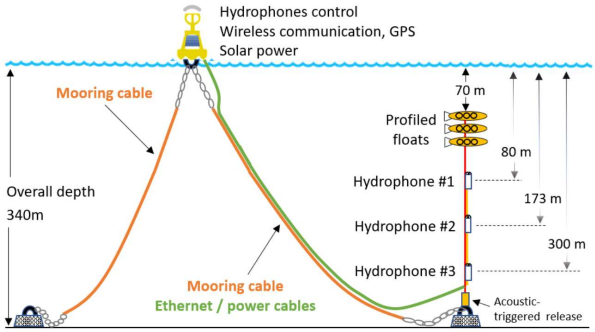

Figure 1: Example of the optimized setup of the hydrophone arrays deployed in 2021 and 2022 with a communicating buoy to transmit recordings.

Acoustic signatures are obtained following the Grade A processing method of ANSI/ASA S12.64-2009 [3]. A spectrogram is computed for the data acquisition window (±30° centered on the CPA as shown in Figure 2) with a timestep of 1s. Background noise adjustments are made by rejecting signal-to-noise ratios less than 10 dB based on the third octaves bands. The transmission losses (TL) are added to the spectrogram which is then averaged on the time axis to produce the ship source levels at a hydrophone. Those spectra are power averaged (1) on each vertical array and the 4 arrays are averaged (2):

$$L_{array\,i} = 10\log_{10}\left(\frac{1}{3}\sum_{j=1}^{3} 10^{L_{hydrophone\,i,j}/10}\right) \quad (1)$$

$$L_{signature} = \frac{1}{n_i}\sum_{i=1}^{n_i} L_{array\,i} \quad (2)$$

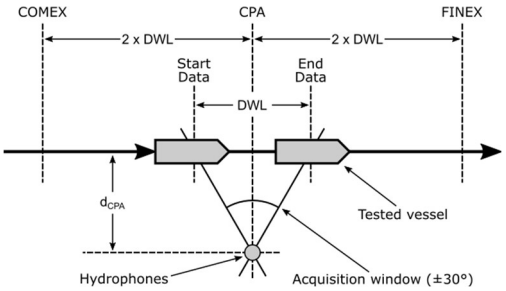

Figure 2: Metrics of a trajectory in front of an array.

Two metrics are used: RNL (Radiated Noise Levels) signatures made using spherical TL, as described by the standards and MSL (Monopole Source Levels) signatures, made using TL obtained with the wavenumber integration model SCOOTER [5].

* Pierre_Mercure-Boissonnault@uqar.ca
† slafrance@imar.ca

An automatic processing system has been developed at ISMER using Matlab R2022 to generate these signatures. Post-processing tools has been developed to allow the manual revision of the ship trajectories, concordance of the CPA with the recordings and platform noise detection to ensure the quality of each signature.

3 Results and discussion

3.1 The MARS database

173 high-quality signatures were made from the passages that followed the optimized trajectory in 2021 and 2022. A few non-partner ships that happened to pass close to the arrays in 2022 were also included. The number of ships by type for these signatures is shown Table 1. Since the fleet of the shipowner partners consisted mostly of bulk carriers, some ship types such as container ships and tanker were underrepresented.

Table 1: Ship types of the optimized trajectory signatures

Ship type	2021	2022
Bulk carrier	25	70
Cargo (general)	4	26
Merchant coastal	3	19
Tanker	5	8
Container ship	0	8
Other	0	5

An additional 983 passages were detected of the remaining traffic in or nearby the upstream shipping. Processing of these data is in progress and will be included to the MARS database after a manual validation have been thoroughly completed. This will allow to have a more extensive view of the shipping noise in the St. Lawrence Estuary and have a better representation of each ship type.

3.2 Comparison to the existing literature

The distribution of the high-quality signatures of the MARS database is presented in Figure 3. It was compared to an extended database of Simard 2016 [6] containing 710 single array signatures and to the MacGillivray 2020 [7] database containing 6295 single hydrophone spectra made with seabed platforms in shallow waters.

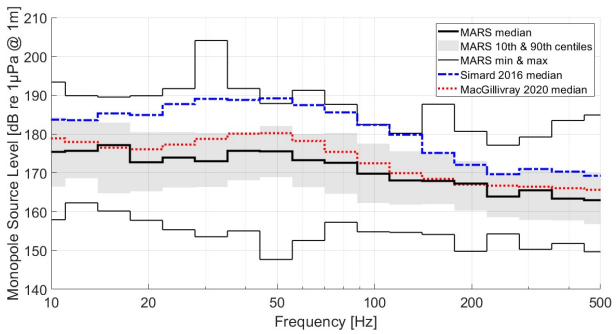

Figure 3: Distribution of the MARS high-quality signatures of the optimized trajectory passages in 2021 and 2022 in comparison to an extended database of Simard 2016 and MacGillivray 2020

We are in concordance with MacGillivray 2020 [7] results with the assumption that the ships measured are longer (thus noisier) for open sea ports that it is for the MARS fleet where a portion of the ships have to go through the Welland Canal locks in the St. Lawrence Seaway that allow a maximum length of 225.6 m. There is a disparity with Simard 2016 [6] where the median MSL is noticeably higher which is currently being investigated.

4 Conclusion

The MARS database provides a reference database of ship acoustic signatures representative of the fleet operating in the St. Lawrence Estuary. Such database is critical to the design and implementation of mitigation measures to reduce the underwater noise radiated by ships. It also allows further scientific analyses such as making new and improved models of ships underwater source levels.

Acknowledgments

The MARS project is co-led by the Institut des sciences de la mer (ISMER) of the Université du Québec à Rimouski (UQAR) and Innovation maritime (IMAR), with the support of MTE Instruments and OpDAQ Systems. It involves a partnership with the shipowners Algoma Central Corporation, CSL, Desgagnés, Fednav and NEAS and is financially supported by Transport Canada, the Quebec Ministry of Economy and Innovation and the St. Lawrence Economic Development Council (SODES).

References

[1] R. E. Francois, G. R. Garrison. Sound absorption based on ocean measurements. Part II: Boric acid contribution and equation for total absorption. J. Acoust. Soc. Am.; 72 (6): 1879–1890, 1982.

[2] O. Robin et al. The MARS project: identifying and reducing underwater noise from Ships in the St. Lawrence estuary. Presented at the Acoustic Week in Canada on Sept. 28th 2022 in St. John's, NL, Canada

[3] ANSI/ASA S12.64-2009/Part 1 (R2019): Quantities and procedures for description and measurement of underwater sound from ships - part 1: General requirements, 21 pp, 2019.

[4] ISO 17208-1:2016: Underwater acoustics — Quantities and procedures for description and measurement of underwater sound from ships — Part 1: Requirements for precision measurements in deep water used for comparison purposes.

[5] Ocean Acoustic Library, Acoustic Toolbox, SCOOTER, https://oalib-acoustics.org/models-and-software/acoustics-toolbox/ (Last viewed July 12, 2023).

[6] Y. Simard et al. Analysis and modeling of 255 source levels of merchant ships from an acoustic observatory along St. Lawrence Seaway. J. Acoust. Soc. Am., 140:2002–2018, 2016.

[7] A.O. MacGillivray et al., Vessel Noise Correlations Phase 2 Study: Final Report. Document 02283, Version 1.0. Technical report by JASCO Applied Sciences, ERM Consultants Canada, and Acentech for Vancouver Fraser Port Authority ECHO Program, 2020

Analysis of the Variability of Ship Acoustic Signatures Measured as a Function of Hydrophone Configuration

Cécile Perrier de la Bathie[*1], Pierre Cauchy [†1], Guillaume St-Onge [‡1], Pierre Mercure-Boissonnault [§1], Cédric Gervaise [¶2], and Sylvain Lafrance [‖3]

[1]Institut des sciences de la mer de Rimouski, Université du Québec à Rimouski, Québec, G5L-3A1, Canada.
[2]CHORUS Research Institute, Phelma Minatec, Grenoble, France
[3]Innovation Maritime, Rimouski, Québec, Canada

1 Introduction

Maritime transport is the main anthropogenic source of noise in the very low frequencies. For conservation purposes, it is critically important to improve understanding of noise pollution and its impact on marine life in order to implement mitigation and regulation programs. The Marine Acoustic Research Station (MARS) project (`www.projet-mars.ca/en`) is dedicated to understanding and measuring the underwater noise radiated by ships and to proposing appropriate mitigation measures to reduce it. Measuring underwater noise emitted by ships is a complex task that is strongly influenced by measurement conditions [1, 2]. The american standard ANSI/ASA S12/64-2009 [3] describes a protocol developed to standardize methods for measuring and calculating underwater noise emitted by ships. However, it is often not possible to comply with its many restrictions, and any modification is likely to add uncertainty to the final measurement [4]. The MARS station is an acoustic measuring station deployed each year in the Laurentian Channel, designed to measure the acoustic signatures of ships as closely as possible to the standard [3]. An experiment was carried out, using the R/V Coriolis II, collecting 113 repeated measurements of its acoustic signature. An analysis of the variability of the measurements with speed, distance from the hydrophones and configuration of the hydrophones highlighted the importance of complying with the measurement protocol to perform an accurate measurement of ship's emitted sound. This study provides qualitative and quantitative insights on the uncertainties associated to the measurement of an acoustic signature, depending on the conditions of the measurement.

2 Method

2.1 Acoustics data : MARS station

The acoustic data comes from the MARS station, which consists of four moorings (E1, E2, W1 and W2) located near the St. Lawrence Seaway off Rimouski (figure 1). These four moorings have been deployed alongside the westward shipping lane, two on the port side (E1 and E2) and the other two on the starboard side (W1 and W2). The E1 array did not comply with the standard due to a deployment problem, these data could not be used.

[*]cecile.perrierdelabathie@uqar.ca
[†]pierre$_{c}auchy@uqar.ca$
[‡]guillaume$_{s}t-onge@uqar.ca$
[§]pierre$_{m}ercure-boissonnault@uqar.ca$
[¶]cedric.gervaise@chorusacoustics.com
[‖]slafrance@imar.ca

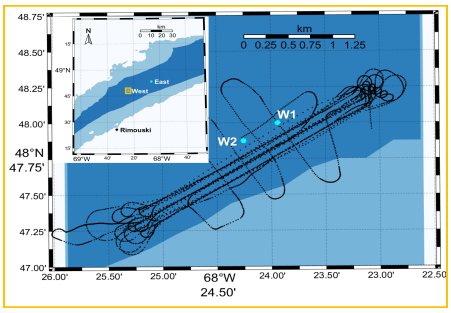

Figure 1: Study area. The locations of the MARS station arrays are specified. Two arrays are located to the east to measure signatures on the port side and two to the west to measure signatures on the starboard side. The zoomed-in area shows an example of the Coriolis II passing over the western array at different distances.

The station is located in a strategic zone for measuring the noise of ships travelling on the St. Lawrence seaway. Each mooring consists of a three hydrophones vertical arrays, at depths of 80, 173 and 300 m. The depths were chosen so that when a vessel passes at 300 m of an array, the angle of measurement of each hydrophone coincides with that recommended by the standard (15°,30° and 45° respectively). The station has been deployed using R/V Coriolis II for the ice-free months of 2021 and 2022.

2.2 R/V Coriolis II repeated measurements

During the arrays deployment and recovery missions, the R/V Coriolis II carried out repeated passages in front of the MARS hydrophone arrays, following the recommendations described in the standard [3]. Each passage was made following a straight line at a specified distance from the arrays, while maintaining constant navigation conditions. The resulting dataset comprises 113 passages, at 200, 300 and 400 m from each array, and at speeds of 2, 6, 8, 10, 12 and 14 knots.

2.3 Data Analysis

For each passage of the R/V Coriolis II, a monopole source level (MSL) spectrum was calculated for each hydrophone, a byproduct of the measurement of acoustic signatures automatically performed as one of the main deliverable of the MARS project. The MSL metric treats the ship's source sound level at 1 m, taking into accounts multiple paths by applying a precise propagation model Between Ship's stern and the measuring hydrophone [5]. In this study, we used MSL spectra on third-octave bands from 20 to 500 Hz. From the MSL spectra calculated for each hydrophone of an array a

MSL spectrum can be built for the array, as the average power of the three hydrophones.

Comparative analyses can be made of the noise spectra emitted by the hydrophones and the array signatures. Given that the Coriolis made passes in front of the two western arrays under the same operating conditions, it is possible to see the uncertainties in the method by comparing the signatures obtained by the two arrays.

3 Results

The R/V Coriolis II made a total of 113 passes in front of three MARS arrays (E2, W1 and W2). This analysis focused on 27 runs, recorded simultaneously by arrays W1 and W2, therefore collecting data in identical operating conditions (i.e. with identical distance to closest point (dCPA) and speed). We analyzed the difference between the signatures of the two arrays (2a), and the difference between the spectrum acquired by each pair of hydrophones at similar depth (i.e top, center and bottom hydrophones of each arrays) (2b).

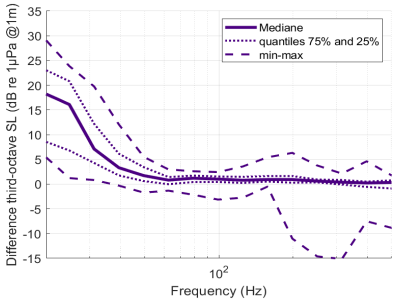

(a)

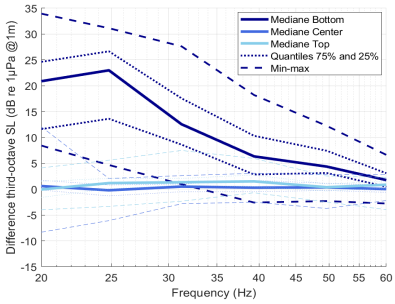

(b)

Figure 2: (a) Median, quartiles, and extrema of the difference between the signatures collected by the arrays W1 and W2, and (b) detail of the difference between the spectrum collected by each pair of hydrophones of similar depth (i.e., W1 top – W2 top, W1 center – W2 center and W1 bottom – W2 bottom), with a zoom on the low frequencies (20 – 60 Hz).

The difference between the signatures provided by W1 and W2 is below 1 dB in the 50 – 500 Hz frequency range. However, there is a clear bias in the low frequencies (20 – 50 Hz), W1 measuring up to 18 dB more than W2 (figure 2a). A similar analysis on each pair of hydrophones of similar depths shows that the bias is generated by measurement differences between the bottom hydrophones only, W1 bottom measuring up to 23 dB more than W2 bottom while the difference between the center and top pairs of hydrophones is below 1 dB on the whole spectrum (figure 2b).

4 Discussion and conclusion

On the 27 compared signatures collected by the arrays W1 and W2, we identified a clear bias at low frequencies (20 – 50 Hz) between the two bottom hydrophones that affects the acoustic signatures and needs to be addressed. Such difference could be caused by higher level of self-noise generated by the bottom part of the W1 mooring. We will also investigate how our sound propagation model would be affected by an error in the mooring localization, that could result in systematic over or under estimation of the low frequencies near the bottom.

Description and quantification of uncertainties in the measurement of acoustic signatures is a necessary task, to allow comparison of measurements taken in different locations and by different acoustic recording stations. This preliminary study highlights the very satisfying agreement (< 1 dB) on the 50 – 500 Hz frequency range between the 27 pairs of signatures compared. A measurement bias was detected from one of the bottom hydrophones at low frequencies (20 – 50 Hz). Further analysis to identify its cause is currently in progress to improve knowledge of our mesurements uncertainties and provide ways to mitigate errors.

Acknowledgments

We sincerely thank the captain, crew and scientific participants of the COR-2023-11 Expedition on board the R/V Coriolis II for the support during the expedition. The MARS project is co-led by the Institut des sciences de la mer (ISMER) of the Université du Québec à Rimouski (UQAR) and Innovation maritime (IMAR), with the support of MTE Instruments and OpDAQ Systems as well as ship owners (Algoma Central Corporation, CSL, Desgagnés, Fednav and NEAS). The project is financially supported by Transport Canada, the Québec Ministry of Economy and Innovation and the St. Lawrence Economic Development Council (SODES).

References

[1] Paul T. Arveson and David J. Vendittis. Radiated noise characteristics of a modern cargo ship. *The Journal of the Acoustical Society of America*, 107(1):118–129, January 2000.

[2] Yvan Simard, Nathalie Roy, Cédric Gervaise, and Samuel Giard. Analysis and modeling of 255 source levels of merchant ships from an acoustic observatory along St. Lawrence Seaway. *The Journal of the Acoustical Society of America*, 140(3):2002–2018, September 2016. Publisher: Acoustical Society of America.

[3] ANSI/ASA s12.64-2009/part 1 (r2019): Quantities and procedures for description and measurement of underwater sound from ships - part 1: General requirements. n. accredited standards committee s12. 2019.

[4] David J. Vendittis and Paul T. Arveson. Ten challenges in measuring and reporting ship noise levels. *JASA Express Letters*, 2(3):036801, March 2022.

[5] Stephen C Wales and Richard M Heitmeyer. An ensemble source spectra model for merchant ship-radiated noise. *The Journal of the Acoustical Society of America*, 111(3):1211–1231, 2002.

Abstracts for Presentations without Proceedings Paper
Résumés des communications sans article

Multi-Domain Approach For Prediction Of Vortex-Induced Hull Pressure Fluctuations On A Model-Scale Ship

Duncan Mcintyre, Shameem Islam, Peter Oshkai

Anthropogenic underwater radiated noise (URN), of which shipping is the largest source, has increasingly become a topic of concern due to its deleterious environmental effects. Shed vorticity in the wake of marine propellers induces fluctuating pressure that contributes to URN and hull vibration both directly and via its influence on cavitation. Accounting for the unsteady pressure in the propeller wake due to shed vorticity is therefore crucial for simulation of acoustic emissions. Historically, accurate prediction of the pressure fluctuations in the wake of a ship propeller has been challenging due the need for both a relatively large computational domain and a high-fidelity turbulence modelling approach to accurately capture the dissipation effects. We present a multi-simulation solution designed as a relatively inexpensive and effective approach to simulating fluctuating pressure in the wake of marine propellers. The methodology relies on three increasingly high-fidelity solutions at decreasing physical length scales. First, flow over a bare hull of the vessel was simulated using the Reynolds-Averaged Navier Stokes (RANS) equations to establish a set of boundary and initial conditions for an Unsteady RANS (URANS) solution for the flow around the propeller and in the near-wake of the hull. Second, the URANS solution was computed using a sliding mesh to determine the initial conditions and the time-dependant boundary conditions suitable for a Delayed Detached-Eddy Simulation (DDES) solution in the wake of the propeller. Finally, the DDES solution was obtained using the time-varying velocity and turbulence boundary conditions from the URANS solution alongside convective pressure boundaries. In practical application, the resulting fluctuating pressure data could be used as an input to an acoustic analogy model for obtaining far-field URN predictions. We applied the multi-domain simulation methodology to a model-scale ship with a generic hull and propeller geometry and compared the numerical fluctuating pressure results to experimental measurements.

Ship Noise Quantification And Source Level Estimation In The Arctic Ocean

Najeem Shajahan, William D Halliday, Stephen J Insley

The melting of ice caused by climate change has resulted in an increase in ships transiting the Arctic region. Increased ship traffic increases underwater noise and poses a significant concern in bioacoustics and marine ecology. The purpose of this study was to quantify the impact of shipping on the Arctic soundscape by using passive acoustic data collected from various locations in the western Canadian Arctic from 2015 to 2022. By combining Automatic Identification System data with acoustic data and a hybrid sound propagation model, a method has been developed to determine the source level of individual ships. A total of 177 measurements were collected from 31 vessels, with research and fishing vessels contributing more to the source-level estimates. A comparison of measured source levels with existing empirical source level models was conducted, and residuals were calculated. By fitting the measured source levels, a ship noise source spectrum model was developed as a function of frequency, speed, and length between 50 Hz and 10 kHz. For a conclusive statistical analysis and to determine if the developed model is suitable for sound mapping in the Arctic, additional opportunistic measurements of ship noise are necessary.

OTHER - AUTRES

ASSESSMENT OF EQUIVALENT PROPERTIES FOR MULTILAYERED PANELS

Diego Martin Tuozzo[*1] **and Noureddine Atalla**[†1]
[1]Département de Génie Mécanique, Université de Sherbrooke, Sherbrooke, Québec, Canada

1 Introduction

The use of lightweight complex heterogeneous structures increased during the last years principally in the transportation sector (i.e., aviation and trains). This sector's technology enhancement pursues reducing long-term CO_2 emissions and increasing efficiency. Lightweight structures may have poor vibro-acoustic behavior and in designs with complex shapes and material heterogeneities, its vibro-acoustic modeling brings new challenges in terms of accuracy and computational cost. Techniques such as model order reduction, homogenization, mesh and meshless methods (with and without periodicity conditions) and energy methods are typically employed to tackle this problem. Within homogenization techniques, an equivalent properties strategy can be utilized to equivalently represent complex structures into more simple ones (for example, a single layer panel). The latter is named equivalent structure or carrier and it is responsible for representing certain conserved quantities of the original structure.

This work aims to stress the use and limitations of two equivalent properties strategies applied to multilayered structures. Limitations provide insight into the potential applicability of these strategies in complex structures. The whole numerical procedure is computed utilizing the General Laminate Model (GLM) [1, and related papers] in a wave and forced response context. In the first homogenization strategy, the carrier is represented by a single layer isotropic plate. In the second one, the carrier is a thin orthotropic plate. To verify the effectiveness of both strategies comprehensive examples of multilayered structures are presented.

2 Method

In this section, the necessary theoretical background of the two carriers utilized for the proposed homogenization strategies is presented.

2.1 Theoretical background

The first carrier is a single layer thin isotropic plate. To obtain the equivalent material properties, the dynamic equations which describes the in-plane and out-of-plane motion of every point within the plate in three perpendicular directions ($u(x,y,t)$, $v(x,y,t)$ and $w(x,y,t)$) are utilized (see e.g., [2, chaps. 13 and 15]). From those equations, after applying a Helmholtz decomposition, the three main wave phase velocities, $c_{\text{ph},i}$, can be obtained and are presented as follows,

$$c^2_{\text{ph},1} = \frac{\omega}{\sqrt{\frac{D}{m_s}}}, c^2_{\text{ph},2} = \frac{E}{2\rho(1+\nu)}, c^2_{\text{ph},3} = \frac{E}{\rho(1-\nu^2)}, \quad (1)$$

where E, ν, ρ, D, ω and $m_s = \rho h$ are the material's Elastic modulus, Poisson ratio and material density, the bending stiffness, the angular frequency, the surface mass and h the plate thickness. Utilizing Eq. 1 and the relation between E and G (the shear modulus) for an isotropic material, $G = E/(2(1+\nu))$, it is possible to obtain (after some algebraic manipulation) five equivalent material properties named, $E_{\text{eq}}, G_{\text{eq}}, \nu_{\text{eq}}, h_{\text{eq}}$ and ρ_{eq}. The latter is obtained considering equal mass between the original and equivalent structure.

The second homogenization strategy proposes the use of a single layer thin orthotropic plate. Then, the three governing dynamic equations utilized for this carrier, after assuming a time harmonic motion for the displacements u, v and w on the form $\mathbf{d} = [\hat{u}, \hat{v}, \hat{w}]e^{\mathrm{j}(k_x x + k_y y - \omega t)}$, are presented as follows,

$$k^2(A_{11}c^2 + A_{66}s^2 + (A_{12}{+}_{66})c\,s) - m_{\text{s}}\omega^2 = 0, \quad (2)$$

$$k^2(A_{66}c^2 + A_{22}s^2 + (A_{12}{+}_{66})c\,s) - m_{\text{s}}\omega^2 = 0 \quad (3)$$

$$k^4 D(\varphi) - m_{\text{s}}\omega^2 = 0, \quad (4)$$

where $k_x = k\cos(\varphi)$ and $k_y = k\sin(\varphi)$ are the x and y components of the wavenumber k, c and s refer to $\cos(\varphi)$ and $\sin(\varphi)$, φ is the heading angle and A_{ij} and $D(\varphi) = D_{11}c^4 + D_{22}s^4 + 2(D_{12}+2D_{66})c^2\,s^2$ are the in-plane and out-of-plane stiffnesses, respectively. Definitions of A_{ij} and D_{ij} can be found in textbooks such as [2].

2.2 Numerical procedure

The numerical procedure applied to both homogenization strategies consists basically in finding the equivalent isotropic/orthotropic properties of the equivalent single layer plate solving the eigenvalue problem of the original structure for each heading angle and each frequency of interest utilizing GLM. The first strategy utilizes Eq. 1 to find the equivalent properties and the second calculates them using Eqs. 2 to 4 and three ellipses that represent the best possible fit to the original dispersion curves. With the equivalent properties, the equivalent global stiffness matrix is built and used to calculate the equivalent forced response indicators. The composite Damping Loss Factor (DLF) of the original structure is calculated and added in the global stiffness matrix of the homogenized or equivalent structure.

[*]diego.martin.tuozzo@usherbrooke.ca
[†]noureddine.atalla@usherbrooke.ca

3 Results

To evaluate the effectiveness of the proposed strategies, both homogenization procedures are evaluated with two representative structures, a bilayer thick asymmetric multilaminate (two different orthotropic layers with non-zero angle lamina) and a highly damped sandwich panel with viscoelastic core (complex and frequency dependent core's material properties and aluminum skins). To characterize the bilayer asymmetric laminate, the total energy and input power, obtained for a point normal load, are presented in Fig. 1 for both homogenization strategies. It can be seen that the orthotropic homogenization performs better than the isotropic strategy (lower relative difference with the original structure's indicators). As a general trend, the relative difference increases with frequency.

Total energy and input power are also presented in Fig. 2 for the case of the sandwich panel. It can be seen that again, the orthotropic homogenization performs better than the isotropic strategy (lower relative difference with the original structure's indicators). However, the relative difference values are considerable higher than the previous less damped structure (i.e, structural damping less than 5 %). As a general trend, the relative difference increases with frequency for the isotropic homogenization and decreases for the orthotropic strategy. The same behavior described here was observed in thick isotropic/orthotropic sandwich panels with soft core (having less relative difference at low frequencies).

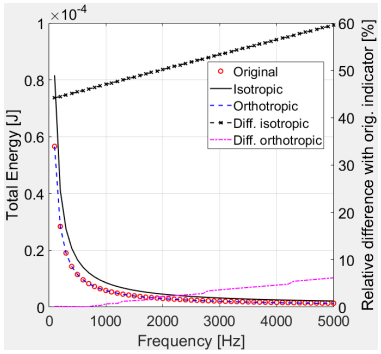

(a)

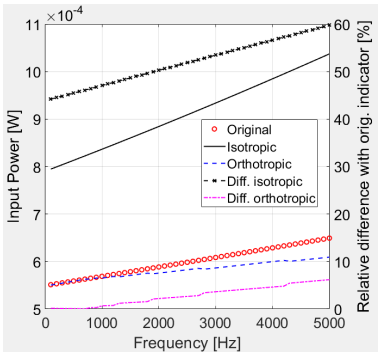

(b)

Figure 1: Total Energy (1a) and Power input (1b) forced indicators of the bilayer asymmetric multilaminate.

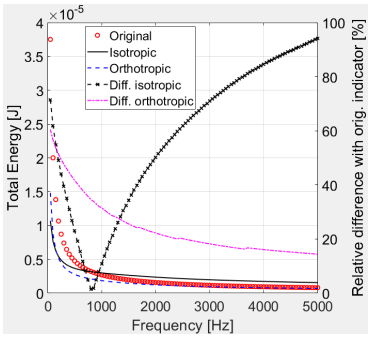

(a)

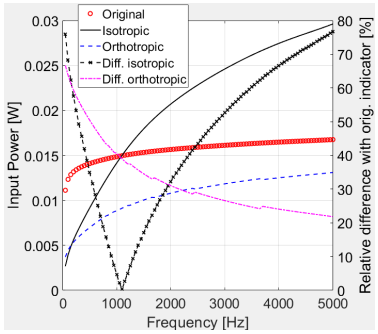

(b)

Figure 2: Total Energy (1a) and Power input (1b) forced indicators of the sandwich with viscoelastic core.

4 Final remarks and discussions

Two different homogenization strategies were presented. The necessary theoretical background utilized by each of these strategies was described. To stress the use and limitations of both strategies, two forced indicators were computed and compared with the original structure's indicators. The results show that the homogenization process (the equivalent properties) affects the equivalent forced quantities and, as a consequence, the composite DLF of the equivalent structure. The better the homogenization approach, the better the agreement between original/equivalent forced indicators such as total energy, injected power and composite DLF. The use of a linear composite damping (equivalently acting only on E and G) probably affects the correct reproduction of the bending behavior of the whole panel in thick or highly damped sandwich type structures. The performance of the strategies in wave (estimation of dispersion curves) and forced analyses is unrelated, highlighting the importance of a forced response assessment. In regards of the potential applicability of the presented strategies to complex structures, the orthotropic homogenization seems to capture the dynamic-anisotropic nature of the original structure (frequency, heading and material spatial properties variations).

References

[1] Sebastian Ghinet and Noureddine Atalla. Modeling thick composite laminate and sandwich structures with linear viscoelastic damping. *Computers & Structures*, 89(15):1547–1561, 2011.

[2] J.-M. Berthelot. *Composite Materials: Mechanical Behavior and Structural Analysis*. Springer New York, NY, 1st.ed., 1999.

ÉTUDE SUR LA FRÉQUENCE D'APPARITION D'APTONYMES ACOUSTIQUES ET MUSICAUX EN FRANCE MÉTROPOLITAINE

Odile Clavier [*1], Nicolas Trompette [†2], Stéphanie Viollon [‡3] et Jérémie Voix [§4]
[1]Creare inc, Hanover, New Hampshire, États-Unis
[2]Acoustique-Expertises, Vandoeuvre-lès-Nancy, Grand Est, France
[3]EDF, Saclay, Île-de-France, France
[4]ÉTS, Université du Québec, Montréal, Québec, Canada

1 Introduction

Cette étude, en marge des activités de recherche habituelles de ses autrices et auteurs, porte sur l'analyse aptonymologique de patronymes reliés aux domaines de l'acoustique, d'une façon générale, et à celui de l'acoustique musicale, en particulier.

Un aptonyme est un « nom de famille d'une personne qui est étroitement lié à son métier ou à ses occupations », selon la définition donnée par le grand dictionnaire terminologique de l'Office québécois de la langue française [1]. Le néologisme *aptonyme*, est composé du radical latin « apte » qui signifie « approprié, qui convient exactement », et de la terminaison « nyme », provenant du grec "onuma", qui signifie « nom », est apparu en 1992 dans l'ouvrage *The Study of Names* [2], mais a été principalement popularisé dès 1995 sur les réseaux sociaux de langue française par le professeur André Bougaïeff de l'Université du Québec à Trois-Rivières [3].

De nombreux auteurs se sont intéressés à l'origine et la signification des patronymes dans différents groupes sociaux [4]. Ainsi, la France compte plusieurs centaines de milliers de patronymes différents, ce qui est à la fois un record du monde et un patrimoine en évolution permanente. Il est donc amusant de voir que quatre personnes oeuvrant dans le domaine de l'acoustique portant chacune un nom en rapport avec l'acoustique ou la musique, intéressant de calculer la probabilité que ces quatre personnes soient coauteurs d'un article scientifique et stupéfiant de réaliser que la probabilité d'une telle occurrence est quasi nulle, rendant donc cette publication d'autant plus méritoire, selon la conviction profonde du dernier auteur [5].

2 Méthodologie

La méthodologie retenue consiste en un croisement entre d'une part les termes propres au domaine de l'acoustique et de la musique et d'autre part les noms communs portés en France métropolitaine depuis 1891, provenant de la base de données de l'Institut national de la statistique et des études économiques (INSEE). Un calcul de fréquence d'apparition portant sur le nombre d'adultes nés entre 1941 et 1990 et enregistrés par l'état civil français est ensuite effectué. Par la suite un calcul similaire est effectué en utilisant la base de données provenant de la Société française d'acoustique (SFA), association professionelle regroupant les professionels du domaine de l'acoustique.

2.1 Base de données des patronymes

Une requête d'accès auprès du Réseau français des centres de données pour les sciences sociales (Réseau Quetelet) nous a permis d'obtenir la base de données « *lil-0697: Fichiers des noms de famille - 1891-2000 - Édition 2008, 2008 (INSEE)* », au format du logiciel statistique propriétaire STATA. Les tables de cette base de données contenaient les années de naissance et patronymes enregistrés par l'état civil français et ont été converties en chiffrier LibreOffice pour être analysées plus simplement par la suite.

2.2 Base de données des termes acoustiques et musicaux

Les termes relevant du lexique acoustique et musical ont été tirés du dictionnaire de musique « Musicmot » [6], dont une extraction hors-ligne et conversion en chiffrier LibreOffice ont été effectuées par les auteurs pour les fins d'analyse croisée.

2.3 Base de données acousticiens français

Une extraction de la liste des participants du Congrès français d'acoustique de 2010 (CFA) a été effectuée, afin d'établir une liste, non-exhaustive mais représentative, de professionels actifs dans le domaine de l'acoustique en France métropolitaine.

3 Résultats

L'analyse de la base de données des patronymes a permis de dénombrer 218 982 patronymes distincts utilisés pour les 40 800 986 personnes nées entre 1941 et 1990, depuis AABI (25 occurrences) à ZYTO (41 occurrences). En recoupant ces patronymes avec la liste des termes acoustiques et musicaux, le tableau 1 ci-dessous est construit.

Au total, selon les données rapportées dans le tableau 1, il y a donc sur le total des 40 800 986 personnes nées entre 1941 et 1990, 14 064 adultes portant un patronyme qui se rapproche d'un terme acoustique ou musical. La probabilité qu'un adulte inscrit à l'état civil français porte un patronyme acoustique ou musical est donc inférieure à 0.03%. La probabilité que quatre personnes portant un tel patronyme (et qui plus est oeuvrant dans le domaine de l'acoustique ou de la musique) est d'environ (14.10^{-15}), soit de l'ordre d'une dizaine

[*] ohc@creare.com
[†] acoustique.expertises@gmail.com
[‡] stephanie.viollon@edf.fr
[§] jeremie.voix@etsmtl.ca

Tableau 1 : Liste des termes acoustiques et musicaux, des patronymes proches ainsi que du nombre **N** d'occurrences combinées.

Terme	Patronyme	N	Terme	Patronyme	N	Terme	Patronyme	N
ACCORDÉON	N/A		COR	COR	215	PIPAUD	PIPAUD	273
ALLEGRO	ALLEGRO	147	CORNEMUSE	CORNEMUSE	19	PIPAULT	PIPAULT	47
ALTO	ALTOT	22	CYMBALES	N/A		PIPAUT	PIPAUT	17
ARCHET	ARCHET	77	DIAPASON	N/A		PISTON	PISTON	82
BANJO	N/A		FANFARD	FANFARD	20	SAXO	SAXOD	98
BARYTON	BARITON	16	FANFARE	FANFARE	25	SON	SON	197
BASSON	BASSON	695	FIFRE	FIFRE	136	SOPRANO	SOPRANO	82
BATTERIE	BATTERY	120	FLUTE	FLUTTE	94	TAMBOUR	TAMBOUR	207
BATTEUR	BATTEUR	194	GRELOTS	GRELOT	421	TAMBOURIN	TAMBOURIN	80
BELVOIX	BELVOIX	101	GUITARE	GUITARD	1996	TENOR	TENOR	25
BELLEVOIX	BELLEVOIX	11	HARPE	HARPE	33	TIMBALE	TIMBAL	41
BEMOL	BEMOL	43	HAUTBOIS	HAUTBOIS	630	TROMPETTE	TROMPETTE	534
BINIOU	N/A		LAFLUTTE	LAFLUTTE	66	TROUBADOUR	TROUBADOUR	10
BOMBARDE	BOMBARDE	205	LATROMPETTE	LATROMPETTE	55	TUBA	N/A	
CAISSE	CAISSE	86	LAVOIX	LAVOIX	335	VIELLE	VIELLE	680
CARILLON	CARILLON	313	LEBATTEUR	LEBATTEUR	65	VIOLE	VIOLE	52
CHANTEUR	CHANTEUR	409	LECHANTEUR	LECHANTEUR	44	VIOLON	VIOLON	144
CHŒUR	CHOEUR	59	LECLAVIER	LECLAVIER	44	VIOLON	VIOLLON	88
CLAIRON	CLAIRON	242	ORGUE	ORGUES	23	VIRTUOSE	VIRTUOSE	19
CLARINETTE	N/A		PIANO	PIANO	105	VOIX	VOIX	78
CLAVIER	CLAVIER	3687	PICCOLO	PICCOLO	499	XYLOPHONE	N/A	
CONTREBASSE	N/A		PIPEAU	PIPEAU	58			

de millionième de milliardième, rendant d'autant plus méritoire cette publication conjointe.

En revanche un calcul de fréquence d'occurence d'un aptonyme parmi les acousticiens français, effectué sur la base de donnée des participants du Congrès français d'acoustique de 2010, révèle que seules 2 personnes, sur les 1287 participants à la conférence CFA2010, portent un aptonyme (en l'occurrence, il s'agit des 2e et 3e auteurs de la présente étude). La fréquence d'apparition parmi les professionel de l'acoustique d'un patronyme lié au domaine de l'acoustique ou de la musique s'élève donc à 0.16%.

4 Discussions et conclusion

Les résultats présentés dans cette étude portent sur la fréquence d'apparition d'aptonymes acoustiques et musicaux en France métropolitaine, selon une méthode originale de croisement de base de données lexicale et sociodémographique. Bien que le dénombrement statistique effectué dans cette étude soit exact, le calcul de probabilité statistique qui en découle est peut-être un peu plus hasardeux. Le biais principal de cette étude étant que les auteurs se sont précisément regroupés pour mener une telle analyse, motivés par l'originalité de porter chacun un aptonyme.

Il reste cependant intéressant de noter que la proportion d'aptonymes reliés aux domaines de l'acoustique et de la musique parmi les professionnels de l'acoustique est plus de quatre fois plus élevée (0.16% vs 0.03%) que parmi la population générale française. Bien qu'il puisse s'agir d'un biais d'échantillonnage statistique, la question de l'influence du nom sur le choix de carrière reste entière, ainsi que de nombreux spécialistes des aptonymes l'ont maintes fois souligné.

Remerciements

Les auteurs remercient l'équipe de diffusion des données du Centre Maurice Halbwachs (Réseau Quetelet) pour l'accès aux bases de données de l'INSEE, Michel Grzebyk, statisticien, pour le travail de croisement des données effectué, Anthony Lister pour ses suggestions de lecture et finalement Jean Lejay pour les discussions sur les limites de l'approche statistique utilisée. Finalement, ce travail a été grandement facilité par l'existence du site Musicmot.com maintenu par Patrick Martial.

Références

[1] Office québécois de la langue française, "Aptonyme | Grand dictionnaire terminologique." [Online]. Disponible : https ://vitrinelinguistique.oqlf.gouv.qc.ca/fiche-gdt/fiche/8364743/aptonyme

[2] F. Nuessel, The Study of Names: A Guide to the Principles andTopics. Bloomsbury Academic, Sep. 1992.

[3] A. Bougaïeff, "Accueil - Aptonymes - UQTR." [Online]. Disponible : https ://www.uqtr.ca/aptonymes

[4] J. Kaplan and A. Bernays, The Language of Names: What We Call Ourselves and Why It Matters. Touchstone, Mar. 1999.

[5] V. Simard, "Aptonymes : Votre nom vous va si bien," La Presse, Dec. 2022. [Online]. Disponible : https ://www.lapresse.ca/societe/2022-12-30/aptonymes/votre-nom-vous-va-si-bien.php

[6] P. Martial, "DICTIONNAIRE DE MUSIQUE EN LIGNE - Dico multim´edia." [Online]. Disponible : https ://www.musicmot.com/

Abstracts for Presentations without Proceedings Paper
Résumés des communications sans article

The Glottal Stop In Garo

Cheman Baira A'gitok

Garo, an understudied Tibeto-Burman language spoken in Northeast India is an atonal language and thus is an exception in the context of its related languages (Burling, 2003; Joseph and Burling, 2001). Garo however, has been described as possessing a phonemic glottal stop in its phonemic inventory (Burling, 1992). Crosslinguistically, it is found that glottal stops are realized a creaky voice quality in a lot of languages (Davidson, 2021), which in turn can affect the F0 on the vowel (Keating et al., 2015). This paper examines the phonetic implementation of the glottal stop in Garo and also examines its effect on the F0 of the adjacent vowels since it has been described as an atonal language. An acoustic analysis of the data recorded from 8 native speakers of Garo (2 male, 6 female) shows that the glottal stop is mostly realized as a creaky voice quality on the adjacent in Garo. The glottal stop is rarely realized as a complete glottal closure. The examination of the F0 of the adjacent vowels also revealed that the presence of the glottal did not substantially lower the F0. A generalized linear mixed model that was fit to the normalized data in R (R Core Team, 2021) showed that F0 was not a significant predictor of the presence of the glottal stop (β = -0.42, SE = 2.63, p = 0.872). The results of this paper show that the glottal stop in Garo is mostly realized as a creaky voice quality which lines up with the crosslinguistic observations. The results of this paper however, reveal that the F0 of the adjacent vowel is not affected thus potentially pointing to the fact that the glottal stop or creakiness is phonetically expresses in terms of other phonetic parameters (Keating et al., 2015).

Use Of Carillons In Building New Musical Instruments

Rama Balike Bhat

Use of Carillon Arrangement in Designing New Musical InstrumentsRama BhatDistinguished Professor EmeritusConcordia University, Montreal, Quebec, CanadaStructure of Musical Instruments:Every musical instrument has three essential functions, (i) conversion of vibration into sound, (ii) transmission of sound and vibration from point to point, and conversion of sound into vibrations again.In this article, discussion is limited to Carnatic Classical Music, which should apply to other musical styles also. While violin, used widely in Western Music, has been accepted with open arms by Carnatic music, Jala Tarang, which uses the vibrations of porcelain bowls filled with water to different levels to produce successive musical notes is virtually unheard of in Western music. West Indian Steel Pan originated in West Indies, and has spread to American continent in the past 50 years, is not familiar to Carnatic music fans. Following the general principles of science of sound, it is possible to visualize new musical instruments in all styles of music by appropriate arrangement of subsystems.The purpose of this presentation is to identify musical instruments by changing the first vibration stage, the middle transmission stage and the final production stage where the sound comes in different forms and different style and flavor of music [1].Conclusions:The oral presentation will include playings of different musical instruments for better appreciation of the proposed design.References:1. Bhat R.B., Vikrutha Panchama Scales in Carnatic Music Containing Fourth and Diminished Fifth, Canadian Acoustical Association Annual Meeting, 2017.

Deaf Gain: Enhancements In Vibrotactile Rhythm Perception For Deaf Individuals

Sean Alexander Gilmore, Frank Russo

The concept of Deaf Gain is used to reframe how we conceive of the consequences of deafness. The aim is to move away from a deficit focus, and towards a focus on enhancement. Research examining enhancements has generally been geared towards visual processing, such as enhanced reaction times to visual targets and heightened acuity to visual motion. The purported mechanism for these enhancements is compensatory plasticity. In the case of an individual with profound hearing loss, the brain undergoes morphological/functional changes in order to accommodate the processing of the preserved senses. Despite the amount of research focused on visual processing, research examining the tactile domain is limited. The current study aims to further our understanding of vibrotactile processing in Deaf individuals with a focus on vibrotactile musical rhythms. The current study used a factorial design to examine sensorimotor synchronization (SMS) and neural entrainment to a series vibrotactile rhythms which varied from a simple metronomic rhythm to a slightly more complex house rhythm. Temporal complexity (metronome, house rhythm), group (i.e., deaf and hearing) and an interaction between the two, were regressed on to SMS and neural entrainment using linear regression models. Results indicate a significant increase in neural entrainment in deaf compared to hearing individuals, no main effect of temporal complexity, and no

interaction. In addition, SMS results suggest a significant enhancement in SMS with deaf individuals showing lower variability compared to hearing. There was a significant interaction, which revealed a pronounced reduction in variability to house rhythms compared to the metronome for deaf individuals, but no differences for hearing individuals. Overall, these results provide new perspective on the enhancements that arise due to the loss of auditory input. Specifically, it suggests the ability to encode and synchronize to vibrotactile rhythms is enhanced following the loss of hearing input.

Assessing Automatic Musical Mode Extraction

Konrad Swierczek, Michael Schutz

Modality (a key aspect of western musical structure) is widely recognized to play a crucial role in conveying emotion. Consequently, psychological models and automated analysis of mode have received considerable attention since the 1970's. While tools such as the mirmode module of MIRtoolbox (Lartillot & Toiviainen, 2007) offer a convenient way of obtaining relative evaluations of a digital audio file's major/minor quality, their accuracy and consistency have not previously been fully tested. Although it is difficult to determine the "ground truth" for a musical passage's mode, in principle different versions of the same passage should have similar computed mode values. Therefore, we analyzed the first eight measures of 14 commercial audio recordings (versions) of preludes from J.S. Bach's Well Tempered Clavier Book 1 with MIRtoolbox's mirmode. In addition, we analyzed MIDI representations of each piece using a MIDI-based recreation of mirmode and included an additional audio version based on MIDI synthesized with a piano timbre. * swierckj@mcmaster.ca † schutz@mcmaster.ca Comparison of MIDI mirmode values to the synthesized version show considerable disagreement, particularly in the case of nominally minor pieces[MS1] . For example, over half of the mode evaluations differed between nominally minor MIDI files and audio synthesized directly from these files. Out of 24 pieces in the set, the algorithm consistently identified only 3 pieces across all versions. Structural features such as tonality and mode are generally thought to be relatively unaffected by changes in surface and expressive features. However, here we show it to be that a computationally extracted feature is inconsistent across different versions of the same piece of music. This method may be a useful framework for testing musical feature extraction more generally: analyzing multiple versions of the same piece of music can determine if an extracted feature is influenced by version-specific changes such as performer defined cues, acoustics, timbre, and recording techniques. [MS1]Interesting - but not clarified/supported by the text here. Do minor pieces have greater discrepancy between MIDI and synthesized audio?

The joint **186th Meeting of the Acoustical Society of America and the 2024 Acoustics Week in Canada conference will be held from May 13-17, 2024,** in downtown Ottawa, Ontario. You are invited to be part of this five days international conference featuring the latest developments in acoustics and vibration.

Shaw Convention Center

Ottawa is Canada's capital, a city that reflects the country's beauty, celebrates its diversity, embodies its spirit, and tells its stories like no other. Located at the confluence of three rivers at the foot of the rugged Canadian shield, Ottawa is home to over one million residents who are proud of their hometown and welcome people in English, French, Indigenous languages, and many more from around the world. The city's urban landscape reveals Canada around every corner, at historic and national sites, monuments, and cultural institutions. It's a city that knows how to celebrate, with annual festivals devoted to things near and dear to the hearts of Canadians, including music, arts and the diverse cultural communities that call Ottawa and Canada home. Unique among G7 capitals, Ottawa is equal parts urban and rural, a city on the edge of nature offering boundless opportunities for adventure and recreation in the great outdoors. Put simply, if Canada were a city, Ottawa would be it.

Venue and Accommodation

The conference will be held at the new Shaw Convention Centre, featuring a sweeping glass façade encasing four floors of state-of-the-art meeting space. This spectacular venue is directly linked to the CF Rideau Centre Mall and a few steps away from recreational paths along the Rideau Canal and the ByWard Market shopping and restaurant district — not to mention 6,000 downtown hotel rooms, all within easy walking distance. Please refer to the conference websites for further registration details: https://awc.caa-aca.ca and https://acousticalsociety.org/meeting-information/.

The Rideau Canal

Plenary, technical sessions

Plenary, technical, and workshop sessions are planned throughout the conference. Each day will begin with a keynote talk of broader interest and relevance to the acoustics community. Technical sessions are planned to cover all areas of acoustics including:

AEROACOUSTICS / ARCHITECTURAL AND BUILDING ACOUSTICS / BIO-ACOUSTICS AND BIOMEDICAL ACOUSTICS / MUSICAL ACOUSTICS / NOISE AND NOISE CONTROL / PHYSICAL ACOUSTICS / PSYCHO- AND PHYSIO-ACOUSTICS / SHOCK AND VIBRATION / SIGNAL PROCESSING / SPEECH SCIENCES AND HEARING SCIENCES / STANDARDS AND GUIDELINES IN ACOUSTICS / ULTRASONICS / UNDERWATER ACOUSTICS

Exhibition and sponsorship

The conference offers opportunities for suppliers of products and services to engage the acoustic community through exhibition and sponsorship.

The tabletop exhibition facilitates in-person and hands-on interaction between suppliers and interested individuals. Companies and organizations that are interested in participating in the exhibition should contact the Exhibition and Sponsorship coordinator for an information package. Exhibitors are encouraged to book early for best selection.

The conference will be offering sponsorship opportunities of various conference features. In addition to the platinum, gold and silver levels, selected technical sessions, social events and coffee breaks will be available for sponsorship. Sponsors can have their logo placed on the conference web site within 10 days of their sponsorship. Additional features and benefits of sponsorship can be obtained from the Exhibition and Sponsorship coordinator or the conference web site.

Registration details

Please refer to the upcoming AWC2024 conference web site: https://awc.caa-aca.ca or to https://acousticalsociety.org/meeting-information/.

Contacts

AWC2024 General Co-Chairs:

- **Dr. Sebastian Ghinet** (Sebastian.Ghinet@nrc-cnrc.gc.ca)
- **Prof. Joana Rocha,** (JoanaRocha@cunet.carleton.ca)

La **186-ème réunion de la Société Américaine d'Acoustique (ASA), conjointement avec la Semaine Canadienne de l'acoustique 2024, aura lieu du 13 au 17 mai 2024, au centre-ville d'Ottawa, en Ontario**. Vous êtes invités à assister à cette conférence internationale de cinq jours durant laquelle les derniers développements en matière d'acoustique et de vibration seront présentés.

Centre de congrès d'Ottawa « Centre Shaw »

Ottawa est la capitale du Canada, une ville qui reflète la beauté du pays, célèbre sa diversité, incarne son esprit et raconte son histoire comme aucune autre. Située à la confluence de trois rivières, au pied du bouclier canadien, Ottawa compte plus d'un million d'habitants, fiers de leur ville natale et accueillent les visiteurs en anglais, en français, en langues autochtones et bien d'autres du monde entier. Le paysage urbain de la ville révèle le Canada à chaque coin de rue, dans les sites historiques et nationaux, les monuments et les institutions culturelles. C'est une ville qui sait comment célébrer, avec des festivals annuels consacrés aux sujets chers au cœur des Canadiens, notamment la musique, les arts et les diverses communautés culturelles qui considèrent Ottawa et le Canada leur chez-soi. Unique parmi les capitales du G7, Ottawa est à parts égales urbaine et rurale, une ville en bordure de la nature offrant d'innombrables opportunités d'aventure et de loisirs en plein air. En résumé, si le Canada était une ville, Ottawa en serait la représentation parfaite.

Lieu et hébergement

La conférence se déroulera au nouveau Centre de congrès d'Ottawa « Centre Shaw », caractérisé par une imposante façade vitrée panoramique enveloppant quatre étages d'espaces de réunion ultramodernes. Ce lieu spectaculaire est directement relié au centre commercial CF Rideau et se trouve à quelques pas des sentiers récréatifs le long du canal Rideau ainsi que du quartier des boutiques et des restaurants du marché By, sans oublier les 6 000 chambres d'hôtel du centre-ville, toutes facilement accessibles à pied. Veuillez consulter les sites web de la conférence pour de plus amples informations sur l'inscription : https://awc.caa-aca.ca et https://acousticalsociety.org/meeting-information/.

Le canal Rideau

Sessions plénières et techniques

Des sessions plénières, techniques et des ateliers sont prévues tout au long de la conférence. Chaque journée débutera par une conférence plénière d'intérêt pour la communauté de l'acoustique. Des sessions techniques sont également prévues pour couvrir tous les domaines de l'acoustique, à savoir:

AEROACOUSTICS / ARCHITECTURAL AND BUILDING ACOUSTICS / BIO-ACOUSTICS AND BIOMEDICAL ACOUSTICS / MUSICAL ACOUSTICS / NOISE AND NOISE CONTROL / PHYSICAL ACOUSTICS / PSYCHO- AND PHYSIO-ACOUSTICS / SHOCK AND VIBRATION / SIGNAL PROCESSING / SPEECH SCIENCES AND HEARING SCIENCES / STANDARDS AND GUIDELINES IN ACOUSTICS / ULTRASONICS / UNDERWATER ACOUSTICS

Exposition et parrainage

La conférence offre aux entreprises fournissant des produits et des services la possibilité de s'engager auprès de la communauté acoustique par le biais d'expositions et de parrainages.

L'exposition des produits et services facilite l'interaction entre les vendeurs et les personnes intéressées. Les entreprises et les organisations souhaitant participer à l'exposition doivent contacter le coordinateur de l'exposition et du parrainage pour obtenir de plus amples informations. Les exposants sont encouragés à réserver le plus tôt possible pour bénéficier des meilleures places.

La conférence offrira des possibilités de parrainage. En plus des niveaux platine, or et argent, certaines sessions techniques, événements sociaux et pauses café pourront être sponsorisées. Les sponsors peuvent ajouter leur logo sur le site web de la conférence dans les 10 jours suivant leur parrainage. D'autres informations et avantages du parrainage peuvent être obtenus auprès du coordinateur des expositions et du parrainage ou sur le site web de la conférence.

Inscription

Pour plus d'informations sur l'inscription, veuillez consulter le site Web de la prochaine conférence AWC2024: https://awc.caa-aca.ca ou au https://acousticalsociety.org/meeting-information/.

Contacts

AWC2024 General Co-Chairs:

- **Dr. Sebastian Ghinet** (Sebastian.Ghinet@nrc-cnrc.gc.ca)
- **Prof. Joana Rocha,** (JoanaRocha@cunet.carleton.ca)

CANADIAN ACOUSTICS ANNOUNCEMENTS - ANNONCES TÉLÉGRAPHIQUES DE L'ACOUSTIQUE CANADIENNE

Looking for a job in Acoustics?

There are many job offers listed on the website of the Canadian Acoustical Association!

You can see them online, under http://www.caa-aca.ca/jobs/

August 5th 2015

Acoustics 2023 (Sydney, Australia)

Early Bird Registration Deadline 5 September, 2023! Make sure you don't miss the lower rate early bird deadline by completing your registration now! There will be no extension to this deadline so do not delay.

On behalf of the Australian Acoustical Society and The Acoustical Society of America, the Organising Committee looks forward to welcoming you to the Acoustics 2023 Conference to be held Monday 4 December to Friday 8 December 2023 at the International Convention Centre Sydney (ICC Sydney), Australia. Early Bird Registration Deadline 5 September, 2023! Make sure you don't miss the lower rate early bird deadline by completing your registration now! There will be no extension to this deadline so do not delay. More information can be found online at https://acoustics23sydney.org/

August 23rd 2023

À la recherche d'un emploi en acoustique ?

De nombreuses offre d'emploi sont affichées sur le site de l'Association canadienne d'acoustique !

Vous pouvez les consulter en ligne à l'adresse http://www.caa-aca.ca/jobs/

August 5th 2015

Why publish in Canadian Acoustics?

Because, it is...

- A respected scientific journal with a 40-year history uniquely dedicated to acoustics in Canada
- A quarterly publication in both electronic and hard-copy format, reaching a large community of experts worldwide
- An Open Access journal, with content freely available to all, 12 months from time of publication
- A better solution for fast and professional review providing authors with an efficient, fair, and constructive peer review process.

Pourquoi publier dans Acoustique canadienne ?

Parce que, c'est...

- Une revue respectée, forte de 40 années de publications uniquement dédiée à l'acoustique au Canada
- Une publication trimestrielle en format papier et électronique, rejoignant une large communauté d'experts à travers le monde
- Une publication "accès libre" dont le contenu est disponible à tous, 12 mois après publication
- Une alternative intéressante pour une évaluation par les pairs, fournissant aux auteurs des commentaires pertinents, objectifs et constructifs

Canadian Acoustical Association
Association canadienne d'acoustique

Application for Membership

CAA membership is open to all individuals who have an interest in acoustics. Annual dues total $120.00 for individual members and $50.00 for student members. This includes a subscription to ***Canadian Acoustics***, the journal of the Association, which is published 4 times/year, and voting privileges at the Annual General Meeting.

Subscriptions to *Canadian Acoustics* or Sustaining Subscriptions

Subscriptions to ***Canadian Acoustics*** are available to companies and institutions at a cost of $120.00 per year. Many organizations choose to become benefactors of the CAA by contributing as Sustaining Subscribers, paying $475.00 per year (no voting privileges at AGM). The list of Sustaining Subscribers is published in each issue of ***Canadian Acoustics*** and on the CAA website.

Please note that online payments will be accepted at http://jcaa.caa-aca.ca

Address for subscription / membership correspondence:

Name / Organization _____

Address _____

City/Province _____ Postal Code _____ Country _____

Phone _____ Fax _____ E-mail _____

Address for mailing Canadian Acoustics, if different from above:

Name / Organization _____

Address _____

City/Province _____ Postal Code _____ Country _____

Areas of Interest: (Please mark 3 maximum)

1. Architectural Acoustics
2. Engineering Acoustics / Noise Control
3. Physical Acoustics / Ultrasound
4. Musical Acoustics / Electro-acoustics
5. Psychological / Physiological Acoustic
6. Shock and Vibration
7. Hearing Sciences
8. Speech Sciences
9. Underwater Acoustics
10. Signal Processing / Numerical Methods
11. Other

For student membership, please also provide:

_____ _____ _____

(University) *(Faculty Member)* *(Signature of Faculty Member)* *(Date)*

I have enclosed the indicated payment for:
[ ] CAA Membership $ 120.00
[ ] CAA Student Membership $ 50.00

Corporate Subscriptions (4 issues/yr)
[ ] $120 including mailing in Canada
[ ] $128 including mailing to USA,
[ ] $135 including International mailing

[ ] Sustaining Subscription $475.00
(4 issues/yr)

Please note that the preferred method of payment is by credit card, online at http://jcaa.caa-aca.ca

For individuals or organizations wishing to pay by check, please register online at *http://jcaa.caa-aca.ca* and then mail your check to:

Executive Secretary, Canadian Acoustical:
Dr. Roberto Racca
c/o JASCO Applied Sciences
2305–4464 Markham Street
Victoria, BC V8Z 7X8 Canada

Association Canadienne d'Acoustique
Canadian Acoustical Association

Formulaire d'adhésion

L'adhésion à l'ACA est ouverte à tous ceux qui s'intéressent à l'acoustique. La cotisation annuelle est de 120.00$ pour les membres individuels, et de 50.00$ pour les étudiants. Tous les membres reçoivent ***l'Acoustique Canadienne***, la revue de l'association.

Abonnement pour la revue *Acoustique Canadienne* et abonnement de soutien

Les abonnements pour la revue ***Acoustique Canadienne*** sont disponibles pour les compagnies et autres établissements au coût annuel de 120.00$. Des compagnies et établissements préfèrent souvent la cotisation de membre bienfaiteur, de 475.00$ par année, pour assister financièrement l'ACA. La liste des membres bienfaiteurs est publiée dans chaque issue de la revue ***Acoustique Canadienne***..

Notez que tous les paiements électroniques sont acceptés en ligne http://jcaa.caa-aca.ca

Pour correspondance administrative et financière:

Nom / Organisation _____

Adresse _____

Ville/Province _____ Code postal_____Pays _____

Téléphone _____ Téléc. _____Courriel _____

Adresse postale pour la revue Acoustique Canadienne

Nom / Organisation _____

Adresse _____

Ville/Province _____ Code postal_____Pays _____

Cocher vos champs d'intérêt: (maximum 3)

1. Acoustique architecturale
2. Génie acoustique / Contrôle du bruit
3. Acoustique physique / Ultrasons
4. Acoustique musicale / Électro-acoustique
5. Physio / Psycho-acoustique
6. Chocs et vibrations
7. Audition
8. Parole
9. Acoustique sous-marine
10. Traitement des signaux /Méthodes numériques
11. Autre

Prière de remplir pour les étudiants et étudiantes:

_____ _____ _____ _____

(Université) (Nom d'un membre du corps professoral) (Signature du membre du corps professoral) (Date)

Cocher la case appropriée:

[ ] Membre individuel 120.00 $
[ ] Membre étudiant(e) 50.00 $

Abonnement institutionnel

[ ] 120 $ à l'intérieur du Canada
[ ] 128 $ vers les États-Unis
[ ] 135 $ tout autre envoi international

[ ] Abonnement de soutien 475.00 $ (comprend l'abonnement à *L'acoustique Canadienne*)

Merci de noter que le moyen de paiement privilégie est le paiement par carte crédit en ligne à *http://jcaa.caa-aca.ca*

Pour les individus ou les organisations qui préféreraient payer par chèque, l'inscription se fait en ligne à *http://jcaa.caa-aca.ca* puis le chèque peut être envoyé à :

Secrétaire exécutif, Association canadienne d'acoustique :
Dr. Roberto Racca
c/o JASCO Applied Sciences
2305–4464 Markham Street
Victoria, BC V8Z 7X8 Canada

Canadian Acoustical Association
Association canadienne d'acoustique

CANADIAN ASSOCIATION
ACOUSTICAL CANADIENNE
ASSOCIATION D'ACOUSTIQUE

Board of Directors - Conseil d'administration

OFFICERS - OFFICIERS

DIRECTORS - ADMINISTRATEURS

SUSTAINING SUBSCRIBERS - ABONNÉS DE SOUTIEN

The Canadian Acoustical Association gratefully acknowledges the financial assistance of the Sustaining Subscribers listed below. Their annual donations (of $475 or more) enable the journal to be distributed to all at a reasonable cost.

L'Association Canadienne d'Acoustique tient à témoigner sa reconnaissance à l'égard de ses Abonnés de Soutien en publiant ci-dessous leur nom et leur adresse. En amortissants les coûts de publication et de distribution, les dons annuels (de 475$ et plus) rendent le journal accessible à tous les membres.

Acoustec Inc.
Jean-Philippe Migneron - 418-496-6600
info@acoustec.qc.ca
acoustec.qc.ca

Acoustex Specialty Products
Mr. Brian Obratoski - 2893895564
Brian@acoustex.ca
www.acoustex.net

AcoustiGuard-Wilrep Ltd.
Mr. William T. Wilkinson - 888-625-8944
wtw@wilrep.com
acoustiguard.com

BKL Consultants Ltd.
Mark Bliss - 604-988-2508
bliss@bkl.ca
www.bkl.ca

dB Noise Reduction
Mehrzad Salkhordeh - 519-651-3330 x 220
mehrzad@dbnoisereduction.com
dbnoisereduction.com

Feltkütur by Alkegen
Gilles Elhadad -
gelhadad@alkegen.com
feltkutur.com

HGC Engineering Ltd.
Mr. Bill Gastmeier -
bill@gastmeier.ca
hgcengineering.com

Hottinger Bruel & Kjaer inc.
Andrew Khoury - 514-695-8225
andrew.khoury@hbkworld.com
bksv.com

Jade Acoustics Inc.
Ms. Dalila Giusti - 905-660-2444
dalila@jadeacoustics.com
jadeacoustics.com

JASCO Applied Sciences (Canada) Ltd
Roberto Racca - +1.250.483.3300 ext.2001
roberto.racca@jasco.com
www.jasco.com

Pliteq Inc.
Wil Byrick - 416-449-0049
wbyrick@pliteq.com
www.pliteq.com

Soft dB Inc.
Dr. Roderick Mackenzie - 514-727-3800 x328
r.mackenzie@softdb.com
softdb.com